

Host plant and immature stages of *Setabara histrionica* (MacGillivray) (Hymenoptera, Tenthredinidae)

Quinlyn Baine¹, David R. Smith², Bill Zakopyko³,
Sapphitah Dickerson⁴, Chris Looney⁴

1 Department of Biology, University of New Mexico, MSC03-2020, Albuquerque, NM 87131, USA
2 Department of Entomology, National Museum of Natural History, Smithsonian Institution, P.O. Box 37012, MRC-168, Washington, DC 20013, USA **3** Renton, WA, USA **4** Washington State Department of Agriculture, 1111 Washington St SE, Olympia WA, 98504, USA

Corresponding author: Chris Looney (clooney@agr.wa.gov)

Academic editor: Marko Prous | Received 16 August 2022 | Accepted 21 November 2022 | Published 20 December 2022

<https://zoobank.org/188516A1-C4DD-41FF-B08B-86B0BF9A77CF>

Citation: Baine Q, Smith DR, Zakopyko B, Dickerson S, Looney C (2022) Host plant and immature stages of *Setabara histrionica* (MacGillivray) (Hymenoptera, Tenthredinidae). Journal of Hymenoptera Research 94: 1–11. <https://doi.org/10.3897/jhr.94.93555>

Abstract

The North American sawfly *Setabara histrionica* (Tenthredinidae: Heterarthrinae) is previously known only from adult collections but has been hypothesized to feed upon trees in the genus *Prunus*. We discovered a population of leaf-mining sawflies in Washington on *Prunus emarginata* and identified it as *S. histrionica* using combined morphological and molecular analysis. We observed preference in oviposition site selection on the host plant, with most eggs deposited on the margin of the basal third of the leaf, and on leaves growing within 1 meter of the ground. We include a description of the egg, larval stages, mine and phenology of *S. histrionica*, and an update to Smith's (1971) key to Heterarthrinae larvae.

Keywords

Heterarthrinae, Leaf miner, *Prunus*, sawfly, Symphyta

Introduction

Setabara Ross, 1951 is a genus of small leaf-mining sawflies in the subfamily Heterarthrinae (Hymenoptera: Symphyta: Tenthredinidae) comprising three described species. *Setabara clypeiambus* Saini & Ahmad, 2013, is known from Arunachal Pradesh, India (Saini and Ahmad 2013), *S. sinica* Wei & Niu, 2014, from Zhejiang, China (Wei and Niu 2014), and *S. histrionica* (MacGillivray, 1909), from western North America (Smith 1971). *Setabara histrionica* is currently known from CA, CO, ID, NV, OR, and WA in the United States (Smith 1971) and BC and MB in Canada (Goulet and Bennett 2021). The host plants have not been confirmed for any of these species, although *Prunus* has long been suspected of being the host of *S. histrionica* based on adult collection data (Smith 1971).

In May 2014, we observed numerous adults of a small black sawfly swarming and mating in a thicket of *Rubus armeniacus* Focke (Himalayan blackberry) and *Prunus emarginata* (Douglas ex Hook.) D. Dietr. (bitter cherry) in a park in Redmond, WA (the *Prunus* species was confirmed using keys in Hitchcock and Cronquist 2018). While the sawflies were initially seen alighting upon blackberry leaves, upon closer examination we determined that this seemed to be out of convenience and numerous females were actually observed ovipositing on the *P. emarginata* leaves. Several specimens were collected and subsequently identified as *S. histrionica* (using Smith 1971), providing strong evidence that *Prunus* spp. is indeed a host genus for this species. We visited the site several times in following years to observe oviposition behavior, phenology, and larvae. Our observations of elements of the species' life history are described herein.

Methods

Phenology

Observations and collections were made in Marymoor Park, Redmond, WA (King County), at the head of the Sammamish River at the north end of Lake Sammamish. The site is located on the northern end of an off-leash dog area of the park and comprises a fairly large stand of *P. emarginata* trees bordered by a gravel parking lot and an open grassy field (47.6599, -122.1114). We visited the site periodically between 2015 and 2020. At each visit the area was surveyed for sawflies, and a selection was collected. We also looked for evidence of leaf mines at these visits. Adult specimens were identified in the lab using Smith (1971).

Oviposition activity

Oviposition of *S. histrionica* was assessed by collecting leaves at varying heights of *P. emarginata*. In 2015, leaves were collected by haphazardly selecting four trees in the stand and clipping branches from three heights: low (<0.75 m), medium (approximately 2 m), and high (2.5–3 m). In 2020 we repeated this sampling with two modifications. Trees were sampled on three transects through the stand: one along the north side, one through the center and one along the south side. Collections were made from

every tree within 1 meter of each transect, by haphazardly selecting a single branch from each of four heights - < 1 m, 1.5 m, 3 m, and \geq 5 m from the ground. In both years every collected leaf was examined, the number of eggs or mines was counted, and their location on the leaf was recorded. Egg or mine location was approximated by dividing the leaf into thirds, (basal, middle, apical), and indicating if the egg was on the margin, along a vein, or along the midvein.

Mine and larval development

We photo-documented mines at the collection site between 30 May and 15 June, 2018. On 15 May, 2020, we collected several *S. histrionica* adults and transferred them to Olympia WA, where they were placed in six groups of three (1 female to 2 males) in mesh bags on short branches (~15 cm) of potted *P. emarginata* plants. Two of the six groups resulted in successful oviposition of 5 and 9 eggs, respectively. The number of eggs on each leaf was counted and the location on the leaf was recorded. After the eggs hatched, mines were examined twice a week to track development. Larvae were sacrificed periodically and preserved in 70% EtOH. Upon each sacrificial event the mine was dissected and searched for head capsules to determine the number of instars up to that point. Measurements of larvae ($n = 30$) and discarded head capsules ($n = 29$) found within captive-reared ($n = 9$) and field-collected mines ($n = 50$) were made under a Leica MXC microscope using the Leica image software package. Five larvae were left to develop in the bagged mines.

Molecular data

Two specimens from the Marymoor collections, one larva and one adult, were selected for mitochondrial *cytochrome oxidase subunit I* (COI) sequencing. We were also provided with a single dead larva from a leaf mine on *Prunus subcordata* Benth. (Klamath plum) collected near Bass Lake, California, in June of 2021 (V. Albu 2021, pers. comm.). DNA from the whole larval bodies, and three legs from the adult, was extracted in 5 μ l to 30 μ l extraction volumes with 10% Chelex, and 4% Proteinase K (20 mg/mL). Samples were incubated at 56 °C for 1 hour, then at 99 °C for 20 min. Each 25 μ l PCR reaction contained 5 μ l of molecular grade water, 12.5 μ l of 2X Platinum II Hot-start Green PCR Master Mix (Invitrogen), 1.25 μ l of MgCl₂ (50 mM), 0.5 μ l of F and R primers (10 μ M), and 2 μ l of DNA template. For the larval extraction, the primer pair LCO1490 and HCO2198 (Folmer et al. 1994) with M13 tails amplified the COI barcode region with cycling conditions as follows: initial denaturation at 95 °C for 1 min., 35 cycles of denaturation at 96 °C for 2 seconds, annealing at 50 °C for 5 seconds, and extension at 72 °C for 20 seconds. Final extension was at 72 °C for 2 minutes. Because adult sample PCR amplification using above primers was unsuccessful, the adult extraction was amplified using primer pair LepF1 and LepR1 (Hebert et al. 2004) with cycling conditions as follows: initial denaturation at 94 °C for 3 min., 40 cycles of denaturation at 94 °C for 20 seconds, annealing at 50 °C for 20 seconds, and extension at 72 °C for 30 seconds. Final extension was at 72 °C for 5 minutes. Amplification controls included a non-template control containing molecular grade water, and a positive control containing *Lymantria dispar dispar*

DNA. Products were visualized via gel electrophoresis using a 1.5% agarose + 1X TBE gel at 160 Volts for 35 minutes. Amplicons of expected size were purified enzymatically using ExoSAP-IT Express (Applied Biosystems) kit per the manufacturer's protocol. Samples were sequenced in both forward and reverse directions using the Big Dye Xterminator cycle sequencing kit v3.1 and BigDye Xterminator BDX clean up kit (Applied Biosystems) on the ABI SeqStudio following manufacturer guidelines. All sequences were manually trimmed for quality to 658 bp using Geneious Prime 2021.2, then aligned using MUSCLE 3.8.425 with 10 iterations. All resulting sequences were submitted to NCBI repository (Washington: ON181656 and ON181654, California: ON181655).

Results

Phenology

Setabara histrionica appears to be univoltine. Adults were active for a period of about 2 weeks during the spring, based on weekly visits to the site between mid-April and late May in 2018, 2019, and 2020 (Table 1). The earliest observations of adults were made on 5 May, 2014, and the latest were 23 May, 2018. Most adults were observed and captured in the understory, although a few adults were also collected by sweeping taller *P. emarginata* within reach (~3m). Over 2/3 of the specimens captured were males, and males outnumbered females at every collecting event except one.

The first mines became visible about two weeks after adult activity was observed. Because of the semi-cryptic nature of leaf-mining larvae, the precise number of days spent in each developmental stage was not recorded. The average number of days from egg hatch to final instar in our captive sawflies was 41 (n = 5). All of these specimens were lost during the final instar. It seems likely that the larvae escaped the mesh rearing bags, perhaps by chewing their way through or by squirming through small creases where the bag was secured to the *Prunus* limbs. Soil from the captive pots was sieved and examined, but no pupae or pre-pupae were located.

Oviposition preference

We collected 61 branches and 489 leaves in 2015, and recorded the location of 292 eggs. In 2020 we collected 114 branches and 1201 leaves, but located only 36 eggs.

Table 1. Collection dates for adult *Setabara histrionica* at Marymoor Park, Washington.

Collection date	male	female
5 May 2014	9	5
14 May 2018	4	2
23 May 2018	2	0
16 May 2019	1	1
15 May 2020	15	7
18 May 2020	4	0

The majority of eggs discovered in both years were located in the lower tree branches (Table 2), with 61% were found within 1 m of the ground. All observed eggs were deposited on the margin of the leaf. Egg frequency decreased from the leaf stem towards the apex of each leaf, with more eggs located in the basal third than the central third, and more in the central third than in the apical third (Table 2).

Larval description

The habitus is typical of leaf-mining Heterarthrinae (Smith 1971): head and body slightly dorsoventrally flattened, prolegs reduced, prognathous. Body white to cream-white. Head capsule slightly wider than long. Larval measurements are reported as averages.

Egg: less than 1 mm in diameter, round or slightly oblong, appearing as a light green blister on the outside of the leaf (Fig. 1).

First instar: body length (n = 3): 2.38 mm, head capsule width (n = 13): 0.38 mm. Head capsule beige to amber, thoracic legs white. Prolegs present on abdominal segments 2–8.

Second instar: body length (n = 2): 2.59 mm, head capsule width (n = 12): 0.51 mm.

Third instar: body length (n = 12): 5.06 mm, head capsule width (n = 18): 0.63 mm.

Final instar: body length (n = 17): 6.70 mm, head capsule width (n = 16): 0.75 mm (Figs 2, 3). Head dark brown, body mostly white with various dark plates. Head: Head capsule dark brown, lighter ventrally and around mouthparts; antenna 2-segmented; each mandible with 3 sharp apical teeth; maxillary palpus with 4 palpomeres, lacinia with row of about 10 subequal short spines; epipharynx with transverse row of about 10 spines on each half; labial palpus with three palpomeres. Thorax: Thoracic legs, large rectangular plate on pronotum, narrow plate on anterior margin of mesonotum, large rectangular plate on prosternum, small central plates on mesosternum and metasternum dark brown; thoracic legs 5 segmented; coxae without tubercles; tarsal claws present, simple. Abdomen: Small central dark brown plate on sternum of first segment (smaller than metasternal plate); prolegs present on segments 2–8 and 10, each proleg with anterior crescent-shaped dark spot, anal proleg with complete, circular dark spot; sometimes tiny supraspiracular spot present.

Table 2. Oviposition sites of *Setabara histrionica* on *Prunus emarginata* leaves.

Branch height from ground	Leaves sampled	Eggs in basal 1/3 leaf	Eggs in middle 1/3 of leaf	Eggs in apical 1/3 of leaf	Mean eggs/leaf
2015					
<0.75 m	173	93	66	19	1.03
~ 2m	158	29	17	5	0.32
2.5–3 m	158	39	18	6	0.4
2020					
<1 m	351	9	10	3	0.06
~1.5 m	397	4	1	0	0.01
~3 m	270	4	1	0	0.02
> 5m	183	1	3	0	0.02

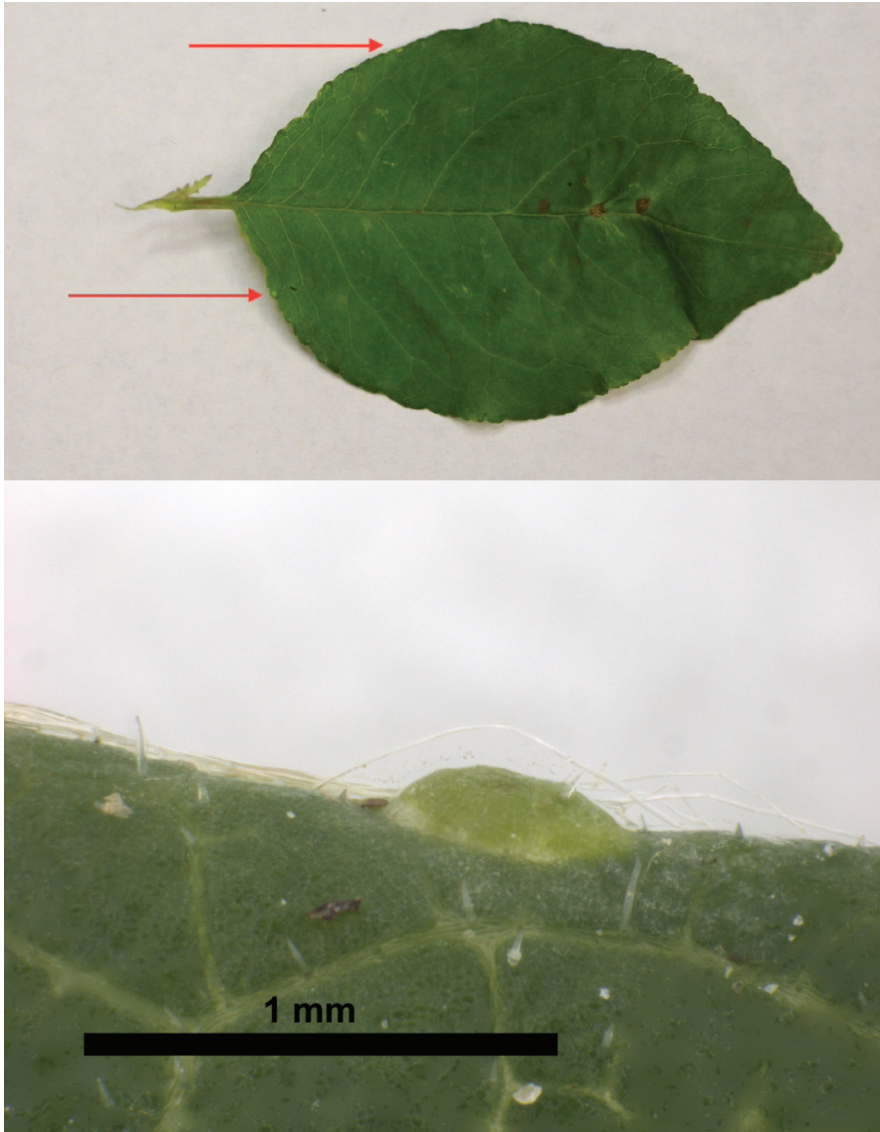


Figure 1. Location of *Setabara histrionica* eggs on a *Prunus emarginata* leaf, and close up of egg.

In Smith’s 1971 key to Heterarthrinae larvae, *Setabara* goes to couplet 6 which includes *Messa* (now *Fenusella*) and *Profenus* (in part). The key can be amended as follows:

- 6 Mesosternum, metasternum, and sternum of first abdominal segment with dark plates (pl. XII, 152, 153; pl.XIV, 164) **6A**
- Mesosternum, metasternum, and sternum of first abdominal segment without plates; on *Crataegus* (pl. XVI, 201, 202) *Profenus* MacGillivray (pt.)

- 6A On *Populus*, *Betula*, *Salix*; 9th sternum with pair of small sound dark spots; Trans-continental; Smith 1971: fig. 153..... *Fenusella* Leach (in key as *Messa*)
- On *Prunus*; 9th sternum without dark spots; western (Fig. 3).....
 *Setabara histrionica*

Mine: After hatching, the larva feeds on leaf tissue in a semi-circular shape moving away from the leaf margin (Fig. 4). Mines continue to be excavated in a blotch pattern, often constrained by the midvein of the leaf, unless near the thinner area at the apex. Frass was distinctly oblong and capsule-shaped, and was broadly dispersed throughout the mine (Fig. 5). The average area at larval maturity was 15.49 mm² (n = 11). Pre-pupae exited the mine through a chewed arced slit in the cuticle, which measured 2.13 mm on average (n = 4) (Fig. 6).

Molecular analysis

The Washington specimens collected in this study were compared with two 421 bp COI sequences from *S. histrionica* specimens housed at the US National Museum of Natural History (USNM), also collected from Marymoor Park (BioProject PRJNA540960, GenBank accessions MW983660 and MW982369). All four trimmed Washington sequences were 100% identical to one another. In contrast, the sequence from the California larva was 95.3% identical to these, with 29 non-identical sites.



Figure 2. Fourth instar, head.

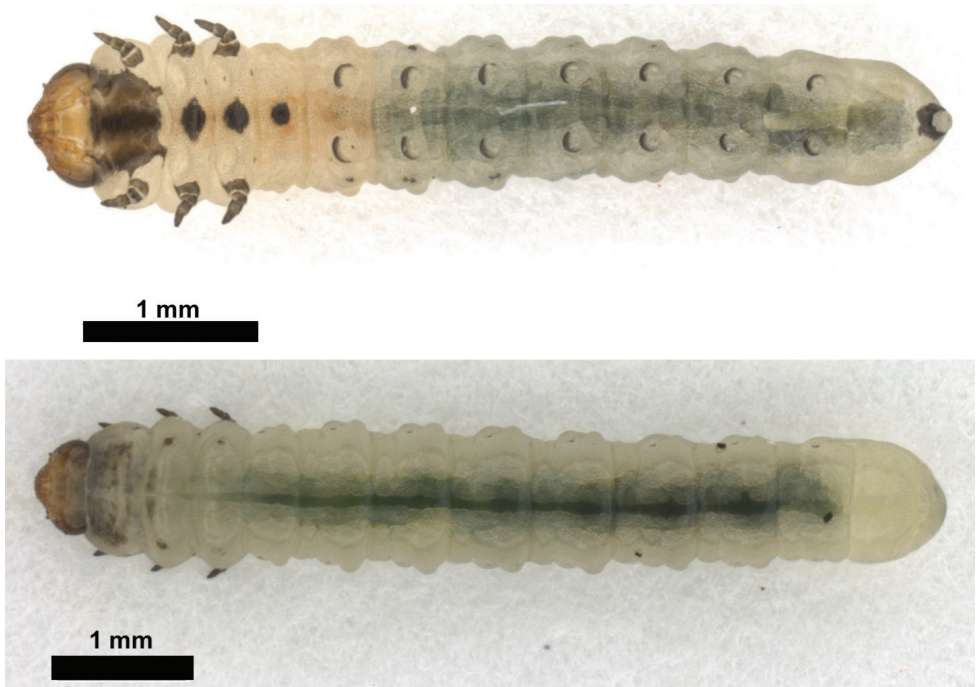


Figure 3. Fourth instar, ventral/dorsal view.



Figure 4. Mines at different stages of development.

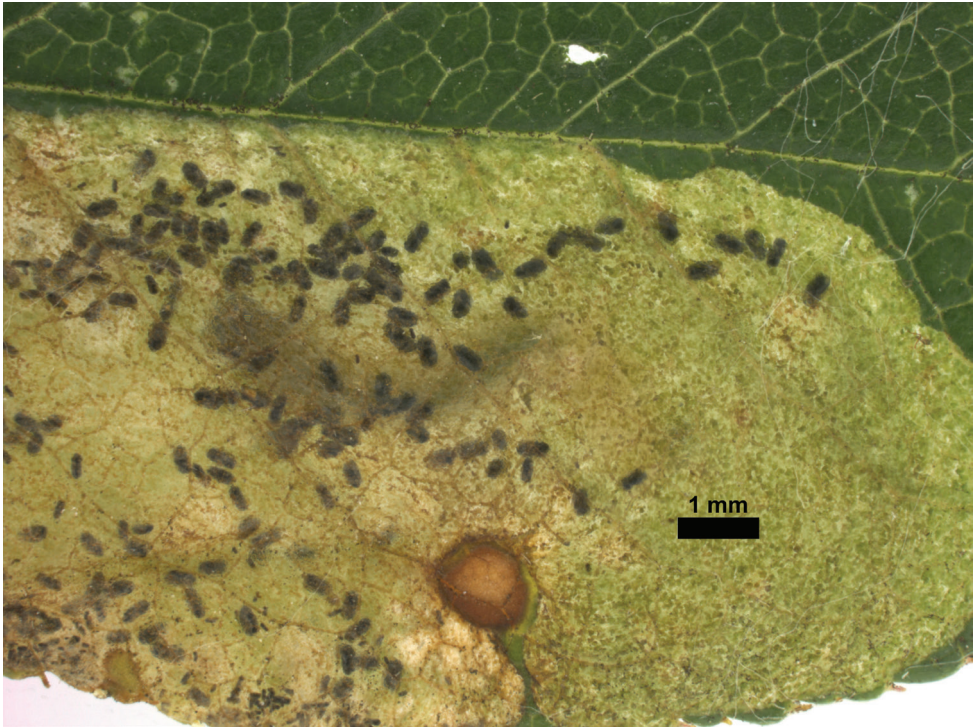


Figure 5. Frass shape and distribution, taken from late instar mine.

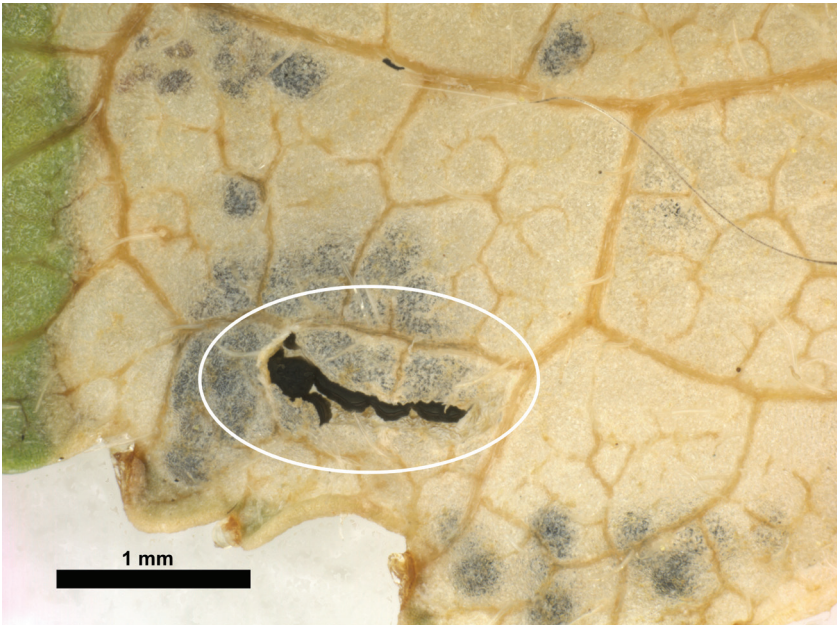


Figure 6. Pre-pupal emergence hole.

Discussion

Larvae of *S. histrionica* are similar in morphology and mining habits to those of the closely-related genus *Fenusella*, species of which mine *Populus*, *Salix*, and *Betula* (Underwood and Titus 1968; Smith 1971). *Metallus* are also very similar and are associated with species of Rosaceae, although not *Prunus* (Eiseman and Smith 2017). Both *Fenusella* and *Metallus* create blotch mines starting from the leaf margin, and exit the mine at maturity to overwinter in the soil below (Underwood and Titus 1968; Smith 1971; Eiseman and Smith 2017), as we observed in *S. histrionica*.

Adults have been collected from *Prunus subcordata*, in Oregon in May, 1964, (Smith 1971), in California from a mixed stand of *P. subcordata* and *P. virginiana* (V. Albu 2021, pers. comm.), and on *P. emarginata* (this study). Eiseman (2019) documents mines on *P. virginiana* in Colorado that appear similar to the mines we observed on *P. emarginata*. However, while the mine shape is similar, the frass within that mine is distinctly long and thin, rather than the capsule-shaped frass we observed in Washington. This difference could be a function of host plant, or the product of a different leaf-mining insect. This subtle difference in mine characteristics and the relatively large difference in COI sequence between the California and Washington specimens raise the possibility that there are two North American species of *Setabara*. This will be explored in future work - the adult specimens collected in California also key to *Setabara*, but a detailed comparison of the different populations has not been made.

One surprising aspect of these data was the heavily male-biased adult collections. Males of many Heterarthrinae are rarely collected, and several species are parthenogenetic. In contrast, reported sex ratios for *Fenusa pumila* and *Heterarthrus vagans* are at, or close to, parity (Digweed et al. 2009; Humble 2010). It is entirely possible that the sex ratio we observed is an artifact of haphazard sampling, rather than an actual aspect of the species' biology. Even so, this is another intriguing possibility that could be explored in greater detail.

Prior to this study, *S. histrionica* was only known from adult specimens and suspected to use *Prunus* as a host plant. These data confirm one host species, *Prunus emarginata*, and are the first description of the egg, larva, mine, and phenology for the genus. Many aspects of life history and morphology are similar to other leaf-mining Heterarthrinae. The potential existence of an undescribed species, and possibility of an unusual sex ratio, indicates that even in this small group discoveries remain to be made in North America.

Acknowledgements

The authors would like to thank the staff of Marymoor Park, Redmond WA, for access to the field site. Telissa Wilson (WSDA) assisted with molecular analysis, and Maggie Freeman (WSDA/ Oregon State University) helped with field work. We are grateful to Valeriu Albu for contacting us and sharing specimens from California. We would also like to Spencer Monckton and an anonymous reviewer who provided valuable feedback and suggestions to improve this article

References

- Digweed SC, MacQuarrie CJK, Langor DW, Williams DJM, Spence JR, Nystrom KL, Morneau L (2009) Current status of invasive alien birch-leafmining sawflies (Hymenoptera: Tenthredinidae) in Canada, with keys to species. *The Canadian Entomologist* 141(3): 201–235. <https://doi.org/10.4039/n09-003>
- Eiseman CS (2019) Leafminers of North America. Self-published e-book, [clii +] 1857 pp.
- Eiseman CS, Smith DR (2017) Nearctic species of *Metallus* Forbes (Hymenoptera: Tenthredinidae): biology and distribution. *Proceedings of the Entomological Society of Washington* 119(4): 551–564. <https://doi.org/10.4289/0013-8797.119.4.551>
- Folmer O, Black M, Hoeh W, Lutz R, Vrijenhoek R (1994) DNA primers for amplification of mitochondrial cytochrome c oxidase subunit I from diverse metazoan invertebrates. *Molecular Marine Biology and Biotechnology* 3: 294–299.
- Goulet H, Bennett AMR (2021) Checklist of the sawflies (Hymenoptera) of Canada, Alaska and Greenland. *Journal of Hymenoptera Research* 82: 21–67. <https://doi.org/10.3897/jhr.82.60057>
- Hebert PD, Penton EH, Burns JM, Janzen DH, Hallwachs W (2004) Ten species in one: DNA barcoding reveals cryptic species in the neotropical skipper butterfly *Astraptes fulgerator*. *Proceedings of the National Academy of Sciences* 101(41): 14812–14817. <https://doi.org/10.1073/pnas.0406166101>
- Hitchcock CL, Cronquist A (2018) *Flora of the Pacific Northwest: an illustrated manual*. University of Washington Press, 750 pp.
- Humble LM (2010) First North American records for *Heterarthrus vagans* (Hymenoptera: Tenthredinidae), a Palaearctic leafmining sawfly of alder. *The Canadian Entomologist* 142: 181–187. <https://doi.org/10.4039/n09-071>
- MacGillivray AD (1909) A synopsis of the American species of Scolioneurinae. *Annals of the Entomological Society of America* 2: 259–271. <https://doi.org/10.1093/aesa/2.4.259>
- Ross HH (1951) Tenthredinidae. In: Muesebeck CFW, Krombein KV, Townes HK (Eds) *Hymenoptera of America North of Mexico, Synoptic Catalog*. U. S. Department of Agriculture, Agriculture Monograph No. 2: 22–64, 66–82.
- Saini MS, Ahmad M (2013) First report of *Profenusa* Macgillivray & *Setabara* Ross with one new species of each genus from India (Hymenoptera: Symphyta: Tenthredinidae). *Annals of Entomology* 31(1): 15–20.
- Smith DR (1971) Nearctic Sawflies. III. Heterarthrinae: Adults and larvae (Hymenoptera: Tenthredinidae). *Technical Bulletin*, U.S. Department of Agriculture 1420: 1–84.
- Underwood GR, Titus FA (1968) Description and seasonal history of a leaf miner on poplar *Messa populifoliella* (Hymenoptera: Tenthredinidae). *Canadian Entomologist* 100: 407–411. <https://doi.org/10.4039/Ent100407-4>
- Wei M, Niu G (2014) *Setabara* Ross, a genus new to China with description of a new species (Hymenoptera: Tenthredinidae). *Entomological News* 124(2): 98–102. <https://doi.org/10.3157/021.124.0204>

From hell's heart I stab at thee! A determined approach towards a monophyletic Pteromalidae and reclassification of Chalcidoidea (Hymenoptera)

Roger Burks¹, Mircea-Dan Mitroiu², Lucian Fusu², John M. Heraty¹,
Petr Janšta^{3,4}, Steve Heydon⁵, Natalie Dale-Skey Papilloud⁶, Ralph S. Peters⁷,
Ekaterina V. Tselikh⁸, James B. Woolley⁹, Simon van Noort^{10,11}, Hannes Baur^{12,13},
Astrid Cruaud¹⁴, Christopher Darling^{15,16}, Michael Haas⁴,
Paul Hanson¹⁷, Lars Krogmann^{4,18}, Jean-Yves Rasplus¹⁴

1 Department of Entomology, University of California Riverside, Riverside, CA, USA **2** Faculty of Biology, Alexandru Ioan Cuza University, Iasi, Romania **3** Department of Zoology, Faculty of Science, Charles University, Prague, Czech Republic **4** Department of Entomology, State Museum of Natural History, Stuttgart, Germany **5** Bobart Museum of Entomology, University of California, Davis, CA, 95616, USA **6** Insects Division, Natural History Museum, London, UK **7** Zoologisches Forschungsmuseum Alexander Koenig, Leibniz Institute for the Analysis of Biodiversity Change, Bonn, Germany **8** Zoological Institute, Russian Academy of Sciences, St. Petersburg, Russia **9** Department of Entomology, Texas A&M University, College Station, TX, USA **10** Research and Exhibitions Department, South African Museum, Iziko Museums of South Africa, PO Box 61, Cape Town 8000 South Africa **11** Department of Biological Sciences, University of Cape Town, Private Bag, Rondebosch, 7701, South Africa **12** Department of Invertebrates, Natural History Museum Bern, Bern, Switzerland **13** Institute of Ecology and Evolution, University of Bern, Bern, Switzerland **14** CBGP, INRAE, CIRAD, IRD, Montpellier SupAgro, University of Montpellier, Montpellier, France **15** Department of Natural History, Royal Ontario Museum, Toronto, ON, M5S 2C6, Canada **16** Department of Ecology and Evolutionary Biology, University of Toronto, Toronto, ON, M5S 1A1, Canada **17** Escuela de Biología, Universidad de Costa Rica, San Pedro de Montes de Oca, San Jose 11501-2060, Costa Rica **18** Institute of Biology, Biological Systematics (190m) University of Hohenheim, Stuttgart, Germany

Corresponding author: Roger Burks (burks.roger@gmail.com)

Academic editor: Miles Zhang | Received 31 August 2022 | Accepted 24 October 2022 | Published 20 December 2022

<https://zoobank.org/6CB80723-9A47-403F-ABEC-9AF8AE7F417F>

Citation: Burks R, Mitroiu M-D, Fusu L, Heraty JM, Janšta P, Heydon S, Papilloud ND-S, Peters RS, Tselikh EV, Woolley JB, van Noort S, Baur H, Cruaud A, Darling C, Haas M, Hanson P, Krogmann L, Rasplus J-Y (2022) From hell's heart I stab at thee! A determined approach towards a monophyletic Pteromalidae and reclassification of Chalcidoidea (Hymenoptera). *Journal of Hymenoptera Research* 94: 13–88. <https://doi.org/10.3897/jhr.94.94263>

Abstract

The family Pteromalidae (Hymenoptera: Chalcidoidea) is reviewed with the goal of providing nomenclatural changes and morphological diagnoses in preparation for a new molecular phylogeny and a book on world fauna that will contain keys to identification. Most subfamilies and some tribes of Pteromalidae are elevated to family level or transferred elsewhere in the superfamily. The resulting classification is a compromise, with the aim of preserving the validity and diagnosability of other, well-established families of Chalcidoidea. The following former subfamilies and tribes of Pteromalidae are elevated to family rank: Boucekiidae, Ceidae, Cerocephalidae, Chalcedectidae, Cleonymidae, Coelocybidae, Diparidae, Epichrysomallidae, Eunotidae, Herbertiidae, Hetreulophidae, Heydeniidae, Idioporidae, Lyciscidae, Macromesidae, Melanosomellidae, Moranilidae, Neodiparidae, Ooderidae, Pelecinnellidae (senior synonym of Leptofoeninae), Pirenidae, Spalangiidae, and Systasidae. The following subfamilies are transferred from Pteromalidae: Chromeurytominae and Keiraninae to Megastigmidae, Elatoidinae to Neodiparidae, Nefoeninae to Pelecinnellidae, and Erotolepsiinae to Spalangiidae. The subfamily Sycophaginae is transferred to Pteromalidae. The formerly *incertae sedis* tribe Lieparini is abolished and its single genus *Liepara* is transferred to Coelocybidae. The former tribe Tomocerodini is transferred to Moranilidae and elevated to subfamily status. The former synonym Tridyminae (Pirenidae) is treated as valid. The following former Pteromalidae are removed from the family and, due to phylogenetic uncertainty, placed as *incertae sedis* subfamilies or genera within Chalcidoidea: Austrosystasinae, Ditropinotellinae, Keryinae, Louriciinae, Micradelinae, Parasaphodinae, *Rivasia*, and Storeyinae. Within the remaining Pteromalidae, Miscogastrinae and Ormocerinae are confirmed as separate from Pteromalinae, the former tribe Trigonoderini is elevated to subfamily status, the former synonym Pachyneurinae is recognized as a distinct subfamily, and as the senior synonym of Austroterobiinae. The tribe Termolampini is synonymized under Pteromalini, and the tribe Uzkini is synonymized under Colotrechnini. Most former Otitesellinae, Sycocinae, and Sycoryctinae are retained in the tribe Otitesellini, which is transferred to Pteromalinae, and all other genera of Pteromalinae are treated as Pteromalini. Eriaporidae is synonymized with Pirenidae, with Eriaporinae and Euryischiinae retained as subfamilies. Other nomenclatural acts performed here outside of Pteromalidae are as follows: Calesidae: elevation to family rank. Eulophidae: transfer of Boucekelimini and Platytetracampini to Opheliminae, and abolishment of the tribes Elasmimi and Gyrolasomyiini. Baeomorphidae is recognized as the senior synonym of Rotoitidae. Khutelchalcididae is formally excluded from Chalcidoidea and placed as *incertae sedis* within Apocrita. Metapelmatidae and Neanastatidae are removed from Eupelmidae and treated as distinct families. *Eopelma* is removed from Eupelmidae and treated as an *incertae sedis* genus in Chalcidoidea. The following subfamilies and tribes are described as new: Cecidellinae (in Pirenidae), Enoggerinae (*incertae sedis* in Chalcidoidea), Erixestinae (in Pteromalidae), Eusandalinae (in Eupelmidae), Neapterolelapinae (*incertae sedis* in Chalcidoidea), Solenurinae (in Lyciscidae), Trisecodinae (in Systasidae), Diconocarini (in Pteromalidae: Miscogastrinae), and Trigonoderopsini (in Pteromalidae: Colotrechninae). A complete generic classification for discussed taxa is provided.

Keywords

New family, taxonomic change

*“Towards thee I roll, thou all-destroying but unconquering whale; to
the last I grapple with thee; from hell’s heart I stab at thee”*
Herman Melville, “Moby Dick”

Introduction

Pteromalidae as defined by Bouček (1988), contains 33 subfamilies and approximately 640 genera, by far the largest count in Chalcidoidea of both categories. However, there has been agreement for decades (Heraty and Darling 1984; Noyes 1990; Gibson et al. 1999) that Pteromalidae has been a polyphyletic “dumping ground” of taxa that do not obviously fit within previously established families of Chalcidoidea. Because of the highly varied morphology and life histories of taxa contained in Pteromalidae, the family has no unifying features. This narrative is complicated by the highly varied morphology and life histories present in the largest pteromalid subfamily, Pteromalinae, which contains by far the most genera and includes parasitoids of hosts across holometabolous insects, and also egg parasitoids of Hemiptera, predators in spider egg sacs, hyperparasitoids and gall-makers. Just as Pteromalidae has not been recently defined in a way that excludes other chalcidoids, the subfamily Pteromalinae, with approximately 315 genera (Noyes 2019) before the publication of this article, has also not been recently diagnosed in a way that excludes other pteromalids. This is presumably because the diversity of Pteromalinae makes definition exceedingly difficult (Graham 1969; Bouček 1988).

The lack of easy characterization of the subfamily Pteromalinae may have contributed to the eventual dumping-ground nature of the family Pteromalidae, but the greatest contributor may instead be the nature of the subfamily Cleonyminae, which contains many morphologically generalized parasitoids of wood-boring beetles. Bouček (1988) indicated that many pteromalid subfamilies could intuitively be derived from early cleonymine-like stock. However, if this early stock is made up entirely of species classified as Cleonyminae, it would cause the subfamily to be paraphyletic.

Inherent in this concept of Pteromalidae is the conclusion that Cleonyminae and Pteromalinae are more closely related to one another than to other Chalcidoidea. However, molecular data have never linked them nor any part of them in a monophyletic group that did not also include most of the other families of Chalcidoidea (Campbell et al. 2000; Munro et al. 2011; Heraty et al. 2013). This does not indicate that Bouček (1988) was incorrect in his hypothesis, but instead allows the possibility that much of the rest of Chalcidoidea outside Pteromalidae may have also been derived from an assemblage of the early cleonymine-like stock that he postulated. Under this scenario, a researcher wishing to find the sister group of almost any distinctive family in Chalcidoidea is forced to consider the possibility that it may be hidden away among the many obscure subfamilies of Pteromalidae or even within one of their tribes.

An arguably generalized part of the early cleonymine-like stock mentioned by Bouček (1988) may be represented in the Cretaceous by Diversinitidae, an extinct family distinguished from most other chalcidoids, but not from Mymaridae, by having multiporous plate sensilla on the true 1st flagellomere (Haas et al. 2018). Given that Mymaridae is hypothesized as the sister group of other Chalcidoidea (Gibson et al. 1999; Munro et al. 2011; Heraty et al. 2013), Diversinitidae may also be part of the outgroup relative to most other Chalcidoidea. Also, given that Diversinitidae are otherwise not particularly unusual relative to most other Chalcidoidea, especially

being similar in habitus to the pteromalid subfamilies Pteromalinae or Louriciinae, it is possible that morphological diagnoses of family-rank lineages from within Pteromalidae will require greater focus upon relatively subtle features that have been previously overlooked or rejected as indicators of deep phylogenetic splits. It also suggests that an elongate body shape with a large mesopleural area and subtriangular metasoma, that together can be called a “pteromaloid habitus” as seen in Diversinitidae and in pteromalid taxa such as Pteromalinae, Cleonyminae, Colotrechninae, and Pireninae, may not always be indicative of membership in Pteromalidae.

Indeed, many families herein removed from Pteromalidae do not have any known members with the pteromaloid habitus as defined here, and this has been one of the many indicators that subfamilies such as Cerocephalinae, Eunotinae, Herbertiinae, Pelecinnellinae (senior synonym of Leptofoeninae), Spalangiinae, and Storeyinae may not be closely related to core Pteromalidae at all. To make matters more confusing, not all core Pteromalinae have the “pteromaloid habitus”, in part because of the diverse life histories of pteromalines. The most conspicuous examples of this are the non-pollinating fig wasps, previously classified in three subfamilies treated as Agaonidae, that have been indicated by molecular data to form a monophyletic group within Pteromalidae (Rasplus et al. 1998). This left open the possibility, when examining morphology alone, that some or all of the morphologically distinctive subfamilies mentioned above could be nothing more than apomorphic members of Pteromalidae that have evolved an unusual habitus due to having different life histories. Several molecular studies have been used to test these morphological hypotheses of phylogenetic relationship and support the results being presented herein (Campbell et al. 2000; Munro et al. 2011; Heraty et al. 2013; Cruaud et al., submitted).

Over the time spent on this project, we have seen that analyses using molecular data alone are not always reliable, and that morphological or life history insights can be helpful in discovering contamination events, or even for suggesting that more rigorous phylogenetic analytical methods may be required (Cruaud et al., submitted). The new classification presented here is therefore not simply a reaction to the results of a new molecular phylogeny. Instead, it is the product of a broader analysis in which morphological investigation and knowledge of natural history have played an active role in a process of reciprocal illumination as described by Hennig (1950 1966). The result is a more credible hypothesis of phylogenetic relationships within Chalcidoidea than has been previously seen, with natural and diagnosable higher taxa being proposed here.

In the course of our molecular studies, interesting monophyletic groups have been discovered, including a “Gall Clade” containing previously unassociated taxa that share a gall association: Cynipencyrtidae, Epichrysomallidae new status, Melanosomellidae new status, Ormyridae, and Tanaostigmatidae (Cruaud et al., submitted; van Noort et al., in prep.). Because these families resemble each other mainly in an overall arched body shape and in other features that could have been dismissed as insignificant, these could have been dismissed as the result of convergence due to shared gall association. Instead, a clade has been revealed that can greatly facilitate evolutionary studies of

many chalcidoid gall associates while excluding other gall-associate chalcidoids that have developed this association independently.

This is not to say that other families of Chalcidoidea have been entirely unaffected by our investigations. While the focus of this publication is to outline changes necessary to produce a new, monophyletic Pteromalidae that is more useful for biological research, necessary changes to other families are discussed here as well. In this respect, we have chosen an approach that preserves previously accepted families such as Signiphoridae and Tanaostigmatidae, whereas an alternative approach could have lumped them into larger families that would prove more difficult to diagnose using easily visible morphological features. This is in keeping with the approach used by Zhang et al. (2022), which preserved the previous concept of Eucharitidae by subdividing Perilampidae and treating Eutrichosomatidae, previously a subfamily of the Pteromalidae, as a separate, but related family.

Finally, a number of taxa are kept as *incertae sedis* in Chalcidoidea, based on two criteria. They have either not been analyzed molecularly and/or they cannot currently be placed with certainty in another family or as separate families. This is carried out as the lesser of evils: to avoid creating a potentially unstable family-level classification, we leave some small and obscure taxa as unplaced in Chalcidoidea, pending future analysis. The present treatment calls attention to these otherwise obscure taxa, but it also avoids unnecessary family names that would be synonymized if the data suggest it.

Materials and methods

Morphological terms generally follow Gibson (1997) and Krogmann and Vilhelmsen (2006). Subforaminal bridge terms follow Heraty et al. (2013) or Burks et al. (2015) with the addition of using hypostoma as defined by Mikó et al. (2007). Terms regarding the antennal cleaner complex of the 1st protarsomere, such as the basitarsal comb and basitarsal notch, are defined by Basibuyuk and Quicke (1994). Mandibles are discussed in the plural, because of their frequent and diagnostically useful asymmetry in tooth count. Metatibial spurs are also discussed in the plural, since their count varies from 1 to 2 in many families. For family-group diagnoses, features are only mentioned if they are useful and relevant for distinction from another family. The word funiculars are used to indicate flagellomeres between the anelli and clava. We treat the term frenal line as indicating a space where the frenal groove, or any other transition indicating a frenum, can occur. Given that the frenal line is indicated through various different means in Chalcidoidea, the frenal line itself is mainly mentioned when it is indicated by something other than a groove. Similarly, the axillula can be set off medially by what is called the axillular sulcus or axillular carina, depending upon which component of it is more strongly expressed. To minimize wordiness in diagnoses, if a feature is highly variable or unknown within a given family, it is not mentioned.

Families emerging from Pteromalidae

Boucekiidae new status

Boucekiini Gibson, 2003. Type genus: *Boucekius* Gibson, 2003.

Diagnosis. Antenna with 8 flagellomeres, including a single anellus and an undivided clava. Eyes ventrally divergent. Clypeus without transverse subapical groove. Labrum hidden behind clypeus. Mandibles with ventral tooth and large dorsal truncation. Mesoscutellum with frenum set off by complete frenal groove, and with axillular sulcus (Fig. 1). Mesopleural area without expanded acropleuron; mesepimeron not extending over anterior margin of metapleuron. All legs with 5 tarsomeres; protibial spur stout and curved; basitarsal comb longitudinal; metafemur with ventral lobe or subapical teeth (Fig. 2). Metasoma with epipygium (Fig. 3), or with syntergum (*Chalcidiscelis* Ashmead).

Discussion. Gibson (2003) described Boucekiidae as a new tribe, although it differed from many species in Cleonyminae (as then defined) in the frenum and potentially the labrum. In habitus boucekiids do resemble former Cleonyminae and other large-bodied Chalcidoidea that have metallic coloration. Out of former Cleonyminae, those with an unambiguous frenal arm (= mesoscutellar arm) laterally are now classified in Solenurinae (Lyciscidae), which differ most notably in having an incomplete frenal line and a flagellum with 2 or 3 clavomeres. Chalcedectidae and Heydeniidae can have either an indistinct frenal groove, a small frenum, or a strongly expanded marginal rim of the mesoscutellum that may resemble a frenum; however, both have a different clava from Boucekiidae, with multiple clavomeres instead of an undivided clava and, in Chalcedectidae, an apical spine in females. Chalcedectidae have a syntergum that is not crossed by a transverse sulcus and otherwise does not have an epipygium. Heydeniidae have a long prepectus that is enlarged both laterally and ventrally. The elongate ovipositor and more or less elongate cerci in females may cause confusion with Torymididae or Megastigmidae, both of which have multiple clavomeres and more than 8 flagellomeres. The narrow, essentially parallel-sided flagellomeres may invite confusion with the antenna in Ceidae or Macromesidae; however, members of both these taxa have multiple clavomeres and much narrower mandibles with no dorsal truncation, and Macromesidae lack a frenum. Pteromalidae and Pelecinnellidae have more than 1 clavomere in nearly all cases, but Pteromalidae with apparently 1 clavomere (some males) have more than one anelliform basal flagellomere.

Ceidae new status

Ceini Bouček, 1961. Type genus: *Cea* Walker, 1837. Treated as Ceinae by Peck, Bouček and Hoffer (1964).

Diagnosis. Antenna with 12 flagellomeres, including a small 4th clavomere. Eyes not ventrally divergent. Clypeus with transverse subapical groove. Labrum subrectangular

and exposed, with marginal setae in a row (Fig. 4). Mandibles with 2 teeth (Fig. 4). Subforaminal bridge with postgena separated by lower tentorial bridge except for a small postgenal bridge dorsal to the hypostoma. Mesoscutellum with frenum indicated at least laterally, and with axillular sulcus. Mesopleural area without an expanded acropleuron. Propodeum with small and circular spiracle separated by more than its own length from the anterior propodeal margin (Fig. 5). All legs with 5 tarsomeres; protibial spur stout and curved; basitarsal comb longitudinal. Metasoma with syntergum, therefore without epipygium.

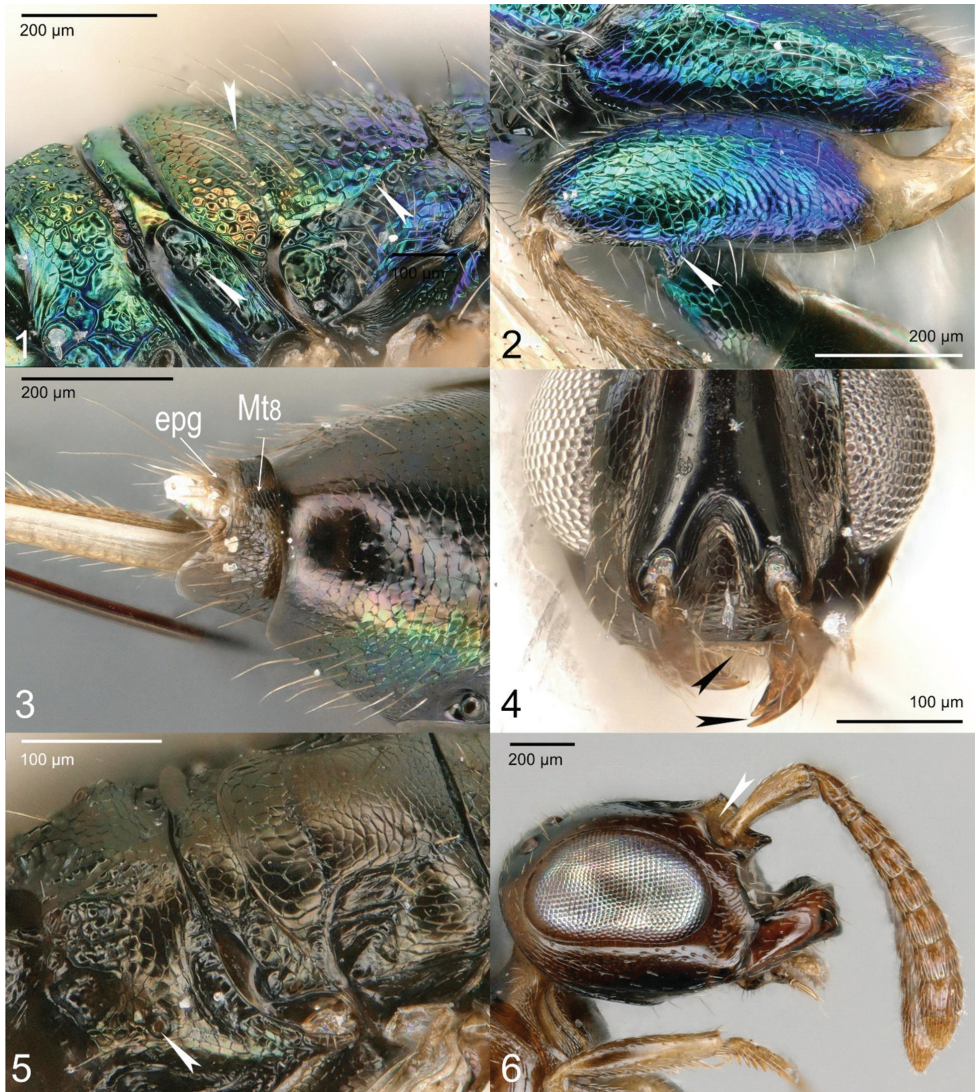
Discussion. Ceidae differs from most other Chalcidoidea in having the propodeal spiracle separated from the anterior propodeal margin by more than its own length. Exceptions to this statement occur in numerous species across many families, including some Pteromalidae. Pteromalidae differ in having more than 2 mandibular teeth except in some fig associates which differ from Ceidae in many other ways. Pteromalidae also lack a transverse subapical clypeal groove, and have a hidden labrum with an elongate median lobe, instead of a subrectangular and exposed labrum. While the subforaminal bridge in Pteromalidae and Ceidae is different, the difference is so slight in many Pteromalidae (such as Colotrechninae and Miscogastrinae) that it should not be relied upon too heavily. Heterulophidae and the single genus of Macromesidae also have propodeal spiracle separated far from the anterior propodeal margin. Heterulophidae differ in having distinctly fewer antennal flagellomeres (9), with a single anellus and united clava, and by having 3 mandibular teeth. Macromesidae differ in having only 4 mesotarsomeres in females, at most 11 antennal flagellomeres, and 3 mandibular teeth.

Cerocephalidae new status

Cerocephalinae Gahan, 1946. Type genus: *Cerocephala* Westwood, 1832.

Diagnosis. Antenna with at most 10 flagellomeres and at most 3 clavomeres. Intertorular prominence present (Fig. 6). Eyes not ventrally divergent. Clypeus without transverse subapical groove. Labrum hidden behind clypeus, flexible. Mandibles with 2 or more teeth. Subforaminal bridge with a postgenal bridge occurring dorsal to the hypostoma. Mesoscutellum with frenum indicated at least laterally, although this may be very subtle. Mesopleural area without an expanded acropleuron; mesepimeron extending over anterior margin of metapleuron (Fig. 7). All legs with 5 tarsomeres; protibial spur stout and curved; basitarsal comb longitudinal. Metasoma with syntergum, therefore without epipygium.

Discussion. Cerocephalidae differ from most other Chalcidoidea in having an intertorular prominence, although a few exceptional taxa exist across the superfamily that have a similar prominence, such as some Haltichellinae (Chalcididae). However, these exceptions can be distinguished from Cerocephalidae using other features mentioned in the diagnosis. Otherwise, Cerocephalidae bear little resemblance to other families, being somewhat similar to Spalangiidae, Storeyinae, and some Eulophidae, but without most diagnostic features of those families.



Figures 1–6. 1–3 *Boucekius* sp. (Boucekiidae) 1 metascutellum, axillula and propodeum 2 hind femur 3 epipygium (epg) and metasomal terga VIII (Mt8) 4, 5 *Spalangiopecta* sp. (Ceidae) 4 clypeus, labrum and mandible 5 metascutellum, axillula and propodeum, arrow shows the propodeal spiracle far separated from the anterior propodeal margin 6 *Muesebeckisia mandibularis* Hedqvist (Cerocephalidae): head and antenna in lateral view, arrow indicating intertorular prominence.

Chalcedectidae new status

Chalcedectinae Ashmead, 1904. Type genus: *Chalcedectus* Walker, 1852.

Diagnosis. Antenna with 11 flagellomeres, including 3 clavomeres, clava with apical spine in females (Fig. 8). Eyes ventrally divergent. Labrum exposed, sclerotized.

Mandibles with 3 teeth. Subforaminal bridge with a postgenal bridge occurring dorsal to the hypostoma, with convergent hypostomal carina, without a postgenal groove or postgenal lamina. Prepectus with dorsal margin at least as long as tegula. Notauli complete; tegula not covering most of humeral plate. Mesoscutellum with variable frenal area: either without a frenum, or having an expanded marginal rim of the mesoscutellum, or with either a frenum indicated mainly by a frenal arm and an indistinct frenal groove, or an ambiguous frenum that can be difficult to interpret; and with axillular sulcus or carina (Fig. 9). Mesopleural area without an expanded acropleuron; mesepimeron not extending over anterior margin of metapleuron (Fig. 9). All legs with 5 tarsomeres; protibial spur stout and curved; basitarsal comb longitudinal; metafemur with ventral teeth (Fig. 10), with metatibial spurs arising from a ventroapical projection (not shown) or absent (Fig. 10). Metasoma with syntergum, therefore without epipygium.

Discussion. Chalcedectidae are most likely to be confused with other Chalcidoidea that have a metafemur with ventral teeth, which occurs in various families and isolated genera across the superfamily. Chalcididae differ in having a small prepectus, the dorsal margin of which is shorter than the tegula, and in that the tegula covers most or all of the humeral plate. In Lyciscidae, the metatibial spurs arise from a truncate apical margin of the metatibia. Leucospidae have, in females, unusual ovipositor sheaths that recurve over the gaster and fit in a notch and, in males, a carapace-like gaster with at most 3 separate terga. Pelecinellidae have an elongate petiole with many lateral setae at a right angle to the longitudinal axis of the petiole, whereas in Chalcedectidae the petiole is small and hardly visible from dorsal view. Boucekiidae have a single clavomere, and either an epipygium or a transverse sulcus across the syntergum immediately anterior to the cerci. A few Melanosomellidae have a toothed metafemur, but they either lack an axillular sulcus or carina or have a reduced and incomplete one, and do not have ventrally divergent eyes. Cleonymidae have incomplete notauli. Some Torymidae have ventral metafemoral teeth, but these have a separate epipygium in females and do not have ventrally divergent eyes. In *Liepara* Bouček (Coelocybidae), the frenum is unambiguously visible dorsally, with a pair of strong setae adjacent to the frenal groove. A few Eulophidae can have ventral teeth on the metafemur, but they have 4 tarsomeres on all legs.

Cleonymidae revived status

Cleonymidae Walker, 1837. Type genus: *Cleonymus* Latreille, 1809.

Diagnosis. Antenna with 9 flagellomeres, including usually a single clavomere, which is sometimes vaguely divided into 3 clavomeres in males, and with a subapical finger-like process or spine extending alongside the clava and/or with an additional apical spine in females. Eyes ventrally divergent. Clypeus with transverse subapical groove. Labrum exposed, sclerotized. Mandibles with 2 or 3 teeth (Fig. 11), sometimes with a truncation in place of the dorsal teeth. Subforaminal bridge with a postgenal bridge

dorsal to the hypostoma and separating the lower tentorial bridge from the convergent hypostomal carina, and without a postgenal groove or postgenal lamina. Pronotum without a smooth median longitudinal line or carina. Prepectus with dorsal margin at least as long as tegula. Notauli incomplete. Tegula not covering most of humeral plate. Mesoscutellum without a frenum, although frenal arm visible only laterally immediately anterior to marginal rim of mesoscutellum; without axillular sulcus. Mesopleural area without an expanded acropleuron. All legs with 5 tarsomeres; protibial spur stout and curved; basitarsal comb longitudinal; metafemur with or without ventral teeth, with apical spurs arising from a truncate metatibial apex when the metafemur has ventral teeth (Fig. 12). Metasoma with syntergum, therefore without epipygium.

Discussion. Cleonymidae in its current, narrow sense represents the former Cleonymini, as characterized by Gibson (2003). It includes *Agrilocida* Steffan new placement, previously placed in Chalcedectini, but which is distinct morphologically and consistently is placed in Cleonymidae in next-generation molecular analyses. This is now a relatively small and narrowly-defined group in comparison with the previous sense of Cleonyminae, and may be confused with other relatively large-bodied taxa that have ventrally divergent eyes.

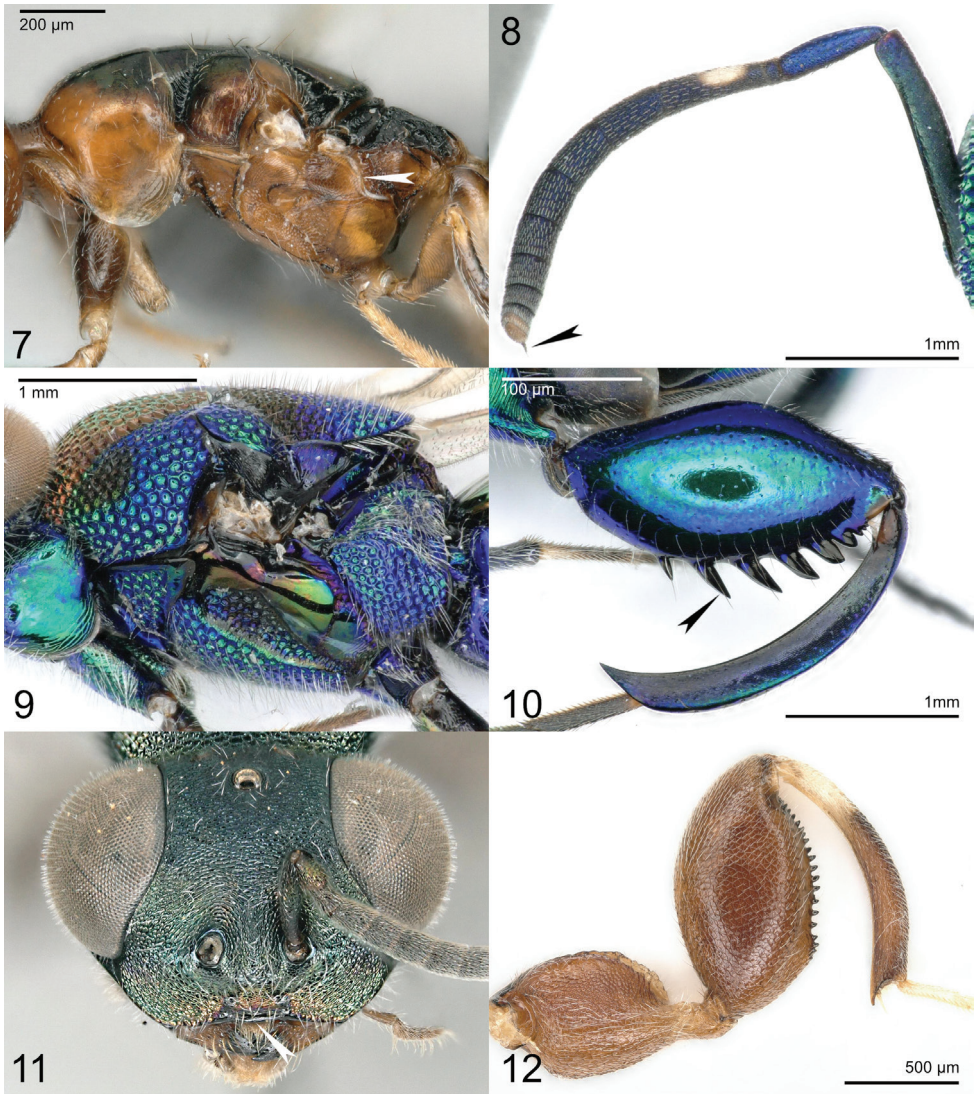
Females of Eupelmidae, Metapelmatidae, Neanastatidae, and *Eopelma* Gibson have an enlarged, convex and pad-like acropleuron that covers most or all of the mesopleural area. Lyciscidae, Chalcedectidae, Ooderidae, Pelecinellidae, and Boucekidae differ from Cleonymidae in having complete notauli. Heydeniidae have a long prepectus with large lateral and ventral surfaces. While some Cleonymidae have ventral teeth on the metafemur, they do not strongly resemble Chalcididae, especially because of the metallic coloration of most Cleonymidae versus the usually non-metallic coloration of Chalcididae, but also because Cleonymidae have incomplete notauli, a larger prepectus, and a smaller tegula that does not cover most of the humeral plate. Coelocybidae usually have non-metallic coloration but also have a distinctive frenum with at least one pair of strong mesoscutellar setae on or nearly adjacent to the frenal groove, whereas the mesoscutellum in Cleonymidae is evenly covered with short and decumbent setae. Additionally, Coelocybidae do not have any spine or finger-like projection on or extending alongside the clava from a previous segment in females.

Coelocybidae new status

Coelocybinae Bouček, 1988. Type genus: *Coelocyba* Ashmead, 1900.

Lieparini Bouček, 1988, new synonymy. Type genus: *Liepara* Bouček, 1988.

Diagnosis. Antenna with 11 flagellomeres. Eyes ventrally divergent. Clypeus with transverse subapical groove (extending from one anterior tentorial pit to the other). Labrum hidden behind clypeus, flexible, subrectangular, with marginal setae in a row. Mandibles with 3 teeth. Subforaminal bridge with postgena separated by



Figures 7–12. **7** *Neocalosoter* sp. (Cerocephalidae): mesosoma in lateral view **8–10** *Chalcedectus* sp. (Chalcedectidae) **8** antenna **9** mesosoma in lateral view **10** hind leg **11** *Cleonymus* sp. (Cleonymidae): head in frontal view **12** *Agrilocida ferrieri* Steffan (Cleonymidae): hind leg.

lower tentorial bridge. Mesoscutellum with frenum indicated and with a pair of strong setae on or adjacent to frenal groove, and with axillular sulcus (Fig. 13). Mesopleural area without an expanded acropleuron; mesepimeron not extending over anterior margin of metapleuron (Fig. 14). All legs with 5 tarsomeres; protibial spur stout and curved; basitarsal comb longitudinal. Metasoma with syntergum, therefore without epipygium.

Discussion. As mentioned by Bouček (1988), Coelocybidae closely resemble what was then known as Cleonyminae, which is now multiple families. Among these, Coelocybidae bear greater resemblance to Cleonymidae and Lyciscidae. Cleonymidae differ from Coelocybidae in lacking a frenum and the accompanying strong setae, the setae also being absent from Lyciscidae. Otherwise, taxa with ventrally divergent eyes have an expanded acropleuron or fewer flagellomeres. Many other taxa have a pair of strong setae on the frenal groove, but not together with ventrally divergent eyes, except *Cecidellis* Hanson (Pirenidae) which has 9 antennal flagellomeres. Nearly all Coelocybidae are from the Southern Hemisphere, with the exception of a single species from India (Narendran 2001).

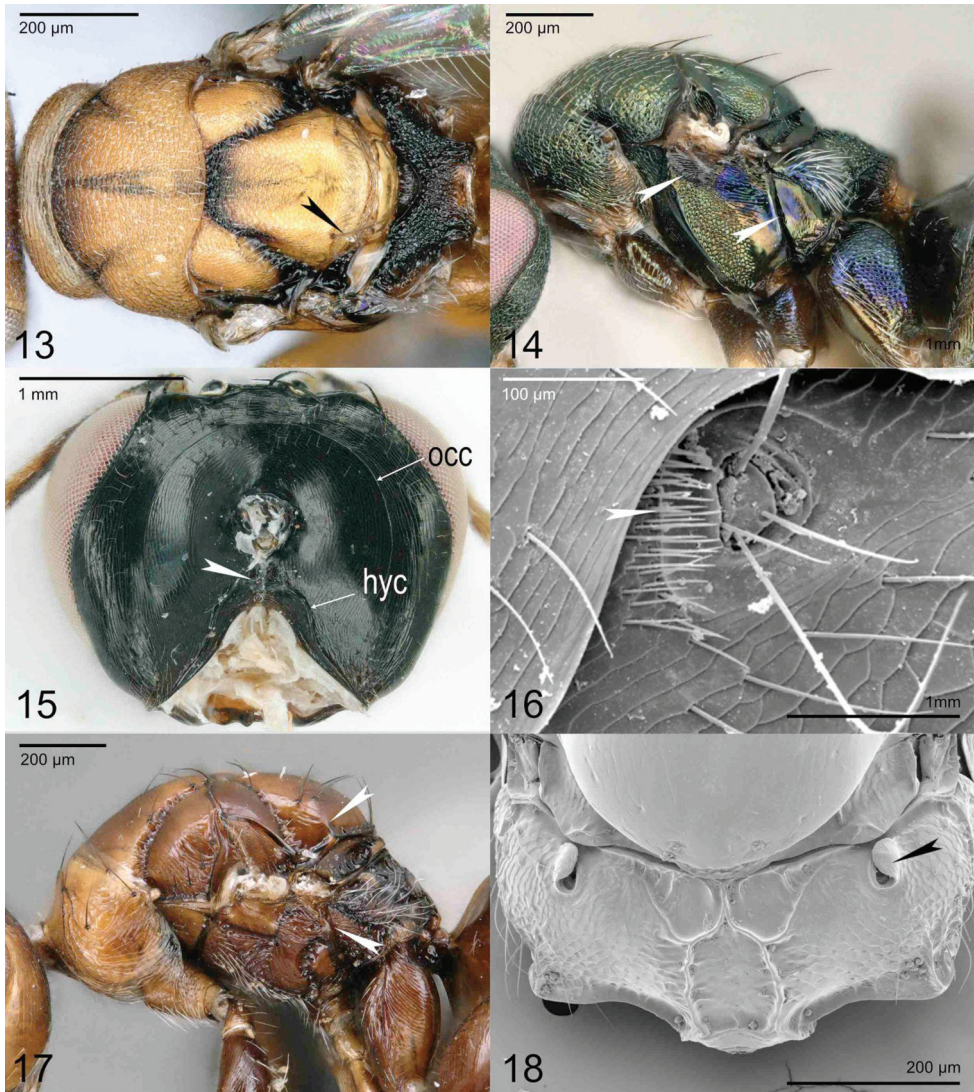
Lieparini new synonym is hereby abolished, and *Liepara* Bouček new placement is transferred here from its *incertae sedis* status (Heraty et al. 2013) because it has consistently been part of the new concept of a monophyletic Coelocybidae in next-generation molecular analyses (Cruaud et al., submitted). While the ventrally toothed metafemur of *Liepara* is distinctive, it is a well-known homoplastic feature in Chalcidoidea. Otherwise, the slightly ventrally divergent eyes, strong setae adjacent to the frenal groove, and non-metallic coloration of *Liepara* indicate that morphology agrees with molecules in this instance. Lieparini does not seem to be a useful tribe to keep as distinct from other coelocybines, although further study may lead to its resurrection once more coelocybids have been analyzed phylogenetically.

Diparidae new status

Diparinae (=Diparides, not Latin) Thomson, 1876. Type genus: *Dipara* Walker, 1833.

Diagnosis. Antenna with 12 flagellomeres, including a small 4th clavomere. Eyes not ventrally divergent. Labrum hidden behind clypeus, flexible, subrectangular, with marginal setae in a row. Mandibles with 3 or 4 teeth. Subforaminal bridge with postgenal bridge occurring dorsal to the hypostoma (Fig. 15). Mesoscutellum with frenum indicated at least laterally, and with axillular sulcus. Mesopleural area without an expanded acropleuron; mesepimeron not extending over anterior margin of metapleuron (except in *Diparisca* Hedqvist). All legs with 5 tarsomeres; protibial spur stout and curved; basitarsal comb longitudinal. Metasoma with syntergum, therefore without epipygium; cercal brush present anterior to cercus (Fig. 16).

Discussion. As discussed by Desjardins (2007), Diparinae have a cercal brush anterior to the cercus (Fig. 16). This feature is not perfectly diagnostic however, because it can also be present in Spalangiidae and Neapterolelapinae, which are recovered as the sister group to Lyciscidae, and Herbertiidae (Cruaud et al., submitted). Spalangiidae differ in having the mesepimeron extending over the anterior margin of the metapleuron. Lyciscidae differ in having an exposed, rigidly sclerotized labrum, and in lacking a frenum (except in Solenurinae). Herbertiidae differ in having at most 10 antennal flagellomeres, and in having an exposed, rigidly sclerotized labrum. In the features



Figures 13–18. **13** *Coelocyboides* sp. (Coelocybidae): mesosoma in dorsal view, arrow indicating setae on or adjacent to frenal groove **14** *Ormyromorpha trifasciata* Girault (Coelocybidae): mesosoma in lateral view **15, 16** *Lelaps* sp. (Diparidae) **15** head posterior view **16** cercal brush **17** *Eufroggattisca polita* (Ashmead) (Epichrysomallidae): mesosoma lateral view **18** *Odontofroggattia* sp. (Epichrysomallidae): propodeum female dorsal view.

listed in the diagnosis, Cerocephalidae may appear similar to Diparidae, although they differ in that Cerocephalidae have an intertorular prominence and at most 10 antennal flagellomeres. *Diparisca* remains in Diparidae as a genus of uncertain placement (Mitroiu 2016), with distinction from Ceinae discussed therein.

Epichrysomallidae new status

Epichrysomallinae Hill & Riek, 1967. Type genus: *Epichrysomalla* Girault, 1915.

Diagnosis. Antenna with 10–12 flagellomeres, including a small 4th clavomere. Eyes not ventrally divergent. Labrum hidden behind clypeus, flexible. Mandibles with 3 teeth. Subforaminal bridge with postgenal bridge separating secondary posterior tentorial pits from hypostoma. Notauli complete. Mesoscutellum with frenum indicated laterally, without axillular sulcus (Fig. 17). Mesopleural area without an expanded acropleuron; mesepimeron extending over anterior margin of metapleuron (Fig. 17). All legs with 5 tarsomeres in most, except tarsi 4-segmented in *Odontofroggattia* Ishii and *Josephiella* Narendran; protibial spur stout and curved; basitarsal comb longitudinal. Metasoma with syntergum, therefore without epipygium.

Discussion. Epichrysomallidae mostly resemble Melanosomellidae in habitus, but do not have a linear mesopleural sulcus. They also have different fore wing venation with a stigmal vein arising at a right angle (excepted in *Acophila* Ishii) and a postmarginal vein that is shorter than the stigmal vein. Epichrysomallidae have a characteristic flap-like expansion of cuticle from the lateral edge of the propodeal spiracle, partially covering the spiracle in dorsal view (Fig. 18) that neither Melanosomellidae nor Ormyridae have. Ormyridae differ further from Epichrysomallidae by having a more conventional fore wing venation, with longer marginal and postmarginal veins, and iridescent coloration in most species.

Eunotidae new status

Eunotinae Ashmead, 1904. Type genus: *Eunotus* Walker, 1834.

Diagnosis. Antenna with at most 11 flagellomeres. Eyes ventrally divergent. Clypeus with transverse subapical groove. Labrum either exposed and well-sclerotized (most species), or hidden behind clypeus (*Epicopterus* Westwood), subrectangular, with marginal setae in a row. Mandibles with 2 or rarely 3 teeth (Fig. 19). Subforaminal bridge with postgena separated by lower tentorial bridge. Pronotum transverse. Mesoscutellum with frenum indicated laterally, with axillular sulcus. Mesopleural area without an expanded acropleuron; mesepimeron not extending over anterior margin of metapleuron; only one mesofurcal pit present (Fig. 20). All legs with 5 tarsomeres; protibial spur stout and curved; basitarsal comb longitudinal (Fig. 21). Metasoma with syntergum, therefore without epipygium.

Discussion. Eunotidae, as defined herein, was previously known as Eunotini (Bouček 1988). Moranilidae, composed of species previously included in Eunotinae, differ in having an oblique basitarsal comb that crosses the area where the basitarsal notch would be, in having pits on the mesopleural area of the mesopectus, and in

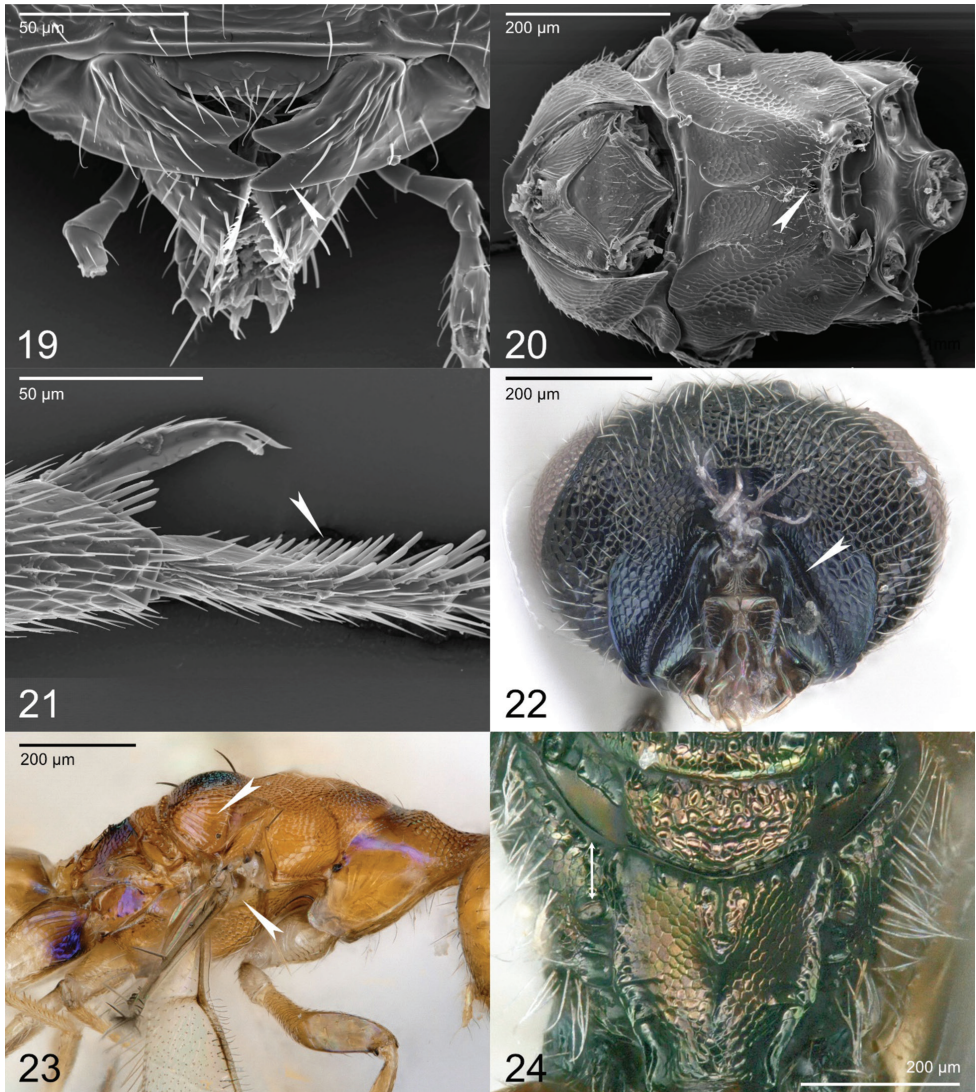
having two mesofurcal pits instead of the single pit usually found in Chalcidoidea. *Idioporus affinis* (Idioporidae) differs in having 4 tarsomeres. Aphelinidae differ in lacking any indication of a frenum, in having a flexible, hidden labrum, usually in having more advanced axilla, and the second phragma extending into the mesosoma. Despite apparent similarities between Aphelinidae and Eunotidae, the two taxa, are seldom confused because Eunotidae have a more strongly sclerotized body, which means that the two families have a very different habitus. Lyciscidae differ in having a subconical pronotum with a median longitudinal carina, whereas the pronotum of Eunotidae is transverse without a visible median carina in dorsal view.

Herbertiidae new status

Herbertiinae Bouček, 1988. Type genus: *Herbertia* Howard, 1894.

Diagnosis. Antenna with 10 flagellomeres, including 3 clavomeres. Clypeus with transverse subapical groove. Labrum exposed, well-sclerotized, subrectangular with marginal setae in a row. Mandibles with 2 teeth. Subforaminal bridge with postgena separated by lower tentorial bridge; head posteriorly with postgenal lamina and postgenal groove (Burks et al. 2018) (Fig. 22). Mesoscutellum with frenum indicated only laterally by the frenal arm, without axillular sulcus. Mesopleural area without an expanded acropleuron, with or without pits. Fore wing marginal vein more than 1.5× stigmal vein length, without elongate uncus. Mesepimeron extending over anterior margin of metapleuron; two mesofurcal pits present. All legs with 5 tarsomeres; protibial spur stout and curved; basitarsal comb oblique. Metasoma with syntergum, therefore without epipygium.

Discussion. The family Herbertiidae has uncertain placement based on both molecular (Cruaud et al., submitted) and morphological data, and is treated as *incertae sedis* in Chalcidoidea pending more consistent phylogenetic resolution. Micradelinae are similar to Herbertiidae in body shape, but differ in having an elongate uncus and much shorter marginal vein relative to the stigmal vein on the fore wing, in having an indicated axillular sulcus, in having only one mesofurcal pit, and in lacking a postgenal lamina and postgenal groove. Erotolepsiinae (Spalangiidae) are similar to Herbertiidae in habitus but differ in having a transverse anterior carina across Gt_1 , and in most species having a long carina encircling most of the face. Eunotidae differ in having a longitudinal basitarsal comb, and in lacking a postgenal lamina and postgenal groove. The presence of two mesofurcal pits is unusual, a feature shared with Moranilidae, Enoggerinae, Asaphesinae, some Eurytominae (Krogmann and Vilhelmsen 2006) and Chalcididae (Haltichellinae and Smicromorphinae, G. Delvare, pers. comm). Moraniidae differ in having an axillular sulcus. Other small-bodied families such as Pirenidae and Systasidae differ in having more than 2 mandibular teeth, and Pirenidae differ in having a concealed, flexible labrum.



Figures 19–24. 19–21 *Eunotus* sp. (Eunotidae) 19 mandible and labrum in frontal view 20 mesosoma ventral view 21 protibial spur and basitarsal comb 22 *Herbertia brasiliensis* Ashmead (Herbertiidae) head posterior view 23 *Hetreulophus* sp. (Hetreulophidae), mesosoma lateral view 24 *Zeala walkerae* Bouček (Hetreulophidae): propodeum.

Hetreulophidae new status

Hetreulophini Girault, 1915. Type genus: *Hetreulophus* Girault, 1915.

Diagnosis. Antenna with 9 flagellomeres, including a 1-segmented clava. Clypeus without transverse subapical groove. Labrum flexible, hidden behind clypeus. Mandibles with 3 teeth. Subforaminal bridge with postgena separated by lower tentorial

bridge except for the small postgenal bridge dorsal to the hypostoma. Mesoscutellum with short frenum, with axillular sulcus, and expanded, convex axillula (Fig. 23). Mesopleural area without an expanded acropleuron; mesepimeron extending over anterior margin of metapleuron (Fig. 23). Propodeum with spiracle small, oval, separated by more than its own length from anterior propodeal margin (Fig. 24). All legs with 5 tarsomeres; protibial spur stout and curved; basitarsal comb longitudinal.

Discussion. Ceidae, another family with propodeal spiracle separated far from the anterior margin of the propodeum, differ in having 12 antennal flagellomeres and only 2 mandibular teeth. Macromesidae share this feature as well, but have at least 10 flagellomeres including multiple clavomeres, 4 mesotarsomeres in females, and the mesepimeron does not extend over the anterior margin of the metapleuron. Otherwise, families that resemble Heterulophidae in habitus have more flagellomeres and multiple clavomeres.

Omphalodipara Girault new placement is transferred from Colotrechninae, Amerostenini (Pteromalidae) to Heterulophidae based on next generation molecular data (Cruaud et al., submitted). Given the 9 antennal flagellomeres with a 1-segmented clava, strongly convex axillula, short frenum, and posteriorly displaced propodeal spiracle shared between *Omphalodipara* and other Heterulophidae, it is reasonable to say that morphology agrees with this placement.

Heydeniidae new status, new placement

Heydenini Hedqvist, 1961. Type genus: *Heydenia* Förster, 1856. Spelling corrected to Heydeniini by Bouček (1988).

Diagnosis. Antenna with 10 or 11 flagellomeres, including 3 clavomeres. Eyes ventrally divergent. Clypeus without transverse subapical groove. Labrum exposed or hidden behind clypeus, sclerotized. Mandibles with 3 teeth. Pronotum expanded laterally and forming a subrectangular or laterally expanded structure from dorsal view (Fig. 67). Prepectus long, with large dorsal and ventral surfaces. Mesoscutellum either without a frenum, or with frenum laterally indicated by a frenal arm, with or without axillular sulcus (Fig. 68). Mesopleural area with acropleuron slightly expanded but occupying less than half its surface; mesepimeron not extending over anterior margin of metapleuron. All legs with 5 tarsomeres; profemur strongly (Fig. 69) or only mildly expanded; protibial spur stout and curved; basitarsal comb longitudinal. Metasoma with syntergum, therefore without epipygium, although terga not well-sclerotized and often difficult to assess.

Discussion. Some species of Heydeniidae are distinctive and resemble Ooderidae, while more generalized species are considerably more difficult to recognize. Ooderidae differ in having multiple rows of spine-like structures on the ventral surface of the always strongly expanded profemur. Heydeniidae have instead at most a single row of crest-like structures ventrally on the profemur. Otherwise, the ventrally elongate prepectus of Heydeniidae is distinctive. When the profemur is not strongly expanded and the pronotum is relatively short and not tent-like, species of *Heydenia* Förster can

be more difficult to recognize. Given the presence of a convex mesoscutellum with a weakly distinct or indistinct frenum and ventrally divergent eyes, generalized Heydeniidae may be confused with Cleonymidae or Lyciscidae, both of which have a much shorter prepectus ventrally.

Idioporidae new status

Idioporini LaSalle, Polaszek & Noyes, 1997. Type genus: *Idioporus* LaSalle & Polaszek, 1997.

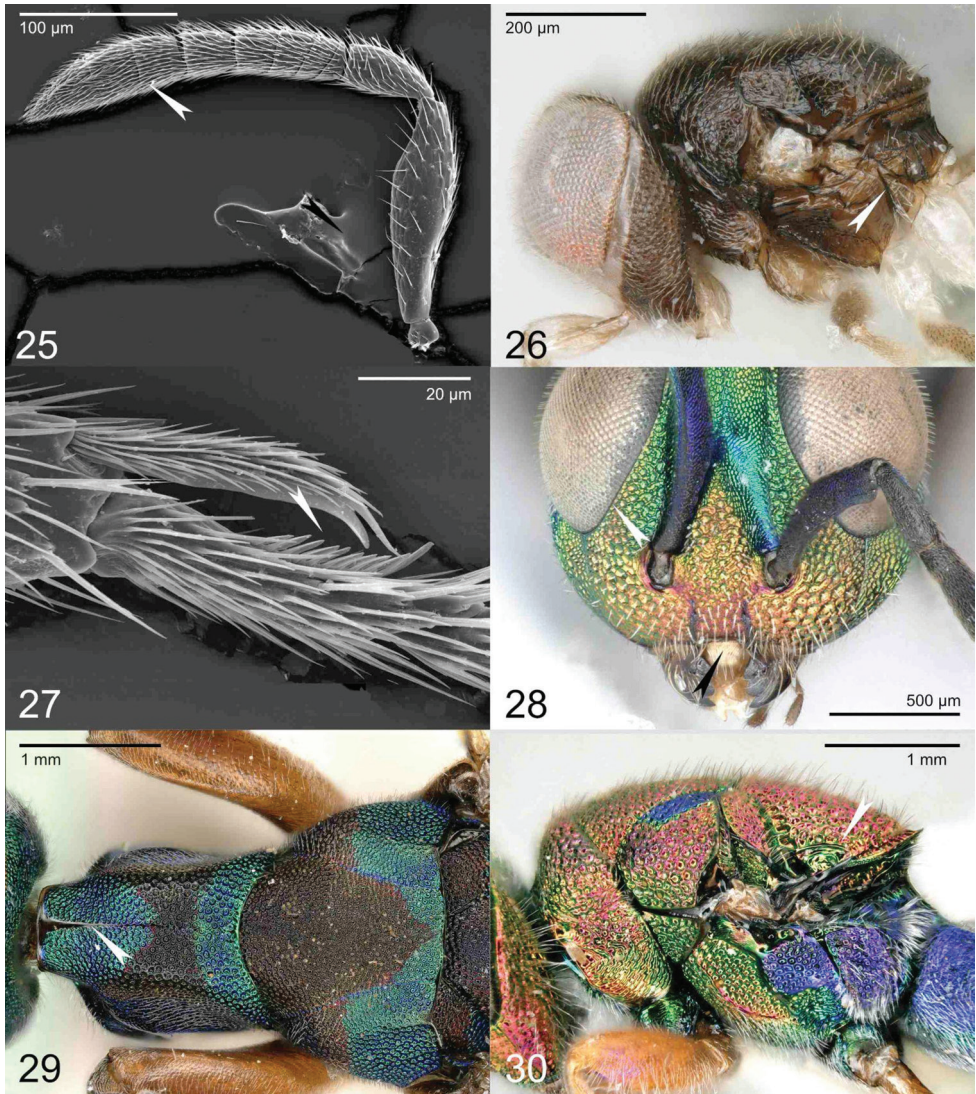
Diagnosis. Antenna with 9 flagellomeres, including 4 distinct clavomeres (Fig. 25). Clypeus with transverse subapical groove. Labrum hidden behind clypeus, flexible, subrectangular, with marginal setae in a row. Mandibles with 2 teeth. Subforaminal bridge with postgena separated by lower tentorial bridge. Mesopleural area without an expanded acropleuron; mesepimeron not extending over anterior margin of metapleuron (Fig. 26). All legs with 4 tarsomeres; protibial spur stout and slightly curved; basitarsal comb longitudinal (Fig. 27).

Discussion. *Idioporus affinis* LaSalle & Polaszek is a highly distinctive species in Chalcidoidea (LaSalle et al. 1997) that has been problematic in placement regardless of whether using morphology or molecules. Relative to most other families discussed here, it is distinct in tarsomere count; only *Zebe* La Salle (Pirenidae) has four tarsomeres, but *Zebe* differs in having most funiculars greatly reduced. *Idioporus* differs from other taxa with 4-segmented tarsi on all legs, such as Eulophidae and Calesidae, and in having a stout and slightly curved protibial spur.

Lyciscidae new status

Lyciscini Bouček, 1958. Type genus: *Lycisca* Spinola, 1840.

Diagnosis. Antenna with 8 or 7 flagellomeres, including usually a single clavomere but sometimes with 2 or (in males) 3 clavomeres. Eyes ventrally divergent (Fig. 28). Clypeus with or without transverse subapical groove. Labrum exposed or hidden behind clypeus, sclerotized and with a row of submarginal setae extending anteriorly (Fig. 28). Mandibles with 2 or 3 teeth, sometimes with a truncation in place of the dorsal teeth. Subforaminal bridge with elongate lower tentorial bridge and secondary tentorial pits that extend to the convergent hypostomal carina, with or without a postgenal groove and postgenal lamina, or (Solenurinae) with a postgenal bridge that externally separates the lower tentorial bridge from the convergent hypostomal carina. Pronotum with a smooth median longitudinal line or carina (Fig. 29). Notauli complete. Mesoscutellum usually without a frenum (Fig. 30) or (Solenurinae) with a frenum indicated by



Figures 25–30. 25–27 *Idioporus affinis* LaSalle & Polaszek (Idioporidae) 25 antenna 26 mesosoma lateral 27 protibial spur and basitarsal comb. 28 *Lycisca nebulipennis* Strand (Lyciscidae) head frontal view 29 *Lycisca ignicaudata* Westwood (Lyciscidae): pronotum and mesonotum dorsal view 30 *Agamerion cleptideum* (Westwood) (Lyciscidae): mesosoma lateral view.

lateral frenal arms (Fig. 32); without or (rarely) with axillular sulcus. Mesopleural area without an expanded acropleuron; mesepimeron not extending over anterior margin of metapleuron. All legs with 5 tarsomeres; protibial spur stout and curved; basitarsal comb longitudinal; metafemur with or without ventral teeth or expansion, with apical spurs arising from a truncate metatibial apex when the metafemur has ventral teeth.

Metasoma with syntergum, therefore without epipygium, although a complex set of carinae sometimes present on syntergum.

Discussion. The family Lyciscidae was potentially a major part of what Bouček (1988) had in mind when describing his concept of Cleonyminae as a monophyletic lineage, being “certainly one of the oldest in Pteromalidae, as seems to be supported by their association with wood-boring beetles.” However, Lyciscidae itself appears to be relatively young and separate from Cleonymidae and all other members of the former sense of Cleonyminae, based upon next-generation molecular data (Cruaud et al., submitted).

Lyciscidae are relatively generalized and are therefore easily confused with many other large-bodied Chalcidoidea. While the longitudinal median smooth strip or carina of the pronotum is distinctive, it can be difficult to assess in some taxa depending on the position of the head. However, Neapterolelapinae differ from Lyciscidae chiefly in the lack of this feature. Many Eupelmidae are similar to Lyciscidae but females and some males have an expanded, convex and pad-like acropleuron that covers most or all of the mesopleural area. In all Chalcedectidae the metafemur has ventral teeth, a feature also present in some Lyciscidae, but in Lyciscidae the metatibia is truncate where the metatibial spurs insert, whereas in Chalcedectidae the spurs are either absent or placed on a ventroapical projection.

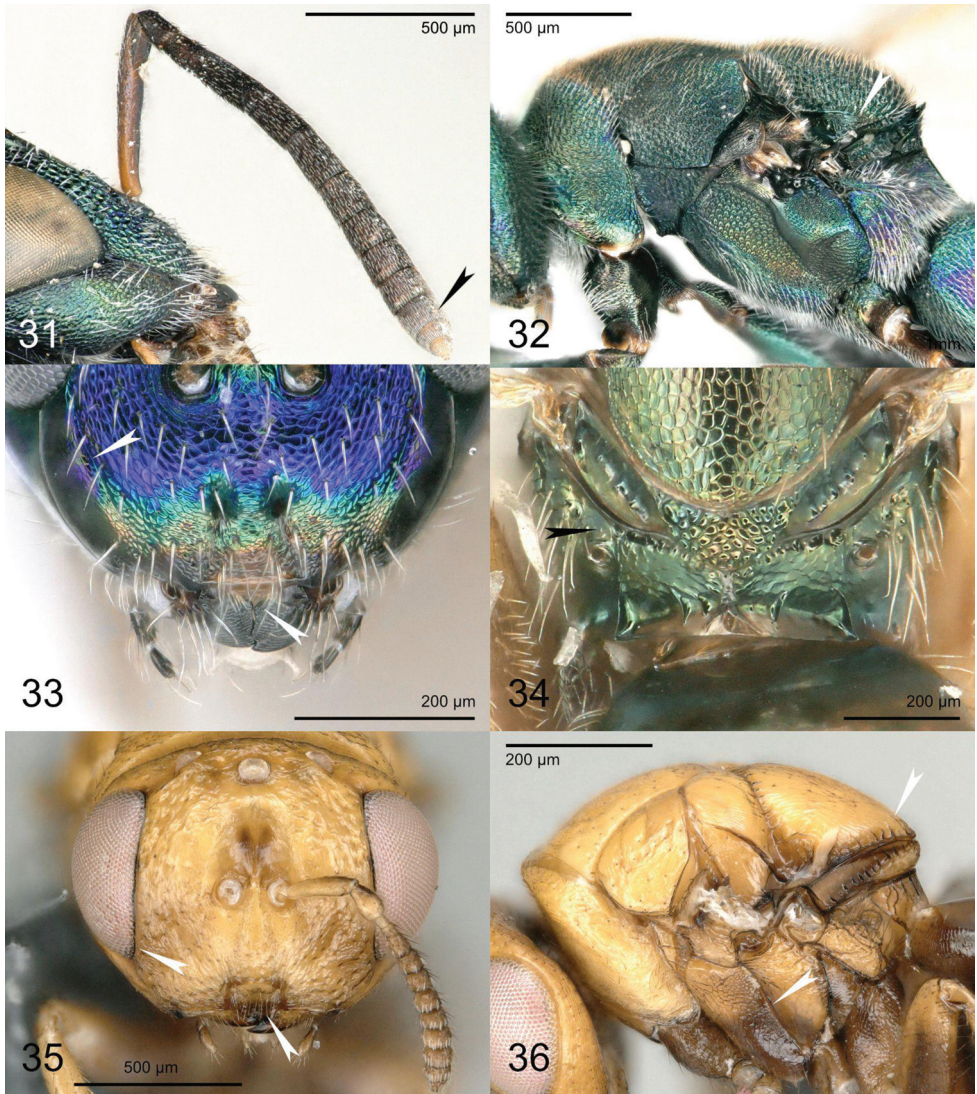
Lyciscidae differ from many other large-bodied Chalcidoidea in lacking a frenum. In Cleonymidae the notauli are incomplete. Pelecinnellidae differ in having an elongate petiole with long setae perpendicular to its longitudinal axis. Macromesidae do not have ventrally divergent eyes, and often instead have ventrally convergent eyes. Eunotidae have a much shorter pronotum without a distinctive anterior neck.

For Solenurinae, identification can be more difficult due to the presence of a frenal arm, which is shared with a greater number of other chalcidoids. While *Solenura* Westwood itself is a highly distinctive genus with an elongate gaster, *Grooca* Sureshan & Narendran has a shorter gaster similar to that of many other Chalcidoidea. Confusion is most likely with other groups that have ventrally divergent eyes, such as Coelocybidae which differ in having strong setae on or nearly adjacent to the frenal groove. Herbertiidae and Micradelinae have a different antenna with 10 or 11 flagellomeres. Ditropinotellinae differ in having a distinctive T-shaped and elongate syntergum that resembles an elongate epipygium. Moranilidae may appear similar to Lyciscidae when comparing the lists of features, but in practice are easily distinguished. Some Moranilidae do not have ventrally divergent eyes (Asaphesinae), while others have a much smaller body with a different antennal flagellum that is strongly clavate and or with transverse funiculars.

Solenurinae Burks & Rasplus, new subfamily

<https://zoobank.org/81F154EA-C0D1-4CDA-9E71-CACC490E2AFA>

Type genus. *Solenura* Westwood, 1868.



Figures 31–36. **31, 32** *Solenura* sp. (Lysicidae, Solenurinae) **31** antenna **32** mesosoma lateral **33** *Macromesus* sp. (Macromesidae): head frontal view **34** *Macromesus amphiretus* Walker (Macromesidae), propodeum **35, 36** *Trichilogaster acaciaelongifoliae* (Froggatt) (Melanosomellidae) **35** head frontal **36** mesosoma lateral view.

Diagnosis. Antenna with 2 or 3 clavomeres (Fig. 31). Clypeus without transverse subapical groove. Labrum exposed small and subrectangular, with marginal setae. Mandibles with 2 similarly-sized teeth. Subforaminal bridge with a postgenal bridge that externally separates the lower tentorial bridge from the convergent hypostomal carina; postgenal groove and postgenal lamina absent. Frenum indicated laterally by frenal arm that is well-separated from the marginal rim of the mesoscutellum (Fig. 32). Metafemur without ventral teeth or expansion. Other features as in Lysicinae.

Macromesidae new status

Macromesinae Graham, 1959. Type genus: *Macromesus* Walker, 1848.

Diagnosis. Antenna with 10 flagellomeres in females, 11 in males. Face between malar sulcus and torulus with a second longitudinal sulcus (Fig. 33). Clypeus without transverse subapical groove. Labrum subrectangular and hidden, with marginal setae in a row. Mandibles with 3 teeth (Fig. 33). Subforaminal bridge with postgena separated by lower tentorial bridge except for a small postgenal bridge dorsal to the hypostoma. Mesoscutellum with frenal arm indicated laterally, and with axillular carina or sulcus. Mesopleural area without an expanded acropleuron. Propodeum with spiracle separated by more than its own length from the anterior propodeal margin (Fig. 34). Fore and hind legs with 5 tarsomeres, middle legs in females with 4 tarsomeres. Protibial spur stout and curved; basitarsal comb longitudinal. Metasoma with syntergum, therefore without epipygium.

Discussion. *Macromesus*, the only genus of Macromesidae, differs from other Chalcidoidea in the tarsomere count of females and the usually conspicuous second longitudinal sulcus on the lower face, although it otherwise bears some resemblance to other large-bodied chalcidoids with metallic coloration. The distance from the propodeal spiracle to the anterior margin of the propodeum may cause it to be confused with Ceidae or Hetrulophidae, but this feature is likely convergent, apparently occurring in Macromesidae because of its unusual propodeum.

Melanosomellidae new status

Melanosomellini Girault, 1913. Type genus: *Melanosomella* Girault, 1913.

Diagnosis. Antenna with 12 flagellomeres, including a small 4th clavomere. Eyes not divergent ventrally (Fig. 35). Clypeus without transverse subapical groove. Labrum hidden, flexible. Mandibles with 3 teeth. Subforaminal bridge with postgena separated by lower tentorial bridge, or with a short apparent postgenal bridge immediately dorsal to the hypostoma. Notauli complete. Mesoscutellum with frenum indicated laterally, either without axillular sulcus or carina, or with it greatly reduced and incomplete (Fig. 36). Mesopleural area without an expanded acropleuron (Fig. 36). All legs with 5 tarsomeres; protibial spur stout and curved; basitarsal comb longitudinal. Metasoma with syntergum, therefore without epipygium, and rigidly convex.

Discussion. Additionally, Melanosomellidae typically have a linear mesopleural sulcus that is more distinct than in most other Chalcidoidea (Fig. 36), although this feature also occurs in various species from other families. There is a strong chance of confusion of Melanosomellidae with Epichrysomallidae and Ormyridae, members of the Gall Clade (Cruaud et al., submitted, van Noort et al., in prep.). Epichrysomallidae are very similar to Melanosomellidae in habitus, but have different fore wing venation, with a nearly straight stigmal vein arising at a right angle from the wing

margin. Furthermore, Epichrysomallidae are strictly associated with *Ficus* (Moraceae) as gall-makers either within figs or on leaves and twigs. Ormyridae are also very similar to Melanosomellidae but have an occipital carina. Pteromalidae almost always have a distinct and complete axillular sulcus or carina. In species where this may not be the case, such as *Nikolskayana mirabilis* Bouček, the notauli are incomplete.

Encyrtocephalus Ashmead is very similar to other genera classified in Melanosomellidae, but molecular data (Cruaud et al., submitted) indicate that it may not belong inside this group. However, the only morphological features that imperfectly separate it from most Melanosomellidae are a large supracoxal flange on the posterior margin of the propodeum (Fig. 37) and a distinctly curved stigmal vein. These features are shared with a few other melanosomellid genera such as *Alyxiaphagus* Riek, with intermediates that would make diagnosis either very difficult or impossible. Therefore, *Encyrtocephalus* is kept in Melanosomellidae.

The fig associate species *Hansonita pertusae* Bouček new placement is transferred here because its fore wing venation resembles that of Melanosomellidae (Fig. 38) more strongly than that of Epichrysomallidae or other fig associates.

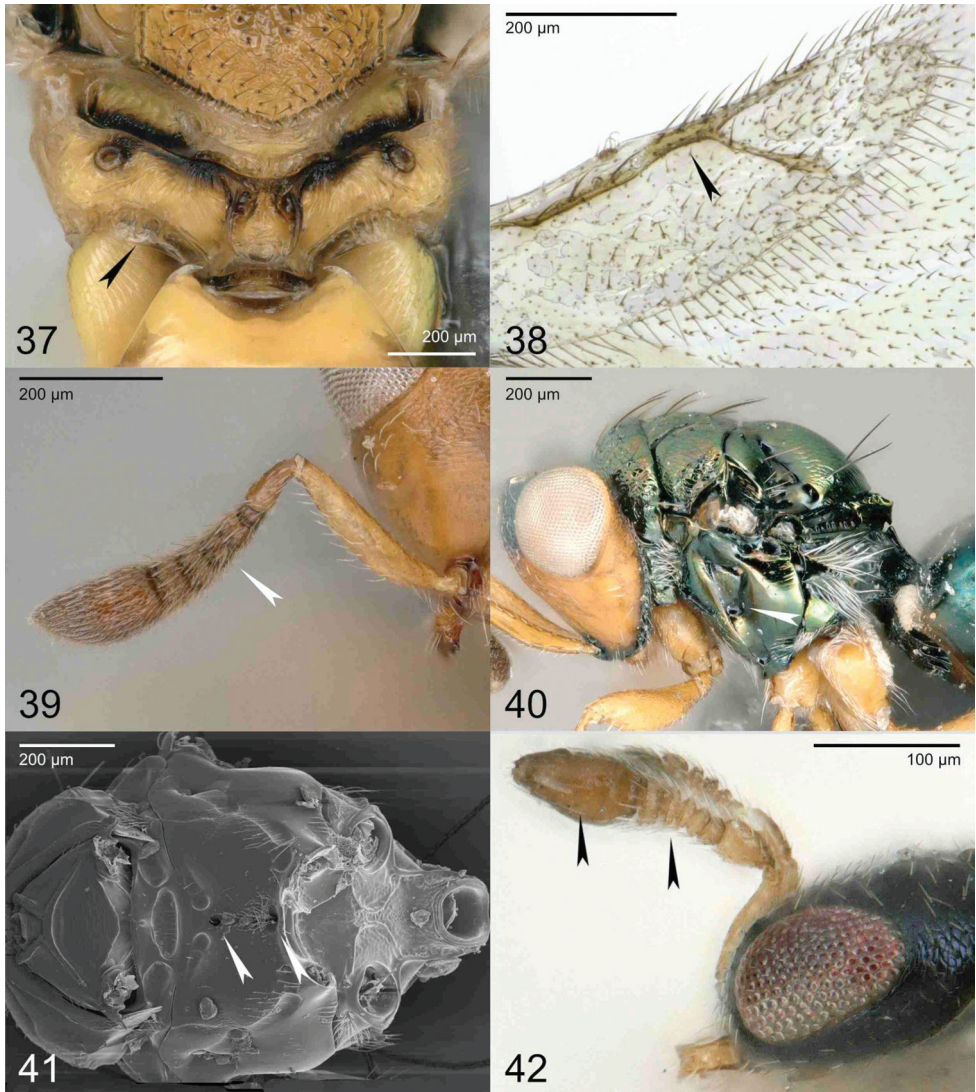
Moranilidae new status

Moranilini Bouček, 1988. Type genus: *Moranila* Cameron, 1883.

Tomocerodini Bouček, 1988. Type genus: *Tomocerodes* Girault, 1916.

Diagnosis. Antenna with 8 flagellomeres, clava undivided or incompletely divided (Fig. 39). Clypeus with transverse subapical groove (Fig. 56b). Labrum exposed, well-sclerotized, subrectangular with marginal setae in a row. Mandibles with 3 teeth. Subforaminal bridge with postgena separated by lower tentorial bridge. Mesoscutellum with frenum indicated at least laterally, with axillular sulcus. Mesopleural area without an expanded acropleuron, with pits (Fig. 40); mesepimeron not extending over anterior margin of metapleuron; two mesofurcal pits present (Fig. 41). All legs with 5 tarsomeres; protibial spur stout and curved; basitarsal comb oblique. Metasoma with syntergum, therefore without epipygium.

Discussion. Moranilidae contains two subfamilies: the former tribe Moranilinae new status and Tomocerodinae new placement, new status, based on morphological similarity since molecular data are absent for Tomocerodinae. Moranilidae differ from almost all other Chalcidoidea in having 2 mesofurcal pits instead of the usual single pit, but this feature appears to be homoplastic within Chalcidoidea. Indeed, some Eurytominae (Eurytomidae) (Krogmann and Vilhelmsen 2006) as well as Smicromorphinae and some Haltichellinae (G. Delvare comm. pers) also have two mesofurcal pits but differ from Moranilidae in many ways, including a different basitarsal comb and subforaminal bridge. These families are not easily confused with one another due to the very different habitus of the much more strongly sclerotized Eurytominae and Chalcididae.



Figures 37–42. **37** *Encyrtoccephalus* sp. (Melanosomellidae): propodeum and supracoxal flange **38** *Hansonita pertusae* Bouček (Melanosomellidae): venation **39** *Moranila californica* (Howard) (Moranilidae): antenna **40** *Moranila viridivertex* (Girault) (Moranilidae): mesosoma lateral view **41** *Moranila californica* (Howard) (Moranilidae): mesosoma ventral view **42** *Neodipara masneri* Bouček (Neodiparidae): head lateral view and antenna.

Herbertiidae, Asaphesinae, and Enoggerinae new subfamily also share 2 mesofurcal pits with Moranilidae. Herbertiidae differ in lacking an axillular sulcus. Asaphesinae have 12 antennal flagellomeres instead of the maximum of 8 in Moranilidae. Enoggerinae lack a temple on the head, thus having the posterior margin of the eye coincident with that of the head dorsally. Micradelinae also resemble Moranilidae, but have only 1 mesofurcal pit instead of 2, and lack pits on the mesopleural area.

Tomocerodinae differ from Moranilinae in features discussed by Bouček (1988), most noticeably in the much shorter Gt_1 , which is the longest tergum in Moranilinae but is much shorter than Gt_2 in *Tomocerodes*.

Neodiparidae new status

Neodiparini Bouček, 1961. Type genus: *Neodipara* Erdős, 1955.

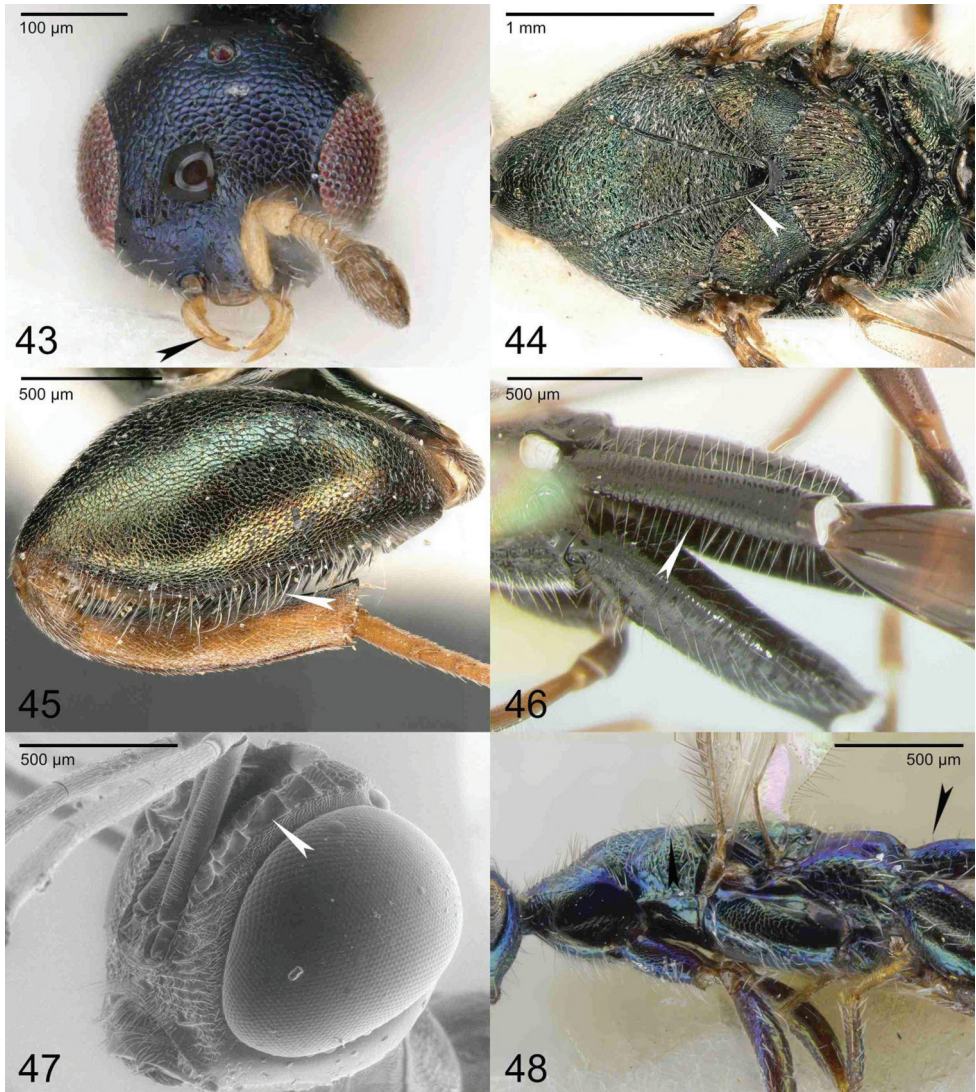
Diagnosis. Antenna with 10 (*Neodipara*) or 11 (*Elatoides*) flagellomeres, including 4 clavomeres (Fig. 42) and an inconspicuous anellus. Clypeus without transverse subapical groove. Labrum hidden, flexible, subcordiform with a median lobe, with marginal setae projecting forward from the lateral lobes (Fig. 43). Mandibles with 2 teeth (Neodiparinae) or with 2 teeth in the left mandible and 3 in the right (Elatoidinae). Subforaminal bridge with postgena separated by lower tentorial bridge. Mesoscutellum with frenum indicated at least laterally, without axillular sulcus. Mesopleural area without an expanded acropleuron; mesepimeron not extending over anterior margin of metapleuron. All legs with 5 tarsomeres; protibial spur stout and curved; basitarsal comb oblique. Metasoma with a separate epipygium.

Discussion. Although similar in habitus to some species with a long petiole from other families, such as Spalangidae or some Pteromalidae, Neodiparidae differ from these in having a small separate epipygium instead of a syntergum, an oblique basitarsal comb, and a relatively large 4th clavomere. Elatoidinae new placement is transferred here, with its single genus *Elatoides* Nikol'skaya, differing from Neodiparinae in having a complete set of 11 flagellomeres instead of 10 and in the right mandible having 3 teeth.

Ooderidae new status

Ooderini Bouček, 1958. Type genus: *Oodera* Westwood, 1874.

Diagnosis. Antenna with 11 flagellomeres, including 3 clavomeres. Eyes ventrally divergent. Clypeus with transverse subapical groove. Labrum exposed, sclerotized. Mandibles with 2 or 3 weakly separated teeth or essentially truncate. Pronotum elongate, with lateral surfaces divergent such that the pronotum is laterally expanded (Fig. 44). Notauli complete, linear except for a short distance anteriorly, and almost meeting posteriorly, forming a distinctive 4-pronged pattern with the also sublinear part of the transscutal articulation that occurs along the anterior edge of the axilla (although this is often broken by a transverse fracture across the sulci) (Fig. 44). Mesoscutellum without a frenum but with an expanded posterior rim of the mesoscutellum that can resemble a frenum; without a distinct axillular sulcus but with some longitudinal sculpture in the axillular area. Mesopleural area without an expanded acropleuron; mesepimeron not extending over anterior margin of metapleuron. All legs with 5 tarsomeres; profemur expanded and with multiple rows of



Figures 43–48. **43** *Neodipara masneri* Bouček (Neodiparidae): head frontal view **44, 45** *Oodera formosa* Giraud (Ooderidae) **44** mesosoma dorsal view **45** fore leg **46** *Leptofoenus stephanoides* (Roman) (Pelecinellidae): petiole **47** *Doddifoenus rex* Bouček (Pelecinellidae): head antero-lateral view **48** *Nefoenus pilosus* Bouček (Pelecinellidae, Nefoeninae): mesosoma lateral view.

ventral spine-like structures (described in detail by Gibson 2003) (Fig. 45); protibial spur stout and curved; basitarsal comb longitudinal; metafemur not expanded and lacking ventral teeth. Metasoma with syntergum, therefore without epipygium.

Discussion. *Oodera* Westwood, the only genus in Ooderidae, is highly distinctive and does not resemble any other Chalcidoidea, especially in mesosomal features. The expanded profemur of *Oodera* can be compared with that of some Heydeniidae, which is also expanded but lacks the additional rows of spine-like structures of *Oodera*,

instead having broad ventral crest-like projections. Additionally, the laterally expanded pronotum also occurs in some Heydeniidae, which can have a somewhat comparable pattern of sulci on the mesoscutal dorsum, even though they are often less distinct in Heydeniidae. Otherwise, Pelecinellinae (Pelecineidae) have parascrobal crests as in *Oodera*, although the two groups are different in many other features.

Pelecineidae new status

Pelecineidae Ashmead, 1895. Type genus: *Pelecineella* Westwood, 1868.

Leptofoeninae Handlirsch, 1925. Type genus: *Leptofoenus* Smith, 1862.

Diagnosis. Antenna with 11 flagellomeres. Clypeus without transverse subapical groove. Mandibles with 3 teeth or with a broad apical truncation. Subforaminal bridge with postgenal bridge. Mesopleural area without an expanded acropleuron; mesepimeron extending over anterior margin of metapleuron. All legs with 5 tarsomeres; protibial spur stout and curved; basitarsal comb longitudinal. Petiole elongate with a row of lateral setae (Fig. 46).

Discussion. Leptofoeninae is here recognized as a junior synonym of Pelecineidae, since Pelecineidae (Ashmead 1895) was described earlier than Leptofoeninae (Handlirsch 1925) and because the situation does not qualify for preserving prevailing usage. Pelecineidae are similar to other large-bodied chalcidoid parasitoids of wood-boring beetles, although they differ radically from all Chalcidoidea morphologically. Nefoeninae new placement is included here as a subfamily distinct from Pelecineidae, on the strength of sharing the elongate petiole with lateral setae (Fig. 46) although it lacks the parascrobal crests present in Pelecineidae (Fig. 47). An elongate petiole with lateral setae is unusual but not unique in Chalcidoidea, being present also in *Polstonia* Heydon (Pteromalidae: Miscogastrinae: Sphegigastrini), some *Spalangia* Latreille (Spalangiidae: Spalangiinae), and in some *Orasema* Cameron (Eucharitidae: Oraseminae) each of these differing greatly from Pelecineidae in many other features. However, the form of the petiole in Nefoeninae (Fig. 48) is somewhat similar to that of Pelecineidae, and the two groups share several other features, including elongation of the pronotum and certain other areas of the mesothoracic dorsum. While Ooderidae also have parascrobal crests, the pattern of sulci present on the mesothoracic dorsum in Ooderidae is unmistakable.

Pirenidae new status

Pireninae Haliday, 1844. Type genus: *Pirene* Haliday, 1833.

Tridyminae Thomson, 1876, new status. Type genus: *Tridymus* Ratzeburg, 1848.

Eriaporidae Ghesquière, 1955, new synonymy. Type genus: *Eriaporus* Waterston, 1917.

Eriaporinae Ghesquière, 1955, new status.

Euryischiinae Shaffee, 1974. Type genus: *Euryischia* Riley, 1889.

Cecidellinae new subfamily. Type genus: *Cecidellis* Hanson, 2005.

Diagnosis. Antenna with at most 11 flagellomeres, including 1 or more visible anellus, not counting any indistinct anelli that are usually present (Fig. 49). Eyes either not ventrally divergent, or diverging linearly (Cecidellinae, Eriaporinae, Euryischiinae), instead of with a concave medial margin in their lower half as in Cleonyminae and others (the exceptions are some male *Macroglenes* Westwood with huge eyes). Clypeus without transverse subapical groove. Labrum hidden, flexible, subrectangular with marginal setae in a row. Mandibles with 3 or 4 teeth, splayed in a characteristic way (Bouček 1988) (Fig. 50). Subforaminal bridge with postgena separated by lower tentorial bridge. Notauli complete. Mesoscutellum with frenum indicated at least laterally, and with axillular sulcus. Mesopleural area without an expanded acropleuron; mesepimeron not extending over anterior margin of metapleuron. All legs with 5 tarsomeres, except in *Zebe* La Salle with 4; protibial spur stout and curved; basitarsal comb longitudinal. Metasoma with syntergum, therefore without epipygium.

Discussion. The family Eriaporidae is synonymized with Pirenidae, with Eriaporinae and Euryischiinae retained as separate subfamilies. Cecidellinae is described for the unusual genus *Cecidellis*.

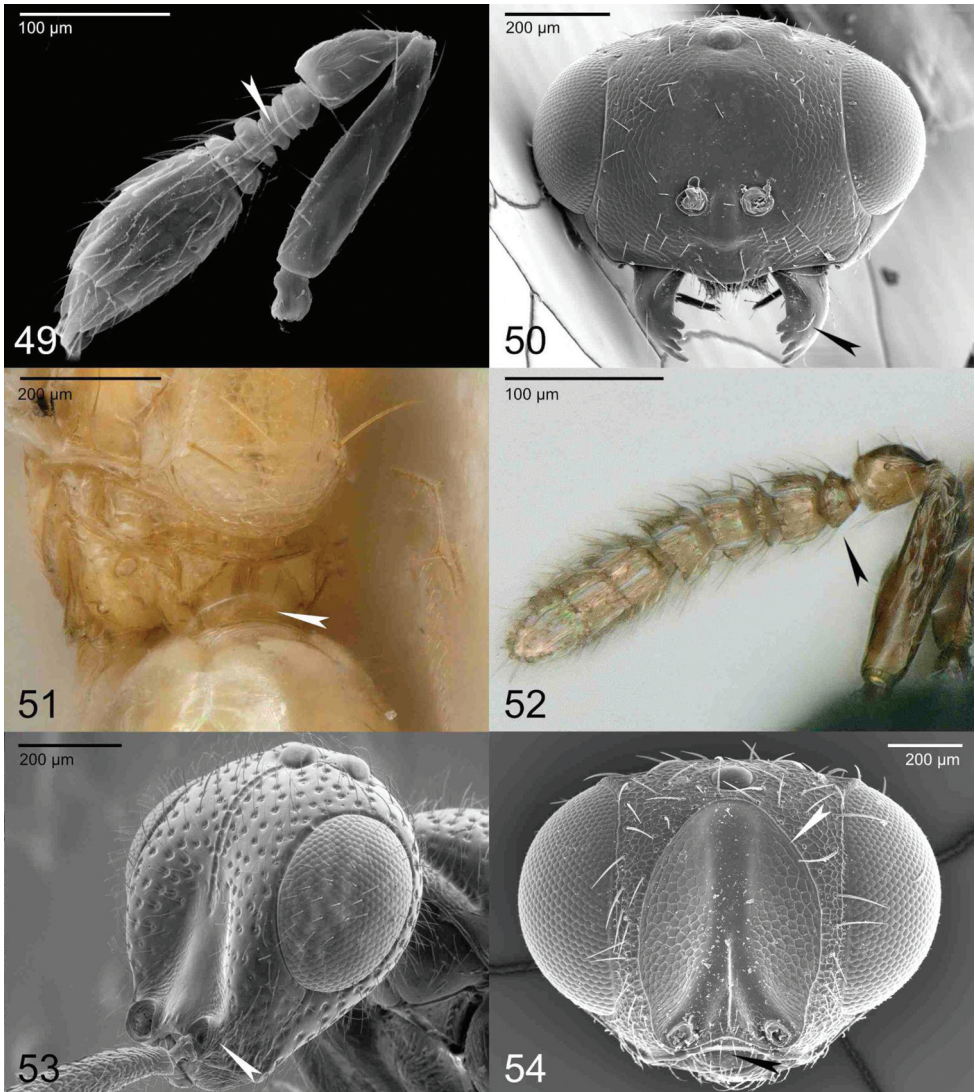
Pirenidae most strongly resemble those few Pteromalidae that have 11 antennal flagellomeres, otherwise differing from most in having 5 funiculars or fewer, without enough visible anelli to bring the total flagellomeres before the clava to the count of 8 that is present in nearly all Pteromalidae. Out of those Pteromalidae with 11 flagellomeres, *Termolampa pinicola* Bouček differs in having incomplete notauli, *Andersena anomala* Andersen differs in having no anelli. *Bugacia* Erdős differs in having the vertex with blunt carina or crest, and *Trigonoderopsis* Girault differs in having 8 flagellomeres between pedicel and clava. Eunotidae differ in having an exposed, rigid labrum and divergent eyes with a concave medial margin in their lower half. While this may make Eunotidae and Pirenidae sound very similar to one another, the habitus of Eunotidae is very different from most Pirenidae, being stout and flattened instead of being more moderate in body proportions and with a deeper mesosoma. Eriaporinae are the pirenids most likely to be confused with Eunotidae, but differ most conspicuously in having stout setae on the parastigma. Moranilidae differ in having 2 mesofurcal pits, in having pits on the mesopleural area of the mesopectus, and in having an oblique basitarsal comb. Herbertiidae and Systasidae differ from Pirenidae in having 2 mandibular teeth, and along with Micradelinae, an exposed, rigidly sclerotized labrum.

Cecidellinae Mitroiu, Rasplus & Burks, new subfamily

<https://zoobank.org/4295BD83-C89D-403E-9BFC-260C63134ADF>

Type genus. *Cecidellis* Hanson, 2005.

Diagnosis. Body pale, white to yellowish or pale brown, without metallic luster. Antenna with 9 flagellomeres, including 4 funiculars and 2 anelli. Eyes linearly diverging in ventral half. Petiole with lamina that overlaps part of the propodeal margin (Heydon and Hanson 2005) (Fig. 51). Otherwise as in Pirenidae.



Figures 49–54. **49** *Macroglenes varicornis* (Haliday) (Pirenidae): antenna **50** *Gastrancistrus* sp. (Pirenidae, Tridyminae): head frontal view **51** *Cecidellis* sp. (Pirenidae, Cecidellinae): petiole with lamina **52** *Spathopus* sp. (Pirenidae, Tridyminae): antenna **53** *Spalangia alycia* Gibson (Spalangiidae): head anterolateral view **54** *Erotolepsia* sp. (Spalangiidae, Erotolepsiinae): head frontal view.

Pireninae

Diagnosis. Body usually dark brownish or metallic. Antenna with at most 3 large flagellomeres and at least 2 anelli before clava (Fig. 49). Eyes usually not or only slightly diverging ventrally (except some males). Marginal vein at least 3.5× as long as the short and mostly straight stigmal vein. Petiole without dorsal lamina.

Discussion. In this new, more restricted sense, Pireninae contains genera that are morphologically similar to *Macroglenes*. They are here distinguished from Tridyminae, which are generally more stout in body shape and differ in features mentioned in diagnoses of both subfamilies, but most prominently in the antennal flagellum and relative lengths of the marginal and stigmal veins of the fore wing.

Tridyminae revived status

Tridymina Thomson, 1876. Type genus: *Tridymus* Ratzeburg, 1848. Treated as Tridyminae by Ashmead (1904).

Diagnosis. Body usually metallic, except *Calyconotiscus* Narendran & Saleem. Antenna with 4 or 5 large flagellomeres and at least one anelliform flagellomere before clava (Fig. 52). Eyes not divergent ventrally. Marginal vein at most 3× as long as the relatively long stigmal vein. Petiole without dorsal lamina.

Discussion. The subfamily Tridyminae is removed from synonymy with Pireninae to include *Gastrancistrus* Westwood new placement and related genera. *Calyconotiscus* Narendran & Saleem new placement, *Ecrizotes* Förster new placement, *Epiterobia* Girault new placement, *Melancistrus* Graham new placement, *Oxyglypta* Förster new placement, *Premiscogaster* Girault new placement, *Sirovena* Bouček new placement, *Spathopus* Ashmead new placement, and *Spinancistrus* Kamijo new placement are here confirmed to belong to this subfamily.

Spalangiidae revived status

Spalangiidae (as Spalangiae, not Latin) Haliday, 1833, revived status. Type genus: *Spalangia* Latreille, 1805.

Erotolepsiinae Bouček, 1988. Type genus: *Erotolepsia* Howard, 1894.

Diagnosis. Antenna usually with 8 flagellomeres, including a 1-segmented clava, with 11 flagellomeres including 3 clavomeres in *Eunotopsia* Bouček. Clypeus without transverse subapical groove. Labrum exposed, well-sclerotized, subrectangular or semicircular with marginal setae in a row (Fig. 53). Mandibles with 2 or 3 teeth, or undivided (in *Eunotopsia*). Subforaminal bridge with postgenal bridge or with postgena separated by lower tentorial bridge. Mesoscutellum with frenum indicated at least laterally, and without axillular sulcus. Mesopleural area without an expanded acropleuron; mesepimeron extending over anterior margin of metapleuron. All legs with 5 tarsomeres; protibial spur stout and curved; basitarsal comb longitudinal. Metasoma with syntergum, therefore without epipygium.

Discussion. There are two distinctive subfamilies in Spalangiidae, Spalangiinae and Erotolepsiinae new placement, both comprised of parasitoids of Diptera. The antennal

toruli are placed very low on the head in most species of both subfamilies (Fig. 54). In most Erotolepsiinae (except *Eunotopsia* where they are placed higher), the toruli are just above the very short clypeus, while in Spalangiinae the toruli are placed on lobes that overhang the clypeus and labrum, rendering them difficult to see. This distinctive antennal placement and the prognathous head make members of Spalangiinae easily identifiable. Most Erotolepsiinae (again, not *Eunotopsia*) are readily identified by the presence of a long carina that encircles most of the face, extending from near the median ocellus to the top of the clypeus (Fig. 54), and have a transverse carina across the anterior part of Gt_1 (Fig. 55). The enigmatic genus *Eunotopsia* shares the transverse carina on Gt_1 with other Erotolepsiinae and can be identified to subfamily using this feature. Erotolepsiinae strongly resemble Herbertiidae and Micradelinae, which differ in lacking the carinae of the face and Gt_1 . Herbertiidae further differ in having an oblique basitarsal comb, although the basitarsal comb of Micradelinae is reduced and difficult to evaluate. Eunotidae are also somewhat similar to Erotolepsiinae, but differ in that the mesepimeron does not overlap the anterior margin of the metapleuron, and in lacking the Gt_1 sculpture of Erotolepsiinae.

Systasidae new status

Systasini Bouček, 1988, new status. Type genus: *Systasis* Walker, 1834.

Trisecodinae new subfamily. Type genus: *Trisecodes* Delvare & LaSalle, 2000.

Diagnosis. Antenna with 7 or 11 flagellomeres, including 1 or more anellus and a small 4th clavomere. Eyes not ventrally divergent. Clypeus without transverse subapical groove. Labrum exposed, well-sclerotized (Fig. 56a). Subforaminal bridge with postgena separated by lower tentorial bridge. Notauli complete. Mesoscutellum with short frenum indicated at least laterally, with axillular sulcus. Mesopleural area without an expanded acropleuron; mesepimeron not extending over anterior margin of metapleuron; mesofurcal pit on mesotrochantal plate directly between the mesocoxal insertions (Fig. 57). Protibial spur curved; basitarsal comb oblique; all legs with either 5 (Systasinae) or 3 (Trisecodinae) tarsomeres. Metasoma with syntergum, therefore without epipygium.

Discussion. Systasinae are most likely to be confused with Pirenidae and Pteromalidae, which differ in having a flexible labrum that is concealed behind the protruding clypeus, whereas the clypeus in Systasinae recedes medially to expose the sclerotized labrum; they also have a longitudinal basitarsal comb, whereas it is oblique in Systasinae. The position of the mesofurcal pit in Systasidae is very unusual, although a leg may need to be removed to see it. Trisecodinae can be confused with Trichogrammatidae based on the 3-segmented tarsi, the head sulci, and the setal lines on the fore wing, and with some Eulophidae, based on the reduced number of flagellomeres, the head sulci, the setal lines on the fore wing, and the very short postmarginal and stigmal veins. From the former, Trisecodinae differ in the longer flagellum, the narrowly attached gaster with phragma

restricted to mesosoma, the different pattern of head sulci, and the shape of the fore tibial spur. From the latter, although *Trisecodes* was preliminary placed in Entedoninae (Delvare & LaSalle, 2000), Trisecodinae differ in various features that do not fit with any current eulophid subfamily. While *Trisecodes* is easy to distinguish from other Systasidae due to the difference in tarsomere count, it is retained in this family to indicate the phylogenetic context provided by both the molecular and morphological data.

Trisecodinae Mitroiu, Rasplus & Burks, new subfamily

<https://zoobank.org/C3DBCDA4-F0C1-4E89-AC82-5BCDC745147D>

Type genus. *Trisecodes* Delvare & LaSalle, 2000.

Diagnosis. Antenna with 7 flagellomeres (Fig. 58); multiporous plate sensilla unusually long and curved; head except malar sulcus with frontal, scrobal and subtorular sulci; anterior tentorial pits absent; toruli at or below the lower ocular line; all legs with 3 tarsomeres.

Former Pteromalidae taxa treated as *incertae sedis* in Chalcidoidea, unplaced to family

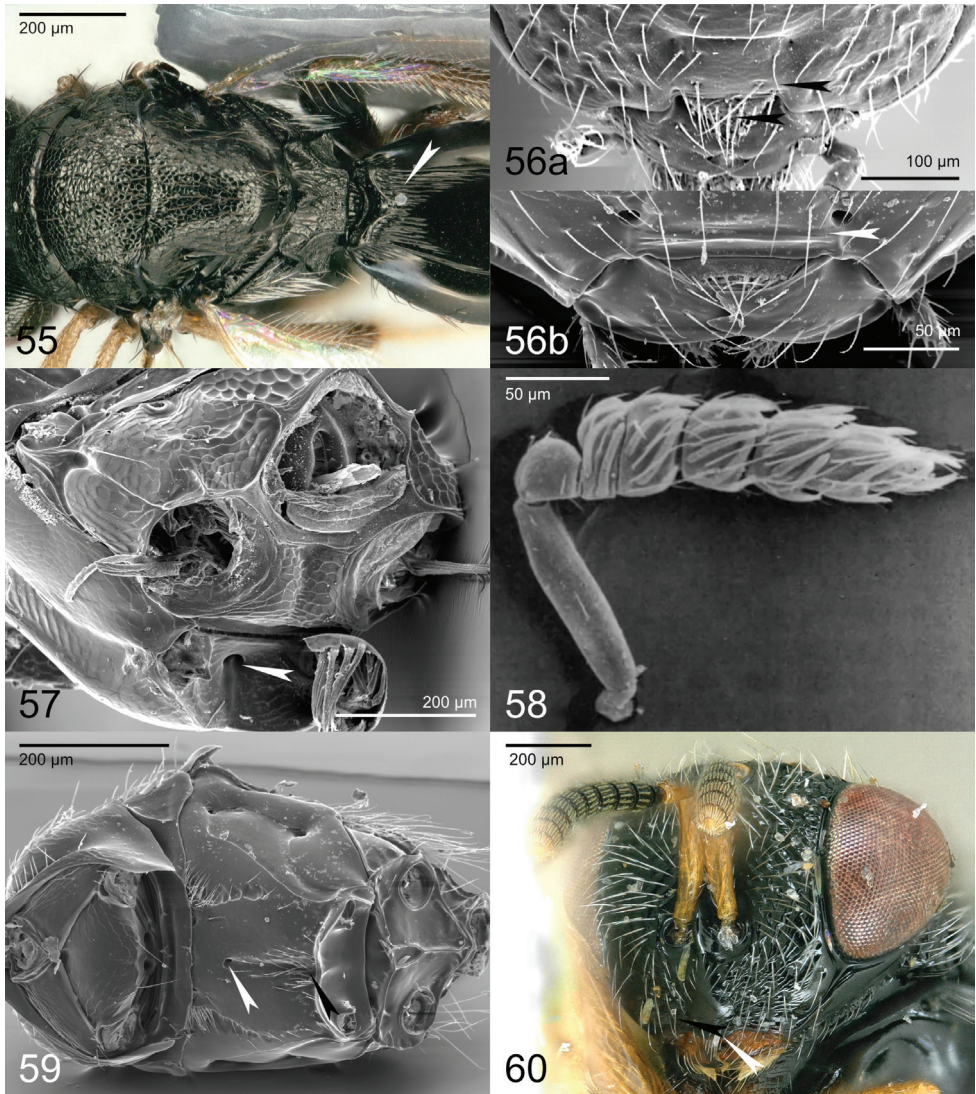
Asaphesinae *incertae sedis* new placement

Asaphinae Ashmead, 1904. Type genus: *Asaphes* Walker, 1834. Junior homonym of Asaphidae Burmeister, 1843.

Asaphesinae Burks & Heraty, 2020, replacement name.

Diagnosis. Antenna with 12 flagellomeres, including a small 4th clavomere. Clypeus with transverse subapical groove. Head dorsally with temple separating posterior margin of eye from that of the head. Labrum exposed, well-sclerotized, subrectangular with marginal setae in a row. Mandibles with 2 or 3 teeth. Subforaminal bridge with postgena separated by lower tentorial bridge; occipital carina present. Mesoscutellum with frenum indicated at least laterally, and with axillular sulcus. Mesopleural area without an expanded acropleuron, with pits; mesepimeron not extending over anterior margin of metapleuron; two mesofurcal pits usually present (Fig. 59) (absent in the fossil genus *Coriotela*). All legs with 5 tarsomeres; protibial spur stout and curved; basitarsal comb oblique. Metasoma with syntergum, therefore without epipygium.

Discussion. The scope of Asaphesinae is much reduced with the removal of Enoggerinae new subfamily to a separate *incertae sedis* subfamily in Chalcidoidea, and *Bairamliia* Waterston to Sphegigastrini (Pteromalidae). Asaphesinae is part of a set of taxa with two mesofurcal pits and some other shared features, but which do not form a clade in molecular analyses (Cruaud et al, submitted), including Enoggerinae, Herbertiidae, and Moranilidae. Asaphesinae differ from Herbertiidae and Moranilidae in having 12 flagellomeres instead of a maximum of 10. Enoggerinae differ in lacking a temple, thus with the posterior margin



Figures 55–60. **55** *Erotolepsia* sp. (Spalangiidae, Erotolepsiinae): mesosoma and base of metasoma dorsal view **56a**, **57** *Systasis* sp. (Systasidae) **56a** apex of clypeus without subapical groove **57** mesosoma ventral, mesotrochantal plate and mesofurcal pit **58** *Trisecodes africanum* Gumovsky (Pirenidae, Trisecodinae): antenna **56b**, **59** *Asaphes* sp. (Asaphesinae, *incertae sedis*) **56b** clypeal subapical groove **59** mesosoma ventral **60** *Austrosystasis atricorpus* Girault (Austrosystasinae, *incertae sedis*) **60** head frontal view, mesosoma lateral view.

of the eye dorsally meeting that of the head. Some Asaphesinae resemble Pteromalidae in habitus, differing in the clypeus, reduced mandibles, labrum, oblique basitarsal comb, and presence of two mesofurcal pits, but also having features that are rarely found in Pteromalidae, such as an occipital carina and the mesopleural area with pits.

Austrosystasinae *incertae sedis* new placement

Austrosystasinae Bouček, 1988. Type genus: *Austrosystasis* Girault, 1924.

Diagnosis. Antenna with 12 flagellomeres, including a small 4th clavomere. Eyes slightly linearly divergent ventrally. Clypeus with transverse subapical groove. Labrum hidden, flexible, with marginal setae in a row (Fig. 60). Subforaminal bridge with postgena separated by lower tentorial bridge, with a short apparent postgenal bridge immediately dorsal to the hypostoma. Mesoscutellum with frenum indicated laterally, with axillular sulcus. Mesopleural area without an expanded acropleuron; mesepimeron not extending over anterior margin of metapleuron (Fig. 61). All legs with 5 tarsomeres; protibial spur stout and curved; basitarsal comb longitudinal. Metasoma with syntergum, therefore without epipygium, rigidly convex.

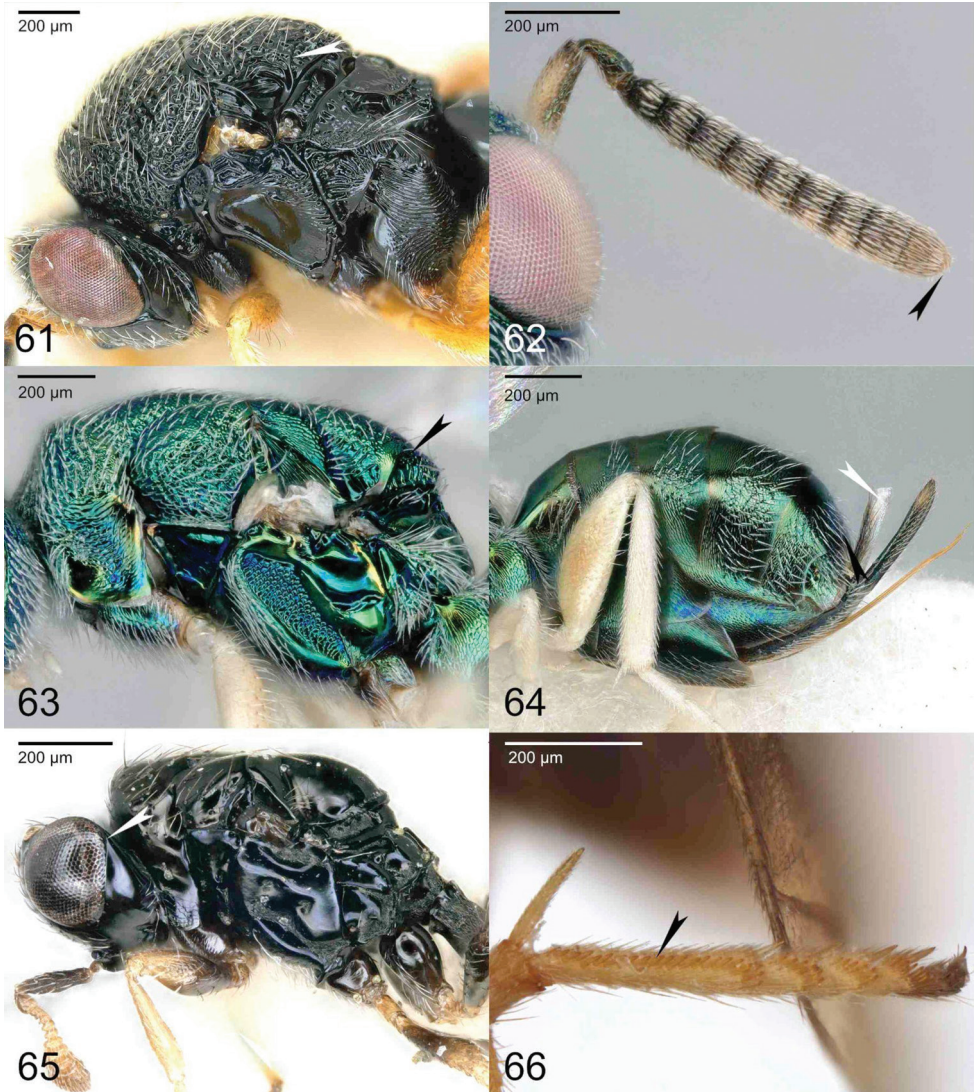
Discussion. *Austrosystasis atricarpus* Girault, the sole species in this subfamily, has not been sequenced, and its place is uncertain given our incomplete knowledge of its morphology. It appears to be a member of the Gall Clade, and it is an associate of galls on *Elaeocarpus* (Elaeocarpaceae) in Australia. It has rough surface sculpture (Fig. 61) that causes it to resemble Eurytomidae (especially Rileyinae), although it has a shorter pronotum. Otherwise, it resembles Melanosomellidae, differing in having a distinct and complete axillular sulcus and distinctive sculpture on the axillula. It also resembles Ormyridae in overall body shape, but this could be attributed to gall association in both taxa. The differing sculpture of the axillula and the posterior surface of the head separate Austrosystasinae from Ormyridae. Given that *A. atricarpus* would complicate the diagnosis of whatever family it could be transferred to, the genus is dealt with here as *incertae sedis* in Chalcidoidea.

Ditropinotellinae *incertae sedis* new placement

Ditropinotellinae Bouček, 1988. Type genus: *Ditropinotella* Girault, 1915.

Diagnosis. Antenna with 11 flagellomeres, without a 4th clavomere (Fig. 62). Eyes slightly divergent ventrally. Clypeus without a transverse subapical groove, with a small median incision. Labrum hidden behind clypeus, flexible. Mandibles with 3 teeth. Occipital carina absent. Subforaminal bridge with a postgenal bridge. Notauli complete. Mesoscutellum with a densely setose frenum that is indicated laterally, without axillular sulcus (Fig. 63). Mesopleural area without an expanded acropleuron; mesepimeron not extending over anterior margin of metapleuron. All legs with 5 tarsomeres; protibial spur stout and curved; basitarsal comb longitudinal. Metasoma with an elongate, T-shaped syntergum in females that may resemble an epipygium because of its shape (Fig. 64).

Discussion. *Ditropinotella* Girault is a morphologically enigmatic Australasian genus of gall associates, transferred out of Torymidae and placed in its own subfamily in



Figures 61–66. **61** *Austrosystasis atricorpus* Girault (Austrosystasinae, *incertae sedis*): mesosoma lateral view **62–64** *Ditropinotella* sp. (Ditropinotellinae, *incertae sedis*) **62** antenna **63** mesosoma lateral view **64** metasoma **65** *Enoggera reticulata* Naumann (Enoggerinae, *incertae sedis*): mesosoma lateral view **66** *Eopelma* sp. (*incertae sedis*): apex of mesotibia and mesotarsus.

Pteromalidae by Bouček (1988). It renders Eupelmidae paraphyletic in next-generation molecular data (Cruaud et al., submitted), although it lacks the expanded acropleuron of that family and lacks the diagnostic features of all genera in Calosotinae. *Ditropinotella* has a broad membranous area posterior to its mesocoxae, although this also occurs in various other chalcidoids that are not related to Eupelmidae. The possibility remains that *Ditropinotella* may be a reduced eupelmid, but morphological

evidence in support of this possibility is lacking. Because of the possible instability of this situation, Ditropinotellinae is removed from Pteromalidae to be treated as *incertae sedis* in Chalcidoidea.

The general habitus, setose frenum, and approximated, slightly advanced axilla of *Ditropinotella* invite comparison with Torymidae, which differ in having a true epipygium in females that is shorter and not so elongate. Males are more difficult to distinguish, differing in the slightly divergent eyes and incised clypeus of *Ditropinotella*, features that do not occur together in Torymidae. Most Megastigmidae also resemble *Ditropinotella*, although most Megastigmidae and Torymidae have an occipital carina. Megastigminae additionally differ from Ditropinotellinae in having an enlarged fore wing stigma and along with Chromeurytominae have a true epipygium in females, while Keiraninae have an occipital carina and do not have an elongate syntergum. Although some pteromalid fig associates have an elongate epipygium that resembles the syntergum of *Ditropinotella*, these differ from *Ditropinotella* in having a larger axillula with a distinct axillular sulcus. Male Eupelminae can strongly resemble those of *Ditropinotella*, but differ in having a distinct frenal arm laterally.

Enoggerinae Burks, new subfamily, *incertae sedis*

<https://zoobank.org/BB289EAC-0821-480F-9E60-B4E75358AE4F>

Type genus. *Enoggera* Girault, 1926.

Diagnosis. Antenna with 9–12 flagellomeres, including either an incompletely divided clava or up to 4 clavomeres, sometimes including a small 4th clavomere. Temple absent, thus posterior margin of eye coincident with the posterior margin of the head dorsally (Fig. 65). Clypeus with transverse subapical groove. Labrum exposed, well-sclerotized, subrectangular, with marginal setae in a row. Mandibles with 3 teeth. Subforaminal bridge with postgena separated by lower tentorial bridge. Mesoscutellum with frenum indicated at least laterally, with axillular sulcus. Mesopleural area without an expanded acropleuron, with pits; mesepimeron not extending over anterior margin of metapleuron; two mesofurcal pits present. All legs with 5 tarsomeres; protibial spur stout and curved; basitarsal comb oblique. Metasoma with syntergum, therefore without epipygium. Egg parasitoids of Chrysomelidae (Coleoptera).

Discussion. Enoggerinae share a pair of mesofurcal pits with a number of other chalcidoid groups, including Herbertiidae, Moranilidae, and Asaphesinae. However, these groups are unstable in molecular analyses and do not form a clade (Cruaud et al., submitted), with Enoggerinae more often as the sister group of Coelocybidae. Therefore, Enoggerinae can be separated from all similar groups by the absence of the temple. With a different biology, Enoggerinae would also represent a discordant element if placed in any of the other groups.

***Eopelma* Gibson *incertae sedis* new placement**

Eopelma Gibson, 1989. Type species. *Eopelma mystax* Gibson, 1989.

Diagnosis. Antenna with 8 flagellomeres, with an undivided clava. Eyes ventrally divergent. Clypeus without transverse subapical groove. Labrum hidden behind clypeus, flexible. Mandibles with 3 teeth or with a ventral tooth and dorsal slightly emarginate truncation. Axilla long, separated anteromedially. Axillular sulcus more or less distinct. Frenum absent. Acropleuron enlarged, convex and pad-like; covering most of mesopleural area, separated from mesocoxa by the lower mesepimeron, metapleuron, and a dorsal extension of the metasternal area. All legs with 5 tarsomeres; protibial spur stout and curved; basitarsal comb longitudinal; ventral membranous area anterior to mesocoxal attachment lacking; mesotibial spur stout; mesotarsus with 1 row of pegs anteroventrally (Fig. 66). Metasoma with syntergum, therefore without epipygium.

Discussion. *Eopelma* is consistently the sister group of another *incertae sedis* taxon, *Storeya* Bouček (Storeyinae), in next-generation molecular analysis (Cruaud et al., submitted). These two groups do not strongly resemble each other in body shape. *Storeya* does not have an expanded acropleuron, and has not previously been indicated as a relative of any eupelmid. They do share an antennal flagellomere count, a long radicle, general coloration, and an undivided clava, but the list of shared features possessed by these two genera is much shorter than the list of differences between them. A new subfamily is not described for *Eopelma* because it is a single genus, the position of which in Chalcidoidea is still in question.

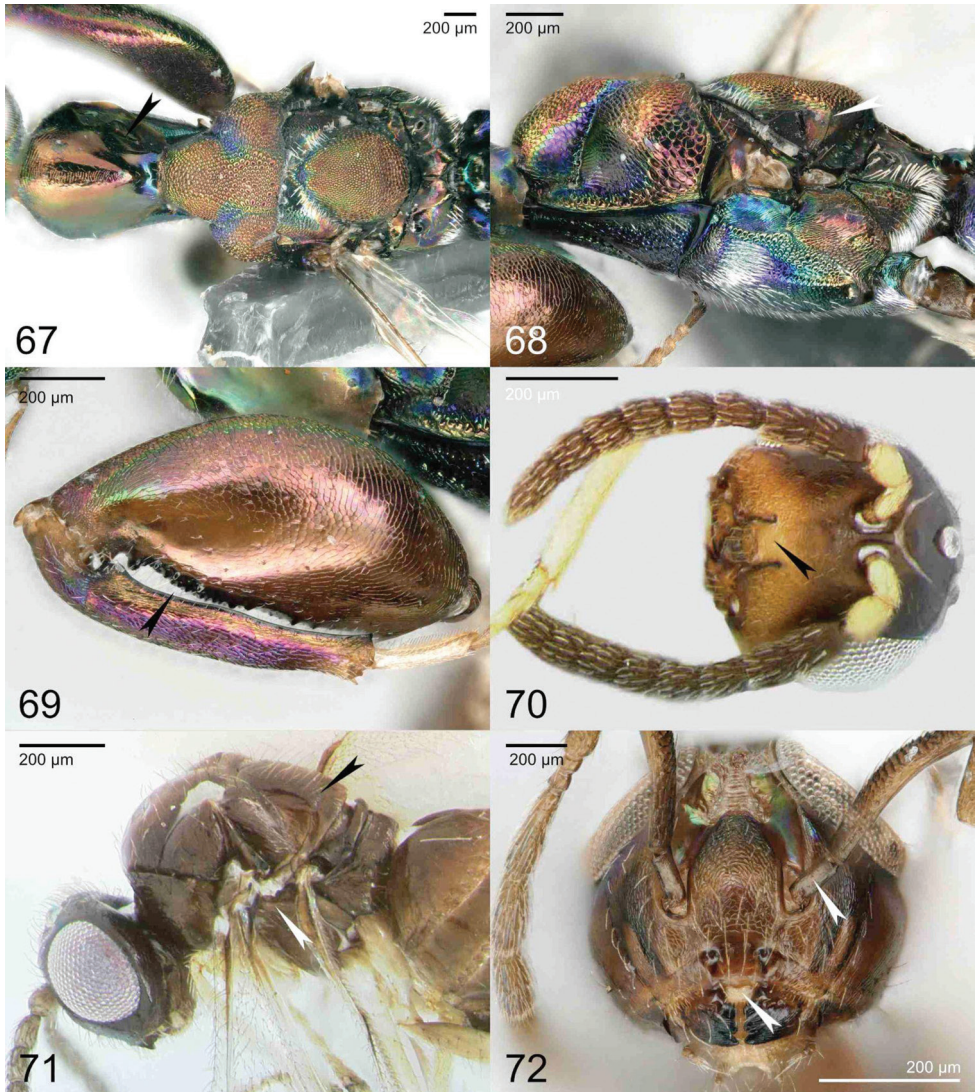
Eopelma vaguely resembles *Neanastatus* Girault in body shape and coloration. *Neanastatus* differs in having a much smaller axilla, which may not be clearly visible.

***Keryinae incertae sedis* new status, new placement**

Keryini Bouček, 1988. Type genus: *Kerya* Bouček, 1988.

Diagnosis. Antenna with 10 flagellomeres, including a single anellus (Fig. 70). Clypeus with lateral sulci but without a dorsal sulcus; ventral margin protruding and slightly convex but not bilobed (Fig. 70). Toruli slightly above center of face, immediately below a forked sulcus that exposes conjunctiva. Trabeculae absent (although sulcus present in middle of upper face). Notauli complete, incised. Frenum present, indicated by a complete frenal sulcus (Fig. 71). Axillular sulcus present. Acropleuron not enlarged (Fig. 71). Fore wing densely setose, without speculum; basal fold pigmented. Legs with 4 tarsomeres on all legs; protibial spur short and straight. Cerci surrounded by conjunctiva.

Discussion. The combination of having just 4 tarsomeres on all legs, 10 flagellomeres, and a frenum, together with a lack of trabeculae, makes *Kerya antennalis* Bouček distinct from all other chalcidoids. It was once placed in Eulophinae (Bouček 1988),



Figures 67–72. **67–69** *Heydenia longicollis* (Cameron) (Heydeniidae) **67** mesosoma dorsal view **68** mesosoma lateral view **69** fore leg **70, 71** *Kerya antennalis* Bouček (Keryinae, *incertae sedis*) **70** head frontal view and antenna **71** mesosoma lateral view **72** *Callimomoides* sp. (Louriciinae, *incertae sedis*): head frontal view.

although analysis of 28S D2 ribosomal DNA indicated that it is not a eulophid and it was moved to Ormocerinae based on the placement of the toruli and the arched body (Gauthier, et al. 2000). Indeed some Melanosomellidae resemble *K. antennalis* in body shape, color, and smooth surface sculpture, but they have 11 or more flagellomeres, a bilobed clypeal margin, 5 tarsomeres, a stout and curved protibial spur, cerci surrounded

by cuticle, no axillular sulcus, and no forked sulcus on the face. Eulophidae and some Aphelinidae also have 4 tarsomeres and are relatively generalized (unlike Calesidae and Idioporidae), but have fewer flagellomeres and no frenum. Given the strong differences between *K. antennalis* and all the taxa with which it has been previously placed, and because it has not been analyzed using next-generation molecular data, Keryini is here elevated to subfamily status and placed as *incertae sedis* in Chalcidoidea.

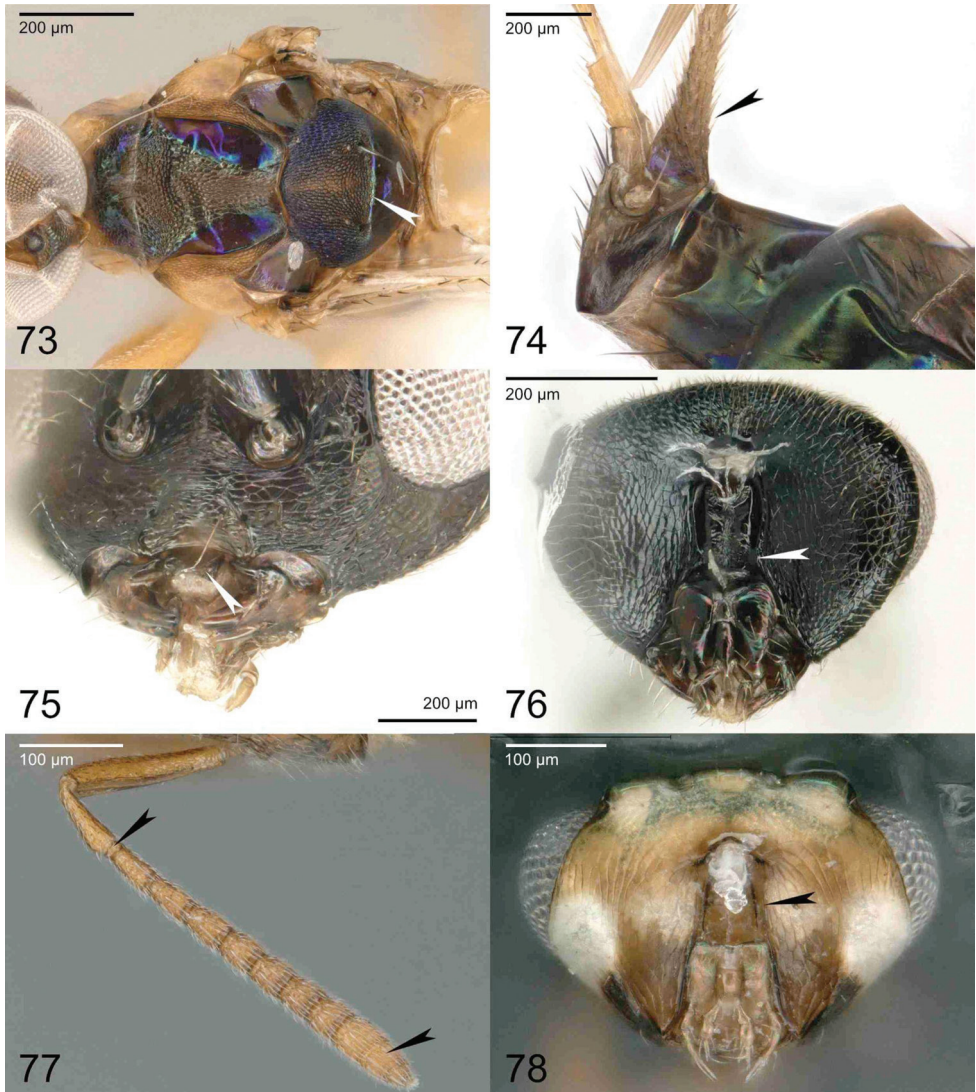
Louriciinae *incertae sedis* new placement

Louriciini Hedqvist, 1961: 92,108. Type genus: *Louricia* Ferrière, 1936. Treated as Louriciinae by Bouček (1988).

Diagnosis. Antenna with 8 flagellomeres, including an undivided clava and 2 anelli; radicle elongate. Eyes ventrally divergent. Face with a network of grooves that is usually concealed by the strongly collapsing head (Fig. 72). Clypeus without transverse subapical groove. Labrum subrectangular and exposed, with marginal setae in a row. Mandibles with 3 teeth. Subforaminal bridge with a postgenal bridge separating the secondary tentorial pits from the hypostoma. Pronotum long, with a slightly expanded lateral surface and therefore somewhat expanded laterally. Notauli complete, linear and incised. Axilla strongly advanced (Fig. 73). Mesoscutellum with frenum indicated at least laterally or by an abrupt transition to smooth surface sculpture, without axillular sulcus (Fig. 73). Mesopleural area without an expanded acropleuron. All legs with 5 tarsomeres; protibial spur stout and curved; basitarsal comb longitudinal. Metasoma in females with elongate syntergum extending over the exerted ovipositor (Fig. 74).

Discussion. Next-generation molecular analysis (Cruaud et al., submitted) consistently recovers the distinctive *Callimomoides* Girault as a member of a strongly supported clade that also includes *Neanastatus* and *Lambdobregma*, with *Callimomoides* as the sister group of *Neanastatus*, which therefore renders Neanastatidae paraphyletic. Morphologically, this relationship is highly debatable and no unique character supports it. However, this strong morphological disparity may be due to difference in life history as *Callimomoides* is an egg parasitoid of Cerambycidae while *Neanastatus* is parasitic in galls of Cecidomyiidae (Diptera) and *Lambdobregma* could be parasitoids of cricket eggs (Gibson 1989). While *Callimomoides* has an enlarged mesotibial spur and a large membranous area posterior to the mesocoxa, these features are not conclusive proof of relationship with Neanastatidae because they are found in various other taxa as well. There are no diagnostic features shared with either *Neanastatus* or *Lambdobregma*.

The highly unusual gestalt of *Callimomoides*, together with the combination of linear notauli, long pronotum, and stout mesotibial spur, prevent it from being easily confused with other Chalcidoidea. Eulophidae can have similar notauli and a weakly sclerotized, collapsing head and body, but differ in having 4 tarsomeres on all legs.



Figures 73–78. **73, 74** *Callimomoides* sp. (Louriciinae, *incertae sedis*) **73** mesosoma dorsal view **74** extremity of metasoma, elongated syntergum **75, 76** *Micradelus acutus* Graham (Micradelinae, *incertae sedis*) **75** head frontal view **76** head posterior view **77** *Neapterolaelaps* sp. (Neapterolelapsinae, *incertae sedis*): antenna **78** *Pseudoceraphron albifrons* (Bouček) (Neapterolelapsinae, *incertae sedis*): head posterior view.

Micradelinae *incertae sedis* new placement

Micradelini Wall, 1972. Type genus: *Micradelus* Walker, 1834. Treated as Micradelinae by Vago (2006).

Diagnosis. Antenna with 10 or 11 flagellomeres, including 3 or 4 clavomeres. Eyes slightly ventrally divergent. Clypeus transverse, with transverse subapical groove. Labrum exposed,

well-sclerotized, subrectangular with marginal setae in a row (Fig. 75). Mandibles with 2 teeth or with a small 3rd dorsal tooth (Fig. 75). Subforaminal bridge with postgena separated by lower tentorial bridge except for a small postgenal bridge dorsal to the hypostoma; posterior surface of head without (Fig. 76) postgenal lamina or postgenal groove. Pronotum transverse in dorsal view. Mesoscutellum with frenum reduced, with frenal arm laterally but sometimes hardly separated from marginal rim of mesoscutellum; axillular sulcus present. Mesopleural area without expanded acropleuron, without pits; mesepimeron extending over anterior margin of metapleuron; one mesofurcal pit present. Fore wing marginal vein subequal to stigmal vein in length; uncus elongate. All legs with 5 tarsomeres; protibial spur stout and curved. Metasoma with syntergum, therefore without epipygium.

Discussion. The former tribe Micradelini was treated as a subfamily by Vago (2006) and we preserve that rank here, although we remove it from Pteromalidae based on both molecular and morphological data (Cruaud et al., submitted). While Micradelinae are very similar to Herbertiidae in body shape, they only occasionally form a monophyletic group and Micradelinae are particularly unstable in phylogenetic placement.

Morphologically, Micradelinae strongly resemble Herbertiidae and the *incertae sedis* genus *Rivasia* Askew & Nieves-Aldrey in habitus and other features. The basitarsal comb of *Micradelus* Walker is reduced and difficult to evaluate, although it may be oblique like that of Herbertiidae. Herbertiidae differ from Micradelinae in having a much shorter stigmal vein relative to the marginal vein, in lacking an axillular sulcus, in lacking the postgenal groove and postgenal sulcus on the back of the head, and in having 2 mesofurcal pits instead of the single pit of Micradelinae. *Rivasia* is very similar to Micradelinae in most features, differing in having a more elongate body including the pronotum, and in having metallic green coloration instead of the short, stout body and brownish coloration of Micradelinae. Eunotidae may appear similar to Micradelidae when comparing lists of features, but in practice are easily distinguished in their different habitus and in having a short fore wing uncus.

Neapterolelapinae Rasplus, Burks & Mitroiu, new subfamily *incertae sedis* new placement

<https://zoobank.org/802C4B39-1937-4EE0-B153-25861437F3DB>

Type genus. *Neapterolelaps* Girault, 1913.

Diagnosis. Antenna with 11 flagellomeres, with 3 clavomeres (Fig. 77). Eyes ventrally divergent. Clypeus with a transverse subapical groove. Labrum exposed, sclerotized, subtriangular with setae. Mandibles with 2 or 3 narrow teeth. Subforaminal bridge with elongate lower tentorial bridge and secondary tentorial pits that extend to the convergent hypostomal carina, with or without a postgenal groove and postgenal lamina (Fig. 78). Pronotum without a smooth median longitudinal line or carina. Mesoscutellum without frenum, at least sometimes with a small axillula indicated by an axillular sulcus or carina. Mesopleural area without an expanded acropleuron; mesepimeron not extending over anterior margin of metapleuron. All legs with 5 tarsomeres; protibial spur stout and curved; basitarsal comb longitudinal; metafemur without ventral teeth or expansion. Metasoma with syntergum, therefore without epipygium; cercal brush present.

Discussion. *Neapterolelaps* and *Pseudoceraphron* Dodd form the sister group of Lyciscidae in next-generation molecular data, although they were previously classified in Diparinae (Bouček 1988; Desjardins 2007; Desjardins et al. 2007). While Desjardins (2004) mentioned the name Neapterolelapini in his doctoral dissertation, it was not mentioned in the two resulting publications. Additionally, it was mentioned by Heraty et al. (2013), although it was not diagnosed in that publication and therefore was not described there. Janšta (2014) also mentioned Neapterolelapini in a doctoral dissertation, but did not diagnose it. None of these previous usages satisfy article 13.1.1 of the ICZN Code, and therefore Neapterolelapinae is described as new here and it is removed from Diparidae to be treated as *incertae sedis* in Chalcidoidea. *Nosodipara* Bouček is also placed here based on morphology.

Given the characters described here, confusion with Lyciscidae is most likely, which differ in having a longitudinal median pronotal carina. However, a lack of metallic coloration on the mesosoma (but sometimes not of the head) of females makes Neapterolelapinae much more likely to be confused with Diparidae, which contains numerous species that resemble this group. Diparidae differ in having a conspicuous frenum in most species, although this may be indistinct or absent in highly derived brachypterous species. These must be distinguished using features of the head, such as the hidden labrum, convex clypeal margin, absence of clypeal subapical groove (excepted in *Dipara*) and striation of metacoxa of Diparidae versus the exposed labrum, concave clypeal margin, presence of clypeal subapical groove and absence of striation on metacoxa in Neapterolelapinae.

The placement of Neapterolelapinae does not conflict with the findings of Desjardins et al. (2007), who also placed *Neapterolelaps* as the sister group of what is now Lyciscidae in molecular analyses. This placement was discussed as “difficulty in uniting” [Diparinae] by Desjardins (2007).

Parasaphodinae *incertae sedis* new placement

Parasaphodinae Bouček, 1988c: 345. Type genus: *Parasaphodes* Schulz, 1906.

Diagnosis. Antenna with 11 flagellomeres, including 1 anellus and 7 funiculars (Fig. 79a). Eyes ventrally not or slightly divergent. Clypeus without transverse subapical groove. Labrum hidden (Fig. 80). Mandibles with 2 teeth. Mesoscutellum with frenum not distinctly indicated, without axillular sulcus. Mesopleural area without an expanded acropleuron, without pits; mesepimeron with posterior margin deeply concave and extending over anterior margin of metapleuron. All legs with 5 tarsomeres; protibial spur stout and curved. Marginal and postmarginal veins widened adjacent to stigmal vein (Fig. 79b).

Discussion. No molecular data are available for Parasaphodinae; moreover, because of the poor preservation of most available specimens, several characters such as the basitarsal comb, the structure of the back of the head, or the mesofurcal pits could not be observed. It is thus very difficult to assess the taxonomic position of Parasaphodinae in relation to other chalcids, therefore we treat it as *incertae sedis* in Chalcidoidea. Similarities with Asaphesinae, Elatoidinae and Herbertiidae have been discussed (Mitroiu 2017), but all these groups differ from Parasaphodinae in many respects.

***Rivasia* Askew & Nieves-Aldrey *incertae sedis* new placement**

Rivasia Askew & Nieves-Aldrey, 2005. Type species: *Rivasia fumariae* Askew & Nieves-Aldrey, 2005

Diagnosis. Antenna with 8 flagellomeres, including an undivided or incompletely divided clava. Eyes slightly ventrally divergent. Clypeus transverse. Labrum exposed, well-sclerotized. Mandibles with 2 teeth. Subforaminal bridge with postgena separated by lower tentorial bridge except for a small postgenal bridge dorsal to the hypostoma; posterior surface of head without postgenal lamina or postgenal groove. Pronotum subconical and elongate in dorsal view. Mesoscutellum with frenum; mesopleural area without an expanded acropleuron, without pits; mesepimeron extending over anterior margin of metapleuron; one mesofurcal pit present. Fore wing marginal vein subequal to stigmal vein in length; uncus elongate. All legs with 5 tarsomeres; protibial spur stout and curved. Metasoma with syntergum, therefore without epipygium.

Discussion. *Rivasia* is usually the sister group of fellow *incertae sedis* taxon Asaphesinae in molecular analyses (Cruaud et al., submitted), although the two groups share few distinctive features morphologically. Instead, *Rivasia* more strongly resembles the subfamily Micradelinae, though never forming a clade with it. *Rivasia* shares no particularly distinctive features with Ormocerinae (Pteromalidae) nor any former part of it, differing from them in numerous features listed in the diagnosis.

Micradelinae can be distinguished from *Rivasia* by having a shorter, transverse pronotum and brownish coloration, in contrast with the longer pronotum and metallic coloration of *Rivasia*. Asaphesinae differ from *Rivasia* in a number of features, including the presence of 8 flagellomeres instead of 12, the lack of an occipital carina, and from extant species in the lack of pits on the mesopleural area.

Storeyinae *incertae sedis* new placement

Storeyinae Bouček, 1988. Type genus: *Storeya* Bouček, 1988.

Diagnosis. Antenna with 8 flagellomeres, including an undivided clava; radicle elongate (Fig. 81). Intertorular prominence absent (Fig. 81). Eyes slightly divergent ventrally. Clypeus without transverse subapical groove. Labrum hidden behind clypeus, flexible, subrectangular and with marginal setae in a row. Mandibles with 3 teeth (may be 2 in some specimens in which it is difficult to see). Subforaminal bridge with a postgena separated by lower tentorial bridge. Notauli incomplete. Mesoscutellum with frenum indicated; with axillular sulcus. Mesopleural area without an expanded acropleuron; mesepimeron extending over anterior margin of metapleuron. Fore wing with a tuft of thickened leaf-shaped setae on the parastigma (Fig. 82). All legs with 5 tarsomeres; protibial spur stout and curved; basitarsal comb longitudinal. Metasoma with syntergum, therefore without epipygium.

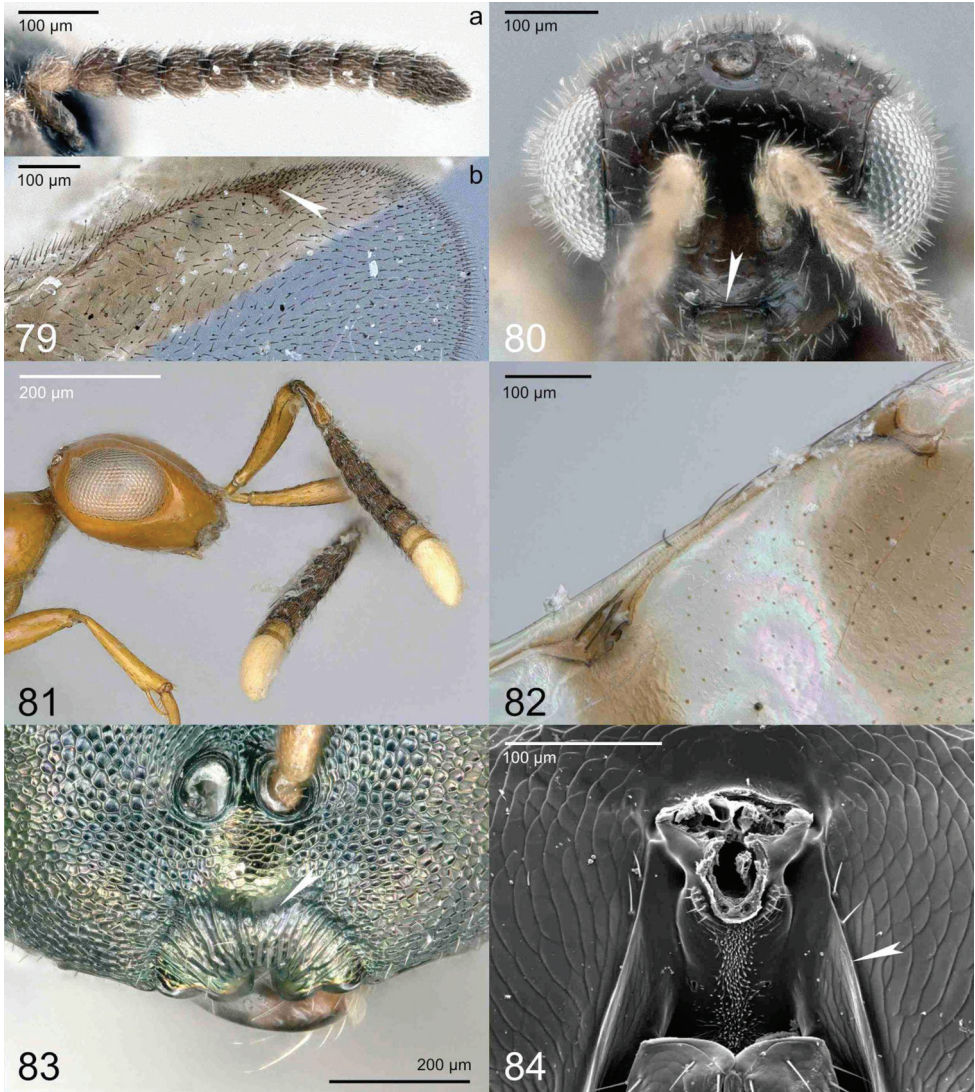
Discussion. Molecular and morphological data do not provide a clear signal on where this subfamily should be placed, and therefore we treat it as *incertae sedis* in Chalcidoidea. The elongate antennal radicle is an unusual feature also shared by its sister group (*Eopelma*) in molecular analyses and, in comparable taxa, is only found in Louriciinae. The enlarged axillula, easily visible dorsally, invites comparison with Colotrechninae and Sycophaginae in Pteromalidae, and with Heteulophidae, although each of these groups differs from Storeyinae in having complete notauli and in many other features as well. The low placement of the toruli may cause Storeyinae to key near Spalangiinae in family keys, although the toruli are not on lobes and the two groups differ in many features. The body coloration (excepted for one undescribed iridescent species) and the tuft of thickened, leaf-shaped setae on the parastigma recall Cerocephalidae, although Storeyinae lack an intertorular prominence and are not placed with cerocephalids using molecular data.

Pteromalidae

Pteromalini Dalman, 1820. Type genus: *Pteromalus* Swederus, 1795. Treated as Pteromalidae by Walker (1834).

Diagnosis. Antenna with 12 flagellomeres in nearly all cases (except in some fig associates, *Amphidocius*, *Andersena anomala*, *Bugacia*, *Trigonoderopsis*, and possibly *Termolampa pinicola*), including a small 4th clavomere; with at least 5 funiculars, and if with 5 then with 2 or more anelli. Eyes not ventrally divergent (although some genera have modified eyes that are difficult to evaluate). Clypeus subquadrate and without ventral transverse groove (Fig. 83). Labrum flexible (Darling 1988) and hidden behind clypeus. Mandibles with 3 or 4 teeth each (except in some fig associates (1–3 teeth) and in *Austroterobia* Girault where the left mandible has 2 teeth but is falcate). Subforaminal bridge with postgena separated by lower tentorial bridge; posterior surface of the head without postgenal lamina or postgenal groove (Fig. 84). Mesoscutellum with frenum indicated at least laterally, with axillular sulcus (except in some fig associates and *Nikolskayana mirabilis*). Mesopleural area without an enlarged acropleuron. All legs with 5 tarsomeres; protibial spur stout and curved; basitarsal comb longitudinal. Gaster, while sometimes rigidly convex, not strongly sclerotized; metasomal apex in most species with a syntergum and therefore without an epipygium (except in some fig associates).

Discussion. Agaonidae are similar to fig-associated Pteromalidae, differing from all in having a mandibular appendage bearing rows of spurs or lamellae in females (*Seres* Waterston, which may appear especially similar to Agaonidae, have an enlarged plate-like mandible, see figs 14–16 in van Noort and van Arden 2006, but do not have a mandibular appendage), and in more or less fused anelli, the last one mostly spine-like (Fig. 85). Male Agaonidae differ from male pteromalid fig wasps in that the metasomal apex is telescoped in a U-shaped arrangement under the body. Eucharitidae differ from most Pteromalidae in that the pronotum is not visible from dorsal view, but also in the flattened marginally digitate labrum. Likewise, most of the members of the Planidial Clade (Zhang et al. 2022) such as Chrysolampidae (digits sometimes ab-



Figures 79–84. **79** *Parasaphodes afer* Mitroiu (Parasaphodinae, *incertae sedis*) **79 a** antenna **b** venation **80** *P. iceryae* (Ashmead) (Parasaphodinae): head frontal view **81, 82** *Storeyia* sp. (Storeyinae, *incertae sedis*) **81** head lateral view and antenna **82** venation **83** *Caenocrepis* sp. (Pteromalidae, Pteromalinae): lower face **84** *Nasonia vitripennis* (Walker) (Pteromalinae): head dorsal view.

sent in Chrysolampinae and labrum plate-like in Philomidinae), Eutrichosomatidae, and Perilampidae have a digitate labrum. Eulophidae differ in having 4-segmented tarsi and a short, straight protibial spur. Some Eurytomidae, such as Rileyinae and *Buresium* Bouček can be similar to a few Pteromalidae, even though nearly all Pteromalidae have a much smaller pronotum; in a few cases where the pronotum is long, e.g. Trigonoderinae, it is not subrectangular in dorsal view, but instead is gradually narrowing anteriorly. Rileyinae and *Buresium* differ from Pteromalidae in having a

postgenal groove and a strongly sclerotized gaster. In practice, Rileyinae and *Buresium* are easily recognized once they are familiar, and no Pteromalidae have the combination of a long pronotum with a rigidly convex gaster. Ormyridae also differ from Pteromalidae in having a carapace-like gaster. Other members of the Gall Clade, such as Epichrysomallidae and Melanosomellidae, can be very similar to those pteromalids with complete notauli, but they differ in having either no indication of an axillular sulcus or carina, or in having a reduced and incomplete one. Pirenidae differ in having fewer flagellomeres: most especially if they have 5 funiculars, then they only have 1 anellus. Torymidae and Megastigmidae differ from most Pteromalidae in having an epipygium in females (except in *Keirana* Bouček which has a transverse sulcus across its syntergum immediately anterior to the cerci), but some pteromalid fig associates have a separate epipygium and a long, exerted ovipositor, therefore strongly resembling both of these families. Torymidae differ from all Pteromalidae in the form of their postgenal bridge, which occurs in the form of postgenal lobes meeting each other over the hypostoma (Burks and Heraty 2015). Most fig-associated Pteromalidae have the postgena separated by the lower tentorial bridge (Rasplus et al. 1998), additionally differing in ways described by Grissell (1995). Those with an elongate head, such as *Sycoecus* Waterston, have rederived a true postgenal bridge but differ from Torymidae in the shape of the highly modified head itself and in the vast number of other unusual features of their highly modified bodies.

From the new families diagnosed above, Pteromalidae can be distinguished using the given diagnoses. Species with 2 mandibular teeth differ in this count from nearly all Pteromalidae except for in the left mandible of *Austroterobia*, but in *Austroterobia* the mandibles are additionally very different in that they are falcate, whereas the bidentate mandibles of other families, such as Ceidae, are small and narrow. A partial exception to this is Neodiparidae, where the mandibles are relatively large but still not the same shape as in *Austroterobia* and are not falcate.

Yusufia Koçak & Kemal and *Ksenoplata* Bouček are kept as unplaced to subfamily in Pteromalidae new placement, because of uncertainty over their molecular placement and difficulty in assigning them to a subfamily morphologically. They would render any other subfamily more difficult to diagnose, although they bear some similarity to Miscogastrinae and Trigonoderinae in having a clypeal margin with a single median tooth.

Subfamilies and tribes of Pteromalidae

Colotrechninae

Colotrechnides Thomson, 1876. Type genus: *Colotrechnus* Thomson, 1878. Treated as Colotrechninae by Ashmead (1899).

Diagnosis. Mandibles not falcate. Scapula not exposed anteriorly by pronotum. Axilla strongly advanced (Fig. 86). Axillula enlarged and convex (Fig. 86). Propodeum with or without plicae. Petiole simple, usually transverse and hardly visible.

Amerostenini

Amerostenini Bouček, 1988. Type genus: *Amerostenus* Girault, 1913.

Diagnosis. Antennal flagellum with 4 anelli and 4 funiculars (Fig. 87). Pronotum not medially divided. Ovipositor sheaths not expanded.

Discussion. Molecular data indicate that the previously mentioned (Bouček 1988) unusual morphology of *Yrka dahmsi* Bouček new placement suggests that it belongs in the tribe Amerostenini in Colotrechninae instead of in Coelocybidae.

Morphology is consistent with this change, given that *Yrka* and some Amerostenini share a count of 4 antennal anelli.

Colotrechnini

Uzkini Bouček, 1988. Type genus: *Uzka* Bouček, 1988.

Diagnosis. Antennal flagellum usually with 3 anelli and 5 funiculars, but sometimes with 2 anelli and 6 funiculars. Pronotum not medially divided. Ovipositor sheaths not expanded.

Discussion. Uzkini new syn. is treated as a synonym of Colotrechnini due to the lack of distinguishing features between them. *Uzka* Bouček has not been analyzed molecularly, but morphologically it is distinguished by a differently shaped head, and therefore seems to be a derived element within Colotrechnini instead of being part of a distinct lineage.

Divnini

Divnini Bouček, 1988. Type genus: *Divna* Bouček, 1988.

Diagnosis. Antennal flagellum with 2 anelli and 5 funiculars. Pronotum medially divided (Fig. 88). Ovipositor sheaths expanded and densely setose.

Discussion. The sole species in Divnini, *Divna hirtura* Bouček, has not been analyzed molecularly, and has only a dubious membership in Colotrechninae or even in Pteromalidae. Divnini is retained in Colotrechninae because we are not aware of any definitive reason to remove it from Pteromalidae, but molecular data or new morphological data may well suggest a change in its placement.

Trigonoderopsini Rasplus & Mitroiu, new tribe

<https://zoobank.org/00E4A87B-E416-4B34-8156-0EAD9B597BC3>

Type genus. *Trigonoderopsis* Girault, 1915.

Diagnosis. Antenna variously with 11 flagellomeres, either with 1 anellus and 5 funiculars, 2 anelli and 5 funiculars, 1 anellus and 6 funiculars, or with 1 anellus and

7 funiculars in some males but then with only 2 clavomeres. Pronotum not medially divided (Fig. 89). Ovipositor sheaths not expanded.

Discussion. Next generation molecular data (Cruaud et al., submitted) place *Trigonoderopsis* Girault and *Bugacia* Erdős new placement in Colotrechninae, as the sister group of Colotrechnini, instead of their previous placements in Pireninae or (in the case of *Bugacia*) dubiously in Ormocerinae. The reduced antennal flagellum helps diagnose this emergent group, and the relatively large mandible with 4 mandibular teeth may also help diagnose the tribe, although this feature is variable in Pteromalidae.

Erixestinae Burks & Rasplus, new subfamily

<https://zoobank.org/49F28424-4F14-4E6E-8FDF-4ED6C5171747>

Type genus. *Erixestus* Crawford, 1910.

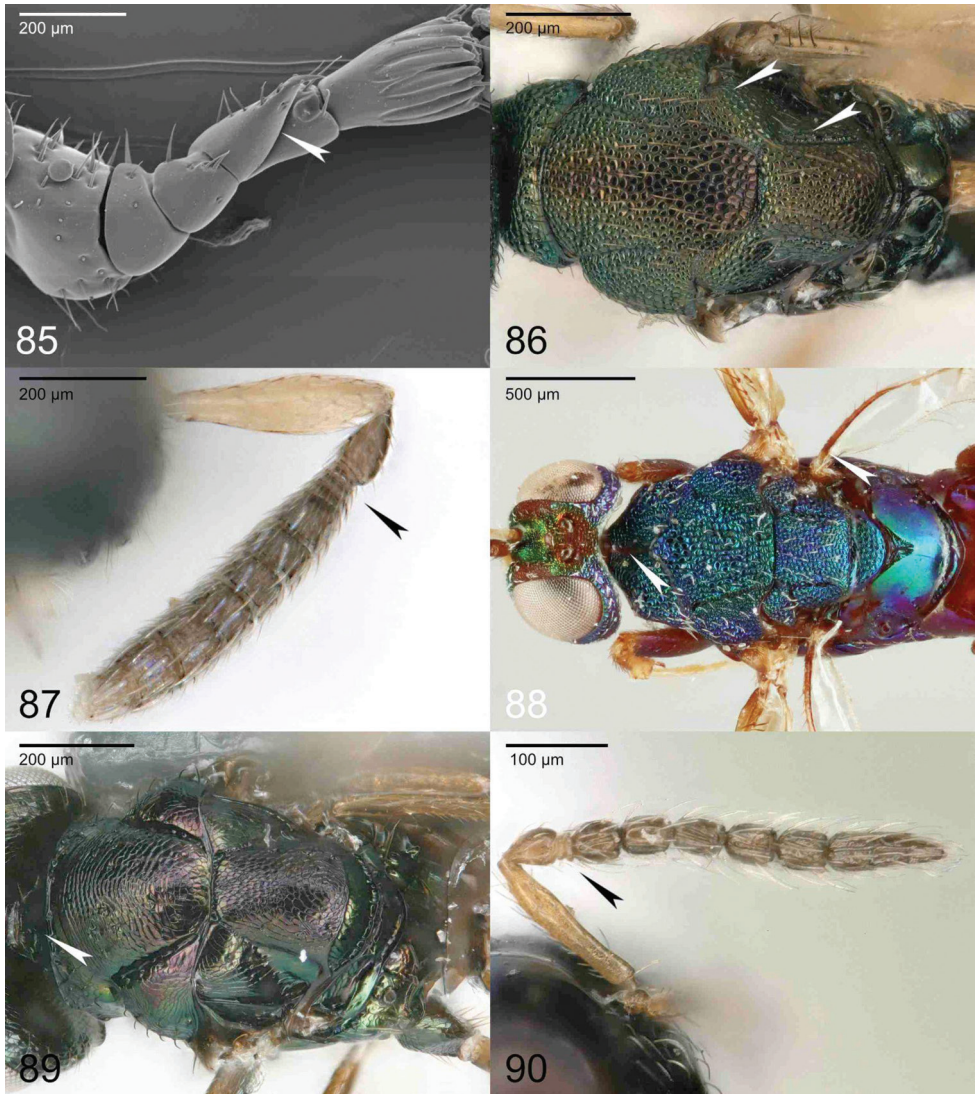
Diagnosis. Antenna with 11 flagellomeres, with 2 anelli and 5 funiculars (Fig. 90). Mandibles falcate. Scapula not anteriorly exposed by pronotum. Axilla not strongly advanced. Axillula not enlarged (Fig. 91). Propodeum with plicae. Petiole transverse.

Discussion. *Erixestus*, containing egg parasitoids of Chrysomelidae, had persisted in uncertain placement since its description, but had apparent affinities with Ormocerini due to the high dorsal placement of the toruli. Next-generation molecular data (Cruaud et al., submitted) suggest that it is the sister group of Pteromalinae plus Pachyneurinae. The falcate mandibles of Erixestinae and Pachyneurinae indicate that this may be a synapomorphy of this entire clade, rather than a synapomorphy of Pachyneurinae alone. Otherwise, features such as the subforaminal bridge do not reject the placement of Erixestinae, but the reduced flagellomere count would be very unusual, though not unknown in the clade. It is likely that divergent features of Erixestinae are due to a life history as egg parasitoids of Chrysomelidae.

Miscogastrinae

Miscogasteridae Walker, 1833. Type genus: *Miscogaster* Walker, 1833. Treated as Miscogasterinae by Ashmead (1904). Spelling corrected to Miscogastrinae by Burks (2012).

Diagnosis. Antenna nearly always with 12 flagellomeres (exception: *Andersena* Bouček). Mandibles usually not falcate, but sometimes enlarged (*Diconocara* Dzhanokmen). Scapula not anteriorly exposed by pronotum. Axilla not strongly advanced. Axillula rarely enlarged, but if so then they are not convex. Propodeum with or without plicae. Petiole variable, either with anterolateral flange extending from ventral surface to form lateral tooth-like protrusions (Fig. 97), or simple. If petiole simple, then clypeal margin asymmetrical (Fig. 94), or concave ventrally and then clypeus enlarged and nearly adjacent to toruli dorsally (Fig. 92).



Figures 85–90. **85** *Blastophaga psenes* (L.) (Agaonidae): antenna part **86** *Bofuria* sp. (Pteromalidae, Colotrechninae): mesosoma dorsal view **87** *Yrka* sp. (Pteromalidae, Colotrechninae, Amerostenini): antenna **88** *Divna hirsuta* Bouček (Pteromalidae, Colotrechninae, Divnini): mesosoma dorsal view **89** *Bugacia* sp. (Pteromalidae, Colotrechninae, Trigonoderopsini) **89** mesosoma dorsal view **90** *Erixestus* sp. (Pteromalidae: Erixestinae): antenna.

Discussion. Distinction of Miscogastrinae from Pteromalinae is best done by tribe, using either the distinctive petiole of Sphegigastrini or the distinctive clypeus of Diconocarini or Miscogastrini. We propose keeping these tribes together as Miscogastrinae, because they form a stable clade in molecular analyses (Cruaud et al., submitted), and because Sphegigastrini also can have an asymmetrical clypeus as in Miscogastrini.

Diconocarini Rasplus, Tselikh & Burks, new tribe

<https://zoobank.org/FFB225F9-1C7F-4735-8B26-CE95F81316DC>

Type genus. *Diconocara* Dzhanokmen, 1986.

Diagnosis. Clypeal margin concave, symmetrical (Fig. 92). Mandibles enlarged. Petiole small but subquadrate, without anterolateral carina (Fig. 93), ventrally narrowly connected and without a flange.

Discussion. *Diconocara* was described as an enigmatic member of Pteromalinae from the Russian Far East (Dzhanokmen 1986). Its position was unclear based on morphology (Heraty et al., 2013), although next-generation molecular data indicate that it is the sister group of all other Miscogastrinae (Cruaud et al., submitted). It does not have any obvious near relatives within Pteromalidae but also bears no resemblance to any other taxa outside Pteromalidae.

Miscogastrini

Diagnosis. Clypeal margin asymmetrical, with 2 or 3 teeth (Fig. 94). Mandibles not enlarged. Petiole variable in length but usually elongate, without the anterolateral carina of Sphegigastrini but often with a small lateral process that does not extend anteriorly (Fig. 95), ventrally either with a membranous gap medially or fused but without a flange.

Discussion. Miscogastrini comprise some of the most easily recognizable miscogastrines, large-bodied and usually with an expanded fore wing stigma.

Sphegigastrini

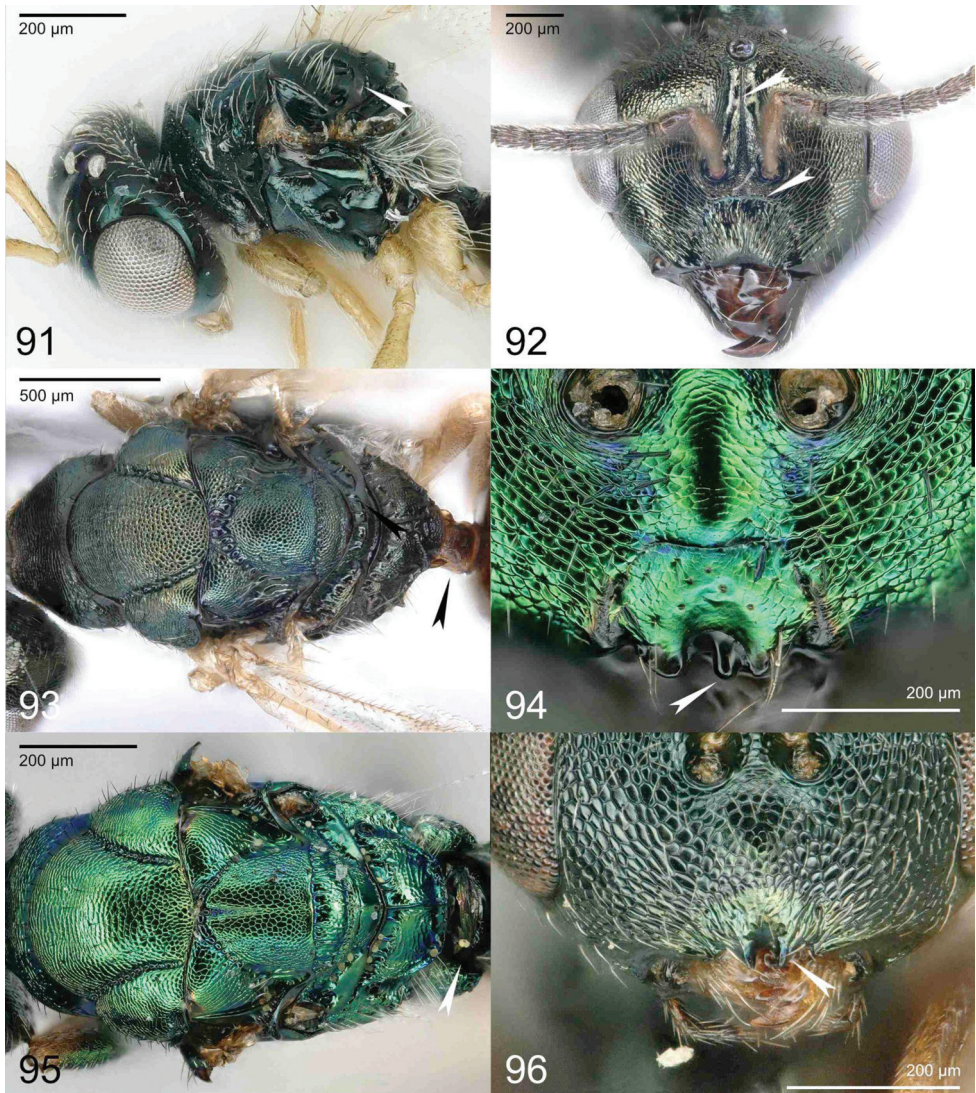
Sphegigastrides Thomson, 1876. Type genus: *Sphegigaster* Spinola, 1811.

Diagnosis. Clypeal margin symmetrical or asymmetrical, with 2 or 3 denticles or uniformly convex (Fig. 96). Mandibles not enlarged. Petiole usually elongate (exception: *Tricyclomischus* Graham), with anterolateral flange that extends anteriorly to flank petiolar insertion (Fig. 97), ventrally closed by the continuation of this flange.

Discussion. The current concept of Sphegigastrini agrees with that presented by Heydon (1988). Specimens of *Bairamlia fuscipes* Waterston new placement were examined morphologically in the course of this study, and were found to belong unambiguously to Sphegigastrini based on the anterolateral petiolar carina. Other genera that we place in Sphegigastrini, based on molecules and/or morphology, are listed in Appendix I.

Ormocerinae

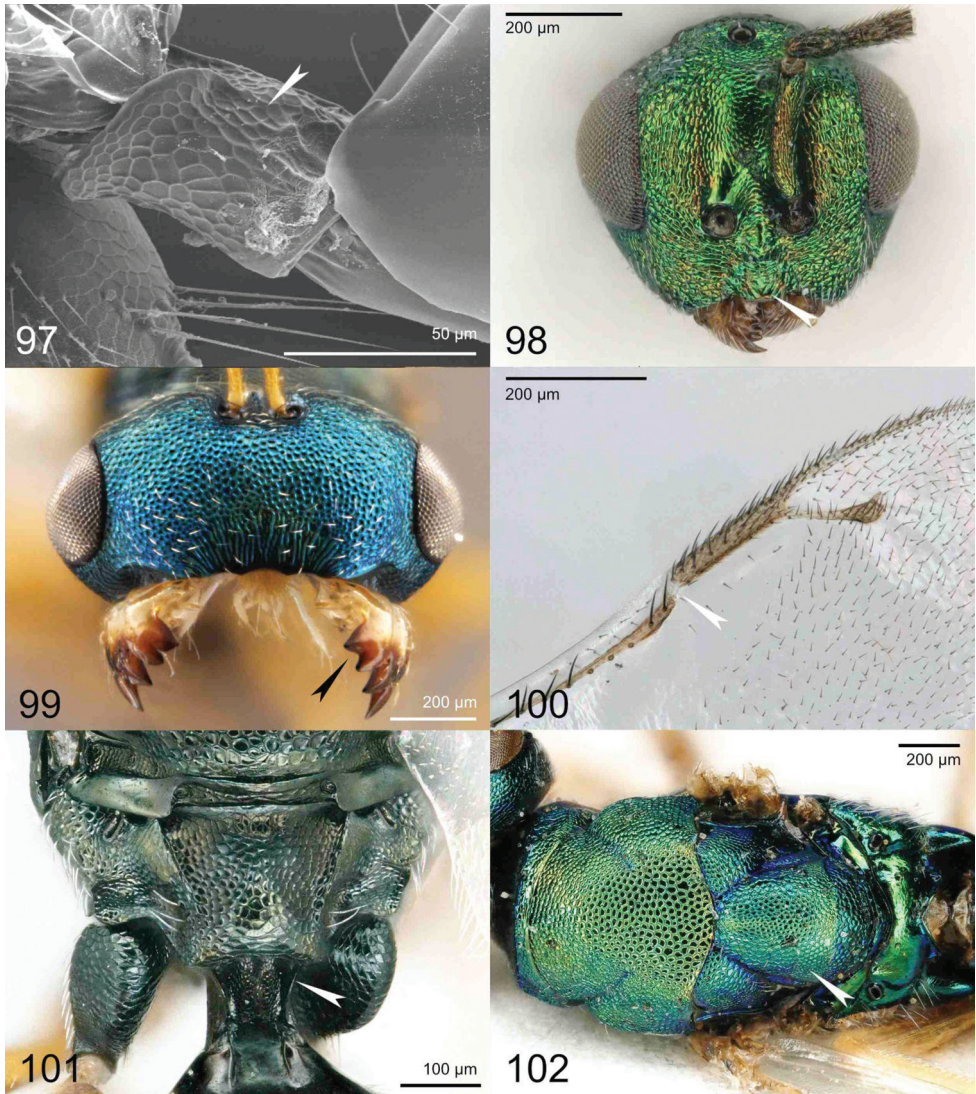
Ormoceridae Walker, 1833. Type genus: *Ormocerus* Walker, 1834. Treated as Ormocerinae by Bouček (1988).



Figures 91–96. **91** *Erixestus winnemana* Crawford (Pteromalidae, Erixestinae): mesosoma lateral view **92, 93** *Diconocara petiolata* Dzhankomen (Pteromalidae, Miscogastrinae, Diconocarini) **92** head frontal view **93** mesosoma dorsal view **94, 95** *Thektogaster aberlenci* Delvare (Pteromalidae, Miscogastrinae, Miscogastrini) **94** clypeus **95** mesosoma dorsal view **96** *Sphegigaster obliqua* Graham (Pteromalidae, Miscogastrinae, Sphegigastrini): lower face frontal view.

Diagnosis. Antenna with 12 flagellomeres. Clypeal margin symmetrical, truncate or uniformly slightly convex (Fig. 98). Mandibles not enlarged. Scapula not anteriorly exposed by pronotum. Notauli complete. Axilla not strongly advanced. Axillula not enlarged. Propodeum without plicae. Petiole transverse, without anterolateral carina.

Discussion. The previous concept of Ormocerinae contained three additional tribes that are now recognized as separate groups in diverse lineages: Melanosomellidae,



Figures 97–102. **97** *Halticoptera* sp. (Sphegigastrini): petiole **98** *Ormocerus latus* Walker (Pteromalidae, Ormocerinae): head frontal view **99** *Acroclisoides sinicus* (Huang & Liao) (Pteromalidae, Pachyneurinae): head frontal and mandibles **100, 101** *Pachycrepoides* sp. (Pachyneurinae) **100** venation **101** propodeum and petiole dorsal view **102** *Chlorocyttus scandolensis* Rasplus (Pteromalidae, Pteromalinae): mesosoma dorsal view.

Systasidae, and the *incertae sedis* tribe Keryini (Bouček 1988; Gauthier et al. 2000). While there was some morphological resemblance between these groups, especially in the position of the toruli and in general gestalt, it became clear that they differed in many ways morphologically, as described in their given sections. Molecular data have suggested that the differences between these groups outweigh their similarities, and indeed Melanosomellidae is morphologically (see discussion of Melanosomellidae in its section above) and molecularly more similar to other members of the Gall Clade

(including Cynipencyrtidae, Epichrysomallidae, Ormyridae, and Tanaostigmatidae) than to other former Ormocerinae. Additionally, *Ormocerus* Walker is much more similar to Pteromalinae than to the aforementioned tribes. This resemblance is strongest with relatively generalized taxa such as *Nodisoplata* Graham new placement that is transferred here from Miscogastrini. The features comprising this resemblance are largely those of gestalt, including enlarged but flat axillula and the nearly equal lengths of fore wing marginal and stigmal veins. The other former members of Ormocerinae, Systasidae and Keryini, are more enigmatic in placement, but differ from the new concept of Ormocerini in features covered in their sections.

Cecidoxenus Ashmead new placement is transferred here from its former position in what is now Melanosomellidae, because of its strong morphological resemblance to *Ormocerus* although with a slightly longer marginal vein. Additionally, *Blascoa* Askew new placement and *Monazosa* Dzhanokmen new placement are transferred here based on morphology.

Ormocerinae strongly resemble some genera of Pteromalini (Pteromalinae) that are retained with some doubt in their current classification because they have not been analyzed molecularly, such as *Fijita* Bouček and *Huberina* Bouček. They differ from Ormocerinae as characterized here by either having features that are conspicuously different from those of ormocerines, such as a median clypeal tooth or pair of teeth, a propodeum with plicae, or an elongate petiole. Other Pteromalinae with complete notauli are fig associates (Otitesellini) that have very different fore wing venation from Ormocerinae.

Pachyneurinae new status

Pachyneurini Ashmead, 1904. Type genus: *Pachyneuron* Walker, 1833.

Austroterobiinae Bouček, 1988 new synonymy. Type genus: *Austroterobia* Girault, 1938.

Diagnosis. Antenna with 12 flagellomeres. Mandibles falcate (Fig. 99). Scapula not anteriorly exposed by pronotum. Axilla not strongly advanced. Axillula not enlarged. Fore wing marginal vein abruptly thickened at parastigmal break relative to submarginal vein thickness (Fig. 100). Propodeum with or without plicae. Petiole (when distinct) anteroventrally either braced by a flange extending from the 1st gastral sternum that reaches anteriorly under the petiolar attachment, e.g. *Pachycrepoides* Ashmead (Fig. 101), or with a more or less developed lateral tooth-like process that extends perpendicular with the longitudinal axis of the petiole, e.g. *Pachyneuron* Walker.

Discussion. Austroterobiinae new syn. was described to contain morphologically divergent parasitoids of margarodid scales (Hemiptera). However, during this study it was observed that they have a recessed subforaminal bridge as in Pteromalinae and Pachyneurinae. Next generation molecular data (Cruaud et al., submitted) place austroterobiines as a derived group inside Pachyneurinae. Although *Austroterobia* Bouček and *Teasienna* Heydon are morphologically divergent from other Pachyneurinae in having complete notauli, this can be attributed to the switch to Margarodidae as hosts. *Austroterobia* and *Teasienna* agree with other Pachyneurinae in having falcate mandibles.

bles. Given the derived position of these genera within Pachyneurinae, we see no value in preserving the group as a tribe. Other genera transferred to Pachyneurinae, based on molecules and/or morphology, are listed in Appendix 1.

Pteromalinae

Diagnosis. Antennal nearly always with 12 flagellomeres (exceptions: some *Otitesellini*, *Amphidocius* Dzhankmen, possibly *Termolampa*). Mandibles usually not falcate (exceptions include some *Apsilocera* Bouček and *Kaleva* Graham). Scapula not anteriorly exposed by pronotum. Notauli usually incomplete, but if complete then clypeus with median tooth or teeth, propodeum with plicae, or petiole distinct and not strongly transverse, e.g., *Fijita*. Axilla variable but usually not strongly advanced (exceptions: *Manineura* Bouček). Axillula usually not enlarged (Fig. 102), but if enlarged then not convex. Fore wing with marginal vein usually slender, if distinctly thickened, e.g. *Rhaphitelus* Walker, then mandibles not falcate. Petiole simple or with small anterolateral processes.

Discussion. Pachyneurinae differ from Pteromalinae in having a combination of falcate mandibles and an abruptly thickened marginal vein base immediately apical to the parastigmal break. Ormocerinae resemble some genera of Pteromalini that are retained with some doubt, but which differ from ormocerines in a number of respects discussed above. The few petiolate Pteromalinae differ from Miscogastrinae as follows: from Diconocarini in having small mandibles; from Miscogastrini in the symmetric clypeus; and from Sphegigastrini in the petiole structure, such as the lack of the characteristic anterolateral petiolar carina.

Otitesellini new status

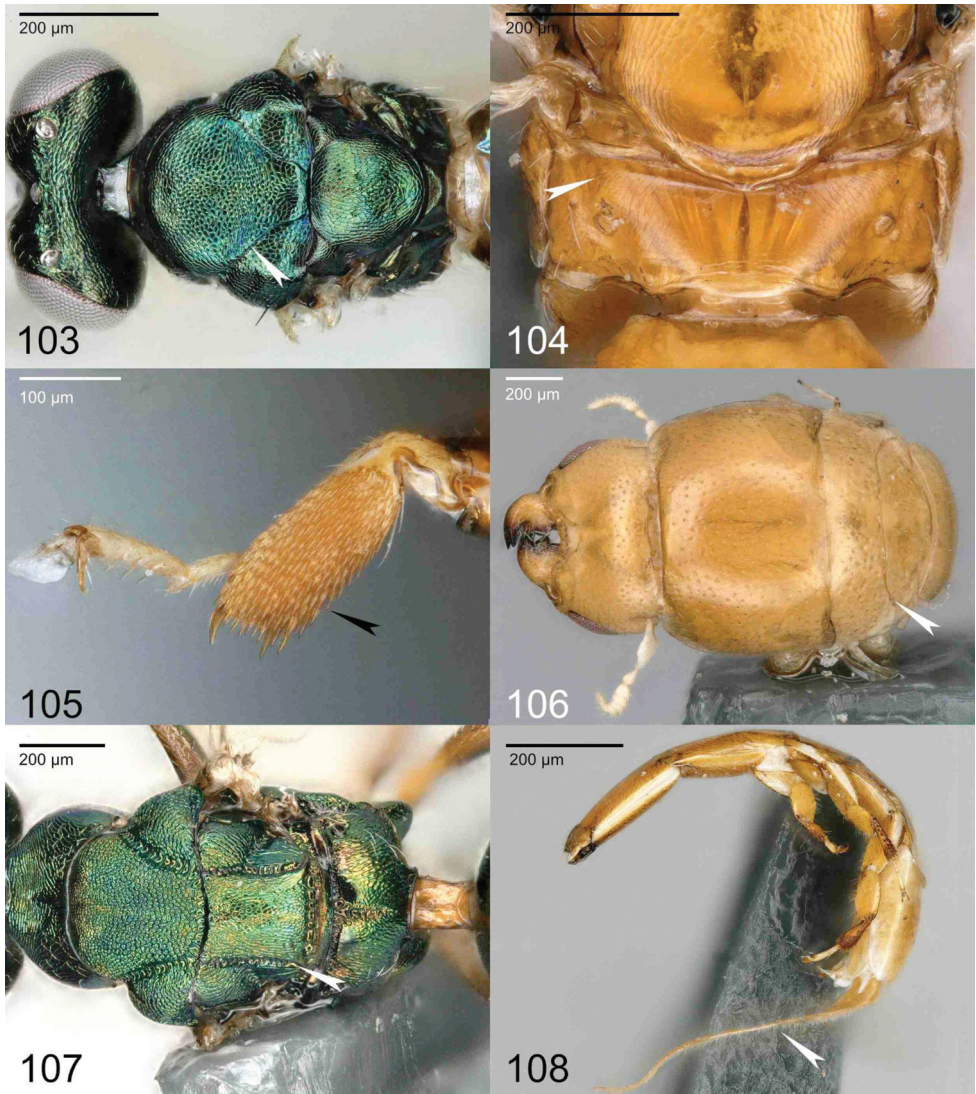
Otitesellini Joseph, 1964. Type genus: *Otitesella* Westwood, 1883.

Sycoryctini Wiebes, 1966 new synonymy. Type genus: *Sycoryctes* Mayr, 1885.

Sycoecini Hill, 1967 new synonymy. Type genus: *Sycoecus* Waterston, 1914.

Diagnosis. Antenna with 10 flagellomeres (*Diaziella* Grandi, *Marginalia* Priyadarshan, *Robertsia* Bouček, *Seres* in part, *Sycoecus*), 11 flagellomeres (*Apocrypta* Coquerel, *Arachonia* Joseph, *Seres* in part, *Otitesella*, *Walkerella* Dalla Torre) or 12 flagellomeres (other genera). Notauli mostly complete (Fig. 103) (absent in *Seres*). Propodeal spiracle usually separated from the anterior propodeal margin by about their own length, or more (except *Marginalia*, some *Walkerella* and *Robertsia*) (Fig. 104). Males usually apterous (except in most members of previous Sycoecinae, some *Watshamiella* Wiebes, and *Sycoryctes* Mayr).

Discussion. This tribe of Pteromalinae contains the previously recognized subfamilies Otitesellinae, Sycoecinae new syn. and Sycoryctinae new syn., all fig associates occurring in the Old World (about 30 genera). It does not contain all the fig associates in Pteromalidae, since Sycophaginae is a separate subfamily of fig associates,



Figures 103–108. **103** *Apocrypta caudata* (Girault) (Pteromalidae, Otitesellini): mesosoma dorsal view **104** *Philotrypesis caricae* L. (Otitesellini): propodeum **105** *Seres wardi* van Noort (Otitesellini): fore tibia **106** *Grandiana* sp. (Otitesellini): male dorsal view **107** *Pseudidarnes minerva* Girault (Pteromalidae, Sycophaginae): metasoma dorsal view **108** *Sycophaga* sp. (Pteromalidae, Sycophaginae): male lateral view.

Podivna Bouček is classified in Colotrechninae, and some New World genera (*Critogaster* Mayr, *Aepocerus* Mayr, *Heterandrium* Mayr, and similar genera) belong to another group of Pteromalinae. Otitesellini possess an amazing morphological disparity. Some genera that enter the fig through the ostiole have a flattened head and smooth cuticle, as well as adaptations to crawl through the bracts filling the fig aperture (mandible lengthened and covered with multiple small teeth, spurs on fore- and hind

legs, enlarged protibial spur etc.) (Fig. 105). Some others oviposit within flowers from the outside once the fig is enlarged and therefore have elongated valves, or with last two tergites lengthened. Most males are greatly transformed, often apterous and sometimes with enlarged mandibles and scapes that are used for fighting for females (Fig. 106). Other genera that we place in Otitesellini based on molecules and/or morphology are listed in Appendix 1.

Pteromalini

Termolampini Bouček, 1961 new synonymy. Type genus: *Termolampa* Bouček, 1961.

Discussion. The previously recognized tribe Termolampini new syn. is abolished here, because it can only be distinguished from other Pteromalini using features that define the genus, and because it seems to be a derived genus within Pteromalini, instead of the sister group of another tribe or set of tribes in Pteromalinae. To resolve previous confusion, *Boucekina* Szelenyi new placement and *Morodora* Gahan new placement belong here according to their morphological resemblance to other Pteromalini, respectively *Neanica* Erdős and *Perniphora* Ruschka. The complete list of genera of Pteromalini are listed in Appendix I, based on molecules and/or morphology. At present the tribe is not diagnosed, because it is the remainder of Pteromalinae excluding Otitesellini. The vast remaining number of genera in Pteromalini makes it unwieldy, and future analysis will be needed to break it up into useful natural tribes that can be more easily diagnosed.

Sycophaginae new placement

Sycophagoidae Walker, 1875. Type genus: *Sycophaga* Westwood, 1840. Treated as Sycophaginae by Ashmead (1904).

Diagnosis. Antennal variable in flagellomere count. Mandibles not falcate. Scapula anteriorly exposed by narrow pronotum. Axilla not strongly advanced. Axillula enlarged and convex (Fig. 107). Petiole simple, transverse. Males usually apterous (except in a few genera), residing inside figs (Fig. 108).

Discussion. The taxonomic placement of the subfamily Sycophaginae has long been controversial. Sycophaginae were previously classified in Torymidae (Wiebes, 1967) and Agaonidae (Bouček 1988; Heraty et al. 2013) as the family shares at least few features with these families. Different strategies to reduce biases in our phylogenetic inference (Cruaud et al., submitted) stabilized the position of Sycophaginae as sister to all other Pteromalidae. This position is corroborated by several features shared with other members of the family and a few others shared with Colotrechninae (large and convex axillula), the next lineage in the Pteromalidae topology. Sycophaginae and Colotrechninae also share a gall-associated biology, indeed most Sycophaginae are ei-

ther gall-makers or parasitoids of gall-makers within figs. We therefore propose to include Sycophaginae in Pteromalidae new placement.

Trigonoderinae new status

Trigonoderini Bouček, 1964. Type genus: *Trigonoderus* Westwood, 1832.

Diagnosis. Antenna with 12 flagellomeres. Mandibles often large but not falcate (Fig. 109). Scapula anteriorly exposed by narrow pronotum. Axilla hardly advanced. Axillula usually not enlarged, but if so (*Plutothrix* Förster), then it is not convex (Fig. 110). Petiole simple, usually transverse and hardly visible.

Discussion. Trigonoderinae are relatively distinctive pteromalids that differ from most others in the family in their long, large bodies in combination with complete notauli and a well-indicated frenal groove (displaced posteriorly in *Platygerrihus* Thomson). Many Pteromalinae are also large-bodied and can be confused superficially with Trigonoderinae, although they have incomplete notauli.

Nomenclatural changes in other chalcidoid families

Baeomorphidae new status

Baeomorphinae Yoshimoto, 1975. Type genus: *Baeomorpha* Brues, 1937. Synonymized with Rotoitidae Bouček & Noyes, 1987 (and inferred synonymy with Rotoitinae) by Gumovsky et al. (2018).

Discussion. The family group name Baeomorphinae was established by Yoshimoto (1975). Rotoitidae was established by Bouček and Noyes (1987). When the two groups were synonymized by Gumovsky et al. (2018), they invoked article 35.5 of the ICZN to conserve the family name Rotoitidae. However, as Baeomorphinae cannot be recognized as a subfamily independent of a Rotoitinae, the family name must be treated with priority and Baeomorphidae recognized over Rotoitidae.

Calesidae new status

Calesinae Mercet, 1929. Type genus: *Cales* Howard, 1907.

Diagnosis. Antenna with radicle 2–4 times as long as broad; 3 or 4 flagellomeres, clava fused and longer than preceding flagellomeres; most species with multiporous plate sensilla raised and not attached along length to flagellomeres. Protibial spur short and straight. All legs with 4 tarsomeres. Axilla extending forward as distinct narrow

scapula (Fig. 111). Mesosoma broadly joined to metasoma, with second phragma extending into metasoma. Hind wing with strongly curved marginal vein. Body pale yellowish or yellowish brown in color.

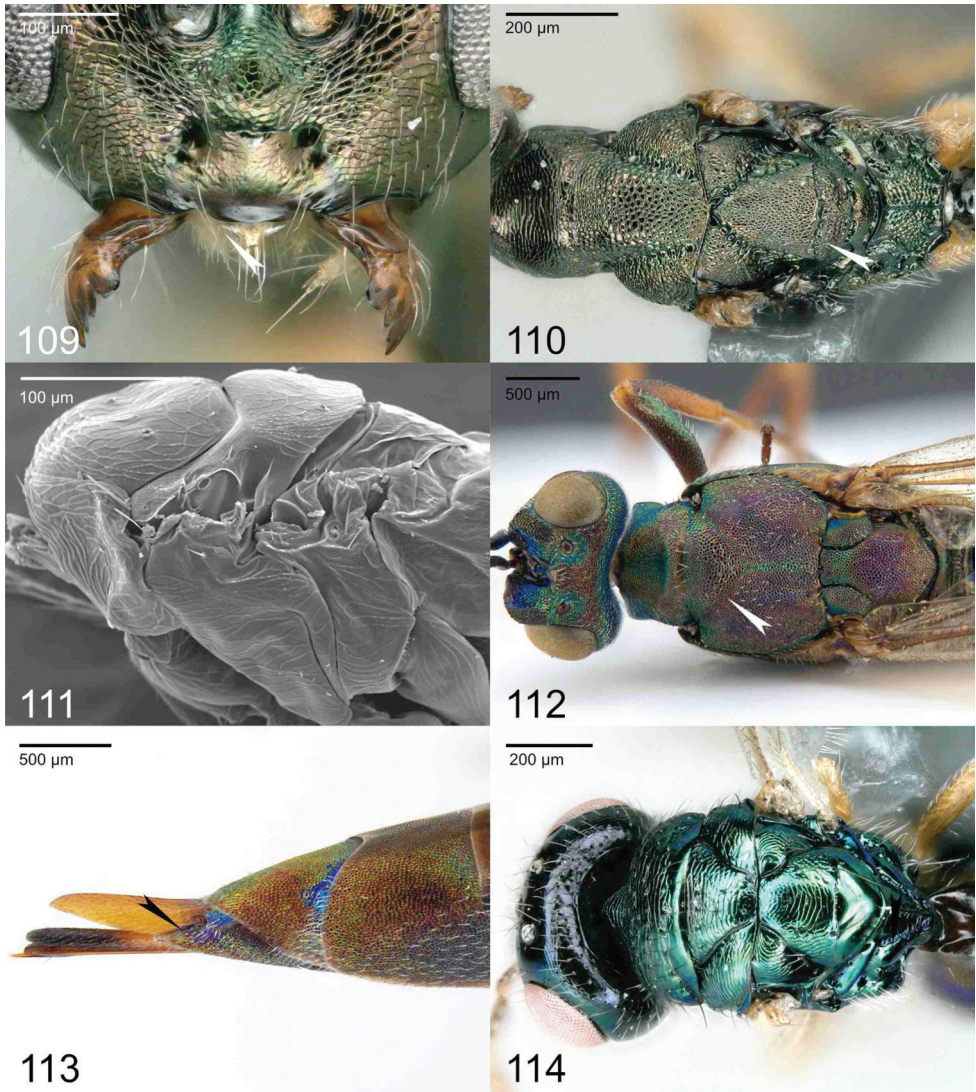
Discussion. Calesinae has been treated as an unusual component of Aphelinidae with no direct affinities to other Aphelinidae (Mottern et al. 2011; Heraty et al. 2013). Next generation molecular data conclusively place the only genus *Cales* Howard as part of a sister group to most other lineages of Chalcidoidea (Cruaud et al., submitted) and not as a member of Aphelinidae. Given that Calesidae is divergent from Aphelinidae both morphologically (Fig. 111) and molecularly, we raise it to family status. Calesidae resemble many Trichogrammatidae in features of the fore wing venation and antennae, but differ from this family by having 4-segmented tarsi. Euderomphalini (Eulophidae) are similar whitefly parasitoids, but these can be distinguished by their narrow petiole with the second phragma restricted to the mesosoma.

Eulophidae

Discussion. The family Eulophidae is not diagnosed here since its limits are not being adjusted, but some taxonomic changes have been carried out as a result of our studies. The Australasian tribe Platytetracammini was described in Entedoninae by Bouček (1988), placed there because of general resemblance to some Euderomphalini. Its placement has been treated as debatable in part because of the relatively large flagellomere count (Bouček 1988; Gauthier, et al. 2000), and it was found to be the sister group of Anselmellini, in what is now Opheliminae, a phylogenetic analysis of 28S D2 ribosomal DNA by Gauthier et al. (2000) and Gumovsky (2002). We suggest that Platytetracammini should be treated as a tribe in Opheliminae new placement, because *Platytetracampe* Girault shares with other ophelimines the placement of fore wing admarginal setae on the ventral side of the marginal vein, and because this transfer renders Entedoninae more definable morphologically, agreeing better with Opheliminae. Although this placement of the admarginal setae is not unique in Eulophidae, we suggest that it may be locally informative for Opheliminae. More definitive placement awaits analysis of next-generation molecular data for *Platytetracampe*, which so far has not been available.

Boucekelimini is a morphologically distinctive group that was treated as an unplaced tribe in Eulophidae by Kim & La Salle (2005). Molecular data for this tribe have not been available, but based again on the placement of the admarginal setae on the ventral side of the marginal vein, and upon the similarity of the antenna of *Boucekelimus* Kim & La Salle (cf. fig. 2) and fore wing stigma shape (Kim and La Salle 2005: figs 11, 12, 19, 20) with that of *Ophelimus* Haliday, we treat Boucekelimini as a tribe within Opheliminae new placement, again awaiting next-generation molecular data for further evaluation of the phylogenetic value of morphological features mentioned here.

Elasmus Westwood was treated in a separate family until molecular data (Gauthier et al. 2000) suggested that it is part of Eulophinae. Elasmmini was therefore reduced to tribe rank within Eulophinae. Rasplus et al. (2020) later found using next-generation



Figures 109–114. **109, 110** *Gastracanthus acutus* (Kamijo) (Pteromalidae, Trigonoderinae) **109** lower face frontal view **110** mesosoma dorsal view **111** *Cales noacki* Howard (Calesidae): mesosoma lateral view **112** *Eusandalum flavipenne* Ruschka: mesosoma dorsal view **113** *Pentacladia elegans* Westwood: Mt8 and Mt9 fused, but delimited by an oblique suture below cercus **114** *Chromeurytoma* sp. (Megastigmidae, Chromeurytominae): head and mesosoma dorsal view.

UCE molecular data that *Sympiesis* Foerster is the sister group of *Elasmus*, rendering recognition of Elasmini problematic versus the now paraphyletic Eulophini, especially since *Sympiesis* is very similar to many other genera of Eulophini morphologically. Given that males of *Elasmus* have branched flagellomeres very much like those of Eulophini, we find the recognition of a separate Elasmini to be an unjustifiable misrepresentation

of the evolutionary timing of the distinctive traits of *Elasmus* relative to the traits that are representative of Eulophini, and therefore Elasmini new syn. is a synonym of Eulophini.

Gyrolasomyiini was described as a separate tribe of Tetrastichinae by Bouček (1988). Molecular data have so far placed *Gyrolasomyia* Girault within Tetrastichini, with instead a *Tetrastichus*-group (Rasplus et al. 2020) being the sister group of remaining Tetrastichinae: the *Aprostocetus*-group including *Gyrolasomyia*. Therefore, recognition of Gyrolasomyiini would necessitate recognition of a separate tribe for the *Aprostocetus*-group or synonymy of Gyrolasomyiini with the oldest available tribe name of the *Aprostocetus*-group. However, this is untenable due to the highly problematic morphological diagnosability of tetrastichine genera and potential tribes. We suggest that both uncertain phylogenetic relationships and the practical difficulties of diagnosing subordinate taxa make recognition of tribes in Tetrastichinae currently inadvisable, and therefore Gyrolasomyiini new syn. is a junior synonym of Tetrastichini.

Eupelmidae

Eusandalinae Fusu, new subfamily

<https://zoobank.org/6A0FAD58-8AD8-45CC-8D4A-604E93E79416>

Type genus. *Eusandalum* Ratzeburg, 1852.

Diagnosis. Antennal flagellum with 9 flagellomeres, clava undivided. Eyes ventrally divergent. Clypeus with truncate apical margin. Labrum subquadrate, exposed. Subforaminal bridge with median area flanked by elongate posterior tentorial attachments; postgenal bridge externally separates the lower tentorial bridge from the hypostomal carina; postgenal groove and postgenal lamina absent. Anterolateral mesoscutal corners projecting shoulder-like on either side of the pronotum (a feature shared with Calosotinae *sensu stricto*). Notauli superficial and convergent, and except for *Archaeopelma*, ending about halfway across mesoscutum (Fig. 112). Axilla approximated (*Archaeopelma* Gibson and *Paraeusandalum* Gibson) or widely separated (*Eusandalum* Ratzeburg, *Licrooides* Gibson and *Pentacladia* Westwood) medially. Axillular groove or carina absent. Frenum absent. Acropleuron expanded and forming the largest surface of the mesopleuron, either comparatively small and not reaching metapleuron and metacoxa (*Archaeopelma*, *Licrooides*) or occupying most of the visible part of the mesopleuron and extending to the metapleuron (the other three genera). All legs with 5 tarsomeres; protibial spur stout and curved; basitarsal comb longitudinal; ventral membranous area anterior to mesocoxal attachment present; mesotibial spur stout except only slightly thickened in *Archaeopelma*. Fore leg with protibial dorsal spicules (except in *Licrooides*). Mesotarsus almost never with row of pegs along both sides, the exception being *Licrooides*: with spine-like setae on both antero- and posteroventral margins (*Archaeopelma*) or a row of pegs on posteroventral margin and a row of spine-like setae along anteroventral margin (remaining three genera). In *Licrooides* there are robust spines on both margins that almost appear as pegs. Metasoma in females with separate Mt8 and Mt9, hence without syntergum (*Eusandalum*) or with Mt8 and Mt9

fused but delimited by a transverse suture between cerci (*Archaeopelma*) or below each cercus (remaining genera; Fig. 113). Sexual dimorphism reduced, limited mainly to primary sexual features and antennal structure.

Discussion. Eusandalinae new subfamily were treated until now as part of Calosotinae, however in next-generation molecular analyses (Cruaud et al., submitted) they were never recovered as monophyletic with the other Calosotinae. Instead, a reduced group of Calosotinae that includes *Balcha* Walker, *Calosota* Curtis and *Tanythorax* Gibson (Calosotinae *sensu stricto*) are sister to *Heydenia* (Heydeniidae) in all final analyses and closer to Eupelminae than to Eusandalinae. Eusandalinae are part of the same large clade containing also the Eupelminae and Calosotinae, but the three Eupelmidae subfamilies never form a monophyletic group since the clade also includes Ditropinotellinae, Heydeniidae and Solenurinae; Eusandalinae are the basal group. Beside the three genera included in these molecular analyses (Cruaud et al., submitted) we also include in Eusandalinae *Archaeopelma* and *Licrooides* based on a UCE analysis with a larger sampling (unpublished data). A possibly biphyletic Calosotinae *sensu lato* was also recognised by Gibson (1989), however with *Licrooides* hypothesized as closer to *Calosota* and allied genera and not to *Eusandalum*, and *Archaeopelma* as the most basal lineage of all Calosotinae. From the morphologically close Calosotinae *sensu stricto*, the Eusandalinae differ mainly in having an undivided clava, convergent notauli, scutellum without axillular groove or carina, mesotarsus almost never with two fully developed rows of pegs and a metasoma with incompletely fused or independent Mt8 and Mt9. In Calosotinae: clava with three clavomeres, notauli present as paramedially parallel lines, axillular groove present and continuing seamlessly with the scuto-scutellar suture and as a result scutellum with a carinated groove extending from base to apex, mesotarsus with a row of pegs on either side, and Mt8 and Mt9 completely fused to form the syntergum. However, all the characteristic features of Eusandalinae are either plesiomorphic or homoplastic. A thorough comparative analysis of all these characters can be found in Gibson (1989).

Khutelchalcididae new placement

Khutelchalcididae Rasnitsyn, Basibuyuk & Quicke, 2004. Type genus: *Khutelchalcis* Rasnitsyn, Basibuyuk & Quicke, 2004.

Discussion. Khutelchalcididae was described as a new family of Chalcidoidea from a compression fossil at an estimated age of around the Jurassic/Cretaceous boundary (Rasnitsyn et al. 2004). Gibson et al. (2007) rejected the placement of Khutelchalcididae in Chalcidoidea on the grounds that the position of the mesothoracic spiracle is not in the location that is apomorphic for Chalcidoidea, but is instead in a position similar to that in Serphitidae. We follow the conclusion from Gibson et al. (2007) here, and officially exclude Khutelchalcididae new placement from Chalcidoidea, to be retained in Apocrita as an *incertae sedis* taxon that is not placed to superfamily.

Megastigmidae

Megastigmidae Thomson, 1876. Type genus: *Megastigmus* Dalman, 1820.

Chromeurytominae Bouček, 1988 new placement. Type genus: *Chromeurytoma* Cameron, 1912.

Keiraninae Bouček, 1988 new placement. Type genus: *Keirana* Bouček, 1988.

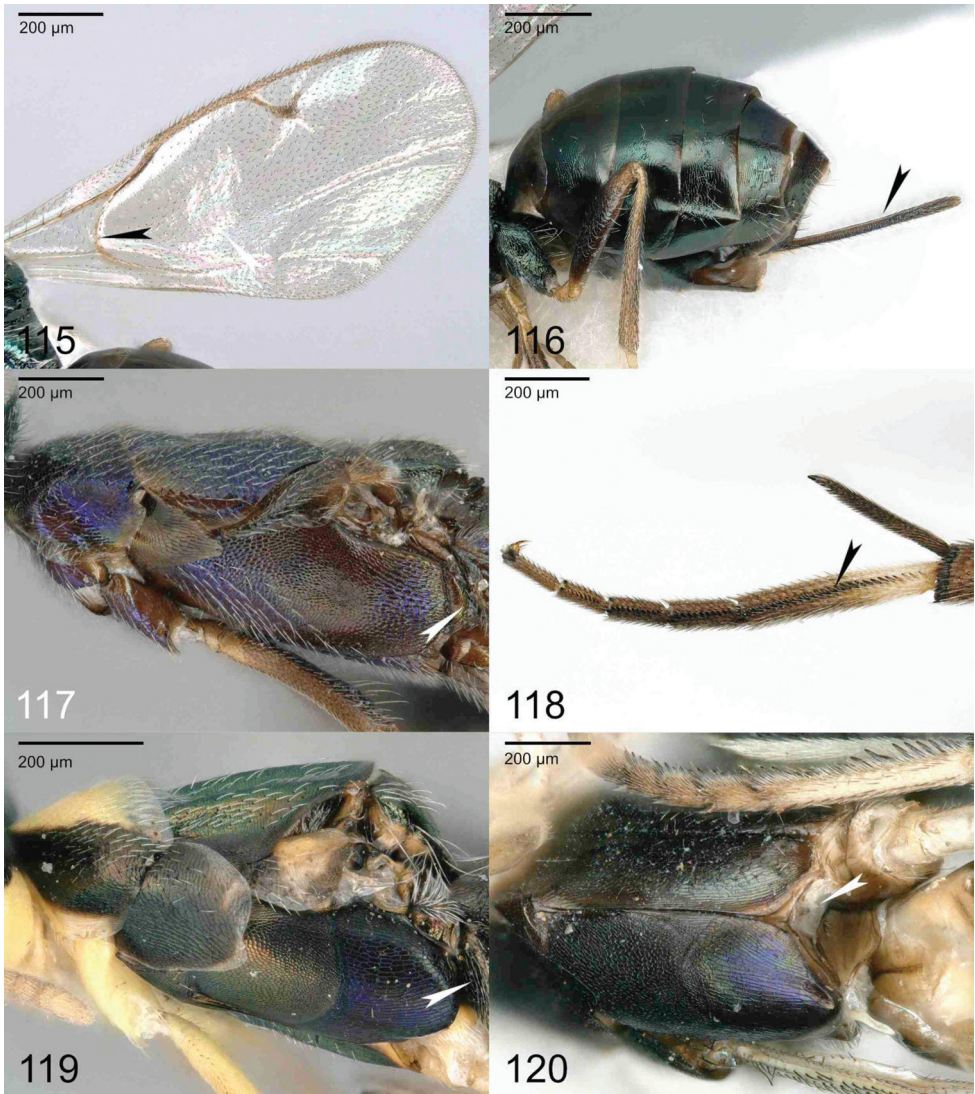
Diagnosis. Antenna with 10 (*Chromeurytoma*) or 12 (Megastigminae and Keiraninae) flagellomeres, including a 4th clavomere. Eyes not or only slightly divergent ventrally. Clypeus bilobed or medially produced, without transverse subapical groove. Labrum flexible and mostly or entirely hidden behind clypeus, divided into several small lobes or subtriangular. Mandibles with 3 teeth. Occipital carina present, at least dorsally in *Chromeurytoma* (Fig. 114), usually high on the head. Pronotum usually elongate, but about as long as mesoscutum or shorter in Chromeurytominae. Notauli complete. Mesoscutellum with frenum defined by a distinct frenal groove, with or without axillular sulcus (Fig. 114). Postmarginal vein longer than stigmal vein (excepted in *Patiyana* Bouček) and frequently longer than marginal vein. Basal fold usually pigmented, in a few genera developed into a basal vein curved outwards (Megastigminae and Keiraninae) (Fig. 115) or rarely basal fold hyaline (Chromeurytominae). All legs with 5 tarsomeres, protibial spur stout and curved; basitarsal comb longitudinal. Gaster, while sometimes rigidly convex, not strongly sclerotized; metasomal apex usually with a separate epipygium in females (in Chromeurytominae and Megastigminae) or with a syntergum that is crossed by a sulcus immediately anterior to the cerci (Keiraninae). Cerci elongate. Ovipositor sheaths long and upcurved in females (Fig. 116).

Discussion. Megastigminae had long been recognized as a monophyletic subfamily of Torymidae and has recently been upgraded to family rank (Janšta et al. 2018). Next-generation molecular analyses (Cruaud et al., submitted) have consistently suggested that two previous subfamilies of Pteromalidae (Chromeurytominae and Keiraninae) were closely related to Megastigmidae. Morphological examination of species of *Chromeurytoma* Cameron and *Keirana* Bouček has confirmed that these clades share several diagnostic features with Megastigmidae and belong to this family. Adding these two entities has increased the morphological disparity within Megastigmidae and has decreased the already low number of apomorphies that define the family. Consequently, Megastigmidae now comprises three subfamilies: Megastigminae including most megastigmid genera (Böhmová et al. 2022), Chromeurytominae new placement (including *Chromeurytoma*, *Asaphoideus* Girault and *Patiyana*) and Keiraninae new placement (with only *Keirana*).

Metapelmatidae revised status

Metapelma Bouček, 1988. Type genus: *Metapelma* Westwood, 1835.

Diagnosis. Antenna with 11 flagellomeres, including 3 clavomeres. Eyes ventrally divergent. Clypeus with truncate apical margin. Labrum subquadrate, exposed. Mandibles



Figures 115–120. **115, 116** *Keirana* sp. (Megastigmidae, Keiraninae) **115** wing **116** metasoma lateral view **117, 118** *Metapelma* sp. (Metapelmatidae) **117** mesosoma lateral view **118** apex of mesotibia and mesotarsus **119, 120** *Neanastatus* sp. (Neanastatidae) **119** mesosoma lateral view **120** mesosoma ventral view.

with a ventral tooth and a dorsal weakly emarginate truncation or with 3 teeth. Subforaminal bridge with postgenal bridge separating secondary posterior tentorial pits from hypostoma; hypostomal carina convergent. Axilla transverse, approximated medially. Mesoscutellum with apex rounded; axillular groove or carina present. Frenum absent. Acropleuron enlarged, convex and pad-like, covering most of mesopleural area but separated from metacoxa by mesepimeron and metapleuron (Fig. 117). All legs with 5 tarsomeres; protibial spur stout and curved; basitarsal comb longitudinal; ventral membranous area anterior to mesocoxal attachment absent; mesotibial spur stout;

mesotarsus with 1 row of pegs anteroventrally (Fig. 118). Metasoma with separate Mt8 and Mt9 in females, without syntergum.

Discussion. Next-generation molecular data (Cruaud et al., submitted) consistently place *Metapelma* Westwood far from its former position in what is now Neanastatidae, instead most frequently as the sister group of Macromesidae + Cleonymidae. There is only minor, and not consistently diagnostic, resemblance between these three groups, and therefore Metapelmatidae revised status is restored from synonymy as a separate family. The difference between Metapelmatidae and Neanastatidae is subtle but present, in that Neanastatidae do not have the mesopleural area separated from the metacoxa by the mesepimeron and metapleuron. *Eopelma* also differs in several respects, including having fewer flagellomeres with an undivided clava, and does not bear any resemblance to *Metapelma*. Eupelmidae differ in ways explained by Gibson (1989, 1995), but notably by having a membranous area anterior to the mesocoxal attachment ventrally. Male Eupelminae additionally do not have an expanded acropleuron and all the associated modifications of the mesosoma and mid legs.

Neanastatidae new status

Neanastatinae Kalina, 1984. Type genus: *Neanastatus* Girault, 1913.

Diagnosis. Antenna with 8, or sometimes apparently 7 flagellomeres in *Neanastatus*, or with 11 in *Lambdobrema* Gibson. Eyes ventrally divergent. Clypeus without transverse subapical groove. Labrum hidden behind clypeus, flexible. Mandibles with 3 teeth. Subforaminal bridge with postgenal bridge separating secondary posterior tentorial pits from hypostoma. Axilla transverse, approximated (*Lambdobrema*) or widely separated (*Neanastatus*) medially. Mesoscutellum with a downwards-projecting hook-like apex; axillular groove or carina present. Frenum apparently absent though the marginal rim of the mesoscutellum may be greatly expanded. Acropleuron enlarged, convex and pad-like; covering mesopleural area (Fig. 119). All legs with 5 tarsomeres; protibial spur stout and curved; basitarsal comb longitudinal; ventral membranous area anterior to mesocoxal attachment absent (Fig. 120); mesotibial spur stout; mesotarsus with 1 row of pegs anteroventrally. Metasoma with syntergum, therefore without epipygium.

Discussion. Neanastatidae, with only *Neanastatus* and *Lambdobrema* remaining, is not related to the formerly included genera *Metapelma* (Metapelmatidae) or *Eopelma* in next-generation molecular analysis (Cruaud et al., submitted). Even then, Neanastatidae is rendered paraphyletic by the *incertae sedis* taxon *Callimomoides* (Louriciinae). Metapelmatidae differ from Neanastatidae in a number of features, including the separate Mt9 in females and the separation of the acropleuron from the mesocoxa by the metapleuron and small mesepimeron in Metapelmatidae. The acropleuron is also separated from the mesocoxa in *Eopelma*, which nevertheless bears the greatest gestalt

resemblance to *Neanastatus* out of all these taxa due to size, coloration, and flagellomere count. Each of these genera differs from Eupelmidae in lacking a membranous area anterior to the mesocoxal attachment ventrally.

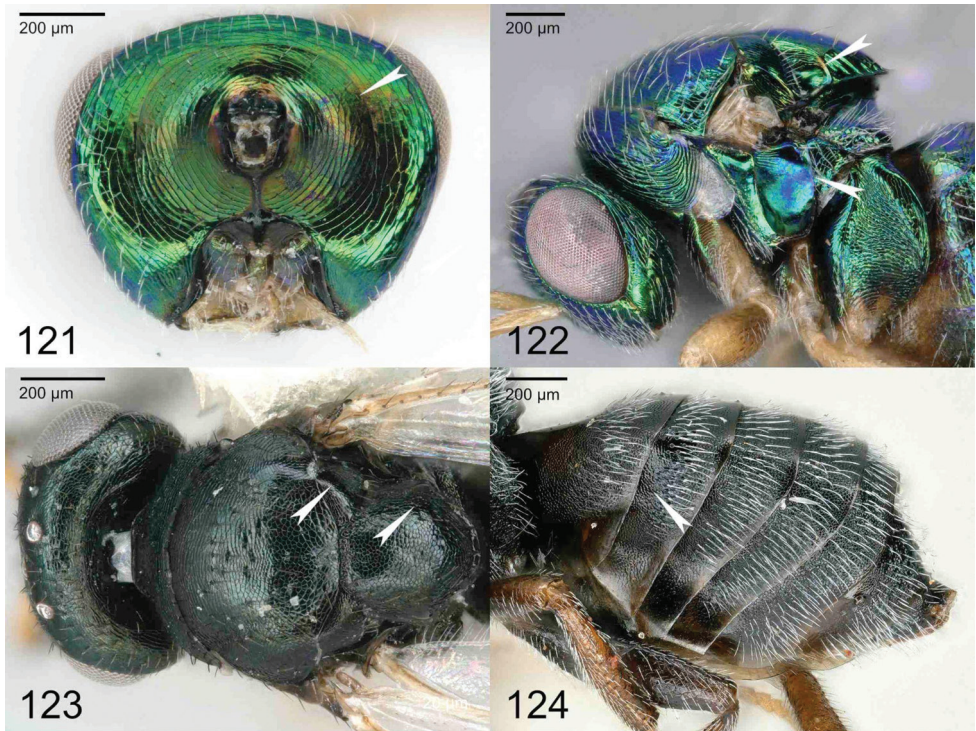
Ormyridae

Ormyridae Foerster, 1856. Type genus: *Ormyrus* Westwood, 1832.

Diagnosis. Antenna with 12 flagellomeres, including a small 4th clavomere. Eyes not ventrally divergent. Clypeus bilobed, without transverse subapical groove. Labrum hidden behind clypeus, flexible, subrectangular with marginal setae in a row. Mandibles with 2 or 3 teeth. Subforaminal bridge with postgenal lobe separating the secondary posterior tentorial pit from the hypostoma and restricting it to the vicinity of the occipital foramen; postgenal bridge present or separated (and therefore lower tentorial bridge reaching or not reaching hypostoma); postgenal lamina usually absent; hypostomal carina usually (but not always) convergent; occipital carina present (Fig. 121). Axilla advanced (Fig. 123). Mesoscutellum with frenum indicated at least laterally, without axillular sulcus. Mesopleural area without an expanded acropleuron; mesepimeron extending over anterior margin of metapleuron (Fig. 122). All legs with 5 tarsomeres; protibial spur stout and curved; basitarsal comb longitudinal. Fore wing stigmal vein not at a right angle with anterior fore wing margin. Metasoma with syntergum and therefore without an epipygium, convex or (more frequently) strongly sclerotized and carapace-like (Fig. 124).

Discussion. *Asparagobius* Mayr has been consistently recovered as the sister group of *Ormyrus* Westwood / *Ormyrus* Bouček with strong support in next-generation molecular analysis (Cruaud et al., submitted). In analysis of morphological characters (van Noort et al., in prep.), we acknowledged the close relationship between *Asparagobius* new placement and Ormyridae. We also propose the inclusion of *Hemadas* Crawford new placement (previously classified in Ormocerinae) in the newly defined Ormyridae.

Ormyridae are most frequently confused with Torymidae because both groups tend to have an arched body and enlarged metacoxa, although torymids have a separate epipygium and usually a long and exerted ovipositor in females whereas that of ormyrids is short. Males of the two groups are usually distinguished using habitus features of genera, and in practice can be easily recognized once the habitus of the two families is learned. Pteromalidae have an axillular sulcus in almost all species, but not in some fig associates that are otherwise highly divergent morphologically and not similar to Ormyridae. Epichrysomallidae have distinctly different fore wing venation from Ormyridae, with a longer stigmal vein that is at approximately a right angle with the anterior fore wing margin, and have a shorter marginal and postmarginal vein. Melanosomellidae lack an occipital carina, and otherwise nearly all species differ in having non-metallic coloration versus the usually metallic Ormyridae (except *Hemadas*).



Figures 121–124. **121, 122** *Ormyrus* sp. (Ormyridae) **121** head dorsal view **122** mesosoma lateral view **123** *Hemadas nubilipennis* (Ashmead) (Ormyridae): mesosoma dorsal view **124** *Asparagobius* sp. (Ormyridae): metasoma lateral view.

Acknowledgements

We thank Gary Gibson, Michael Gates, Christer Hansson, John Huber, Ana Dal Molin, Jason Mottern, John Noyes, Andy Polaszek, Alex Gumovsky, Gérard Delvare, Krissy Dominguez, Robert Kresslein, and Ryan Perry for many helpful comments on the classification. We thank Daniel Alejandro Aquino (Museo de La Plata), Fernando H. A. Farache (Rio Verde), Jeremy Frank (Bishop Museum), and Ryan Perry (UC Santa Barbara) for helpful photographs of type specimens. We thank Nicole Fisher and Juanita Rodriguez Arrieta (ANIC, Canberra) as well as Christine Lambkin, Chris Burwell and Susan Wright (QM, Brisbane) for the loan of multiple Australian specimens. We acknowledge the Queensland government for collecting permits (WITK18248017 - WITK18278817). Grant support was provided in part by NSF DEB-1555808 to J. Heraty, J.B. Woolley and M. Yoder. This work was also partly supported by the ANR projects TRIPTIC (ANR-14-CE18-0002), BIDIME (ANR-19-ECOM-0010) and recurring funding of the INRAE to A. Cruaud and J.Y. Rasplus.

References

- Ashmead WH (1895) On the genus *Pelecinnella*, Westwood, and its position among the Chalcididae. *Proceedings of the Entomological Society of Washington* 3: 230–233.
- Ashmead WH (1899) On the genera of the Cleonymidae. *Proceedings of the Entomological Society of Washington* 4: 200–206.
- Ashmead WH (1904) Classification of the chalcid flies, or the superfamily Chalcidoidea, with descriptions of new species in the Carnegie Museum, collected in South America by Herbert H. Smith. *Memoirs of the Carnegie Museum* 1: i–xi, 225–551. [pls xxxi–xxxix] <https://doi.org/10.5962/bhl.title.10341>
- Basibuyuk H, Quicke DL (1994) Evolution of antennal cleaner structure in the Hymenoptera (Insecta). *Norwegian Journal of Agricultural Sciences Supplement No 16*: 199–206.
- Böhmová J, Rasplus J-Y, Taylor GS, Janšta P (2022) Description of two new Australian genera of Megastigmidae (Hymenoptera, Chalcidoidea) with notes on the biology of the genus *Bortesia*. *Journal of Hymenoptera Research* 90: 75–99. <https://doi.org/10.3897/jhr.90.82582>
- Bouček Z (1988) Australasian Chalcidoidea (Hymenoptera). A biosystematic revision of genera of fourteen families, with a reclassification of species. CAB International, Wallingford, UK, 832 pp.
- Burks RA (2012) Formation of family group names using the stem *-gaster*, with special reference to names based on *Miscogaster* and *Sphegigaster* (Hymenoptera: Chalcidoidea: Pteromalidae). *Zootaxa* 3389: 61–64. <https://doi.org/10.11646/zootaxa.3389.1.7>
- Burks RA, Heraty JM (2015) Subforaminal bridges in Hymenoptera (Insecta), with a focus on Chalcidoidea. *Arthropod Structure & Development* 44: 173–194. <https://doi.org/10.1016/j.asd.2014.12.003>
- Burks RA, Krogmann L, Heraty JM (2018) Simultaneous discovery and taxonomic placement of new extant and fossil genera of Herbertiinae (Hymenoptera: Chalcidoidea: Pteromalidae). *Insect Systematics and Diversity* 2(5): 1–8. <https://doi.org/10.1093/isd/ixy012>
- Campbell B, Heraty J, Rasplus J-Y, Chan K, Steffen-Campbell J, Babcock C (2000) Molecular systematics of the Chalcidoidea using 28S-D2 rDNA. In: Austin AD, Downton M (Eds) *Hymenoptera: Evolution, Biodiversity and Biological Control*. CSIRO Publishing, Melbourne, Australia, 59–73. <https://doi.org/10.1071/9780643090088>
- Cruaud A, Rasplus J-Y, Zhang J, Burks R, Delvare G, Fusu L, Gibson GAP, Gumovsky A, Hanson P, Huber JT, Janšta P, Mitroiu M-D, Noyes JS, van Noort S, Baker A, Böhmová J, Baur H, Blaimer BB, Brady SG, Bubeníková K, Chartois M, Copeland RS, Dale-Skey Papilloud N, Dal Molin A, Darling C, Dominguez C, Fisher N, Gates MW, Gebiola M, Guerrieri E, Haas M, Hansson C, Heydon S, Kresslein RL, Krogmann L, Moriarty Lemmon E, Mottern J, Murray E, Nidelet S, Nieves Aldrey JL, Perry R, Peters RS, Pinto JD, Polaszek A, Sauné L, Schmidt S, Torrén J, Triapitsyn S, Tselikh EV, Ubaidillah R, Yoder M, Lemmon A, Woolley JB, Heraty JM (2022) The Chalcidoidea bush of life—a massive radiation blurred by mutational saturation. Submitted. *bioRxiv*, 1–74. <https://doi.org/10.1101/2022.09.11.507458>

- Darling DC (1988) Comparative morphology of the labrum in Hymenoptera: the digitate labrum of Perilampidae and Eucharitidae (Chalcidoidea). *Canadian Journal of Zoology* 66: 2811–2835. <https://doi.org/10.1139/z88-409>
- Delvare G, LaSalle J (2000) *Trisecodes* gen. n., (Hymenoptera: Eulophidae: Entedoninae), the first eulophid with three tarsal segments. *Journal of Hymenoptera Research* 9(2): 305–312.
- Desjardins CA, Regier JC, Mitter C (2007) Phylogeny of pteromalid parasitic wasps (Hymenoptera: Pteromalidae): initial evidence from four protein-coding nuclear genes. *Molecular Phylogenetics and Evolution* 45(2): 454–469. <https://doi.org/10.1016/j.ympev.2007.08.004>
- Desjardins CA (2004) Systematics of Diparinae (Hymenoptera: Pteromalidae), and their position within the broader context of pteromalid phylogeny. PhD Thesis. University of Maryland, College Park, 1–259.
- Desjardins CA (2007) Phylogenetics and classification of the world genera of Diparinae (Hymenoptera: Pteromalidae). *Zootaxa* 1647: 1–88. <https://doi.org/10.11646/zootaxa.1647.1.1>
- Dzhanokmen KA (1986) New genera and species of pteromalids (Hymenoptera, Pteromalidae) from the Soviet Far East. In: Ler PA, Belokobylskii AS, Storozheva NA (Eds) *Pereponchatokrikiye Vostochnoy Sibiri i Dalinego Vostoka*, 49–54.
- Gauthier N, LaSalle J, Quicke DLJ, Godfray HCJ (2000) Phylogeny of Eulophidae (Hymenoptera: Chalcidoidea), with a reclassification of Eulophinae and the recognition that Elasmidae are derived eulophids. *Systematic Entomology* 25: 521–539. <https://doi.org/10.1046/j.1365-3113.2000.00134.x>
- Gibson GAP (1989) Phylogeny and classification of Eupelmidae, with a revision of the world genera of Calosotinae and Metapelmatinae (Hymenoptera: Chalcidoidea). *Memoirs of the Entomological Society of Canada* 149: 1–121. <https://doi.org/10.4039/entm121149fv>
- Gibson GAP (1995) Parasitic wasps of the subfamily Eupelminae: classification and revision of world genera (Hymenoptera: Chalcidoidea: Eupelmidae). *Memoirs on Entomology, International* 5: [v +] 421.
- Gibson GAP (1997) Annotated Keys to the Genera of Nearctic Chalcidoidea (Hymenoptera) Chapter 2. Morphology and Terminology. In: Gibson GAP, Huber JT, Woolley JB (Eds) *National Research Council of Canada, NRC Research Press, Ottawa Canada*, 16–44.
- Gibson GAP (2003) Phylogenetics and classification of Cleonyminae (Hymenoptera: Chalcidoidea: Pteromalidae). *Memoirs on Entomology, International* 16: [v +] 339.
- Gibson GAP, Heraty JM, Woolley JB (1999) Phylogenetics and classification of Chalcidoidea and Mymarommatoidea - a review of current concepts (Hymenoptera, Apocrita). *Zoologica Scripta* 28: 87–124. <https://doi.org/10.1046/j.1463-6409.1999.00016.x>
- Gibson GAP, Read J, Huber JT (2007) Diversity, classification and higher relationships of Mymarommatoidea (Hymenoptera). *Journal of Hymenoptera Research* 16(1): 51–146.
- Graham MWR de V (1969) The Pteromalidae of north-western Europe (Hymenoptera: Chalcidoidea). *Bulletin of the British Museum (Natural History) (Entomology) Supplement* 16: 1–908. <https://doi.org/10.5962/p.258046>
- Grissell EE (1995) Toryminae (Hymenoptera: Chalcidoidea: Torymidae): a redefinition, generic classification and annotated world catalogue of species. *Memoirs on Entomology, International* 2, 474 pp.

- Gumovsky A (2002) Monophyly and preliminary phylogeny of Entedoninae (Hymenoptera, Chalcidoidea, Eulophidae) with notes on related groups: 28S D2 rDNA considerations and morphological support. In: Austin AD, Dowton M (Eds) CSIRO Publishing, Collingwood, Victoria. Parasitic Wasps: Evolution, Systematics, Biodiversity and Biological Control, 193–219.
- Gumovsky A, Perkovsky E, Rasnitsyn A (2018) Laurasian ancestors and “Gondwanan” descendants of Rotoitidae (Hymenoptera: Chalcidoidea): what a review of Late Cretaceous *Baeomorpha* revealed. *Cretaceous Research* 84: 286–322. <https://doi.org/10.1016/j.cretres.2017.10.027>
- Haas M, Burks RA, Krogmann L (2018) A new lineage of Cretaceous jewel wasps (Chalcidoidea: Diversinitidae). *PeerJ* 6(e4633): 30. <https://doi.org/10.7717/peerj.4633>
- Handlirsch A (1925) Systematische übersicht. In: *Handbuch der Entomologie*. Gustav Fischer Verlag, Jena, Germany, 711–825.
- Hennig W (1950) *Grundzuge einer Theorie der phylogenetischen Systematik*. Deutscher zentralverlag, Berlin, 370 pp.
- Hennig W (1966) *Phylogenetic systematics*. Urbana, USA. University of Illinois Press, 263 pp.
- Heraty JM, Burks RA, Cruaud A, Gibson GA, Liljeblad J, Munro JB, Rasplus J-Y, Delvare G, Janšta P, Gumovsky A, Huber JT, Woolley JB, Krogmann L, Heydon SL, Polaszek A, Schmidt S, Darling DC, Gates M, Mottern J, Murray E, Dal Molin A, Triapitsyn SV, Baur H, Pinto JD, Van Noort S, George JN, Yoder MJ (2013) A phylogenetic analysis of the megadiverse Chalcidoidea (Hymenoptera). *Cladistics* 29: 466–542. <https://doi.org/10.1111/cla.12006>
- Heraty JM, Darling DC (1984) Comparative morphology of the planidial larvae of Eucharitidae and Perilampidae (Hymenoptera: Chalcidoidea). *Systematic Entomology* 9: 309–328. <https://doi.org/10.1111/j.1365-3113.1984.tb00056.x>
- Heydon SL (1988) *The Sphegigasterini: A cladistic analysis and generic classification with reviews of selected genera (Hymenoptera: Pteromalidae)*. PhD Thesis. University of Illinois at Urbana-Champaign.
- Heydon SL, Hanson PE (2005) A first review of the Coelocybinae of the New World (Hymenoptera: Pteromalidae). *Acta Societatis Zoologicae Bohemoslovenicae* 69(1–2): 147–166.
- Janšta P (2014) *Phylogeny of parasitic wasps of Torymidae (Hymenoptera: Chalcidoidea) and evolution of their life-strategies*. PhD Thesis. Charles University in Prague.
- Janšta P, Cruaud A, Delvare G, Genson G, Heraty J, Křížková B, Rasplus J-Y (2018) Torymidae (Hymenoptera, Chalcidoidea) revised: molecular phylogeny, circumscription and reclassification of the family with discussion of its biogeography and evolution of life-history traits. *Cladistics* 34: 627–651. <https://doi.org/10.1111/cla.12228>
- Kim I-K, La Salle J (2005) *Boucekelimini trib. nov.*, with genera *Boucekelimus* gen. nov. and *Tatiana* gen. nov. (Hymenoptera: Eulophidae) from Western Australia. *Acta Societatis Zoologicae Bohemicae* 69: 185–192.
- Krogmann L, Vilhelmsen L (2006) Phylogenetic implications of the mesosomal skeleton in Chalcidoidea (Hymenoptera, Apocrita)—tree searches in a jungle of homoplasy. *Invertebrate Systematics* 20: 615–674. <https://doi.org/10.1071/IS06012>
- Miko I, Vilhelmsen L, Johnson NF, Masner L, Penzes Z (2007) Skeletomusculature of Scelionidae (Hymenoptera: Platygastroidea): head and mesosoma. *Zootaxa* 1571: 1–78. <https://doi.org/10.11646/zootaxa.1571.1.1>

- Mitroiu M-D (2016) Review of world genera of Ceinae, with the description of two new Palearctic species of *Spalangioelta* Masi (Hymenoptera, Chalcidoidea, Pteromalidae). *European Journal of Taxonomy* 251: 1–15. <https://doi.org/10.5852/ejt.2016.251>
- Mitroiu M-D (2017) Revision of world Austroterobiinae and Parasaphodinae (Hymenoptera: Chalcidoidea: Pteromalidae), parasitoids of giant scales (Hemiptera: Coccoidea: Monophlebidae). *Zootaxa* 4301: 1–63. <https://doi.org/10.11646/zootaxa.4301.1.1>
- Mottern JL, Heraty JM, Hartop E (2011) *Cales* (Hymenoptera: Chalcidoidea): morphology of an enigmatic taxon with a review of species. *Systematic Entomology* 36(2): 267–284. <https://doi.org/10.1111/j.1365-3113.2010.00557.x>
- Munro JB, Heraty JM, Burks RA, Hawks D, Mottern J, Cruaud A, Rasplus J-Y, Jansta P (2011) A molecular phylogeny of the Chalcidoidea (Hymenoptera). *PLoS ONE* 6: e27023. <https://doi.org/10.1371/journal.pone.0027023>
- Narendran TC (2001) A new record of the genus *Erotolepsiella* Girault (Hymenoptera: Pteromalidae) from the Oriental region with description of a new species from India. *Zoos' Print Journal* 16(2): 418–420. <https://doi.org/10.11609/JoTT.ZPJ.16.2.418-20>
- Noyes JS (1990) A word on chalcidoid classification. *Chalcid Forum*, 6–7.
- Noyes JS (2019) Universal Chalcidoidea Database. <https://www.nhm.ac.uk/our-science/data/chalcidoids/>
- Peck O, Bouček Z, Hoffer A (1964) Keys to the Chalcidoidea of Czechoslovakia (Insecta: Hymenoptera). *Memoirs of the Entomological Society of Canada* 96: 1–121. <https://doi.org/10.4039/entm9634fv>
- Rasnitsyn A, Quicke D, Basibuyuk H (2004) A basal chalcidoid (Insecta: Hymenoptera) from the earliest Cretaceous or latest Jurassic of Mongolia. *Insect Systematics & Evolution* 35: 123–135. <https://doi.org/10.1163/187631204788912391>
- Rasplus JY, Kerdelhué C, Clainche I, Mondor G (1998) Molecular phylogeny of fig wasps. Agaonidae are not monophyletic. *Comptes Rendus de l'Académie des Sciences, Paris (III) (Sciences de la Vie)* 321(6): 517–527. [https://doi.org/10.1016/S0764-4469\(98\)80784-1](https://doi.org/10.1016/S0764-4469(98)80784-1)
- Rasplus J-Y, Blaimer BB, Brady SG, Burks RA, Delvare G, Fisher N, Gates M, Gauthier N, Gumovsky AV, Hansson C, Heraty JM, Fusu L, Nidelet S, Pereira RAS, Sauné L, Ubaidillah R, Cruaud A (2020) A first phylogenomic hypothesis for Eulophidae (Hymenoptera, Chalcidoidea). *Journal of Natural History* 54: 597–609. <https://doi.org/10.1080/00222933.2020.1762941>
- Vago J-L (2006) Revision of the collections of Chalcidoidea Pteromalidae (Hymenoptera) of the Belgian Royal Institute of Natural Sciences and the university faculty of agronomic sciences of Gembloux, and the discovery of 145 new species for Belgium. *Bulletin de la Société Royale Belge d'Entomologie* 142(1–6): 73–99.
- Van Noort S, Harten A van (2006) The species richness of fig wasps (Hymenoptera: Chalcidoidea: Agaonidae, Pteromalidae) in Yemen. *Fauna of Arabia* 22: 449–472.
- Walker F (1834) *Monographia chalciditum* (continued). *Entomological Magazine* 2: 286–309.
- Wiebes JT (1967) Redescription of Sycophaginae from Ceylon and India, with designation of lectotypes, and a world catalogue of the Otitesellini (Hymenoptera: Chalcidoidea, Torymidae). *Tijdschrift voor entomologie* 110: 399–442.

Zhang J, Heraty JM, Darling DC, Kresslein RL, Baker AJ, Torr ns J, Rasplus J-Y, Lemmon AR, Lemmon EM (2022) Anchored phylogenomics and a revised classification of the planidial larva clade of jewel wasps (Hymenoptera: Chalcidoidea). *Systematic Entomology* 47(2): 329–353. <https://doi.org/10.1111/syen.12533>

Appendix I

Classification of genera in families discussed here

Boucekiidae: *Boucekius* Gibson, *Chalcidiscelis* Ashmead

Calesidae: *Cales* Howard

Ceidae: *Bohpa* Darling, *Cea* Walker, *Spalangiopelta* Masi

Cerocephalidae: *Acercephala* Gahan, *Cerocephala* Westwood, *Choetospilisca* Hedqvist, *Dominocephala*[†] Krogmann, *Gahanisca* Hedqvist, *Gnathophorisca* Hedqvist, *Laesthiola* Bou ek, *Muesebeckisia* Hedqvist, *Neocalosoter* Girault & Dodd, *Neosciatheras* Masi, *Paracerocephala* Hedqvist, *Paralaesthia* Cameron, *Pteropilosa*[†] Bl ser, Krogmann & Peters, *Sciatherellus* Masi, *Tenuicornis*[†] Bl ser, Krogmann & Peters, *Theocolax* Westwood

Chalcedectidae: *Chalcedectus* Walker

Cleonymidae: *Agrilocida* Steffan, *Callocleonymus* Masi, *Cleonymus* Latreille, *Dasycleonymus* Gibson, *Notanisus* Walker, *Zolotarewskyia* Risbec

Coelocybidae: *Acoelocyba* Bou ek, *Ambogaster* Heydon, *Ariasina* Heydon, *Coelocyba* Ashmead, *Coelocyboides* Girault, *Cooloolana* Bou ek, *Cytopella* Bou ek, *Erotolepsiella* Girault, *Eucoelocybomyia* Girault, *Fusiterga* Bou ek, *Lanthanomyia* De Santis, *Lelapsomorpha* Girault, *Liepara* Bou ek, *Nerotolepsia* Girault, *Ormyromorpha* Girault, *Paratomicobia* Girault, *Tomicobomorphella* Girault

Diparidae: *Cerodipara* Desjardins, *Chimaerolelaps* Desjardins, *Conodipara* Hedqvist, *Conophorisca* Hedqvist, *Dipara* Walker, *Diparisca* Hedqvist, *Dozodipara* Desjardins, *Hedqvistina* Ko ak, H seyinoglu & Kemal, *Lelaps* Walker, *Myrmicolelaps* Hedqvist, *Netomocera* Bou ek

Epichrysomallidae: *Acophila* Ishii, *Asycobia* Bou ek, *Camarothorax* Mayr, *Epichrysomalla* Girault, *Eufroggattisca* Ghesqu re, *Herodotia* Girault, *Josephiella* Narendran, *Lachaisea* Rasplus, *Leeuweniella* Ferri re, *Meselatus* Girault, *Neosycophila* Grandi, *Odontofroggattia* Ishii, *Parasycobia* Abdurahiman & Joseph, *Sycobia* Walker, *Sycobiomorphella* Abdurahiman & Joseph, *Sycomacophila* Rasplus, *Sycophilodes* Joseph, *Sycophilomorpha* Joseph & Abdurahiman, *Sycotetra* Bou ek

Eulophidae (altered genera only): **Eulophinae:** **Eulophini:** *Elasmus* Westwood.

Opheliminae: **Boucekelimini:** *Boucekelimus* Kim & La Salle, *Tatiana* Kim & La Salle; **Platytracampini:** *Platytracampe* Girault. **Tetrastichinae:** **Tetrastichini:** *Gyrolasomyia* Girault

Eunotidae: *Butiokeras*[†] Burks & Heraty, *Cavitas* Xiao & Huang, *Cephaleta* Motschulsky, *Epicopterus* Westwood, *Eunotus* Walker, *Mesopeltita* Ghesqu re, *Scutellista* Motschulsky

- Eupelmidae** (altered genera only): **Eusandalinae**: *Archaeopelma* Gibson, *Eusandalum* Ratzeburg, *Licrooides* Gibson, *Paraeusandalum* Gibson, *Pentacladia* Westwood
- Herbertiidae**: *Exolabrum* Burks, *Herbertia* Howard, *Versolabrum*[†] Burks & Krogmann
- Hetreulophidae**: *Hetreulophus* Girault, *Omphalodipara* Girault, *Zeala* Bouček
- Heydeniidae**: *Heydenia* Förster, *Heydeniopsis*[†] Hedqvist
- Idioporidae**: *Idioporus* LaSalle & Polaszek
- Lyciscidae**: **Lyciscinae**: *Agamerion* Haliday, *Amazonisca* Hedqvist, *Chadwickia* Bouček, *Epistenia* Westwood, *Eupelmophotismus* Girault, *Hadroepistenia* Gibson, *Hedqvistia* Gibson, *Lycisca* Spinola, *Marxiana* Girault, *Mesamotura* Girault, *Neboissia* Bouček, *Neoepistenia* Hedqvist, *Nepistenia* Bouček, *Paralycisca* Hedqvist, *Parepistenia* Dodd, *Proglochis* Philippi, *Proshizonotus* Girault, *Protoepistenia* Gibson, *Riekisura* Bouček, *Romanisca* Hedqvist, *Scaphepistenia* Gibson, *Shedoepistenia* Gibson, *Striatacanthus* Gibson, *Thaumasura* Westwood, *Urolycisca* Roman, *Westwoodiana* Girault. **Solenurinae**: *Grooca* Sureshan & Narendran, *Solenura* Westwood
- Macromesidae**: *Macromesus* Walker
- Megastigmidae** (transferred subfamilies only): **Chromeurytominae**: *Asaphoideus* Girault, *Chromeurytoma* Cameron, *Patiyana* Bouček. **Keiraninae**: *Keirana* Bouček
- Melanosomellidae**: *Aditrochus*, Rübsaamen, *Aeschylia*, Girault, *Alloderma*, Ashmead, *Alyxiaphagus*, Riek, *Australicesa*, Koçak, &, Kemal, *Brachyscelidiphaga*, Ashmead, *Encyrtocephalus*, Ashmead, *Epelatus*, Girault, *Espinosa*, Gahan, *Eurytomomma*, Girault, *Hansonita*, Bouček, *Hubena*, Bouček, *Indoclava*, Gupta, Khan, &, Agnihotri, *Krivena*, Bouček, *Lincolna*, Girault, *Lisseurytoma*, Cameron, *Mayrellus*, Crawford, *Megamelanosoma*, Girault, *Nambouria*, Bouček, *Neochalcissia*, Girault, *Neoperilampus*, Girault, &, Dodd, *Perilampella*, Girault, &, Dodd, *Perilampomyia*, Girault, *Plastobelyta*, Kieffer, *Queenslandia*, Koçak, &, Kemal, *Systolomorpha*, Ashmead, *Terobiella*, Ashmead, *Trichilogaster*, Mayr, *Westra*, Bouček, *Wubina*, Bouček, *Xantheurytoma*, Cameron
- Metapelmatidae**: *Metapelma* Westwood
- Moranilidae**: **Moranilinae**: *Amoturella* Girault, *Aphobetus* Howard, *Australeunotus* Girault, *Australurios* Girault, *Eunotomyia* Girault, *Globonila* Bouček, *Hirtonila* Bouček, *Ismaya* Bouček, *Kneva* Bouček, *Mnoonema* Motschulsky, *Moranila* Cameron, *Ophelosia* Riley, *Tomicobiella* Girault, *Tomicobomorpha* Girault.
- Tomocerodinae**: *Tomocerodes* Girault
- Neanastatidae**: *Lambdobregma* Gibson, *Neanastatus* Girault
- Neodiparidae**: **Elatoidinae**: *Elatoides* Nikol'skaya. **Neodiparinae**: *Neodipara* Erdős
- Ooderidae**: *Oodera* Westwood
- Ormyridae**: *Asparagobius* Mayr, *Hemadas* Crawford, *Ormyrulus* Bouček, *Ormyrus* Westwood
- Pelecinellidae**: **Nefoeninae**: *Nefoenus* Bouček. **Pelecinellinae**: *Doddifoenus* Bouček, *Leptofoenus* Smith
- Pireniidae**: **Cecidellinae**: *Cecidellis* Hanson; **Eriaporinae**: *Eunotiscus* Compere, *Promuscidea* Girault. **Euryischiinae**: *Euryischia* Riley, *Euryischomyia* Girault, *Myiocnema* Ashmead. **Pireninae**: *Ecrizotomorpha* Mani, *Kesia* Mitroiu, *Lasallea*

Bouček, *Macroglenes* Westwood, *Papuaglenes* Mitroiu, *Petipirene* Bouček, *Velepirene* Bouček, *Watshamia* Bouček, *Zebe* La Salle. **Tridyminae:** *Calyconotiscus* Narendran & Saleem, *Ecrizotes* Förster, *Epiterobia* Girault, *Gastrancistrus* Westwood, *Melancistrus* Graham, *Oxyglypta* Förster, *Premiscogaster* Girault, *Sirovena* Bouček, *Spathopus* Ashmead, *Spinancistrus* Kamijo

Pteromalidae: **Colotrechninae:** **Amerostenini:** *Amerostenus* Girault, *Errolia* Bouček, *Glorimontana* Bouček, *Yrka* Bouček; **Colotrechnini:** *Baridobius* Heydon, *Bofuria* Hedqvist, *Bomburia* Hedqvist, *Cameronella* Dalla Torre, *Colotrechnus* Thomson, *Dipachystigma* Crawford, *Dvalinia* Hedqvist, *Elachertodomyia* Girault, *Pachyneuronella* Girault, *Podivna* Bouček, *Uriellopteromalus* Girault, *Uzka* Bouček; **Divnini:** *Divna* Bouček; **Trigonoderopsini:** *Bugacia* Erdős, *Trigonoderopsis* Girault. **Erixestinae:** *Erixestus* Crawford. **Miscogastrinae:** **Diconocarini:** *Diconocara* Dzhankmen; **Miscogastrini:** *Collentis* Heydon, *Drailea* Huang, *Glyphognathus* Graham, *Lamprotatus* Westwood, *Miscogaster* Walker, *Neoskeloceras* Kamijo, *Paralamprotatus* Liao, *Seladerma* Walker, *Sphaeripalpus* Förster, *Stictomischus* Thomson, *Telepsogina* Hedqvist, *Thektogaster* Delucchi, *Tumor* Huang, *Xestomnaster* Delucchi; **Sphegigastrini:** *Acroclisis* Förster, *Ammelia* Delucchi, *Andersena* Bouček, *Ardilea* Graham, *Bairamliia* Waterston, *Bubekia* Dalla Torre, *Bubekiana* De Santis, *Callicarolyntia* Heydon, *Callimerismus* Graham, *Ceratetra* Dzhankmen, *Cryptoprymna* Förster, *Cyrtogaster* Walker, *Haliplogeton* De Santis, *Halticoptera* Spinola, *Harrizia* Delucchi, *Kazina* Bouček, *Maorita* Bouček, *Mauleus* Graham, *Merismus* Walker, *Notoglyptus* Masi, *Notoprymna* De Santis, *Novitzkyanus* Bouček, *Paracroclisis* Girault, *Ploskana* Bouček, *Polstonia* Heydon, *Rhincocoelia* Graham, *Schimitschekia* Bouček, *Sorosina* Dzhankmen, *Sphegigaster* Spinola, *Syntomopus* Walker, *Thinodytes* Graham, *Toxeuma* Walker, *Tricyclomischus* Graham, *Trigonogastrella* Girault, *Vespita* Bouček. **Ormocerinae:** *Blascoa* Askew, *Cecidoxenus* Ashmead, *Monazosa* Dzhankmen, *Nodisoplata* Graham, *Ormocerus* Walker. **Pachyneurinae:** *Acroclisoides* Girault & Dodd, *Amblyharma* Huang & Tong, *Austroterobia* Girault, *Canada* Koçak & Kemal, *Coruna* Walker, *Euneura* Walker, *Fusta* Xiao & Ye, *Goidanichium* Bouček, *Golovissima* Dzhankmen, *Inkaka* Girault, *Metastenus* Walker, *Nazgulia* Hedqvist, *Neotoxeumorpha* Narendran, *Oomara* Delucchi, *Oricoruna* Bouček, *Ottaria* Hedqvist, *Pachycrepoideus* Ashmead, *Pachyneuron* Walker, *Parabruchobius* Risbec, *Platecrizotes* Ferrière, *Teasienna* Heydon, *Toxeumorpha* Girault. **Pteromalinae:** **Otitesellini:** *Adiyodiella* Priyadarsanan, *Apocrypta* Coquerel, *Arachonia* Joseph, *Bouceka* Koçak & Kemal, *Comptoniella* Wiebes, *Crossogaster* Mayr, *Diaziella* Grandi, *Dobunabaa* Bouček, *Eujacobsonia* Grandi, *Grandiana* Wiebes, *Grasseiana* Abdurahiman & Joseph, *Guadalia* Wiebes, *Lipothymus* Grandi, *Marginalia* Priyadarsanan, *Micranisa* Walker, *Micrognathophora* Grandi, *Otitesella* Westwood, *Philosycella* Abdurahiman & Joseph, *Philosycus* Wiebes, *Philoverdance* Priyadarsanan, *Philotrypsis* Förster, *Robertisia* Bouček, *Seres* Waterston, *Sycoecus* Waterston, *Sycoryctes* Mayr, *Sycosapter* Saunders, *Walkerella* Westwood, *Watshamiella* Wiebes; **Pteromalini:** *Ablaxia* Delucchi, *Abomalus* Bouček, *Acaenacis* Girault, *Acroclisella* Girault, *Acroclisissa* Girault, *Acroclypa* Bouček, *Acrocormus* Förster, *Aepocerus* Mayr, *Afropsilocera* Bouček, *Aggelma* Delucchi,

Agiommatus Crawford, *Aiemea* Bouček, *Allocricellius* Yang, *Alticornis* Bouček, *Amandia* Graham, *Amblypachus* De Santis, *Amphidocius* Dzhankmen, *Angulifrons* Xiao & Huang, *Anisopteromalus* Ruschka, *Ankaratrella* Risbec, *Anogmoides* Askew, *Anogmus* Förster, *Anorbanus* Bouček, *Apelioma* Delucchi, *Apsilocera* Bouček, *Apycnetron* Bouček, *Arachnopteromalus* Gordh, *Arriva* Bouček, *Arthrolytus* Thomson, *Asoka* Bouček, *Atrichomalus* Graham, *Boharticus* Grissell, *Bonitoa* Bouček, *Boucekina* Szelenyi, *Brachycaudonia* Ashmead, *Bupronotum* Xiao & Huang, *Caenacis* Förster, *Caenocrepis* Thomson, *Calliprymna* Graham, *Callitula* Spinola, *Canberrana* Bouček, *Capellia* Delucchi, *Catolaccus* Thomson, *Cecidolampa* Askew, *Cecidostiba* Thomson, *Cheiopachus* Westwood, *Chlorocyclus* Graham, *Chrysoglyphe* Ashmead, *Coelopisthia* Förster, *Conigastrus* Bouček, *Conomorium* Masi, *Cratomus* Dalman, *Critogaster* Mayr, *Cyclogastrella* Bukovskii, *Cyrtophagoides* Narendran, *Cyrtopyx* Delucchi, *Dasyneurophaga* Hedqvist, *Delisleia* Girault, *Delucchia* Koçak & Kemal, *Dibrachoides* Kurdjumov, *Dibrachys* Förster, *Diglochis* Förster, *Dimachus* Thomson, *Dinarmoides* Masi, *Dinarmolaelaps* Masi, *Dinarmus* Thomson, *Dineuticida* Bouček, *Dinotiscus* Ghesquière, *Dinotoides* Bouček, *Diourbelia* Risbec, *Dirhincus* Thomson, *Doganlaria* Koçak & Kemal, *Dorcatomophaga* Kryger, *Elderia* Hedqvist, *Endomychobius* Ashmead, *Epanogmus* Girault, *Epicatolaccus* Blanchard, *Epipteromalus* Ashmead, *Erdoesina* Graham, *Erythromalus* Graham, *Eulonchetron* Graham, *Eumacepolus* Graham, *Eurydinota* Förster, *Eurydinoteloides* Girault, *Eurydinotomorpha* Girault, *Euteloida* Bouček, *Ezgia* Koçak & Kemal, *Fedelia* Delucchi, *Ficicola* Heydon, *Fijita* Bouček, *Frena* Bouček, *Gbelcia* Bouček, *Genangula* Bouček, *Globimesosoma* Xiao & Hui, *Grissellium* Bouček, *Guancheria* Hedqvist, *Gugolzia* Delucchi & Steffan, *Guinea* Koçak & Kemal, *Guolina* Heydon, *Gyrinophagus* Ruschka, *Habritella* Girault & Dodd, *Habritys* Thomson, *Habromalina* Dzhankmen, *Halomalus* Erdős, *Halticopterella* Girault & Dodd, *Halticopteroides* Girault, *Helocasis* Wallace, *Heterandrium* Mayr, *Heteroprymna* Graham, *Heteroschema* Gahan, *Hillerita* Bouček, *Hlavka* Bouček, *Hobbya* Delucchi, *Holcaeus* Thomson, *Homoporus* Thomson, *Huberina* Bouček, *Hypopteromalus* Ashmead, *Ischyroptyx* Delucchi, *Isocyrptella* Risbec, *Isocyrptus* Walker, *Isoplatoides* Girault, *Jaliscoa* Bouček, *Kaleva* Graham, *Klabonosa* Bouček, *Kratka* Bouček, *Kukua* Bouček, *Kumarella* Sureshan, *Lampoterma* Graham, *Lariophagus* Crawford, *Laticlypa* Bouček, *Lenka* Bouček, *Leodamus* Masi, *Leptomeraporus* Graham, *Licteria* Risbec, *Lomonosoffiella* Girault, *Lonchetron* Graham, *Longinucha* Bouček, *Lyrcus* Walker, *Lysirina* Heydon, *Lyubana* Bouček, *Makaronesa* Graham, *Mazinawa* Bouček, *Megadicylus* Girault, *Merallus* Masi, *Meraporus* Walker, *Merismoclea* De Santis, *Merismomorpha* Girault, *Merisus* Walker, *Mesopolobus* Westwood, *Metacolus* Förster, *Meximalus* Bouček, *Mimencyrtus* De Santis, *Mirekia* Bouček, *Miristhma* Bouček, *Mokrzeckia* Mokrzecki, *Monoksa* Bouček, *Morodora* Gahan, *Muscidifurax* Girault & Sanders, *Nadelaia* Bouček, *Narendrella* Sureshan, *Nasonia* Ashmead, *Neanica* Erdős, *Nedinotus* Bouček, *Neocatolaccus* Ashmead, *Neolyubana* Sureshan, *Neopolycystus* Girault, *Nephelomalus* Graham, *Nikolskayana* Bouček, *Norbanus* Walker, *Nuchata* Bouček, *Oaxa* Bouček, *Obalana* Bouček, *Olchon* Tselikh, *Oniticellobia* Bouček, *Ottawita* Bouček, *Oxyharma* Bouček, *Oxytychus*

Delucchi, *Pandelus* Förster, *Panstenon* Walker, *Paracarotomus* Ashmead, *Paradinarmus* Masi, *Paraiemea* Sureshan & Narendran, *Paroxyharma* Huang & Tong, *Pegopus* Förster, *Peridesmia* Förster, *Perilampidea* Crawford, *Perniphora* Ruschka, *Pestra* Bouček, *Pezilepsis* Delucchi, *Phaenocyttus* Graham, *Platneptis* Bouček, *Platypteromalus* Bouček, *Procallitula* De Santis, *Propicroscytus* Szelenyi, *Propodeia* Bouček, *Pseudanogmus* Dodd & Girault, *Pseudetroxys* Masi, *Pseudocatolaccus* Masi, *Psilocera* Walker, *Psilonotus* Walker, *Psychophagoides* Graham, *Psychophagus* Mayr, *Pterapicus* Dzhankmen, *Pterisemoppa* Girault, *Pteromalus* Swederus, *Pterosemigastra* Girault & Dodd, *Pterosemopsis* Girault, *Ptinocida* Bouček, *Pycnetron* Gahan, *Quercanus* Heydon, *Rakosina* Bouček, *Raspela* Bouček, *Rhaphitelus* Walker, *Rhopalicus* Förster, *Rohatina* Bouček, *Roptrocerus* Ratzeburg, *Sceptrothelys* Graham, *Schizonotus* Ratzeburg, *Sedma* Bouček, *Sigynia* Hedqvist, *Sisyridivora* Gahan, *Spaniopus* Walker, *Sphbegigastrella* Masi, *Sphbegipterosema* Girault, *Sphbegipterosemella* Girault, *Spilomalus* Graham, *Spintherus* Thomson, *Spodophagus* Delvare & Rasplus, *Staurothyreus* Graham, *Stenetra* Masi, *Stenomalina* Ghesquière, *Stenoselma* Delucchi, *Stichocrepis* Förster, *Stinoplus* Thomson, *Strejcekia* Bouček, *Synedrus* Graham, *Systellogaster* Gahan, *Szelenyinus* Bouček, *Tachingousa* Tselikh, *Tanina* Bouček, *Tanzanicesa* Koçak & Kemal, *Termolampa* Bouček, *Thureonella* Gijswijt, *Tomicobia* Ashmead, *Toxeumella* Girault, *Toxeumelloides* Girault, *Trichargyrus* Dzhankmen, *Trichokaleva* Bouček, *Trichomalopsis* Crawford, *Trichomalus* Thomson, *Tricolus* Bouček, *Trimeromicrus* Gahan, *Trinotiscus* Bouček, *Tritneptis* Girault, *Trjapitzinia* Dzhankmen, *Trychnosoma* Graham, *Tsela* Bouček, *Unicypea* Bouček, *Urolepis* Walker, *Usubaia* Kamijo, *Veltrusia* Bouček, *Vrestovia* Bouček, *Xiphydriophagus* Ferrière, *Yancheppia* Bouček, *Yosemitea* Bouček, *Zdenekiana* Huggert. **Sycophaginae**: *Anidarnes* Bouček, *Conidarnes* Farache & Rasplus, *Eukoebelea* Ashmead, *Idarnes* Walker, *Neoekoebelea* Lal, Farooqi & Husain, *Pseudidarnes* Girault, *Sycidiphaga* Liu, Rasplus & Huang, *Sycophaga* Westwood. **Trigonoderinae**: *Erdoesia* Bouček, *Eutelisca* Hedqvist, *Gastracanthus* Westwood, *Janssoniella* Kerrich, *Miscogasteriella* Girault, *Neolelaps* Ashmead, *Ogloblinisca* Hedqvist, *Platygerrius* Thomson, *Plutothrix* Förster, *Trigonoderus* Westwood. **Incertae sedis (unplaced to subfamily)**: *Calolelaps* Timberlake, *Hemitrichus* Thomson, *Ksenoplata* Bouček, *Mesolelaps* Ashmead, *Stictolelaps* Timberlake, *Yusufia* Koçak & Kemal

Spalangiidae: **Erotolepsiinae**: *Balrogia* Hedqvist, *Erotolepsia* Howard, *Eunotopsia* Bouček, *Papuopsia* Bouček. **Spalangiinae**: *Playaspalangia* Yoshimoto, *Spalangia* Latreille

Systasidae: **Systasinae**: *Semiotellus* Westwood, *Systasis* Walker. **Trisecodinae**: *Trisecodes* Delvare & LaSalle

***incertae sedis* taxa in Chalcidoidea not placed to family**

Asaphesinae: *Asaphes* Walker, *Coriotela*[†] Burks & Heraty, *Hyperimerus* Girault

Austrosystasinae: *Austrosystasis* Girault

Ditropinotellinae: *Ditropinotella* Girault

Eopelma Gibson

Enoggerinae: *Ausasaphes* Bouček, *Enoggera* Girault

Keryinae: *Kerya* Bouček

Louriciinae: *Callimomoides* Girault

Micradelinae: *Micradelus* Walker

Neapterolelapinae: *Neapterolelaps* Girault, *Nosodipara* Bouček, *Pseudoceraphron* Dodd

Parasaphodinae: *Parasaphodes* Schulz

Rivasia Askew & Nieves-Aldrey

Storeyinae: *Storeya* Bouček

Genera inquirenda unplaced to family

Elachertoidea Girault, *Eubeckerella* Narendran, *Glyphotoma* Cameron, *Promerisus* Kieffer, *Pyramidophoriella* Hedqvist, *Selimnus* Walker, *Sennia* De Stefani, *Tripteromalus* Kieffer

Encarsia hera Lahey & Andreason (Hymenoptera, Aphelinidae): a charismatic new parasitoid of *Aleurocybotus* Quaintance & Baker (Hemiptera, Aleyrodidae) from Florida

Zachary Lahey¹, Alvin M. Simmons¹, Sharon A. Andreason¹

¹ United States Department of Agriculture, Agricultural Research Service, U.S. Vegetable Laboratory, Charleston, South Carolina 29414, USA

Corresponding authors: Sharon A. Andreason (sharon.andreason@usda.gov), Zachary Lahey (zachary.lahey@usda.gov)

Academic editor: Petr Janšta | Received 9 September 2022 | Accepted 8 November 2022 | Published 20 December 2022

<https://zoobank.org/18EA5CA5-AA6D-4D47-8046-D5CF392B5840>

Citation: Lahey Z, Simmons AM, Andreason SA (2022) *Encarsia hera* Lahey & Andreason (Hymenoptera, Aphelinidae): a charismatic new parasitoid of *Aleurocybotus* Quaintance & Baker (Hemiptera, Aleyrodidae) from Florida. Journal of Hymenoptera Research 94: 89–104. <https://doi.org/10.3897/jhr.94.94677>

Abstract

A new, biparental species of the genus *Encarsia* Förster (Hymenoptera: Aphelinidae), *E. hera* Lahey & Andreason, **sp. nov.**, is characterized based on morphological and molecular data. The parasitoid was reared from the puparia of its host, an undescribed species of the grass-feeding aleyrodine genus *Aleurocybotus* Quaintance & Baker (Hemiptera: Aleyrodidae) collected in Gainesville, Florida. The same whitefly is newly recorded from Charleston, South Carolina, where it is a pest of ornamental Muhly grass [*Muhlenbergia capillaris* (Lam.) Trin. (Poaceae)]. A phylogenetic analysis based on a fragment of 28S ribosomal DNA in 34 *Encarsia* species placed *E. hera*, **sp. nov.**, within the *E. luteola*-group, a result concordant with its morphology. A key to the *Encarsia* species reared from *Aleurocybotus* is provided.

Keywords

DNA, new species, phylogenetics, whitefly

Introduction

Florida is home to the largest number of whitefly (Hemiptera: Aleyrodidae) species in the United States (Hodges and Evans 2005; L. Deeter, pers. comm.). While many of these species have been described, the discovery of new aleyrodid species is not uncommon, nor is the establishment of extralimital, adventive whiteflies [e.g., *Aleurodicus rugioperculatus* Martin; *Asiothrixus antidesmae* (Takahashi); *Singhiella simplex* (Singh)] (Stocks 2013). It has been known for several years that an undescribed species of the genus *Aleurocybotus* Quaintance & Baker exists in Florida (G. Evans, pers. comm.). The undescribed species can be separated from its congeners by a combination of morphological characters found in the immature and adult stage (G. Evans and N. von Ellenrieder, pers. comm.).

Species of *Aleurocybotus* are unusual among whiteflies in that they feed exclusively on grasses (Poaceae) and sedges (Cyperaceae) (Russell 2000). Among four known species, *A. cereus* Martin was described from Belize (Martin 2005). The remaining three described species are recorded from the west and east coasts of the United States (Quaintance 1899; Russell 1964; von Ellenrieder and Bailey 2022), and two of these, *A. graminicolus* (Quaintance) and *A. occiduus* Russell, have been collected in Florida.

Natural enemies associated with *Aleurocybotus* include several species of chalcidoid parasitoid Hymenoptera in four genera: *Encarsia* Förster and *Eretmocerus* Haldeman (Aphelinidae) (Myartseva et al. 2009); *Metaphycus* Mercet (Encyrtidae) (Myartseva and Cancino 2010); and *Euderomphale* Girault (Eulophidae) (LaSalle and Schauff 1994). The latter three genera are infrequently collected from *Aleurocybotus*; for discussions of those species, the reader is referred to the above references.

The genus *Encarsia* contains approximately 450 described species (Kresslein et al. 2020), although conservative estimates of the number of species is 10× that number (Polaszek et al. 2009). The primary hosts of *Encarsia* are whiteflies, although other groups of sternorrhynchous Hemiptera and insect eggs may also be attacked (Polaszek 1991; Evans et al. 1995; Heraty et al. 2008; Polaszek and Luft Albarracin 2011). Several species have been at the center of successful biological control programs, which makes this genus of considerable economic importance (Clausen and Berry 1932; Hart et al. 1978; Sailer et al. 1984; Hoddle et al. 1998). The purpose of this study is to describe a new species of *Encarsia* reared from a pestiferous, undescribed species of *Aleurocybotus* from the southeastern United States, place the *Encarsia* species within the context of the genus based on a phylogenetic analysis of 28S ribosomal DNA, and provide a key to the species of *Encarsia* known to attack *Aleurocybotus*.

Materials and methods

Specimen collection

Immature and adult *Aleurocybotus* were collected in 2022 from infested ornamental Muhly grass [*Muhlenbergia capillaris* (Lam.) Trin. (Poales: Poaceae)] in Gainesville, Florida (Alachua County) and Charleston, South Carolina (Charleston County), USA.

Representative series of unparasitized puparia and other whitefly life stages were collected into 95% ethanol and slide-mounted following the protocol of Martin (2004), except that clearing of specimens took place in an ATL lysis buffer-Proteinase K solution, the first step in a non-destructive DNA extraction protocol that retains the cuticle of the insect for subsequent morphological examination. Parasitoid specimens were reared directly from their host. Parasitized whitefly puparia were excised from portions of leaf tissue using a cork borer (5 mm diameter), placed in size 0 gelatin capsules (Pure Planet Products, Scottsdale, Arizona), and monitored daily for emergence. Reared parasitoid specimens were killed directly in 95% ethanol and stored at -20 °C until DNA extraction.

DNA Extraction & PCR

Genomic DNA was extracted from *Aleurocybotus* puparia, adults, and single wasps using a DNeasy Blood and Tissue Kit (Qiagen, Hilden, Germany). Individual specimens were first removed from ethanol and allowed to air dry on a Kimwipe for approximately 30 s. The specimen was then transferred to an Eppendorf tube containing 90 µl ATL lysis buffer to which 20 µl proteinase K was added. Tissue digestion was achieved by incubating the reaction mixture for 8 hrs at 56 °C. Tubes were agitated periodically, by hand, to ensure the specimen remained in the reaction mixture at the bottom of the tube. Most specimens were satisfactorily cleared after 8 hrs in the reaction mixture, but some were left for 24 hrs without damaging the specimen. Following tissue digestion, specimens were removed from the reaction mixture directly into distilled water where they remained until slide-mounting. Extracted parasitoids were placed on microscope slides following the protocol of Polaszek et al. (2013). The extract was then processed per the manufacturer's instructions except that the AE buffer used in the final elution step was warmed to 55 °C, and the final elution volume per sample was 50 µl. DNA extracts were then stored at -20 °C until use in PCR.

The standard 5' barcode region of the cytochrome c oxidase subunit I (COI) gene (Folmer et al. 1994) and the 28S D2 and D3 domains of the 28S large ribosomal subunit (28S-D2-3) were targeted for amplification by PCR. The standard barcode primers (HCO2198/LCO1490) do not adequately amplify this region from many chalcidoids. Therefore, we utilized the two primer sets from Fusu and Polaszek (2017) that produce overlapping 'mini-barcode' sequences that can be assembled into a full consensus barcode. Primer sequences for each genomic region are listed in Table 1. The thermocycling conditions for the 28S-D2-3 region followed Andreason et al. (2019) and that of COI followed Fusu and Polaszek (2017) and Polaszek et al. (2022). PCR amplicons were visualized on a 1.5% agarose gel in 1X TAE buffer stained with SYBR Safe DNA Gel Stain (Invitrogen, Carlsbad, CA, USA) and a TrackIT 1 Kb Plus DNA Ladder (Invitrogen, Waltham, MA, USA) to estimate product sizes. Both strands of each amplicon were sequenced on an ABI 3730xl DNA Analyzer by Eton Bioscience, Inc. (Research Triangle Park, NC, USA). Forward and reverse sequences of each amplicon were assembled with the Geneious assembler at the Highest Sensitivity/Slow setting in Geneious Prime (version 2022.0.2). Newly generated sequences for all *Encarsia* species used in the phylogenetic analyses have been deposited in GenBank (Table 2).

Table 1. PCR primer sets used in this study.

Primer	Orientation	Region	Sequence (5'–3')	Reference
MChaF1	Forward	COI A	CCTCGAATAAATAATATAAGATT	Fusu and Polaszek 2017
HCO2198	Reverse		TAAACTTCAGGGTGACCAAAAAATCA	Folmer et al. 1994
LCO1490M	Forward	COI B	CAACAAATCATAAAGATATTGG	Fusu and Polaszek 2017; Folmer et al. 1994
MChaR1	Reverse		CCYGTTCCTCAAYAAATATTCT	Fusu and Polaszek 2017
D23F	Forward	28S-D2-3	GAGAGTTCAAGAGTACGTG	Park and O'Foighil 2000
D3B	Reverse		TCGGAAGGAACCAGCTACTA	Nunn et al. 1996; Whiting et al. 1997

Table 2. CUIDs, host records, GenBank accession numbers, and sequence lengths associated with the *Encarsia* specimens newly sequenced for this study.

Taxon	CUID	Host	GenBank Accession	Sequence Length (bp)
<i>Encarsia citrella</i>	OSUC 835434	<i>Aleuroplatus</i> sp.	OP133209 (28S)	901
<i>Encarsia protransvena</i>	OSUC 835443	<i>Parabemisia myricae</i>	OP133210 (28S)	742
<i>Encarsia</i> sp.	OSUC 835445	<i>Tetraleurodes</i> sp.	OP133211 (28S)	746
	OSUC 835446		OP133212 (28S)	745
<i>Encarsia lahorensis</i>	OSUC 835456	<i>Dialeurodes citri</i>	OP133213 (28S)	1,085
<i>Encarsia</i> sp. ^a	OSUC 863826	Unknown	OP133214 (28S)	713
<i>Encarsia hera</i>	OSUC 863846	<i>Aleurocybotus</i> sp.	OP146609 (28S)	494
			OP270223 (COI)	673
	OSUC 863847		OP133215 (28S)	750
			OP270224 (COI)	674

^a Specimen was collected with a sweep net.

Phylogenetic analyses

Phylogenetic analyses were conducted following Polaszek et al. (2021). Maximum likelihood phylogenies were estimated for the 28S-D2-3 region of 34 *Encarsia* species using IQ-TREE (v. 2.1.3) (Minh et al. 2020). This gene region in *Encarsia* is fast-evolving and accumulates mutations at a rate that provides sufficient phylogenetic signal to delimit species and species-groups with minimal noise (Heraty 2004; Polaszek et al. 2009). Sequences were aligned with MAFFT (v. 7.429) (Katoh et al. 2013) using the E-INS-i algorithm. The best nucleotide substitution model was selected with ModelFinder (Kalyaanamoorthy et al. 2017), and branch support was estimated by 1000 ultrafast bootstrap replicates with the `-bnni` flag enabled to reduce the negative impact of model violations (Hoang et al. 2018). We performed 25 independent tree searches and present the tree with the best (greatest) log-likelihood score. Two coccophagine aphelinids were selected as outgroups: *Coccophagoides fuscipennis* (Girault) (GenBank: AF254248.1) and *Pteroptrix chinensis* (Howard) (GenBank: KF778628.1).

Databasing

The specimens listed in the Material Examined section of the species description have been accessioned in The Ohio State University's Museum of Biological Diversity data-

base (<https://mbd-db.osu.edu/>). The numbers prefixed with “OSUC” are unique identifiers for the individual specimens. Details of the data associated with these specimens may be accessed at the above URL by entering the unique specimen identifier (e.g., OSUC 863846) in the form (note the blank space after the acronym).

Morphology

Morphological terminology follows Schmidt and Polaszek (2007). Relative lengths of morphological features were taken from the slide-mounted holotype and paratype as depicted in Heraty and Polaszek (2000).

Imaging

Slide-mounted specimens were imaged with a Keyence BZ-X810. Photographs of card-mounted insects were captured using a Macroscopic Solutions Macropod Micro Kit, with optical slices rendered in Helicon Focus. Composite images from each imaging system were imported into Adobe Photoshop 2022 to correct for brightness and contrast.

Collections

The slide-mounted holotype (OSUC 863846) and paratype (OSUC 863847) of *E. hera*, sp. nov., are deposited in the Smithsonian National Museum of Natural History (USNM), Washington, DC, USA. The two card-mounted paratypes (OSUC 863886; OSUC 863887) are deposited in the Florida State Collection of Arthropods (FSCA), Gainesville, Florida, USA.

Results

Taxonomy

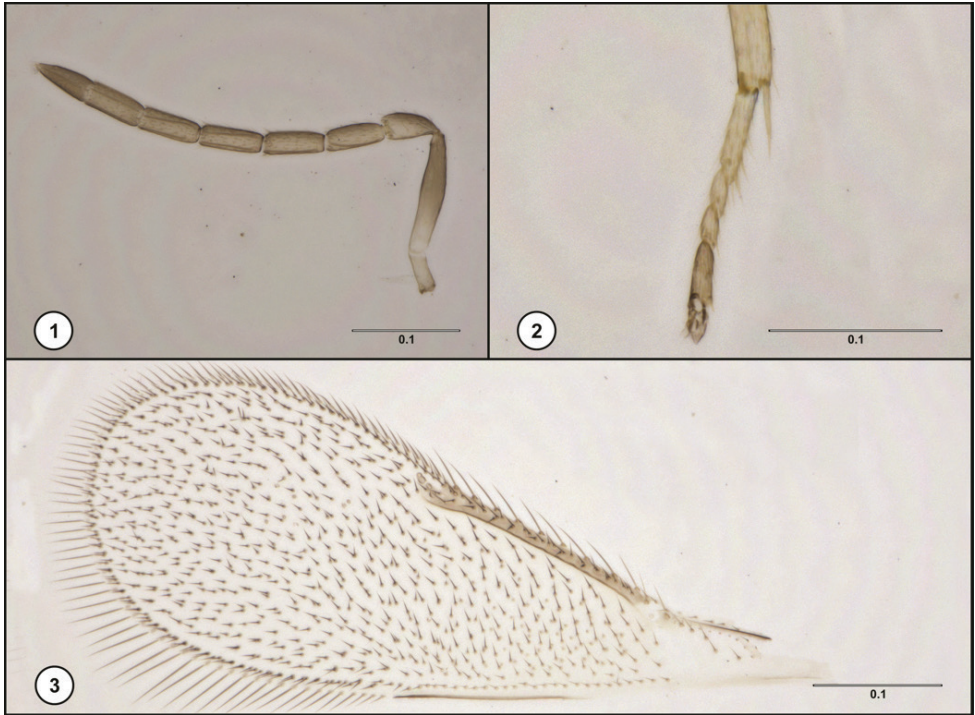
Encarsia hera Lahey & Andreason, sp. nov.

<https://zoobank.org/3C75DFAF-5FFF-44A1-947F-E34DF7F9DF3C>

Figs 1–5

Species-group placement. *Encarsia luteola*-group.

Diagnosis. *Encarsia hera*, sp. nov., can be differentiated from other members of the *E. luteola*-group by outstanding coloration of the mesoscutellum and metasoma. Most *E. luteola*-group species have a concolorous mesoscutellum and a predominately yellow metasoma. *Encarsia hera*, sp. nov., differs from these species by the paired brown patches in the posterior half of the mesoscutellum and the predominantly brown metasoma of the female. *Encarsia guadeloupae* Viggiani also has a dark metasoma; however, in that species T1 is completely dark and the clava is 2-merous, whereas the lateral portions of T1 are yellow and the clava is 3-merous in *E. hera*, sp. nov.



Figures 1–3. *Encarsia hera* Lahey & Andreason, female holotype (OSUC 863846) **1** Antenna, lateral view **2** Mesotarsus, dorsal view **3** Fore wing, lateral view. Scale bars in millimeters.



Figure 4. *Encarsia hera* Lahey & Andreason, female paratype (OSUC 863886), habitus, dorsal view. Scale bar in millimeters.

Description (female). *Coloration.* Body: predominately dark brown. Head: dark brown, except for pale areas on frons adjacent to compound eyes and a transverse strip on vertex anterior to ocellar bars. Antenna: yellow, except for fuscous apical clavomere (F6). Mesosoma: dark brown, except for yellow lateral and posteromedial margin of

mesoscutum, mesoscutal side lobe, anterodorsal portion of acropleuron, and most of mesoscutellum. Mesoscutellum: predominately yellow with two conspicuous brown spots in posterolateral half. Fore and hind wings: hyaline, venation fuscous. Legs: pale yellow, except for fuscous apical tarsomere (tarsomeres 4 + 5 fused) on midleg and apical three tarsomeres on hindleg. Metasoma: dark brown, except for lateral portions of T1 which appear transparent/opalescent. Ovipositor: third valvulae yellow.

Head. Antennal formula: 1-1-3-3. Length of pedicel relative to F1: 0.8. Length of F1 relative to F2: 0.9. Length of F2 relative to F3: approximately equal. Number of multiporous plate sensilla on F1–F6: 1-2-2-3-3-3. Sculpture of stemmaticum: aciculate. Sculpture of frons ventral to transfacial line: indiscernible. Sculpture of frons dorsal to transfacial line: transversely imbricate.

Mesosoma. Number of setae on midlobe of mesoscutum: 16. Number of setae on side lobe of mesoscutum: 2. Number of setae on axilla: 1. Proximity of campaniform sensilla on mesoscutellum: ≥ 5 sensillar widths apart. Distance between anterior pair of mesoscutellar setae: equal to distance between posterior pair of mesoscutellar setae. Length of mesoscutellar setae: anterior pair distinctly shorter than posterior pair. Tarsal formula: 5-4-5. Length of midtibial spur: $0.8\times$ length of midbasitarsus.

Metasoma. Number of paired setae on T1–T6: 0-1-2-1-3-3. Length of ovipositor: $0.8\times$ length of midtibia. Apical portion of 3rd valvulae: chisel-tipped, inner margin longer than outer margin. Length of 3rd valvulae relative to 2nd valvifer: $0.7\times$.

Wings. Length of fore wing: $2.7\times$ width. Asetose area below stigma vein: absent. Length of marginal fringe: $0.3\times$ maximum width of disc. Number of setae in basal cell region: 5. Arrangement of setae in basal cell: linear, originating and forming a 45° angle with submarginal vein. Number of setae on submarginal vein: 2. Number of setae along anterior of marginal vein: 8; 9.

Description (male). **Coloration.** Same as female, except for the darker mesoscutellum and T1 is dark throughout.

Morphology. Sculptural patterns very similar to female. Mesoscutellar sculpture: weak medially, large reticulations laterally. Number of antennomeres: 8. Condition of F6: articulate with F5, not fused or partially fused.

Distribution. Florida (USA).

Host. *Aleurocybotus* sp. nr. *cereus* (Hemiptera: Aleyrodidae).

Etymology. Named for the Hera of Greek mythology, one of the Twelve Olympians, Queen of the Gods, and protector of women from harm during childbirth.

Material Examined. **Holotype**, female: **USA:** Florida, Gainesville, $29^\circ36'3''\text{N}$, $82^\circ25'13''\text{W}$, 19.vi.2022, ex. *Aleurocybotus* n. sp. on ornamental Muhly grass (*Muhlenbergia capillaris*), Z. Lahey, OSUC 863846 (deposited in USNM). **Paratypes:** **USA:** collection data identical to holotype, 1 female, 2 males, OSUC 863847 (USNM); OSUC 863886, 863887 (FSCA).

Phylogenetic analyses. The alignment of the 28S-D2-3 region in the 36 taxa was 1,037 characters long (base pairs plus gaps) and the model of nucleotide evolution was SYM+I+G4. In all analyses, the *E. luteola*-group was recovered as monophyletic with maximum ultrafast bootstrap support (UFBS = 100; Fig. 9). *Encarsia hera*, sp. nov., was nested within the *E. luteola*-group, as the sister taxon to *E. formosa* Gahan (UFBS = 99; Fig. 9), and *E. luteola*

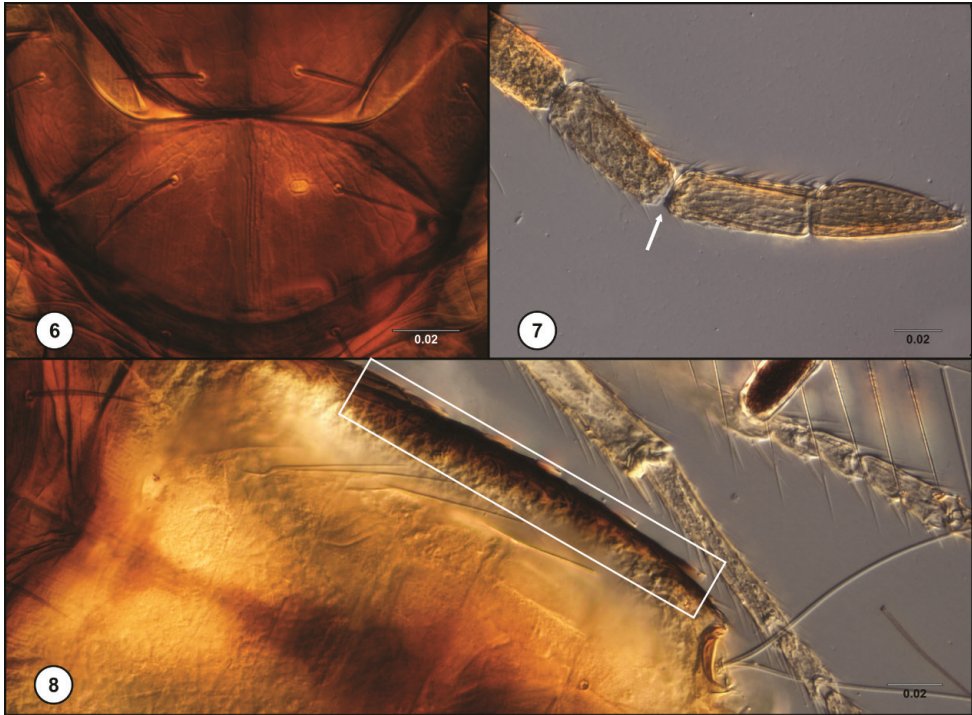


Figure 5. *Encarsia hera* Lahey & Andreason, male paratype (OSUC 863887), habitus, dorsolateral view. Scale bar in millimeters.

Howard was recovered as the sister taxon to *E. hera* sp. nov. + *E. formosa* (UFBS = 95; Fig. 9). An expanded analysis of the same gene region with additional *Encarsia* species recovered the same sister group relationships between *E. luteola*, *E. hera* sp. nov., and *E. formosa* as those in Fig. 9 (Suppl. material 1), as did a trimmed version (495 characters) of the original dataset (Suppl. material 2). While this article was in press, we were alerted that two taxa (three sequences) used in the phylogenetic analyses are misidentified in GenBank. The sequences corresponding to accessions AF223366.1 and AF223367.1 belong to *E. californica* Polaszek and AY360217.1 corresponds to *E. dispersa* Polaszek. Both *E. meritoria* Gahan and *E. haitiensis* Dozier have never been sequenced (A. Polaszek, pers. comm.).

Comments. Members of the *E. luteola*-group are recognized by having 4 mesotarsal segments and a fully setose wing disc (Gahan 1924; Polaszek et al. 1992). This species group has been recovered as monophyletic in several phylogenetic analyses of 28S rDNA (Babcock et al. 2000; Schmidt et al. 2006), although no analysis has yet to include all described species.

The sister group relationship between *E. formosa* and *E. hera*, sp. nov., recovered in our study breaks the longstanding paradigm that *E. formosa* and *E. luteola* are likely each other's most closely related living relative (Babcock and Heraty 2000). This is an



Figures 6–8. *Encarsia longitarsis* Myartseva, female paratype **6** Mesoscutellum, dorsal view **7** Antennal clava, lateral view, with arrow at the constriction between the last funicular and first claval segment **8** Metasoma, dorsal view, coloration of lateral metasoma boxed in white. Scale bars in millimeters.

interesting finding given the morphological similarity between the two taxa, with certain specimens impossible to distinguish as either species (Polaszek et al. 1992). Schauff et al. (1996) even mentioned the possibility that *E. formosa* and *E. luteola* are conspecific based on the lack of morphological characters that can readily define them. Our analysis brings to light at least one character mentioned by Babcock and Heraty (2000) that allows for the unambiguous identification of *E. formosa*: the presence of multiporous plate sensilla (MPS) on funicle (F) 1 and 2. *Encarsia hera*, sp. nov., also possesses this character, whereas *E. luteola* lacks MPS on F1 and F2, lending morphological credence to the relationships between these three taxa recovered in the molecular analysis.

Key to species of *Encarsia* Förster reared from *Aleurocybotus* Quaintance & Baker

- 1 Tarsus of midleg 5-merous; head, mesosoma, and metasoma yellow *Encarsia protransvena* Silvestri
- Tarsus of midleg 4-merous (Fig. 2); head and mesosoma completely or partially dark (Figs 4, 5) **2**

- 2 Mesoscutellum with two brown markings in posterior half (Fig. 4); clava 3-merous (Fig. 1) ***Encarsia hera* Lahey & Andreason, sp. nov.**
- Mesoscutellum concolorous throughout (Fig. 6); clava 2-merous (Fig. 7) ... **3**
- 3 Dorsolateral surface of metasoma light yellow, concolorous with remainder of metasoma ***Encarsia luteola* Howard**
- Dorsolateral surface of metasoma brown, contrasting with remainder of metasoma (Fig. 8) ***Encarsia longitarsis* Myartseva**

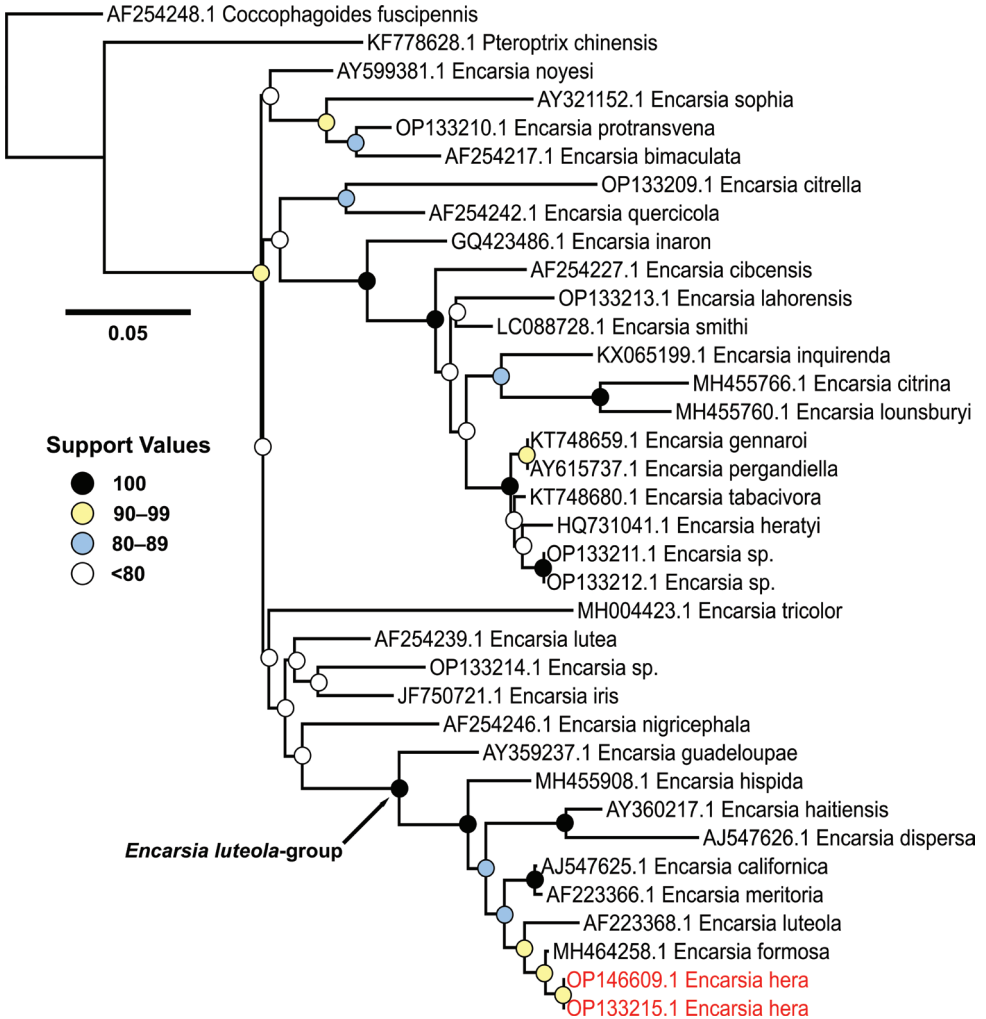


Figure 9. Maximum likelihood phylogeny of the 28S-D2-3 region in 34 *Encarsia* and two outgroup species. The number under the scale bar indicates the number of expected nucleotide substitutions per site. Ultrafast bootstrap supports values are indicated by colored circles at nodes. GenBank accession numbers beginning with OP correspond to specimens newly sequenced for this study.

Discussion

The arthropod fauna of Florida is in a constant state of flux, notably because of its position as a botanical import hub of the countries that comprise the Caribbean, South America, Europe, and Asia (Stocks 2013). Each of these regions harbors exotic whitefly species with the potential to become invasive and effect economic losses in the United States. The provenance of the new species of *Aleurocybotus*, first found in Florida, and now found in South Carolina, as well as its parasitoid, is uncertain. The earliest collections of this whitefly are from January 1988 in Wabasso, Florida, on Muhly grass (L. Deeter, pers. comm.). Muhly grass is a common perennial ornamental that is native to eastern North America and is the only reported host of this whitefly species.

The evidence for the undescribed whitefly as adventive is based on a comparison of its morphology with other described species of the genus. Puparia of the new *Aleurocybotus* secrete copious amounts of flocculent wax, a characteristic exhibited by both *A. cereus* and *A. mojaviensis* von Ellenrieder & Bailey, species from Belize and California, respectively (Martin 2005; von Ellenrieder and Bailey 2022). These species share a glandular zone on the dorsal submedian area of the nymphal stages that is not present in either named species known to occur in Florida (von Ellenrieder and Bailey 2022).

Surveys of parasitoid Hymenoptera primarily associated with *Bemisia* Quaintance & Baker in Florida, the Caribbean, and Latin America failed to recover *E. hera*, sp. nov., from that host (Stansly et al. 1997; Schuster et al. 1998). Lahey (2014) built upon these efforts by expanding the taxon sampling to additional whitefly genera in Florida. *Encarsia hera*, sp. nov., was not reared from the 13 non-*Bemisia* genera collected over a 6-year period, but these collections did not include *Aleurocybotus* (Lahey 2014; Stocks 2016; Lahey and Polaszek 2017). Given that this parasitoid has not been reared from any other whitefly genus in Florida, it apparently established with its host on infested plant material and has persisted since the original introduction, sometime before 1988. Alternatively, *E. hera*, sp. nov., may be a recent introduction or have expanded its host range to include *Aleurocybotus*. Testing either hypothesis will require continued sampling of whiteflies and their parasitoids from a broad geographic range.

The discovery of a new *Encarsia* species is not surprising. *Encarsia* is the most speciose genus in the family Aphelinidae and has been labeled ‘megadiverse’ based on a suite of morphological, genetic, and biological characteristics that account for the estimated 4,000 plus species thought to exist in nature (Polaszek et al. 2009). This estimate may even be considered conservative in that it does not consider the lack of knowledge regarding the biodiversity of their hosts, mostly whiteflies (approx. 1,600 described species; Martin and Mound 2007) and armored scale insects (2,700 described species; García Morales et al. 2016), new species of which are frequently uncovered. Based on these numbers and that Florida is home to the most diverse assemblage of whiteflies in the United States, we expect the number of new *Encarsia* and whiteflies to grow as scouting for these economically important pests, and their natural enemies, continues.

Acknowledgements

We thank Greg Evans (USDA-APHIS) and Natalia von Ellenrieder (California Department of Food and Agriculture) for confirming the species status of the *Aleurocybotus* specimens from Florida and South Carolina. Lily Deeter (FDACS-DPI-FSCA) kindly provided a tally for the number of whitefly genera and species in Florida, and Natalia von Ellenrieder did the same for California. Andrew Polaszek (Natural History Museum) is thanked for discussions on the morphology of *Encarsia*, the status of the *E. luteola*-group, and for constructive criticism during the review process. Luke Kresslein (University of California, Riverside) is thanked for taking images of the *E. longitarsis* paratype. Petr Janšta (Naturkundemuseum Stuttgart) kindly handled the review process and provided valuable feedback. The first author is a participant of the Oak Ridge Institute for Science and Education (ORISE) Agricultural Research Service (ARS) Research Participation Program, supported by the USDA-ARS, U.S. Vegetable Laboratory in Charleston, SC, USA. This work has been funded by the USDA. Mention of trade names or commercial products in this article is solely for the purpose of providing specific information and does not imply recommendation or endorsement by the USDA.

References

- Andreason SA, Triapitsyn SV, Perring TM (2019) Untangling the *Anagyrus pseudococci* species complex (Hymenoptera: Encyrtidae), parasitoids of worldwide importance for biological control of mealybugs (Hemiptera: Pseudococcidae): genetic data corroborates separation of two new, previously misidentified species. *Biological Control* 129: 65–82. <https://doi.org/10.1016/j.biocontrol.2018.09.010>
- Babcock CS, Heraty JM (2000) Molecular markers distinguishing *Encarsia formosa* and *Encarsia luteola* (Hymenoptera: Aphelinidae). *Annals of the Entomological Society of America* 93: 738–744. [https://doi.org/10.1603/0013-8746\(2000\)093\[0738:MMDEFA\]2.0.CO;2](https://doi.org/10.1603/0013-8746(2000)093[0738:MMDEFA]2.0.CO;2)
- Babcock CS, Heraty JM, De Barro PJ, Driver F, Schmidt S (2001) Preliminary phylogeny of *Encarsia* Förster (Hymenoptera: Aphelinidae) based on morphology and 28S rDNA. *Molecular Phylogenetics and Evolution* 18: 306–323.
- Clausen CP, Berry PA (1932) The citrus blackfly in Asia, and the importation of its natural enemies into Tropical America. US Department of Agriculture Technical Bulletin 320: 1–58.
- Evans GA, Polaszek A, Bennett FD (1995) The taxonomy of the *Encarsia flavoscutellum* species-group (Hymenoptera: Aphelinidae) parasitoids of Hormaphididae (Homoptera: Aphidoidea). *Oriental Insects* 29: 33–45. <https://doi.org/10.1080/00305316.1995.10433740>
- Folmer O, Black M, Hoeh W, Lutz R, Vrijenhoek R (1994) DNA primers for amplification of mitochondrial cytochrome c oxidase subunit I from diverse metazoan invertebrates. *Molecular Marine Biology and Biotechnology* 3: 294–299.
- Fusu L, Polaszek A (2017) Description, DNA barcoding and phylogenetic placement of a remarkable new species of *Eopelma* (Hymenoptera: Eupelmidae) from Borneo. *Zootaxa* 4263: 557–566. <https://doi.org/10.11646/zootaxa.4263.3.7>

- Gahan AB (1924) Some new parasitic Hymenoptera with notes on several described forms. *Proceedings of the United States National Museum* 65: 1–23. <https://doi.org/10.5479/si.00963801.2517>
- García Morales M, Denno BD, Miller DR, Miller GL, Ben-Dov Y, Hardy NB (2016) ScaleNet: a literature-based model of scale insect biology and systematics. *Database* 2016: bav118. <https://doi.org/10.1093/database/bav118>
- Hart WG, Selhime A, Harlan DP, Ingle SJ, Sanchez RM, Rhode RH, Garcia CA, Caballero J, Garcia RL (1978) The introduction and establishment of parasites of citrus blackfly, *Aleurocanthus woglumi* in Florida [Hem.: Aleyrodidae]. *Entomophaga* 23: 361–366. <https://doi.org/10.1007/BF02373053>
- Heraty JM, Polaszek A (2000) Morphometric analysis and descriptions of selected species in the *Encarsia strenua* group (Hymenoptera: Aphelinidae). *Journal of Hymenoptera Research* 9: 142–169.
- Heraty JM, Polaszek A, Schauff ME (2008) Systematics and biology of *Encarsia*. In: Gould J, Hoelmer K, Goolsby J (Eds) *Classical biological control of Bemisia tabaci in the United States – a review of interagency research and implementation*. *Progress in Biological Control* 4: 71–87. https://doi.org/10.1007/978-1-4020-6740-2_4
- Hoang DT, Chernomor O, Von Haeseler A, Minh BQ, Vinh LS (2018) UFBoot2: improving the ultrafast bootstrap approximation. *Molecular Biology and Evolution* 35: 518–522. <https://doi.org/10.1093/molbev/msx281>
- Hoddle MS, Van Driesche RG, Sanderson JP (1998) Biology and use of the whitefly parasitoid *Encarsia formosa*. *Annual Review of Entomology* 43: 645–669. <https://doi.org/10.1146/annurev.ento.43.1.645>
- Hodges GS, Evans GA (2005) An identification guide to the whiteflies of the southeastern United States. *Florida Entomologist* 88: 518–534. [https://doi.org/10.1653/0015-4040\(2005\)88\[518:AIGTTW\]2.0.CO;2](https://doi.org/10.1653/0015-4040(2005)88[518:AIGTTW]2.0.CO;2)
- Kalyanamoorthy S, Minh BQ, Wong TK, von Haeseler A, Jermini LS (2017) ModelFinder: fast model selection for accurate phylogenetic estimates. *Nature Methods* 14: 587–589. <https://doi.org/10.1038/nmeth.4285>
- Katoh K, Standley DM (2013) MAFFT multiple sequence alignment software version 7: improvements in performance and usability. *Molecular Biology and Evolution* 30: 772–780. <https://doi.org/10.1093/molbev/mst010>
- Kresslein RL, Heraty J, Woolley J, Polaszek A (2020) *Catalog of the Encarsia Förster of the World*, 1–117. <https://hymenoptera.ucr.edu/Encarsia.cat.pdf>
- Lahey ZJ (2014) Parasitoids of an invasive *Bemisia tabaci* species (Hemiptera: Aleyrodidae) in southwest Florida: faunal composition, host-plant associations, and interspecific competition. Master's Thesis. University of Florida, Gainesville, Florida.
- Lahey ZJ, Polaszek A (2017) *Baeoentedon balios* (Hymenoptera: Eulophidae): a parasitoid of ficus whitefly, *Singhiella simplex* (Singh) (Hemiptera: Aleyrodidae), new to the United States. *International Journal of Pest Management* 63: 349–351. <https://doi.org/10.1080/109670874.2016.1269222>
- LaSalle J, Schauff ME (1994) Systematics of the tribe Euderomphalini (Hymenoptera: Eulophidae): parasitoids of whiteflies (Homoptera: Aleyrodidae). *Systematic Entomology* 19: 235–258. <https://doi.org/10.1111/j.1365-3113.1994.tb00589.x>

- Martin JH (2005) Whiteflies of Belize (Hemiptera: Aleyrodidae) Part 2 – a review of the subfamily Aleyrodinae Westwood. *Zootaxa* 1098: 1–116. <https://doi.org/10.11646/zootaxa.1098.1.1>
- Martin JH, Mound LA (2007) An annotated check list of the world's whiteflies (Insecta: Hemiptera: Aleyrodidae). *Zootaxa* 1492: 1–84. <https://doi.org/10.11646/zootaxa.1492.1.1>
- Minh BQ, Schmidt HA, Chernomor O, Schrepf D, Woodhams MD, von Haeseler A, Lanfear R (2020) IQ-TREE 2: new models and efficient methods for phylogenetic inference in the genomic era. *Molecular Biology and Evolution* 37: 1530–1534. <https://doi.org/10.1093/molbev/msaa015>
- Myartseva SN, Ruíz-Cancino E (2010) Una nueva especie de *Metaphycus* Mercet (Hymenoptera: Encyrtidae) de México y clave de especies del género que parasitan mosquitos blancos (Hemiptera: Aleyrodidae) en la región neotropical. *Acta Zoológica Mexicana* 26: 17–24. <https://doi.org/10.21829/azm.2010.261676>
- Myartseva SN, Vejar-Cota G, Cortez-Mondaca E (2009) A new species of the genus *Encarsia* (Hymenoptera: Aphelinidae) – parasitoid of *Aleurocybotus occiduus* Russell (Hemiptera: Aleyrodidae) from Mexico. *Russian Entomological Journal* 18: 123–126.
- Nunn GB, Theisen BF, Christensen B, Arctander P (1996) Simplicity correlated size growth of the nuclear 28S ribosomal RNA D3 expansion segment in the crustacean order Isopoda. *Journal of Molecular Evolution* 42: 211–223. <https://doi.org/10.1007/BF02198847>
- Park JK, O' Foighil D (2000) Sphaeriid and corbiculid clams represent separate heterodont bivalve radiations into freshwater environments. *Molecular Phylogenetics and Evolution* 14: 75–88. <https://doi.org/10.1006/mpev.1999.0691>
- Polaszek A (1991) Egg parasitism in Aphelinidae (Hymenoptera: Chalcidoidea) with special reference to *Centrodora* and *Encarsia* species. *Bulletin of Entomological Research* 81: 97–106. <https://doi.org/10.1017/S0007485300053293>
- Polaszek A, Evans GA, Bennett FD (1992) *Encarsia* parasitoids of *Bemisia tabaci* (Hymenoptera: Aphelinidae, Homoptera: Aleyrodidae): a preliminary guide to identification. *Bulletin of Entomological Research* 82: 375–392. <https://doi.org/10.1017/S0007485300041171>
- Polaszek A, Hernández-Suárez EM, Manzari S, Pedata PA, Schmidt S (2009) Megadiversity of *Encarsia* (Chalcidoidea, Aphelinidae): macroevolution in a microhymenopteran. *Memoria de Taller Internacional sobre Recursos Naturales* 21: 87–92.
- Polaszek A, Gill R (2011) A new species of whitefly (Hemiptera: Aleyrodidae) and its parasitoid (Hymenoptera: Aphelinidae) from desert lavender in California. *Zootaxa* 2750: 51–59. <https://doi.org/10.11646/zootaxa.2750.1.5>
- Polaszek A, Albarracín EL (2011) Two new *Encarsia* species (Hymenoptera: Aphelinidae) reared from eggs of Cicadellidae (Hemiptera: Auchenorrhyncha) in Argentina: an unusual new host association. *Journal of Natural History* 45: 55–64. <https://doi.org/10.1080/00222933.2010.520169>
- Polaszek A, Ayshford T, Effendi B, Fusu L (2013) *Wallaceaphytis*: an unusual new genus of parasitoid wasp (Hymenoptera: Aphelinidae) from Borneo. *Journal of Natural History* 48: 1111–1123. <https://doi.org/10.1080/00222933.2013.852264>
- Polaszek A, Al-Riyami A, Lahey Z, Al-Khatiri SA, Al-Shidi RH, Hardy ICW (2021) *Telenomus nizwaensis* (Hymenoptera: Scelionidae), an important egg parasitoid of the pomegranate

- butterfly *Deudorix livia* Klug (Lepidoptera: Lycaenidae) in Oman. PLoS ONE 16: e0250464. <https://doi.org/10.1371/journal.pone.0250464>
- Polaszek A, Fusu L, Viggiani G, Hall A, Hanson P, Polilov AA (2022) Revision of the world species of *Megaphragma* Timberlake (Hymenoptera: Trichogrammatidae). Insects 13: 561. <https://doi.org/10.3390/insects13060561>
- Quaintance AL (1899) New or little known Aleurodidae II. Canadian Entomologist 31: 89–93. <https://doi.org/10.4039/Ent3189-4>
- Russell LM (1964) A new species of *Aleurocybotus* (Homoptera: Aleyrodidae). Proceedings of the Entomological Society of Washington 66: 101–102.
- Russell LM (2000) Notes on the family Aleyrodidae and its subfamilies: redescription of the genus *Aleurocybotus* Quaintance and Baker and description of *Vasdavidius*, a new genus (Homoptera: Aleyrodidae). Proceedings of the Entomological Society of Washington 102: 374–383.
- Sailer RI, Brown RE, Munir B, Nickerson JCE (1984) Dissemination of the citrus whitefly (Homoptera: Aleyrodidae) parasite *Encarsia lahorensis* (Howard) (Hymenoptera: Aphelinidae) and its effectiveness as a control agent in Florida. Bulletin of the Entomological Society of America 30: 36–39. <https://doi.org/10.1093/besa/30.2.36>
- Schmidt S, Driver F, De Barro P (2006) The phylogenetic characteristics of three different 28S rRNA gene regions in *Encarsia* (Insecta, Hymenoptera, Aphelinidae). Organisms Diversity & Evolution 6: 127–139. <https://doi.org/10.1016/j.ode.2005.07.002>
- Schmidt S, Polaszek A (2007) The Australian species of *Encarsia* Förster (Hymenoptera, Chalcidoidea: Aphelinidae), parasitoids of whiteflies (Hemiptera, Sternorrhyncha, Aleyrodidae) and armoured scale insects (Hemiptera, Coccoidea: Diaspididae). Journal of Natural History 41: 2099–2265. <https://doi.org/10.1080/00222930701550766>
- Schuster DJ, Evans GA, Bennett FD, Stansly PA, Jansson RK, Leibe GL, Webb SE (1998) A survey of the parasitoids of *Bemisia* spp. whiteflies in Florida, the Caribbean, and Central and South America. International Journal of Pest Management 44: 255–260. <https://doi.org/10.1080/096708798228194>
- Stansly PA, Schuster DJ, Liu T-X (1997) Apparent parasitism of *Bemisia argentifolii* (Homoptera: Aleyrodidae) by Aphelinidae (Hymenoptera) on vegetable crops and associated weeds in south Florida. Biological Control 9: 49–57. <https://doi.org/10.1006/bcon.1997.0504>
- Stocks I (2013) Recent adventive scale insects (Hemiptera: Coccoidea) and whiteflies (Hemiptera: Aleyrodidae) in Florida and the Caribbean region. In: Peña JE (Ed.) Potential invasive pests of agricultural crops. CABI International, Wallingford (UK), 342–362. <http://doi.org/10.1079/9781845938291.0342>
- Stocks I (2016) A new continental record whitefly in Florida. Florida Department of Agriculture and Consumer Services, Division of Plant Industry, Pest Alert. FDACS-P-02066.
- von Ellenrieder N, Bailey J (2022) *Aleurocybotus mojavensis* (Hemiptera: Sternorrhyncha: Aleyrodidae), a new whitefly species from California. Zootaxa 5174: 294–300. <https://doi.org/10.11646/zootaxa.5174.3.7>
- Whiting MF, Carpenter JC, Wheeler QD, Wheeler WC (1997) The Strepsiptera problem: phylogeny of the holometabolous insect orders inferred from 18S and 28S ribosomal DNA sequences and morphology. Systematic Biology 46: 1–68. <https://doi.org/10.2307/2413635>

Supplementary material 1

Maximum likelihood cladogram of the 28S-D2-3 region in 71 *Encarsia* and two outgroup species (1,070 sites, SYM+R3)

Authors: Zachary Lahey, Alvin M. Simmons, Sharon A. Andreason

Data type: image (svg file)

Explanation note: Maximum likelihood cladogram of the 28S-D2-3 region in 71 *Encarsia* and two outgroup species (1,070 sites, SYM+R3). Ultrafast bootstrap supports values are indicated on branches. GenBank accession numbers beginning with OP correspond to specimens newly sequenced for this study. Branches in red correspond to members of the *E. luteola*-group.

Copyright notice: This dataset is made available under the Open Database License (<http://opendatacommons.org/licenses/odbl/1.0/>). The Open Database License (ODbL) is a license agreement intended to allow users to freely share, modify, and use this Dataset while maintaining this same freedom for others, provided that the original source and author(s) are credited.

Link: <https://doi.org/10.3897/jhr.94.94677.suppl1>

Supplementary material 2

Maximum likelihood cladogram of a trimmed version of the 28S-D2-3 dataset analyzed in Fig. 9 (495 sites, GTR+F+G4)

Authors: Zachary Lahey, Alvin M. Simmons, Sharon A. Andreason

Data type: image (svg file)

Explanation note: Maximum likelihood cladogram of a trimmed version of the 28S-D2-3 dataset analyzed in Fig. 9 (495 sites, GTR+F+G4). Ultrafast bootstrap supports values are indicated on branches. GenBank accession numbers beginning with OP correspond to specimens newly sequenced for this study. Branches in red correspond to members of the *E. luteola*-group.

Copyright notice: This dataset is made available under the Open Database License (<http://opendatacommons.org/licenses/odbl/1.0/>). The Open Database License (ODbL) is a license agreement intended to allow users to freely share, modify, and use this Dataset while maintaining this same freedom for others, provided that the original source and author(s) are credited.

Link: <https://doi.org/10.3897/jhr.94.94677.suppl2>

Electronoyesella antiqua Simutnik, gen. et sp. nov. (Chalcidoidea, Encyrtidae) from Rovno amber

Serguei A. Simutnik¹, Evgeny E. Perkovsky¹, Dmitry V. Vasilenko^{2,3}

1 I.I. Schmalhausen Institute of Zoology, National Academy of Sciences of Ukraine, Kiev 01601, Ukraine

2 A.A. Borissiak Paleontological Institute, Russian Academy of Sciences, Moscow 117647, Russia **3** Cherepovets State University, Cherepovets, Vologda Region 162600, Russia

Corresponding author: Serguei A. Simutnik (simutnik@gmail.com)

Academic editor: Petr Janšta | Received 12 September 2022 | Accepted 13 October 2022 | Published 20 December 2022

<https://zoobank.org/D9DDB53D-4A3E-430D-B3B7-8FDDBBE0260D>

Citation: Simutnik SA, Perkovsky EE, Vasilenko DV (2022) *Electronoyesella antiqua* Simutnik, gen. et sp. nov. (Chalcidoidea, Encyrtidae) from Rovno amber. Journal of Hymenoptera Research 94: 105–120. <https://doi.org/10.3897/jhr.94.94773>

Abstract

Electronoyesella antiqua Simutnik, **gen. et sp. nov.**, is described and illustrated based on a female specimen from late Eocene Rovno amber. Like most previously described Eocene Encyrtidae, the new taxon differs from the majority of extant ones in a number of features. Sclerotised metasomal structures, similar to the paratergites of extant Tetracneminae, are seen here for the first time in fossils. The new genus is characterized also by the frontovertex with four vertical rows of piliferous punctures and the face also with intricate sculpture; notauli are present as small but distinct depressions, only anteriorly; the apex of metatibia with a peg originating from a round, deep pit; and the unusual setation of the hind wing.

Keywords

cerci, Eocene, evolution of Encyrtidae, metatibial peg, paratergites

Introduction

To date, 16 species in 14 extinct genera of Encyrtidae have been described from Rovno, Baltic, and Danish ambers and several undescribed encyrtids have been reported by Noyes and Hayat (1994) and Manukyan (1999) from Baltic amber. Extinct Encyrtidae demonstrate remarkable morphological differences from extant representatives of the

family (Simutnik et al. 2014, 2021a, b, 2022a, b; Simutnik 2015a, 2021; Simutnik and Perkovsky 2018). Most examined European amber Encyrtidae differ from the majority of extant ones by their relatively long marginal vein in the forewing, a distinctly thickened but not triangular parastigma, a short radicle, and a seta marking the apex of the postmarginal vein not longer than any other on this vein. Many have cerci positioned apically or subapically (Simutnik 2021).

One species of the extant genus *Copidosoma* Ratzeburg, 1844, *C. archeodominica* Zuparko & Trjapitzin, 2014, has been described from Miocene Dominican amber (Zuparko and Trjapitzin 2014).

According to the molecular analysis of Peters et al. (2018), Encyrtidae had already split into two subfamilies in the middle Eocene. Encyrtidae with filum spinosum (the presence of which is one of the main features of Encyrtinae; Trjapitzin 1968) are known since late Eocene (Simutnik et al. 2014, 2020), not from middle Eocene Sakhalinian amber (Simutnik 2015b, 2021). Further, although paratergites (their presence between the syntergum and the outer plates of the ovipositor is one of the main features of Tetracneminae; Trjapitzin 1968) have not been previously found in fossil encyrtids, at least similar structures are reported here for the first time.

Materials and methods

The studied specimen is housed in the collection of the Schmalhausen Institute of Zoology of the National Academy of Sciences of Ukraine, Kiev (SIZK). The amber piece containing the holotype (0.95 grams after primary preparation) was found in the Pugach quarry (Klesov) (fauna of the deposit reviewed by Mitov et al. 2021), Sarny District, Rovno Region.

The specimen was examined using the equipment and techniques described in Simutnik et al. (2022a). Photographs were taken using a Leica Z16 APO stereomicroscope equipped with a Leica DFC 450 camera and processed with LAS Core and Adobe Photoshop software (brightness and contrast only).

Terminology and abbreviations follow Sharkov (1985), Gibson (1997), and Heraty et al. (2013). For the identification, comparison, and description of the new taxon, we also used the keys of V.A. Trjapitzin (1989); J.S. Noyes, J.B. Woolley, and G. Zolnerowich (in Gibson 1997); and the genus description of *Oesol* Noyes & Woolley, 1994 (Noyes, Woolley 1994). We use the following abbreviations: **FS** = filum spinosum; **F1**, **F2**, **etc.** = funicular segments 1, 2, etc.; **LOL** = minimum distance between the anterior ocellus and a posterior ocellus; **mps** = multiporous plate sensilla; **OOL** = minimum distance between an eye margin and the adjacent posterior ocellus; **OCL** = minimum distance between a posterior ocellus and the occipital margin; **POL** = minimum distance between the posterior ocelli; **OPO** = outer plates of the ovipositor. Other abbreviations are explained in figure captions.

Results

Systematic paleontology

Chalcidoidea Latreille, 1817

Encyrtidae Walker, 1837

Tetracneminae Howard, 1892

Genus *Electronoyesella* Simutnik, gen. nov.

<https://zoobank.org/5BFACFC4-6923-4E7B-B034-95DEEE352D78>

Type species. *Electronoyesella antiqua* Simutnik, sp. nov.

Species composition. Type species only.

Etymology. The new genus is named in honor of John Stuart Noyes, who first saw the presence of the structures similar to paratergites in the new fossil. The name is a combination of “electrum” (Latin: *electrum* = amber) and “Noyes”. The genus name is a feminine noun.

Diagnosis. Female. Body not flattened; frontovertex as long as broad, with four vertical rows of piliferous punctures (Fig. 3A); ocelli forming right angled triangle; horizontal row of three large, deep cells under each torulus (Fig. 4); clypeus and interantennal prominence intricately sculptured; mandibles tridentate with middle tooth longest; scape much more than 3× as long as broad; F1 a little longer than broad to quadrate; notauli present only anteriorly as small but distinct depressions (Fig. 3B: arrow), without visible lines; filum spinosum absent; covering setae present; marginal vein 5× as long as broad; postmarginal vein 1.5× as long as marginal; costal cell of hind wing with line of long setae (Fig. 5C: ls1), longest of which located alongside parastigma (Fig. 5C: pst); row of thickened setae present alongside hyaline spur vein of hind wing (Fig. 5C: ls2, spv); apex of metatibia with one peg (Fig. 2A: arrows); cerci located in apical third of metasoma; paratergite-like, sclerotized, separated part of Mt8 present alongside margin of syntergum (Figs 6A, B, 7C: ptrg?); apex of hypopygium reaching a little way past apex of last gastral tergum.

Male. Unknown.

Remarks. Placement of *Electronoyesella* gen. nov. in Tetracneminae is supported by the absence of the filum spinosum of linea calva, the tridentate mandibles with the middle tooth being the longest, the hypopygium reaching a little way past the apex of the syntergum, and the presence of the sclerotized, ribbon-like, separated part of Mt8 along the margin of the syntergum (Figs 6A, B, 7C: ptrg?). This structure closely resembles the paratergites of extant Tetracneminae (Fig. 7A, B: ptrg) and may be morphological evidence for the existence of this subfamily in the late Eocene.

The hind wing of the new genus has a single line of long setae alongside the entire costal cell (Fig. 5C: ls1) as in most extant Tanaostigmatidae. These setae vary in length, the longest located along the parastigma of the hind wing. In fossil Encyrtidae, the

same line of long setae has been recorded in *Eocencnemus sugonjaevi* Simutnik, 2002, *Sulia glaesaria* Simutnik, 2015 (Simutnik et al. 2021), and is also known in several undescribed specimens without filum spinosum. These differ from the new genus by the absence of a vertical rows of large piliferous punctures on the frontovertex. *E. sugonjaevi* also differs by its short, ring-like F1.

The same line of long setae alongside the costal cell of the hind wing is present in few extant Encyrtinae: *Exoristobia* Ashmead, 1904 (Simutnik et al. 2021), *Rhytidothorax* Ashmead, 1900, and some other Bothriothoracini Howard, 1895 (J. S. Noyes, pers. comm. 2022). In *Aphycooides* Mercet, 1921 these setae are sparser and shorter. Within Tetracneminae, a somewhat similar line of setae is present in *Ericydnus* Walker, 1837 and *Moraviella* Hoffer, 1954, but their setae do not vary in length. A line or several lines of setae are present in *Aenasius* Walker, 1846; *Blepyrus* Howard, 1898; *Monodiscodes* Hoffer, 1953, but they are also short.

A line of long setae, but sparser and more or less equal in length originating from the membrane of the costal cell, similar to these of *Ericydnus*, are also found in the earliest known Sakhalinian amber encyrtids: *Sugonjaevia* Simutnik, 2015, *Encyrtoides* Simutnik, 2021, and *Sakhalinencyrtus* Simutnik, 2021. This character state seems to be a feature of the stem group of Encyrtidae.

The first funicular segment seen in the majority of known Eocene encyrtid females, including the oldest described female from middle Eocene Sakhalinian amber (Simutnik 2021), had an annular shape, or at least is broader than long. Of the 27 examined females of European and Sakhalinian ambers (some of which might belong to the same species), some undescribed, few have an F1 longer than broad. Among Eocene females without the filum spinosum (supposedly Tetracneminae), only in *Sulia* Simutnik, 2015 and *Rovnopositor* Simutnik, 2022, is F1 about 1.5× as long as broad (the latter differs from the new genus by the absence of vertical rows of piliferous punctures on the frontovertex, its shorter marginal vein, the reduced gonostyli, and by its long, curved ovipositor stylet). F1 in *Electronoyesella* is slightly longer than broad (Fig. 3A, B).

The new taxon further differs from most known Encyrtidae by the presence of a peg or spicule originating from the round, deep pit at the apex of metatibia (Fig. 2A, arrows); and a row of thickened setae alongside the spur vein of the hind wing (Figs 5C, 6B: spv). Such a row of setae is also absent in the middle Eocene encyrtids from the Sakhalinian amber.

***Electronoyesella antiqua* Simutnik, sp. nov.**

<https://zoobank.org/E78EBF78-2533-4025-98F2-B486BA6E3736>

Figs 1–6, 7C

Material. *Holotype*, SIZK K-27005, 1 ♀, Klesov, Sarny District, Rovno Region, Ukraine; Rovno amber; late Eocene (deposited in SIZK). The inclusion is in a reddish-yellow and clear, parallelepiped piece of amber (ca. 7 × 6.5 × 4 mm). It is well preserved, but its left side is obscured by a large air bubble (Figs 1B, 2).

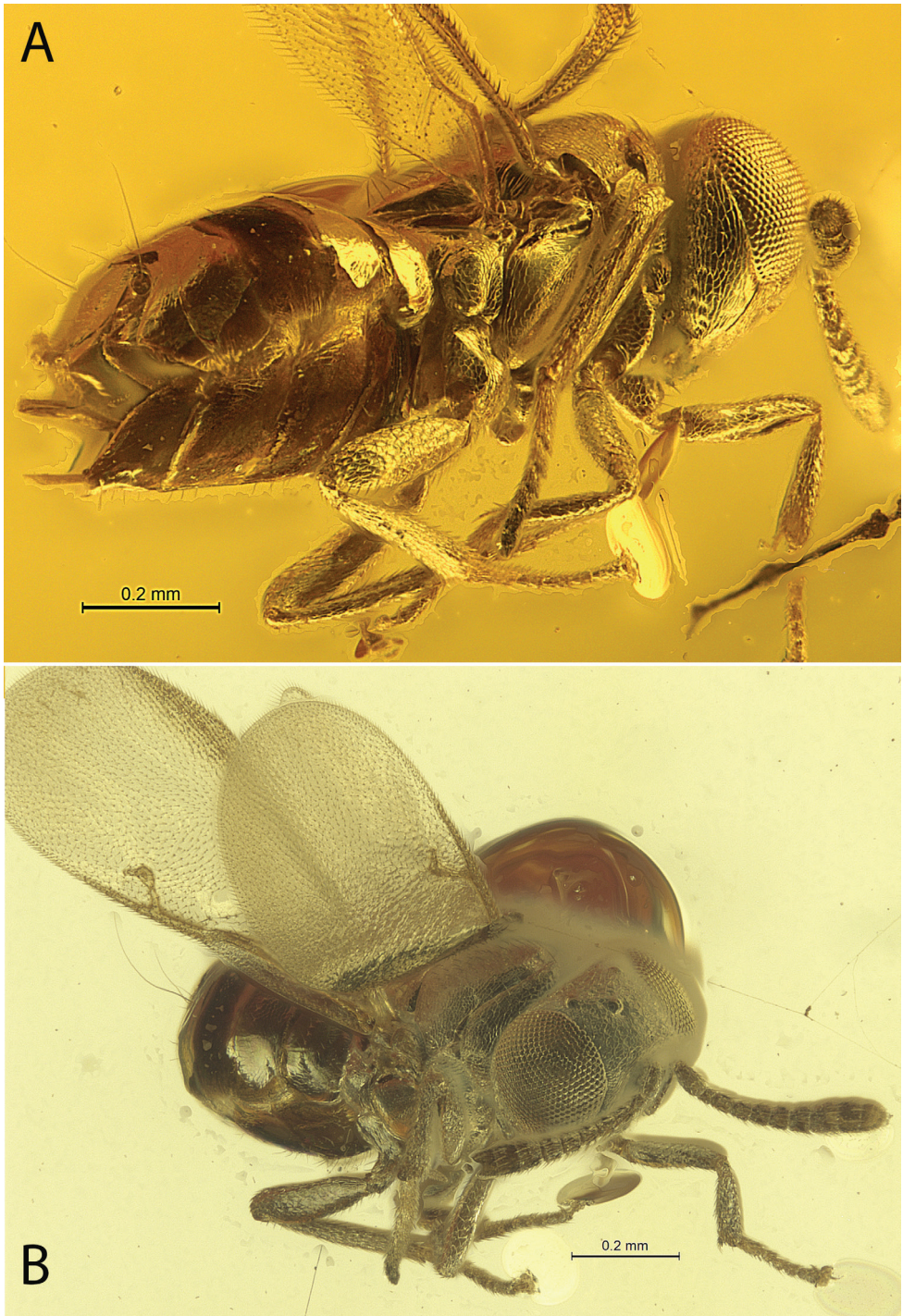


Figure 1. *Electronyesella antiqua* gen. et sp. nov., holotype female **A** body, lateral view **B** body, antero-dorsolateral view.

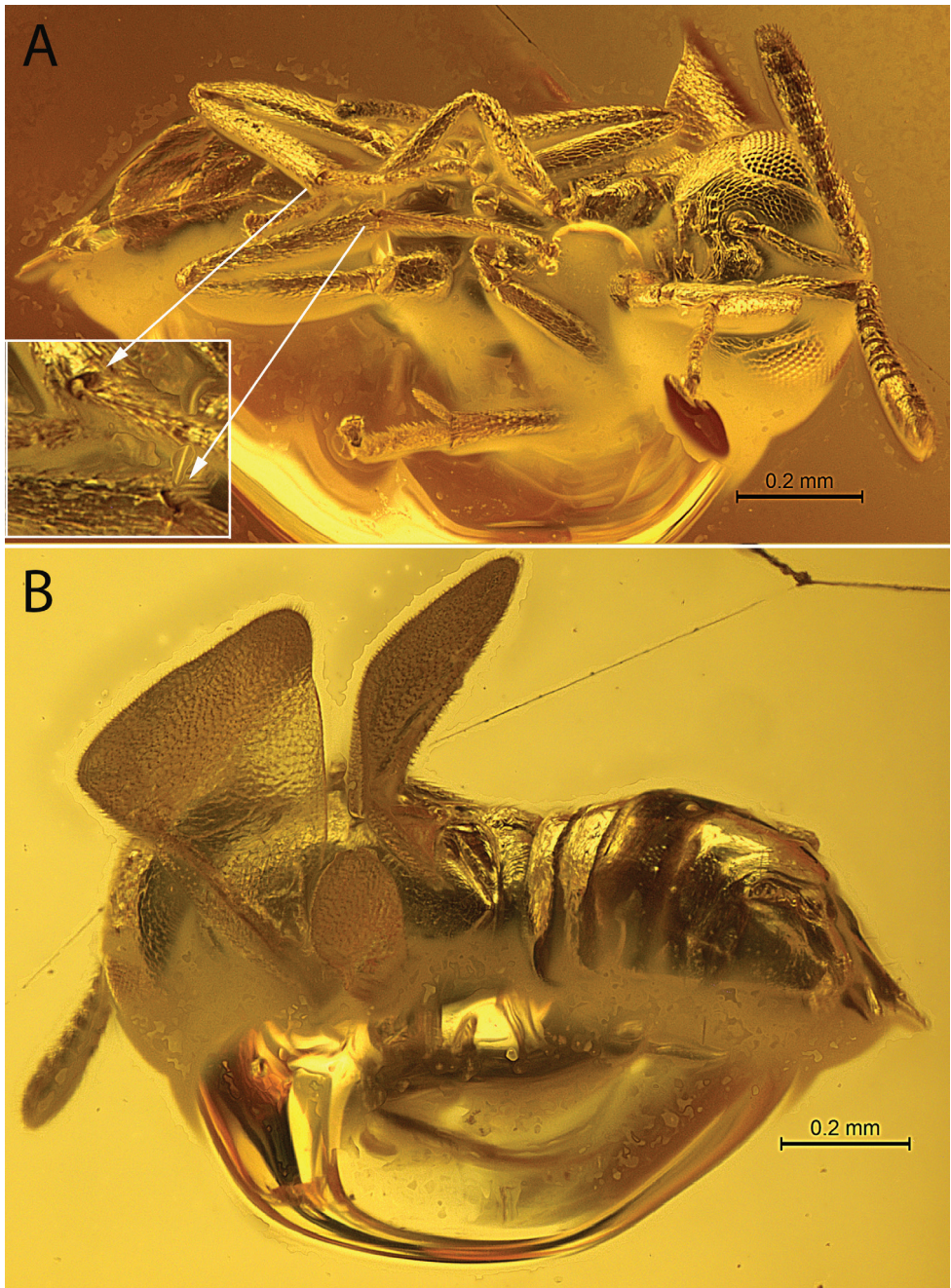


Figure 2. *Electronyoesella antiqua* gen. et sp. nov., holotype female **A** body, ventral (arrows indicate the metatibial pegs in inset) **B** body, posterodorsal.

Syninclusions. Nematocera, spider web.

Etymology. The specific epithet means ancient in Latin.

Description. Female. Habitus as in Figs 1, 2. Body length 1.3 mm.

Coloration. Head, thorax, gaster dorsally, tegula, and all femora black; antenna uniformly dark brown; gaster ventrally dark brown; venation brown; mesotibial spur and tarsi pale yellow; surface of frontovertex, thorax, legs shiny due to presence of a thin layer of air, without metallic shine.

Sculpture. Head, pronotum and mesoscutum rough reticulate, but surface of head only sparsely punctate – frontovertex with 4 vertical rows of large but shallow piliferous punctures (Fig. 3A), outer row separated from eye margin by a distance equal to or more than diameter of this punctures; scape, pedicel, scutellum, tegula, mesopleuron, coxae, legs, and gaster also relatively similarly but more smoothly reticulate; sculpture of face as in Fig. 4 – horizontal row of three large, deep cells located under each torulus, lateral to clypeus, also intricately sculptured.

Head. Lenticular, slightly wider than thorax in dorsal view; occipital margin sharp, but not carinate (Fig. 2B); frontovertex curved to posterior ocelli; broadly rounded in frontal view, not vaulted above eyes; eyes bare, without visible setae, with inner orbits parallel over much of height but ventrally divergent (Figs 3B, 4); frontovertex as long as broad, minimum distance between eyes about $0.4\times$ head width; ocelli forming a right angled triangle, posterior ones closer to eye than occipital margin; OOL about equal to posterior ocellar diameter; OOL:POL:LOL:OCL about 3:11:8:4; eye reaching occipital margin (Figs 1A, 3); antennal scrobes as in Figs 3, 4, v- or u-shaped and meeting dorsally, not extended to anterior ocellus, in dorsal view anterior ocellus about equidistant from occipital margin and from upper margin of scrobal depression; interantennal prominence presents (Fig. 4); antennal toruli located about at level of lower eye margin, separated from mouth margin by distance equal to their own width (Fig. 4); distance between toruli equal to distance between torulus and eye, about $1.5\times$ width of torulus, about $0.5\times$ length of malar space; malar space with complete malar sulcus (Fig. 4), about $2\times$ shorter than height of eye; clypeus strongly emarginate, with short lateral margins; mandible 3-dentate, with middle tooth longest (Fig. 4).

Antenna. Geniculate, 11-segmented, without differentiated anelli, with 6 funicular segments and 3-segmented clava; radicle short, about $2\times$ as long as broad (Fig. 2B); antennal scape $\sim 4\times$ as long as broad; pedicel conical, little longer than first two funicular segments combined, longer than any segment of funicle; F1 subquadrate, slightly longer than broad, F2 and F3 distinctly longer than broad, F4–F6 subquadrate, F3–F6 slightly flattened; width of flagellomeres slightly increases toward apex; F5 and F6 noticeably wider than F2–F4 (Fig. 4); all segments of funicle, at least F2–F6, and two basal segments of clava with mps; clava a little shorter than F3–F6 combined, with small oblique truncation at apical segment only (Figs 3, 4), wider than F6; flagellum and clava clothed in very short setae.

Mesosoma. Pronotum short, not conspicuously narrower than mesoscutum, almost vertical (in lateral view), with posterior edge only slightly emarginate (Fig. 3B); mesoscutum as broad as long or nearly to (in dorsal view); mesothoracic spiracle open, not concealed beneath pronotum (Fig. 1A); notauli present as depressions at extreme antero-lateral margin of mesoscutum (Figs 3A, B: arrow); meeting of axillae not visible; scutellum flat, apically pointed, with several long, vertical setae at own apex (Fig. 2B); mesopleuron enlarged posteriorly; metapleuron triangular, narrow, without visible setation (Fig. 1A); propodeum bare, with relatively large lateral parts, touching hind coxa (Fig. 1A).

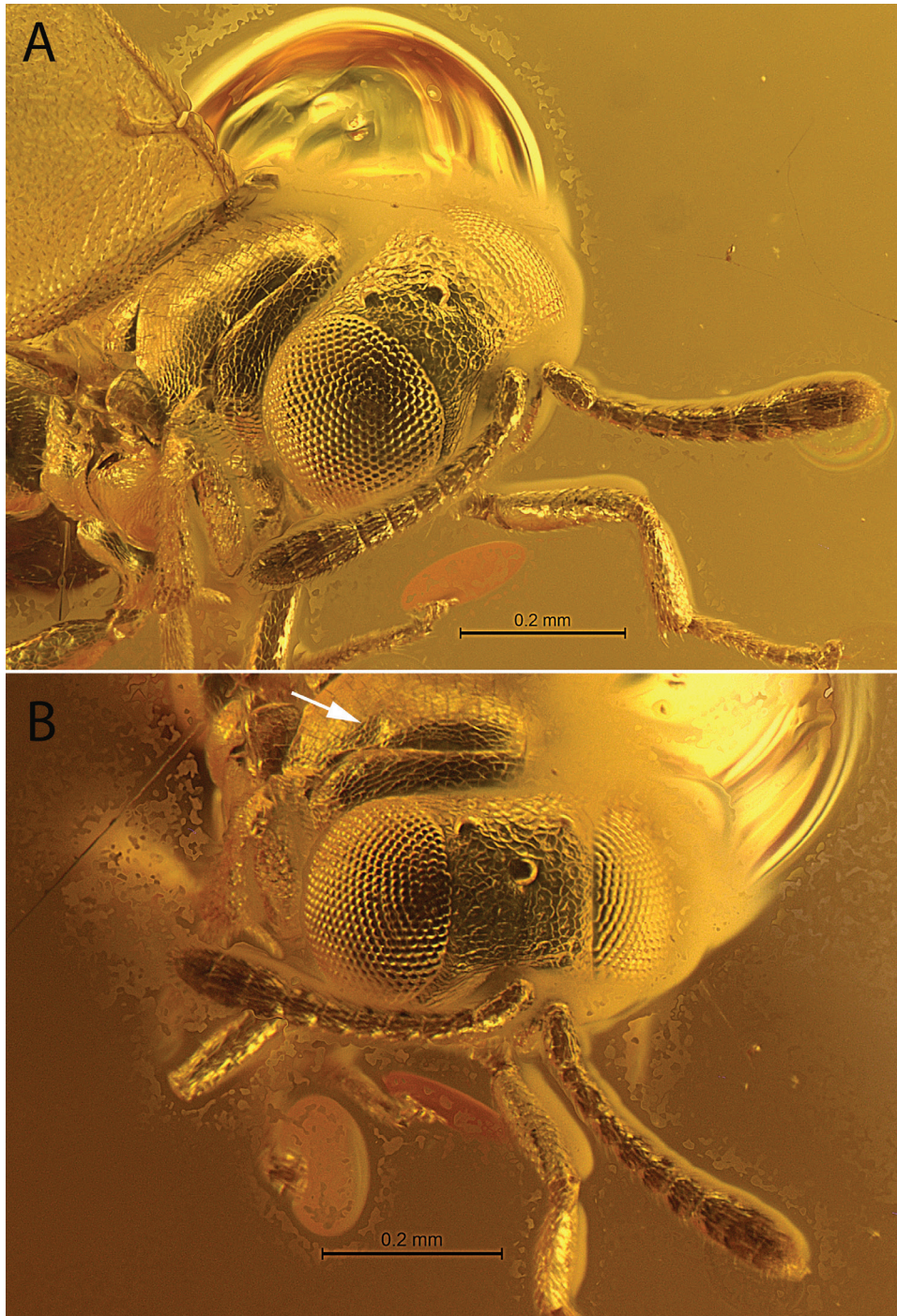


Figure 3. *Electronoyesella antiqua* gen. et sp. nov., holotype female **A** head, antennae, part of mesosoma, anterodorsolateral view **B** head, antennae, part of mesosoma, anterodorsal view (arrow indicates the notaular depression).

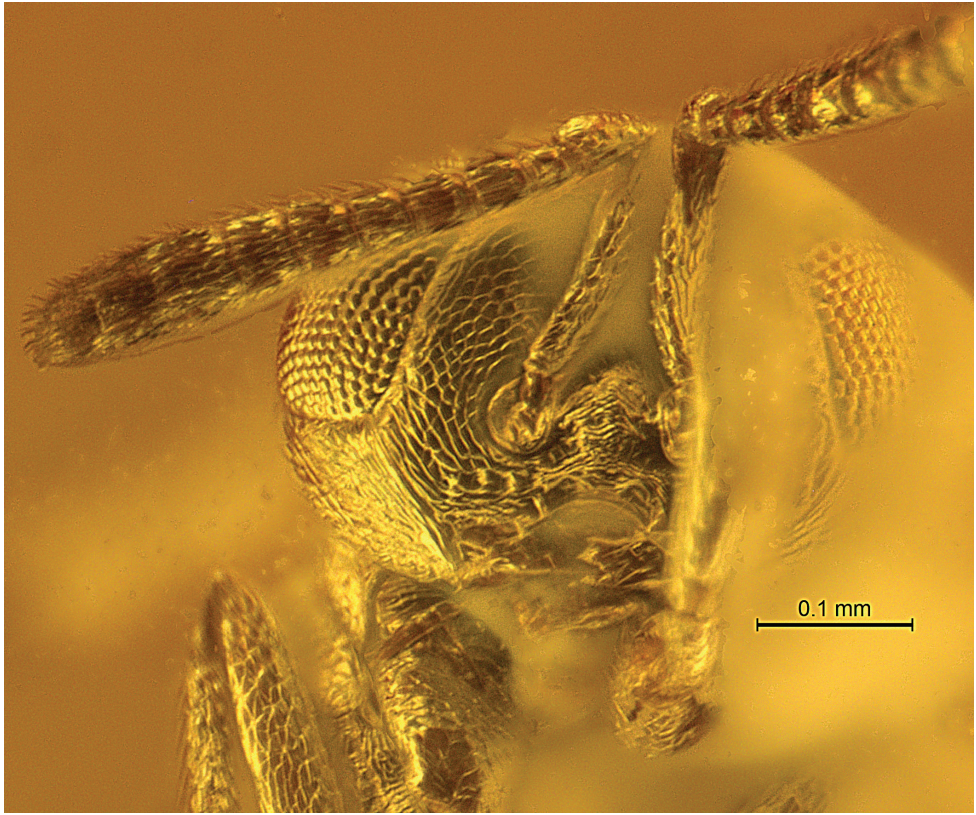


Figure 4. *Electronoyesella antiqua* gen. et sp. nov., holotype female, antennae, head anteroventral.

Wings. Fully developed, hyaline. Forewing $2.5\times$ as long as broad; linea calva not interrupted but closed on posterior margin, without filum spinosum, with well-developed line of long setae alongside basal margin of dorsal surface (Figs 5A, B); parastigma thickened, hyaline break (unpigmented area) present; marginal vein $5\times$ as long as broad; stigmal vein as long as marginal, with long narrow uncus consisting row of 4 uncal sensilla (Fig. 5B); postmarginal vein $1.5\times$ as long as marginal vein, enlarged seta marking apex of postmarginal vein of forewing absent (as long as others on this vein); setae of marginal fringe short. Hindwing relatively wide; membrane of costal cell along submarginal vein with line of long setae (Fig. 5C: ls1); spur vein originating from submarginal vein visible as differentiated hyaline process, alongside this a row of 5 thickened setae (Fig. 5C: spv, ls2); apex of marginal vein with 3 hamuli; marginal fringe $\sim 0.2\times$ as long as wing width.

Legs. Mid tibial spur about as long as basal mid tarsal segment or slightly shorter, both relatively long; mesotibia with row of pegs along anteroapical edge (Figs 1B, 2A); ventral surface of mesobasitarsus and each next tarsomere with differentiated setation along anteroventral edge (Fig. 2A); apex of metatibia with one peg originating from round, deep pit and row of spine-like setae (Fig. 2A: arrows); tarsi 5-segmented.

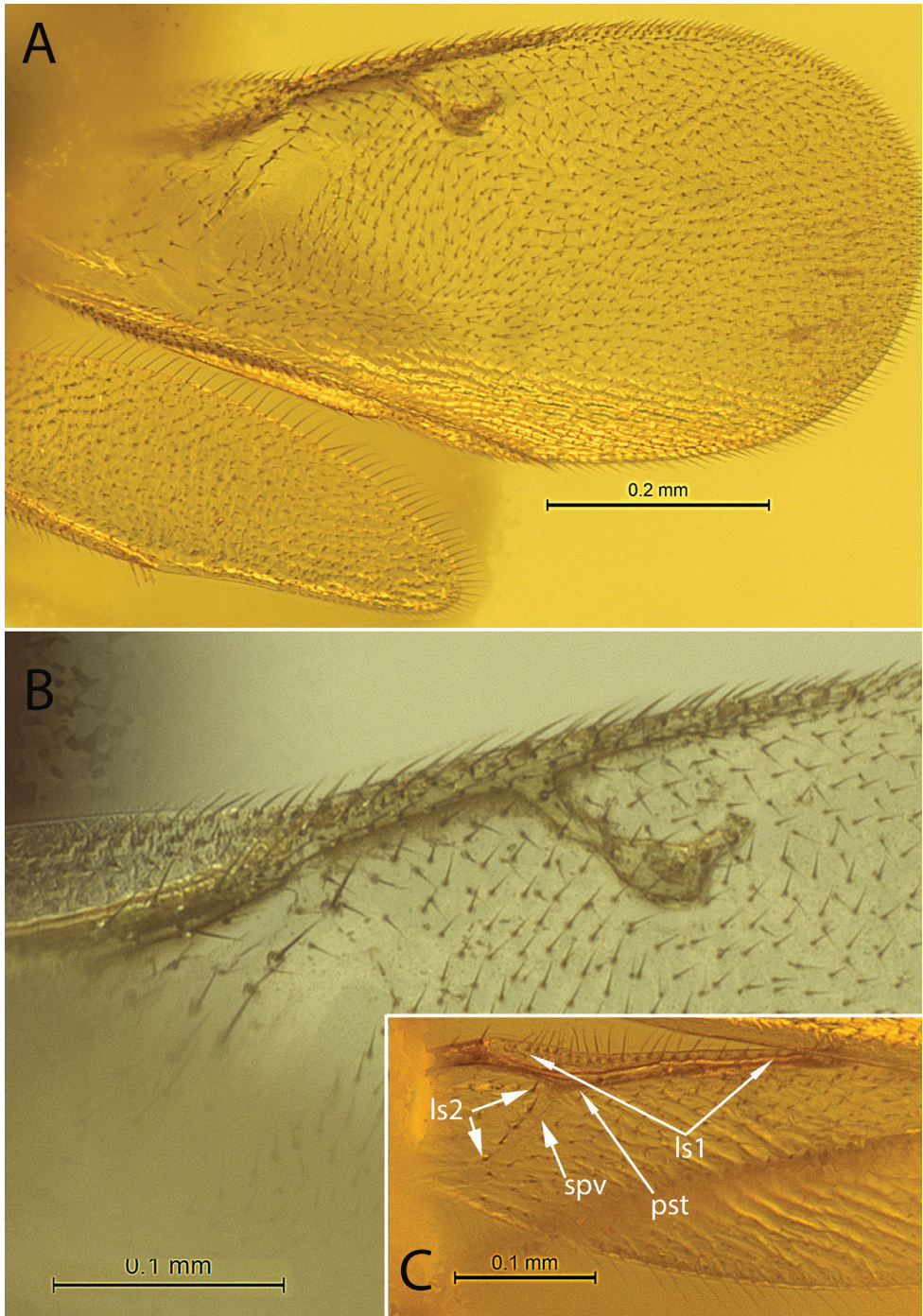


Figure 5. *Electronoyesella antiqua* gen. et sp. nov., holotype female **A** wings **B** forewing venation **C** hind wing venation (ls1, 2 – lines of setae, spv – spur vein, pst – parastigma). Scale bars: 0.2 mm (**A**); 0.1 mm (**B, C**).

Metasoma. As long as head and mesosoma together; cerci situated in apical third of metasoma, with long vertical setae (or bristles) (Figs 1A, B, 6B); syntergum (Mt8 + Mt9) v-shaped, no longer than 1/3 of metasoma; posterior margins of Mt2–Mt5 straight, parallel; Mt6 and Mt7 slightly produced, M-shaped, U-like between cerci; apex of hypopygium with developed mucro, reaching apex of syntergum (Fig. 6B); lateral margin of hypopygium bare, without row of setae; ovipositor stylet thick; ovipositor sheaths (gonostyli or third valvulae) visible in dorsal view (Fig. 6A, B: osh (v3)), as long as mesobasitarsus, connect at some angle with second valvifers (inner plates of the ovipositor, Fig. 6B: vr2), apparently, movably fused; outer plates of ovipositor not visible but (as J. S. Noyes, pers. comm. 2022, suggested) appear very slender, appear to have filamentous connection to paratergite (Fig. 6B: fc, ptrg?) running forwards to outside of cercal plate, similar to that of *Ericydnus* (Fig. 7).

Male. Unknown.

Genus composition. Type species only.

Remark. *Electronoyesella antiqua* gen. et sp. nov. from Rovno amber is the 23th non-ant hymenopteran genus (from 57, 40.4%) and 50th non-ant hymenopteran species (from 73, 68.5%), unknown from Baltic amber (Olm 2022a, b).

Discussion. Late Eocene and extant encyrtid faunas differ (Simutnik 2021). For example, fossil Encyrtidae with reduced or shortened wings are unknown. The presence of the filum spinosum (*FS*), one of the main features of the subfamily Encyrtinae, have been found in about one third (22) of the 64 examined Eocene encyrtid specimens (males and females). In extant Encyrtidae, the number of species of Encyrtinae (with *FS*) is approximately three times more than the number of Tetracneminae species (without *FS*). The venation of the forewings and the structure of the linea calva in the fossil described here, as well as in other known Eocene Encyrtidae without *FS*, most closely resemble those of *Savzdargia* Trjapitzin, 1979; *Moraviella* Hoffer, 1954; *Monodiscodes* Hoffer, 1954; possibly some species of *Ericydnus*; and some other extant Tetracneminae. At the same time, distinct paratergites (the presence of which is one of the main features of the Tetracneminae: Trjapitzin 1968) have not been previously found in fossil females. Therefore, there is not enough morphological evidence to classify them as members of the Tetracneminae (Simutnik and Perkovsky 2018; Simutnik et al. 2022a). *Electronoyesella* has a sclerotized, ribbon-like, separated part of Mt8 along the lateral edge of the syntergum (Figs 6B, 7C: ptrg?). This structure closely resembles the paratergites of extant Tetracneminae (Fig. 7A, B: ptrg).

One of the most intriguing things in the evolution of encyrtids is what happens to the connection of tergite IX of the abdomen (Mt8) and the outer plates of the ovipositor (*OPO*) (J. S. Noyes, pers. comm. 2022). The *OPO* are completely separated from the syntergum behind the cercal plate in Encyrtinae. In Tetracneminae they are connected by the paratergite. Both features almost certainly result from advancement of cerci (Noyes 2004).

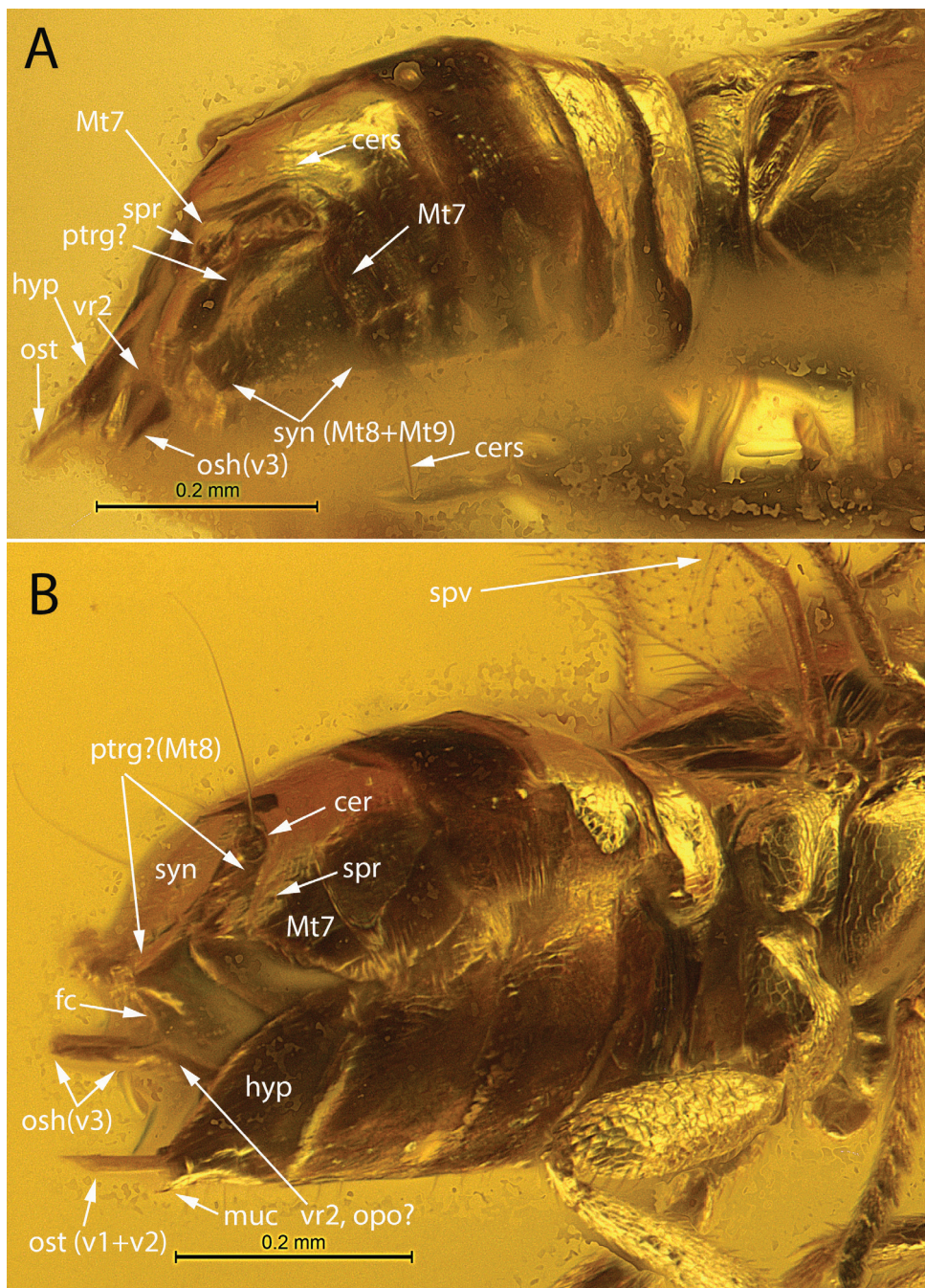


Figure 6. *Electronoyesella antiqua* gen. et sp. nov., holotype female **A** metasoma, part of mesosoma, posterodorsal (cers – cercal seta, hyp – hypopygium, osh – ovipositor sheaths, ost – ovipositor stylet, ptrg? – paratergite?, spr – spiracle, syn – syntergum, vr2 – second valvifer) **B** metasoma, part of mesosoma, posterolateral (cer – cercus, fc – filamentous connection, muc – mucro, opo? – possible, outer plate of the ovipositor, spv – hyaline spur vein; osh(v3) – ovipositor sheaths).

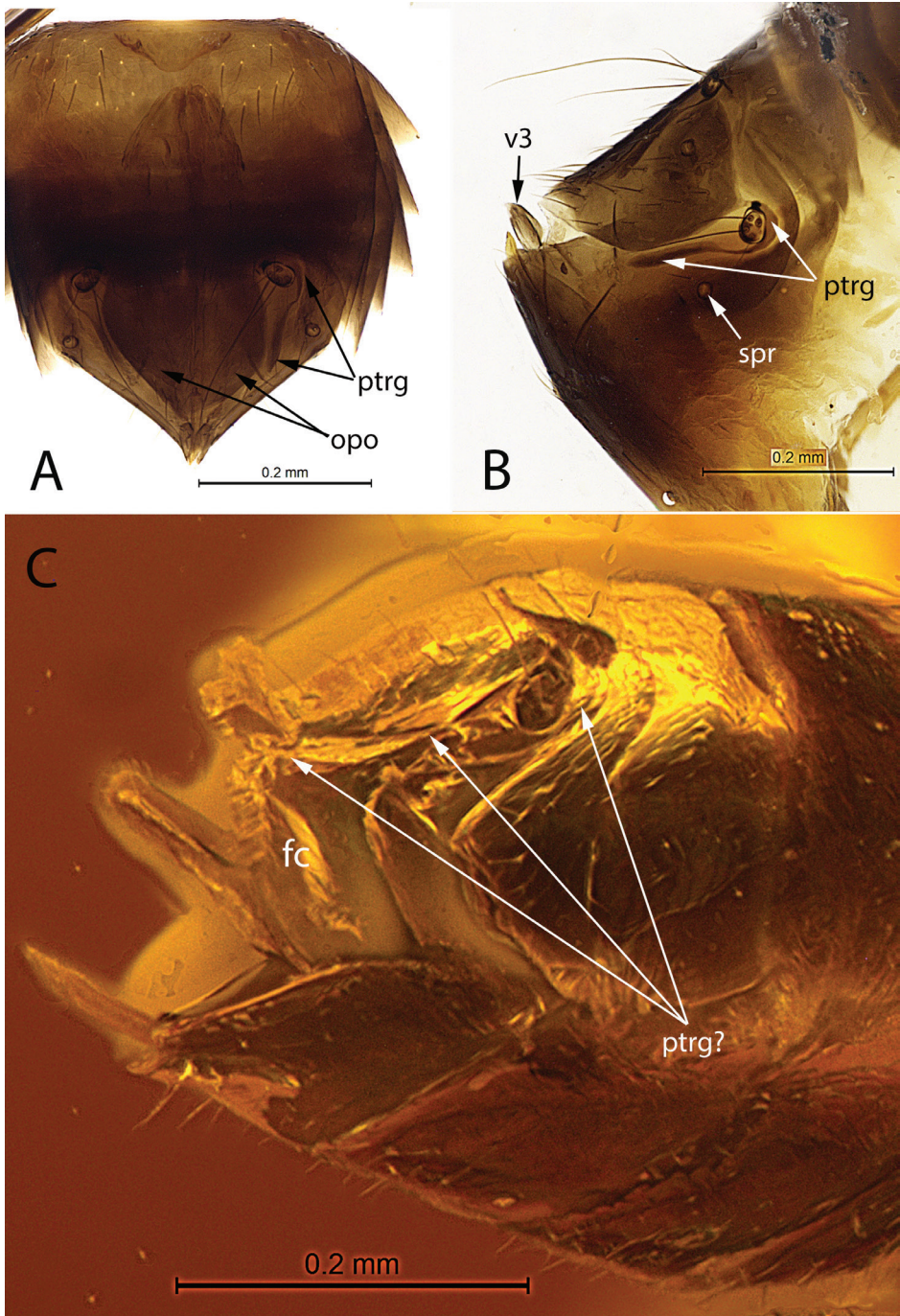


Figure 7. A, B *Ericydnus* sp., female **A** metasoma, dorsal (opo – outer plates of ovipositor, ptrg – paratergite) **B** apex of metasoma, lateral (spr – spiracle on the lateral lobe of the Mt7, v3 – ovipositor sheaths) **C** *Electronoyesella antiqua* gen. et sp. nov., holotype female, apex of metasoma, lateral (fc – filamentous connection). Scale bars: 0.2 mm.

Cerci of the earliest known middle Eocene Encyrtidae from Sakhalinian amber are close to each other, located at the very top of the gaster, similar to the ground plan state for Chalcidoidea. Then, tentatively in late Eocene, they began to shift towards the base of the gaster and the distance between them began to increase (figs 12–14 in Simutnik 2021). This process was most likely the result of adaptation to parasitization of the host, probably by Coccinea (for example, *Archaeocercoides puchkovi* Simutnik, 2022 from Rovno amber was fossilized near an undescribed crawler, see fig. 1C, D in Simutnik et al. 2022a). As the cerci advanced forward, Mt8 (or syntergum Mt8+Mt9) and then the previous terga began to separate into a dorsal part and lateral lobes (Fig. 7).

The process of cercus advancement in both Encyrtinae and Tetracneminae occurred independently and in parallel, and it began precisely in the late Eocene, since the cerci still remain in the apical or subapical position in most encyrtids from European ambers. Cerci extremely advanced to the base of the metasoma, as in many extant taxa, have not been found in known Eocene Encyrtidae.

The elongate sclerotized strip (paratergite) in Tetracneminae apparently separated from the lateral margin of the syntergum when the latter became long enough and the cercal plates advanced significantly towards the base of the gaster. The true paratergite must directly maintain a connection to tergite IX (Mt8). This connection is traceable in many species of extant *Ericydnus* around the side and anterior of the cercal plate (Fig. 7A, B) but not in any other genera where the connection, at most is at best tenuous (J. S. Noyes, pers. comm. 2022). What is possibly the paratergite of *Electronoyesella* running anteriorly to the outside of the cercal plate is very similar to the paratergite of *Ericydnus* and may provide morphological evidence for the existence of the subfamily Tetracneminae in the late Eocene.

Acknowledgements

We are sincerely grateful to John S. Noyes, S. Bruce Archibald, Aleksandr P. Rasnitsyn, and Petr Janšta for their help and valuable comments, and to Anatoly P. Vlaskin (SIZK) for cutting and polishing the sample. This work was supported by grant NRFU No. 2020/02/0369 (to S.A. Simutnik).

References

- Gibson GAP (1997) Chapter 2, Morphology and terminology. In: Gibson GAP, Huber JT, Woolley JB (Eds) Annotated keys to the genera of Nearctic Chalcidoidea (Hymenoptera). NRC Research Press, Ottawa, 16–45. [794 pp.]
- Heraty JM, Burks RA, Cruaud A, Gibson GA, Liljeblad J, Munro J, Rasplus JY, Delvare G, Janšta P, Gumovsky A, Huber JT, Woolley JB, Krogmann L, Heydon S, Polaszek A, Schmidt S, Darling DC, Gates MW, Mottern J, Murray E, Dal Molin A, Triapitsyn S, Baur H, Pinto JD, van Noort S, George J, Yoder M (2013) A phylogenetic analysis of the megadiverse Chalcidoidea (Hymenoptera). *Cladistics* 29: 466–542. <https://doi.org/10.1111/cla.12006>

- Manukyan AR (1999) New data on fossil faunas of chalcidoids of the families Encyrtidae and Tetracampidae (Hymenoptera, Chalcidoidea). International Conference “The biodiversity of terrestrial and soil invertebrates in the North”, Syktyvkar, September 15–17. Abstracts, Syktyvkar, 132–134. [in Russian]
- Mitov PG, Perkovsky EE, Dunlop JA (2021) Harvestmen (Arachnida: Opiliones) in Eocene Rovno amber (Ukraine). *Zootaxa* 4984: 43–72. <https://doi.org/10.11646/zootaxa.4984.1.6>
- Noyes JS (2004) Encyrtidae of Costa Rica (Hymenoptera: Chalcidoidea), 2. *Metaphycus* and related genera, parasitoids of scale insects (Coccoidea) and whiteflies (Aleyrodidae). *Memoirs of the American Entomological Institute* 73: 1–459.
- Noyes JS, Hayat M (1994) Oriental mealybug parasitoids of the Anagyrini (Hymenoptera: Encyrtidae). Wallingford, Oxon: CAB International, [viii +] 554 pp.
- Noyes JS, Woolley JB (1994) North American encyrtid fauna (Hymenoptera: Encyrtidae): taxonomic changes and new taxa. *Journal of Natural History* 28: 1327–1401. <https://doi.org/10.1080/00222939400770681>
- Oلمي M, Guglielmino A, Vasilenko DV, Perkovsky EE (2022a) Discovery of the first apterous pincer wasp from amber, with description of a new tribe, genus and species of Apodyryniinae (Hymenoptera, Dryinidae). *Zootaxa* 5162(1): 54–66. <https://doi.org/10.11646/zootaxa.5162.1.3>
- Oلمي M, Eggs B, Capradossi L, van de Kamp T, Perkovsky EE, Guglielmino A, Vasilenko DV (2022b) A new species of *Bocchus* from upper Eocene Rovno amber (Hymenoptera, Dryinidae). *Journal of Hymenoptera Research* 92: 257–272. <https://doi.org/10.3897/jhr.92.87084>
- Peters RS, Niehui O, Gunkel S, Bläser M, Mayer C, Podsiadlowski L, Kozlov A, Donath A, van Noort S, Liu Sh, Zhou X, Misof B, Heraty J, Krogmann L (2018) Transcriptome sequence-based phylogeny of chalcidoid wasps (Hymenoptera: Chalcidoidea) reveals a history of rapid radiations, convergence, and evolutionary success. *Molecular Phylogenetics and Evolution* 120: 286–296. <https://doi.org/10.1016/j.ympev.2017.12.005>
- Sharkov AV (1985) Encyrtids (Hymenoptera, Chalcidoidea, Encyrtidae) of the southern Far East of the USSR [dissertation]. Extended Abstract of Cand. Sci. (Biol.). Leningrad. [in Russian]
- Simutnik SA (2015a) A new fossil genus of Encyrtidae (Hymenoptera: Chalcidoidea) from late Eocene Danish amber. *Russian Entomological Journal* 24(1): 73–75. <https://doi.org/10.15298/rusentj.24.1.07>
- Simutnik SA (2015b) Description of two new monotypical genera of encyrtid wasps (Hymenoptera, Chalcidoidea: Encyrtidae), based on males from the middle Eocene Sakhalin amber. *Entomological Review* 95(7): 937–940. <https://doi.org/10.1134/S0013873815070118>
- Simutnik SA (2021) The earliest Encyrtidae (Hymenoptera, Chalcidoidea). *Historical Biology*. 33(11): 2931–2950. <https://doi.org/10.1080/08912963.2020.1835887>
- Simutnik SA, Perkovsky EE (2018) *Archaeocercus* gen. nov. (Hymenoptera, Chalcidoidea, Encyrtidae) from late Eocene Rovno amber. *Zootaxa* 4441(3): 543–548. <https://doi.org/10.11646/zootaxa.4441.3.8>
- Simutnik SA, Perkovsky EE, Gumovsky AV (2014) Review of the Late Eocene Encyrtidae (Hymenoptera, Chalcidoidea) with a description of the first fossil genus with filum spinosum. *Paleontological Journal* 48(1): 65–73. <https://doi.org/10.1134/S0031030114010122>

- Simutnik SA, Perkovsky EE, Vasilenko DV (2020) *Efesus trufanovi* Simutnik gen. et sp. n. (Hymenoptera: Chalcidoidea: Encyrtidae) from late Eocene Danish amber. Russian Entomological Journal 29(3): 298–302. <https://doi.org/10.15298/rusentj.29.3.10>
- Simutnik SA, Perkovsky EE, Vasilenko DV (2021a) *Sakhalinencyrtus leleji* Simutnik gen. et sp. nov. of earliest Encyrtidae (Hymenoptera, Chalcidoidea) from Sakhalinian amber. Journal of Hymenoptera Research 84: 361–372. <https://doi.org/10.3897/jhr.84.66367>
- Simutnik SA, Perkovsky EE, Khomych MR, Vasilenko DV (2021b) First record of the *Sulia glaesaria* Simutnik, 2015 (Hymenoptera, Chalcidoidea, Encyrtidae) from Rovno amber. Journal of Hymenoptera Research 88: 85–102. <https://doi.org/10.3897/jhr.88.75941>
- Simutnik SA, Perkovsky EE, Khomych MR, Vasilenko DV (2022a) Two new genera of Encyrtidae (Hymenoptera, Chalcidoidea) with reduced ovipositor sheaths. Journal of Hymenoptera Research 89: 47–60. <https://doi.org/10.3897/jhr.89.79180>
- Simutnik SA, Perkovsky EE, Vasilenko DV (2022b) *Protaphycus shuvalikovi* Simutnik gen. et sp. n. (Chalcidoidea, Encyrtidae, Encyrtinae) from Rovno amber. Journal of Hymenoptera Research 91: 1–9. <https://doi.org/10.3897/jhr.91.81957>
- Trjapitzin VA (1968) The problems of morphological evolution and the classification of the family Encyrtidae (Hymenoptera, Chalcidoidea). Readings in Memory of N.A. Kholodkovsky (1967), 44–62. [in Russian]
- Trjapitzin VA (1989) Parasitic Hymenoptera of the Fam. Encyrtidae of Palaearctics. Opre-deliteli po faune SSSR, izdavaemiye Zoologicheskim institutom AN SSSR 158: 1–489. [in Russian]
- Zuparko RL, Trjapitzin VA (2014) *Copidosoma archeodominnica* (Hymenoptera: Encyrtidae), a new species from Dominican amber. The Pan-Pacific Entomologist 89(4): 230–233. <https://doi.org/10.3956/2013-24.1>

***Protelenomus* Kieffer is a derived lineage of *Trissolcus* Ashmead (Hymenoptera, Scelionidae), with comments on the evolution of phoresy in Scelionidae**

Cheng-Jin Yan¹, Elijah Talamas², Zachary Lahey³, Hua-Yan Chen⁴

1 Institute of Agriculture and Biotechnology, Wenzhou Vocational College of Science and Technology, Wenzhou, 325006, China **2** Florida Department of Agriculture and Consumer Services, Division of Plant Industry, Gainesville, Florida, USA **3** USDA-ARS, U.S. Vegetable Laboratory, Charleston, South Carolina 29414, USA **4** Key Laboratory of Plant Resources Conservation and Sustainable Utilization, South China Botanical Garden, Chinese Academy of Sciences, Guangzhou 510650, China

Corresponding authors: Hua-Yan Chen (huayanc@scbg.ac.cn), Elijah Talamas (elijah.talamas@fdacs.gov)

Academic editor: Miles Zhang | Received 4 October 2022 | Accepted 5 November 2022 | Published 20 December 2022

<https://zoobank.org/6E9DA437-FFAD-4B50-A2EC-09D3A451872F>

Citation: Yan C-J, Talamas E, Lahey Z, Chen H-Y (2022) *Protelenomus* Kieffer is a derived lineage of *Trissolcus* Ashmead (Hymenoptera, Scelionidae), with comments on the evolution of phoresy in Scelionidae. Journal of Hymenoptera Research 94: 121–137. <https://doi.org/10.3897/jhr.94.95961>

Abstract

Species of the genus *Protelenomus* Kieffer (Platygastridae, Scelionidae) are phoretic egg parasitoids of coreid bugs. The discovery, DNA sequencing, and molecular phylogenetic analysis of a *Protelenomus* species phoretic on *Cletus punctiger* (Dallas) (Hemiptera, Coreidae) shows that *Protelenomus* is a derived lineage of *Trissolcus* Ashmead. *Protelenomus* is treated as a junior synonym and a new species of phoretic *Trissolcus*, *T. siliangae* Yan, Chen & Talamas, is described from China.

Keywords

Coreidae, egg parasitoid, Hemiptera, integrated taxonomy, phylogenetics

Introduction

Scelionid parasitoids of hemipteran eggs are the subject of active study, driven by the economic damage caused by a variety of bug pests, and by recent works that accelerate further advancement. These include progress in the taxonomy and systematics of these parasitoids, which underlie accurate identification and classification (Talamas et al. 2017; Talamas et al. 2019; Tortorici et al. 2019; Talamas et al. 2021). *Protelenomus*

Copyright Cheng-Jin Yan et al. This is an open access article distributed under the terms of the CC0 Public Domain Dedication.

Kieffer, a genus of egg parasitoids that are phoretic on Coreidae, was recently revised by Veenakumari et al. (2019), who described six new species, tripling the size of the genus. This treatment significantly expanded the known diversity of *Protelenomus* and brought attention to its uncertain generic status. Presently, *Protelenomus* cannot be unambiguously separated from *Trissolcus* Ashmead. Indeed, all of the characters used to define *Protelenomus* can be found in *Trissolcus*: T2 is longer than wide in *T. ancon* Johnson (Johnson 1991), *T. hyalinipennis* Rajmohana & Narendran has 4 clavomeres (Talamas et al. 2017), facial striae are found on species from both North America and Asia (Talamas et al. 2015; Talamas et al. 2017), and notauli are absent in many species (Johnson 1985; Talamas et al. 2017). In addition, *Trissolcus* species exhibit a wide range of sculpture on the frons, from coarsely rugose (*T. painei* (Ferrière)) to mostly smooth and shining (*T. perepelovi* (Kozlov)).

Even modification of the legs, which is pronounced in some species (e.g., *P. tibialis* Veenakumari), is not ubiquitous in *Protelenomus*. Given the nebulous boundary between *Protelenomus* and *Trissolcus*, we investigated the possibility that *Protelenomus* is a lineage derived from within *Trissolcus*, an idea first proposed by Masner (1976). The acquisition of freshly collected specimens, phoretic on Coreidae in China, combined with data made available by Talamas et al. (2019) and Vasilița et al. (2021), provided the opportunity to determine the placement of *Protelenomus* using molecular analysis.

Materials and methods

During a survey of insect pests and their parasitoids in a corn field in Wenzhou, Zhejiang Province, China, in the autumn of 2021, four female coreid bugs were found to each harbor a phoretic wasp dorsally on the head near the base of the antennae Fig. 1. Both the host and wasp specimens were collected and preserved in 100% ethanol until further study. The coreids were identified as *Cletus punctiger* (Dallas) using the key and description by Gupta and Singh (2013). All specimens are deposited in the Insect Collection of South China Botanical Garden, Chinese Academy of Sciences, Guangzhou, China (**SCBG**) and the Insect Collection of Wenzhou Vocational College of Science and Technology, Wenzhou, China (**WVCST**).

Morphological terms

Abbreviations and morphological terms used in text: **A1**, **A2**, ... **A12**: antennomere 1, 2, ... 12; **OOL**: ocellar-ocular length; **POL**: posterior ocellar length; **OD**: ocellar diameter; **T1**, **T2**, ... **T7**: metasomal tergite 1, 2, ... 7; **S1**, **S2**, ... **S7**: metasomal sternite 1, 2, ... 7. Morphological terminology otherwise generally follows Mikó et al. (2007), Talamas et al. (2017), and Tortorici et al. (2019).

Character annotations

sasu	subacroleural sulcus (Fig. 4B);
mtnm	metanotum (Figs 4A, 5B);
mtpm	metapostnotum (Figs 4A, 5B);
pl	parapsidal line (Fig. 5A, B);
ppm	propodeum (Figs 4A, 5B).

Molecular analysis

Genomic DNA was extracted using a TIANamp Micro DNA Kit (Tiangen Biotech (Beijing), Co., Ltd), following the nondestructive DNA extraction protocol described in Taekul et al. (2014). Four molecular markers were amplified: two nuclear ribosomal (18S and 28S D2-3), one mitochondrial protein (COI), and one single-copy nuclear protein (wingless). Polymerase chain reactions were performed using Tks Gflex DNA Polymerase (Takara) with primer pairs shown in Table 1 and conducted in a T100 Thermal Cycler (Bio-Rad). Thermocycling conditions consisted of an initial denaturing step at 94 °C for 5 min, followed by 35 cycles of 94 °C for 30 s, 50 °C for 30 s, 72 °C for 30 s and an additional extension at 72 °C for 5 min. Amplicons were directly sequenced in both directions with forward and reverse primers on an Applied Biosystems (ABI) 3730XL by Guangzhou Tianyi Huiyuan Gene Technology Co., Ltd. (Guangzhou, China). Chromatograms were assembled with Geneious 11.0.3. The assembled sequence was translated to amino acids using the invertebrate mitochondrial code to check for stop codons and frame shifts and was compared via BLAST against the GenBank database to check for contamination and pseudogenes (e.g., nuclear mitochondrial DNA, NUMT) as implemented in Geneious 11.0.3. The sequences generated from this study are deposited in GenBank (accession numbers are shown in Suppl. material 1).

Phylogenetic analysis

Multiple sequence alignments for each gene were performed with MAFFT v7.490 (Katoh and Standley 2013) by the E-INS-i strategy for 18S and 28S, and the L-INS-i strategy for COI and wingless. Maximum likelihood phylogenetic analyses were conducted in IQ-TREE (v. 2.1.3) (Minh et al. 2020) following the methodology of Chen et al. (2021). Eight partitions were specified in the original concatenated alignment: one for each ribosomal gene and three for each codon position in COI and wingless (Chernomor et al. 2016). ModelFinder was employed to determine the best nucleotide substitution model for each partition and to merge partitions to increase overall model fit (Kalyaanamoorthy et al. 2017). Branch support was estimated with 1000 ultrafast bootstrap replicates (Hoang et al. 2018). Ten independent tree searches were conducted, and we present the tree with the greatest log-likelihood score. *Maruzza japonica* Mineo was selected as the outgroup.

Table 1. Primer pairs used in this study.

Gene	Primer name	Primer sequence 5' to 3'	Reference
<i>18S</i>	ai	CTGAGAAACGGCTACCACATC	Whiting et al. (1997)
<i>18S</i>	18S-5R	CTTGGCAAATGCTTTCGC	Giribet et al. (1996)
<i>28S</i>	D23F	GAGAGTTCAAGAGTACGTG	Whiting et al. (1997)
<i>28S</i>	28Sb	TCGGAAGGAACCAGCTACTA	Whiting et al. (1997)
<i>COI</i>	HCO-2198	TAAACTTCAGGGTGACCAAAAAATCA	Folmer et al. (1994)
<i>COI</i>	LCO-1490	GGTCAACAAATCATAAAGATATTGG	Folmer et al. (1994)
<i>Wingless</i>	ScwWgIF-1	GTAAGTGTACACGGGATGTC	Chen et al. (2021)
<i>Wingless</i>	ScwWgIR-1	TTGACTTCACAGCACCAGT	Chen et al. (2021)

Imaging

Photographs of live specimens were taken with a Canon 5D Mark III (Tokyo, Japan) camera with a 100 mm macro lens. Multifocal images of mounted specimens were made using a Nikon SMZ25 microscope with a Nikon DS-Ri 2 digital camera system and a Macropod Microkit photography system. All image stacks were rendered using Helicon Focus. Scanning electron micrographs were produced using a Phenom Pro Desktop SEM. Images were post-processed with Adobe Photoshop CS6 Extended.

Results

The phylogenetic analysis retrieved *Trissolcus siliangae* Yan, Chen & Talamas sp. nov. embedded within *Trissolcus*, as the sister taxon to a clade comprising (*T. vindicius* + *T. cultratus*) + (*T. corai* + (*T. japonicus* + *T. plautiae*)) (Fig. 6).

Treatment of *Protelenomus* as a derived lineage of *Trissolcus* is also supported by a morphological character, the subacroleural sulcus. Talamas et al. (2017) proposed that this sulcus had value for circumscribing *Trissolcus* and noted that it was present in all Palearctic *Trissolcus* except for *T. exerrandus* Kozlov & Lê. Notably, a preliminary phylogenetic analysis indicates that *T. exerrandus* does not belong in *Trissolcus*, although its destination is presently unclear. In their synonymy of *Latoni* Kononova, Vasilița et al. (2021) reported that *T. planus* (Kononova) does not have a subacroleural sulcus. In the figures provided in the revision of *Protelenomus* by Veena-kumari et al. (2019), the subacroleural sulcus is present in *T. anoplocnemidis* (Ghesquière), *T. gajadanta* (Veenakumari), *T. maasai* (Veenakumari), *T. tibialis* (Veenakumari), and *T. zulu* (Veenakumari), whereas it is clearly absent in *T. flavicornis* (Kieffer). This character can be difficult to assess in species with coarse sculpture and from images with glare on the specimens. In *T. siliangae* sp. nov., the subacroleural sulcus is clearly visible in Figs 3F and 4B. Given that this sulcus appears to be absent in some highly derived species, we consider that it may still be a synapomorphy for

the genus, albeit with secondary losses. The subacroleural sulcus thus remains useful for affirming placement in *Trissolcus*, but its absence cannot be used to exclude species from the genus.

Synonymy

Trissolcus Ashmead

Trissolcus Ashmead, 1893: 161 (original description. Type: *Telenomus brochymenae* Ashmead, by original designation. Key to species).

Asolcus Nakagawa, 1900: 17 (original description. Type: *Asolcus nigripedius* Nakagawa, by monotypy. Synonymized with *Trissolcus* by Masner (1964)).

Protelenomus Kieffer syn. nov., 1906: 6 (original description. Type: *Protelenomus flavicornis* Kieffer, by monotypy).

Aphanurus Kieffer, 1912: 10, 69 (original description. Type: *Teleas semistriatus* Nees von Esenbeck, by original designation. Preoccupied by *Aphanurus* Looss (1907) (Trematoda).

Immsia Cameron, 1912: 104 (original description. Type: *Immsia carinifrons* Cameron, by monotypy. Synonymized with *Microphanurus* Kieffer by Nixon (1938)).

Microphanurus Kieffer: Kieffer 1926: 16, 91 (replacement name for *Aphanurus* Kieffer. Type: *Teleas semistriatus* Nees von Esenbeck, by substitution of *Microphanurus* for *Aphanurus*. Description, keyed, key to species. Synonymized with *Asolcus* Nakagawa by Watanabe (1951)).

Epinomus Ghesquière, 1948: 324 (original description. Type: *Epinomus anoplocnemidis* Ghesquière, by monotypy and original designation. Synonymized with *Protelenomus* by Masner (1976)).

Latoni Kononova, 1982: 76 (original description. Type: *Latoni* *planus* Kononova, by monotypy and original designation. Synonymized with *Trissolcus* by Vasilița et al. (2021)).

Kozlotelenomus Mineo, O'Connor & Ashe, 2009: 193 (original description. Type: *mopsus* Nixon, by monotypy and original designation. Synonymized with *Trissolcus* by Talamas and Buffington (2015)).

Ioseppinella Mineo, O'Connor & Ashe, 2010: 267 (original description. Type species *Ioseppinella serena* Mineo, O'Connor & Ashe, by monotypy and original designation. Synonymized with *Trissolcus* by Vasilița et al. (2021)).

Generic transfers

Trissolcus anoplocnemidis (Ghesquière), comb. nov.

Epinomus anoplocnemidis Ghesquière, 1948: 325 (original description); Risbec 1950: 568, 576 (description, keyed).

Protelenomus anoplocnemidis (Ghesquière): Masner 1976: 77 (generic transfer); Johnson 1992: 565 (cataloged, type information); Rajmohana 2013: 3 (description); Veenakumari et al. 2019: 384, 389 (diagnosis, keyed).

***Trissolcus areolatus* (Rajmohana), comb. nov.**

Protelenomus areolatus Rajmohana, 2013: 2 (original description, diagnosis); Veenakumari et al. 2019: 384 (keyed).

***Trissolcus flavicornis* (Kieffer), comb. nov.**

Protelenomus flavicornis Kieffer, 1906: 7 (original description); Kieffer 1926: 22 (description); Bin 1974: 458 (type information); Johnson 1992: 565 (cataloged, type information); Veenakumari and Mohanraj 2015: 306 (description, new distribution record for India); Veenakumari et al. 2019: 384, 389 (description, diagnosis, keyed).

***Trissolcus gajadanta* (Veenakumari), comb. nov.**

Protelenomus gajadanta Veenakumari, 2019: 384 (original description, keyed)

***Trissolcus lutuli* (Veenakumari), comb. nov.**

Protelenomus lutuli Veenakumari, 2019: 384, 385 (original description, keyed)

***Trissolcus maasai* (Veenakumari), comb. nov.**

Protelenomus maasai Veenakumari, 2019: 384, 386 (original description, keyed)

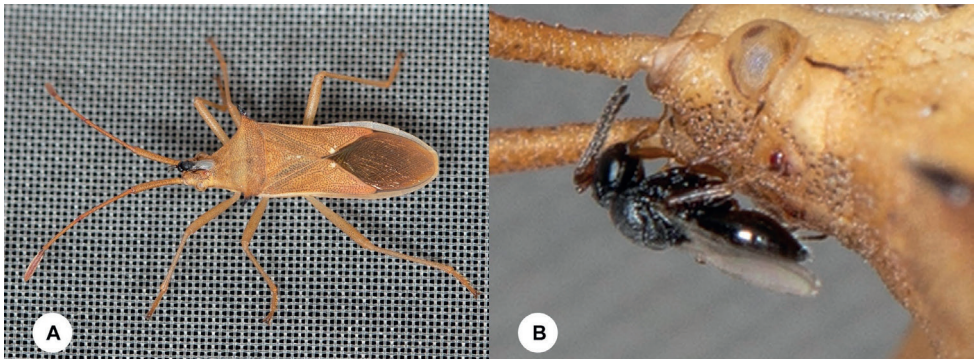


Figure 1. **A** female *Trissolcus siliangae* on *Cletus punctiger* **B** closeup of *T. siliangae* on *C. punctiger* from Fig. 1A.

***Trissolcus tibialis* (Veenakumari), comb. nov.**

Protelenomus tibialis Veenakumari, 2019: 384, 387 (original description, keyed)

***Trissolcus yao* (Veenakumari), comb. nov.**

Protelenomus yao Veenakumari, 2019: 384, 388 (original description, keyed)

***Trissolcus zulu* (Veenakumari), comb. nov.**

Protelenomus zulu Veenakumari, 2019: 384, 388 (original description, keyed)

Species description

***Trissolcus siliangae* Yan, Chen & Talamas, sp. nov.**

<https://zoobank.org/DAD99C7C-D538-43D9-A43B-577A27D1C9B3>

Figs 1–4

Description. Female body length: 1.28 mm (n = 4). Body color: head, mesosoma, and metasoma black, shining. Mandible color: red-brown. Leg color: coxae and tarsi dark brown, rest of legs yellow-brown. Tegulae yellow-brown. Antennal color: radicle and A1–A2 yellow to brown, darker dorsally; A3–A11 dark brown.

Head. Length of radicle: less than width of clypeus. Claval formula: A8–A11:1-1-1-1. Facial striae: present. Number of clypeal setae: 4. Shape of gena in lateral view: moderately wide, bulging. Genal carina: absent. Malar striae: absent. Sculpture of malar sulcus: smooth. Orbital furrow: expanded at intersection with malar sulcus, medial margin of furrow poorly defined. Macrosculpture of frons directly dorsal to the antennal scrobe: absent. Preocellar pit: absent. Setation of lateral frons: sparse. Punctuation of lateral frons: absent. Sculpture directly ventral to preocellar pit: coriaceous microsculpture. Rugae on lateral frons: absent. OOL: about one ocellar diameter. Hyperoccipital carina: absent. Macrosculpture of posterior vertex: absent. Microsculpture on posterior vertex along occipital carina: coriaceous. Anterior margin of occipital carina: crenulate. Medial part of occipital carina in dorsal view: rounded.

Mesosoma. Epomial carina: present. Macrosculpture of lateral pronotum directly anterior to netrion: finely rugulose. Netrion sulcus: incomplete, only weakly defined ventrally. Pronotal suprahumeral sulcus in posterior half of pronotum: absent. Number of episternal foveae: 2. Course of episternal foveae ventrally: abutting dorsal apex of acetabular carina. Course of episternal foveae dorsally: distinctly separate from mesopleural pit. Subacropleurial sulcus: present. Speculum: transversely strigose. Mesopleural pit: simple. Mesopleural carina: absent. Sculpture of femoral depression: smooth. Patch of striae at posteroventral end of femoral depression: present, striae orthogonal to long axis of femoral depression. Setal patch at posteroventral end of femoral depression:

present as a line of setae. Microsculpture of anteroventral mesopleuron: present in anterior portion, smooth posteriorly. Macrosculpture of anteroventral mesopleuron: absent. Postacetabular sulcus: present as a smooth furrow. Mesopleural epicoxal sulcus: indicated by shallow foveae. Setation of posteroventral metapleuron: absent. Sculpture of dorsal metapleural area: rugulose. Posterodorsal metapleural sulcus: undifferentiated. Paracoxal sulcus in ventral half of metapleuron: absent. Length of anteroventral extension of metapleuron: short, not reaching base of mesocoxa. Metapleural epicoxal sulcus: indistinguishable from rugose sculpture. Mesoscutal humeral sulcus: comprised of shallow foveae. Median mesoscutal carina: absent. Microsculpture of mesoscutum: coriaceous. Mesoscutal suprahumeral sulcus: comprised of shallow foveae. Length of mesoscutal suprahumeral sulcus: about two-thirds the length of anterolateral edge of mesoscutum. Parapsidal line: present. Notaulus: absent. Median protuberance on anterior margin of mesoscutellum: absent. Shape of dorsal margin of anterior lobe of axillar crescent: flat. Sculpture of anterior lobe of axillar crescent: dorsoventrally strigose. Area bound by axillar crescent: smooth. Macrosculpture of mesoscutellum: absent. Microsculpture on mesoscutellum: coriaceous. Median mesoscutellar carina: absent. Setation of posterior scutellar sulcus: absent. Form of metascutellum: broad, short, rugose projection. Metanotal trough: foveate, foveae occupying less than half of metanotal height. Metapostnotum: invaginated laterally, propodeum and metanotum directly adjacent. Anteromedial portion of metasomal depression: rugulose.

Wings. Length of postmarginal vein: about twice as long as stigmal vein. Fore wing apex: reaching beyond T6.

Legs. Color: coxae and distal tarsomeres dark brown to black, otherwise yellow to light brown. Anteroventral area of hind femora: not covered by setae. Femur and tibia not enlarged. Basitarsi of fore leg with a row of densely stout bristles at basal half. Claws well developed, curved.

Metasoma. Width of metasoma: about equal to width of mesosoma. Longitudinal striae on T1 posterior to basal costae: present. Number of sublateral setae (on one side): 0. Setation of laterotergite 1: absent. Striation on T2: extending about half the length of the tergite, weakly indicated. Setation of T2: present along lateral margin. Setation of laterotergite 2: present. Striation on S2 striate: present laterally, length of striae extending up to anterior half, remainder smooth. S2 felt fields: present. Sculpture of S3–S6: setigerous punctate.

Male. Unknown.

Diagnosis. Moniliform antennae in females are rare in Scelionidae, shared in *Trissolcus* by *T. siliangae*, *T. flavicornis*, *T. gajadanta*, and *T. planus*; these species also have a single papillary sensillum on each clavomere. Care should be taken to count the antennomeres (11 in females, 12 in males) so that female specimens are not mistaken for males. Clavomeres that are only slightly wider than the preceding flagellomeres are more common, found in many species of the former *Protelenomus* and in more typical *Trissolcus* such as *T. sipioides*.

Trissolcus siliangae has a laterally invaginated metapostnotum, as in *T. hullensis* (Johnson 1985), which is found in a minority of *Trissolcus* species. In Veenakumari et

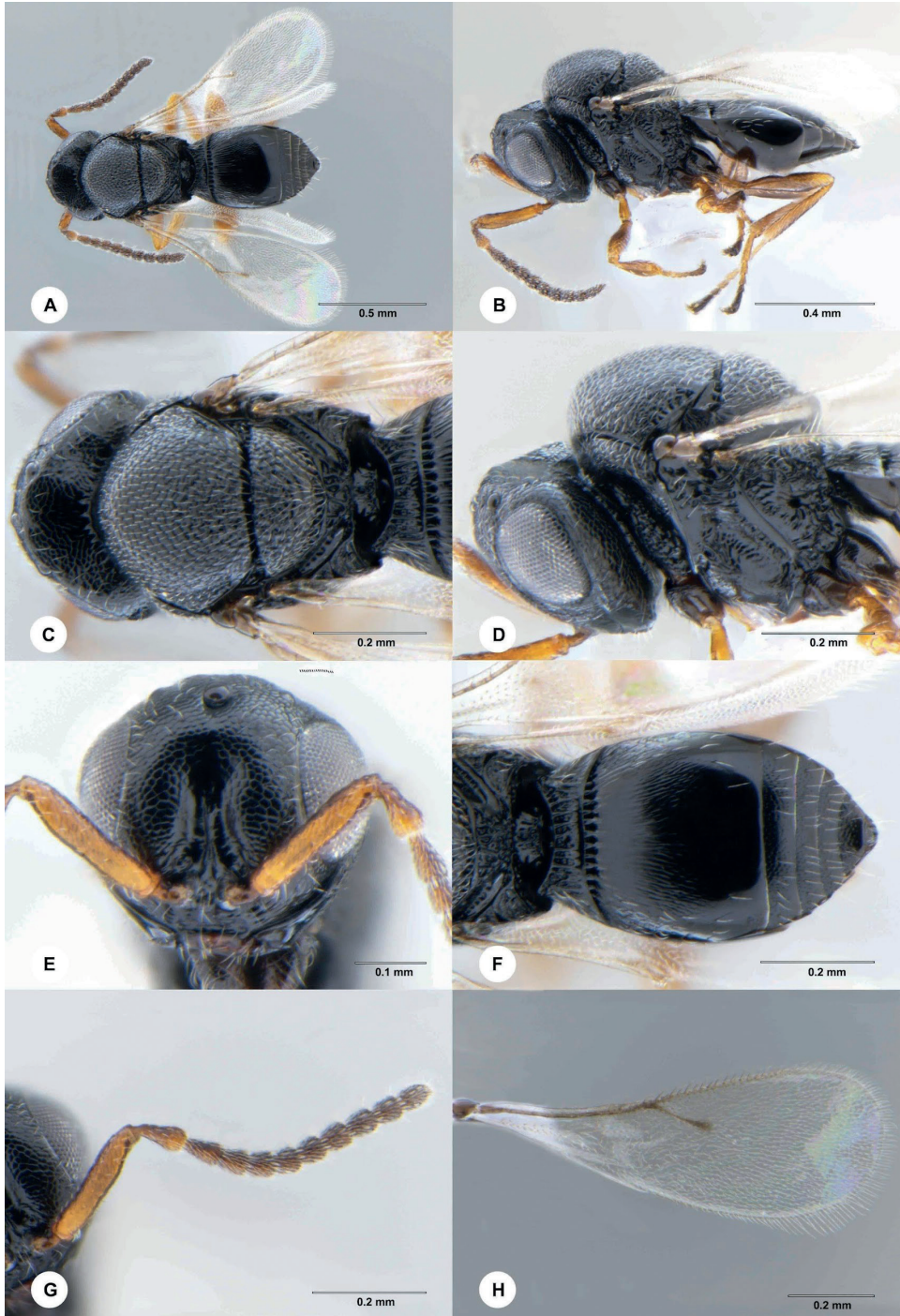


Figure 2. *Trissolcus siliangae*, paratype, female (SCAU 3042799) **A** dorsal habitus **B** lateral habitus **C** head and mesosoma, dorsal view **D** head and mesosoma, lateral view **E** head, anterior view **F** meta-soma, dorsal view **G** antenna **H** fore wing.

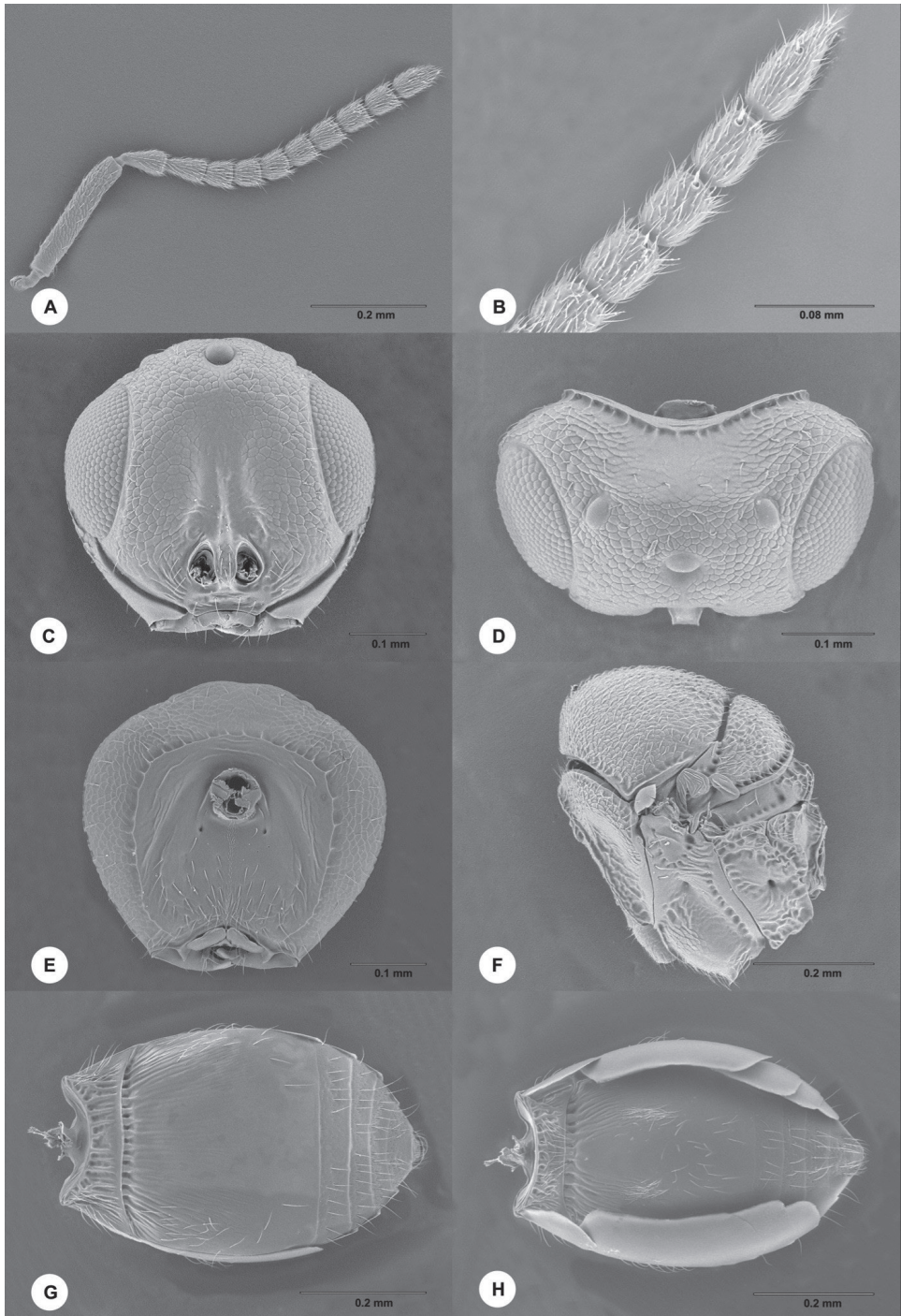


Figure 3. *Trissolcus siliangae*, paratype, female (SCAU 3042799) **A** antenna **B** apical antennal segments **A** head, anterior view **D** head, dorsal view **E** head, ventral view **F** mesosoma, lateral view **G** metasoma, dorsal view **H** metasoma, ventral view.

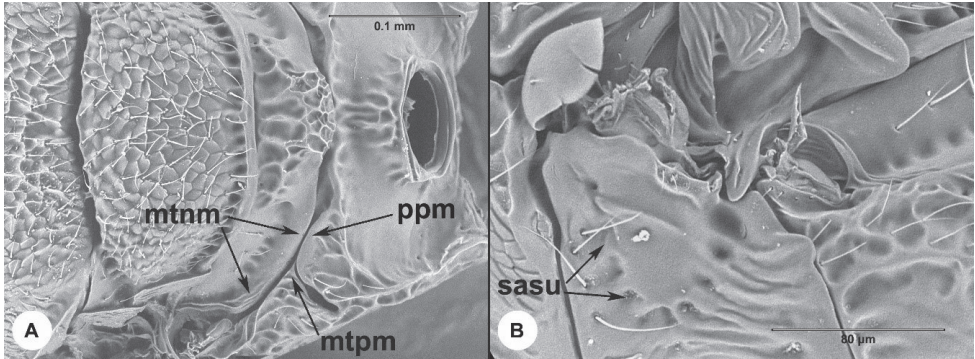


Figure 4. *Trissolcus siliangae*, paratype, female (SCAU 3042799) **A** mesosoma, dorsal view **B** dorsal mesopleuron, lateral view.

al. (2019), the metapostnotum in *T. flavicornis* appears to extend medially, separating the propodeum from the metanotum until it reaches the vicinity of the lateral margin of the metascutellum (see figures 27, 29, and 31 of that publication). We find this to be the case for *T. gajadanta* as well, based on examination of a specimen from Ivory Coast (Fig. 5). *Trissolcus siliangae* can thus be separated by the combination of the moniliiform antennae, claval formula (1-1-1-1), and lateral invagination of the metapostnotum. Additionally, *T. siliangae* can be separated from the very similar *T. gajadanta* by the striation on T2: robust in the anterior $\frac{2}{3}$ of the tergite in *T. gajadanta* and only weakly present in *T. siliangae*; and by the robust parapsidal lines in *T. gajadanta*, which are not indicated in *T. siliangae*. Notably, the posterior head in *T. gajadanta* has two concavities lateral to a dorsoventral median ridge, with the dorsal part of the occipital carina located low on the posterior head (Fig. 5B).

Etymology. This species is named after one of its collectors, Dr. Siliang Wang, for her discovery of this species.

Material examined. *Holotype*, female: **CHINA:** Zhejiang, Wenzhou, corn field, 27.609301°N, 120.508985°E, phoretic on *Cletus punctiger* Dallas, 10.IX.2021, Cheng-jin Yan, SCAU 3042644 (deposited in SCBG). *Paratypes:* (3 females) **CHINA:** 2 females, same data as holotype, SCAU 3042799, 3041198 (SCBG); 1 female, **CHINA:** Zhejiang, Wenzhou, corn field, 27.609301°N, 120.508985°E, phoretic on *Cletus punctiger* Dallas, 10.IX.2021, Siliang Wang, SCAU 3044000 (WVCST).

Distribution. China (Zhejiang).

Discussion

The phenomenon of phoresy has been documented in a variety of scelionids: *Paratelenomus anu* Rajmohana, Sachin & Talamas (Rajmohana et al. 2019), *Thoronella* Masner (Carlow 1992), *Synoditella* Muesebeck (Lanham and Evans 1958), *Scelicerdo* Muesebeck (Brues 1917), *Scelio* Latreille (Ramachandra Rao

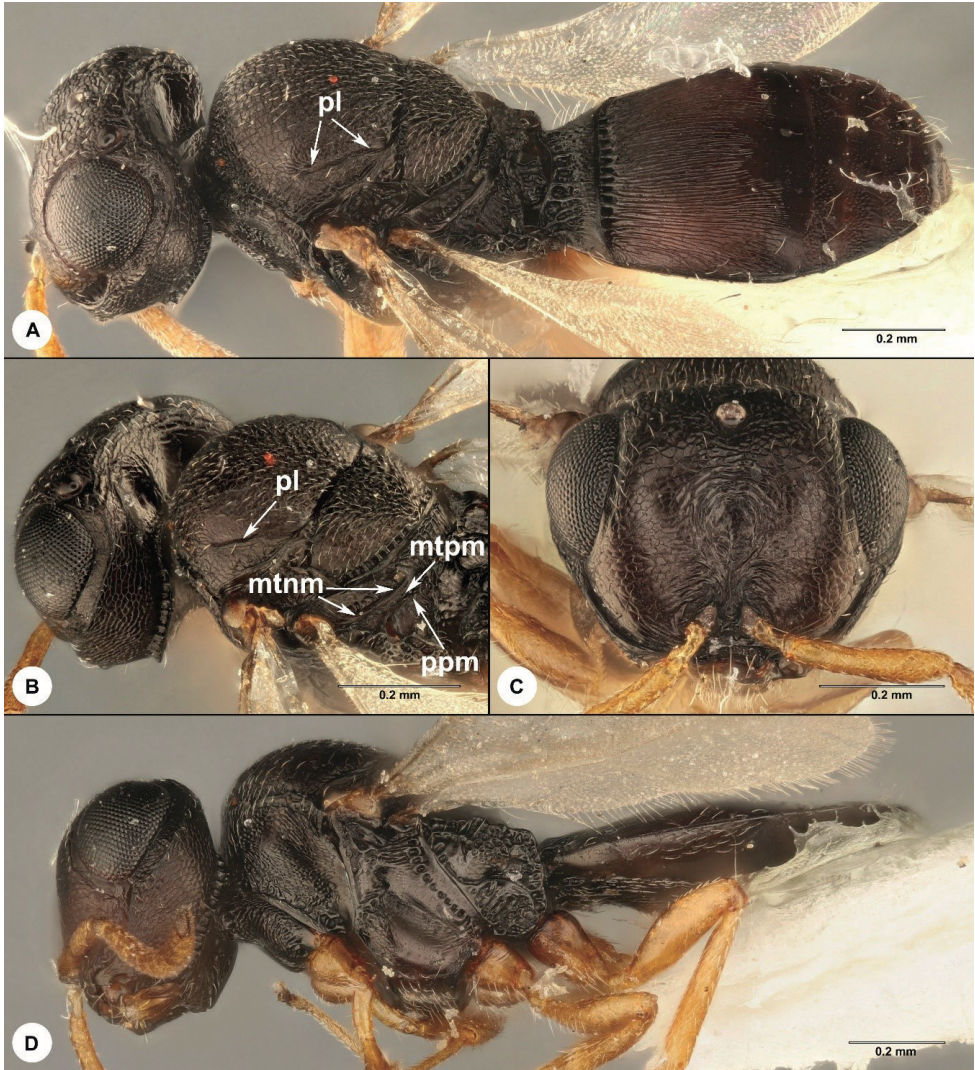


Figure 5. *Trissolcus gajadanta*, female (OSUC 398371) **A** head, mesosoma, metasoma, dorsolateral view **B** head and mesosoma, posterolateral view **C** head, anterior view **D** head, mesosoma, metasoma, lateral view.

1952), *Mantibaria* Kirby (Maglić and Žikić 2021), *Telenomus* (Orr et al. 1986; Arakaki et al. 1995), and *Trissolcus*. These taxa are distantly related within Scelionidae and present examples of evolutionary convergence. Phoresy occurs in *Trissolcus*, *Paratelenomus*, and some *Telenomus* that parasitize heteropteran eggs and are part of a scelionid radiation on Hemiptera (Chen et al. 2021). The scelionids not associated with Hemiptera are more distantly related and they also attack more distantly related hosts: Orthoptera, Mantodea, Lepidoptera, and Odonata, although it should be noted that phoretic parasitoids of Lepidoptera can be found within *Telenomus* (Arakaki et al. 1995). Detailed examination of this assortment of relationships may

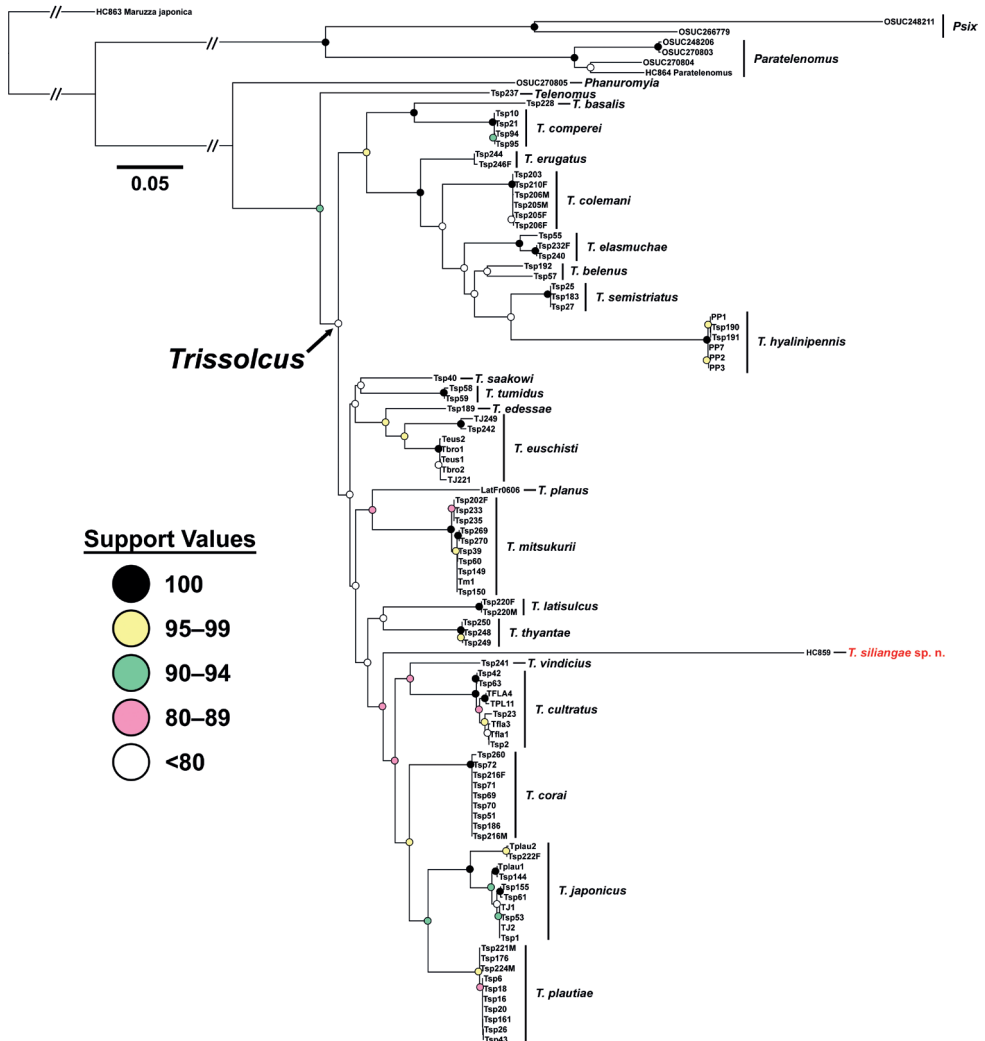


Figure 6. Four-gene maximum likelihood phylogenetic analysis of a modified dataset of Talamas et al. (2019) and Vasilița et al. (2021). Scale bar in the expected number of nucleotide substitutions per site. Ultrafast bootstrap support values indicated by colored circles at nodes. Some nodes were not annotated due to short branch lengths.

yield information on the selection pressures for phoresy, which may include finding the eggs or reaching the eggs at a stage sufficiently early for parasitoid development to occur, or to have a competitive advantage. In *Trissolcus*, interspecific competition is common, and being the first parasitoid may yield an advantage for intrinsic (larval) competition. Phoresy in *Trissolcus* is worth further examination, both in terms of behavioral studies that will illuminate its benefits, and further phylogenetic analysis to determine if it has evolved more than once in the genus, and to identify sister taxa to phoretic lineages.

Acknowledgements

This study was supported by the National Natural Science Foundation of China (31900346, 32100360), the Major Scientific and Technological Innovation Project of Wenzhou (ZN2019002), the Wenzhou Agricultural Harvest Found (FSJH2021004), the Science and Technology Commissioner Project of Wenzhou (X20210058) and the Wencheng County's Second Phase of Innovation and Entrepreneurship Seed Fund (2019NKY09). We thank Lubomir Masner (CNCI) for generously donating a specimen of *Trissolcus gajadanta* and Natalie McGathey (FDACS/DPI) for photographing it. Zachary Lahey is a participant of the Oak Ridge Institute for Science and Education (ORISE) Agricultural Research Service (ARS) Research Participation Program, supported by the USDA-ARS U.S. Vegetable Laboratory in Charleston, SC, USA. Elijah Talamas was supported by the Florida Department of Agriculture and Consumer Services, Division of Plant Industry. Mention of trade names or commercial products in this article is solely for the purpose of providing specific information and does not imply recommendation or endorsement by the USDA.

References

- Arakaki N, Wakamura S, Yasuda T (1995) Phoresy by an egg parasitoid, *Telenomus euproctidis* (Hymenoptera: Scelionidae), on the tea tussock moth, *Euproctis pseudoconspersa* (Lepidoptera: Lymantriidae). *Applied Entomology and Zoology* 30(4): 602–603. <https://doi.org/10.1303/aez.30.602>
- Ashmead WH (1893) A monograph of the North American Proctotrypidae. *Bulletin of the United States National Museum* 45: 1–472. <https://doi.org/10.5962/bhl.title.38713>
- Bin F (1974) The types of Scelionidae [Hymenoptera: Proctotrupoidea] in some Italian collections (Museums of Genoa and Florence, Institute of Portici). *Entomophaga* 19: 453–466. <https://doi.org/10.1007/BF02372781>
- Brues CT (1917) Adult Hymenopterous Parasites Attached to the Body of Their Host. *Proceedings of the National Academy of Sciences* 3: 136–140. <https://doi.org/10.1073/pnas.3.2.136>
- Cameron JC (1912) On the parasitic Hymenoptera reared at Dehra Dun, northern India, from the lac (*Tachardia*) and sal insects. *Indian Forest Records* 4: 91–110.
- Carlow T (1992) *Thoronella* sp. (Hymenoptera: Scolionidae) discovered on the thorax of an Aeshnidae (Anisoptera). *Notulae Odonatologicae* 3: 149–150.
- Chen H, Lahey Z, Talamas EJ, Valerio AA, Popovici OA, Musetti L, Klompen H, Polaszek A, Masner L, Austin AD, Johnson NF (2021) An integrated phylogenetic reassessment of the parasitoid superfamily Platygastroidea (Hymenoptera: Proctotrupomorpha) results in a revised familial classification. *Systematic Entomology* 46(4): 1088–1113. <https://doi.org/10.1111/syen.12511>
- Chernomor O, von Haeseler A, Minh BQ (2016) Terrace aware data structure for phylogenomic inference from supermatrices. *Systematic Biology* 65(6): 997–1008. <https://doi.org/10.1093/sysbio/syw037>

- Folmer O, Black M, Hoeh W, Lutz R, Vrijenhoek R (1994) DNA primers for amplification of mitochondrial cytochrome c oxidase subunit I from diverse metazoan invertebrates. *Molecular Marine Biology and Biotechnology* 3: 294–299.
- Ghesquière J (1948) Contribution a l'étude des microhyménoptères du Congo belge. Xii. Un proctotrupien phoretique nouveau (Hym. Scelionidae). *Revue de Zoologie et de Botanique Africaines* 30: 323–327.
- Giribet G, Carranza S, Bagui J, Riutort M, Ribera C (1996) First molecular evidence for the existence of a Tardigrada + Arthropoda clade. *Molecular Biology and Evolution* 13: 76–84. <https://doi.org/10.1093/oxfordjournals.molbev.a025573>
- Gupta R, Singh D (2013) Taxonomic notes on five species of the genus *Cletus* Stal (Heteroptera: Coreidae) from northern India with particular reference to their female genitalia. *Journal of Entomology and Zoology Studies* 1(6): 44–45.
- Hoang DT, Chernomor O, Von Haeseler A, Minh BQ, Vinh LS (2018) UFBoot2: improving the ultrafast bootstrap approximation. *Molecular Biology and Evolution* 35: 518–522. <https://doi.org/10.1093/molbev/msx281>
- Johnson NF (1985) Systematics of New World *Trissolcus* (Hymenoptera: Scelionidae): species related to *T. basalis*. *The Canadian Entomologist* 117: 431–445.
- Johnson NF (1992) Catalog of world Proctotrupeoidea excluding Platygasteridae. *Memoirs of the American Entomological Institute* 51: 1–825. <https://doi.org/10.4039/Ent117431-4>
- Kalyaanamoorthy S, Minh BQ, Wong TK, von Haeseler A, Jermini LS (2017) ModelFinder: fast model selection for accurate phylogenetic estimates. *Nature Methods* 14: 587–589. <https://doi.org/10.1038/nmeth.4285>
- Katoh K, Standley DM (2013) MAFFT multiple sequence alignment software version 7: improvements in performance and usability. *Molecular Biology and Evolution* 30: 772–780. <https://doi.org/10.1093/molbev/mst010>
- Kieffer JJ (1912) Proctotrypidae (3e partie). Species des Hyménoptères d'Europe et d'Algérie 11: 1–160. <https://doi.org/10.3406/lsoc.1980.1236>
- Kieffer JJ (1926) Scelionidae. *Das Tierreich*. Vol. 48. Walter de Gruyter & Co., Berlin, 885 pp.
- Kohno, K (2002) Phoresy by an egg parasitoid, *Protelenomus* sp. (Hymenoptera: Scelionidae), on the coreid bug *Anoplocnemis phasiana* (Heteroptera: Coreidae). *Entomological Science*, 5(3): 281–285.
- Kononova SV (1982) A new genus and species of egg parasite (Hymenoptera, Scelionidae) from the south of the USSR. *Vestnik Zoologii* 1982(3): 76–78.
- Lanham UN, Evans FC (1958) Phoretic Scelionids on Grasshoppers of the Genus *Melanoplus* (Hymenoptera: Scelionidae). *The Pan-Pacific Entomologist* 34: 213–214.
- Maglić R, Žikić V (2021) Presence of *Mantibaria seefeldiana* (de Stefani) (Hymenoptera: Scelionidae) in Croatia: a pseudoparasitoid of praying mantis. *Acta Entomologica Serbia* 26: 59–65.
- Masner L (1964) A comparison of some Nearctic and Palearctic genera of Proctotrupeoidea (Hymenoptera) with revisional notes. *Casopis Československé Společnosti Entomologické* 61: 123–155.
- Masner L (1976) Revisionary notes and keys to world genera of Scelionidae (Hymenoptera: Proctotrupeoidea). *Memoirs of the Entomological Society of Canada* 97: 1–87. <https://doi.org/10.4039/entm10897fv>

- Mikó I, Vilhelmsen L, Johnson NF, Masner L, Péntzes Z (2007) Skeletomusculature of Scelionidae (Hymenoptera: Platygastridae): head and mesosoma. *Zootaxa* 1571: 1–78. <https://doi.org/10.11646/zootaxa.1571.1.1>
- Mineo G, O'Connor JP, Ashe P (2009) A new genus of Telenominae from Africa (Hym., Platygastridae: Scelionidae). *Entomologist's Monthly Magazine* 145: 193–196.
- Minh BQ, Schmidt HA, Chernomor O, Schrempf D, Woodhams MD, von Haeseler A, Lanfear R (2020) IQ-TREE 2: new models and efficient methods for phylogenetic inference in the genomic era. *Molecular Biology and Evolution* 37: 1530–1534. <https://doi.org/10.1093/molbev/msaa015>
- Nakagawa H (1900) [Illustrations of some Japanese Hymenoptera parasitic on insect eggs. I.] Special Report, Agricultural Experimental Station, Tokyo. No. 6, 26 pp.
- Nixon GEJ (1938) Asiatic species of *Microphanurus* (Hym., Proctotrupoidea). *Annals and Magazine of Natural History* (11)2: 122–139. <https://doi.org/10.1080/03745481.1938.9755445>
- Orr DB, Russin JS, Boethel DJ, Jones WA (1986) Stink bug (Hemiptera: Pentatomidae) egg parasitism in Louisiana soybeans. *Environmental Entomology* 15: 1250–1254. <https://doi.org/10.1093/ee/15.6.1250>
- Rajmohana K (2013) On a new species of *Protelenomus* Kieffer, 1906 (Hymenoptera-Platygastridae-Telenominae) from Arunachal Pradesh, being the first record of the genus from India. *Colemania* 38: 1–7.
- Rajmohana K, Sachin JP, Talamas EJ, Shamyasree MS, Jalali SK, Rakshit O (2019) *Paratelenomus anu* Rajmohana, Sachin & Talamas (Hymenoptera, Scelionidae): description and biology of a new species of phoretic egg parasitoid of *Megacopta cribraria* (Fab.) (Hemiptera, Plataspidae). In: Talamas E (Ed.) *Advances in the Systematics of Platygastridae II*. *Journal of Hymenoptera Research* 73: 103–123. <https://doi.org/10.3897/jhr.73.34262>
- Ramachandra Rao Y (1952) Scelionids as parasites of eggs of Orthoptera. *The Indian Journal of Entomology* 14: 174–175.
- Risbec J (1950) Contribution a l'étude des Proctotrupidae (Serphiidae). (II) in Risbec. *Travaux du Laboratoire d'Entomologie du Secteur Soudanais de Recherches Agronomiques. Gouvernement Général de l'Afrique Occidentale Française*, Paris, 511–639.
- Talamas E, Johnson N, Buffington M (2015) Key to Nearctic species of *Trissolcus* Ashmead (Hymenoptera, Scelionidae), natural enemies of native and invasive stink bugs (Hemiptera, Pentatomidae). *Journal of Hymenoptera Research* 43: 45–110. <https://doi.org/10.3897/JHR.43.8560>
- Talamas E, Buffington M, Hoelmer K (2017) Revision of Palearctic *Trissolcus* Ashmead (Hymenoptera: Scelionidae). In: Talamas EJ, Buffington ML (Eds) *Advances in the Systematics of Platygastridae*. *Journal of Hymenoptera Research* 56: 3–185. <https://doi.org/10.3897/jhr.56.10158>
- Talamas EJ, Bon M-C, Hoelmer KA, Buffington ML (2019) Molecular phylogeny of *Trissolcus* wasps (Hymenoptera, Scelionidae) associated with *Halyomorpha halys* (Hemiptera, Pentatomidae). In: Talamas E (Ed.) *Advances in the Systematics of Platygastridae II*. *Journal of Hymenoptera Research* 73: 201–217. <https://doi.org/10.3897/jhr.73.39563>

- Talamas E, Bremer J, Moore M, Bon MC, Lahey Z, Roberts C, Combee L, van Noort S, McGathey N, Timokhov A, Hougardy E, Hogg B (2021) A maximalist approach to the systematics of a biological control agent: *Gryon aetherium* Talamas, sp. n. (Hymenoptera, Scelionidae). In: Lahey Z, Talamas E (Eds) Advances in the Systematics of Platygastroidea III. Journal of Hymenoptera Research 87: 323–480. <https://doi.org/10.3897/jhr.87.72842>
- Tortorici F, Talamas EJ, Moraglio ST, Pansa MG, Asadi-Farfar M, Tavella L, Caleca V (2019) A morphological, biological and molecular approach reveals four cryptic species of *Trissolcus* Ashmead (Hymenoptera, Scelionidae), egg parasitoids of Pentatomidae (Hemiptera). In: Talamas E (Ed.) Advances in the Systematics of Platygastroidea II. Journal of Hymenoptera Research 73: 153–200. <https://doi.org/10.3897/jhr.73.39052>
- Vasiḷa C, Popovici OA, Talamas E, Johnson N, Masner L, Tortorici F, Fusu L (2021) Molecular analysis reveals *Latonius planus* Kononova to be a derived species of *Trissolcus* Ashmead. In: Lahey Z, Talamas E (Eds) Advances in the Systematics of Platygastroidea III. Journal of Hymenoptera Research 87: 267–289. <https://doi.org/10.3897/jhr.87.63533>
- Veenakumari K, Notton DG, Polaszek A (2019) World Revision of the Genus *Protelenomus* Kieffer (Hymenoptera: Scelionidae: Telenominae). Annales Zoologici 69(2): 381–406. <https://doi.org/10.3161/00034541ANZ2019.69.2.006>
- Veenakumari K, Mohanraj P (2015) Redescription of *Protelenomus flavicornis* Kieffer (Platygastroidea: Platygastriidae) from India. Entomofauna, Zeitschrift für Entomologie, 36: 305–312.
- Watanabe C (1951) On five scelionid egg-parasites of some pentatomid and coreid bugs from Shikoku, Japan (Hymenoptera: Proctotrupoidea). Transactions of the Shikoku Entomological Society 2: 17–26.
- Whiting M, Carpenter JM, Wheeler QD, Wheeler WC (1997) The Strepsiptera problem: phylogeny of the holometabolous insect orders inferred from 18S and 28S ribosomal DNA sequences and morphology. Systematic Biology 4: 1–68. <https://doi.org/10.1093/sysbio/46.1.1>

Supplementary material I

Sequenced taxa and GenBank accession numbers

Authors: Cheng-Jin Yan, Elijah Talamas, Zachary Lahey, Hua-Yan Chen

Data type: table

Copyright notice: This dataset is made available under the Open Database License (<http://opendatacommons.org/licenses/odbl/1.0/>). The Open Database License (ODbL) is a license agreement intended to allow users to freely share, modify, and use this Dataset while maintaining this same freedom for others, provided that the original source and author(s) are credited.

Link: <https://doi.org/10.3897/jhr.94.95961.suppl1>

Hadronotus pubescens (Motschoulsky) (Hymenoptera, Scelionidae): Redescription, biological attributes, and parasitism on eggs of *Riptortus pedestris* (Fab.) (Hemiptera, Alydidae)

Md. Rasel Raju¹, Mst. Arifunnahar¹, Md. Munir Mostafiz²,
Md. Abdul Alim¹, Md. Alamgir Hossain¹, Elijah J. Talamas³

1 Department of Entomology, Hajee Mohammad Danesh Science and Technology University, Dinajpur-5200, Bangladesh **2** Division of Applied Biosciences, College of Agriculture and Life Sciences, Kyungpook National University, Daegu, 41566, Republic of Korea **3** Division of Plant Industry, Florida Department of Agriculture and Consumer Services, Gainesville, FL, USA

Corresponding authors: Md. Abdul Alim (alim@hstu.ac.bd), Elijah J. Talamas (elijah.talamas@fdacs.gov)

Academic editor: Miles Zhang | Received 15 August 2022 | Accepted 17 October 2022 | Published 20 December 2022

<https://zoobank.org/26A6BC19-E361-433F-A8F1-C1C1EEF9E604>

Citation: Raju MdR, Arifunnahar M, Mostafiz MdM, Alim MdA, Hossain MdA, Talamas EJ (2022) *Hadronotus pubescens* (Motschoulsky) (Hymenoptera, Scelionidae): Redescription, biological attributes, and parasitism on eggs of *Riptortus pedestris* (Fab.) (Hemiptera, Alydidae). Journal of Hymenoptera Research 94: 139–161. <https://doi.org/10.3897/jhr.94.93512>

Abstract

Riptortus pedestris (Fab.) (Hemiptera, Alydidae) is one of the most damaging insects of leguminous crops in Eastern Asia but has only recently emerged as a pest in Bangladesh. Eggs, nymphs and adults of *R. pedestris* are here reported from mung bean (*Vigna radiata* (L.)) fields in Bangladesh. Two parasitoid species were reared from field-collected eggs of *R. pedestris*, the solitary *Hadronotus pubescens* (Motschoulsky) (Hymenoptera, Scelionidae) and a gregarious species of *Ooencyrtus* Ashmead (Hymenoptera, Encyrtidae). Here we redescribe *H. pubescens*, treat *H. hogenakalensis* (Sharma) as a junior synonym, and report aspects of its biology that were investigated under laboratory conditions. The number of eggs parasitized by *H. pubescens* was constant with eggs up to 48 hours in age, decreasing by 14% for 96 hour-old eggs. As host egg age increased, the parasitoid mean development time increased and the longevity of the parasitoids decreased.

Keywords

bean bug, biological control, egg parasitoid, mass rearing, mung bean

Introduction

Riptortus pedestris (Fab.) (Hemiptera, Alydidae) is a destructive pest on a wide range of crop plants in Korea and Japan (Honda 1986; Son et al. 2000; Kang et al. 2003; Lee et al. 2004) and has infested many leguminous crops in Bangladesh (Arifunnahar et al. 2019, 2021). It is also an important hemipteran pest of soybean (*Glycine max* (L.) Merr.) (Osakabe and Honda 2002; Choi et al. 2005) and fruit trees (Chung et al. 1995). *Riptortus pedestris* is a major pest of many grains, including sorghum (*Sorghum bicolor* (L.) Moench), foxtail millet (*Setaria italica* (L.) P. Beauvois), and barley (*Hordeum vulgare* L.) in the reproductive stages (Chung et al. 1995; Mainali et al. 2014), as well as other field crops in Asian countries (Kang et al. 2003; Wada et al. 2006). Nymphs and adults of *R. pedestris* feed preferentially on seeds by piercing and sucking (Choi et al. 2005). Their polyphagous nature, as well as the preferential feeding on seeds, make crop plants highly vulnerable to damage (Choi et al. 2005). Both adults and nymphs feed on the fluids from seed pods, causing them to fail to mature, turn brown, shrivel and die. Generally, when such pods are opened, the seeds inside are shriveled, undersized, or malformed. These unhealthy seeds often succumb to secondary fungal infections like yeast-spot disease (*Eremothecium coryli* (Peglion) Kurtzman) (Kimura et al. 2008) which can lead to the complete abortion of seeds in the entire field (Li et al. 2019). Many legume growers spray insecticides to control *R. pedestris*, but this is not economically effective with mung bean (*Vigna radiata* (L.)) in Bangladesh due to its relatively low cash value. Chemical insecticides are a useful component of integrated pest management (IPM) systems when they are quick and easy to apply, economically viable, and have reliable effectiveness against the targeted insect pest (Endo and Tsurumachi 2001). However chemical insecticides often negatively impact natural enemies and may cause pest resurgence and other environmental side effects (Schwab et al. 1995). Therefore, chemical insecticides may not be economically feasible due to the higher cost of production and environmental concerns. While most chemical insecticides are fast-acting, the high mobility of these insects makes them difficult to control (Choi et al. 2005; Wada et al. 2006). In light of these difficulties, cultural practices such as delayed seeding and use of resistant varieties have been suggested for the management of various stink bugs (Bowers 1990; Wada et al. 2006). Biological control has been successfully employed against various stink bugs by introduction or augmentation of egg parasitoids (Weber et al. 1996; Orr 1998; Alim and Lim 2011) and may be an option for *R. pedestris* in Bangladesh.

Previously reported parasitoids of *R. pedestris* eggs in soybean fields in east Asia include *Hadronotus japonicus* (Ashmead) (reported as *Gryon japonicum* (Ashmead)), *Hadronotus nigricornis* (Dodd) (reported as *Gryon nigricorne* (Dodd)) (Hymenoptera, Scelionidae) and *Ooencyrtus nezarae* Ishii (Hymenoptera, Encyrtidae) (Noda 1989; Hirose et al. 1996; Mizutani et al. 1996; Son et al. 2009). Species of *Hadronotus* Förster are known to parasitize the eggs of hemipteran pests, including pentatomids such as

Piezodorus hybneri (Gmelin), *Dolycoris baccarum* (L.), *Nezara antennata* Scott and *Halyomorpha halys* (Stål) (Hirose et al. 1996; Mizutani et al. 1996; Zhang et al. 2005). However, the effective use of *Hadronotus* species for biological control requires the ability to accurately identify them. In many cases, this involves time-consuming taxonomic research, creating delays for field and laboratory studies and the publication of their results. Some recent advances in the taxonomy of the group include the work of Komeda et al. (2020), who revised some species-groups in Japan, and Talamas et al. (2021), who resurrected *Hadronotus* and provided images for many primary types of *Gryon* Haliday and *Hadronotus*.

Hadronotus pubescens is a solitary egg parasitoid reported from Sri Lanka and India, especially Karnataka (Sharma et al. 1982), but not previously recorded in Bangladesh. The biological parameters of this parasitoid are largely unknown, and to date no research on either *H. pubescens* or the egg parasitoids of *R. pedestris* has been conducted in Bangladesh. In this study, biological parameters of *H. pubescens* on *R. pedestris* eggs were evaluated in laboratory conditions to determine the parasitoid's potential as a biological control agent. These parameters included emergence rate, development time, sex ratio, adult longevity and size variation of the adult wasps.

Materials and methods

Experiments were conducted in the laboratory of the Department of Entomology, Hajee Mohammad Danesh Science and Technology University (HSTU), Dinajpur and different mung bean fields near HSTU campus from December 2019 to June 2020. The taxonomic portion of the study was conducted at the Florida State Collection of Arthropods, Gainesville, Florida, USA.

Imaging

Photographs were captured using a Macropod Microkit (Macroscopic Solutions) imaging system and rendered with Helicon Focus. In some cases, multiple images were stitched together in Photoshop to produce larger images at high resolution and magnification. Dissections for scanning electron microscopy were performed with a minuten probe and forceps. Body parts were mounted to a 12 mm slotted aluminum mounting stub using a carbon adhesive tab and sputter coated with approximately 70 nm of gold/palladium using a Denton IV sputter coater. Micrographs were captured using a Phenom XL G2 Desktop SEM.

Morphological terms

Terminology for carinae on the posterior head follows Mineo (1980) and for other characters follows Mikó et al. (2007), Lahey et al. (2021) and Talamas et al. (2021).

Abbreviations and characters annotated in the figures

atc	acetabular carina (Fig. 9)
ec	epiclypeal carina (Figs 2, 6)
hoc	hyperoccipital carina (Fig. 4)
mc	mesopleural carina (Fig. 9)
mac	median carina on the vertex (Fig. 4)
mhp	mesoscutal humeral pit (Fig. 10)
oc	occipital carina (Fig. 4);
spf	sulcus of the propodeal foramen (Fig. 11)
tcmd	transverse carina of the metasomal depression (Fig. 11)
tsmd	transverse sulcus of the metasomal depression (Fig. 11)
vplc	ventral mesopleural carina (Fig. 9)
vprc	ventral propodeal carina (Fig. 11)

Collections

Specimens on which this work is based are deposited in the following repositories with abbreviations used in the text:

- FSCA** Florida State Collection of Arthropods, Gainesville, Florida, USA
SAMC Iziko Museums of South Africa, Cape Town, South Africa
USNM National Museum of Natural History, Washington, District of Columbia, USA
ZMMU Zoological Museum of Lomonosov Moscow State University, Moscow, Russia

Data deposition

The data associated with the specimens in this study are deposited at mbd-db.osu.edu and are retrievable via the collecting unit identifier (CUID) for each specimen. Images of the holotype specimens of *Muscidea pubescens* Motschoulsky and *Gryon hogenakalensis* Sharma were made available by Talamas et al. (2021) and Talamas et al. (2017), respectively, and direct links to these images are provided in the species treatment.

DNA barcoding

Genomic DNA was nondestructively isolated from whole specimens using the Qiagen DNeasy kit (Hilden, Germany) as described by Giantsis et al. (2016). PCRs were carried out to amplify the DNA barcode region of the cytochrome oxidase subunit I (COI) using the LCO/HCO primers of Folmer et al. (1994). The PCRs were performed in a 25 µL reaction volume using the KAPA HiFi Hotstart Ready Mix (Roche) per the manufacturer's standard protocol. PCR conditions were as follows: 95 °C for 2 min, followed by 32 cycles of 95 °C for 30 s, 50 °C for 40 seconds, 72 °C for 1 min with a final extension at 72 °C for 7 min. The fragments to be amplified by PCR were

separated by electrophoresis on 1.5% agarose gels. After verification, the samples were sequenced at the Florida Department of Agriculture and Consumer Services, Division of Plant Industry, Gainesville, Florida. GenBank accession numbers for the newly generated barcodes for *H. pubescens* and sequences from Talamas et al. (2021) are listed in Table 2.

Rearing of *R. pedestris*

Adults of *Riptortus pedestris* were collected from infested country bean (*Lablab purpureus* L.) fields near the HSTU campus during 2019 and the colony was maintained in the laboratory as described by Alim and Lim (2009). Briefly, the nymphs and adults were kept in acrylic cages (40 L × 40 W × 40 H cm), each with windows on three lateral sides covered with mesh screens for ventilation. The insects were reared at a constant temperature (30 °C ± 2) and relative humidity 75% ± 4 and with a natural photoperiod. Temperature and relative humidity were monitored by the Hydro-thermometer (HTC-1). Ascorbic acid was dissolved in water and provided to the adult *R. pedestris* in dishes along with soybean seeds. Nymphs were fed with soybean seeds and bean plants with cotyledonous leaves. Oviposition substrates were prepared by placing a few pieces of gauze fabric in the top and bottom corners inside the adult cages. The gauze was replaced every day and the eggs were collected to continue the colony. The cage was cleaned two times per week.

Rearing of *H. pubescens*

Hadronotus pubescens were reared from field-collected eggs of *R. pedestris* from country bean fields. The parasitoids were reared under laboratory conditions as described in the previous section. The males and females of *H. pubescens* were placed into plastic centrifuge tubes (50 mL) (SPL Life Sciences Co. Ltd, Korea) and provided with honey on the inner surface of the tube and a piece of moistened cotton. Moistened cotton and honey were replaced every three days.

Abundance of *R. pedestris* and its egg parasitoids at different locations

To determine the parasitism rate of field-laid eggs, 10 mung bean plants were randomly selected in plots at three locations (Table 1). These plants were examined every 10 days from February to April, 2020, to collect eggs of *R. pedestris* and record the numbers of nymphs and adults. Eggs were brought to the laboratory, individually placed in microtubes (2 mL capacity), and kept in the laboratory. The numbers of newly hatched *R. pedestris* and parasitoids were recorded daily. Additionally, the sex of the newly emerged parasitoids was recorded. Eggs that produced neither a host nymph nor an adult parasitoid were dissected under a stereomicroscope. Host eggs containing parasitoids that failed to develop or emerge were considered parasitized. Each sampling plot was spaced 200 meters apart at each location.

Table 1. Study site and coordinates for the present study.

Site number	Location	Coordinates
Site 1	Kornai	25°42'9.172N, 88°38'26.449E
Site 2	Shadipur	25°42'46.08N, 88°39'45.036E
Site 3	HSTU Campus	25°41'50.748N, 88°39'9.792E

Table 2. Specimens of *H. pubescens* and a closely related specimen with COI barcodes.

Species	CUID	GenBank Accession	Locality
<i>Hadronotus pubescens</i>	FSCA 00094687	MZ513578	Taiwan
<i>Hadronotus pubescens</i>	FSCA 00094882	MZ147017	Bangladesh
<i>Hadronotus pubescens</i>	FSCA 00094879	MZ147018	Bangladesh
<i>Hadronotus</i> sp.	SAM-HYM-P093638	MZ513595	South Africa

Monitoring of *R. pedestris* and its egg parasitoids by pheromone traps

Aggregation pheromone traps were made locally with an iron frame covered with mosquito netting (32 L × 13 D cm). Each trap had two separate openings that enabled entry of *R. pedestris*. Inside the traps were aggregation pheromone lures (Green Agro-Tech Co. Ltd., Kyungsan, Republic of Korea, 50 µL/lure). [Myristyl isobutyrate, (*E*)-2-hexenyl (*E*)-2-hexenoate and (*E*)-2-hexenyl (*Z*)-3-hexenoate at the ratio 1:5:1], and the traps were suspended in the mung bean canopy from a cord attached to the end of a bamboo pole. Inside the trap, a cord was affixed to provide a substrate for egg laying by *R. pedestris* adults. Three pheromone traps were installed at each location (Table 1). Adults and nymphs of *R. pedestris* were recorded at 10-day intervals and the eggs laid by adult *R. pedestris* were collected, brought into the laboratory, placed in micro tubes individually and kept at ambient temperature. The hatching of host insects and the emergence of adult parasitoids were recorded daily.

Effects of host egg age on host acceptance behavior by *H. pubescens*

After 0, 24, 48, 72 and 96 hours from the time that the eggs were laid, eggs were placed in an insect breeding Petri dish (4 H × 10 D cm) at room temperature. Then, a single, mated and naive, 4-day old female *H. pubescens* was introduced into each Petri dish. Host acceptance behaviors were observed under a stereomicroscope (AmScope SM-2TZ LWD, USA) and categorized as drumming, drilling, marking, and oviposition (Strand and Vinson 1983; Noda 1993). The time spent performing each behavior was recorded for each of the eggs when the parasitoid displayed complete host acceptance behavior. The entire procedure was repeated with 10 female parasitoids at each time interval.

Effect of host eggs age on the biological parameters of *H. pubescens*

After 0, 24, 48, 72 and 96 hours from the time that the eggs were laid, 10 eggs of *R. pedestris* were placed on an insect breeding dish (4 H × 10 D cm), and a 4-day old, mated *H. pubescens* female was allowed to parasitize the eggs for 24 hours at ambient conditions.

After 24 hours the female was withdrawn, and the eggs were then placed individually in 2 mL micro tubes with a drop of honey. The eggs were checked daily for the emergence of parasitoids. The number of host eggs parasitized, adult emergence, sex ratio, development time and longevity of male and female *H. pubescens* were recorded. Host eggs containing parasitoids that failed to develop or emerge were also considered parasitized, as determined by dissection of each egg. These procedures were replicated 10 times for each age period.

Each parasitoid that emerged was collected and placed in a 50 mL rearing tube. To maximize longevity, fresh honey and moistened cotton were provided every three days, and the parasitoids were transferred to new tubes as needed. To determine the effect of time on the size of the emerged parasitoids, a total of 30 individuals, both males and females, were randomly selected in each group and their hind tibia lengths were measured under a stereomicroscope (Am Scope, China.) using a micrometer.

Statistical analyses

Emergence rate, adult sex ratio and seasonal parasitism rate were subjected to a chi-square test of a contingency table and a Tukey-type multiple comparison test for post hoc analysis (Zar 2010). The number of parasitized host eggs, number of emerged parasitoids, development time, and hind tibia length of parasitoids was analyzed by a Kruskal-Wallis single factor analysis of variance by rank. If significance was detected, multiple comparisons were conducted using the Duncan test (Zar 2010). The number of eggs, nymphs and adults recorded in the field were analyzed by a univariate analysis of variance by rank. If significance was detected, multiple comparisons were conducted using the Duncan test (Zar 2010). Statistical analyses were performed in IBM SPSS Statistics for Windows.

Results

Taxonomy

Hadronotus pubescens (Motschoulsky)

Figs 1–11

Muscidea pubescens Motschoulsky, 1863: 70 (original description).

Gryon pubescens (Motschoulsky): Masner 1976: 57 (generic transfer, type information); Johnson 1992: 395 (cataloged, type information).

Gryon hogenakalensis Sharma, 1982: 329, 336 (original description, keyed); Lê, 1997: 23 (keyed); Lê, 2000: 99, 118 (description, keyed, type information).

Gryon hogenakalense Sharma: Johnson 1992: 384 (cataloged).

Hadronotus pubescens (Motschoulsky): Talamas et al. 2021: 441 (generic transfer).

Hadronotus hogenakalensis (Sharma) syn. nov.: Talamas et al. 2021: 423 (generic transfer).

Images of holotype specimens. *Muscidea pubescens*: <https://zenodo.org/record/4924954#.YkMH-PnMJJaQ>. *Gryon hogenakalensis*: USNMENT01197123.

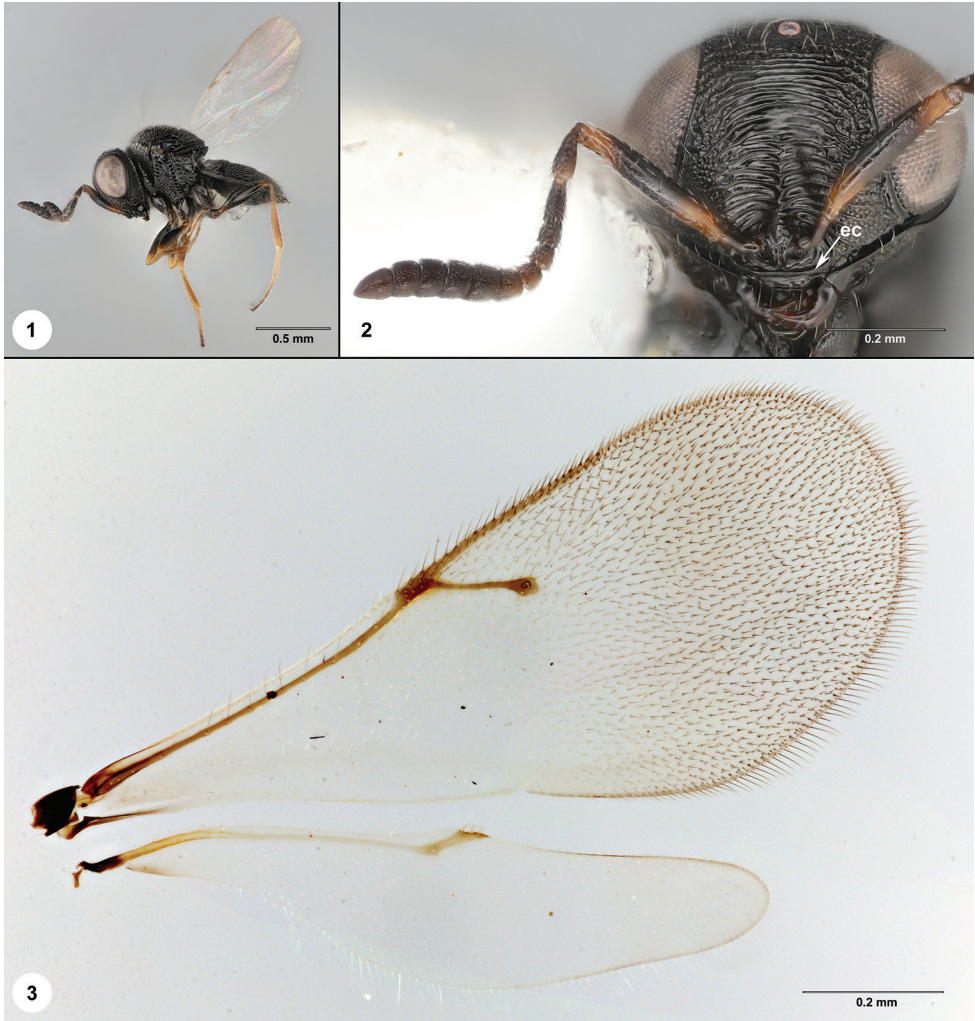
Description. Color of body: dark brown to black. Color of antenna in female: radicle black, A1–A6 yellow-brown with scape darker in middle, A7–A12 black. Color of legs: coxae and femora brown; trochanters, tibiae and tarsi yellow to pale brown. Body length of female: 1.07–1.43 mm (n = 12). Body length of male: 1.34–1.38 mm (n = 2).

Head: Claval formula: A12–A7: 1-2-2-2-2. Number of mandibular teeth: 3. Size of mandibular teeth: small, middle tooth the smallest. Shape of clypeus: transverse, not projecting ventrally, apex flat. Number of clypeal setae: 6, lateral pair very short; medial pairs approximately equal in length; Epiclypeal carina: present. Facial striae: absent. Central keel: present in lower portion of frons. Line of setae above interantennal process: absent. Sculpture of ventral frons: strigose, strigae arching slightly ventrally from central keel, sometimes extending to inner orbit. Sculpture of dorsal frons: transversely strigose medially, weakly rugulose along inner orbit of compound eye. Preocellar pit: absent. Malar striae: absent. Sculpture of gena directly above mandibles: smooth. Genal carina: absent. Occipital carina: continuous medially, with sharp corner behind dorsal apex of compound eye. Anterior margin of occipital carina on gena: crenulate. Anterior margin of occipital carina on posterior head: simple. Hyperoccipital carina: present. Marginal carina: present. Sculpture of occiput: arched, parallel rugae.

Mesosoma: Epomial carina: present. Sculpture of pronotum posterior to epomial carina: transversely rugose. Sculpture of pronotum anterior to epomial carina: smooth. Sculpture of pronotum dorsal to epomial carina: pustulate-punctate. Netrion sulcus: absent. Pronotal suprahumeral sulcus: absent. Setation of lateral pronotum: white; uniformly dense dorsal topomial carina, with small setal patch directly anterior to epomial carina. Mesoscutal suprahumeral sulcus: absent. Mesoscutal humeral sulcus: indicated by a shallow smooth furrow. Mesoscutal humeral pit: present. Sculpture of mesoscutum: reticulate-punctate, with longitudinal rugae in posteromedial portion. Setation of mesoscutum: white, mostly uniform in density, slightly sparser lateral to parapsidal line. Scutoscutellar sulcus: smooth furrow medially, striate laterally. Sculpture of mesoscutellar disc: longitudinally rugose medially, with coarse microsculpture throughout. Posterior mesoscutellar sulcus: foveate.

Posterior margin of mesoscutellum: not extending over metanotum, metascutellum visible in dorsal view. Posterior margin of metascutellum: convex. Sculpture on posteroventral surface of metascutellum: finely strigose. Sculpture of metanotal trough: foveate. Lateral propodeal area: narrow, deeply foveate with white setation. Lateral propodeal carina: extending laterally to metapleural carina, forming flange around metasomal depression. Sculpture of metasomal depression: radially rugulose. Sulcus of the propodeal foramen: foveate.

Postacetabular sulcus: crenulate. Posterior limit of acetabulum: intersecting with ventral mesopleural carina. Mesopleural epicoxal sulcus: composed of shallow foveae. Episternal foveae: absent. Mesopleural carina: present, parallel to acetabular carina. Sculpture of mesopleuron above mesopleural carina: transversely rugose. Femoral depression: not indicated. Prespecular sulcus: composed of large foveae. Sculpture of speculum: transversely rugose. Shape of subalar pit: roughly circular. Mesepimeral



Figures 1–3. *Hadronotus pubescens*, female (FSCA 00094879) **1** lateral habitus **2** head, anterior view **3** wings.

sulcus: foveate, foveae of uniform size. Posterior mesepimeral area: smooth, narrow. Paracoxal sulcus: foveate, absent in ventral part of metapleuron. Metapleural epicoxal sulcus: foveate. Dorsal metapleural area: smooth, with white setation posteriorly. Ventral metapleural area: irregularly rugulose, setose. Posterodorsal metapleuron sulcus: foveate, present along entirety of metapleural carina.

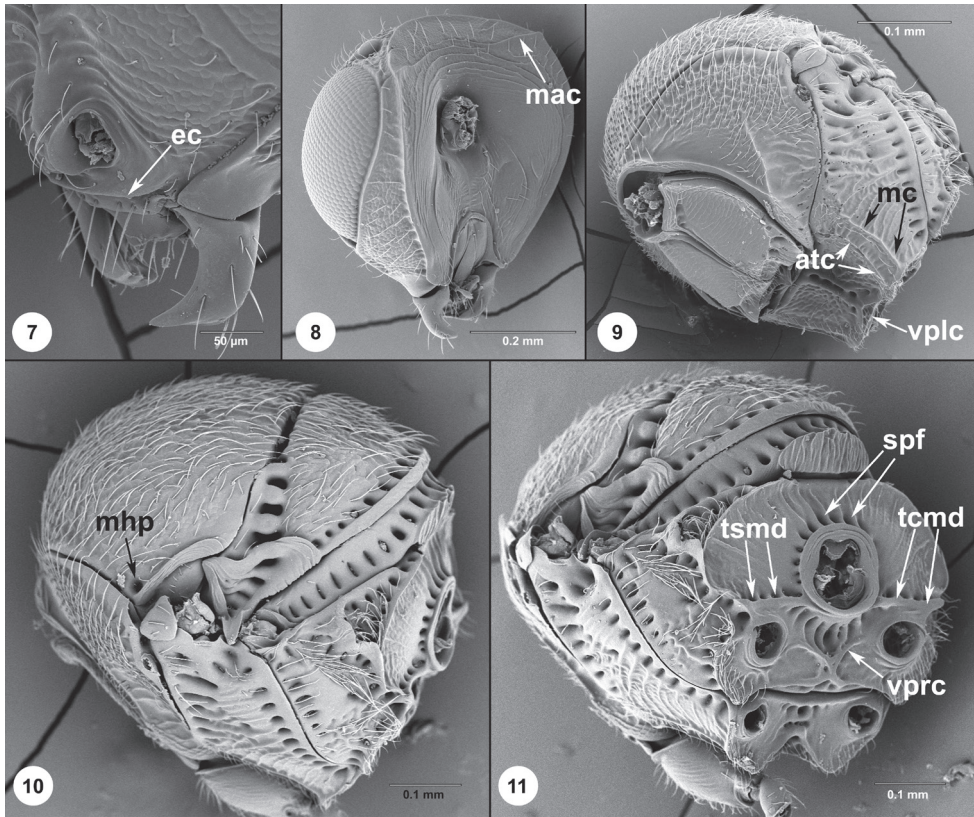
Wings: Length of postmarginal vein in fore wing: almost twice as long as stigmal vein. Length of marginal vein in fore wing: about one third as long as stigmal vein. Color of wing disc: hyaline. Color of fore wing setation: brown in distal half, white in basal half. Color of hind wing setation: white throughout. Shape of submarginal vein: shallowly curved, nearly parallel to wing margin, without sharp bend.



Figures 4–6. *Hadronotus pubescens*, female (FSCA 00094879) **4** head, mesosoma, metasoma, dorsal view **5** head and mesosoma, lateral view **6** head, mesosoma, metasoma, posterolateral view.

Metasoma: Basal foveae: present on T1–T2, S1–S2. Setation of T1–T3: present on lateral portions of tergite. Setation of T2–T5: dense in lateral part of tergite, absent medially except for a transverse line of sparse setae along posterior margin. Sculpture of T1: longitudinally striate, smooth along posterior margin. Sculpture of T2–T4: finely reticulate with a smooth band along posterior margin. Posterior margin of T5: concave. Setation of laterotergites: present. Sculpture of ventral metasoma: reticulate microsculpture throughout. Setation of ventral metasoma: absent from anterolateral S2, otherwise evenly setose throughout.

Intraspecific variation: The specimens examined here are phenotypically uniform, with slight variation occurring in the degree to which transverse striation is developed on the frons and how far the striation extends laterally. The specimens from Bangladesh showed little variation in size, with females ranging from 1.25–1.43 mm. The female specimen from Taiwan was significantly smaller (1.07 mm).



Figures 7–11. *Hadronotus pubescens*, female (FSCA) **7** ventral frons, anterolateral view **8** head, postero-lateral view **9** mesosoma, ventrolateral view **10** mesosoma, dorsolateral view, **11** mesosoma, posterolateral view. Scale bars in millimeters.

Material examined. *Holotype*, female, *Muscidea pubescens* Motchoulsky: **SRI LANKA:** Nuwara Eliya, ZMMU 0001 (ZMMU). *Holotype*, female, *Gryon hogenakalensis* Sharma: **INDIA:** Hogenakal, 1-FEB-1977, coll. Mani, M. S., USNM01137123 (USNM). **BANGLADESH:** 12 females, 2 males, DPI_FSCA 00008722, FSCA 00034113–00034118, 00034090–00034094, 00094879, 00094882 (FSCA). **TAIWAN:** 1 female, FSCA 00094687 (FSCA).

Comments. *Hadronotus pubescens* is a widespread species, ranging at least from Sri Lanka to Taiwan based on the specimens examined here. The COI sequences from the Taiwanese and Bangladesh specimens share 99.83% sequence identity, providing strong molecular support that they are conspecific. However, a more comprehensive examination of the species limits of *H. pubescens* is still needed and will require analysis of specimens from an even greater geographic range. We examined specimens from South Africa that are morphologically very similar to *H. pubescens* in Asia, pres-

ently separable only by the color of the appendages, yet their COI sequences differ by nearly 13%.

Hadronotus pubescens belongs to a lineage, the *pubescens* species group, that Mineo (1980) defined primarily by the presence of a “marginal carina” (Figs 4, 8, *mac*), which extends medially from the hyperoccipital carina. Two characters provide evidence that this lineage is close to the *charon* species group: the mesoscutal humeral pit (Fig. 10, mhp) and the epiclypeal carina (Figs 2, 7, *ec*). The mesoscutal humeral pit was first documented by Chen et al. (2020) in *H. ancinla* (Kozlov & Lê) and is present in all species of the *charon* group that we have examined. The antennal scrobe in the *charon* group is entirely delimited by a continuous carina. We consider the ventral, transverse portion of this carina to be homologous with the epiclypeal carina, as is found in *H. pubescens*. The taxon sampling in the multi-gene phylogeny presented in Fig. 2 of Talamas et al. (2021) does not allow for analysis of the monophyly or delimitation of these two species groups. The systematics of *Hadronotus* is ongoing and treatment of species groups within the genus is a research priority.

The metapectal propodeal complex contains morphological characters that have yet to be fully exploited in *Hadronotus*. Carinae and sulci on the metasomal depression vary remarkably among species that we have examined and are likely to become more informative as they are studied in greater detail. The ventral mesopleural carina delimits the posterior margin of the metapleuron on the venter and may be interrupted by the foramen of the hind coxa, as in *H. pubescens* (Figs 9, 11). A transverse carina often extends from the propodeal foramen across the metasomal depression and may be accompanied by a sulcus (Fig. 11). Talamas et al. (2021) provided the term “sulcus of the propodeal foramen” for *Gryon aetherium* Talamas, which is present only dorsally. In *H. pubescens*, foveae are present ventral to the transverse carina on the metasoma depression. It is presently unclear if these foveae are a continuation of the sulcus of the propodeal foramen or an independent structure.

Biological parameters

Abundance of *R. pedestris* and its egg parasitoids in different locations

All life stages of *R. pedestris* were found throughout the sampling period. The occurrence of *R. pedestris* eggs, nymphs, and adults started in February and peaked in the month of April. The seasonal number of eggs ($H_C = 11.201$, $df = 8$, $P = 0.076$), nymphs ($H_C = 11.028$, $df = 8$, $P = 0.284$) and adults ($H_C = 3.00$, $df = 8$, $P = 0.876$) of *R. pedestris* was not significantly different among the three different locations (Fig. 12). The number of both unparasitized and parasitized eggs was higher in the mung bean field in Shadipur compared to the other two locations (Fig. 13). The number of unparasitized eggs ($H_C = 1.192$, $df = 8$, $P = 0.981$) and parasitized eggs ($H_C = 8.998$, $df = 8$, $P = 0.98$) were not significantly different among the three locations (Fig. 13). The total parasitism rate of natural host eggs at each sampling site was separated by parasitoid species, i.e., solitary parasitoid *Hadronotus pubescens* and gregarious parasitoids like *Ooencyrtus* sp. Throughout the sampling period, the total parasitism rate

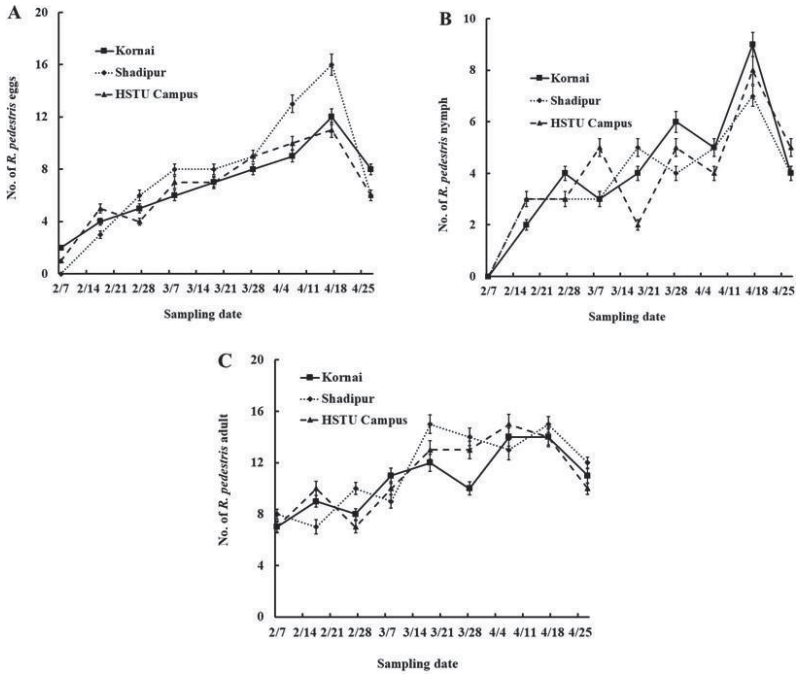


Figure 12. Mean number of eggs (A), nymphs (B), and adults (C) of *R. pedestris* sampled from three different study sites. Analyses were conducted on the seasonal data using Kruskal-Wallis single factor analysis of variance by rank.

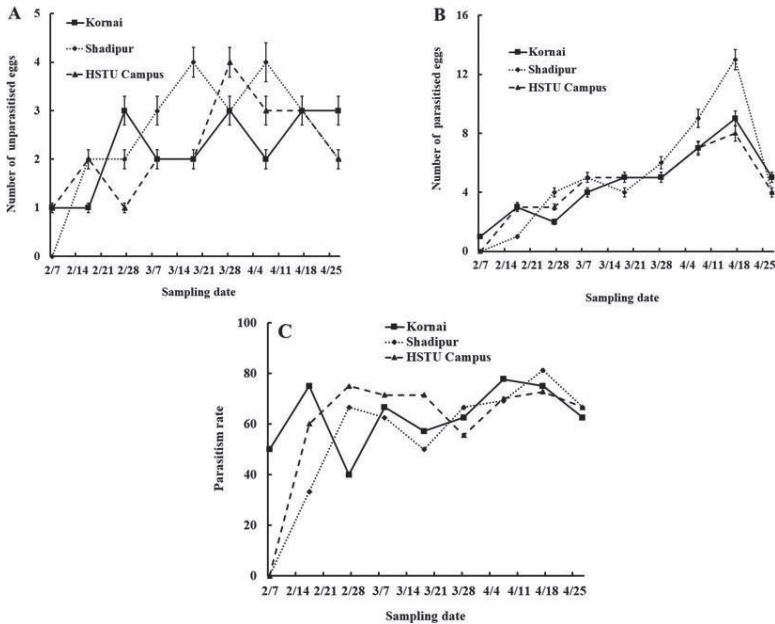


Figure 13. Parasitism rate (%) of natural *R. pedestris* eggs collected from three different study sites. Analyses were conducted on the seasonal data using Kruskal-Wallis single factor analysis of variance by rank.

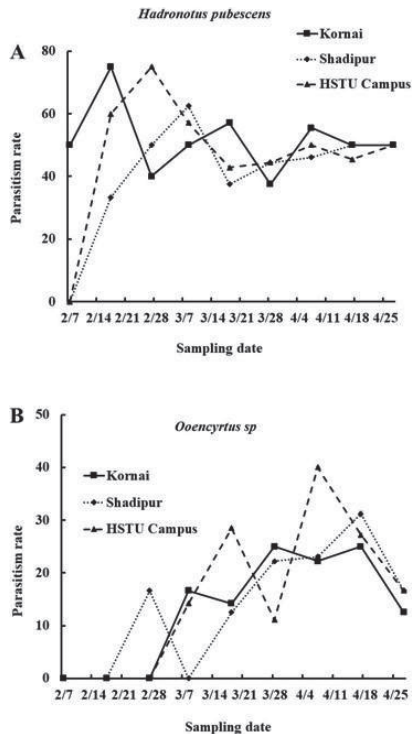


Figure 14. Parasitism rates by *H. pubescens* (A) and *Ooencyrtus* sp. (B) on natural eggs collected from three different study sites.

by both species was found to be higher in Kornai compared to HSTU campus and Shadipur mung bean field ($\chi^2 = 0.005$, $df = 2$, $P = 0.997$) (Fig. 13). The total parasitism rates by both parasitoid species were higher in the month of April, when the mung bean seeds were maturing. The parasitism rate by *H. pubescens* on naturally-laid host eggs was higher in Kornai than in Shadipur or the HSTU Campus ($\chi^2 = 5.371$, $df = 8$, $P = 0.639$) (Fig. 14). On the other hand, the parasitism rate of *Ooencyrtus* sp. alone ($\chi^2 = 9.746$, $df = 8$, $P = 0.201$) was highest in the HSTU campus among the three study sites (Fig. 14).

Monitoring of *R. pedestris* and its egg parasitoids by pheromone traps

Throughout the sampling period, the number of eggs, nymphs, and adults of *R. pedestris* found in the pheromone traps differed between the sites. The seasonal numbers of eggs ($H_c = 7.513$, $df = 8$, $P = 0.341$), nymphs ($H_c = 10.096$, $df = 8$, $P = 0.268$), and adults ($H_c = 14.415$, $df = 8$, $P = 0.254$) of *R. pedestris* were not significantly different among the study sites (Fig. 15). However, the numbers of eggs, nymphs, and adults of *R. pedestris* caught by pheromone traps was higher on the HSTU campus than at the other two sites in the month of April. The number of unparasitized eggs was higher

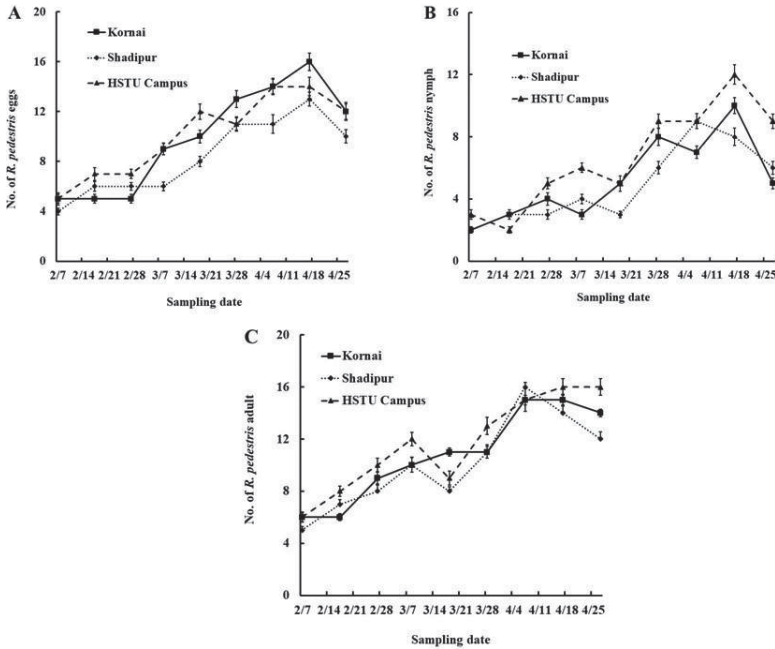


Figure 15. Mean number of eggs (A), nymphs (B), and adults (C) of *R. pedestris* collected from aggregation pheromone traps from three different study sites. Analyses were conducted on the seasonal data using Kruskal-Wallis single factor analysis of variance by rank.

on the HSTU campus compared to the other two sites, and the number of parasitized eggs was higher in Kornai compared to other locations in the month of April. The seasonal numbers of unparasitized eggs ($H_C = 0.507, df = 8, P = 1.00$) and parasitized eggs ($H_C = 6.302, df = 8, P = 0.330$) were not significantly different among the three different locations (Fig. 16). Throughout the sampling period, the total parasitism rate was not significantly different but was higher in the month of April in Kornai compared to the other sites ($\chi^2 = 0.862, df = 2, P = 0.649$) (Fig. 16).

The total parasitism rate on natural host eggs at each sampling site was separated by parasitoid species, i.e., *H. pubescens* and *Ooencyrtus* sp. The overall parasitism rate by *H. pubescens* peaked in February and was lowest in April, whereas parasitism by *Ooencyrtus* sp. peaked in April and was lowest in February. The parasitism rate of both *H. pubescens* ($\chi^2 = 2.440, df = 8, P = 0.827$) and *Ooencyrtus* sp. ($\chi^2 = 7.745, df = 8, P = 0.357$) were not statistically different among sites and were highest in Kornai (Fig. 17).

Effects of host egg age on host acceptance behavior by *H. pubescens*

All *H. pubescens* showed a complete process of host acceptance behaviors on the eggs of *R. pedestris*. Each phase consisted of one or more bouts. The duration of host acceptance behaviors displayed by the egg parasitoids is shown in Table 3. Drumming was

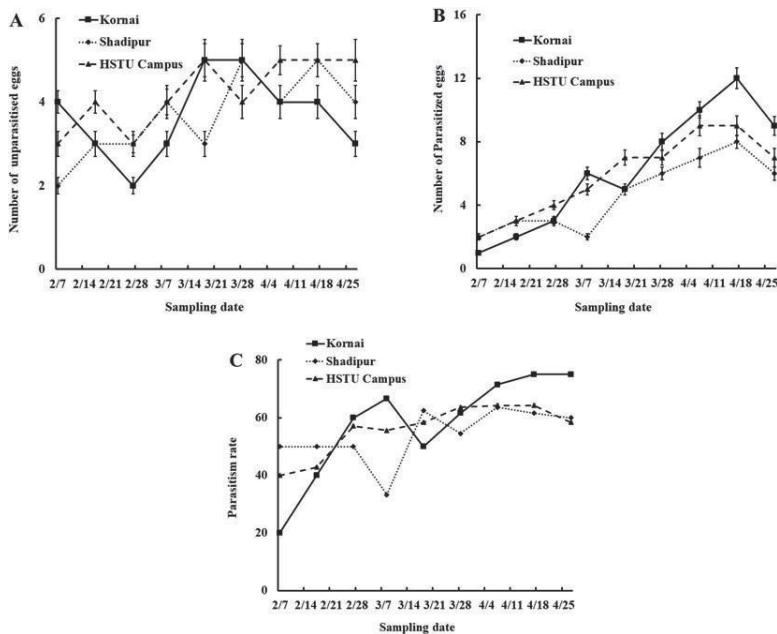


Figure 16. Parasitism rate of natural *R. pedestris* eggs collected from aggregation pheromone traps from three different study sites. Analyses were conducted on the seasonal data using Kruskal-Wallis single factor analysis of variance by rank.

characterized by moving antennae up and down over the exposed surface of the eggs while the female remained still, standing over the eggs. The duration of drumming increased as the age of the host egg increased ($H_C = 43.562$, $df = 4$, $P < 0.001$) (Table 3). The 96 hr old eggs of *R. pedestris* received the longest duration of drumming by the parasitoid. The female parasitoid started drilling after the drumming by inserting her ovipositor into the host eggs. After head pumping, the female remained motionless for 10–15 seconds until oviposition was completed. The mean time spent on drilling and oviposition increased as the age of the host egg increased. The eggs of *R. pedestris* at 96 hours showed the longest duration of drilling and oviposition by the parasitoid. ($H_C = 47.063$, $df = 4$, $P < 0.001$) (Table 3). Similarly, females of *H. pubescens* spent more time marking eggs that were 96 hours old compared to eggs of other ages ($H_C = 47.059$, $df = 4$, $P < 0.001$) (Table 3).

Table 3. Duration (seconds \pm SE) of host acceptance behaviors in different ages of *R. pedestris* eggs. Numbers in each row followed by the same letter are not significantly different ($P > 0.05$).

Behaviors	Age of host eggs (hours)				
	0 (Control)	24	48	72	96
Drumming	37.58 \pm 0.68 d	47.09 \pm 0.30 b	40.88 \pm 0.67 c	48.89 \pm 0.96 b	58.30 \pm 0.68 a
Drilling & Oviposition	413.11 \pm 0.98 e	490.04 \pm 0.88 c	437.53 \pm 1.15 d	549.85 \pm 1.03 b	588.91 \pm 0.77 a
Marking	137.53 \pm 1.22 e	148.98 \pm 1.11 d	171.67 \pm 0.94 c	190.25 \pm 0.91 b	210.74 \pm 0.72 a

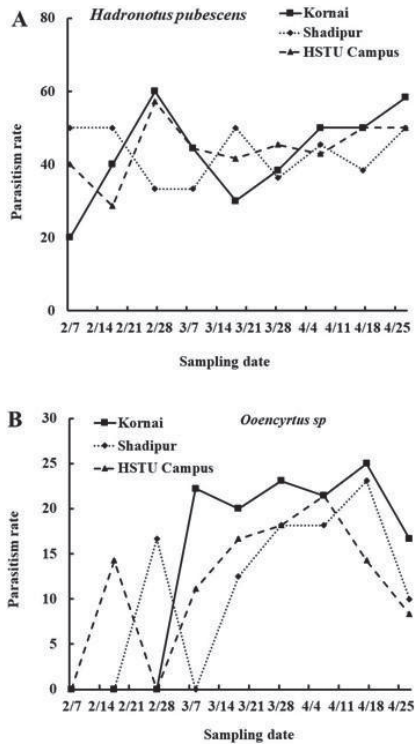


Figure 17. Parasitism rate by *H. pubescens* (A) and *Ooencyrtus* sp. (B) on natural eggs collected from three different study sites from inside the aggregation pheromone traps.

Effect of host egg age on the biological attributes of *Hadronotus pubescens*

The number of eggs parasitized by *H. pubescens* was influenced by the age of the host eggs. *Hadronotus pubescens* can successfully parasitize host eggs up to 48 hours old without a change in the parasitism rate ($H_c = 10.813, df = 4, P = 0.029$) (Table 4). However, for the host eggs 96 hours old, the parasitism rate decreased approximately 14% compared to the control (Table 4). The emergence rate ($H_c = 8.802, df = 4, P = 0.662$) and the sex ratio ($\chi^2 = 6.416, df = 4, P = 0.170$) of *H. pubescens* were unaffected by host egg ages (Table 4). However, the total number of parasitoids that emerged from parasitized eggs significantly decreased with the increase in the host egg age. The sex ratios of the emerged parasitoids were all female biased. The mean development time (from egg to adult) of *H. pubescens* males and females increased significantly as host egg age increased (male $H_c = 14.288, df = 4, P < 0.001$; female $H_c = 105.398, df = 4, P < 0.001$) (Table 4). The highest mean development time for both males and females was found in eggs 96 hours in age and was lowest in the control (0 hours). The longevity of male and female *H. pubescens* decreased significantly when host egg age increased (male $H_c = 41.432, df = 4, P < 0.001$; female $H_c = 192.442, df = 4, P < 0.001$) (Table 4). The highest longevity was found at 0 hours of age (control) compared to the other treatments.

Table 4. Biological attributes of *H. pubescens* on different age of *R. pedestris* eggs. Numbers in each row followed by the same letter are not significantly different ($P > 0.05$).

	Age of host eggs (hours)				
	0	24	48	72	96
Number parasitized host eggs /female \pm SE	9.10 \pm 0.27 a	8.60 \pm 0.52 ab	8.40 \pm 0.26 ab	8.30 \pm 0.36 ab	7.70 \pm 0.15 b
Proportion of male	0.13 (12/91)	0.10 (9/86)	0.21 (18/84)	0.14 (12/83)	0.10 (9/86)
Emergence rate	0.90 (90/100)	0.83 (83/100)	0.82 (82/100)	0.82 (82/100)	0.74 (74/100)
Development time, day \pm SE					
Male	14.75 \pm 0.16 b	14.88 \pm 0.14 b	15.12 \pm 0.12 ab	15.22 \pm 0.10 ab	15.58 \pm 0.14 a
Female	14.88 \pm 0.06 c	14.91 \pm 0.06 c	15.41 \pm 0.08 b	15.19 \pm 0.04 b	15.72 \pm 0.05 a
Longevity, day \pm SE					
Male	23.16 \pm 0.18 a	22.42 \pm 0.20 a	20.75 \pm 0.81 a	15.25 \pm 0.45 b	15.50 \pm 0.86 b
Female	25.12 \pm 0.10 a	24.50 \pm 0.18 a	24.27 \pm 0.30 a	20.61 \pm 0.44 b	17.60 \pm 0.41 c

Discussion

Throughout the sampling period, eggs, nymphs, and adults of *R. pedestris* were found in the three mung bean fields that we sampled. All life stages of *R. pedestris* were observed early in the mung bean season (February) and increased in abundance in April. Son et al. (2008) reported *R. pedestris* in different fruit orchards starting in the last week of April and found the highest abundance in June and October. *Riptortus pedestris* populations were found to start infesting soybeans in the second week of August, with a population peak occurring in the first half of September (Kim and Lim 2010). In the present study, nymphs were caught in pheromone traps during the whole experimental period at the three different locations. The highest number of nymphs was attracted by pheromone traps in the month of April. The synthetic pheromone was effective in attracting second instar *R. pedestris* nymphs only. Leal et al. (1995) speculated that older nymphs do not respond because they may not need information to locate a food source as they have already reached the host plant. The *R. pedestris* adults were attracted to pheromone traps starting in the month of February and showed the highest levels of attraction in the middle of April. Adults of *R. pedestris* were found in traps on barley in the second week of April. The population then increased and peaked in the last week of August on soybeans, and sharply decreased in October (Mainali and Lim 2012).

In this study, we confirmed that the solitary egg parasitoid *H. pubescens* appears in mung bean fields from the first week of February to the last week of April. On the other hand, gregarious parasitoids *Ooencyrtus* sp. appear in mung bean fields from the middle of February to the end of April.

The differential pattern of occurrence, i.e., *H. pubescens* during spring and *Ooencyrtus* sp. during summer, is a new finding in mung bean fields in Bangladesh. Differences in the temporal patterns of each parasitoid's occurrence could be the result of adaptation to certain environmental conditions such as temperature or humidity. Patterns observed in our survey demonstrated that *H. pubescens* probably perform better in the spring and early summer, when humidity is low, compared to *Ooencyrtus* sp., whose abundance was greatest in the summer when higher humidity was recorded

in Bangladesh. The effects of weather conditions on the timing of occurrence and on biological attributes have been reported for other parasitoid species (Ouedraogo et al. 1996; Rousse et al. 2009; Sorribas et al. 2010).

Another factor that could affect the abundance of adult populations is interspecific competition inside the host eggs. Takasu et al. (1998) found that interactions between adults of *Ooencyrtus* sp. and *Hadronotus* spp. did not influence the reproduction of either species (Takasu et al. 1998). Given that some species of *Ooencyrtus*, eg., *O. nezarae*, are facultative hyperparasitoids, use of these species as biological control agents may reduce the population of other parasitoids in the system, such as *H. pubescens*.

The emergence rate and the sex ratio of *H. pubescens* were unaffected by host egg ages. This, in combination with the increased time spent on host assessment and the lower parasitism rate associated with older eggs, suggests that females of *H. pubescens* discriminate and reject eggs that are too old to be viable for their progeny. The sex ratios of the emerged parasitoids were all female-biased without statistical significance among the different periods. The highest mean development time (male and female) was found at 96 hours of age and the lowest in control (0 hours), which might be due to the lower nutritional quality attributed to older host eggs that can slow the offspring development rate (Godfray 1994). Male and female *H. pubescens* had shorter lifespans as age of the the host eggs increased, perhaps due to reduced nutritional quality of the eggs (Alim and Lim 2009).

Conclusion

This study provides baseline data on the parasitism of *R. pedestris* eggs by *H. pubescens* and a species of *Ooencyrtus* and indicates that *H. pubescens* has potential as a biological control agent. It also showcases the necessity of integrating taxonomy with field studies so that the biological parameters of a species can be confidently associated with a species name. In the case of *H. pubescens*, the species-level treatment provided here is the first since its original description in 1863 and was facilitated by the holotype images and molecular data provided in Talamas et al. (2021). We hope that this paradigm of integration will continue to be employed as additional studies on parasitoids of hemipteran eggs are conducted.

Acknowledgements

We express sincere thanks to Professor Dr. Kazunori Matsuo, Kyushu University, Japan for the identification of the genus of the parasitoids, to Matthew Moore and Natalie McGathey (Florida Department of Agriculture and Consumer Services, Division of Plant Industry) for DNA barcoding and imaging support, respectively. We acknowledge the Ministry of Science and Technology (Project no. 39.00.0000.009.14.011.20-1332 (ES-388), The People Republic of Bangladesh for financial support. Elijah Talamas was supported by the Florida Department of Agriculture and Consumer Services, Division of Plant Industry.

References

- Alim MA, Lim UT (2011) Refrigerated eggs of *Riptortus clavatus* (Hemiptera: Alydidae) added to aggregation pheromone traps increase field parasitism in soybean. *Journal of Economic Entomology* 104: 1833–1893. <https://doi.org/10.1603/EC11143>
- Alim MA, Lim UT (2009) Refrigeration of *Riptortus clavatus* (Hemiptera: Alydidae) eggs for the parasitization by *Gryon japonicum* (Hymenoptera: Scelionidae). *Biocontrol Science and Technology* 19: 315–325. <https://doi.org/10.1080/09583150902752020>
- Arifunnahar M, Ahmed MBU, Hossain MA, Alim MA (2019) Varietal susceptibility of mungbean to pod borer (*Maruca vitrata*), bean bug (*Riptortus pedestris*) and epilachna beetle (*Epilachna decastigma*). *Bangladesh Journal of Entomology* 29: 49–58.
- Arifunnahar M, Khatun MM, Hossain MA, Alim MA (2021) Toxicity evaluation of different chemical pesticides against *Riptortus pedestris* (Hemiptera: Alydidae) under laboratory condition in Bangladesh. *Journal of the Bangladesh Agricultural University* 19: 192–197. <https://doi.org/10.5455/JBAU.72976>
- Chen H, Talamas EJ, Bon M-C, Moore MR (2020) *Gryon ancinclae* Kozlov & Lê (Hymenoptera: Scelionidae): host association, expanded distribution, redescription and a new synonymy. *Biodiversity Data Journal* 8: e47687. <https://doi.org/10.3897/BDJ.8.e47687>
- Choi MY, Lee GH, Paik CH (2005) Feeding preference, nymphal development time, body-weight increase, and survival rate of the bean bug, *Riptortus clavatus* (Thunberg) (Hemiptera: Alydidae), on soybean varieties. *Korean Journal of Applied Entomology* 44: 287–292.
- Chung BK, Kang SW, Kwon JH (1995) Damages, occurrences and control of hemipterous insects in non-astringent persimmon orchards. *Journal of Agricultural Science* 37: 376–382.
- Folmer O, Black M, Hoeh W, Lutz R, Vrijenhoek R (1994) DNA primers for amplification of mitochondrial cytochrome c oxidase subunit I from diverse metazoan invertebrates. *Molecular Marine Biology and Biotechnology* 3: 294–299.
- Giantsis IA, Chaskopoulou A, Bon MC (2016) Mild-Vectolysis: A nondestructive DNA extraction method for vouchering sand flies and mosquitoes. *Journal of Medical Entomology* 53: 692–695. <https://doi.org/10.1093/jme/tjv236>
- Higuchgi H, Suzuki Y (1996) Host handling behavior of the egg parasitoid *Telenomus triptus* to the egg mass of the stink bug *Piezodorus hybneri*. *Entomologia Experimentalis et Applicata* 80: 475–479. <https://doi.org/10.1111/j.1570-7458.1996.tb00962.x>
- Hirose Y, Takasu K, Takagi M (1996) Egg parasitoids of phytophagous bugs in soybean: Mobile natural enemies as naturally occurring biological control agents of mobile pests. *Biological control* 7: 84–94. <https://doi.org/10.1006/bcon.1996.0069>
- Honda K (1986) Estimation of the number of damaged soybean seeds caused by the bean bug, *Riptortus clavatus* Thunberg. *Tohoku Agricultural Research* 39: 157–158.
- Johnson NF (1992) Catalog of world Proctotrupeoidea excluding Platygasteridae. *Memoirs of the American Entomological Institute* 51: 1–825.
- Kang CH, Huh HS, Park CG (2003) Review on true bugs infesting tree fruits, upland crops, and weed in Korea. *Korean Journal of Applied Entomology* 42: 269–277.
- Kim S, Lim UT (2010) Seasonal occurrence pattern and within-plant egg distribution of bean bug, *Riptortus pedestris* (Fabricius) (Hemiptera: Alydidae), and its egg parasitoids in soy-

- bean fields. Applied Entomology and Zoology 45: 457–464. <https://doi.org/10.13031/aez.2010.457>
- Kimura S, Tokumaru S, Kikuchi A (2008) Carrying and transmission of *Eremothecium coryli* (Peglion) Kurtzman as a causal pathogen of yeast-spot disease in soybeans by *Riptortus clavatus* (Thunberg), *Nezara antennata* (Scott), *Piezodorus hybneri* (Gmelin) and *Dolycoris baccarum* (Linnaeus). Japanese Journal of Applied Entomology and Zoology 52: 13–18. <https://doi.org/10.13031/jjaez.2008.13>
- Lahey Z, Talamas E, Masner L, Johnson NF (2021) Revision of the Australian genus *Alfredella* Masner & Huggert (Hymenoptera, Platygastridae, Sceliotrachelinae). In: Lahey Z, Talamas E (Eds) Advances in the Systematics of Platygastridae III. Journal of Hymenoptera Research 87: 81–113. <https://doi.org/10.3897/jhr.87.58368>
- Lê XH (1997) Ong ky sinh ho Scelionidae (Hymenoptera) ky sinh trong trung bo xit (Heteroptera) o Viet Name. Tap Chi Sinh Hoc 19: 23–28.
- Lê XH (2000) Egg-parasites of family Scelionidae (Hymenoptera). Fauna of Vietnam, vol. 3. Science and Technics Publishing House. Hanoi, 386 pp.
- Leal WS, Higuchi H, Mizutani N, Nakamori H, Kadosawa T, Ono M (1995) Multifunctional communication in *Riptortus clavatus* (Heteroptera: Alydidae): conspecific nymphs and egg parasitoid *Ooencyrtus nezarae* use the same adult attractant pheromone as chemical cue. Journal of Chemical Ecology 21: 973–985. <https://doi.org/10.1007/BF02033802>
- Lee GH, Paik CH, Choi MY, Oh TJ, Kim DH, Na SY (2004) Seasonal occurrence, soybean damage and control efficacy of bean bug, *Riptortus clavatus* Thunberg (Hemiptera: Alydidae) at soybean field in Honam Province. Korean Journal of Applied Entomology 43: 249–255.
- Li K, Zhang XX, Guo JQ, Hannah P, Wu TT, Li L, Jiang H, Chang LD, Wu CX, Han TF (2019) Feeding of *Riptortus pedestris* on soybean plants, the primary cause of soybean staygreen syndrome in the Huang-Huai-Hai river basin. The Crop Journal 7: 360–367. <https://doi.org/10.1016/j.cj.2018.07.008>
- Mainali BP, Kimand HJ, Bae SD (2014) Infestation of *Riptortus pedestris* Fabricius decreases the nutritional quality and germination potential of soybean seeds. Journal of Asia-Pacific Entomology 17: 477–481. <https://doi.org/10.1016/j.aspen.2014.04.006>
- Mainali BP, Lim UT (2012) Annual pattern of occurrence of *Riptortus pedestris* (Hemiptera: Alydidae) and its egg parasitoids *Ooencyrtus nezarae* Ishii and *Gryon japonicum* (Ashmead) in Andong, Korea. Crop Protection 36: 37–42. <https://doi.org/10.1016/j.cropro.2012.01.016>
- Masner L (1976) Revisionary notes and keys to world genera of Scelionidae (Hymenoptera: Proctotrupoidea). Memoirs of the Entomological Society of Canada 97: 1–87. <https://doi.org/10.4039/entm10897fv>
- Mikó I, Vilhelmsen L, Johnson NF, Masner L, Péntzes Z (2007) Skeletomusculature of Scelionidae (Hymenoptera: Platygastridae): head and mesosoma. Zootaxa 1571: 1–78. <https://doi.org/10.11646/zootaxa.1571.1.1>
- Mineo G (1980) Studies on the Scelionidae (Hym. Proctotrupoidea). XI. A revision of the Palearctic species of *Gryon* Haliday: the *insulare* and *pubescens* groups. Bollettino dell'Istituto di Entomologia Agraria e dell'Osservatorio di Fitopatologia di Palermo 10: 213–226.

- Mizutani N, Hirose Y, Higuchi H, Wada T (1996) Seasonal abundance of *Ooencyrtus nezarae* Ishii (Hymenoptera: Encyrtidae), an egg parasitoid of phytophagous bugs, in summer soybean fields. Japanese Journal of Applied Entomology and Zoology 40: 199–204. <https://doi.org/10.1303/jjaez.40.199>
- Motschoulsky VI (1863) Essai d'un catalogue des insectes de l'île Ceylan. Bulletin de la Société Imperiale des Naturalistes de Moscou. 36(2): 1–153.
- Noda T (1989) Seasonal occurrence of egg parasitoids of *Riptortus clavatus* (Thunberg) (Heteroptera: Alydidae) on several leguminous plants. Japanese Journal of Applied Entomology and Zoology 4: 257–259. <https://doi.org/10.1303/jjaez.33.257>
- Noda T (1993) Ovipositional strategy of *Gryon japonicum* (Hymenoptera: Scelionidae). Bulletin of the National Institute of Agro-Environmental Sciences 9: 1–51.
- Osakabe M, Honda K (2002) Influence of trap and barrier crops on occurrence of and damage by stink bugs and lepidopterous pod borers in soybean fields. Japanese Journal of Applied Entomology and Zoology 46: 233–241. <https://doi.org/10.1303/jjaez.2002.233>
- Orr DB (1998) Scelionid wasps as biological control agents: A review. Florida Entomologist 71: 506–527. <https://doi.org/10.2307/3495011>
- Ouedraogo PA, Sou S, Sanon A, Monge JP, Huignard J, Tran B, Credland PF (1996) Influence of temperature and humidity on populations of *Callosobruchus maculatus* (Coleoptera: Bruchidae) and its parasitoid *Dinarmus basalis* (Pteromalidae) in two climatic zones of Burkina Faso. Bulletin of Entomological Research 86: 695–702. <https://doi.org/10.1017/S0007485300039213>
- Rabb RL, Bradley JR (1970) Marking host eggs by *Telenomus sphingis*. Annals of the Entomological Society of America 63: 209–215. <https://doi.org/10.1093/aesa/63.4.1053>
- Rousse P, Gourdon F, Roubaud M, Chiroleu F, Quilici S (2009) Biotic and abiotic factors affecting the flight activity of *Fopius arisanus*, an egg-pupal parasitoid of fruit fly pests. Environmental Entomology 38: 896–903. <https://doi.org/10.1603/022.038.0344>
- Schwab AI, Jager I, Stoll G, Gorgen R, Schwab SP, Altenburger R (1995) Pesticides in Tropical Agriculture: Hazards and alternatives. PAN, ACTA, Tropical Agro Ecology, 131 pp.
- Sharma SK (1982) On some Scelionidae (Proctotrupeoidea: Hymenoptera) from India. Records of the Zoological Survey of India 79: 319–342. <https://doi.org/10.26515/rzsi/v79/i3-4/1981/161730>
- Son C, Park SG, Hwang YH, Choi B (2000) Field occurrence of stink bug and its damage in soybean. Korean Journal of Crop Science 45: 405–410.
- Son JK, Nguyen XD, Park CG (2008) Seasonal parasitism of *Riptortus clavatus* Thunberg (Heteroptera: Alydidae) Thunberg by *Dionaea magnifrons* (Herting) (Diptera: Tachinidae). Journal of Asia-Pacific Entomology 11: 191–194. <https://doi.org/10.1016/j.aspen.2008.08.001>
- Son JK, Choo HY, Choi JY, Paik CH, Park CG (2009) Enhancement of *Riptortus clavatus* (Thunberg) (Hemiptera: Alydidae) egg parasitism by a component of the bugs aggregation pheromone. Journal of Asia-Pacific Entomology 12: 159–163. <https://doi.org/10.1016/j.aspen.2009.02.009>
- Sorribas J, Rodriguez R, Garcia-Mari F (2010) Parasitoid competitive displacement and coexistence in citrus agroecosystems: linking species distribution with climate. Ecological Applications 20: 1101–1113. <https://doi.org/10.1890/09-1662.1>

- Strand MR, Vinson SB (1983) Host acceptance behavior of *Telenomus heliothidis* (Hymenoptera: Scelionidae) toward *Heliothis virescens* (Lepidoptera: Noctuidae). *Annals of the Entomological Society of America* 76: 781–785. <https://doi.org/10.1093/aesa/76.4.781>
- Takasu K, Hirose Y, Takagi M (1998) Occasional interspecific competition and within plant microhabitat preference in egg parasitoids of the bean bug, *Riptortus clavatus* (Hemiptera: Alydidae) in soybean. *Applied Entomology and Zoology* 33: 391–399. <https://doi.org/10.1303/aez.33.391>
- Talamas EJ, Thompson J, Cutler A, Fitzsimmons Schoenberger S, Cuminale A, Jung T, Johnson NF, Valerio AA, Smith AB, Haltermann V, Alvarez E, Schwantes C, Blewer C, Bodenreider C, Salzberg A, Luo P, Meislin D, Buffington ML (2017) An online photographic catalog of primary types of Platygastroidea (Hymenoptera) in the National Museum of Natural History, Smithsonian Institution. In: Talamas EJ, Buffington ML (Eds) *Advances in the Systematics of Platygastroidea*. *Journal of Hymenoptera Research* 56: 187–224. <https://doi.org/10.3897/jhr.56.10774>
- Talamas EJ, Bremer JS, Moore MR, Bon M-C, Lahey Z, Roberts CG, Combee LA, McGathey N, van Noort S, Timokhov AV, Hougardy E, Hogg B (2021) A maximalist approach to the systematics of a biological control agent: *Gryon aetherium* Talamas, sp. nov. (Hymenoptera, Scelionidae). In: Lahey Z, Talamas E (Eds) *Advances in the Systematics of Platygastroidea III*. *Journal of Hymenoptera Research* 87: 323–480. <https://doi.org/10.3897/jhr.87.72842>
- Wada T, Endo N, Takahashi M (2006) Reducing seed damage by soybean bugs by growing small-seeded soybeans and delaying sowing time. *Crop Protection* 25: 726–731. <https://doi.org/10.1016/j.cropro.2005.10.003>
- Weber CA, Smilanick JM, Ehler LE, Zalom FG (1996) Ovipositional behavior and host discrimination in three scelionid egg parasitoids of stink bugs. *Biological Control* 6: 245–252. <https://doi.org/10.1006/bcon.1996.0031>
- Wiedemann LM, Canto-Silva CR, Romanowski HP, Redaelli LR (2003) Oviposition behaviour of *Gryon gallardoi* (Hymenoptera.; Scelionidae) on eggs of *Spartocera dentiventris* (Hemiptera; Coreidae). *Brazilian Journal of Biology* 63: 781–785. <https://doi.org/10.1590/S1519-69842003000100018>
- Zar JH (2010) *Biostatistical Analysis*, 5th Edn. Prentice Hall, Upper Saddle River, NJ, 555–565.
- Zhang YZ, Li W, Huang, DW (2005) A Taxonomic study of Chinese species of *Ooencyrtus* (Insecta: Hymenoptera: Encyrtidae). *Zoological Studies* 44: 347–360.

A remarkable new family of stinging wasps from the Cretaceous of Myanmar and China (Hymenoptera, Aculeata)

Anderson Lepeco^{1,2}, Diego N. Barbosa¹, Gabriel A. R. Melo¹

1 *Laboratório de Biologia Comparada de Hymenoptera, Departamento de Zoologia, Universidade Federal do Paraná, Curitiba, Brazil* **2** *Laboratório de Biologia Comparada e Abelhas, Departamento de Biologia, Faculdade de Filosofia, Ciências e Letras de Ribeirão Preto, Universidade de São Paulo, Ribeirão Preto, Brazil*

Corresponding author: Anderson Lepeco (al.lepeco@gmail.com)

Academic editor: Michael Ohl | Received 20 April 2022 | Accepted 23 November 2022 | Published 20 December 2022

<https://zoobank.org/0EA310AF-8084-4448-AEDA-4CD39772A98B>

Citation: Lepeco A, Barbosa DN, Melo GAR (2022) A remarkable new family of stinging wasps from the Cretaceous of Myanmar and China (Hymenoptera, Aculeata). *Journal of Hymenoptera Research* 94: 163–190. <https://doi.org/10.3897/jhr.94.85613>

Abstract

Burmese amber provides a unique window to the Cretaceous entomofauna, being the most prolific source of fossil insects for the period. Presently, about 61% of the Hymenoptera described from amber deposits in Myanmar are stinging wasps (Aculeata), including eight families known solely from Burmese amber. In the present work we describe the aculeate family †Trifionyichidae **fam. nov.**, as well as three new genera: †*Prionaspidion* **gen. nov.**, including †*Prionaspidion brevidens* **sp. nov.** and †*P. nanus* **sp. nov.**; †*Trifionyx* **gen. nov.**, including †*Trifionyx pilosus* **sp. nov.**; and †*Trifionyximus* **gen. nov.**, including †*Trifionyximus cracens* **sp. nov.** We also reinterpret the fossil genus †*Mirabythus*, described based on rock impressions from the Yixian formation in China and originally attributed to Scolebythidae. †*Mirabythus* is moved to the new family, based mainly on the characteristic mandible; the large clypeus with a series of small denticles on the apical margin; the frons protruding over lateral portions of clypeus, directing the antennal sockets downwards below ocular level; and the presence of nine flagellomeres. Based on resemblances with fossil impressions attributed to †Bethylonymidae, we tentatively include the new family within the superfamily †Bethylonymoidea. Discovery of †Trifionyichidae **fam. nov.** adds a novel lineage to the pool of aculeate families from the Cretaceous which did not survive to the present day.

Keywords

Burmese amber, fossil, morphology, paleoentomology, sting, Yixian formation

Introduction

Stinging wasps (Aculeata) represent over 60,000 species, corresponding to ~43% of the total diversity of Hymenoptera (Aguiar et al. 2013). They are characterized by the possession of a sting, a unique evolutionary novelty among insects used for defense and preying, being a modification of the ovipositor to deliver venom instead of laying eggs (Snodgrass 1935). Aculeata have long been recognized as a monophyletic group supported by both morphological and molecular data (Oeser 1961; Rasnitsyn 1988; Vilhelmsen et al. 2010; Johnson et al. 2013; Peters et al. 2017).

Traditionally, these wasps are divided into three superfamilies: Chrysoidea, Vespoidea and Apoidea, based on the phylogenetic analysis of Brothers (1975), Brothers and Carpenter (1993), and Brothers (1999). The Chrysoidea include mostly small parasitoid wasps with reduced wing venation, with the extant diversity composed of three larger families: Bethyridae, Chrysididae and Dryinidae, as well as four rarely collected families with mostly tropical distributions (i.e., Embolemidae, Plumariidae, Sclerogibbidae, and Scolebythidae). Vespoidea is composed by a diverse assemblage of parasitoid and predatory wasps, including the highly eusocial vespids and ants, as well as the spider wasps and velvet ants. Finally, the Apoidea comprise the bees and a large array of predatory wasp lineages, and, together with the Vespoidea, are referred to as the Aculeata *sensu stricto*.

Although Brothers' (1975) classification still is in use today, recent phylogenetic analyses based on molecular data have put in doubt the monophyly of Chrysoidea and Vespoidea (Pilgrim et al. 2008; Heraty et al. 2011; Johnson et al. 2013; Branstetter et al. 2017; Pauli et al. 2021). The families Dryinidae, Embolemidae and Sclerogibbidae, which form a clade supported by both morphology and molecules (Carpenter, 1986; Brothers and Carpenter 1993; Brothers 2011; Branstetter et al. 2017), have been recovered either as sister group of the Aculeata *s. str.* (Branstetter et al. 2017) or being the sister clade of a group formed by the remaining Chrysoidea families plus the Aculeata *s.str.* (Pauli et al. 2021). On the other hand, the Vespoidea can be split in at least three lineages, with the Formicidae being consistently recovered as sister group to the Apoidea (Pilgrim et al. 2008; Johnson et al. 2013; Branstetter et al. 2017; Peters et al. 2017).

Incongruence between molecular and morphological hypotheses complicates the assessment of the phylogenetic position of fossil aculeate families in relation to the extant taxa. At present, thirteen fossil families are attributed to Aculeata. Two families from the Cretaceous are recognized in Chrysoidea: †Chrysothyridae and †Plumalexidae, both with phylogenetic affinities to the extant families Chrysididae and Plumariidae, respectively (Brothers 2011; Melo and Lucena 2020; Brothers and Melo 2021). Within the Apoidea the fossil families †Allommationidae, †Angarosphecidae, †Cirrosphecidae, and †Spheciellidae, from the Cretaceous, are recognized (Rosa and Melo 2021). The families †Bryopompilidae, †Burmusculidae, †Falsiformicidae, †Holopsenellidae, †Melittosphecidae, and †Panguidae are either tentatively associated to Vespoidea or considered as *incertae sedis* within Aculeata, due to lack of obvious synapomorphies linking them to extant lineages (Rodríguez et al. 2015; Zhang et al. 2018a; Li et al. 2020;

Rasnitsyn et al. 2020; Rosa and Melo 2021; Lepeco and Melo 2022). Finally, the †Bethylonymidae are considered as stem aculeates, with a fossil record dating back to the Middle Jurassic (Rasnitsyn 1975, 1988; Grimaldi and Engel 2005).

Aculeate wasps, including Formicidae, comprise about 61% of all Hymenoptera described from amber deposits in Myanmar, which currently represents the richest source of Cretaceous insects (Rasnitsyn et al. 2016). The fauna found in Burmese amber is remarkable for its endemic aspect, revealing a rich paleoenvironment with no counterparts elsewhere in the globe (Zhang et al. 2018b). Regarding aculeate wasps, eight families are known solely from inclusions in Burmese amber, not being recorded at any other fossil deposit or in the extant fauna. Fossiliferous amber from Myanmar was usually gathered from several mines in the Hukawng Valley, Kachin state, with an estimated age of ca. 99 my (Shi et al. 2012). More recently, other deposits have been explored commercially, including mines in the Sagaing Region, near the township of Hkamti (Liu 2018). Amber from Hkamti is older in relation to Kachin amber, with an estimated age of ca. 110 my (Xing and Qiu 2020).

In the present study, we describe a new family of stinging wasps from the Cretaceous, including three new genera from Burmese amber. We also reinterpret the identity of the fossil genus †*Mirabythus*, described by Cai et al. (2012) based on rock impressions from the Yixian formation, China, and originally attributed to the family Scolebythidae. Key characteristics linking †*Mirabythus* to the newly described family are evidenced.

Methods

The amber pieces containing the new taxa described here were obtained from dealers established in Thailand and China. Pieces are derived from amber mines in northern Myanmar (Hukawng Valley, Kachin state and Hkamti, Sagaing region). A map containing the localities from where the amber was obtained can be found in Xing and Qiu (2020). The examined material, including type specimens, is permanently deposited at the Departamento de Zoologia (DZUP) of the Universidade Federal do Paraná (UFPR) under care of the senior author. In order to have a better view of the inclusions, the pieces were manually trimmed with a jewelry saw and ground with wet emery paper (grit sizes of 800 to 3000). Final polishing was obtained using a sanding sponge pad (grit size of 5000), followed by rubbing in soft cloth.

General morphological terminology mostly follows Huber and Sharkey (1993). The abbreviations F, S and T are employed for flagellomeres, metasomal sterna, and metasomal terga, respectively. We refer to the section of vein Rs enclosing the first submarginal cell as 2Rs. Veins 2r-m and 3r-m are referred to as 2rs-m and 3rs-m respectively. For structures related to the sting apparatus we follow Barbosa et al. (2021), except that the numbering of structures follows the metasomal ordering and not abdominal ordering. Observations and descriptions were made using a Leica M125 stereomicroscope. The color images were obtained by a Leica DFC295 digital camera attached to the stereomicroscope, following the illumination scheme developed by

Kawada and Buffington (2016). The resulting images were merged with the software Zerene Stacker (Zerene Systems, LLC). The figures were enhanced using the free software GIMP 2.8.16 (The GIMP Team). Line drawings of the presently described taxa were made with the aid of a camera lucida. All measurements are given in millimeters (mm). Measurements were taken at an angle that provided the most accurate view of the structure being measured; in the case of body length, when necessary, separate measurements for head, mesosoma and metasoma were summed to provide the total value. Setae were measured relative to the size of the mid ocellus. We used “tiny” for setae shorter than ocellar diameter; “short” for setae not surpassing twice ocellar diameter, “medium-sized” for setae with about 2–3 times ocellar diameter, and “long” for setae surpassing 3 times ocellar diameter. Proportions and measurements of head parts are provided in reference to the anterior-posterior axis.

Results

Systematic paleontology

Hymenoptera Linnaeus, 1758

Apocrita Gerstaecker, 1867

Aculeata Latreille, 1802

†Bethylonymoidea Rasnitsyn, 1975

†Trifionychidae Lepeco & Melo, fam. nov.

<https://zoobank.org/C8401C22-05F8-4797-96FF-B5FE8F1A45F4>

Type genus. †*Trifionyx* Lepeco & Melo, gen. nov.

Included genera. †*Prionaspidion* Lepeco & Melo, gen. nov., †*Trifionyx* Lepeco & Melo, gen. nov., †*Trifionyximus* Lepeco & Melo, gen. nov., †*Mirabythus* Cai, Shih & Ren.

Diagnosis. The following set of characters differentiate †Trifionychidae fam. nov. from other aculeate lineages: falciform mandible, apex abruptly tapering and becoming strongly curved at distal two-thirds; apex of clypeus widely rounded and projecting over mandibles; frons protruding over lateral portion of clypeus, forming tube in which antennal radicle is inserted; antennal socket directed laterally on head, below ocular level; both sexes with nine flagellomeres; partial or complete fusion of veins C and Sc+R on forewing; and base of the metasoma forming small petiole (more easily visualized in ventral view). Other helpful diagnostic characters found in all family members are the percurrent notauli, strongly diverging anteriorly; dorsal surface of propodeum posteriorly delimited by transverse carina; and third valvula very elongated, undivided, and exposed at rest. Additional features unique to some members of the family are the clypeal apex sometimes with serial indentations, giving it a serrate aspect (†*Mirabythus*, †*Prionaspidion* gen. nov. and, to a lesser extent, †*Trifionyx* gen. nov.) and trifid tarsal claws (†*Trifionyx* gen. nov. and †*Trifionyximus* gen. nov.).

Description. *Head.* Large, as wide as or wider than mesosoma; prognathous to obliquely hypognathous. Palps shorter than mandible. Mandible wide basally, with well-delimited depressed region between anterior condyle and posterior acetabulum; distally tapering and curved. Labrum very reduced, inconspicuous. Clypeus large; apex widely rounded and projected over mandibles. Malar space width between one or two times the diameter of scape. Frons protruding over lateral portion of clypeus, forming tube concealing antennal radicle. Compound eye ovoid, bulging. Three ocelli present. Hypostomal bridge long, at least as long as basal mandibular width; anteriorly delimited by strong and curved carina between bases of mandibles. Occipital carina well developed, complete. Antennal socket directed laterally on head, anterior to ocular level; dorsal rim slightly projecting over radicle. *Antenna.* Scape long, tubular, at least twice as long as its maximum width; main shaft of scape forming angle of about 45° in relation to insertion of radicle. Pedicel long, narrowed at base, at least twice as long as its maximum width. Flagellum with nine flagellomeres. *Mesosoma.* Pronotum anteriorly declivitous; pronotal flange well developed, covering propleuron in dorsal view; dorsolateral lobe reaching tegula; posterolateral corner narrow, strongly projecting towards procoxa. Propleuron with percurrent carina dorsally; dorsal and ventral edges completely abutting; posterior edges not diverging; epicoxal lobe present. Basisternum small, most of external portion of prosternum facing backwards. Notaulus well developed, indicated as percurrent sulcus; notauli strongly diverging anteriorly. Parapsidial lines absent. Scutellum shorter than mesoscutum; anteriorly with broad and deep sulcus posterior to transscutal articulation; axillae small. Prepectus absent, mesepisternum forming a continuous sclerite. Ventral portion of mesepisternum anteriorly marked by strong transverse angulation; mesocoxal foramina small, separated from each other by more than twice their width. Metanotum short, not covered by scutellum medially. Metepisternum broadly separating metacoxae ventrally, but not forming plate; submetapleural carina well developed above metacoxa. Metacoxal foramen small. Propodeum long, at least as long as mesoscutum; dorsal and posterior surfaces well defined; spiracle positioned on transition between lateral and dorsal portions of the sclerite; propodeal foramen separated from metacoxal foramina by sclerotized bridge. *Legs.* Coxae small and globose. Femora broad. Protrochanter elongated; inserted posteriorly on procoxa. Meso- and metatrochanters very small, globose. *Forewing.* Veins C and Sc+R partially fused, costal cell obliterated. With one or no submarginal cell enclosed by tubular veins. Veins 3rs-m and 2m-cu absent. Veins not reaching distal margin of wing. *Metasoma.* Basally with small petiole; with seven exposed terga and eight exposed sterna on males; less segments exposed on females. T1 small, forming convex, rounded plate; posterior margin entire; lateral line absent. T2-T6 wider than long, posterior margins widely rounded. S1 rounded, relatively reduced; S2-S5 wider than long, posterior margins widely rounded. Without constriction or specialized articulation between first and second metasomal segments. *Sting apparatus.* Well developed. Seventh sternum enclosing most of sting. Second valvifer very narrow. Third valvula longer than wide, narrow; as a unique piece, without articulation; permanently exposed in some of the taxa. Terebra curving upwards. First and second valvulae of equal size. Furcula well developed, V-shaped, with very short posterior arm.

Key to the genera of †Trifionyichidae fam. nov.

- 1 Forewing without cells enclosed by tubular veins, marginal cell absent; head distinctly enlarged, far wider than mesosoma (mid-Cretaceous Burmese amber) **2**
- Forewing with radial and first cubital cells enclosed by tubular veins, marginal cell present, either open or closed; head not distinctly enlarged, slightly wider than mesosoma **3**
- 2 Tarsal claws simple or bifid; eyes glabrous; mesotibia with none or only a single spur; dorsal surface of propodeum without depression between spiracles; lower margin of lateral ocelli well-above upper eye level; disc of clypeus almost flat †*Prionaspidion* Lepeco & Melo, **gen. nov.**
- Tarsal claws trifid; eyes covered with erect setae; mesotibia with two spurs; dorsal surface of propodeum with transverse depression between spiracles; ocellar triangle below upper eye level; disc of clypeus convex †*Trifonyx* Lepeco & Melo, **gen. nov.**
- 3 Clypeus well developed, projecting well ahead of mandibular bases, its apex denticulate; submarginal cell relatively short, less than 1.5 times as long as wide, distally closed by vein 2Rs (distal limit of submarginal cell confluent with m-cu); body length above 6 mm (Early Cretaceous of China) †*Mirabythus* Cai et al.
- Clypeus relatively short, slightly projected over mandibular bases, its apex entire, without denticles; submarginal cell relatively long, about twice as long as wide, distally closed by vein 2rs-m, which is distanced from vein m-cu by about its length; body length below 5 mm (mid-Cretaceous Burmese amber) †*Trifonyximus* Lepeco & Melo, **gen. nov.**

†*Prionaspidion* Lepeco & Melo, **gen. nov.**

<https://zoobank.org/DB1E645C-2016-4079-A941-20A780DFB298>

Type species. †*Prionaspidion brevidens* Lepeco & Melo, sp. nov.

Included species. †*Prionaspidion brevidens* Lepeco & Melo, sp. nov., †*Prionaspidion nanus* Lepeco & Melo, sp. nov.

Diagnosis. Species in the new genus are characterized by the combination of the following characters: absence of enclosed cells in the forewing; enlarged head, which is far wider than the mesosoma; vertex flat in frontal view; lower margin of lateral ocelli well-above upper eye level; and metasoma shortened, with telescopic segments. Additional diagnostic features are the relatively small eyes in comparison to the head size and the tibial spur formula: 1-1-1 or apparently 1-0-1. Females have simple tarsal claws, while the only known male has bifid claws. In the type species, it seems that the apical portion of the third valvulae is permanently exposed.

Description. Head. Enlarged, far wider than mesosoma; prognathous. Apical margin of clypeus completely filled with indentations or denticles; disc of clypeus about as large as compound eye, almost flat. Frons wider than eye length, flat.

Frontal line indicated as shallow sulcus near mid ocellus. Compound eye relatively small, bulging, glabrous. Vertex flat in frontal view; extending behind lateral ocelli for at least 1.5 times length of ocellar triangle. Lower margin of mid ocellus near upper tangent of compound eye. Lower margin of lateral ocelli well-above upper eye tangent. **Antenna.** F1-F8 about twice as long as maximum width; F1 about as long as F2. **Mesosoma.** Pronotal collar relatively long, at least as long as mesoscutum; anterior surface of pronotum somewhat rounded in dorsal view, with transverse sulcus at mid-height; surface near posterior edge without transverse depression. Surface of mesoscutum between notauli flat, at the same level as lateral surfaces. Mesepisternum with a shallow transverse sulcus above mesepisternal pit. Metanotum with few short carinae on sublateral surfaces. Propodeum with box-like aspect, posterior slope abrupt; dorsal surface not depressed between spiracles. **Legs.** Arolia not enlarged. Tibial spur formula 1-1-1 or apparently 1-0-1. **Forewing.** Without enclosed cell. Veins C and Sc+R completely fused. Pterostigma vestigial. Vein M+Cu nebulous. Vein cu-a absent. Distal portion of vein Cu absent. Vein A spectral. **Hindwing.** Vein C present, nebulous. Vein A absent. **Metasoma.** Short, far shorter than lengths of head and mesosoma combined; segments telescoped within each other.

Etymology. The name is derived from Ancient Greek, being a combination of *prion*, which means “saw”, and *aspidion*, meaning “small shield”, in reference to the clypeus with a series of denticles along its apical margin. It is a neuter name.

†*Prionaspidion brevidens* Lepeco & Melo, sp. nov.

<https://zoobank.org/A83B2DA0-1665-4188-97A4-94D4DBA6FE95>

Fig. 1

Type material. Holotype female in amber piece DZUP Bur-1919. The specimen integument is structurally well preserved, but part of its body was lost due to breaking of the amber piece. The mouthparts are broken; a set of two and another of three palpomeres can be distinguished, but we could not identify if they belong to maxillar or labial palps; the right mandible and the apex of the left one was sanded off. The left antenna is disarticulated, but intact. The right antenna is disarticulated and is represented only by F3 to F9. The right fore and mid legs were sanded off. Parts of the hind wings are present, but we could not identify its shape or venation. The metasoma is compacted, perhaps due to a telescopic capacity of its segments. Syninclusions: the apex of a leaf, which is slightly larger than the specimen; two unidentified mites; stellate trichomes; spores; and debris.

Diagnosis. The species can be separated from †*P. nanus* sp. nov. by the larger body size (over 4 mm); presence of a carina adjacent to inner orbit, reaching dorsal rim of antennal socket (Fig. 1D); denticles on the apical margin of clypeus well defined, at least on sublateral surfaces (Fig. 1C, D); and the relatively slender profemur, about 4.2 times as long as maximum width.

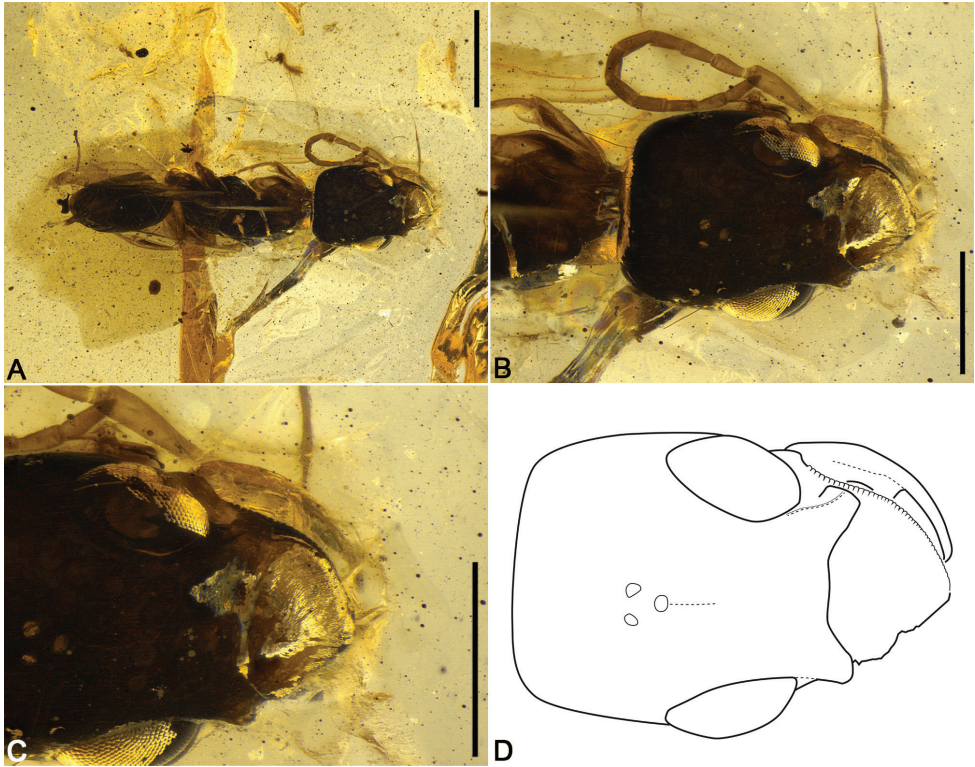


Figure 1. Holotype female of †*Prionaspidion brevidens* sp. nov. (DZUP Bur-1919) **A** habitus, dorsal view **B** dorsal view of head **C** close-up of clypeus. Scale bar: 0.5 mm. **D** line drawing of head, dorsal view, not in scale. Scale bar: 1 mm (**A**); 0.5 mm (**B, C**).

Description. Female. Measurements: approximate body length: 4.2 mm; maximum head length: 1.1 mm; maximum head width: 0.9 mm; medial clypeus length: 0.3 mm; approximate forewing length: 2.0 mm. **Color.** Poorly preserved, body apparently brown. Wings hyaline, veins light brownish. **Pubescence.** Head, metasoma and most of mesosoma apparently glabrous. Mesepisternum with sparse coverage of tiny setae on lateral surface. Short bristles visible on apex of tarsomeres; first tarsomere of all legs densely covered by small setae. Forewing with homogeneous coverage of tiny setae; anterior margin with dense tiny setae, setae as long as half width of vein C+Sc+R. **Sculpturing.** Smooth overall. Head apparently with tiny scattered punctures. Lateral portion of mesepisternum with sparse punctures. Metapostnotum filled with rugae delimiting wide spaces; medially with a straight longitudinal carina; dorsal surface of propodeum rugose posteriorly. **Structure.** Palps not distinguishable. Clypeal disc about twice as wide as long, larger than compound eye; apical margin with homogeneously sized, deep, blunt indentations. Frons with strong carina adjacent to inner orbit and reaching dorsal rim of antennal socket. Eyes separated medially by about 1.4 times eye length. Mid ocellus separated from lateral ocellus by about its diameter. Lateral

ocellus distanced from inner orbit of eye by about 2.5 times ocellar triangle length. Vertex extending behind lateral ocelli for about twice the length of ocellar triangle. Hypostomal bridge as long as 1.5 times basal mandibular width. Scape about 4 times as long as maximum width; pedicel about as long as F1. Metapostnotum visible externally, occupying most of the dorsal surface of propodeum medially. Profemur about 4.2 times as long as maximum width. Basitarsomere of fore leg as long as 0.7 times protibial length. Tibial spur formula apparently 1-0-1. Basitarsomere of hind leg about 0.6 times metatibial length. Tarsal claws simple.

Etymology. The name is a combination of the Latin *brevis*, meaning “short”, and *dens*, meaning “tooth”. The name is an allusion to the presence of a series of short denticles on the clypeal margin. It is a noun in apposition.

†*Prionaspidion nanus* Lepeco & Melo, sp. nov.

<https://zoobank.org/29966B39-4973-40C8-9471-66D79BB77EBE>

Figs 2–4

Type material. Holotype male in amber piece DZUP Bur-2265 (Fig. 2). The specimen is almost fully articulated, except for part of the right metatarsus, and a detached metasomal sclerite, near the metasoma. Syninclusions: an unidentified mite and a large number of debris and plant trichomes. Paratype specimen (apparently a female, judging by the simple tarsal claws) in amber piece DZUP Bur-1127 (Figs 3, 4). The specimen is relatively well preserved, fully articulated, with the exception of the distal portion of the metasoma and the hind wings. No sting or genitalia are present on the piece. A bubble hinders the visualization of the propodeum. Syninclusions: five unidentified mites and debris.

Diagnosis. The species can be separated from †*P. brevidens* sp. nov. by the smaller body size (forewing length between 1.3 and 1.4 mm in the examined specimens); carina on the dorsal rim of antennal socket not reaching the inner orbit; poorly defined and irregularly sized denticles on the apical margin of clypeus; and the relatively robust profemur, about 2.5 times as long as maximum width.

Description. Holotype male. Measurements. Approximate body length: 2.3 mm; maximum head length: 0.7 mm; maximum head width: 0.5 mm; medial clypeus length: 0.2 mm; approximate forewing length: 1.4 mm. **Color.** Poorly preserved, body apparently dark brown. Legs yellowish. Wings hyaline, veins light brownish. **Pubescence.** Head mostly glabrous, except for short erect setae on mandible and clypeus. Mesosoma and most of metasoma apparently glabrous. Legs mostly with short setae; apex of tarsomeres with two to five short bristles. Apex of T4 and T5 with sparse long setae. Forewing with homogeneous coverage of tiny setae; anterior margin with dense tiny setae, setae as long as half width of vein C+Sc+R. **Sculpturing.** Smooth, where preserved. Metapostnotum apparently occupying most of dorsal surface of propodeum medially, without basal rugae. **Structure.** Maxillary palp with at least three palpomeres. Labial palpomeres not distinguishable. Mandible tridentate, upper tooth larger than lower teeth. Clypeal disc

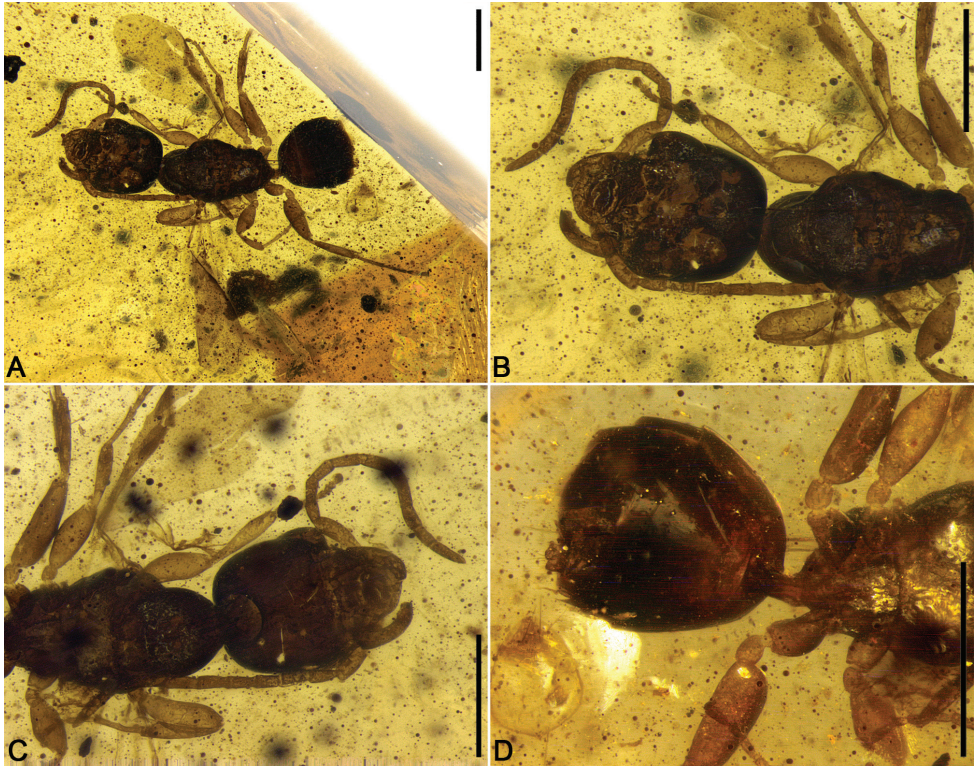


Figure 2. Holotype male of †*Prionaspidion nanus* sp. nov. (DZUP Bur-2265) **A** habitus, dorsal view **B** dorsal view of head and mesosoma **C** ventral view of head and mesosoma **D** ventral view of metasoma. Scale bars: 0.5 mm.

about as wide as long, slightly smaller than compound eye; apical margin with irregular, weak, blunt denticles. Frons without strong carina adjacent to inner orbit; dorsal rim of antennal socket with low carina directed towards frons. Eyes separated medially by about eye length; lower orbits slightly converging. Mid ocellus separated from lateral ocelli by about 1.5 times its diameter. Lateral ocellus separated from inner orbit of eye by about 3 times ocellar triangle length. Vertex extending behind lateral ocelli for about 1.5 times the length of ocellar triangle. Hypostomal bridge 3.5 times as long as basal mandibular width. Scape about 4 times as long as maximum width; pedicel about 1.3 times as long as F1. Profemur about 2.5 times as long as maximum width. Basitarsomere of fore leg as long as 0.5 times protibial length. Tibial spur formula 1-1-1. Basitarsomere of hind leg about as long as 0.7 times metatibial length. Tarsal claws bifid.

Paratype female. As for the male, except: **Measurements.** Approximate body length: 2.0 mm; maximum head length: 0.6 mm; maximum head width: 0.5 mm; medial clypeus length: 0.1 mm; approximate forewing length: 1.3 mm. **Color.** Poorly preserved, body apparently brown. **Pubescence.** Head, mesosoma and most of metasoma

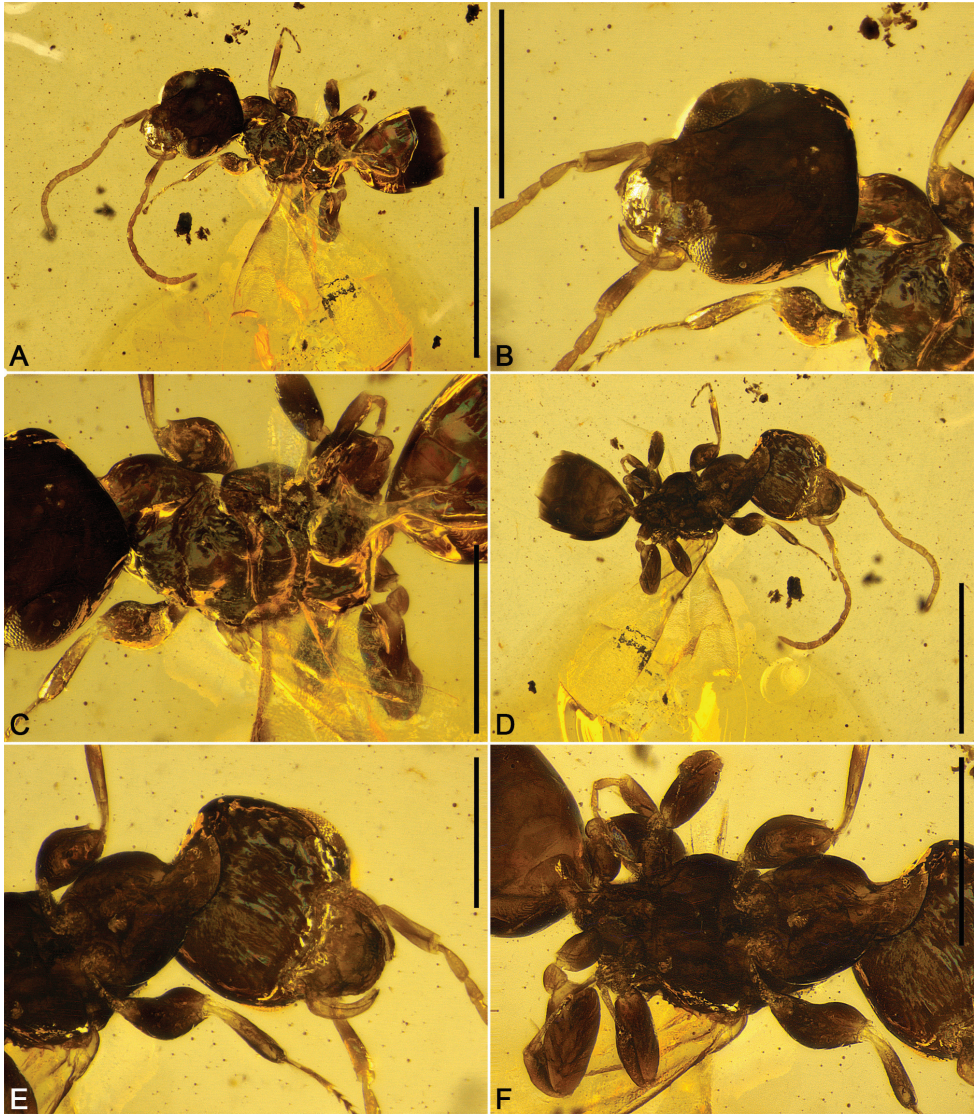


Figure 3. Paratype (apparently female) of †*Prionaspidion nanus* sp. nov. (DZUP Bur-1127) **A** habitus, dorsal view **B** head, dorsal view **C** mesosoma, dorsal view **D** habitus, ventral view **E** head, ventral view **F** mesosoma, ventral view. Scale bar: 1 mm (**A, D**); 0.5 mm (**B, C, E, F**).

apparently glabrous. Apex of T4 and T5 with sparse setae. **Sculpturing.** Head apparently with tiny scattered punctures. **Structure.** Head slightly shorter than that of male; tibial spur formula apparently 1-0-1; tarsal claws simple.

Etymology. The name is derived from the Latin *nanus*, meaning “dwarf”, in allusion to the relatively small size of the species. The name is an adjective.



Figure 4. Paratype (apparently female) of †*Prionaspidion nanus* sp. nov. (DZUP Bur-1127). Habitus, ventral view. Scale bar: 1 mm.

†*Trifionyx* Lepeco & Melo, gen. nov.

<https://zoobank.org/C7CFFCD0-D5DF-43EF-9514-E5A12EFADBA5>

Type species. †*Trifionyx pilosus* Lepeco & Melo, sp. nov.

Diagnosis. The single species allocated in this genus is differentiated from †*Mirabythus* and †*Trifionyximus* gen. nov. by the absence of cells enclosed by tubular veins in the forewing (Fig. 5F) and the enlarged head, which is far wider than mesosoma. From †*Prionaspidion* gen. nov. it can be differentiated by the trifid tarsal claws (Fig. 5G); tibial spur formula 1-2-2; dorsal surface of propodeum with a transverse depression between spiracles (which may correspond to the metapostnotum); ocellar triangle below upper eye level and convex clypeus disc. †*Trifionyx* gen. nov. is unique within †Trifionychidae fam. nov. in having the body with conspicuously developed pubescence, including on the compound eyes.

Description. Head. Enlarged, far wider than mesosoma; prognathous. Entire apical margin of clypeus with small denticles; disc of clypeus relatively large, convex. Frons wider than twice eye length, flat. Frontal line not indicated. Compound eye relatively small, bulging, covered with erect setae. Vertex arcuate in frontal view; extending behind lateral ocelli for at least 1.5 times length of ocellar triangle. Mid ocellus

far below upper tangent of compound eye. Lower margin of lateral ocelli below upper eye tangent. **Antenna.** F1 3 times as long as maximum width, longer than F2; F2–F8 about twice as long as maximum width. **Mesosoma.** Pronotal collar relatively short, as long as half-length of mesoscutum; anterior surface of pronotum somewhat rounded in dorsal view, with transverse sulcus at mid-height; surface near posterior edge with transverse depression. Surface of mesoscutum between notauli slightly convex, level with lateral surfaces. Mesepisternum with a shallow transverse sulcus above mesepisternal pit. Metanotum with few short carinae on sublateral surfaces. Propodeum without box-like aspect, posterior slope convex; dorsal surface depressed transversally between spiracles. **Legs.** Arolia not enlarged. **Forewing.** Veins C and Sc+R completely fused. Pterostigma present. Marginal cell absent. Submarginal cell not enclosed by tubular veins. Radial, first cubital, and medial cells defined by nebulous veins. Vein M+Cu nebulous. Vein cu-a nebulous. Distal portion of vein Cu nebulous. Vein A spectral. **Hindwing.** Vein C present, nebulous. Vein A absent. **Metasoma.** Apparently short, shorter than mesosoma; segments apparently not telescoped within one another.

Etymology. The name is derived from Latin and results from the combination of *trifidus*, meaning “cleft into three”, and *onyx*, meaning “claw”. The name is masculine.

† *Trifionyx pilosus* Lepeco & Melo, sp. nov.

<https://zoobank.org/CD33CC38-52EE-43F2-99CE-9144030EF0A5>

Fig. 5

Type material. Holotype female in amber piece DZUP Bur-1906. The specimen is fully articulated, but part of the left fore leg, apex of forewings, and part of metasoma were sanded off. As the metasoma is curved frontwards, it retains part of the sting apparatus. There are no visible syninclusions.

Diagnosis. As for the genus.

Description. **Holotype female.** **Measurements:** approximate body length: 4.5 mm; maximum head length: 0.9 mm; maximum head width: 1.1 mm; medial clypeus length: 0.2 mm; approximate forewing length: 2.2 mm. **Color.** Poorly preserved, apparently dark brown. Apical margin of clypeus darkened, apparently black. Wings hyaline, veins brown. **Pubescence.** Head mostly covered with medium-sized setae, except for frons and vertex, apparently glabrous. Setae on hypostomal bridge relatively longer. Antenna densely covered with tiny decumbent setae. Mesosoma mostly with sparse medium-sized setae. Legs mostly covered by short setae; femora with longer setae on inner surface. Forewing with homogeneous coverage of tiny setae; anterior margin with dense tiny setae, setae as long as one-half C+Sc+R width. Apex of metasoma with very long erect setae. **Sculpturing.** Smooth, where preserved. **Structure.** Maxillary palp with five palpomeres. Labial palp slightly shorter than maxillary palp, apparently with four palpomeres. Mandible simple, without preapical teeth. Clypeus disc wider than medial length, slightly larger than compound eye; denticles on apical margin barely distinguishable. Frons without carina adjacent to inner orbit; dorsal rim of antennal socket with slight carina directed towards frons. Mid ocellus

separated from lateral ocelli by about twice its diameter. Lateral ocellus distanced from inner orbit of eye by about 1.5 times ocellar triangle length. Vertex extending behind lateral ocelli for about 1.5 times ocellar triangle. Hypostomal bridge 3 times as long as basal mandibular width. Scape about 3 times as long as maximum width; pedicel less than 0.5 times as long as F1. Metapostnotum not indicated by sculpturation externally. Profemur about 2.7 times as long as maximum width. Tibial spur formula 1-2-2. Basitarsomere of fore leg as long as 0.8 times protibial length. Basitarsomere of hind leg about as long as 0.8 times metatibial length. Tarsal claws trifid.

Etymology. The specific epithet means “pilose”, in allusion to the abundant pilosity of the type species. The name is an adjective.

† *Trifionyximus* Lepeco & Melo, gen. nov.

<https://zoobank.org/B883DD04-525B-4FC8-9995-32AA463818A4>

Type species. † *Trifionyximus cracens* Lepeco & Melo, sp. nov.

Diagnosis. The new genus is distinguished from the other genera described from Burmese amber by the presence of enclosed cells in the forewing (Fig. 6E); and head comparatively small. From † *Mirabythus*, it differs in having the clypeus relatively short with a smooth apex, without denticles; and submarginal cell relatively long, about twice as long as wide, distally closed by vein 2rs-m (in † *Mirabythus* the cell is closed distally by vein 2Rs, judging by its confluence with m-cu), which is distanced from vein m-cu by about its length. An additional difference between both genera is the smaller size of † *Trifionyximus* gen. nov., not surpassing 5 mm.

Description. Head. Not enlarged, slightly wider than mesosoma; obliquely hypognathous. Apical margin of clypeus entire, without denticles; disc of clypeus smaller than compound eye, strongly convex. Frons gently convex. Frontal line inconspicuous. Compound eye relatively large, occupying most of lateral surface of head, glabrous. Vertex arcuate, short, extending behind lateral ocelli for less than length of ocellar triangle. Lower margin of lateral ocelli below upper eye tangent. **Antenna.** F1–F8 about 1.5 times as long as maximum width; F1 about as long as F2. **Mesosoma.** Pronotal collar longer than mesoscutum; anterior surface somewhat narrowed medially in dorsal view, with transverse sulcus at mid-height; surface near posterior edge depressed transversally. Surface of mesoscutum between notauli convex, bulging in relation to lateral surfaces. Mesepisternum without transverse sulcus above mesepisternal pit. Metanotum without carinae on sublateral surfaces. Propodeum without box-like aspect, posterior slope convex; dorsal surface not depressed between spiracles. **Legs.** Arolia enlarged. **Forewing.** Veins C and Sc+R partially fused. Vein C nebulous, costal cell very narrowed and obscured at its mid-length. Pterostigma well developed, small. Marginal cell open, distal portion of vein Rs ending as nebulous vein near distal margin of wing. Submarginal cell posteriorly closed by 2rs-m. Medial cell posteriorly closed by nebulous veins. Vein M+Cu tubular. Vein cu-a tubular. Distal portion of vein Cu ending as a nebulous vein near distal margin of wing. Vein A tubular. **Hindwing.** Vein C present, tubular for at least basal third of wing, becoming nebulous distally. Vein A present,

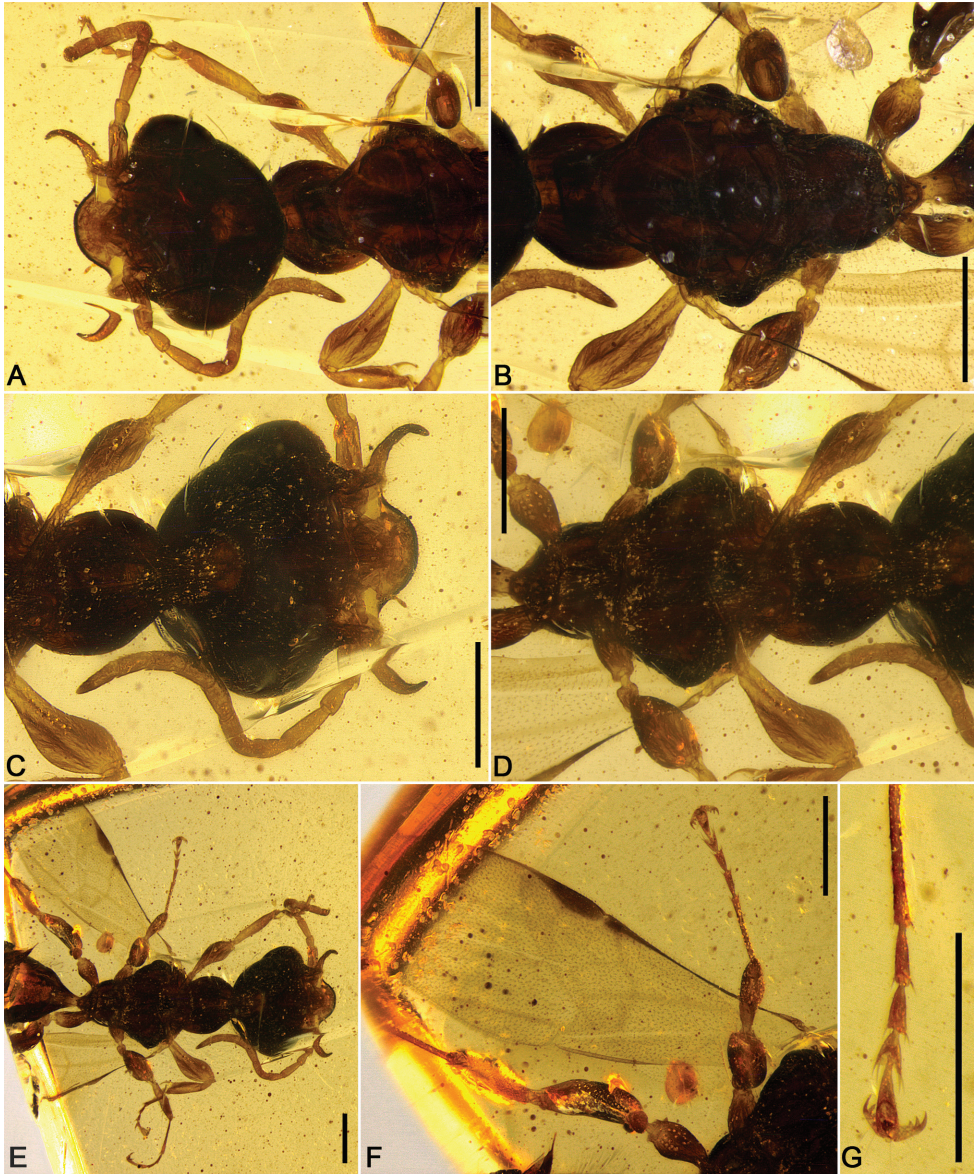


Figure 5. †*Trifionyx pilosus* sp. nov. Holotype female (DZUP Bur-1906) **A** dorsal view of head and mesosoma **B** dorsal view of mesosoma **C** ventral view of head **D** ventral view of mesosoma, habitus, ventral view **E** wings **F** detail of mesotarsal claw. Scale bars: 0.5 mm.

short. *Metasoma*. Long, but shorter than lengths of head and mesosoma combined; segments not distinctly telescopic within each other.

Etymology. The name is derived from the type genus of the family with the addition of the Latin suffix *-imus*, meaning “pertaining to” or “related to”. The name is masculine.

† *Trifionyximus cracens* Lepeco & Melo, sp. nov.

<https://zoobank.org/EE0362A0-0A7F-43CD-B84C-475AB469BA66>

Fig. 6

Type material. Holotype female in amber piece DZUP Bur-828. The specimen is fully articulated, but part of the right antenna was sanded off. The right forewing apex is fragmented. The left side of the head, the posterior portion of the mesosoma and parts of the metasoma are covered by calcite. There are no syninclusions except for scattered debris. The paratype male is in amber piece DZUP Bur-1386. The specimen is fully articulated, but parts of the mesosoma and the legs are diaphanized. Part of the right antenna was sanded off during preparation. A large calcite bubble obstructs the view of part of the left side of the mesosoma. Syninclusions: a small psocid.

Diagnosis. As for the genus.

Description. Female Holotype. Measurements: approximate body length: 3.6 mm; maximum head length: 0.7 mm; approximate forewing length: 1.9 mm. **Color.** Poorly preserved, apparently dark brown. Wings hyaline, veins brown. **Pubescence.** Head sparsely covered with short setae. Forewing with homogeneous coverage of tiny setae; anterior margin with dense tiny setae, setae as long as half width of veins C+Sc+R. **Sculpturing.** Smooth, where preserved. **Structure.** Maxillary palp with at least three palpomeres. Labial palp not distinguishable. Mandible quadridentate, with three preapical teeth with similar sizes, lower tooth larger than preapical teeth. Clypeus disc about as wide as long, far smaller than compound eye. Frons without carina adjacent to inner orbit; dorsal rim of antennal socket without carina directed towards frons. Mid ocellus separated from lateral ocelli by about its diameter. Lateral ocellus distanced from inner orbit of eye by about ocellar triangle length. Vertex extending behind lateral ocelli for about the width of mid ocellus. Hypostomal bridge 3 times as long as basal mandibular width. Scape about twice as long as maximum width; pedicel about 1.5 times as long as F1. Metapostnotum obstructed. Profemur about 1.2 times as long as maximum width. Tibial spur formula 1-2-2. Basitarsomere of fore leg as long as 0.5 times protibial length. Basitarsomere of hind leg about as long as 0.7 times metatibial length. Tarsal claws trifold.

Male Paratype. As for the female, except: **Measurements:** approximate body length: 3.0 mm; maximum head length: 0.5 mm; maximum head width: 0.6 mm; medial clypeus length: 0.1 mm; approximate forewing length: 1.8 mm. **Color.** Head black. Color not preserved in legs and mesosoma, due to diaphanization. Metasomal sclerites apparently dark brown. Wings hyaline, slightly darkened near marginal cell, veins dark brown. **Pubescence.** Head, mesosoma and most of metasoma apparently glabrous. Apical metasomal sclerites with sparse erect setae. **Sculpturing.** Smooth, where preserved. **Structure.** Upper tooth of mandible smaller than lower tooth. Scape about 3 times as long as maximum width. Profemur about twice as long as maximum width.

Etymology. From the Latin *cracens*, meaning “slender”, in allusion to the body shape of the type specimens. The name is an adjective.

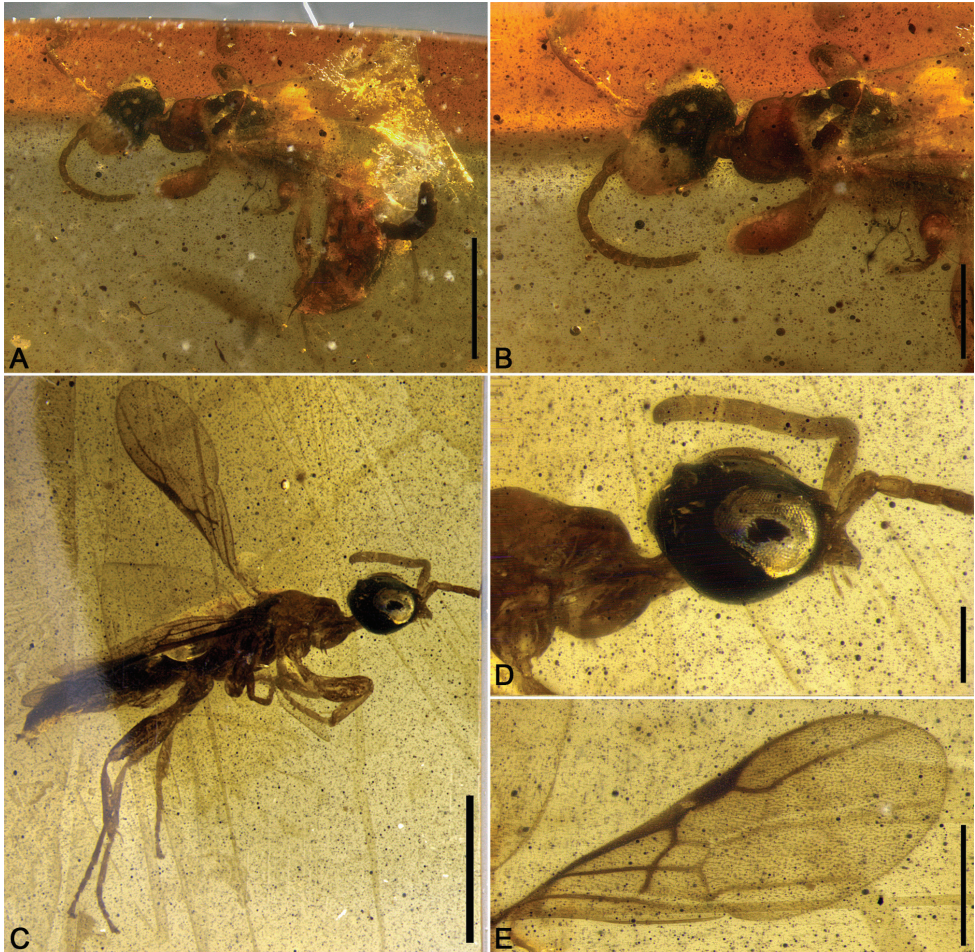


Figure 6. †*Trifionyximus cracens* sp. nov. **A, B** holotype female (DZUP Bur-828) **A** habitus, dorsolateral view **B** dorsolateral view of head and mesosoma **C–F** paratype male (DZUP Bur-1386) **C** habitus, lateral view **D** head, lateral view **E** forewing. Scale bar: 1 mm (**A, C**); 0.5 mm (**B**); 0.2 mm (**D**); 0.4 mm (**E**).

†*Trifionychidae* sp. indet.

Fig. 7

Comments. We refer here to a female belonging to †*Trifionychidae* fam. nov., found in amber piece DZUP Bur-332 and represented by the head, most of the mesosoma and fragments of the metasoma. The female is clearly a representative of the new family due to the presence of nine flagellomeres; characteristically curved mandibles; frons protruding over lateral portions of clypeus; and trifold tarsal claws. The specimen is interesting for the presence of a dissected sting apparatus and for having the head plus

the propleura and fore legs detached from the remainder of the body. The parts are very close to the body, and are congruent to what is found in other representatives of the family. The anterior portion of its mesopleura can be observed without obstruction and it is possible to see that it lacks a prepectus. The whole region forms an entire sclerite without any indication of articulation or line of fusion of the prepectus with the mesopleura. In relation to the sting apparatus, although most of the sclerites associated to the sting are lost or scattered through the piece, the characteristic upward curvature of the sting shaft can be visualized (Fig. 7D). We opted to not describe this inclusion as a new taxon or assign it to any species of †Trifionychidae fam. nov., due to the absence of forewings, which are essential to differentiate genera within the family. Nevertheless, the specimen seems to be more related to †*Tryfionyximus* gen. nov., due to the relatively small clypeus, trifid claws and the propodeum lacking a box-shape aspect and without transverse depression between spiracles.

†*Mirabythus* Cai, Shih & Ren

Figs 8, Suppl. material 1: figs S1–S5

†*Mirabythus* Cai, Shih & Ren, 2012 in Cai et al. (2012): 58. Type species: †*Mirabythus lechrius* Cai, Shih & Ren, 2012.

Comments. In the original description, Cai et al. (2012) considered that the mandibles of †*Mirabythus* had a series of small notches on the anterior surface. We interpret that these notches correspond in fact to the apical margin of the clypeus, a condition also found in †*Prionaspidion* gen. nov. and †*Trifionyx* gen. nov. (more evident in †*P. brevidens* sp. nov.). The clypeus of †*Mirabythus* is large, comprising nearly one-third of the entire head length, as indicated by the position of the epistomal groove (Fig. 8C, D). The apical margin of the clypeus and the anterior surface of the mandibles are aligned in the type specimens, and this is also observed in specimens from Burmese amber. The antennal sockets of †*Mirabythus* are directed towards the apical margin of the clypeus, below the lower eye tangent (Fig. 8C, D). Cai et al. (2012) represent with dashed lines at least fourteen articles in the antennae of †*M. liae*. For us, it is nearly impossible to count the number of antennomeres in the holotype. In the case of †*M. lechrius*, we can clearly see nine flagellomeres in the holotype, with the first two being far longer than the remaining flagellomeres (Fig. 8A, B).

It is difficult to determine whether the anterior flange of the pronotum is well developed, but none of the specimens exhibit a long propleura with a wide membranous area medially, as is found in most Scolebythidae. We interpret that the propleura are covered in dorsal view and, therefore, the pronotal flange is present. In both type specimens the legs are curled below the body, hindering the interpretation of structures in the ventral surface of the mesosoma, but two main characteristics can be observed. First, the structure originally interpreted as a large prosternum seems to

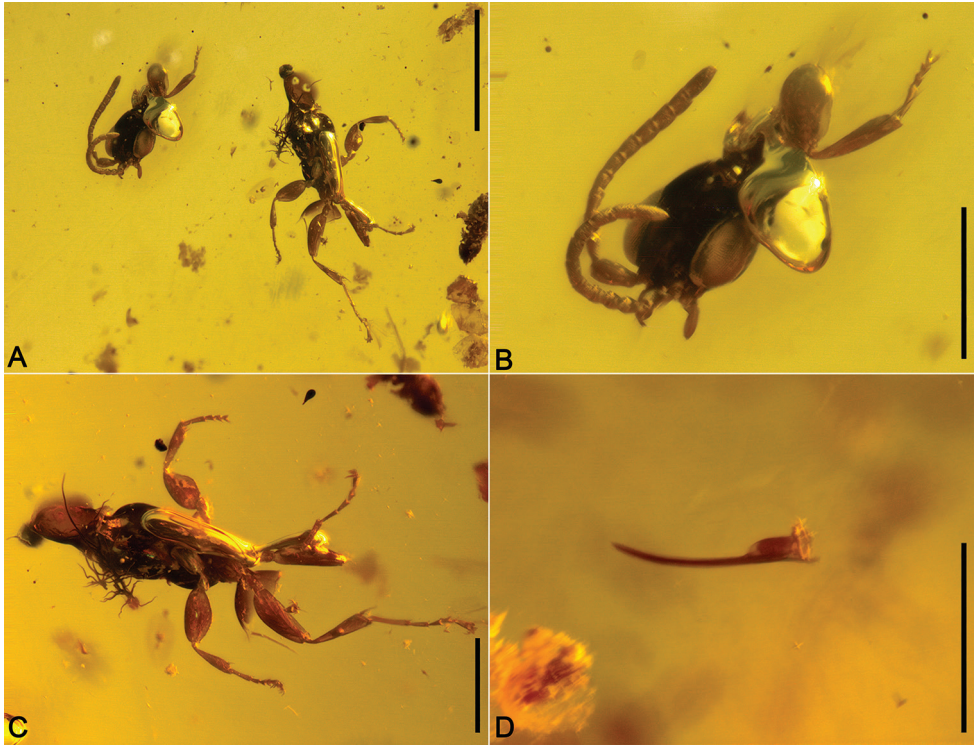


Figure 7. †Trifonychidae *sp. indet.* (DZUP Bur-332) **A** general view of head and mesosoma **B** head, dorsal view **C** mesosoma, ventral view **D** detail of sting. Scale bar: 1 mm (**A**); 0.5 mm (**B–D**).

represent a void area, where the anterior portion of the mesosoma has detached from the mesepisternum (Fig. 8A, B). In †*M. liae* this detachment is more evident than in †*M. lechrius*. We interpret that the basisternum (the ventrally exposed portion of the prosternum) is not as large as in scolebythids, for both species, similar to what is observed in †*Prionaspidion nanus* *sp. nov.* Second, a transverse dark line can be seen crossing the mesepisternum of both type specimens (more conspicuous in †*M. liae*), which probably represents the angulation of the mesepisternum found in Burmese amber trifonychids (Fig. 8A, B). This angulation is not found in Scolebythidae. The propodeum has a transverse angulation marking its posterior declivity in both specimens, a characteristic found in the new family, but not in Scolebythidae. The point of insertion of the trochanters on the procoxae is difficult to interpret in both specimens, but it is clearly not basal as in all Scolebythidae. At least one tibial spur is visible in the hind leg of the holotype of †*M. lechrius*. In none of the specimens of †*Mirabythus* it is possible to identify a costal cell on the forewing, and we interpret that, as in the species from Burmese amber, the veins C and Sc+R are fused along most of the anterior margin of the wing (Fig. 8A, B).

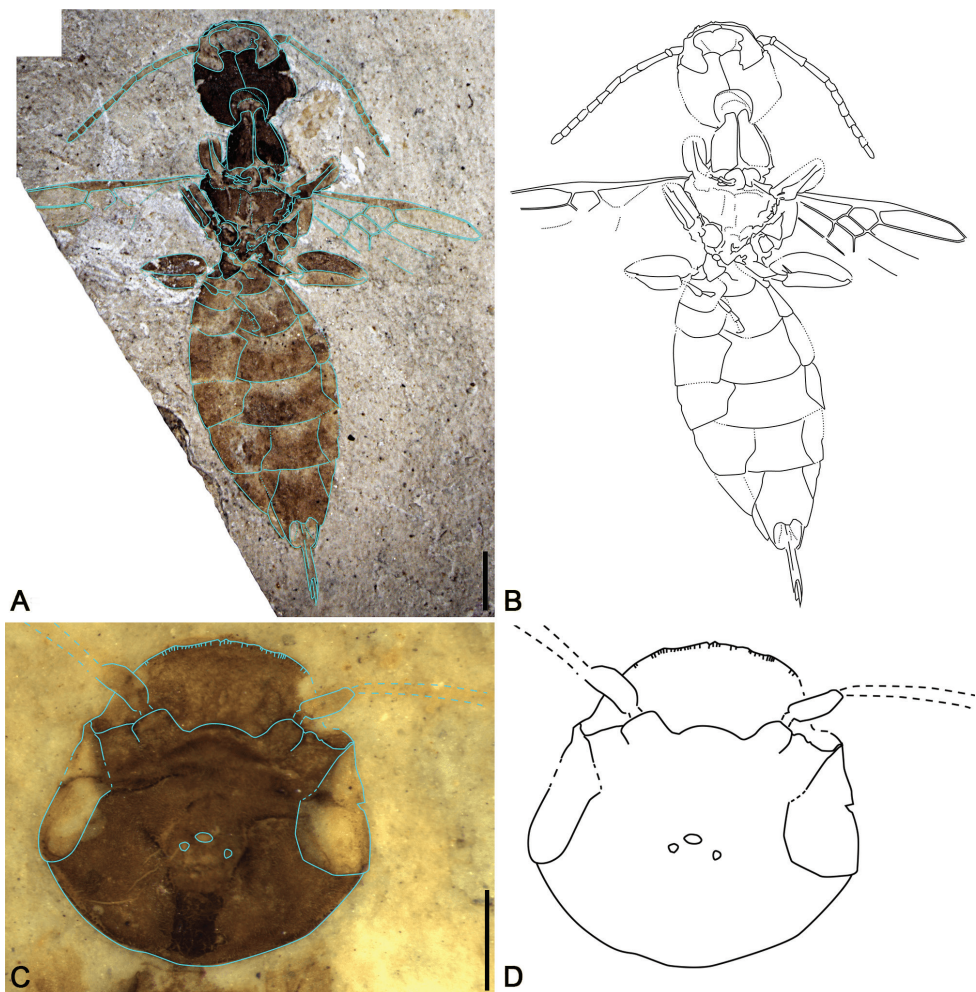


Figure 8. †*Mirabythus* Cai et al. **A, B** †*Mirabythus lechrius* Cai et al. 2012 **A** photograph of habitus, ventral view, line drawing superimposed **B** habitus, ventral view, line drawing isolated **C, D** †*Mirabythus liae* Cai et al. 2012 **C** photograph of head, dorsal view, line drawing superimposed **D** head, dorsal view, line drawings isolated. Photograph credits: Taiping Gao and Yaping Cai. Scale bar: 2 mm (**A, B**); 1 mm (**C, D**).

Part of the sting apparatus is evident in both specimens, including most of the third valvula, which is unsegmented and apparently has its apical portion permanently exposed. The terebra in the holotype of †*M. lechrius* also apparently curves upward, as in other †Trifionychidae fam. nov. In Scolebythidae the terebra is curved downward. The third valvula and terebra of †*Mirabythus* are distinctly elongated, relatively longer in comparison to females of Scolebythidae and other chrysidoids. The two unidentified specimens illustrated by Cai et al. as †*Mirabythus indet* are putative members of †Trifionychidae gen. nov. as well, although many characters are not clearly visible. Additional figures of †*M. lechrius* and †*M. liae* are available at Suppl. material 1: figs S1–S5.

Discussion

The new taxa described herein add to the pool of fossil lineages of aculeate wasps and improve our understanding about the Cretaceous entomofauna. Based on these species and on the reinterpretation of †*Mirabythus*, the novel family comprises at least four distinct genera and six species described, indicating that †Trifionychidae fam. nov. were a prolific lineage that thrived at least in the eastern landmasses of the globe during the first-half of the Cretaceous period. Unfortunately, no putative members of the family have been found in other fossil deposits besides the Burmese amber and the Yixian formation, limiting the amount of information we have about this lineage.

The two species of the genus †*Mirabythus* were misinterpreted as scolebythid wasps, but undoubtedly belong in †Trifionychidae fam. nov. Placement of the genus within the new family is supported by the characteristic curvature and tapering of the mandible; the large clypeus with a series of denticles on the apical margin (as in species of †*Prionaspidion* gen. nov. and †*Trifonyx* gen. nov.); the frons protruding over lateral portions of clypeus, directing the antennal sockets downwards below ocular level; and the presence of nine flagellomeres. The reinterpretation of †*Mirabythus* narrows the fossil record of Scolebythidae in the Early Cretaceous to three species from the Barremian, described from inclusions in Lebanese amber (Prentice et al. 1996; Engel and Grimaldi 2007). Concomitantly, the fossil record of Scolebythidae is now represented only by amber inclusions, since †*Mirabythus* was the only taxon attributed to the family with representatives preserved as rock impressions.

At the present moment, it is not possible to indicate with certainty the phylogenetic placement of †Trifionychidae fam. nov. The presence of an equal number of flagellomeres in both sexes, seven exposed metasomal terga and lack of specialized articulation or constriction between the first two metasomal segments rule out the positioning of the family among lineages of Aculeata *s. str.* (see Brothers 1975; Brothers and Carpenter 1993). In addition, members of the new family do not resemble any extant or extinct group belonging to Aculeata *s. str.* Even so, the similarity with Chrysoidea is derived from a combination of plesiomorphic and independently acquired apomorphic characters, and the new family also does not exhibit obvious synapomorphies relating it to families within Chrysoidea.

The flagellum with nine articles is an unusual feature among Chrysoidea. All representatives of Scolebythidae, †Plumalexiidae and †Chrysobythidae, as well as most species of Bethyloidea, Chrysididae and Plumariidae have antennae with eleven flagellomeres (Finnamore and Brothers 1993; Melo and Lucena 2020; Brothers and Melo 2021; Lepeco and Melo, unpublished data), with reductions to ten or eight flagellomeres occurring in rather derived lineages (Brothers 1975; Azevedo et al. 2018; Lucena and Almeida 2022). On the other hand, Dryinidae and Embolemidae usually have eight flagellomeres, while Sclerogibbidae may exhibit a multiarticulate flagellum, with at least twelve flagellomeres (Finnamore and Brothers 1993; Perkovsky et al. 2020). Therefore, the number of flagellomeres does not link †Trifionychidae fam. nov. with any specific lineage of Aculeata.

The same can be said of the wing venation. The fusion of veins C and Sc+R on the forewing is unusual among aculeate wasps. †*Mirabythus* has a relatively well-developed forewing venation, with marginal cell closed, as well as submarginal, medial and second cubital cells enclosed by tubular or nebulous veins. †*Trifionyximus* gen. nov. has a similar condition, except for the marginal cell, which is open distally, and the apparent presence of the 2rs-m enclosing the submarginal cell distally instead of the 2Rs. †*Prionaspidium* gen. nov. exhibits the most reduced forewing venation of the family, without closed cells and a vestigial pterostigma. Simplification of wing venation is a trend within Hymenoptera (Sharkey and Roy 2002; Klopstein et al. 2015), and occurred repeatedly within basal lineages of Aculeata (Melo and Lucena 2020). Assuming monophyly of †Trifionyichidae fam. nov., the presence of species with different levels of complexity on forewing venation indicates that the family represents another event of reduction within Aculeata. As far as we could observe, all members of the family lack closed cells in the hind wing, a condition shared with most chrysidoid wasps.

The morphology of the sting apparatus in †Trifionyichidae fam. nov. resembles that of Chryridoidea rather than other aculeate groups. Nevertheless, a furcula is present, differentiating the new family from the clade formed by Dryinidae, Embolemidae and Sclerogibbidae, which completely lacks this structure (Carpenter 1986; Barbosa et al. 2021). This ‘chrysidoid-like’ appearance of their sting is likely due to a plesiomorphic condition, with no obvious similarity with the sting of other aculeate families. Two additional interesting characters possessed by the new family, an undivided and permanently exposed third valvula, are features common with non-aculeate wasps (Smith 1972; Rasnitsyn 1980; Kumpanenko et al. 2019). In aculeate wasps the third valvulae are represented by a pair of sheaths that form a tube allocating the terebra (shaft of the sting), used in assisting its movements, and are kept hidden within the metasoma together with the remainder of the sting apparatus. Although the division of the third valvula in proximal and distal regions is considered as one of the synapomorphies of Aculeata (Rasnitsyn 1980; Ronquist et al. 1999), Barbosa et al. (2021) have shown that in all Chryridoidea this structure is undivided. Therefore, a divided third valvula should be considered a synapomorphy for Aculeata *s. str.* only (see Kumpanenko et al. 2019 for reversal cases within this group).

The presence of undivided and exposed third valvulae is a characteristic also found in the Mesozoic wasp family †Bethylonymidae, considered as precursors of stinging wasps and frequently recovered as sister group of Aculeata (Rasnitsyn 1975, 1980, 1988; Ronquist et al. 1999; Grimaldi and Engel 2005). Although Rasnitsyn (1975) discarded the presence of sting in †Bethylonymidae and used the exposure of the ovipositor as a character differentiating the family from Aculeata, the structure and conformation of the third valvulae are very similar to what is observed in females of †Trifionyichidae fam. nov., especially †*Mirabythus*. In common with †Trifionyichidae fam. nov., bethylonymids also exhibit reductions in the number of antennomeres, with a minimum of six flagellomeres in †*Bethylonymellus* (Rasnitsyn 1975). Another character shared at least with some bethylonymids is the fusion of the vein C with Sc+R in the forewing, that can be inferred based on photographs of †*Bethylonymus magnus* Rasnitsyn, 1975 and

†*Bethylonymellus bethyloides* Rasnitsyn, 1975. Unfortunately, this character is difficult to verify in fossils, especially in those from rock impressions, since the anterior margin of the wing may bend or fragment during the process of fossilization.

An important characteristic found in stinging wasps is the third valvula overlapping the terebra distally, with the apical portion of the terebra concealed within the third valvula. This anatomical conformation would facilitate quick and accurate movements of the interlocked first and second valvulae, that compose the terebra (Kumpanenko and Gladun 2017). The ovipositor described and illustrated by Rasnitsyn (1975) for †*Bethylonymidae* apparently exhibit the same conformation, and thus presence of a sting in these wasps cannot be discarded, since the terebra could be hidden between the large third valvulae or be absent due to preservation processes. Presence of sting would indicate that †*Bethylonymidae* are, in fact, the oldest aculeate lineage known from the fossil record. This, in accordance with the plesiomorphic characters of the new family and morphological similarity between †*Trifionychidae* fam. nov. and †*Bethylonymidae*, may indicate that both families are closely related. Alternatively, these families may compose a grade leading to Aculeata, with bethylonymids as sister group to the remaining stinging wasps. Nevertheless, we tentatively maintain †*Trifionychidae* fam. nov. within the superfamily †*Bethylonymoidea*. We consider that reevaluation of the type specimens of †*Bethylonymoidea*, as well as inclusion of species of †*Trifionychidae* fam. nov. in future cladistic analyses will be essential to elucidate the phylogenetic relationships among basal lineages of aculeate Hymenoptera.

Regarding the biological traits of the new family, species of †*Mirabythus* and *Scolebythidae* could have exhibited similar foraging habits, judging by the overall similarity between the body shape of both families. *Scolebythidae* are ectoparasitoids of beetle larvae living concealed within wood (Brothers 1981; Melo 2000), having an elongated and dorso-ventrally flattened body, as well as short and strong appendages. On the other hand, †*Trifionychidae* fam. nov. have been most commonly found in clear amber pieces, without massive amounts of debris. Inclusions in Burmese amber belonging to *Scolebythidae* and †*Holopsenellidae*, among other wasp lineages that presumably attacked wood-boring larvae, are frequently observed in pieces with considerable larger amounts of plant debris and beetle frass (Lepeco and Melo 2022; *personal observation*). Use of beetle larvae living in concealed conditions would be expected for basal clades of Aculeata, since this is considered the groundplan habit for the group (Melo et al. 2011).

Conclusions

We reaffirm the importance of describing the Burmese amber fauna. With the continued study of the ever-increasing amount of material from amber deposits in Myanmar, new insect inclusions have been described, enhancing our knowledge about mid-Cretaceous entomofauna. Observation and description of the new taxa has clarified the identity of †*Mirabythus*, an enigmatic wasp genus originally attributed to the

chrysidoid family Scolebythidae. Perhaps, without the newly described material, we would not be able to infer the non-scolebythid identity of †*Mirabythus*. Nevertheless, the peculiar mosaic of derived and plesiomorphic characters of the new family suggests that the Cretaceous diversity of aculeates may have been composed of many other elements that did not survive to the present day. These lineages are prone to be discovered through deeper investigation of the massive undescribed diversity trapped in Burmese amber. Given the apparent basal position of the new family, untangling its probable behavior will be of great importance to understand the behavioral evolution at early steps of the diversification of aculeate wasps.

Acknowledgements

We sincerely thank Dr. Chung Kun Shih, Dr. Taiping Gao and Ms. Yaping Cai, who kindly provided photographs of the type material of †*Mirabythus* and allowed us to use the photographs in the present publication. We also thank the reviewers Alexandr Rasnitsyn, André Martins and Volker Lohrmann for their careful reading of the manuscript and suggestions to improve it. Financial support has been provided by CNPq.

References

- Aguiar AP, Deans AR, Engel MS, Forshage M, Huber JT, Jennings JT, Johnson NF, Lelej AS, Longino JT, Lohrmann V, Mikó I, Ohl M, Rasmussen C, Taeger A, Yu DSK (2013) Order Hymenoptera. *Zootaxa* 3701: 51–62. <http://doi.org/10.11646/zootaxa.3703.1.12>
- Azevedo CO, Alencar IDCC, Ramos MS, Barbosa DN, Colombo WD, Vargas JMR, Lim J (2018) Global guide of the flat wasps (Hymenoptera, Bethyloidea). *Zootaxa* 4489: 1–294. <https://doi.org/10.11646/zootaxa.4489.1.1>
- Barbosa DN, Vilhelmsen L, Azevedo CO (2021) Morphology of sting apparatus of Chryridoidea (Hymenoptera, Aculeata). *Arthropod Structure & Development* 60: 100999. <https://doi.org/10.1016/j.asd.2020.100999>
- Branstetter MG, Danforth BN, Pitts JP, Faircloth BC, Ward PS, Buffington ML, Gates MW, Kula RR, Brady SG (2017) Phylogenomic insights into the evolution of stinging wasps and the origins of ants and bees. *Current Biology* 27: 1019–1025. <https://doi.org/10.1016/j.cub.2017.03.027>
- Brothers DJ (1975) Phylogeny and classification of the aculeate Hymenoptera, with special reference to Mutillidae. *University of Kansas Science Bulletin* 50(11): 483–648.
- Brothers DJ (1981) Note on the biology of *Ycaploca evansi* (Hymenoptera: Scolebythidae). *Journal of the Entomological Society of Southern Africa* 44 (1): 107–108.
- Brothers DJ (1999) Phylogeny and evolution of wasps, ants and bees (Hymenoptera, Chryridoidea, Vespoidea and Apoidea). *Zoologica Scripta* 28 (1–2): 233–250. <https://doi.org/10.1046/j.1463-6409.1999.00003.x>

- Brothers DJ (2011) A new Late Cretaceous family of Hymenoptera, and phylogeny of the Plumariidae and Chrysoidea (Aculeata). *ZooKeys* 130: 515–542. <https://doi.org/10.3897/zookeys.130.1591>
- Brothers DJ, Carpenter JM (1993) Phylogeny of Aculeata: Chrysoidea and Vespoidea (Hymenoptera). *Journal of Hymenoptera Research* 2: 227–304.
- Brothers DJ, Melo GAR (2021) Re-evaluation of the Cretaceous family Plumalexiidae and its relationships (Hymenoptera: Chrysoidea). *Palaeoentomology* 4(6): 584–591. <https://doi.org/10.11646/palaeoentomology.4.6.7>
- Cai YP, Zhao YY, Shih CK, Ren D (2012) A new genus of Scolebythidae (Hymenoptera: Chrysoidea) from the Early Cretaceous of China. *Zootaxa* 3504(56): e66. <https://doi.org/10.11646/zootaxa.3504.1.2>.
- Carpenter JM (1986) Cladistics of the Chrysoidea (Hymenoptera). *Journal of the New York Entomological Society* 94: 303–330.
- Engel MS, Grimaldi DA (2007) Cretaceous Scolebythidae and phylogeny of the family (Hymenoptera: Chrysoidea). *American Museum Novitates* 3568(2007): 1–16. [https://doi.org/10.1206/0003-0082\(2007\)475\[1:CSAPOT\]2.0.CO;2](https://doi.org/10.1206/0003-0082(2007)475[1:CSAPOT]2.0.CO;2)
- Finnamore AT, Brothers DJ (1993) Superfamily Chrysoidea. In: Goulet H, Huber JT (Eds) *Hymenoptera of the world: an identification guide to families*. Agriculture Canada Publications (Ottawa): 130–160.
- Grimaldi D, Engel MS (2005) *Evolution of the Insects*. Cambridge University Press, Cambridge.
- Heraty J, Ronquist F, Carpenter JM, Hawks D, Schulmeister S, Dowling AP, Murray D, Munro J, Wheeler WC, Schiff N, Sharkey M (2011) Evolution of the hymenopteran mega-radiation. *Molecular Phylogenetics and Evolution* 60: 73–88. <https://doi.org/10.1016/j.ympev.2011.04.003>
- Huber JT, Sharkey MJ (1993) Chapter 3. Structure. In: Goulet H, Huber JT (Eds) *Hymenoptera of the World: an Identification Guide to Families*. Agriculture Canada Publication, Ottawa, 13–59.
- Johnson BR, Borowiec ML, Chiu JC, Lee EK, Atallah J, Ward PS (2013) Phylogenomics resolves evolutionary relationships among ants, bees, and wasps. *Current Biology* 23(20): 2058–2062. <https://doi.org/10.1016/j.cub.2013.08.050>
- Kawada R, Buffington ML (2016) A scalable and modular dome illumination system for scientific microphotography on a budget. *PLoS ONE* 11(5): e0153426. <https://doi.org/10.1371/journal.pone.0153426>
- Klopstein S, Vilhelmsen L, Ronquist F (2015) A nonstationary Markov model detects directional evolution in hymenopteran morphology. *Systematic biology* 64(6): 1089–1103. <https://doi.org/10.1093/sysbio/syv052>
- Kumpanenko AS, Gladun DV (2018) Functional morphology of the sting apparatus of the spider wasp *Cryptocheilus versicolor* (Scopoli, 1763) (Hymenoptera: Pompilidae). *Entomological Science* 21(1): 124–132. <https://doi.org/10.1111/ens.12288>.
- Kumpanenko A, Gladun D, Vilhelmsen L (2019) Functional morphology and evolution of the sting sheaths in Aculeata (Hymenoptera). *Arthropod Systematics & Phylogeny* 77(2): 325–338.

- Lepeco A, Melo GAR (2022) The wasp genus †*Holopsenella* in mid-Cretaceous Burmese amber (Hymenoptera: †Holopsenellidae stat. nov.). *Cretaceous Research* 131: 105089. <https://doi.org/10.1016/j.cretres.2021.105089>
- Li L, Rasnitsyn AP, Shih C, Li D, Ren D (2020) Two new rare wasps (Hymenoptera: Apocrita: Panguidae and Burmusculidae) from mid-Cretaceous amber of Northern Myanmar. *Cretaceous Research* 109: 104220. <https://doi.org/10.1016/j.cretres.2019.104220>
- Liu SI (2018) Burmese Amber from Khamti, Sagaing Region. *The Journal of Gemmology* 36(2): 107–111.
- Lucena DA, Almeida EAB (2022) Morphology and Bayesian tip-dating recover deep Cretaceous-age divergences among major chrysidid lineages (Hymenoptera: Chrysididae). *Zoological Journal of the Linnean Society* 194(1): 36–79. <https://doi.org/10.1093/zoolinnea/zlab010>
- Melo GAR (2000) Biology of an extant species of the scolebythid genus *Dominibythus* (Hymenoptera: Chryridoidea: Scolebythidae), with description of its mature larva. In: Austin AD, Downton M (Eds) *Hymenoptera: evolution, biodiversity and biological control*, CSIRO Collingwood, 281–284.
- Melo GAR, Lucena DAA (2020) †Chrysoebythidae, a new family of chrysidoid wasps from Cretaceous Burmese amber (Hymenoptera, Aculeata). *Historical Biology* 32(8): 1143–1155. <https://doi.org/10.1080/08912963.2019.1570184>
- Melo GAR, Hermes MG, Garcete-Barrett BR (2011) Origin and occurrence of predation among Hymenoptera: a phylogenetic perspective. In: Polidori C (Ed.) *Predation in the Hymenoptera: an evolutionary perspective*. Trivandrum: Transworld Research Network, 1–22.
- Oeser R (1961) Vergleichend-morphologische Untersuchungen über den Ovipositor der Hymenopteren. *Mitteilungen aus dem Museum für Naturkunde in Berlin. Zoologisches Museum und Institut für Spezielle Zoologie (Berlin)* 37(1): 3–119. <https://doi.org/10.1002/mmz.19610370102>
- Pauli T, Meusemann K, Kukowka S, Sann M, Donath A, Mayer C, Oeyen JP, Ballesteros Y, Berg A, Van den Berghe E, Escalona HE, Guglielmino A, Niehuis M, Olmi M, Podsiadlowski L, Polidori C, De Rond J, Rosa P, Schmitt T, Strumia F, Wurdack M, Liu S, Zhou X, Misof B, Peters RS, Niehuis O (2021) Analysis of RNA-Seq, DNA target enrichment, and Sanger nucleotide sequence data resolves deep splits in the phylogeny of cuckoo wasps (Hymenoptera: Chrysididae). *Insect Systematics and Diversity* 5: 1–14. <https://doi.org/10.1093/isd/ixaa018>
- Perkovsky EE, Martynova KV, Mita T, Olmi M, Zheng Y, Müller P, Zhang Q, Gantier F, Perichot V (2020) A golden age for ectoparasitoids of Embioidea: Cretaceous Sclerogibbidae (Hymenoptera, Chryridoidea) from *Kachin* (Myanmar), *Charentes* (France) and *Choshi* (Japan) ambers. *Gondwana Research* 87: 1–22. <https://doi.org/10.1016/j.jgr.2020.06.004>
- Peters RS, Krogmann L, Mayer C, Donath A, Gunkel S, Meusemann K, Kozlov A, Podsiadlowski L, Petersen M, Lanfear R, Diez PA, Heraty J, Kjer KM, Klopstein S, Meier R, Polidori C, Schmitt T, Liu S, Zhou X, Wappler T, Rust J, Misof B, Niehuis O (2017) Evolutionary history of the Hymenoptera. *Current Biology* 27: 1013–1018. <https://doi.org/10.1016/j.cub.2017.01.027>
- Pilgrim EM, Von Dohlen CD, Pitts JP (2008) Molecular phylogenetics of Vespoidea indicate paraphyly of the superfamily and novel relationships of its component families

- and subfamilies. *Zoologica Scripta* 37(5): 539–560. <https://doi.org/10.1111/j.1463-6409.2008.00340.x>
- Prentice MA, Poinar Jr GO, Milki R (1996) Fossil scolebythids (Hymenoptera: Scolebythidae) from Lebanese and Dominican amber. *Proceedings of the Entomological Society of Washington* 98(4): 802–811.
- Rasnitsyn AP (1975) Vysshyie pereponchatokrylyie mezozoya [Hymenoptera Apocrita of Mesozoic]. *Transactions of the Palaeontological Institute* 147: 1–133.
- Rasnitsyn AP (1980) Origin and evolution of Hymenoptera. *Transactions of the Paleontological Institute of the Academy of Sciences of the USSR* 174: 1–192.
- Rasnitsyn AP (1988) An outline of evolution of the hymenopterous insects (order Vespida). *Oriental Insects* 22(1): 115–145. <https://doi.org/10.1080/00305316.1988.11835485>
- Rasnitsyn AP, Bashkuev AS, Kopylov DS, Lukashevich ED, Ponomarenko AG, Popov YA, Rasnitsyn DA, Ryzhkova OV, Sidorchuk EA, Sukatsheva ID, Vorontsov DD (2016) Sequence and scale of changes in the terrestrial biota during the Cretaceous (based on materials from fossil resins). *Cretaceous Research* 61: 234–255. <https://doi.org/10.1016/j.cretres.2015.12.025>
- Rasnitsyn AP, Zhang Q, Müller P, Zhang HC (2020) On the identity and limits of Falsiformicidae (Insecta: Hymenoptera, Vespoidea sl). *Palaeoentomology* 3(6): 582–596. <https://doi.org/10.11646/PALAEOENTOMOLOGY.3.6.10>
- Rodriguez J, Waichert C, Von Dohlen CD, Poinar GO, Pitts JP (2015) Eocene and not Cretaceous origin of spider wasps: Fossil evidence from amber. *Acta Palaeontologica Polonica* 61(1): 89–96. <https://doi.org/10.4202/app.00073.2014>
- Ronquist F, Rasnitsyn AP, Roy A, Eriksson K, Lindgren M (1999) Phylogeny of the Hymenoptera: a cladistic reanalysis of Rasnitsyn's (1988) data. *Zoologica Scripta* 28(1–2): 13–50. <https://doi.org/10.1046/j.1463-6409.1999.00023.x>
- Rosa BB, Melo GAR (2021) Apoid wasps (Hymenoptera: Apoidea) from mid-Cretaceous amber of northern Myanmar. *Cretaceous Research* 122: 104770. <https://doi.org/10.1016/j.cretres.2021.104770>
- Sharkey MJ, Roy A (2002) Phylogeny of the Hymenoptera: a reanalysis of the Ronquist et al. (1999) reanalysis, emphasizing wing venation and apocritan relationships. *Zoologica Scripta* 31(1): 57–66. <https://doi.org/10.1046/j.0300-3256.2001.00081.x>
- Shi GH, Grimaldi DA, Harlow GE, Wang J, Wang J, Yang MC, Lei WY, Li QL, Li XH (2012) Age constraint on Burmese amber based on U-Pb dating of zircons. *Cretaceous Research* 37: 155–163. <https://doi.org/10.1016/j.cretres.2012.03.014>.
- Smith EL (1972) Biosystematics and morphology of Symphyta – III. External genitalia of *Euura* (Hymenoptera: Tenthredinidae): sclerites, sensilla, musculature, development and oviposition behavior. *International Journal of Insect Morphology and Embryology* 1(4): 321–365. [https://doi.org/10.1016/0020-7322\(72\)90016-5](https://doi.org/10.1016/0020-7322(72)90016-5)
- Snodgrass RE (1935) *Principles of Insect Morphology*. McGraw-Hill publications in the zoological sciences, New York/London.
- Vilhelmsen L, Miko I, Krogmann L (2010) Beyond the wasp-waist: structural diversity and phylogenetic significance of the mesosoma in apocritan wasps (Insecta: Hymenoptera). *Zoological Journal of the Linnean Society* 159(1): 22–194. <https://doi.org/10.1111/j.1096-3642.2009.00576.x>

- Xing L, Qiu L (2020) Zircon U-Pb age constraints on the mid-Cretaceous Hkamti amber biota in northern Myanmar. *Palaeogeography, Palaeoclimatology, Palaeoecology* 558: 109960. <https://doi.org/10.1016/j.palaeo.2020.109960>.
- Zhang Q, Rasnitsyn AP, Zhang H (2018a) *Burmusculidae*, a new and basal family of pompiloid wasps from the Cretaceous of Eurasia (Hymenoptera: Pompiloidea). *Cretaceous Research* 91: 341–349. <https://doi.org/10.1016/j.cretres.2018.07.004>
- Zhang Q, Rasnitsyn AP, Wang B, Zhang H (2018b) Hymenoptera (wasps, bees and ants) in mid-Cretaceous Burmese amber: a review of the fauna. *Proceedings of the Geologists' Association* 129(6): 736–747. <https://doi.org/10.1016/j.pgeola.2018.06.004>

Supplementary material I

Additional figures of †*Mirabythus lechrius* Cai et al., 2012 and †*Mirabythus liae* Cai et al., 2012.

Authors: Anderson Lepeco, Diego N. Barbosa, Gabriel A. R. Melo

Data type: images (zip file)

Explanation note: †*Mirabythus lechrius* Cai et al., 2012, dorsal view of head and mesosoma, †*Mirabythus lechrius* Cai et al., 2012, dorsal view of head, †*Mirabythus lechrius* Cai et al., 2012, detail of clypeus. †*Mirabythus liae* Cai et al., 2012, habitus, dorsal view, †*Mirabythus liae* Cai et al., 2012, dorsal view of head.

Copyright notice: This dataset is made available under the Open Database License (<http://opendatacommons.org/licenses/odbl/1.0/>). The Open Database License (ODbL) is a license agreement intended to allow users to freely share, modify, and use this Dataset while maintaining this same freedom for others, provided that the original source and author(s) are credited.

Link: <https://doi.org/10.3897/jhr.94.85613.suppl1>

Review of the *Epeolus julliani* species group (Hymenoptera, Apidae, *Epeolus* Latreille, 1802), with descriptions of two new species

Yulia V. Astafurova¹, Maxim Yu. Proshchalykin²

1 Zoological Institute, Russian Academy of Sciences, Saint Petersburg 199034, Russia **2** Federal Scientific Center of the East Asia Terrestrial Biodiversity, Far East Branch of the Russian Academy of Sciences, Vladivostok 690022, Russia

Corresponding author: Maxim Yu. Proshchalykin (proshchalikin@biosoil.ru)

Academic editor: Michael Ohl | Received 17 October 2022 | Accepted 23 November 2022 | Published 20 December 2022

<https://zoobank.org/8DFD8F12-63C7-46B4-BD26-C498A83BBF6F>

Citation: Astafurova YuV, Proshchalykin MYu (2022) Review of the *Epeolus julliani* species group (Hymenoptera, Apidae, *Epeolus* Latreille, 1802), with descriptions of two new species. Journal of Hymenoptera Research 94: 191–213. <https://doi.org/10.3897/jhr.94.96429>

Abstract

The nine species of the *Epeolus julliani* species group from the Palaearctic region are reviewed. Two new species are described and illustrated: *Epeolus rasmonti* Astafurova & Proshchalykin, **sp. nov.** (Russia, Mongolia, China) and *E. kyzylkumicus* Astafurova, **sp. nov.** (Central Asia). *Epeolus julliani* Pérez, 1884 and *E. laticauda* Bischoff, 1930 are newly recorded from Kazakhstan and *E. seraxensis* Radoszkowski, 1893 is newly recorded from Kazakhstan and Tajikistan. An identification key for both sexes of all members of this species group is presented.

Keywords

Anthophila, Apiformes, cleptoparasites, Palaearctic region, taxonomy

Introduction

In recent years, significant progress has been made towards a better understanding of the taxonomy of the species of *Epeolus* Latreille, 1802 from the Palaearctic region, in particular Europe (Bogusch and Hadrava 2018; Le Divelec 2021), the Middle East and North Africa (Bogusch 2021), Turkey (Bogusch 2018), and Central Asia and Mongolia (Astafurova and Proshchalykin 2021a, b, c, 2022). In total, about 45 species

are now known from the Palaearctic. Based on specimens from several collections, the present work aims to complement these studies by providing a review of the *Epeolus julliani* species group.

The *julliani* species group includes *Epeolus fasciatus* Friese, 1895, *E. iranicus* Bogusch, 2021, *E. julliani* Pérez, 1884, *E. laticauda* Bischoff, 1930, *E. seraxensis* Radoszkowski, 1893, *E. siculus* Giordani Soika, 1944, and *E. transitorius* Eversmann, 1852.

Here, we add two new species to this group: *Epeolus rasmonti* Astafurova & Proshchalykin, sp. nov. from the East Palaearctic and *E. kyzylkumicus* Astafurova, sp. nov. from Central Asia.

This paper is meant as a further step towards a better documentation of the species of *Epeolus* and their distribution patterns in the wider Palaearctic region and adjacent areas. As previous years have shown, a greater number of undescribed species can be expected, particularly in the eastern, central and southern Palaearctic, where so far relatively little material has been available for study.

Materials and methods

The results presented in this paper are based on 257 specimens in the *Epeolus julliani* species group currently housed in the Zoological Institute, Russian Academy of Sciences (St. Petersburg, Russia, **ZISP**); Zoological Museum of the Moscow State University (Moscow, Russia, **ZMMU**); Federal Scientific Center of the East Asia Terrestrial Biodiversity, Far Eastern Branch of Russian Academy of Sciences (Vladivostok, Russia, **FSCV**); and Oberösterreichisches Landesmuseum, Biologiezentrum (Linz, Austria, **OLBL**).

The taxonomy and synonymy of species generally follow those of Bogusch and Hadrava (2018), except we regard *E. julliani* and *E. transitorius* as separate species, following Le Divelec (2021). Morphological terminology follows that of Michener (1944, 2007) and Engel (2001). The density of integumental punctures is described using the following formula: puncture diameter (in μm) / ratio of distance between punctures to average puncture diameter, e.g., 15–20 μm / 0.5–1.5.

Abbreviations **T** and **S** are used for metasomal tergum and metasomal sternum, respectively.

The species are listed alphabetically. We have used the following abbreviations for collectors: **AF** – A. Fateryga, **MP** – M. Proshchalykin; **SB** – S. Belokobylskij; **VG** – V. Gussakovskij, **VL** – V. Loktionov.

Specimens were studied with an Olympus SZ51 stereomicroscope and photographs were taken with a combination of stereomicroscope (Olympus SZX10) and digital camera (Olympus OM-D). Final images are stacked composites generated using Helicon Focus 7.7.4 Pro. All images were post-processed for contrast and brightness using Adobe Photoshop. New distributional records are noted with an asterisk (*).

The map was generated using an online tool for producing publication-quality point maps, SimpleMappr (Shorthouse 2010).

Taxonomy

Genus *Epeolus* Latreille, 1802

Epeolus Latreille, 1802: 427. Type species: *Apis variegata* Linnaeus, 1758, monobasic.

Epeolus julliani species group

Diagnosis. Labrum with apical margin straight and without medial tooth; apically or near apical margin (as opposed to medially, as in species in the *Epeolus variegatus* species group, or sub-apically, as in species in the *E. cruciger* species group) with two sharply carinate, triangular (as seen as lateral view) teeth (tubercles). Axilla large with short apical tooth (extending well beyond midlength of scutellum but not as far back as its posterior margin).

Species included. *Epeolus fasciatus* Friese, 1895, *E. iranicus* Bogusch, 2021, *E. julliani* Pérez, 1884, *E. kyzylkumicus* Astafurova, sp. nov., *E. laticauda* Bischoff, 1930, *E. rasmonti* Astafurova & Proshchalykin, sp. nov., *E. seraxensis* Radoszkowski, 1893, *E. siculus* Giordani Soika, 1944, *E. transitorius* Eversmann, 1852.

Remarks. Le Divelec (2021) also included *Epeolus flavociliatus* Friese, 1899 to this species group, but this species clearly differs from species *julliani* group by small (ill-defined) labral tubercles and elongate (longer than mesoscutellum) axillae. Additionally, the placement of *E. flavociliatus* in this group is not supported by recent phylogenetic studies (see Onuferko et al. 2019; Lim et al. 2022). Together with *E. priesneri* Bogusch, 2021, *E. subrufescens* Saunders, 1908, *E. warnckeii* Bogusch, 2018 and *E. ruficornis* Morawitz, 1875 this species rather belongs to another group.

Key to the species of the *E. julliani* species group

- 1 Anteromedial area of mesepisternum with deep depression (Fig. 8A, B).....2
- Anteromedial area of mesepisternum normal, more or less flat.....3
- 2 Subpleural signum positioned on a small elevated plate (Fig. 8C) and the mesepisternum lateral to anteromedian depression with a strong sharp carina (Fig. 8B)*E. rasmonti* sp. nov.
- Subpleural signum not elevated under mesepisternum; mesepisternum lateral to anteromedian depression with weak rounded corners (Fig. 8A)
.....*E. transitorius* Eversmann
- 3 Female 4
- Male 10
- 4 Apical bands of metasomal terga uninterrupted 5
- Apical bands of metasomal terga interrupted medially (at least on T2–T4) 6

- 5 Mesoscutum entirely reddish; F1 slightly longer than F2 (ca 1.5 vs 1.3–1.4 times as long as wide)..... *E. kyzylkumicus* **sp. nov.**
- Mesoscutum entirely black or largely black; F1 slightly shorter than F2 (ca 1.2 vs 1.3–1.4 times as long as wide) *E. seraxensis* **Radoszkowski**
- 6 Pubescence on S2 discs dense, obscuring integument..... *E. laticauda* **Bischoff**
- Pubescence on S2 discs sparse, sculpture of integument clearly visible.....7
- 7 Mesoscutum and terga reddish..... *E. iranicus* **Bogusch**
- Mesoscutum and terga black. Mesoscutum sometimes reddish along margins but never predominantly reddish **8**
- 8 F2 1.6–1.7 times longer than F3. Integument mostly black, labrum and axilla usually black. Mesepisternum sparsely punctate *E. fasciatus* **Friese**
- F2 slightly longer than F3. Integument with well developed red body coloration, labrum and axillae red. Mesepisternum densely punctate..... **9**
- 9 Metasomal terga with bright yellow bands of tomentum; propodeum forms obtuse angle with mesoscutellum [known only from Sicily]
..... *E. siculus* **Giordani Soika**
- Metasomal terga with pale-yellow or whitish bands of tomentum; propodeum forms right angle with mesoscutellum [widespread] *E. julliani* **Pérez**
- 10 Apical bands of metasomal terga interrupted medially (at least on T2–T4)..... **11**
- Apical bands of metasomal terga uninterrupted **14**
- 11 Metasomal terga reddish *E. iranicus* **Bogusch**
- Metasomal terga black **11**
- 12 Apical bands of T1 uninterrupted *E. fasciatus* **Friese**
- Apical bands of T1 interrupted **13**
- 13 Metasomal terga with yellowish bands of tomentum; propodeum forms obtuse angle with mesoscutellum [known only from Sicily]
..... *E. siculus* **Giordani Soika**
- Metasomal terga with whitish bands of tomentum; propodeum forms right angle with mesoscutellum [widespread] *E. julliani* **Pérez**
- 14 Mesoscutum and terga reddish. Pygidium narrower, 1.05–1.1 times wider than long *E. kyzylkumicus* **sp. nov.**
- Mesoscutum and terga black or brownish. Pygidium wide, 1.4–1.7 times wider than long..... **15**
- 15 Labral teeth positioned directly on apical margin. Hind basitarsus bordered by dense fringe of plumose setae. Pygidium wide, 1.6–1.7 times wider than long, apically distinctly bilobed. Lateral lobes of penis (best seen in dorsal view) small, triangular, extending to mid-length of penis valve (Fig. 9A, B, arrow) *E. seraxensis* **Radoszkowski**
- Labral teeth usually positioned near apical margin. Hind basitarsus bordered by sparse fringe of simple setae. Pygidium narrow, 1.4 times wider than long, apically slightly bilobed or rarely straight. Lateral lobes of penis (best seen in dorsal view) large, petal shaped, elongate, extending to tip of penis valve (Fig. 9I, J, arrow) *E. laticauda* **Bischoff**

***Epeolus fasciatus* Friese, 1895**

Epeolus fasciatus Friese, 1895: 208, ♀, ♂ (type locality: Hungary, Budapest [Pest]; Museum für Naturkunde, Berlin; Muséum National d'Histoire Naturelle, Paris; ZISP).

Material examined. HUNGARY, Pest [Budapest], 2.VII.1886 (1 ♂, syntype), Friese [ZISP].

Distribution. Southern and Central Europe, Turkey (Bogusch 2018).

***Epeolus iranicus* Bogusch, 2021**

Epeolus iranicus Bogusch, 2021: 52, ♀, ♂ (type locality: Kuhre-Sefid, Bazuft, Iran; OLBL).

Material examined. None.

Distribution. Iran (Bogusch, 2021).

***Epeolus julliani* Pérez, 1884**

Fig. 9E, F

Epeolus julliani Pérez, 1884: 318–322, ♀ (type locality: Marseille, France; Muséum National d'Histoire Naturelle, Paris).

Material examined. AUSTRIA, Wien, (1 ♀), coll. F. Morawitz, *transitorius* Eversm. [Morawitz det.] [ZISP]; AZERBAIJAN, Lenkoran, 28.VII.1930, (1 ♀), A. Shestakov [ZISP]; GEORGIA, Lagodehy, (1 ♀), coll. F. Morawitz [ZISP]; IRAN, Shaku, Elbrus Mts., VI.1914, (1 ♀), Kirichenko [ZISP]; Tularud, 11.V.1916, (1 ♂), B. Ilyin [ZISP]; Kerman Prov., 8 km N of Bordsir, 200 m, 29°95'N, 56°58'E, 6.VI.2010, (1 ♂), Mi. Halada (OLBL); MOLDOVA, Leovo, 25.VII.1913, (1 ♂), Chernavin [ZISP]; KAZAKHSTAN, Kokshetau Mts., 1. VII, 3.VIII.1958, (2 ♀), V. Rudolf [ZISP]; Aktobe, Berchogur [Birshoghyr], 26.VI.1910, (7 ♀, 3 ♂), L. Bubyar [ZISP]; RUSSIA, Dagestan Rep., 20 km W of Makhachkala, Sarykum, 23–24.V.2019, (1 ♂), MP, VL [FSCV]; CRIMEA, Mukhalatka, VII.1902, (1 ♀), N. Kuznetsov [ZISP]; Sevastopol, 28.VII.1916, (1 ♀), Pliginski [ZISP]; idem, 7.VII.2015, (1 ♀), V. Zhidkov [ZISP]; Tarkhankut, Atlesh, 29.VII.2008, (1 ♂), AF [ZISP]; Tarkhankut, Bolshoy Kastel, 25.VII.2015, (7 ♀), AF [ZISP]; idem, on *Jurinea stoechadifolia*, 8.VIII.2015, (1 ♀), V. Zhidkov [ZISP]; idem, 9.VIII.2020, (2 ♀), S. Ivanov [ZISP]; Tarkhankut, Kipchak, 16.IV.2016, (3 ♀, 1 ♂), V. Zhidkov [ZISP]; Tarkhankut, Dzhangul, 26.VII.2017, (3 ♀), AF [ZISP]; Feodosia, Karadag, 15.VI.2015, (1 ♀), AF [ZISP]; Lukull Cape, 8.VII.2015, (3 ♀), AF [ZISP]; near Sudak, 27.V.2016, (1 ♂), AF [ZISP]; Krasnodar Terr., Anapa, Bolshoy Utrish, 2.VII.2018, (1 ♀), AF [ZISP]; Orenburg Prov., Orenburg, (1 ♂), coll. F. Morawitz, *Epeolus transitorius* Eversm. [Morawitz det.] [ZISP]; SPAIN, Andalusia, 26.VI. (1 ♀, 1 ♂) [ZISP]; UKRAINE, Akkerman [=Bilhorod-Dnistrovskyi], (1 ♂), 21.VIII.1921, Petrovich [ZISP].

Remarks. The main differences between *Epeolus julliani* and *E. transitorius* are outlined by Le Divelec 2021, who removed the former from synonymy with the latter. Here, we describe the structure of the male genitalia (Table 1).

The integument coloration and variability are closest to *E. transitorius* (see below). Unlike *E. transitorius*, all studied female specimens of *E. julliani* have a sparsely pubescent or almost glabrous clypeus (vs on that is often obscured by dense tomentum), and the lower mesepisternum is always pubescent (vs often glabrous).

Distribution. North Africa, Middle East, Europe, Caucasus, Russia (south of European part, south Ural), *Kazakhstan, Iran (Bischoff 1930; Le Divelec 2021; current data).

Table 1. Main differences between species of the *Epeolus julliani* group.

	<i>seraxensis</i>	<i>iranicus</i> (according to Bogusch 2021)	<i>julliani</i> + <i>siculus</i>	<i>kyzylkumicus</i>	<i>laticauda</i>	<i>transitorius</i> + <i>rasmonti</i>
Both sexes						
Anteromedial area of mesepisternum	normal, more or less flat					with deep depression
Apical bands of metasomal terga	uninterrupted	interrupted medially on T2–T4	interrupted medially	uninterrupted	narrowly interrupted medially in female, uninterrupted in male	interrupted medially
Coloration of tergal discs	varies from brownish to reddish in female and from black to brownish in male	reddish	black	reddish	varies from dark brown to red-brown in female and from black to brownish in male	black
Female						
Length of flagellomeres (ratio L/W)	F1 little shorter than F2 (ca 1.2 vs 1.3–1.4); remaining flagellomeres distinctly longer than wide	F1 distinctly shorter than F2 (1.05–1.1 vs 1.35); remaining flagellomeres slightly longer than wide	F1 equal or little shorter than F2 (1.2 vs 1.2–1.3); remaining flagellomeres distinctly longer than wide	F1 little longer than F2 (ca 1.5 vs 1.3–1.4); remaining flagellomeres distinctly longer than wide	F1 little shorter than F2 (1.2–1.3 vs 1.4–1.5); remaining flagellomeres distinctly longer than wide	F1 distinctly shorter than F2 (ca 1.5 vs 1.0–1.1); remaining flagellomeres slightly longer than wide
Pubescence on S2 disc	dense, obscuring integument	sparse, sculpture of integument well-visible	sparse, sculpture of integument well-visible	moderate, almost obscuring integument	dense, obscuring integument	sparse, sculpture of integument well-visible
Male						
Lateral lobes of penis (dorsal view)	Small, triangular, extending mid-length of penis valve (Fig. 9C, D, arrow)	not studied	Small, petal shaped, extending mid-length of penis valve (Fig. 9E, F, arrow)	Medium sized, petal shaped, not extending tip of penis valve (Fig. 9C, D, arrow)	Large, petal shaped, elongate, extending tip of penis valve (Fig. 9G–J, arrow)	
Pygidium	very wide, 1.6–1.7 times wider than long, apically distinctly bilobed	1.3 times wider than long, apically rounded	1.25–1.35 times wider than long, apically rounded, sometimes slightly bilobed	1.05–1.1 times wider than long, apically rounded	1.4 times wider than long, apically slightly bilobed or rarely straight	1.1–1.2 times wider than long, apically rounded, sometimes slightly bilobed

***Epeolus kyzylkumicus* Astafurova, sp. nov.**

<https://zoobank.org/0DE6C379-8F69-40B6-9C77-BF90BFA4BD3E>

Figs 1–3, 8D, 9G, H

Material examined. Holotype: ♀, UZBEKISTAN, Kyzyl-kum [Kyzylkum desert], 10 km SW Arnasay [Lakes], 27.VIII.1979, Yu. Pesenko [ZISP]. **Paratypes:** 3 ♂, the same label as in the holotype; 1 ♀, KAZAKHSTAN, Perowsk[=Qyzylorda], Syr-Darja Geb., 17.VII.1909, W. Nikolsky [ZISP]; 1 ♀, TAJIKISTAN, Farap, NW Bukhara, 5.VII.1928, V. Gussakovskij [ZISP].

Diagnosis. This species is most similar to *Epeolus iranicus*, especially with regard to the extensive red integument coloration, but can be separated from it by the uninterrupted apical bands on the metasomal terga, dense pubescence of sterna, and longer antennae (flagellomeres distinctly longer than wide in both sexes vs slightly longer than wide in females and slightly shorter than wide in males of *E. iranicus*). The differences between *E. kyzylkumicus* sp. nov. and other species of the *julliani* group are outlined in Table 1.

Description. Female. Total body length 8.0 mm (Figs 1A, 2A); forewing length (without tegula) 6.0 mm.

Structure and sculpture: Head (Fig. 2B) 1.3 times as wide as long. Labrum (Fig. 2D) 1.65 (holotype) to 1.75 times (paratypes) as wide as long, angulated basally, rounded laterally and weakly concave medially, apical margin straight without medial tooth; close to apex (but not directly) with two well-visible teeth (tubercles); integument shiny, densely punctate (10–30 µm / confluent–2). Clypeus densely and finely punctate (10–15 µm / confluent–0.5), narrowly impunctate along apical margin. Frons with developed frontal keel. Frons and vertex areolate punctate (15–30 µm). Flagellomeres long, F1 1.5 times as long as wide, succeeding flagellomeres ca 1.3–1.4 times as long as wide. Mesoscutum and mesoscutellum coarsely and densely punctate (30–70 µm / confluent–0.5), small interspaces between punctures shiny and smooth. Axilla convex, apically with distinct short tooth. Mesoscutellum with deep medial longitudinal impression distinctly divided mesoscutellum on two slightly convex lobes; posterior margin scarcely extending over propodeum. Mesepisternum areolate-punctate (sculpture not visible under pubescence). Propodeal triangle shagreened. Metasomal terga densely and finely punctate (10–15 µm / 0.5–1), interspaces shiny and smooth; marginal zones (apical impressed area) wide, equal to length of discs. Pseudopygidial area triangular. Pygidial plate trapezoidal, apically truncate (Fig. 2C). Processes on sides of S6 normal, with short projections (Fig. 8D). Metasomal terga and sterna with punctures more or less equally dense.

Integument coloration: Body mostly reddish, but paraocular and genal areas, frons and vertex black.

Pubescence: Body with dense and mostly white tomentum (brownish only on medial part of tergal discs). Labrum with mixed thin and plumose setae. Face and genal area with dense tomentum obscuring integument, vertex with sparser and short

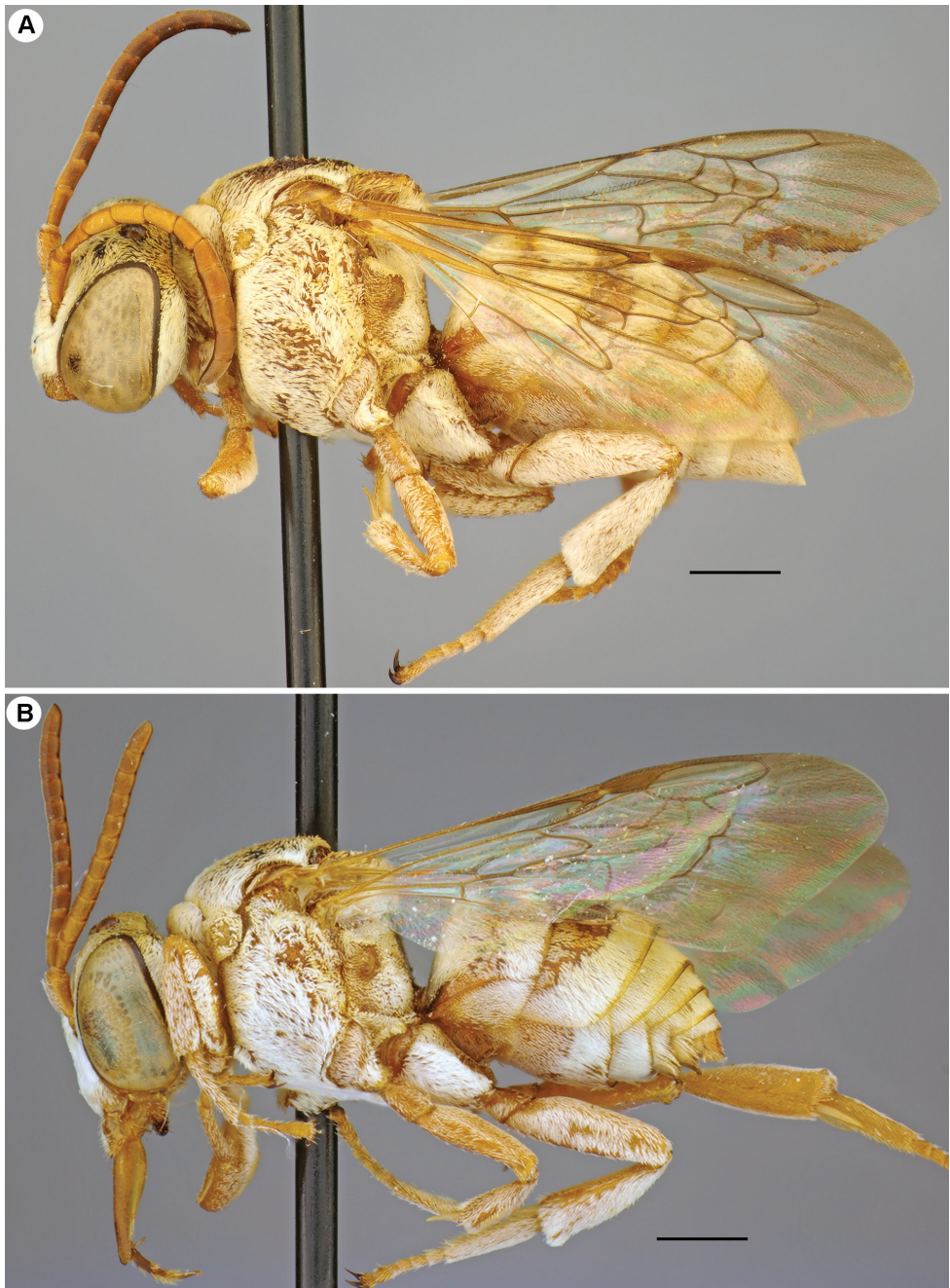


Figure 1. *Epeolus kyzylkumicus* Astafurova, sp. nov., holotype, female (**A**), paratype, male (**B**) **A, B** habitus, lateral view. Scale bars: 1.0 mm.

setae. Pronotum dorsally with tomentum obscuring integument. Mesoscutum with dense tomentum peripherally and with wide paramedial strips. Metanotal integument entirely obscured by tomentum. Lower and lateral parts of thorax and propodeum

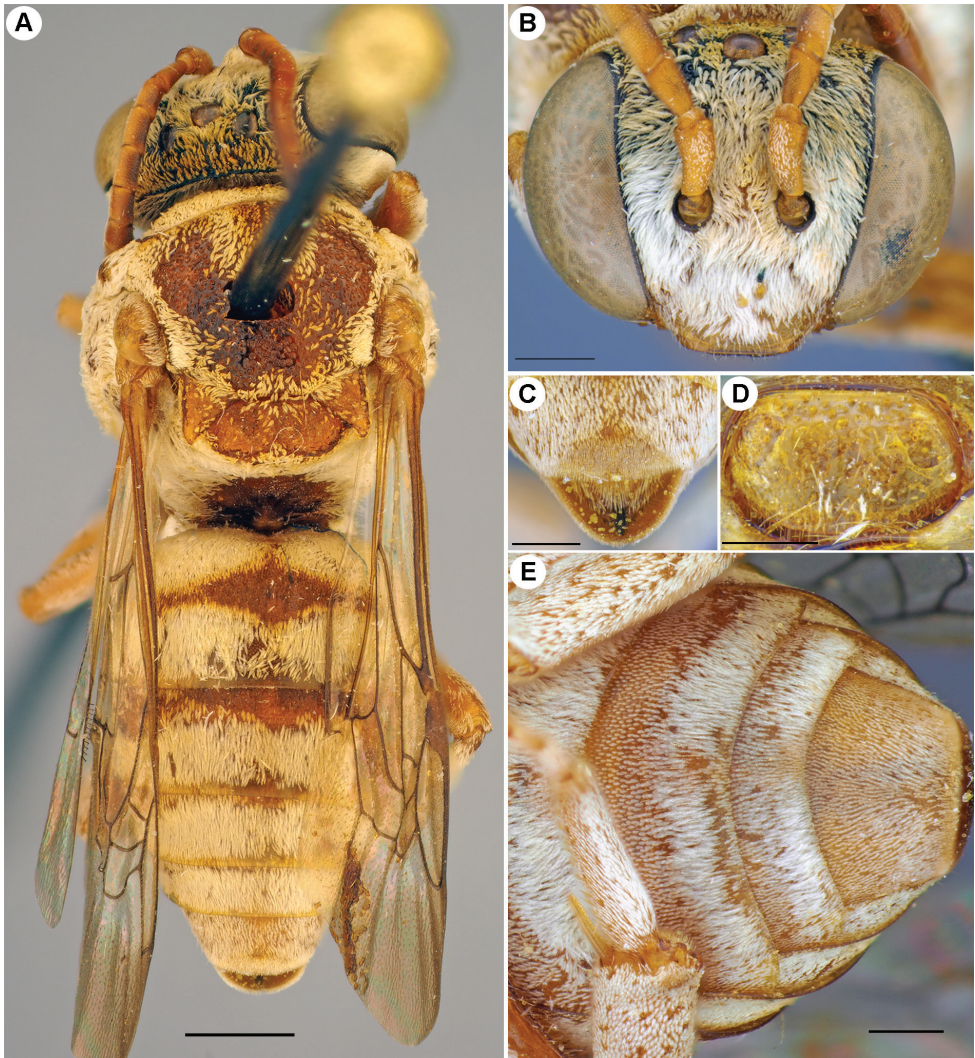


Figure 2. *Epeolus kyzylkumicus* Astafurova, sp. nov., holotype, female **A** habitus, dorsal view **B** head, frontal view **C** S6, ventral view **D** labrum, frontal view **E** metasoma, ventral view. Scale bars: 1.0 mm (**A**, **E**); 0.5 mm (**B**, **C**); 0.3 mm (**D**).

laterally entirely obscured by tomentum. Legs with dense tomentum. T1 with wide basal band of tomentum connected with apical band laterally; margins of T1–T4 with uninterrupted bands of tomentum. T1–T4 discs with tomentum dense and laterally similar to that on apical margins, but somewhat sparser and brownish medially. T5 entirely obscured by tomentum. Pseudopygidial area with golden pubescence. Sterna entirely obscured by tomentum, moderate on discs and distinctly denser and longer on margins (Fig. 2E).

Male. Structure, sculpture, coloration and pubescence are similar to those of the female (Figs 1B, 3A). Total body length 6.0–7.0 mm; forewing length (without tegula)

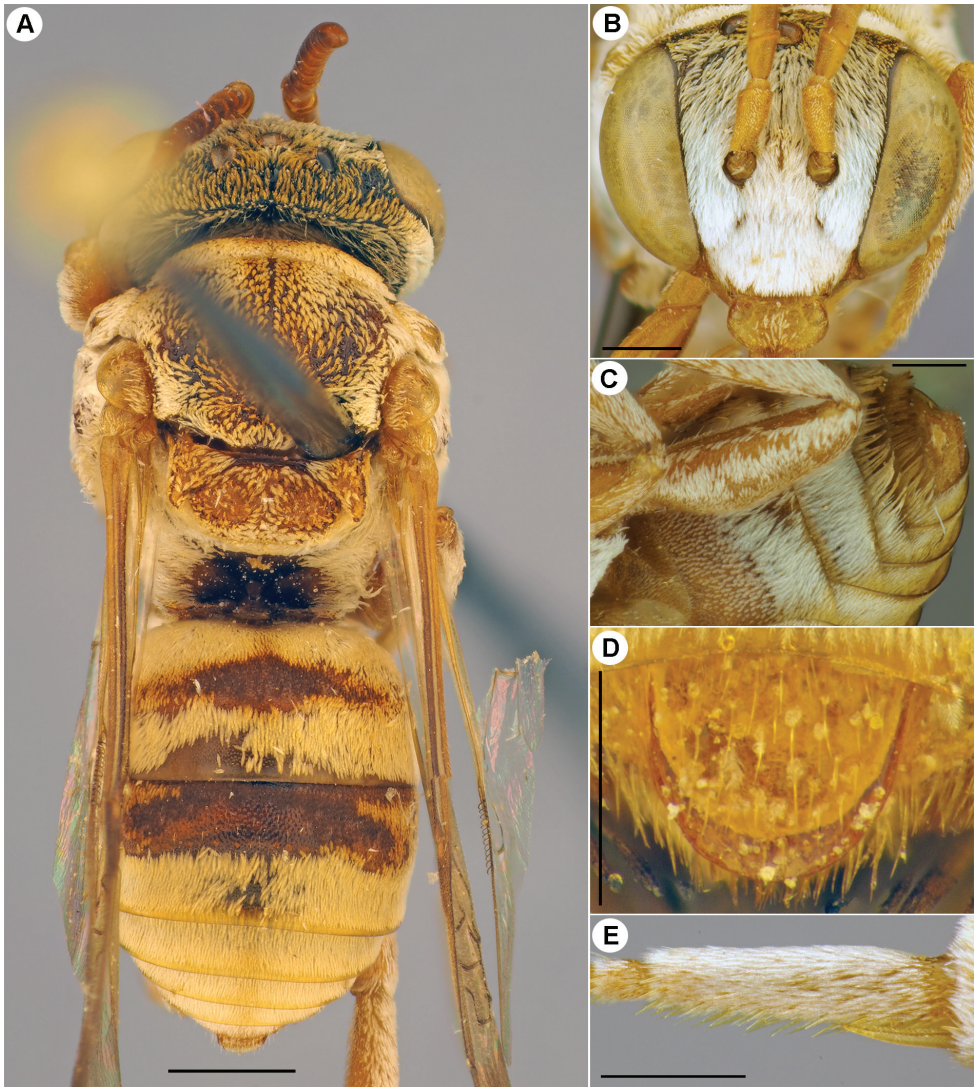


Figure 3. *Epeolus kyzylkumicus* Astafurova, sp. nov., paratype, male **A** habitus, dorsal view **B** head, frontal view **C** metasoma, ventral view **D** T7, dorsal view **E** hind basitarsus, dorsal view. Scale bars: 1.0 mm (**A**, **C**); 0.5 mm (**B**, **E**); 0.3 mm (**D**).

5.5 mm. Head (Fig. 3B) ca 1.2 times as wide as long. Labrum flatter and wider than in female, 1.9 times as wide as long. F1 ca 1.3 times as long as wide, succeeding flagellomeres ca 1.2 times as long as wide. Clypeus with dense tomentum obscuring integument. Mesoscutum entirely covered by plumose setae, denser peripherally and in anterior half. Hind basitarsus boarded by sparse fringe of pale short setae (Fig. 3E). Pygidial plate (T7) shiny, coarsely and densely punctate, 1.05–1.1 times wider than

long, slightly narrowed toward apex; apical margin rounded (Fig. 3D). Margins of S2 and S3 with dense uninterrupted white tomentum bands; S4 and S5 normal, with cream long setae (Fig. 3C). Genitalia as in Fig. 9C, D.

Etymology. The specific name “*kyzylkumikus*” is an adjective in the nominative singular and refers to the occurrence of this species in Kyzylkum desert of Central Asia.

Distribution. Kazakhstan (Qyzylorda Prov.), Kyrgyzstan, Tajikistan.

Epeolus laticauda Bischoff, 1930

Fig. 9I, J

Epeolus laticauda Bischoff, 1930: 13, ♂ (type locality: “Monda, Mongolei” [Mondy, Buryatia Republic, Russia]; Natural History Museum, Berlin).

Material examined. KAZAKHSTAN, Kulandy, Aral Sea, 13.VII.1900, (1 ♀, 1 ♂), L. Berg (ZMMU); Mergenevo, Ural River, 12.VII.1951, (1 ♀), Romadina [ZISP]; TAJIKISTAN, Kulyab, 7.VIII.1933, (2 ♀), V. Popov [ZISP]; Dzhili-Kul, Vakhsh River, 12.VI.1934, (1 ♀), VG [ZISP]; Kabadian, 2.VII.1934, (1 ♀, 2 ♂), VG; Ayvadh, 8.VIII.1934, (1 ♀), VG; Stalinabad [=Dushanbe], Botanical garden, 21.VII–8.VIII.1943, (9 ♀, 9 ♂), V. Popov [ZISP]; Kurgan-Tuybe, 14.VIII.1948, (1 ♀), V. Popov [ZISP]; TURKMENISTAN, Ashgabat, (1 ♀), coll. F. Morawitz, *transitorius* Eversm. [Morawitz det.] [ZISP]; Kara-Kala, 27.V.1953, (1 ♂), Steinberg [ZISP]; UZBEKISTAN, Farab, 31.V.1912, (1 ♀, 3 ♂), Golbek [ZISP]; Bukhara, 26.VI.1926, (1 ♀), V. Yakhontov [ZISP]; Khiva, 15.VI.1927, (6 ♀), VG [ZISP]; idem, 18–22.VI.1927, (1 ♀, 9 ♂), VG [ZISP]; Kattakurgan, 12.VII.1931, (1 ♀), VG [ZISP]; Dzhuma, 25–29.VI.1937, (15 ♀, 7 ♂), V. Popov [ZISP].

Distribution. Russia (Buryatia Rep.), *Kazakhstan, Tajikistan, Turkmenistan, Uzbekistan (Popov 1935, 1949, 1967; current data).

Variability. Labral tubercles in both sexes are positioned, typically, more or less close to the apical margin and rarely directly thereupon.

Females have well developed red body coloration. The labrum, clypeus, pronotal lobe, tegulae, mesepisternum, axillae, mesoscutellum, metanotum, legs, pygidial plate and sterna are always reddened. The antennae are mostly reddish, but with terminal flagellomeres usually brownish. The pronotum varies from reddish to partially black. The mesoscutum is mostly black, but red patterning sometimes also occurs laterally, or rarely it is almost entirely red-brownish. The propodeum varies from black to reddish. The metasomal terga vary from dark brown to red-brown with golden marginal zones; T5 is usually reddish.

Males are mostly black (excepting a red labrum, scape, pedicel, F1, pronotal lobe, tegulae, legs and pygidial plate). The clypeus is red (entirely or only in apical half). The mesepisternum, axillae and mesoscutellum are typically black, but sometimes can be partially or entirely red. The sterna vary from brownish to reddish. The pygidial plate apical margin is typically more or less bilobed, sometimes rather straight.

***Epeolus rasmonti* Astafurova & Proshchalykin, sp. nov.**

<https://zoobank.org/B08677BE-9224-4C08-8E10-45B1F3DDAAAA>

Figs 4–7, 8B, C, 9G, H, 10

Material examined. *Holotype*: ♀, RUSSIA, Buryatia Republic, Gusinoye Lake, Baraty, 25.VII.2007, A. Lelej, M. Proshchalykin, V. Loktionov [ZISP]; *Paratypes*: 1 ♀, 1 ♂, the same label as in the holotype [FSCV/ZISP]; 6 ♀, 1 ♂, the same label as in the holotype, but 26.VII.2007 [FSCV/ZISP]; 1 ♂, Naushki, Selenga River, 30.VII.2007, A. Lelej, M. Proshchalykin, V. Loktionov [ZISP].

Additional material. CHINA, Beijing, park of the Summer Palace, 18.VIII.1954, (1 ♀), G. Bey-Bienko [ZISP]; MONGOLIA, Khutag, Selenga River, 25.VII.1975, (1 ♂), E. Narchuk [ZISP]; 200 km SEE of Baruun-Urt, Moltsoy Els, 1250 m, 27.VII.2007, (3 ♀, 14 ♂), M. Kadlecova, M. Halada, P. Tymer [OLBL]; 100 km NE of Ondorkhaan, Kerulen River, 970 m, 22.VII.2007, (3 ♂), M. Kadlecova [OLBL]; 100 km W Choibalsan, 820 m, 23.VII.2007, (1 ♂), M. Halada [OLBL]; 15 km W Choibalsan, Kerulen River, 770 m, 24.VII.2007, (1 ♂), M. Halada [OLBL].

Diagnosis. This species is most similar to *Epeolus transitorius*, with which it uniquely shares a deep depression in the anteromedian area of the mesepisternum, but can be separated from it by the position of the subpleural signum on a small elevated plate (Fig. 8C) and the presence of a strong, sharp carina on the mesepisternum lateral to the anteromedian depression (Fig. 8B) (vs weak rounded corners, Fig. 8A). The differences between *Epeolus rasmonti* sp. nov., *E. transitorius* and other species of the *julliani* group are outlined in Table 1.

Description. Female. Total body length 7.0–9.0 mm (Figs 4, 5A); forewing length (without tegula) 6.0–7.0 mm.

Structure and sculpture: Head (Fig. 5B) 1.3 times as wide as long. Labrum (Fig. 5C) 1.55 times as wide as long, more or less rounded basally and laterally, weakly concave medially, apical margin straight without medial tooth; apically with two well-visible carina-shaped teeth (tubercles); integument shiny, areolate punctate (10–30 µm). Clypeus densely and finely punctate (10–15 µm / confluent–0.5), narrowly impunctate along apical margin. Frons with developed frontal keel. Frons and vertex coarsely and areolate punctate (30–40 µm). F1 long, ca 1.5 times as long as wide, F2 distinctly shorter than F1 (1.0–1.1 times as long as wide), succeeding flagellomeres slightly longer than wide (ca 1.2 times). Mesoscutum and mesoscutellum coarsely and mostly areolate punctate (30–70 µm), a few small interspaces between punctures shiny and smooth. Axilla slightly convex laterally, apically with distinct short tooth. Mesoscutellum with shallow medial longitudinal impression; posterior margin scarcely extending over propodeum. Mesepisternum areolate punctate on upper half and with dull, delicately shagreened interspaces on lower part; anteromedian area with deep depression, laterally from anteromedian depression with strong sharp carina (Fig. 8B). Propodeal triangle shagreened. Metasomal terga densely and finely punctate (10–15 µm / confluent–1), interspaces shiny; marginal zones wide, equal to length of discs. Pseudopygidial area narrow, linear. Pygidial plate trapezoidal, apically truncate. Processes on sides of S6 normal, with short projections. Metasomal terga and sterna with punctures more or less equally dense (Fig. 5D).

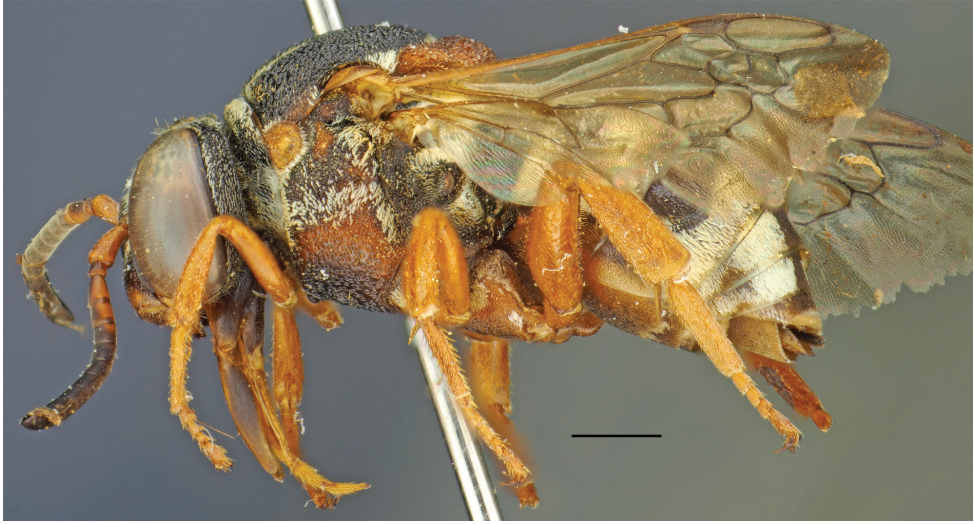


Figure 4. *Epeolus rasmonti* Astafurova & Proshchalykin, sp. nov., holotype, female, habitus, lateral view. Scale bar: 1.0 mm.

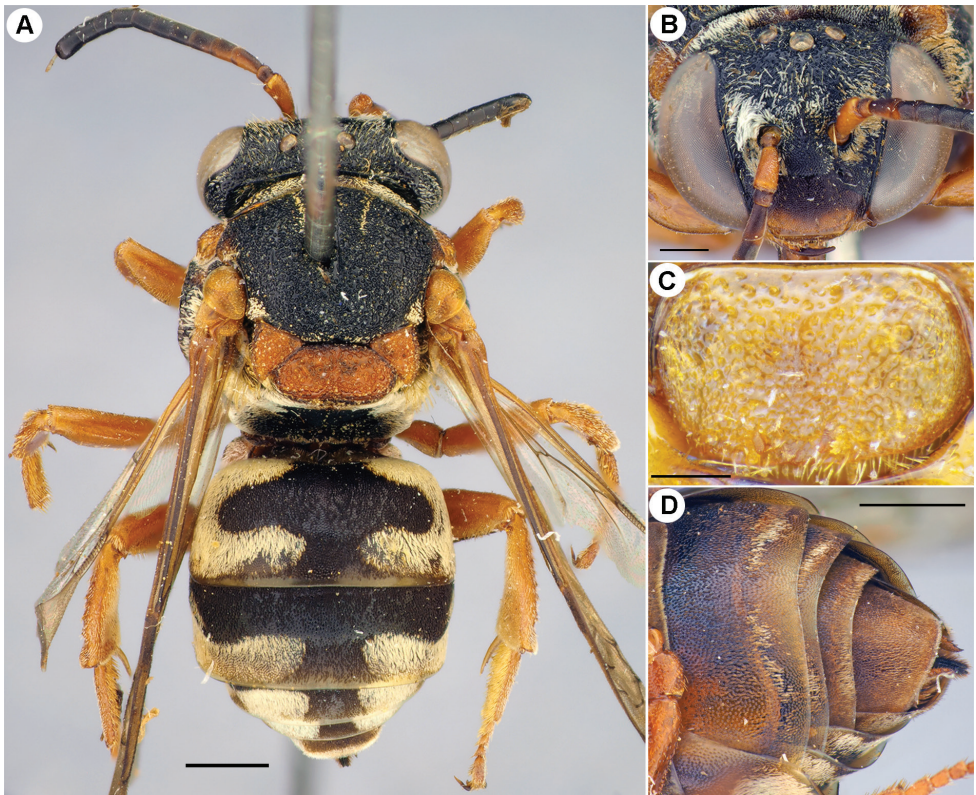


Figure 5. *Epeolus rasmonti* Astafurova & Proshchalykin, sp. nov., holotype, female **A** habitus, dorsal view **B** head, frontal view **C** labrum, frontal view **D** metasoma, ventral view. Scale bars: 1.0 mm (**A**, **D**); 0.5 mm (**B**); 0.3 mm (**C**).

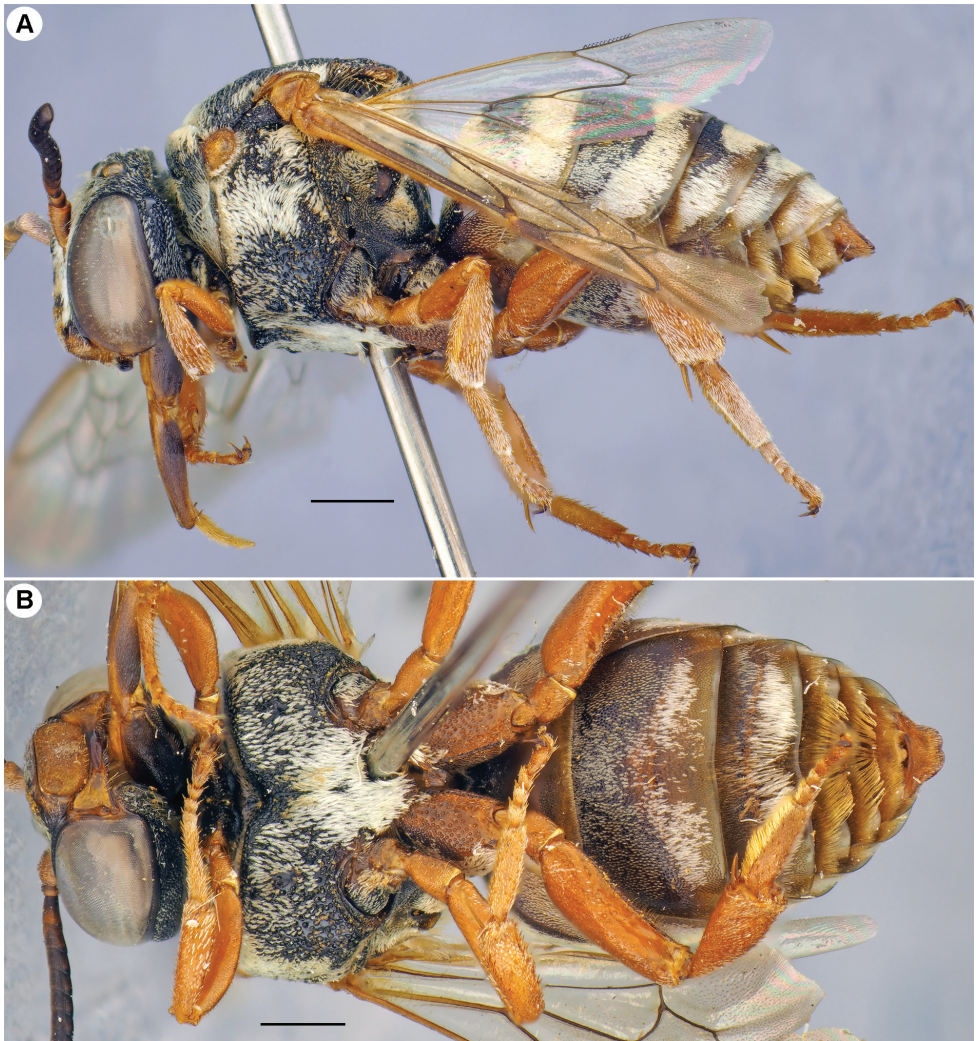


Figure 6. *Epeolus rasmonti* Astafurova & Proshchalykin, sp. nov., paratype, male **A, B** habitus, lateral view (**A**) ventral view (**B**). Scale bars: 1.0 mm.

Integument coloration: Head mostly black, but mandibles (excluding darker apex), labrum, clypeus along apical margin, scape and F1 reddish (amber). Mesosoma mostly black; pronotal lobe, tegulae, axillae, mesoscutellum, metanotum medially and legs (including spurs) reddish (amber); wings with brownish darkening, stigma and veins brown. Mesepisternum partially reddish (usually in middle part, lower scobal area). Metasomal terga black; marginal zones brownish to dark-golden apically. Pygidial plate reddish with brownish edging. Sterna brownish to reddish; margins golden.

Pubescence: Body with relatively sparse pubescence; tomentum white, except black on tergal discs. Labrum with thin sparse setae. Paraocular area with dense tomentum

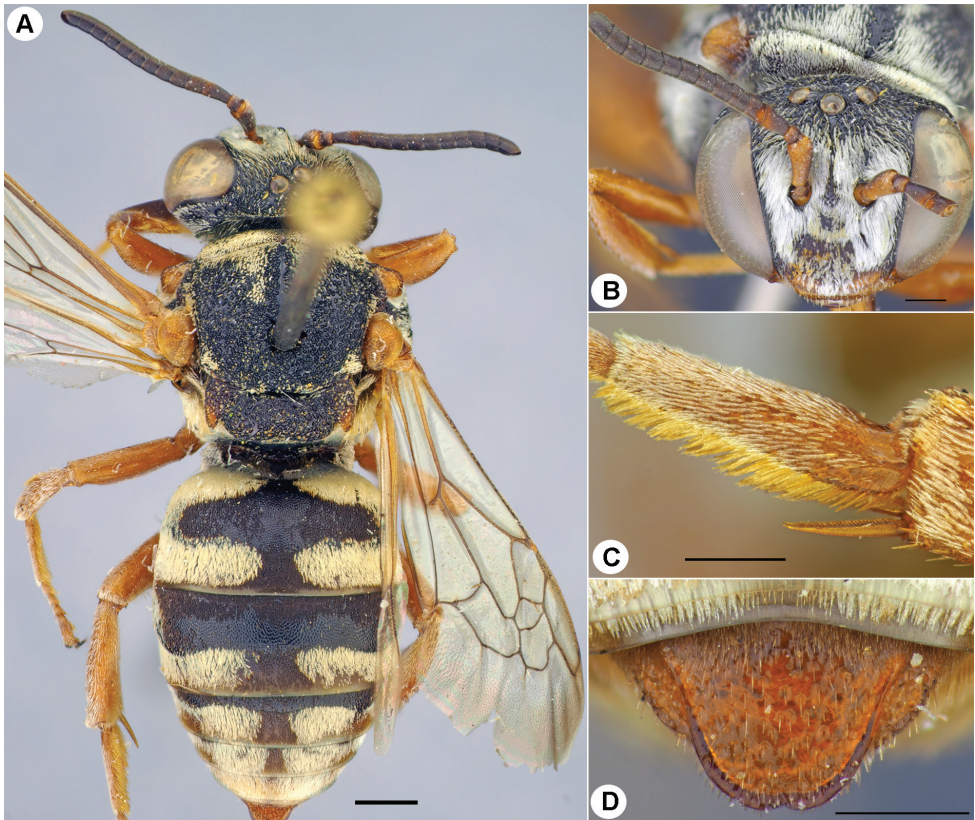


Figure 7. *Epeolus rasmonti* Astafurova & Proshchalykin, sp. nov., paratype, male **A** habitus, dorsal view **B** head, frontal view **C** hind basitarsus, dorsal view **D** T7, dorsal view. Scale bars: 1.0 mm (**A**); 0.5 mm (**B–D**).

obscuring integument; remaining part of face and vertex with sparse thin pubescence. Upper half of frons with relatively long erect simple setae mixed with adpressed sparse plumose pubescence. Genal area with relatively dense plumose setae, but not obscuring integument. Pronotum dorsally with tomentum obscuring integument, but medially setae sparse and short. Mesoscutum with dense tomentum peripherally and with narrow paramedial strips. Mesepisternum with sparse, short plumose pubescence or glabrous on lower part and with relatively dense and longer plumose pubescence on upper half. Metanotal integument obscured by tomentum except medially. Legs with sparse pubescence. T1 with basal band of tomentum interrupted medially and connected with apical band laterally; margins of T1–T4 with widely interrupted bands of tomentum. Black tomentum on T1–T4 discs and in interrupted area sparser than pale tomentum. T5 obscured by white tomentum laterally and black medially. Pseudopygidial area with white pubescence. Discs of metasomal sterna with short brownish plumose setae, sparse on S2 and entirely obscured by tomentum on S3–S5; margins with dense and pale tomentum interrupted medially.

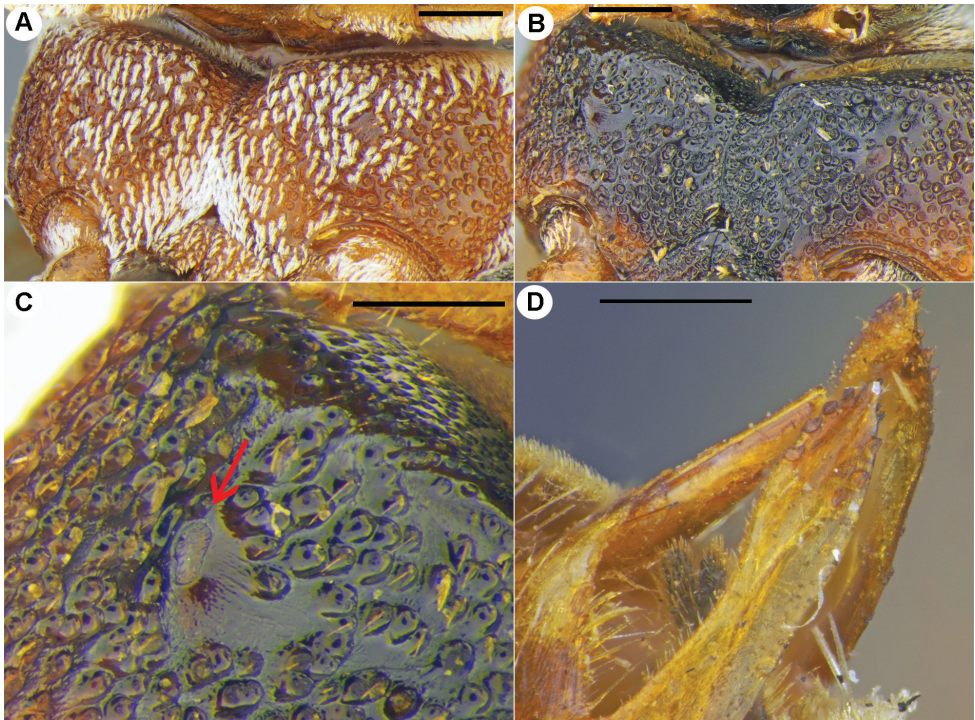


Figure 8. *Epeolus transitorius* Eversmann, 1852, female (**A**), *E. rasmonti* Astafurova & Proshchalykin, sp. nov., paratype, female (**B**, **C**), *E. kyzylkumicus* Astafurova, sp. nov., female (**D**) **A**, **B** lower mesepisternum, ventral view **C** subpleural signum (arrow), ventral view **D** S6, lateral view. Scale bars: 0.5 mm (**A**, **B**); 0.3 mm (**C**, **D**).

Male. Structure, sculpture, coloration and are similar to those of the female (Figs 6, 7), but pubescence more developed. Total body length 5.5–8.0 mm; forewing length (without tegula) 6.0–6.5 mm. F1 1.3–1.4 times as long as wide, succeeding flagellomeres ca 1.1 times as long as wide. Labrum with dense, plumose setae medially. Face obscured by plumose tomentum, but on upper frons sparser and mixed with long setae (Fig. 7B). Mesoscutum with paramedial strips wider than in female. Axillae and mesoscutellum black or reddish. Mesepisternum mostly areolate-punctate, with shiny, smooth interspaces on lower part; entirely obscured by tomentum. Hind basitarsus boarded by dense fringe of long golden setae (Fig. 7C). Metasomal terga with apical bands narrower interrupted than in female. Pygidial plate (T7) reddish, shiny, coarsely and densely punctate, ca 1.2 times wider than long, narrowed toward apex; apical margin rounded, slightly bilobed or almost straight (Fig. 7D). Margins of S2 and S3 with dense uninterrupted white tomentum bands; S4 and S5 normal, with gold long setae. Genitalia as on Fig. 9G, H.

Etymology. The specific epithet is a patronym honoring our colleague and friend Prof. Pierre Rasmont (University of Mons, Belgium) on the occasion of his 65th birthday and in recognition of his many contributions to the study of bee diversity.

Distribution (Fig. 10). Russia (Buryatia Rep.), Mongolia (Bulgan, Dornod, Khentii, Sukhbaatar), China (Beijing).

***Epeolus seraxensis* Radoszkowski, 1893**

Fig. 9A, B

Epeolus transitorius var. *seraxensis* Radoszkowski, 1893: 54–55, ♀, ♂ (lectotype: ♀, designated by Bogusch 2021: 59, Serax, Turkmenistan; Natural History Museum, Berlin).

Material examined. AZERBAIJAN, Araxesthal [=Nakhchivan Republic, near Ordubad], (1 ♀), Reitter leg. [ZISP]; KAZAKHSTAN, Tartugay, 3–15.VI.1929, (3 ♀, 2 ♂), A. Shestakov [ZISP]; Charyn valley, W Chundza, 650 m, 43°37'N, 79°21'E, 29–31.V.2001, (2 ♀), M. Hauser [OLBL]; 30 km ENE Shelek, 43°41.24'N, 78°38.50'E, 500 m, on *Tamarix* sp., 2.VIII.2002, (1 ♂), M. Kuhlmann [OLBL]; 3 km NE Boradysu, 30 km E Shelek, 19.VI.2003, (1 ♀), V. Kazenas [ZISP]; Charyn valley, 12 km W Chundzha, 12.VI.2004, (1 ♀, 1 ♂), V. Kazenas [ZISP]; TAJIKISTAN, Dushanbe, 1931, (1 ♀, 1 ♂), N. Fursov [ZISP]; TURKMENISTAN, Kopetdag, 12 km SW Kyzyl-Arvat, 24.V.1953, (1 ♂), Odintzova [ZISP].

Distribution. Azerbaijan, *Kazakhstan, *Tajikistan, Turkmenistan, Iran, Israel (Bogusch 2021; current records).

Remarks. Records from Bogusch (2021: 59) from Iran (“Anaesthal”) belong to specimens collected in Araxesthal, Azerbaijan, near Ordubad (see, Reitter 1890, 1905).

Variability. Females have well developed red body coloration, including the labrum, clypeus, pronotal lobe, tegulae, mesepisternum, axillae, mesoscutellum, metanotum, legs, pygidial plate and sterna. The antennae are brownish with the scape, pedicel and F1 entirely reddish. The mesoscutum is mostly black, sometimes with small red patterning peripherally and a pair red stripes posteriorly. The propodeum varies from entirely reddish to entirely black. The tergal discs vary from brownish to reddish. The males are mostly black, except the red labrum, scape, pedicel, F1, pronotal lobe, tegulae, legs and pygidial plate. The axillae and mesoscutellum are black or red. Tergal discs vary from black to brownish, and sterna from brownish to reddish.

***Epeolus siculus* Giordani Soika, 1944**

Epeolus siculus Giordani Soika, 1944: 20, ♀ (type locality: Messina, Sicily, Italy; holotype is lost).

Material examined. ITALIA, Sicilia, (2 ♀), coll. F. Morawitz [ZISP]; Sicilia, 35 km SW Ragusa, 18–22.VI.2002, (1 ♂), J. Halada (OLBL).

Distribution. Italia (Sicilia) (Giordani Soika 1944).

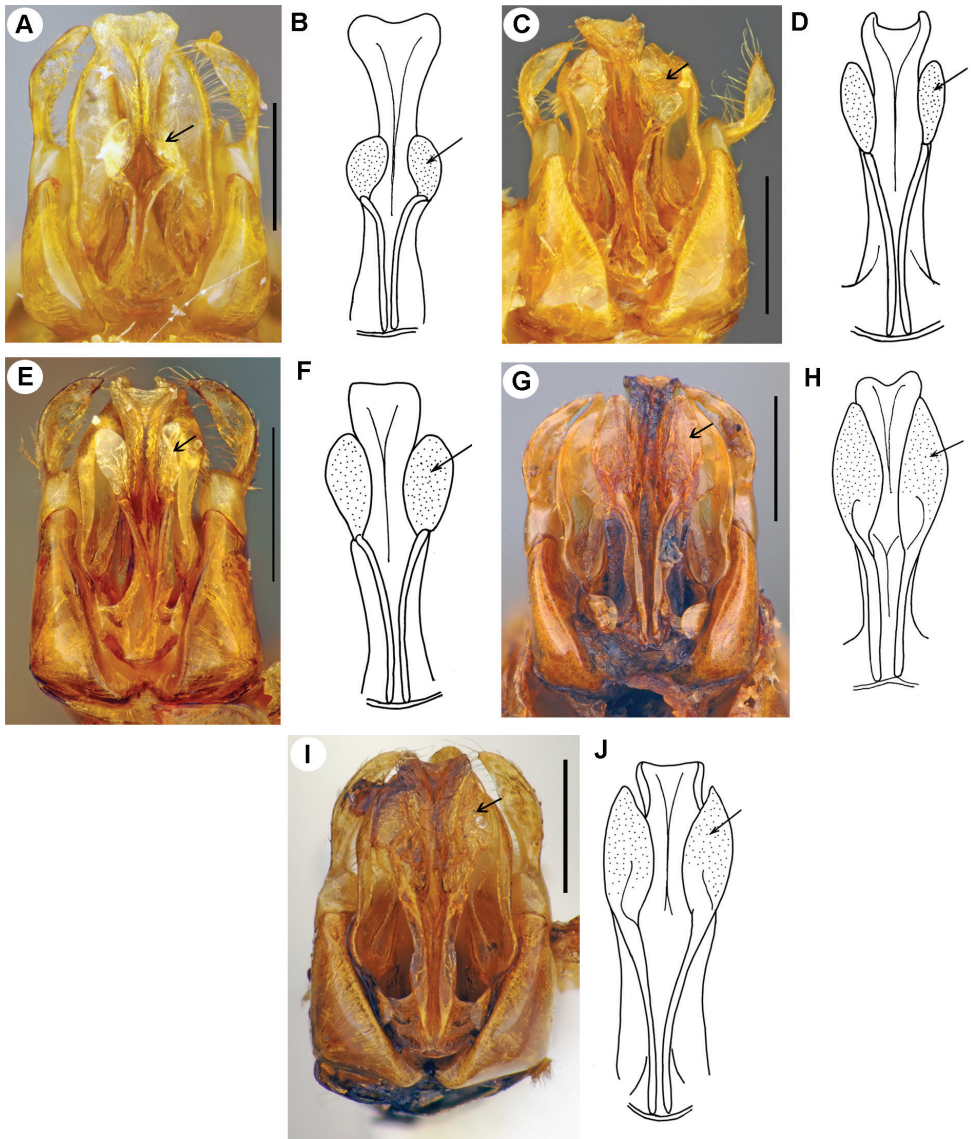


Figure 9. Male, genitalia **A, C, E, G, I** genital capsule, dorsal view **B, D, F, H, J** penis, dorsal view **A, B** *Epeolus seraxensis* Radoszkowski, 1893 **C, D** *Epeolus kyzylkumicus* Astafurova, sp. nov. **E, F** *E. julliani* Pérez, 1884 **G, H** *E. rasmonti* Astafurova & Proshchalykin, sp. nov. **I, J** *E. laticauda* Bischoff, 1930. Scale bars: 0.5 mm.

***Epeolus transitorius* Eversmann, 1852**

Figs 8A, 10

Epeolus transitorius Eversmann, 1852: 102 (lectotype: ♀, designated by Le Divelec 2021: 16, Indersk District, Atyrau Province, Kazakhstan; ZISP).

Material examined. GEORGIA, Tiflis[=Tbilisi], (1 ♀), coll. F. Morawitz, *transitorius* Eversm. [Morawitz det.] [ZISP]; KAZAKHSTAN, Zaysan, IX.1908, (1 ♂), coll. Gussakovskij [ZISP]; Fort Aleksandrovsk[=Fort-Shevchenko], 5.VII.1909, (1 ♂), Nasonov [ZISP]; Berchogur[=Birshoghyr], 26.VI.1910, (1 ♂), L. Bubyar [ZISP]; Chernoretsk, 11.VII.1925, (2 ♂), coll. Gussakovskij [ZISP]; near Chelkar Lake, Bolshiye Barsuki desert, 20.VI–10.VII., (1 ♀) [ZMMU]; Yanvartsevo, 19.VI–17.VIII.1950, (1 ♀, 5 ♂), V. Rudolf [ZISP]; 10 km N Zharkol Lake, 9.VII.1950, (2 ♀), V. Rudolf [ZISP]; Tengiz Lake, 3.VII.1957, (2 ♂), V. Rudolf [ZISP]; Kokshetau, on *Allium glabrosum*, 11.VII.1958, (1 ♀), V. Rudolf [ZISP]; 50 km E Balkhash Lake, 26–27.VI.1992, (1 ♀, 2 ♂), J. Halada [OLBL]; 5 km W Shardara, 250 m, 41°16'N, 67°53'E, 23–24.V.2016, (1 ♀, 1 ♂), J. Halada [OLBL]; RUSSIA, Astarakhan Prov., 35 km NNE of Astrakhan, 26.VII.2015, (1 ♀, 6 ♂), MP, VL, S. Belokobylskij, M. Mokrousov [ZISP]; Altai Terr., Novovoznesenka, 11.VII.1922, (2 ♂), A. Reygardt [ZISP]; CRIMEA, 8 km N of Dmitrovka, 5.VI.2018, (1 ♀), V. Savchuk [ZISP]; Mirny, Donuslav Lake, 17.VII.2017, (1 ♀), AF [ZISP]; Dagestan Rep., 20 km W of Makhachkala, Sarykum, 20–29.V.2019, (2 ♀, 1 ♂), MP, VL [FSCV]; Kalmykia Rep., 22 km E of Yashkul, 16–18.VII.2015, (1 ♀, 2 ♂) MP, VL, S. Belokobylskij, M. Mokrousov [FSCV/ZISP]; 17 km SWW of Artezian, Kuma River, 18–24.VII.2015, (2 ♀, 9 ♂), MP, VL, S. Belokobylskij, M. Mokrousov [FSCV/ZISP]; Orenburg Prov., Mayachnaya, 4.VIII.1993, (1 ♀), L. Zimin [ZMMU]; Orenburg, 9.VIII–3.IX.1926, (6 ♀, 1 ♂), P.A. Vorontzovskiy [ZISP]; Volgograd Prov., Sarepta, (2 ♀, 2 ♂), coll. F. Morawitz [ZISP]; Tinguta, 11.VIII.1952, (2 ♂), G. Viktorov [ZMMU]; TAJIKISTAN, Yagnob River, (1 ♂), coll. F. Morawitz, *transitorius* Eversm. [Morawitz det.] [ZISP]; Stalinabad[=Dushanbe], 18.VII.1936, (2 ♀), VG [ZISP]; idem, 15.VII.1943, (2 ♀, 1 ♂), V. Popov [ZISP]; UKRAINE, Yareski, 21.VII.1922, (2 ♀), coll. V. Gussakovskij [ZISP]; Kharkov, (1 ♂), coll. F. Morawitz, *transitorius* Eversm. [Morawitz det.] [ZISP]; UZBEKISTAN, Kurgan-Tyube[=Kurgantepa], Fergana, 27.V., 17.VII.1938, (1 ♀, 1 ♂), V. Popov [ZISP].

Variability. Females typically have well developed red body coloration. The labrum, pronotal lobe, tegulae, metanotum (medially), legs, and sterna are always red. The clypeus is usually red, but rarely can be mostly black or dark brownish (except with a red apical margin). The antennae are typically brownish with a red scape, pedicel and F1. The pronotum varies from black to partially red. The mesoscutum is mostly black, but red patterning sometimes also occurs laterally. Coloration of the mesepisternum varies from entirely red to partially black. The axillae and mesoscutellum are usually red, but rarely black peripherally. The terga are black or brownish, but T5 apically is typically red; sometimes red patterning occurs also on the anterior half of T1 and along margins. Pubescences of female is moderate. The face (except upper half of frons) is often obscured by dense tomentum, but 45% of specimens examined have the clypeus with sparse pubescence or almost glabrous. The mesepisternum is densely tomentose on the upper half and with sparse pubescence or glabrous below the scobal suture.

The males do not show significant variability. The body is mostly black, but the labrum, scape, pedicel, pronotal lobe, tegulae, legs and pygidial plate are red. The clypeus is black or with red patterning apically. The axillae and mesoscutellum are

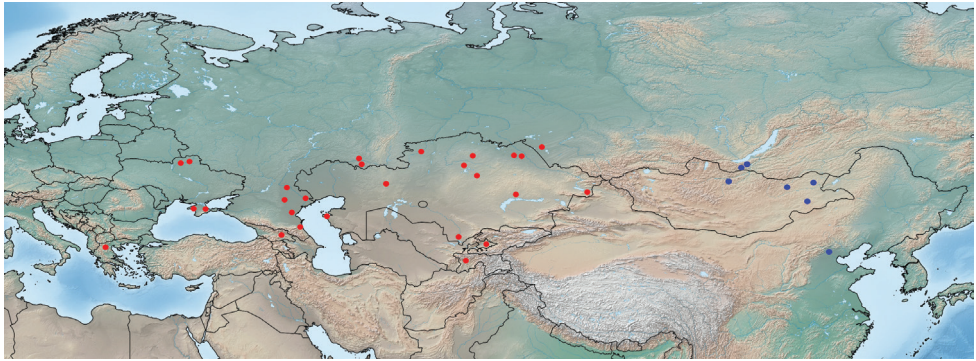


Figure 10. Distribution of *Epeolus transitorius* Eversmann (red dots) and *E. rasmonti* Astafurova & Proshchalykin, sp. nov. (blue dots).

usually black, often with red axillar teeth, sometimes partially red on mesoscutellum. The sterna are black or brownish to red along margins; marginal zones are golden. The pygidial plate is apically rounded, sometimes more or less straight or slightly bilobed.

Distribution (Fig. 10). Greece, Georgia, Ukraine, Russia (south of European part, south Ural, SW Siberia), Kazakhstan, Uzbekistan, Tajikistan (Le Divelec 2021; current data).

Remarks. The previous records of *Epeolus transitorius* from North Africa, Europe, Caucasus and Iran (Friese 1893, 1895; Bischoff 1930; Popov 1967; Bogusch and Hadrava 2018; Bogusch 2021) are mostly wrong (see Le Divelec 2021). Records from Morawitz (1875: 144, from Tajikistan [=Levchenko et al. 2017: 317, as Uzbekistan]) belongs to *E. michailovi* Astafurova & Proshchalykin, 2021; records from Turkmenistan (Levchenko et al. 2017: 317) refer to *E. seraxensis* Radoszkowski, 1893.

Discussion

The *Epeolus julliani* species group is distributed only in the southern Palearctic, ranging from northern Africa to China. Eight of the nine species occur in the Western Palearctic, and only *Epeolus rasmonti* sp. nov. is known only from the Eastern Palearctic. There are no species with a Trans-Palearctic range. *Epeolus julliani* is the most widespread species in this group, occurring from North Africa and Southern Europe east to the Middle East and Central Asia and north to the Urals. *Epeolus transitorius* occurs from Eastern Europe and Central Asia to Western Siberia. *Epeolus seraxensis* is distributed from the Middle East and Caucasus to Central Asia. *Epeolus fasciatus* Friese, 1895 occurs from Southern Europe to Turkey. The remaining species are endemics—*Epeolus siculus* – Sicily; *E. laticauda* Bischoff, 1930 and *E. kyzylkumicus* sp. nov. – Central Asia; *E. iranicus* – Iran.

Species of the group do not demonstrate as much intraspecific variation as has been observed within those in the *E. cruciger* species group (Astafurova and Proshchalykin

2022). The main combination of features to distinguish species in the *julliani* group is coloration and pubescence of the body, length of flagellomeres, and shape/width of the male pygidial plate (Table 1). The shape of the lateral lobes of the penis is an additional feature that can reliably distinguish species in this group (Fig. 9).

Acknowledgements

We are grateful to Maximilian Schwarz (Ansfelden, Austria), Esther Ockermueller (OLBL) and Alexander Antropov (ZMMU) for providing *Epeolus* specimens and Michael Orr (Beijing, China) for checking the English grammar, as well as to the subject editor (Michael Ohl, Berlin, Germany) and two reviewers (Thomas Onuferko, Ottawa, Canada and Petr Bogusch, Hradec Králové, Czech Republic) for their valuable comments, which helped to improve the quality of this paper.

This investigation was supported by the Russian Funds for Basic Research (grant number 20–54–44014), and the state research projects 122031100272-3 and 121031000151-3.

References

- Astafurova YuV, Proshchalykin MYu (2021a) Review of the *Epeolus tarsalis* species group (Hymenoptera: Apidae, *Epeolus* Latreille, 1802), with description of a new species. *Zootaxa* 5006(1): 26–36. <https://doi.org/10.11646/zootaxa.5006.1.6>
- Astafurova YuV, Proshchalykin MYu (2021b) New and little-known bees of the genus *Epeolus* Latreille, 1802 (Hymenoptera, Apidae, Nomadinae) from Mongolia. *Journal of Hymenoptera Research* 84: 11–28. <https://doi.org/10.3897/jhr.84.67150>
- Astafurova YuV, Proshchalykin MYu (2021c) A new species of the genus *Epeolus* Latreille, 1802 (Hymenoptera, Apoidea: Apidae) from the Pamirs, with a checklist of Central Asian species. *Far Eastern Entomologist* 437: 10–15. <https://doi.org/10.25221/fee.437.3>
- Astafurova YuV, Proshchalykin MYu (2022) Review of the *Epeolus cruciger* species group (Hymenoptera: Apidae, *Epeolus* Latreille, 1802) of Asia, with the description of two new species. *Journal of Hymenoptera Research* 92: 305–328. <https://doi.org/10.3897/jhr.92.90098>
- Bischoff H (1930) Beitrag zur Kenntnis palaarktischer Arten der Gattung *Epeolus*. *Deutsche entomologische Zeitschrift* 1930: 1–15. <https://doi.org/10.1002/mmnd.193019300102>
- Bogusch P (2018) Three new species and new records of cuckoo bees of the genus *Epeolus* in Turkey (Hymenoptera: Apidae: Nomadinae). *Acta Entomologica Musei Nationalis Pragae* 58: 127–135. <https://doi.org/10.2478/aemnp-2018-0010>
- Bogusch P (2021) The cuckoo bees of the genus *Epeolus* Latreille, 1802 (Hymenoptera, Apidae) from the Middle East and North Africa with descriptions of two new species. *Journal of Hymenoptera Research* 84: 45–68. <https://doi.org/10.3897/jhr.84.67049>
- Bogusch P, Hadrava J (2018) The bees of the genera *Epeolus* Latreille, 1802 and *Triepeolus* Robertson, 1901 (Hymenoptera: Apidae: Nomadinae: Epeolini) of Europe: taxonomy,

- identification key, distribution, and ecology. *Zootaxa* 4437(1): 1–60. <https://doi.org/10.11646/zootaxa.4437.1.1>
- Engel MS (2001) A monograph of the Baltic amber bees and evolution of the Apoidea (Hymenoptera). *Bulletin of the American Museum of Natural History* 259: 1–192. [https://doi.org/10.1206/0003-0090\(2001\)259<0001:AMOTBA>2.0.CO;2](https://doi.org/10.1206/0003-0090(2001)259<0001:AMOTBA>2.0.CO;2)
- Eversmann E (1852) Fauna hymenopterologica volgo-uralensis (Continuatio). *Bulletin de la Société impériale des Naturalistes de Moscou* 25(2/3): 3–137.
- Friese H (1893) Die Bienenfauna von Deutschland und Ungarn. R. Friedländer & Sohn, Berlin, 79 pp.
- Friese H (1895) Die Bienen Europa's (Apidae europaeae) nach ihren Gattungen, Arten und Varietäten auf vergleichend morphologisch-biologischer Grundlage. Theil I: Schmarotzerbienen R. Friedländer, Berlin, 218 pp. <https://doi.org/10.5962/bhl.title.160173>
- Giordani Soika A (1944) Contributo alla conoscenza dei Vespidi solitari e sociali della regione etiopica. *Atti del Regio Istituto Veneto di Scienze* 103: 149–178.
- Latreille PA (1802) Histoire naturelle, generale et particuliere, des Crustaces et des Insectes. *Historie naturelle des Crustaces et des Insectes* 3: 1–467. <https://doi.org/10.5962/bhl.title.15764>
- Le Divelec R (2021) The West Palaearctic *Epeolini* Linsley & Michener, 1939 housed in the Muséum national d'Histoire naturelle (Paris) with some taxonomic notes (Hymenoptera: Apidae: Nomadinae). *Annales de la Société entomologique de France (N.S.)* 57(4): 313–345. <https://doi.org/10.1080/00379271.2021.1942206>
- Lim K, Lee S, Orr M, Lee S (2022) Harrison's rule corroborated for the body size of cleptoparasitic cuckoo bees (Hymenoptera: Apidae: Nomadinae) and their hosts. *Scientific Reports* 12: 10984. <https://doi.org/10.1038/s41598-022-14938-9>
- Levchenko TV, Byvaltsev AM, Proshchalykin MYu (2017) Family Apidae. In: Lelej AS, Proshchalykin MYu, Loktionov VM (Eds) *Annotated Catalogue of the Hymenoptera of Russia. Volume I. Symphyta and Apocrita: Aculeata*. Proceedings of the Zoological Institute RAS, Supplement 6: 263–276.
- Michener CD (1944) Comparative external morphology, phylogeny, and a classification of the bees. *Bulletin of the American Museum of Natural History* 82: 151–326.
- Michener CD (2007) *The Bees of the World* (2nd edn.). Johns Hopkins University Press, Baltimore, 953 pp. [+ 20 pls] <http://base.dnsgb.com.ua/files/book/Agriculture/Beekeeping/Thep-Bees-of-the-World.pdf>
- Morawitz F (1875) A travel to Turkestan by the member-founder of the society A. P. Fedtschenko, accomplished from the Imperial Society of Naturalists, Anthropologists, and Ethnographers on a Commission from the General-Governor of Turkestan K. P. von Kaufmann (Issue 9). Vol. II. Zoogeographical Investigations. Pt. V. (Division 7). Bees (Mellifera). Pt. I [Apidae genuinae]. *Izvestiya Imperatorskogo Obshchestva Lyubiteley Estestvoznaniya, Anthropologii i Ethnografii* 21(3): 1–160. [in Russian]
- Onuferko TM, Bogusch P, Ferrari R, Packer L (2019) Phylogeny and biogeography of the cleptoparasitic bee genus *Epeolus* (Hymenoptera: Apidae) and cophylogenetic analysis with its host bee genus *Colletes* (Hymenoptera: Colletidae). *Molecular Phylogenetics and Evolution* 141: e106603. <https://doi.org/10.1016/j.ympev.2019.106603>

- Pérez J (1884) Contribution a la faune des Apiaires de France. Actes de la Société linnéenne de Bordeaux 37: 257–378.
- Popov VB (1935) Contributions to the bee fauna of Tajikistan (Hymenoptera, Apoidea). Trudy Tajikskoi Basy Akademii Nauk SSSR 5: 351–408. [in Russian]
- Popov VB (1949) Notes on the bee fauna of Tajikistan (Hymenoptera, Apoidea). Trudy Zoologicheskogo Instituta Akademii Nauk SSSR 8: 688–699. [in Russian]
- Popov VB (1967) The bees (Hymenoptera, Apoidea) of Middle Asia and their associations with angiosperm plants. Trudy Zoologicheskogo Instituta Akademii Nauk SSSR 38: 11–329. [in Russian]
- Radoszkowski O (1893) Faune hyménoptérologique transcaspienne. (Suite et Fin). Horae Societatis Entomologicae Rossicae 27(1/2): 38–81.
- Reitter E (1890) Eine neue mit Athous verwandte Elateriden. Gattung aus russisch Armenien. Entomologische-Nachrichten 16: 247–248.
- Reitter E (1905) Neun neue Coleopteren aus der palaearktischen Fauna. Wiener Entomologische Zeitung 24(5–6): 201–206.
- Shorthouse DP (2010) SimpleMappR, an online tool to produce publication-quality point maps. <https://www.simplemappR.net/> [accessed 12 October 2022]

A metabarcoding framework for wild bee assessment in Luxembourg

Fernanda Herrera-Mesías^{1,2}, Imen Kharrat Ep Jarboui¹, Alexander M. Weigand¹

1 *Musée National d'Histoire Naturelle de Luxembourg, Zoology Department, Luxembourg* **2** *Ruhr-Universität, Department of Animal Ecology, Evolution and Biodiversity, Bochum, Germany*

Corresponding author: Alexander M. Weigand (alexander.weigand@mnhn.lu)

Academic editor: Michael Ohl | Received 30 March 2022 | Accepted 19 October 2022 | Published 20 December 2022

<https://zoobank.org/1F2CA60D-E91C-4B05-98A5-A6C29C78B114>

Citation: Herrera-Mesías F, Ep Jarboui IK, Weigand AM (2022) A metabarcoding framework for wild bee assessment in Luxembourg. *Journal of Hymenoptera Research* 94: 215–246. <https://doi.org/10.3897/jhr.94.84617>

Abstract

Wild bees are crucial organisms for terrestrial environments. Their ongoing decline could cause irreparable damage to ecosystem services vital to plant reproduction and human food production. The importance of taking swift action to prevent further declines is widely acknowledged, but the current deficit of reliable taxonomic information complicates the development of efficient conservation strategies targeting wild bees. DNA metabarcoding can help to improve this situation by providing rapid and standardized mass identification. This technique allows the analysis of large numbers of specimens without the need for specialized taxonomic knowledge by matching high-throughput sequencing reads against public DNA barcode reference libraries. However, the validation of this approach for wild bees requires the evaluation of potential error sources on a regional scale. Here we analyzed the effects of three potential error sources on a metabarcoding pipeline customized for the wild bee fauna of Luxembourg. In an *in silico* study, we checked the completeness of the BOLD reference library for 349 species found in the country, the correspondence between molecular and morphological species delimitation for these taxa, and the amplification efficiency of three commonly used metabarcoding primer pairs (mICOLintF/HCO2198, LepF1/MLepF1-Rev and BF2/BR2). The detection power of the pipeline was evaluated based on the species recovery rates from mock communities of known composition under variable DNA concentration treatments. The reference barcode library evaluation results show that 97% of the species have at least a single barcode in BOLD Systems (minimal length 196 bp) and that 85% of species have ≥ 5 barcodes in the public domain. The mICOLintF/HCO2198 target fragment presented the highest coverage (77.94% of the species with full barcode sequences), followed by the target fragments of LepF1/MLepF1-Rev (77.65%) and BF2/BR2 (68.48%). Only 60% of the morphospecies presented a complete coverage of the prominent Folmer region (658 bp). The *in silico* amplification efficiency analysis shows that the BF2/BR2 primer pair has the best-predicted amplification performance, but none of the primer combinations evaluated can be expected to efficiently amplify all local wild bee genera. Finally, all species detection rates in the mock communities, except for the sample with the most discrepant

DNA concentrations, were above 97%, with no significant differences found among treatments. These results indicate that the detection capacity of the pipeline is robust enough to be used for the reliable assessment of local wild bee biodiversity, even if species from various size categories are pooled together. Primer bias has a major effect on species detection, which can be acknowledged with a preliminary assessment of primer-template mismatch and sophisticated methodological designs (e.g. mock community controls, replicates). Overall, the metabarcoding pipeline here described provides a suitable tool for quick and reliable taxonomic identification of the regional wild bee fauna to aid conservation initiatives in Luxembourg – and beyond.

Keywords

biodiversity, COI, conservation, molecular taxonomic tools, pollinators, primer evaluation

Introduction

Bees (Hymenoptera, Anthophila) are important insect pollinators of Angiosperms with critical ecological functions and high economic value (Brown and Paxton 2009). Their pollination services have a crucial impact on the reproduction of both wild flowering plants and cultivated crops (Potts et al. 2010a; Rafferty 2017). Over 75% of the crops grown worldwide benefit to some degree from insect-mediated pollination and wild bees participate directly in the reproduction of about 42% of the leading food crops grown for human consumption (Klein et al. 2007; Potts et al. 2010a). Moreover, the global annual economic value of insect pollination, most of which is performed by bees, has been estimated on at least 153 billion euros (Potts et al. 2010a).

Despite the high importance of the ecological services provided by insects (Losey and Vaughan 2006), several studies have reported large declines in insect diversity, abundance and biomass over the past few decades (Dirzo et al. 2014; Hallmann et al. 2017; Hausmann et al. 2020), a trend from which bees are not excluded. Consistent evidence has been found of ongoing decline in Europe for honey bees and bumblebees (Rasmont and Mersch 1988; Goulson et al. 2008; Potts et al. 2010a, b). Rarefaction analyses performed on records from national entomological databases in the UK and The Netherlands suggest that wild bee biodiversity has significantly declined after 1980 in landscapes of both countries, with a special emphasis on species with narrow habitat requirements (Biesmeijer et al. 2006). Similar trends are likely to be true for nearby regions and similarly urbanized locations, but important documentation gaps complicate the evaluation of the extent and characteristics of this potential decline of wild bee species in Europe.

According to the European Red List of Bees, 1,101 species (57% of the total) are classified as “data deficient” (Nieto et al. 2014). This lack of scientific information makes it difficult to assess vulnerability and extinction risk for individual taxa. This is important as there are considerable differences in pollination effectiveness and floral specialization (oligolecty vs. polylecty) among genera and species are observed (Dogterom et al. 1998; Cane and Sipes 2006). The misinformation regarding regional wild bee species diversity and distribution has been accompanied by the persistent decline of traditional professional and amateur taxonomic experts since the mid-20th century, a

situation that threatens the future of conservation efforts (Hopkins et al. 2002; Wägele et al. 2011).

DNA-based approaches and in particular DNA metabarcoding might act as a game changer for wild bee assessments (Taberlet et al. 2012; Piper et al. 2019). This tool can generate and process large quantities of data, providing at the same time a way to distinguish cryptic or hard to identify sister species. Moreover, it allows identifying complicated cases such as when facing juveniles or incomplete organisms. Despite its overall potential, the development and applicability of DNA metabarcoding approaches is still a work in progress that has to be evaluated on a case-by-case and regional basis (Leese et al. 2018; van der Loos and Nijland 2020). Metabarcoding datasets are sensitive to multiple factors which can introduce false negative (e.g. gaps in reference libraries, variable primer efficiencies among target taxa, i.e. primer-bias, and variable biomass among specimens and species compromising detection rates) or false positive results (e.g. cross-contamination, tag-switching and a priori identification errors in barcode libraries) (Clarke et al. 2014; Elbrecht and Leese 2015; Weigand et al. 2019; Zinger et al. 2019).

In this study, we tested the suitability of a DNA metabarcoding approach customized for the assessment of the wild bee biodiversity of the Grand Duchy of Luxembourg. Early metabarcoding data already indicate a potential benefit of this approach for assessing Central European wild bees (Gueuning et al. 2019, for Switzerland), but its methodological performance has yet to be evaluated for the regional fauna and for different primer pairs separately. By 2021, 349 wild bee species had been described as present in Luxembourg (Cantú-Salazar et al. 2021; Herrera-Mesías and Weigand 2021), a number that is expected to increase over the next years as a result of increased sampling efforts to develop pollinator monitoring programs. Compared to adjacent countries, this amount is similar to the number of species registered in Belgium (398 species) and The Netherlands (366 species), about one third of the species described from France (949 species) and more than half of the species of Germany (over 550 species) (Westrich et al. 2011; Rasmont et al. 2017; Schneider 2018; Vereecken 2018).

Our central aim here is to propose an effective DNA metabarcoding approach, which ultimately can provide robust data on the wild bee species diversity and distribution in Luxembourg, while preserving bulk samples of wild bees as vouchers. Although this at first glance contradicts the often-highlighted “time-and-cost” benefits of DNA metabarcoding approaches, this strategy will enable subsequent morphological investigations in case of peculiar or doubtful findings, and allows the integration of selected specimens in the reference collection of the National Museum of Natural History Luxembourg (MNHNL).

From a technical point of view, the following methodological aspects were evaluated:

- a. Completeness of the barcode reference library of Luxembourgish wild bees
The commonly used Cytochrome C Oxidase Subunit I (COI) barcode region has a high species discrimination power in Hymenoptera (Smith et al. 2008) and a barcoding library for Central European wild bee species has been available for some time (Schmidt et al. 2015, based on the fauna of Germany). Moreover, new wild bee sequences are being uploaded to the Barcode of Life Data system

- (BOLD; Ratnasingham and Hebert 2007) on a regular basis, providing a constantly growing reference library. We thus evaluated the proportion of all regionally cataloged bees having available barcode fragments in general, and more specifically, for three widely applied metabarcoding primer pairs in the study of insects.
- b. Effect of primer bias on detectability (*in silico* evaluation)

Numerous primers targeting the COI region have been designed for or applied in metabarcoding studies of insects (e.g. Brandon-Mong et al. 2015; Marquina et al. 2019; Piñol et al. 2019). We compared the *in silico* performance of three promising metabarcoding primer pairs from the literature to select appropriate combinations for wild bees.
 - c. Effect of biomass bias on detectability

Wild bees are a phenotypically diverse pollinator group with considerable interspecific variation in body size (Michener 2007). As such, wild bee bulk samples might be susceptible to detection biases due to differences in individual biomass. This has been shown in metabarcoding pipelines of wild bees, where strong correlations between read numbers and estimated biomass have been found (Gueuning et al. 2019). Since passive sampling strategies such as pan and malaise trapping are commonly used to collect wild bees despite their body size variations, it is not unlikely that biomass-rich and biomass-low specimens get mixed in bulk samples, potentially obscuring the identification of smaller specimens in a parallel analysis. Adding to this, the effects of primer bias and biomass bias can be synergistic or antagonistic for individual species. We thus examined the effect of biomass in the detection capacity of our metabarcoding approach by using mock communities of known composition under different treatments.

Thus, for this study, *in silico*, and *in vitro* approaches were combined to evaluate the sensitivity of a customized metabarcoding pipeline targeting regional wild bee species to common potential error sources: reference library completeness, primer and biomass-related bias. We compared the *in silico* performance of three popular metabarcoding primer pairs from the literature and then tested these expectations in the laboratory using mock communities. With this strategy, we aim to determine the best candidate for regional wild bee metabarcoding and to evaluate the suitability of the proposed workflow as a potential identification tool to be used in national conservation initiatives in Luxembourg.

Materials and methods

Barcode reference library coverage analyses

Barcode coverage analyses were performed for three different metabarcoding primer pairs: BF2/BR2, mlCOLintF/HCO2198 and LepF1/MLepF1-Rev (Table 1). The selected primer combinations correspond to primer pairs from the literature that have been previously tested for metabarcoding arthropod samples, showing promising

Table 1. Overview of primer pairs evaluated in the *in silico* analysis.

Primer name	Orientation	Fragment length (bp)	Sequence (5'-3')	Reference
mIColintF	forward	313	GGWACWGGWTGAACWGTWTAYCCYCC	Leray et al. (2013)
HCO2198	reverse		TAAACTTCAGGGTGACCAAAAAATCA	Folmer et al. (1994)
BF2	forward	421	GCHCCHGAYATRGCHTTYCC	Elbrecht and Leese (2017b)
BR2	reverse		TCDGGRTGNCCRAARAAYCA	Elbrecht and Leese (2017b)
LepF1	forward	218	ATCAACCAATCATAAAGATATTGG	Hebert et al. (2004)
MLepF1-Rev	reverse		CGTGGAAAWGCTATATCWGGTG	Brandon-Mong et al. (2015)
LCO1490	forward	658	GGTCAACAAATCATAAAGATATTGG	Folmer et al. (1994)
HCO2198	reverse		TAAACTTCAGGGTGACCAAAAAATCA	Folmer et al. (1994)

amplification success rates for insect taxa, in particular for hymenopterans and bees (Hebert et al. 2004; Brandon-Mong et al. 2015; Elbrecht and Leese 2017a; Gueuning et al. 2019). All pairs included at least one degenerate primer (either forward or reverse), with the BF2/BR2 pair presenting the highest combined primer degeneracy.

Since the DNA barcode sequences deposited in the BOLD reference library may cover different regions of the COI gene, the coverage of the specific amplicon of each primer pair was individually checked for the local wild bee fauna. Additionally, the coverage of the prominent COI Folmer region (i.e. the traditional 658 bp long DNA barcode fragment used for animal barcoding) was also checked.

For this purpose, the R package PrimerMiner version 0.18 (Elbrecht and Leese 2017a) was executed under R version 3.6.2 (R Core Team 2019) to batch download COI sequence data from BOLD (data retrieved on 26-05-2021, minimal barcode length of 196 bp) for the considered 349 Luxembourgish morphospecies, thereby generating the overall barcode coverage report of the public library. As a first step, all available barcode fragments corresponding to the target wild bee species based on their BOLD record details were downloaded and counted. Species were classified into three categories depending on the number of available barcodes (no barcode; 1–4 barcodes; ≥ 5 barcodes).

From this original dataset, identical sequences were automatically reduced to singletons and clustered into Molecular Operational Taxonomic Units (MOTUs) based on a 3% sequence similarity threshold to reduce the bias introduced by unequal representation of sequences in the database (Elbrecht and Leese 2017a).

To further validate the correspondence of each MOTU consensus sequence with the taxonomic data from the BOLD record details of the original barcodes, the resulting fasta files were compared against BOLD Systems using BOLDigger (Buchner and Leese 2020). Taxonomic identification was conducted based on the following sequence similarity thresholds: over 85% of match for identification to the level of order, 90% to family, 95% to genus and 98% to species.

Even if only sequences uploaded under regional wild bee species binomial names were downloaded, the best BOLD match for some MOTU consensus sequences was

not a wild bee present in Luxembourg. For example, OTU 416 consists of a single sequence (BOLD Process ID NOBEE085-09). Even if this sequence was downloaded as *Lasioglossum fratellum*, the available barcode matches the mosquito *Aedes canadensis*. Problematic MOTUs such as this one were deleted from the dataset, keeping only consensus sequences matching Luxembourgish wild bees up to species level.

These validated MOTU consensus sequences representing each target species were subsequently analyzed thus to determine their COI coverage for all three metabarcoding primer-pairs (Suppl. material 1: table a). Finally, the congruence of species delimitation (taxonomic splitting or lumping) was evaluated for each of the 349 morphospecies by tracing back the accession numbers of the original batch downloaded sequences assigned to each Linnaean species across the MOTUs generated in the previous step (Suppl. material 1: tables b, c).

In silico primer evaluation

The PrimerMiner package was used to perform an *in silico* evaluation of the amplification efficiency of each metabarcoding primer based on the dataset of validated MOTU consensus sequences. Scores for primer-template mismatches were assigned based on position and mismatch type under default settings, using the tables included in the package. These scores were summed up to calculate individual penalty scores for each primer or primer pair (Elbrecht and Leese 2017a).

Consensus sequences were visualized with Mesquite v3.6 (Maddison and Maddison 2019) and aligned against a reference “backbone” sequence, obtained by combining wild bee mitochondrial genomes from GenBank into a consensus sequence using MAFFT v7.450 (Katoh et al. 2002). A penalty score of 100 was defined as the threshold (value taken from the package documentation) to determine if a particular primer or primer pair was suitable for the amplification of a specific taxonomic unit. Primers with penalty scores above this threshold were considered inappropriate for metabarcoding. The Folmer primers (LCO1490 and HCO2198) were included in the analysis for comparison. Amplification success rates for each primer were calculated based only on the scores of MOTU consensus sequences with complete sequence data in their respective primer binding sites. Therefore, analogous calculations for the primer pair could only be achieved when complete sequence data was available for both the forward and reverse primer.

To compare the overall performance of the primers across different taxonomic groups, mean penalty scores were calculated by averaging the penalty scores of all the MOTUs within each wild bee genus. Mean values were transformed with a Tukey’s Ladder of Powers transformation ($\lambda = 0.375$) to correct for skewness caused due to the presence of outliers (Suppl. material 2). The R packages *car* (Fox et al. 2016) and *rcompanion* (Mangiafico and Mangiafico 2017) were used to calculate Shapiro-Wilk and Levene’s tests to account for the assumptions of normality and homocedasticity.

To determine whether there were significant differences among the primer pairs regarding their mean *in silico* scores across the wild bee genera, the transformed values

were compared with a weighted One-Way ANOVA, using the number of MOTUs in each genus as weights and the primer pairs as the grouping variable. A Tukey Honest Significant Differences (Tukey's HSD) test was used to calculate pairwise-comparisons between the mean scores of the primer pairs. Both tests were performed in the R package "stats".

Sampling, identification and laboratory processing of specimens

Wild bees were sorted from collections taken in spring and summer 2019 across Luxembourg and the nearby Federal State of Rhineland-Palatinate (Germany) using sweep netting, opportunistic sampling of dead specimens and different kinds of passive trapping (pan traps, vane traps and malaise traps). Wild bee specimens were morphologically identified to the level of species or genus using the taxonomic keys of Amiet et al. (1999, 2001, 2004, 2007), Scheuchl (2000) and Falk (2015).

In the case of the wild bees from Luxembourg, samples were collected over several days using traps filled with 80% propylene glycol and soap or soapy water (Weigand et al. 2021). Individually collected specimens were immediately stored in 96% ethanol. Bees were separated from by-catch in the laboratory.

Wild bees collected in Rhineland-Palatinate were stored in 80% ethanol after sampling, pinned by the end of the field season and kept dry in a drawer. Except for *Ceratina chalybea*, all the specimens from Germany corresponded to species present in Luxembourg (Suppl. material 3: table a). This species was added since no other regional *Ceratina* specimen was available. In total, 32 specimens were selected from the 2019 field work campaigns for the mock community setup. Additionally, a single pinned specimen from the reference collection of the MNHNL and 10 dried specimens opportunistically collected in 2018 and 2019 (found dead in the field) were added as well. This experimental design intended to include representatives from as many of the available genera found in the country as possible in the mock communities, considering only one specimen per species, so that sequencing reads could be easily traced back to a single specimen.

For validation purposes, as well as to check the general suitability of the obtained tissue material for molecular analysis, all specimens were individually Sanger-sequenced using the Folmer primer pair LCO1490/HCO2198. All DNA extractions were performed by grinding a single mid-leg of each specimen in a Retsch TissueLyser Mixer Mill model MM200 using 3 mm beads made of either plastic (41 specimens) or metal (2 specimens), as described in the laboratory protocols of Weigand and Herrera-Mesías (2020). Polymerase chain reaction (PCR), PCR purification and Sanger sequencing were also done according to the protocols described in this publication. In the case of specimens for which it was not possible to get reliable individual barcode sequences using the Folmer primers, molecular identifications were obtained using the LepF1/MlepF1-Rev or the BF2/BR2 primer pairs, using the same PCR thermal profile. Molecular species identification was performed by comparing the obtained sequences against BOLD Systems.

The final assortment of specimens used for the mock community design included 43 adult females. Of them, 28 specimens (25 fresh and 3 dry) were used for “concentration adjustment” mock communities and 14 specimens (7 fresh and 7 dry) for “regular” bulk extraction mock communities, plus a single dry specimen that was used for both treatments (Suppl. material 3: table a). Specimens were classified into three categories based on the overall pre-PCR DNA concentration. Specimens with a concentration below the first quartile of the group were grouped in the small (“S”) category, specimens with concentrations between the first and the third quartile were included in the medium (“M”) category and specimens with concentrations above the third quartile were assigned to the large (“L”) category (Suppl. material 3: table b). DNA concentrations were quantified using a Microvolume Spectrophotometer Trinean Xpose with the A260 dsDNA setting.

Mock community design

To study the *in vitro* effect of primer bias and the impact of biomass differences on the metabarcoding pipeline detection capacity, three experimental set-ups (“mock communities”) were designed (Suppl. material 3: table a).

The first mock community (homogeneous, HOMO) was arranged by pooling 10 ng of DNA of each species. In two cases (*Hylaeus nigrinus* and *Lasioglossum morio*), just 5 to 6 ng were added due to a lack of further tissue material. This roughly homogeneous treatment provides a theoretically biomass-related bias free scenario, in which differences in the detection rates are more likely to be caused by factors such as primer bias and the stochasticity of the PCR process.

The second mock community (heterogeneous, HETE) was assembled by pooling 1 ul of variable DNA concentration obtained from a single mid-leg from each specimen. This setup provides information regarding the detection limits of the pipeline when DNA from one leg per specimen is analysed and as such, how species are recovered by metabarcoding when the amount of species-specific template DNA is unequal in the PCR. In this case, false negatives are expected to be caused by biomass-related bias under unaltered conditions.

The third mock community (gradient, GRAD) uses the same specimens as in the two previous mock communities, but modifying their concentrations based on the concentration categories previously assigned to each specimen. The DNA of the bees from the “S” category was diluted with buffer in a proportion of 1:100. Six bees from the “M” category were randomly selected and their isolated DNA was diluted to approach concentrations similar to the bees from the “S” category. The bees belonging to the “L” category were not modified. This treatment creates a gradient of DNA concentrations to test the effectiveness of the pipeline under variable DNA concentrations, indicating the impact of the biomass-related bias under more extreme conditions.

Additionally, two “regular mock communities” (RmockA and RmockB) were analyzed for reference purposes (Suppl. material 3). In this case, legs from eight specimens per sample, without repetition of species within the sample, were combined to produce bulk samples from which DNA was isolated.

Metabarcoding PCR, replication strategy, library preparation and sequencing

Three PCR replicates for each mock community (i.e. of HETE, HOMO, GRAD, RmockA and B) were set-up and sequenced. The 16 samples (15 mock community replicates plus a negative control) were amplified using the primer set showing the best performance in the *in silico* evaluation. A two-step PCR protocol was used. The first PCR reaction consisted of 1× Master Mix (GoTaq G2 Hot Start Colorless), 0.5 μM of each primer, 25 ng of DNA and Nuclease-Free H₂O to a final volume of 25 μl. For the second PCR, 1 μl of the amplicon (without cleanup) was used as template and the amount of reagents was modified to a final volume of 50 μl. Both PCRs were run on an Eppendorf Mastercycler nexus eco thermocycler using thermal profiles based on the ones described in Elbrecht and Steinke (2019). The first PCR started with an initial denaturation step at 94 °C for 5 minutes, followed by 34 cycles of denaturation for 30 seconds at 94 °C with annealing for 30 seconds at 50 °C and extension at 65 °C for 50 seconds; and a final extension for 5 minutes at 65 °C. The program for the second PCR followed the same steps, but with 19 cycles instead and an extension time of 2 minutes. The tag combination used for the second PCR are described in Elbrecht and Leese (2017b) (Suppl. material 4). PCR success was verified by electrophoresis and the products were purified with a NucleoSpin Gel and PCR Clean-up kit (Macherey-Nagel™). The DNA concentrations of the purified products were measured for equimolarly pooling into the final library (40 μl, 64.3 ng/μl). The cleaned library was sequenced on one lane of an Illumina MiSeq System (2 × 250 bp) at the Luxembourg Centre for Systems Biomedicine (Belval, Luxembourg).

Quality filtering, MOTU clustering and taxonomic assignment

Dereplication of the samples in the same sequencing run based on inline tag combinations was done using scripts (“Demultiplexer”) developed by the Aquatic Ecosystem Research Group of the University of Duisburg-Essen. Reads that were unmatched after this module were mapped against PhiX to check for the presence of virus genome. The demultiplexed data was further processed using the JAMP (“Just Another Metabarcoding Pipeline”) R package (<https://github.com/VascoElbrecht/JAMP>). This package consists of a modular metabarcoding pipeline that provides extended quality filtering options and automatically generated summary statistics, integrating different functions from external programs to produce the output of the different steps (Elbrecht et al. 2018). JAMP 0.67 was run using R version 3.6.2 (R Core Team 2019), relying on Usearch v11.0.667 (Edgar 2010), Vsearch v2.14.2 (Rognes et al. 2016) and Cutadapt 2.8 (Martin 2011). Settings were adjusted so that 25% mismatches were allowed to overlap. Any read that did not match the expected length of the BF2/BR2 amplicon (421bp ± 10bp) was removed. After MOTU clustering based on 3% sequence similarity, a default 0.01% abundance filter was applied twice (i.e. first based on the overall dataset and second based on the results of each individual sample) to the initial MOTU table to produce the final dataset.

Taxonomic sorting was performed by comparing the resulting MOTU fasta files against sequences stored in BOLD Systems using BOLDigger. The same thresholds for taxonomic identification used in the *in silico* evaluation were used here. The resulting data were pruned using TaxonTableTools (Macher et al. 2021) to remove all non-Hymenoptera MOTUs, as well as Hymenoptera MOTUs present in only one out of the three PCR replicates.

The detection capacity of the metabarcoding pipeline was evaluated based on the percentage of intentionally pooled species retrieved from each treatment (“detection rates”). Kruskal-Wallis and Wilcoxon rank sum tests (both default R package “stats 3.6.2”) were used to determine whether there were significant differences among the HETE, HOMO and GRAD mock communities regarding the average read numbers per species obtained after combining the sequencing results of all replicates.

Results

Barcode coverage

Of the 349 wild bee species evaluated, 96.84% presented at least one COI barcode sequence available in the BOLD Systems public library (Fig. 1); 84.81% of all morphospecies were represented by at least five barcodes and 12.03% by one to four barcodes. Only eleven species (3.15%) had not barcodes in the database.

The 7,317 de-replicated sequences considered (i.e. after removing identical sequences from the set of 11,810 downloaded sequences) were clustered into 558 MOTUs. From them, the consensus sequences of 433 were included in the final dataset based on the combined assessment of their 20 top matches using BOLDigger, and supporting their identification as local wild bee taxa.

Barcode coverage of the regions targeted by the three considered metabarcoding primer pairs presented little variation (Fig. 2). The mlCOLintF/HCO2198 target fragment was completely covered for 77.94% of the morphospecies, partially covered for 9.74% and it was missing for 12.32%. LepF1/MLepF1-rev presented a complete coverage in 77.65% of morphospecies, a partial coverage for 10.60% and for 11.75% the target region was missing in BOLD. The BF2/BR2 target fragment was complete for 68.48% of the species, partially covered for 20.34% and missing in 11.18%. Full-length (complete) barcode coverage for the traditional animal barcoding Folmer primer pair LCO1490/HCO2198 target region was the lowest (59.89%).

Species delimitation congruence

Only 39.05% (132/338) of the morphospecies considered in the final dataset fulfilled the expected correspondence of one MOTU per Linnaean species (Suppl. material 7). In all the other cases, some sort of incongruence was observed (Suppl. material 1: table b).

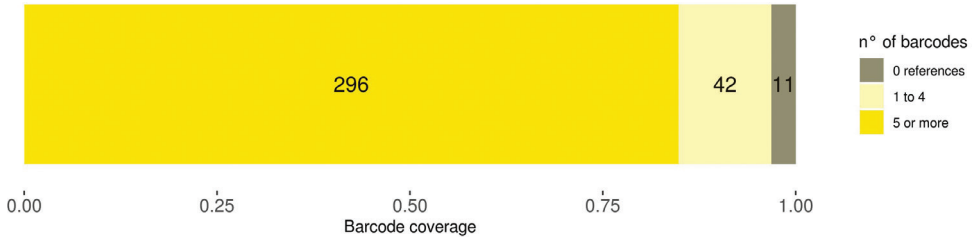


Figure 1. Overall COI barcode coverage in the BOLD public library for the 349 Luxembourgish wild bee species considered.

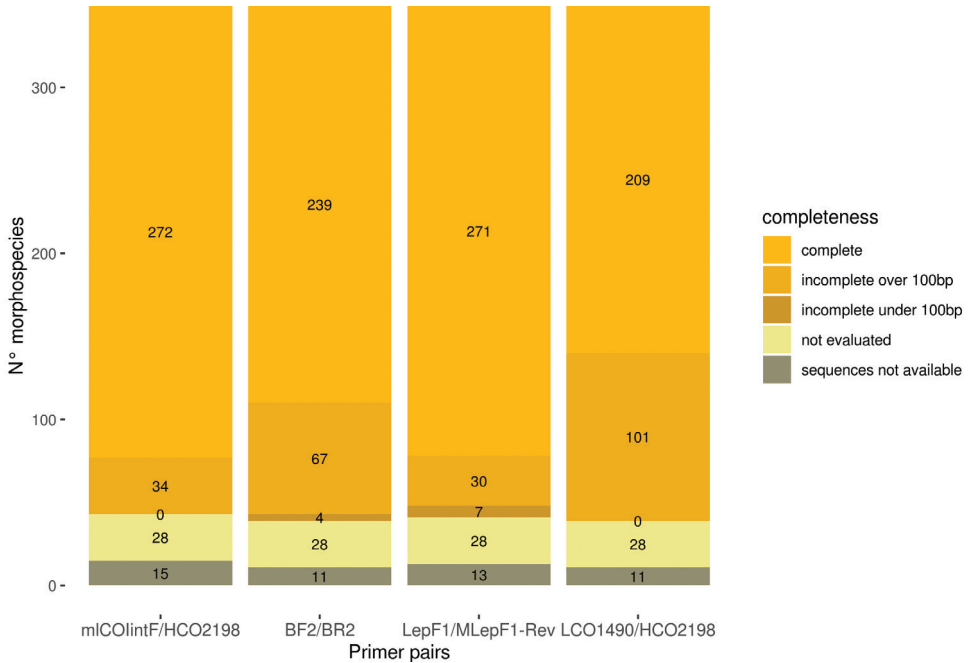


Figure 2. Coverage of (meta)barcoding primer pairs considered in this study for the targeted 349 Luxembourgish wild bee species.

The clustering process either split sequences belonging to one species into multiple MOTUs (29.29% of the cases; mostly into two MOTU) or lumped sequences from different morphospecies into a single MOTU (8.88% of the cases). While lumping might lead to false negatives or unresolved metabarcoding results, splitting of a nominal species into multiple MOTUs generally does not bias metabarcoding outcomes. Finally, in 22.78% of the cases, the 3% clustering threshold split the sequences of a Linnaean species and then lumped them with sequences corresponding to another morphospecies. This process created MOTUs that combined sequences from several species.

In silico primer evaluation

The results of the *in silico* analysis of the metabarcoding primers were first sorted by genera to assess their performances across different taxonomic groups of interest. When all MOTUs are considered, the expected amplification success rates of the individual primers varied across 25 wild bee genera. However, in the majority of the cases the combined outcomes of the metabarcoding primer pairs were higher or equal to the ones of the standard Folmer barcoding primers (Suppl. material 8). Exceptions to this were the genera *Sphecodes*, *Osmia*, *Hoplitis*, *Halictus*, *Megachile*, *Chelostoma*, *Colletes* and *Dasygaster*, for which the Folmer primers outperformed one or more metabarcoding primer pairs.

The BF2/BR2 primer pair had the highest mean *in silico* amplification success rate (86.52% of the species with binding site sequence data were expected to correctly amplify), while LepF1/MLepF1-Rev (16.88% of the species) and LCO1490/HCO2198 (17.65% of the species) had the lowest success rates. The primer pair mlCOIintF/HCO2198 showed an intermediate *in silico* performance (amplification is expected successful for 37.50% of the species). The expected amplification success rates of the primer pairs mlCOIintF/HCO2198 and BF2/BR2 were identical for 48.57% of the wild bee genera considered. However, BF2/BR2 consistently outperforms mlCOIintF/HCO2198 in 83.33% of the remaining cases, while mlCOIintF/HCO2198 only shows higher amplification success rates than BF2/BR2 in three genera: *Nomada*, *Heriades* and *Melitta*.

Regarding the average penalty scores obtained from all the MOTUs within each wild bee genus, the transformed scores for BF2/BR2 were within the accepted values of amplification success, with the exception of the mean penalty scores of *Anthophora*, *Eucera*, *Halictus*, *Melitta* and *Nomada* (Fig. 3). In contrast, the average penalty scores of only nine genera were below the threshold for mlCOIintF/HCO2198 and of only two genera for LepF1/MLepF1-Rev. Moreover, the BF2/BR2 mean score calculated from all genus average penalty scores was the only one below the threshold. The results of the weighted One-Way ANOVA indicated that there was a statistically-significant difference in the genera average transformed penalty scores by metabarcoding primer pair ($f(2) = 42.98$, $p < 0.001$). The Tukey's HSD test indicated that the differences were statistically significant for all primer comparisons ($p < 0.001$ for all pairwise comparisons). Data is normally distributed and homocedastic at a 95% level of confidence (Shapiro-Wilk test: $W = 0.98$, $p = 0.241$; Levene's Test: $F(2) = 2.47$, $p = 0.092$).

The results of the *in silico* analysis vary slightly when only the MOTU with the best score for a distinctive morphospecies (in the case of "multi-MOTU" species) is considered as an outcome (Suppl. material 9). Under this assumption, the metabarcoding primer pair with the highest amplification success rate is BF2/BR2 (87.05%), followed by mlCOIintF/HCO2198 (36.09%) and finally LepF1/MLepF1-Rev (17.44%).

Overall, multi-MOTU morphospecies presented congruent results for the same primer pair, despite variable penalty scores for each of their MOTUs. The exception to this were four species (*A. plumipes*, *B. terrestris*, *S. albilabris*, and *S. geoffrellus*), which presented MOTUs with scores both above and below the threshold for one or more primer combinations. *Bombus terrestris* presented discrepancies for all primer pairs but

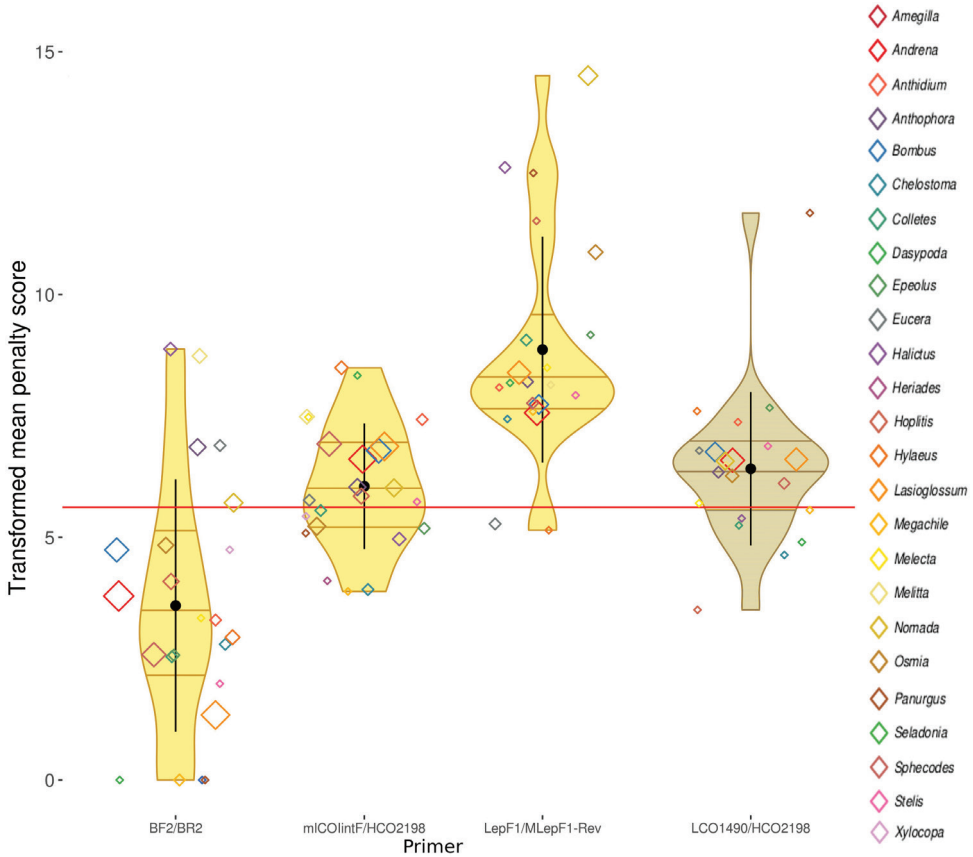


Figure 3. Distribution of transformed mean penalty scores by primer pair and genus. The sizes of the diamonds that represent the mean of the genera are proportional to the number of MOTUs in each genus. The overall mean value and standard deviations for each primer pair are shown in black. Means with a penalty above the red line (penalty score of 100) are considered *in silico* performance failures. The LCO1490/HCO2198 primer pair is indicated for reference purposes only, and not included in the statistical analysis.

LepF1/MLepF1-Rev. Two species (*A. plumipes*, and *S. geoffrellus*) showed discrepancies for mlCOIintF/HCO2198 and BF2/BR2. Finally, *S. albilabris* only presented discrepancies for mlCOIintF/HCO2198.

Bioinformatic analysis of mock communities and detection rates

A total of 6,902,568 high quality reads from the original 11,701,736 read pairs remained after trimming and quality filtering (Short Read Archive bioproject number PRJNA867321). The percentage corresponding to PhiX found in the unassigned reads (64% of the 2,251,231 reads in “no match”) was in agreement with the procedures of the sequencing center. From the original 328 MOTUs generated, 118 MOTUs

remained after the 0.01% abundance filters (Suppl. material 5). 1,126 chimeras were discarded during clustering. The sample presented a moderate level of resolution, with 70% of the MOTUs identified at least up to the level of genus and 52% to the level of species.

For species detection rate assessment within mock communities, 53 Hymenoptera MOTUs – identified to species level and present in at least two replicates – were considered (Suppl. material 6). The detection rate of input species was 97% for both the HETE and HOMO mock communities, but only 72% in the GRAD mock community. The single missing species in the HETE sample corresponded to a “S” category species (*L. morio*) that was only found in the first replicate of the sample with 53 reads, while the missing bee in the HOMO sample corresponded to a “L” category museum specimen (*T. byssina*), whose DNA was potentially already degraded. All the missing species in the GRAD mock community belonged to the “S” category (*H. langobardicus*, *C. afra*, *L. morio*, *L. nitidulum*, *E. alticineta*, *H. tumulorum*, *L. laticeps* and *H. nigritus*), except for *T. byssina*, which was found only in the first replicate of the sample with 110 reads. Bee specimens in the “M” category were detected in all three set-ups, even when diluted in a proportion of 1:100 (GRAD mock community). Both regular set-ups (RmockA and RmockB) had a detection rate of input species of 100%. However, a false positive (*Halictus confusus*) was found in both, likely due to pre-PCR contamination.

In the main three experimental set-ups (HETE, HOMO, GRAD), sequence reads of *Andrena cineraria* dominated the results, with over 30% of the average reads in all three mock communities and replicates (Fig. 4). In the HETE and GRAD mock communities, *Bombus lapidarius* and *Dasygaster hirtipes* were both highly represented (*B. lapidarius*: 25% to 21% of the reads, *D. hirtipes*: 15% to 13%), but not in the HOMO mock community (*B. lapidarius*: 11%, *D. hirtipes*: 6%). The number of reads corresponding to the wild bee with the highest biomass among all specimens pooled in the mock communities (*Xylocopa violacea*) was neither particularly high in the HETE nor in the GRAD treatment, and it has considerably less reads than *A. cineraria*.

The results of the Kruskal-Wallis rank sum test and Wilcoxon rank sum test indicate the presence of significant differences in average read numbers per species only between the GRAD and the HOMO mock community at a 95% confidence level (Kruskal-Wallis $\chi^2(2) = 8.12$, $p = 0.017$; Wilcoxon rank sum test with Bonferroni correction $p < 0.05$ only for GRADxHOMO comparison). No significant differences in average read numbers per species were found between the HETE mock community and the two other treatments. Data is not normally distributed but homoscedastic (Shapiro-Wilk test: $W = 0.46$, $p = 2.597e^{-16}$, Levene’s Test: $F(2) = 0.004$, $p = 0.96$). Also, it is important to mention that nine morphospecies were represented by multiple MOTUs in the metabarcoding results, despite only one specimen being pooled in the mock community mixtures (Suppl. material 6): *A. carantonica*, *B. lapidarius*, *B. terrestris*, *C. afra*, *C. cunicularius*, *D. hirtipes*, *E. interrupta*, *H. tumulorum* and *O. bicornis*.

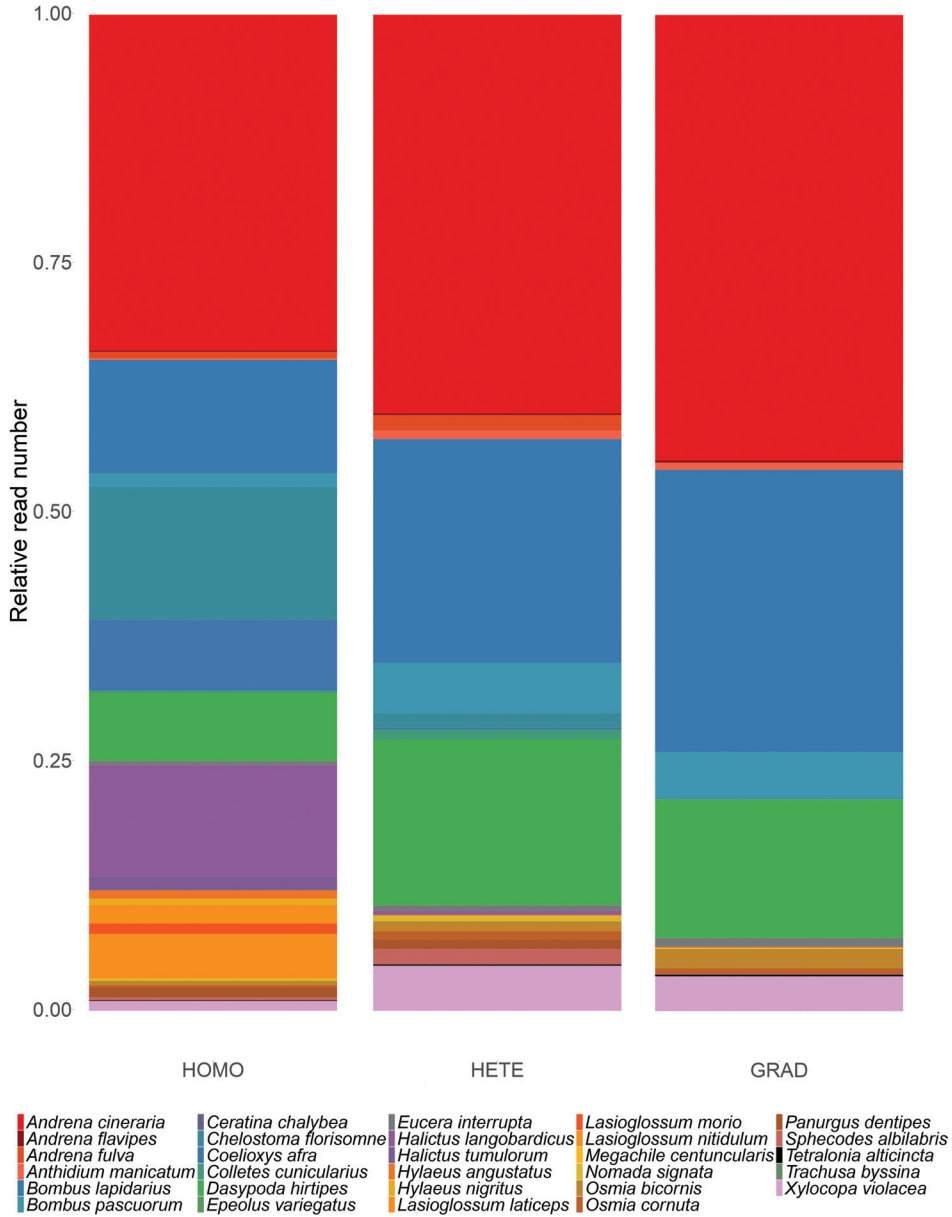


Figure 4. Proportion of sequencing reads per species in each mock community. Each community was assembled from the DNA of the same 29 specimens (25 fresh ones and 4 dry ones), all of them belonging to different species; the HOMO community was based on equimolar pools of the individual DNA extractions; the HETE community was assembled by pooling 1 ul of isolated DNA from a single leg from each specimen and the GRAD community was made by modifying the original concentrations of each species based on their concentration categories in order to exaggerate existing biomass differences. Relative read numbers were obtained by averaging absolute read numbers from all three replicates of each mock community and then correcting by the total number of reads in each treatment. A significant difference was found only between GRAD and HOMO (see text for details).

Non-Hymenoptera metazoan MOTUs found in the samples, such as *Parus major* and *Nephrotoma appendiculata*, are likely the result of contamination with organisms present in the field. The fungi and plant DNA found in the samples are also likely to be due to carry over from the field or rather contaminations with materials from other research groups at the laboratory of the MNHNL.

Discussion

Barcode coverage analysis

The availability of reference barcode sequences is a central requirement when evaluating the performance power of a DNA-based identification method for a certain taxonomic group, geographical region or environment (Weigand et al. 2019). The barcode coverage analysis here performed shows that missing barcodes are not a general limitation for DNA metabarcoding analysis of the local wild bee fauna of Luxembourg. In total, 338 morphospecies (97%) were represented by at least one COI barcode sequence in BOLD systems. Among them, 296 species are particularly well covered (>5 sequences available). However, these results only indicate the presence in the database of one or more COI sequences with over 196 bp of length for the target taxa, regardless of their specific location within the COI gene and prominent Folmer region. To properly evaluate the suitability of the proposed metabarcoding approach, the coverages of the selected target fragments had to be evaluated case-by-case. The coverage analyses of the target fragments of the three selected metabarcoding primer pairs shows that a full length fragment can only be expected for 68%–78% of the species, despite the primer pair combination. If species with partial coverage (>100 bp) are added to the primer pair-specific evaluations (“mini-barcodes”, Meusnier et al. 2008), over 85% of the wild bees currently described in Luxembourg have a reference in BOLD, regardless of which metabarcoding primer pair is used. Since PrimerMiner is only able to batch download publicly available sequences, the number of BOLD reference sequences might even be slightly higher when comparisons make use of the full database (incl. non-public records). Moreover, a few morphospecies were omitted by the automated metabarcoding pipeline due to i) alignment artifacts in Mesquite, ii) clustering of a morphospecies into multiple MOTUs with different taxonomic IDs (this was only the case for *N. striata*), and iii) an extreme difference between the original annotation of a MOTU consensus sequence and its BOLDigger re-identification. The latter problem may be partly related to limitations of the PrimerMiner algorithm generating the consensus sequences, which was primarily developed and is frequently used for MOTU consensus sequence construction at the taxonomic level of order and/or family.

Congruence of MOTUs with morphospecies

With the applied clustering threshold value of 3% sequence similarity, only 39% (132/338) of the evaluated wild bee species met the expectation of one MOTU per

morphospecies based on a Linnaean species delimitation concept. In 29% of the cases, a morphospecies split into multiple MOTUs, while in 9% of the cases sequences from multiple morphospecies lumped together. Additionally, 23% of the cases showed a variable combination of both effects, including multiple barcodes merging into mixed species MOTUs. For example, the COI barcodes downloaded for *Andrena bimaculata* split into two MOTUs. Three barcodes clustered together with *Andrena tibialis* in MOTU 203, while the remaining five formed a mixed species MOTU (MOTU 345). These deviations are in agreement with the incongruences described by Creedy et al. (2020) for the wild bee fauna of the United Kingdom. Their phylogenetic analyses suggested that these deviations could be due to closely related taxonomic groups and/or to the geographical range of available DNA barcodes (Creedy et al. 2020). The effect of this latter factor might be avoided by only considering DNA barcodes from local sources (Bergsten et al. 2012), which was not possible in our case but must be aimed at.

It is worth noticing that at least part of the splitting and lumping situation observed here is potentially the result of sequences uploaded under incorrect species annotation into BOLD. Outstanding examples can be found in the DNA barcode material of *Nomada striata*, which split into three MOTUs and then lumped with different morphospecies in each mixed MOTU (MOTU20: *N. ruficornis* and *N. fulvicornis*; MOTU259: *N. alboguttata*; MOTU310: *N. zonata*). Furthermore, the BOLD_BIN ABY7961 of *N. striata* not only includes annotated specimens of this species, but *N. villosa* (4 specimens) and *N. symphyti* (1) -two species so far not reported for Luxembourg (Cantú-Salazar et al. 2021; Herrera-Mesías and Weigand 2021) and hence not considered by us. A single specimen can be found in BOLD_BIN AAF3496, identified as *N. striata* but most likely corresponding to *N. zonata* based on their genetic data. Improved quality control of DNA barcode voucher material and its associated metadata is advisable to reduce potential noise in the database (Weigand et al. 2019). A well-curated regional database for the wild bee fauna of Luxembourg comprising a few but high-quality entries per species might help to overcome similar MOTU annotation problems in the future.

Pipeline evaluation and potential error sources

Even in cases when a reliable reference barcode library is available for the target taxa, primer bias can lead to false negatives and/or reduced detection rates (Elbrecht and Leese 2015). False negative results can also be generated when a low-biomass specimen is analyzed in parallel with high-biomass specimens or in a generally biomass-rich sample (Elbrecht and Leese 2015). Hence, it is of paramount importance to understand the effects of non-equal primer binding (amplification) efficiencies and variable biomass differences for the taxonomic groups under study. Our *in silico* evaluation of three metabarcoding primer pairs consistently identified the BF2/BR2 primer pair as the top performer for local wild bee assessment: over 85% of all MOTUs and morphospecies for which complete binding site sequence data was available are expected to efficiently amplify based on their simulated amplification success rates. However, deviations from these expectations set by the *in silico* analysis can potentially be found in laboratory set-

ups due to several factors. Even if primer-template mismatch has been experimentally shown to have a disproportionate effect over amplification success in mock communities (Piñol et al. 2015; Piñol et al. 2019), other factors such as annealing temperature, PCR cycle number or blocking oligonucleotide concentration can also affect species relative abundance in metabarcoding analyses (Piñol et al. 2015). Interestingly, species from genera predicted to present amplification troubles based on their mean penalty scores (i.e. *Anthophora*, *Eucera*, *Halictus*, *Melitta* and *Nomada*) correctly amplified in our mock communities and were easily detected among the pipeline results. Further laboratory experiments are needed to evaluate the actual amplification efficiency of the BF2/BR2 primer pair in potentially troubling wild bee taxa, thus to adjust expectations and uncover other potential factors affecting metabarcoding results.

COI metabarcoding approaches rely on degenerate primers such as BF2/BR2 to maximize taxon recovery, as this allows matching at variable binding sites and the amplification of as many (target) input sequences as possible (Linhart and Shamir 2002; Elbrecht et al. 2018). However, high degeneracy increases the chances of co-amplifying non-target sequences, potentially losing specificity (Linhart and Shamir 2002). Even if these non-target sequences (NUMTs, pseudogenes or parasitic/bacterial contaminants) may be bioinformatically filtered out, such procedure can reduce the recovery of target sequences (Elbrecht et al. 2018), affecting the overall detection capacity of the pipeline. Whenever possible, the susceptibility of specific degenerate primer combinations to this bias should be evaluated and taken into consideration for the experimental design, based on the taxa of interest. In the case of BF2/BR2, laboratory validations performed on invertebrate mock communities indicate that the amplification of non-target regions is minimal when this primer pair is used for insect taxa metabarcoding, with less than 0.5% of all resulting sequences deviating from the expected length (Elbrecht and Leese 2017b). However, conclusions regarding this aspect must be drawn carefully, as subsequent studies have also shown that the BF2 primer is also susceptible to primer slippage, which depending on the target taxa analyzed, may result in part of the amplicon sequences to be a few bp longer or shorter than expected (Elbrecht et al. 2018).

In principle, it must be highlighted that a highly degenerate primer pair can generally perform well in an *in silico* analysis, but might mal-perform *in vitro* due to the co-amplification of non-target taxa.

In our study, we tested the predictions of the *in silico* analysis by sequencing five distinct mock communities using our best performing primer pair (i.e. homogeneous, heterogeneous, gradient and two regular mock communities). The final detection rates of input species for the HOMO and HETE mock communities were the same (97%), while the detection rate of the GRAD mock community was considerably lower (72%). The missing species in the HOMO mock community (*T. byssina*, “L” category) likely represents an artifact, considering that a 7-year-old museum sample with unknown initial preservation conditions was used. This hypothesis is supported by the fact that the fresh specimen of *T. byssina* used for bulk extraction in the regular mock communities was found in all replicates. DNA degradation over time in insect museum samples is a well-known phenomenon and models have been developed to characterize

the level of molecular damage (Zimmermann et al. 2008). Therefore, metabarcoding projects working with preserved insect specimens (i.e. confirming the presence of a species from damaged historical samples to complete museum databases) should be aware of potential DNA damage that may bias their results. All missing species in the GRAD mock community correspond to bees from the “S” category. The samples in this category are bees from the genera *Halictus*, *Coelioxys*, *Hylaeus* and *Lasioglossum*. Originally, all of them had an overall pre-PCR DNA concentration between 4.5 and 1.2 ng/ul, but in the GRAD treatment, they were diluted in a proportion 1:100. This artificial concentration is often well below the expected DNA concentration of a full leg after isolation, even of the smallest Central European wild bee specimen. However, particularly specimen-rich bulk samples containing several *Bombus* spp. and honey bees may complicate the detection of a single small-sized bee species if it is represented by just a few specimens (e.g. *Lasioglossum* spp.), due to the magnitude of the difference between their template DNA compared to the total DNA of the sample.

Since a single specimen per species was pooled in our mock communities, the proportion of sequence reads per species should be similar in all experimental set-ups, unless error sources (i.e. primer mismatch, biomass bias, etc) were biasing the relative read abundances, favoring some taxonomic groups over others (Braukmann et al. 2019). Therefore, the differences observed in the proportion of sequences from each taxonomic group in the mock community supports that one or more error sources are affecting the results of the pipeline.

In all three main mock communities (HETE, HOMO, GRAD), 30% to 45% of all reads corresponded to *A. cineraria*, a species that has a considerable biomass (pre-PCR DNA concentration: 48.8 ng/ml, dry weight: 31.9 mg) and a very low primer-template mismatch (penalty score: 18.32). In the GRAD and HETE mock communities, biomass-rich species from the “L” category tended to have higher overall read numbers. However, no significant differences were found in detection rates or in read numbers per species among the HOMO and the HETE mock communities. Therefore, there is no evidence suggesting that correcting for biomass differences (e.g. size-sorting) has a significant effect in the general assessment outcome of our wild bee metabarcoding approach, at least under the conditions here proposed. Hence, isolating a single leg from each wild bee specimen should be sufficient for its detection in an average bulk sample under the described sequencing depth. Nevertheless, it is important to acknowledge that challenging bulk sample mixtures consisting of few small-sized taxa and an overabundance of large-sized bees might result in further problems not evaluated in this study.

In summary, the comparison between the results of the HETE and the HOMO mock communities suggest that the differences found in the proportion of read numbers per species are likely due to differential amplification resulting from primer bias. In the case of the GRAD community, the proportion of input species read numbers was not significantly different from the HETE mock community and the overall detection rate was only mildly affected. Overall, these results suggest that primer bias was the principal driver behind the unequal representation of species in the mock communities, with biomass differences only adding to the effect as a secondary factor.

Quantitative estimations from metabarcoding results: Is it possible?

The results found in the HETE mock community suggest a general trend of biomass-rich bee taxa to have higher read numbers. However, it is unlikely that this information can be used to retrieve accurate quantitative results regarding species biomass or specimen abundances. If PCR-based approaches are used in a metabarcoding set-up, the effect of differential amplification efficiency would make extremely difficult to estimate any of these parameters based on the final read numbers (Piñol et al. 2015, 2019; Elbrecht and Leese 2015). Numerical experiments done with computational simulations using insect datasets indicate that the capacity of providing quantitative estimates regarding the composition of the original sample will largely depend on the primer pair used for amplification and on the characteristics of the species community analyzed (Piñol et al. 2019). In the particular case of BF2/BR2, a significant correlation between pre- and post-PCR DNA concentrations has been reported for insect taxa, suggesting that it would be theoretically possible to quantify the initial abundance of each species in a bulk sample using customized equations, given that the species composition and number of primer-template mismatches are known (Piñol et al. 2019). However, the metabarcoding pipeline here developed should only be used for the qualitative assessment of wild bee fauna, at least until this hypothesis is experimentally tested and further data regarding quantitative estimations using the BF2/BR2 primer pair become publicly available.

Multiple MOTUs originating from single specimens

It is noteworthy that multiple MOTUs from the same species were found among the mock community metabarcoding results, despite a single specimen being used for the design. The presence of multiple MOTUs may have been caused by the effect of mitochondrial heteroplasmy or by nuclear copies of mtDNA (numts). The presence of multiple mitochondrial DNA haplotypes coexisting in a single organism remains a potential problem for the use of DNA (meta)barcoding as a molecular taxonomic tool (Rubinoff et al. 2006). Even if maternal mitochondrial DNA inheritance is considered the general rule for eukaryotes, it has been observed that paternal mtDNA transfer can happen during polyspermic fertilization in honeybees, a fraction of which is partially retained in later developmental stages (Meusel and Moritz 1993). In the case of wild bees, high proportions of heteroplasmic species have been described for Hawaiian *Hylaeus* spp. (Magnacca and Brown 2010), indicating that mtDNA heteroplasmy can occur in wild bees and that it might be more common than originally thought. To the best of our knowledge, this is the only study suggesting heteroplasmy in wild bees and further research would be needed to confirm its findings, especially as it can be difficult to distinguish heteroplasmy from the presence of highly similar NUMTS. In our mock communities, three MOTUs (separated by 3% sequence divergence) originated from a single *Dasygaster hirtipes* female, showing a sequence similarity of 100%, 99.49% and 99.45% with their best BOLD matches. This high sequence similarity and the

congruent detection of those MOTUs in all three replicates of every mock community excludes PCR and sequencing errors as the primary source for the anomaly.

Alternatively, these peculiarities in the dataset may be explained by nuclear mitochondrial DNA (NUMT) sequences. NUMTs are the result of non-translated and non-transcribed regions from the mitochondrial DNA transferred to the nuclear genome, which can be amplified if effective primer binding sites are still existing (Cristiano et al. 2012). This causes the amplification of non-functional nuclear copies of COI together with real mitochondrial DNA, producing a mix of copies that will result in several MOTUs originating from the same specimen (Cristiano et al. 2012). Molecular phylogenetic analysis in an extended dataset including the species here described might be useful to search for evidence of potential COI-like NUMTs in the target taxa. Sample contamination as an explanation for this anomaly (e.g. environmental DNA carry over) seems very improbable, as this would have also likely introduced new species and not only inflated the number of MOTUs of species already present in the mock communities.

Further studies should determine the presence and the potential impact of heteroplasmy and NUMTs in the effectiveness of barcoding identification of potentially heteroplasmic wild bees of both sexes, as well as the impact of multiple MOTUs originating from single specimens on diversity estimates.

Conclusion

The *in silico* and *in vitro* analyses highlight the influence of primer bias on the performance of the proposed metabarcoding approach. However, it is possible to reduce its effect by selecting the most suitable primer combinations for the taxa of interest. This can be achieved by comparing the *in silico* amplification efficiency of primer pair candidates and then experimentally testing the capacity of the best performing pairs in the laboratory. Among the metabarcoding primer pairs here evaluated, no combination can be expected to correctly amplify all wild bee taxa and some genera in particular are predicted to be prone to amplification problems, ultimately translating into a higher probability of producing false negatives. Therefore, primers have to be evaluated on a case-by-case basis against the target taxa at hand. Nevertheless, from the combinations available, the highly degenerate primer pair BF2/BR2 provided the best results for our regional wild bee fauna, with over 85% of available MOTUs and morphospecies expected to correctly amplify when this primer pair is used. Our experimental set-ups support these results as over 97% of the species were retrieved from four out of five mock community trials using the metabarcoding approach that incorporates this primer pair.

A deficiency of DNA barcodes in the public reference library BOLD does not seem to be a major error source for the identification of the regional wild bee species using molecular taxonomic tools. In total, 97% of the currently known morphospecies in Luxembourg present at least one barcode in BOLD, and 85% of them can be considered well covered. However, for the ~30% of the taxa whose identification might be

obscured due to lumping with other wild bee species, the definition of potentially diagnostic barcodes or a multi-marker DNA metabarcoding approach (i.e. incorporating nuclear markers) may be considered as alternative strategies to discriminate lumped species. Finally, new sampling campaigns and collection revisions are likely to provide material to fill the few remaining gaps in the database, as well as to produce barcodes originating from regional specimens.

The results of the mock community experiments indicate that the overall output of the metabarcoding pipeline is expected to be robust, despite biomass differences among the wild bee specimens. Even if these biomass differences affect the number of reads per taxonomic group, the detection rates of input species (i.e. taxalists) remained stable, with the exception of the gradient treatment. Biomass-related bias is likely to have a higher impact under more extreme scenarios, where the size difference of the pooled specimens is higher (e.g. in Malaise traps). Moreover, due to the small numbers of specimens included in this analysis, a higher effect of this type of bias in bulk samples combining numerous biomass-rich specimens and few biomass-low ones cannot be ruled out. However, strategies can be used to compensate for this issue under reasonable conditions. In general, processing separately the fraction of smallest wild bee specimens in a sample should provide an appropriate countermeasure to avoid false negative results due to biomass differences, especially for genera with negative primer bias (e.g. *Nomada* spp.). Moreover, as the proposed metabarcoding pipeline only uses one leg for bulk extraction, the voucher specimens can be traced back for complementary analysis with Sanger sequencing or traditional morphotaxonomy, thus to provide identifications validated by multiple approaches.

Even if only a few specimens were used here to set up the mock community trial, the layout of the metabarcoding pipeline in this study can be used to analyze much larger samples. Sequencing costs for a HTS run on an Illumina platform remain stable independently of how many individuals are included in each bulk sample, and the BF2/BR2 tagging primer combinations allow the tagging of up to 288 samples within the same run (Elbrecht and Steinke 2019). Therefore, the current metabarcoding approach can potentially be used to analyze hundreds of bulk samples containing several dozens of wild bees on a single run without incurring in substantial modifications to the workflow or significantly higher costs.

Overall, our customized metabarcoding pipeline represents a promising alternative taxonomic identification tool to analyze large numbers of wild bees in the context of local conservation biology initiatives. As such, the further improvement of this technique would benefit projects dealing with many specimens to be swiftly analyzed, as well as restricted time frames and limited access to taxonomic specialists.

Acknowledgements

We thank Joana Margarida Teixeira Lopes, Claude Kolwelter and Dylan Thissen for their help during the wild bee fieldwork in 2019, as well as Sophie Ogan for providing the samples from the Rhineland-Palatinate state used in this work. Nico Schneider is ac-

knowledge for his feedback on the taxonomic identification of wild bees and Gerhard Haszprunar for his collaboration. We would also like to thank Rashi Halder from the Luxembourg Centre for Systems Biomedicine in Belval for her work on the high-throughput sequencing of the library and the Aquatic Ecosystem Research Group of the University of Duisburg-Essen for their help with the bioinformatic analysis. We also thank the Zoology department at the Musée national d'histoire naturelle Luxembourg (MNHNL), especially Amanda Luttringer and Stéphanie Lippert for their useful comments on the manuscript.

Finally, we would also like to thank Christophe Praz for the constructive feedback during the revision of this manuscript. Financial support was received under the Bauer and Stemmler foundations programme "FORSCHUNGSGEIST! Next Generation Sequencing in der Oekosystemforschung". Collection permit was issued by the Ministère de l'Environnement, du Climat et du Développement durable (MECDD) Luxembourg.

References

- Alberdi A, Aizpurua O, Gilbert MTP, Bohmann K (2018) Scrutinizing key steps for reliable metabarcoding of environmental samples. *Methods in Ecology and Evolution* 9(1): 134–147. <https://doi.org/10.1111/2041-210X.12849>
- Amiet F, Herrmann M, Müller A, Neumeyer R (2007) *Fauna Helvetica* 20: Apidae 5: *Ammobates*, *Ammobatooides*, *Anthophora*, *Blastes*, *Ceratina*, *Dasygaster*, *Epeoloides*, *Epeolus*, *Eucera*, *Macropis*, *Melecta*, *Melitta*, *Nomada*, *Pasites*, *Tetralonia*, *Thyreus*, *Xylocopa*. Centre suisse de cartographie de la Faune, Neuchâtel, Switzerland, 356 pp.
- Amiet F, Herrmann M, Müller A, Neumeyer R (2004) *Fauna Helvetica* 9. Apidae 4: *Anthidium*, *Chelostoma*, *Coelioxys*, *Dioxys*, *Heriades*, *Lithurgus*, *Megachile*, *Osmia*, *Stelis*. Centre Suisse de Cartographie de la Faune, Neuchâtel, Switzerland, 273 pp.
- Amiet F, Herrmann M, Müller A, Neumeyer R (2001) *Fauna Helvetica* 9. Apidae 3: *Lasioglossum*, *Halictus*. Centre Suisse de Cartographie de la Faune, Neuchâtel, Switzerland. 208 pp.
- Amiet F, Müller A, Neumeyer R (1999) *Fauna Helvetica* 9. Apidae 2 : *Colletes*, *Dufourea*, *Hylaeus*, *Nomia*, *Nomioides*, *Rhophitoides*, *Rophites*, *Sphcodes*, *Systropha*. Centre Suisse de Cartographie de la Faune, Neuchâtel, Switzerland, 219 pp.
- Bergsten J, Bilton DT, Fujisawa T, Elliott M, Monaghan MT, Balke M, Vogler AP (2012) The effect of geographical scale of sampling on DNA barcoding. *Systematic Biology* 61(5): 851–869. <https://doi.org/10.1093/sysbio/sys037>
- Biesmeijer JC, Roberts SP, Reemer M, Ohlemüller R, Edwards M, Peeters T, Settele J (2006) Parallel declines in pollinators and insect-pollinated plants in Britain and the Netherlands. *Science* 313(5785): 351–354. <https://doi.org/10.1126/science.1127863>
- Brandon-Mong GJ, Gan HM, Sing KW, Lee PS, Lim PE, Wilson JJ (2015) DNA metabarcoding of insects and allies: an evaluation of primers and pipelines. *Bulletin of Entomological Research* 105(6): 717–727. <https://doi.org/10.1017/S0007485315000681>
- Braukmann TW, Ivanova NV, Prosser SW, Elbrecht V, Steinke D, Ratnasingham S, Hebert PD (2019) Metabarcoding a diverse arthropod mock community. *Molecular Ecology Resources* 19(3): 711–727. <https://doi.org/10.1111/1755-0998.13008>

- Brown MJ, Paxton RJ (2009) The conservation of bees: a global perspective. *Apidologie* 40(3): 410–416. <https://doi.org/10.1051/apido/2009019>
- Buchner D, Leese F (2020) BOLDigger - a Python package to identify and organise sequences with the Barcode of Life Data systems. *Metabarcoding and Metagenomics* 4: 19–21. <https://doi.org/10.3897/mbmg.4.53535>
- Cane JH, Sipes S (2006) Characterizing floral specialization by bees: analytical methods and a revised lexicon for oligolecty. *Plant-Pollinator Interactions: From Specialization To Generalization* 99: 122.
- Cantú-Salazar L, Vray S, L'Hoste L, Jakubzik A, Herrera-Mesías F (2021) An addition to the list of wild bee fauna of Luxembourg: *Nomada kohli* Schmiedeknecht, 1882 (Hymenoptera, Apidae), with a list of the species of the genus *Nomada* Scopoli, 1770 recorded in the country. *Bulletin de la Société des Naturalistes Luxembourgeois* 123: 195–204.
- Clarke LJ, Soubrier J, Weyrich LS, Cooper A (2014) Environmental metabarcodes for insects: in silico PCR reveals potential for taxonomic bias. *Molecular Ecology Resources* 14(6): 1160–1170. <https://doi.org/10.1051/apido/2009019>
- Creedy TJ, Norman H, Tang CQ, Qing Chin K, Andujar C, Arribas P, Vogler AP (2020) A validated workflow for rapid taxonomic assignment and monitoring of a national fauna of bees (Apiformes) using high throughput DNA barcoding. *Molecular Ecology Resources* 20(1): 40–53. <https://doi.org/10.1111/1755-0998.13056>
- Cristiano MP, Fernandes-Salomão TM, Yotoko KS (2012) Nuclear mitochondrial DNA: an Achilles' heel of molecular systematics, phylogenetics, and phylogeographic studies of stingless bees. *Apidologie* 43(5): 527–538. <https://doi.org/10.1007/s13592-012-0122-4>
- Dirzo R, Young HS, Galetti M, Ceballos G, Isaac NJ, Collen B (2014) Defaunation in the Anthropocene. *Science* 345(6195): 401–406. <https://doi.org/10.1126/science.1251817>
- Dogterom MH, Matteoni JA, Plowright RC (1998) Pollination of greenhouse tomatoes by the North American *Bombus vosnesenskii* (Hymenoptera: Apidae). *Journal of Economic Entomology* 91(1): 71–75. <https://doi.org/10.1093/jee/91.1.71>
- Edgar RC, Flyvbjerg H (2015) Error filtering, pair assembly and error correction for next-generation sequencing reads. *Bioinformatics* 31(21): 3476–3482. <https://doi.org/10.1093/bioinformatics/btv401>
- Elbrecht V, Leese F (2017a) PrimerMiner: an R package for development and in silico validation of DNA metabarcoding primers. *Methods in Ecology and Evolution* 8(5): 622–626. <https://doi.org/10.1111/2041-210X.12687>
- Elbrecht V, Leese F (2017b) Validation and development of COI metabarcoding primers for freshwater macroinvertebrate bioassessment. *Frontiers in Environmental Science* 5: 11. <https://doi.org/10.3389/fenvs.2017.00011>
- Elbrecht V, Leese F (2015) Can DNA-based ecosystem assessments quantify species abundance? Testing primer bias and biomass-sequence relationships with an innovative metabarcoding protocol. *PLoS ONE* 10(7): 0130324. <https://doi.org/10.1371/journal.pone.0130324>
- Elbrecht V, Hebert PDN, Steinke D (2018) Slippage of degenerate primers can cause variation in amplicon length. *Scientific Reports* 8: 10999. <https://doi.org/10.1038/s41598-018-29364-z>
- Elbrecht V, Steinke D (2019) Scaling up DNA metabarcoding for freshwater macrozoobenthos monitoring. *Freshwater Biology* 64(2): 380–387. <https://doi.org/10.7287/peerj.preprints.3456v5>

- Elbrecht V, Vamos EE, Steinke D, Leese F (2018) Estimating intraspecific genetic diversity from community DNA metabarcoding data. *PeerJ* 6: e4644. <https://doi.org/10.7717/peerj.4644>
- Falk SJ (2015) Field guide to the bees of Great Britain and Ireland. Bloomsbury, London.
- Folmer O, Black M, Hoeh W, Lutz R, Vrijenhoek R (1994) DNA primers for amplification of mitochondrial cytochrome c oxidase subunit I from diverse metazoan invertebrates. *Molecular Marine Biology and Biotechnology* 3: 294–299.
- Fox J, Weisberg S, Adler D, Bates D, Baud-Bovy G, Ellison S, Graves S (2016) R. Package ‘car’. Companion to applied regression. R Package version 2-1.
- Goulson D, Lye GC, Darvill B (2008) Decline and conservation of bumble bees. *Annual Review of Entomology* 53: 191–208. <https://doi.org/10.1146/annurev.ento.53.103106.093454>
- Gueuning M, Blaser GD, Albrecht SM, Knop E, Praz C, Frey JE (2019) Evaluating next-generation sequencing (NGS) methods for routine monitoring of wild bees: Metabarcoding, mitogenomics or NGS barcoding. *Molecular Ecology Resources* 19(4): 847–862. <https://doi.org/10.1111/1755-0998.13013>
- Hebert PD, Penton EH, Burns JM, Janzen DH, Hallwachs W (2004) Ten species in one: DNA barcoding reveals cryptic species in the neotropical skipper butterfly *Astraptes fulgerator*. *Proceedings of the National Academy of Sciences* 101(41): 14812–14817. <https://doi.org/10.1073/pnas.0406166101>
- Herrera-Mesías F, Weigand AM (2021) Updates to the checklist of the wild bee fauna of Luxembourg as inferred from revised natural history collection data and fieldwork. *Biodiversity Data Journal* 9: e64027. <https://doi.org/10.3897/BDJ.9.e64027>
- Hallmann CA, Sorg M, Jongejans E, Siepel H, Hofland N, Schwan H, Goulson D (2017) More than 75 percent decline over 27 years in total flying insect biomass in protected areas. *PLoS ONE*, 12(10): e0185809. <https://doi.org/10.1371/journal.pone.0185809>
- Hausmann A, Segerer AH, Greifenstein T, Knubben J, Morinière J, Bozicevic V, Habel JC (2020) Toward a standardized quantitative and qualitative insect monitoring scheme. *Ecology and Evolution* 10(9): 4009–4020.
- Hopkins GW, Freckleton RP (2002) Declines in the numbers of amateur and professional taxonomists: implications for conservation. In *Animal Conservation Forum*. Cambridge University Press 5(3): 245–249. <https://doi.org/10.1017/S1367943002002299>
- Katoh K, Misawa K, Kuma KI, Miyata T (2002) MAFFT: a novel method for rapid multiple sequence alignment based on fast Fourier transform. *Nucleic Acids Research* 30(14): 3059–3066. <https://doi.org/10.1093/nar/gkf436>
- Klein AM, Vaissière BE, Cane JH, Steffan-Dewenter I, Cunningham SA, Kremen C, Tscharntke T (2007) Importance of pollinators in changing landscapes for world crops. *Proceedings of the Royal Society B: Biological Sciences* 274: 303–313. <https://doi.org/10.1098/rspb.2006.3721>
- Leese F, Bouchez A, Abarenkov K, Altermatt F, Borja A, Bruce K, Ekrem T, Čiampor F, Čiamporová-Zaťovičová Z, Costa F, Duarte S, Elbrecht V, Fontaneto D, Franc A, Geiger M, Hering D, Kahlert M, Stroil BK, Kelly M, Keskin E, Liška I, Mergen P, Meissner K, Pawłowski J, Penev L, Reyjol Y, Rotter A, Steinke D, Wal B, Vitecek S, Zimmermann J, Weigand AM (2018) Why we need sustainable networks bridging countries, disciplines, cultures and generations for aquatic biomonitoring 2.0: a perspective derived from the

- DNAqua-Net COST action. *Advances in Ecological Research* 58: 63–99. <https://doi.org/10.1016/bs.aecr.2018.01.001>
- Leray M, Yang JY, Meyer CP, Mills SC, Agudelo N, Ranwez V, Boehm JT, Machida RJ (2013) A new versatile primer set targeting a short fragment of the mitochondrial COI region for metabarcoding metazoan diversity: Application for characterizing coral reef fish gut contents. *Frontiers in Zoology* 10: 34. <https://doi.org/10.1186/1742-9994-10-34>
- Linhart C, Shamir R (2002) The degenerate primer design problem. *Bioinformatics* 18: S172–S181. https://doi.org/10.1093/bioinformatics/18.suppl_1.S172
- Losey JE, Vaughan M (2006) The economic value of ecological services provided by insects. *Bioscience* 56(4): 311–323. https://doi.org/10.1093/bioinformatics/18.suppl_1.S172
- Macher TH, Beerermann AJ, Leese F (2021) TaxonTableTools: A comprehensive, platform-independent graphical user interface software to explore and visualise DNA metabarcoding data. *Molecular Ecology Resources* 21(5): 1705–1714. <https://doi.org/10.1111/1755-0998.13358>
- Maddison WP, Maddison DR (2019) Mesquite: a modular system for evolutionary analysis. Version 3.61 <http://www.mesquiteproject.org>
- Magnacca KN, Brown MJ (2010) Mitochondrial heteroplasmy and DNA barcoding in Hawaiian *Hylaeus* (*Nesoprosopis*) bees (Hymenoptera: Colletidae). *BMC Evolutionary Biology* 10(1): 174. <https://doi.org/10.1186/1471-2148-10-174>
- Mangiafico S, Mangiafico MS (2017) Package ‘rcompanion’. *Cran Repos* 20: 1–71.
- Marquina D, Andersson AF, Ronquist F (2019) New mitochondrial primers for metabarcoding of insects, designed and evaluated using in silico methods. *Molecular Ecology Resources* 19(1): 90–104.
- Martin M (2011) Cutadapt removes adapter sequences from high-throughput sequencing reads. *EMBnet Journal* 17(1): 10–12. <https://doi.org/10.14806/ej.17.1.200>
- Meusel MS, Moritz RF (1993) Transfer of paternal mitochondrial DNA during fertilization of honeybee (*Apis mellifera* L.) eggs. *Current Genetics* 24(6): 539–543. <https://doi.org/10.1007/BF00351719>
- Meusnier I, Singer GA, Landry JF, Hickey DA, Hebert PD, Hajibabaei M (2008) A universal DNA mini-barcode for biodiversity analysis. *BMC Genomics* 9(1): 214. <https://doi.org/10.1186/1471-2164-9-214>
- Michener CD (2007) *Bees of the World*. 2nd Edn. Johns Hopkins University press. Baltimore, MD.
- Nieto A, Roberts SPM, Kemp J, Rasmont P, Kuhlmann M, García Criado M, Biesmeijer JC, Bogusch P, Dathe HH, De la Rúa P, De Meulemeester T, Dehon M, Dewulf A, Ortiz-Sánchez FJ, Lhomme P, Pauly A, Potts SG, Praz CQ, Window J, Michez D (2014) IUCN Global Species Programm European Red List of Bees, 1–98. <https://doi.org/10.2779/77003>
- Piñol J, Senar MA, Symondson WO (2019) The choice of universal primers and the characteristics of the species mixture determine when DNA metabarcoding can be quantitative. *Molecular Ecology* 28(2): 407–419. <https://doi.org/10.1111/mec.14776>
- Piñol J, Mir G, Gomez-Polo P, Agustí N (2015) Universal and blocking primer mismatches limit the use of high-throughput DNA sequencing for the quantitative metabarcoding of arthropods. *Molecular Ecology Resources* 15(4): 819–830. <https://doi.org/10.1111/1755-0998.12355>

- Piper AM, Batovska J, Cogan NO, Weiss J, Cunningham JP, Rodoni BC, Blacket MJ (2019) Prospects and challenges of implementing DNA metabarcoding for high-throughput insect surveillance. *GigaScience* 8(8): giz092. <https://doi.org/10.1093/gigascience/giz092>
- Potts SG, Biesmeijer JC, Kremen C, Neumann P, Schweiger O, Kunin WE (2010a) Global pollinator declines: trends, impacts and drivers. *Trends in Ecology and Evolution* 25(6): 345–353. <https://doi.org/10.1016/j.tree.2010.01.007>
- Potts SG, Roberts SP, Dean R, Marris G, Brown MA, Jones R, Settele J (2010b) Declines of managed honey bees and beekeepers in Europe. *Journal of Apicultural Research* 49(1): 15–22. <https://doi.org/10.3896/IBRA.1.49.1.02>
- R Core Team (2019) R: A language and environment for statistical computing. R Foundation for Statistical Computing, Vienna, Austria. <https://www.R-project.org/>
- Rafferty NE (2017) Effects of global change on insect pollinators: multiple drivers lead to novel communities. *Current Opinion in Insect Science* 23: 22–27. <https://doi.org/10.1016/j.cois.2017.06.009>
- Rasmont P, Genoud D, Gadoum S, Aubert M, Dufrene E, Le Goff G, Gilles Mahe G, Michez D, Pauly A (2017) Hymenoptera Apoidea Gallica: liste des abeilles sauvages de Belgique, France, Luxembourg et Suisse. Edition Atlas Hymenoptera, Université de Mons, Mons, Belgium.
- Rasmont P, Mersch P (1988) Première estimation de la dérive faunique chez les bourdons de la Belgique (Hymenoptera: Apidae). In *Annales de la Société Royale zoologique de Belgique* 118(2): 141–147.
- Ratnasingham S, Hebert PD (2007) BOLD: The Barcode of Life Data System (<http://www.barcodinglife.org>). *Molecular Ecology Notes* 7(3): 355–364. <https://doi.org/10.1111/j.1471-8286.2007.01678.x>
- Rognes T, Flouri T, Nichols B, Quince C, Mahé F (2016) VSEARCH: a versatile open source tool for metagenomics. *PeerJ* 4: e2584. <https://doi.org/10.7717/peerj.2584>
- Rubinoff D, Cameron S, Will K (2006) A genomic perspective on the shortcomings of mitochondrial DNA for “barcoding” identification. *Journal of Heredity* 97(6): 581–594. <https://doi.org/10.1093/jhered/esl036>
- Scheuchl E (2006) *Illustrierte Bestimmungstabellen der Wildbienen Deutschlands und Österreichs*. Apollo books, 192 pp.
- Schmidt S, Schmid-Egger C, Morinière J, Haszprunar G, Hebert PD (2015) DNA barcoding largely supports 250 years of classical taxonomy: identifications for Central European bees (Hymenoptera, *Apoidea partim*). *Molecular Ecology Resources* 15(4): 985–1000. <https://doi.org/10.1111/1755-0998.12363>
- Schneider N (2018) Recension ouvrage: Découvrir and protéger nos abeilles sauvages. *Bulletin de la Société des Naturalistes Luxembourgeois* 120: 163–164.
- Taberlet P, Coissac E, Pompanon F, Brochmann C, Willerslev E (2012) Towards next-generation biodiversity assessment using DNA metabarcoding. *Molecular Ecology* 21: 2045–2050. <https://doi.org/10.1111/j.1365-294X.2012.05470.x>
- van der Loos LM, Nijland R (2021) Biases in bulk: DNA metabarcoding of marine communities and the methodology involved. *Molecular Ecology* 30(13): 3270–3288. <https://doi.org/10.1111/mec.15592>
- Vereecken N (2018) *Découvrir and protéger nos abeilles sauvages*. Glénat.

- Wägele H, Klussmann-Kolb A, Kuhlmann M, Haszprunar G, Lindberg D, Koch A, Wägele JW (2011) The taxonomist-an endangered race. A practical proposal for its survival. *Frontiers in Zoology* 8(1): 25. <https://doi.org/10.1186/1742-9994-8-25>
- Weigand AM, Herrera-Mesías F (2020) First record of the wild bee *Eucera (Tetralonia) alticincta* (Lepeletier, 1841) in Luxembourg. *Bulletin de la Société des Naturalistes Luxembourgeois* 122: 141–146.
- Weigand AM, Desquiotz N, Weigand H, Szucsich N (2021) Application of propylene glycol in DNA-based studies of invertebrates. *Metabarcoding and Metagenomics* 5: e57278. <https://doi.org/10.3897/mbmg.5.57278>
- Weigand H, Beermann AJ, Čiampor F, Costa FO, Csabai Z, Duarte S, Ekrem T (2019) DNA barcode reference libraries for the monitoring of aquatic biota in Europe: Gap-analysis and recommendations for future work. *Science of the Total Environment* 678: 499–524. <https://doi.org/10.1016/j.scitotenv.2019.04.247>
- Weigand AM, Macher JN (2018) A DNA metabarcoding protocol for hyporheic freshwater meiofauna: Evaluating highly degenerate COI primers and replication strategy. *Metabarcoding and Metagenomics* 2: e26869. <https://doi.org/10.3897/mbmg.2.26869>
- Westrich P, Frommer U, Mandery K, Riemann H, Ruhnke H, Saure C, Voith J (2011) Rote Liste und Gesamtartenliste der Bienen (Hymenoptera, Apidae) Deutschlands (5. Fassung, Dezember 2011) [Red List and complete species list of bees in Germany]. Bundesamt für Naturschutz (Ed.) Rote Liste der gefährdeten Tiere, Pflanzen und Pilze Deutschlands. Band 3: Wirbellose Tiere (Teil 1) [Red List of threatened animals, plants and fungi of Germany], 371–416.
- Zimmermann J, Hajibabaei M, Blackburn DC, Hanken J, Cantin E, Posfai J, Evans TC (2008) DNA damage in preserved specimens and tissue samples: a molecular assessment. *Frontiers in Zoology* 5(1): 18. <https://doi.org/10.1186/1742-9994-5-18>
- Zinger L, Bonin A, Alsos IG, Bálint M, Bik H, Boyer F, De Barba M (2019) DNA metabarcoding—Need for robust experimental designs to draw sound ecological conclusions. *Molecular ecology* 28(8): 1857–1862. <https://doi.org/10.1111/mec.15060>

Supplementary material I

***In silico* penalty scores, barcode coverage and congruency analysis of the wild bee species of Luxembourg**

Authors: Fernanda Herrera-Mesías, Imen Kharrat Ep Jarboui, Alexander M. Weigand
Data type: tables (excel file)

Explanation note: *In silico* scores, barcode coverage and species delimitation congruence of the 349 wild bee species from Luxembourg evaluated in this study.

Copyright notice: This dataset is made available under the Open Database License (<http://opendatacommons.org/licenses/odbl/1.0/>). The Open Database License (ODbL) is a license agreement intended to allow users to freely share, modify, and use this Dataset while maintaining this same freedom for others, provided that the original source and author(s) are credited.

Link: <https://doi.org/10.3897/jhr.94.84617.suppl1>

Supplementary material 2

Mean wild bee genus penalty scores sorted by primer pair

Authors: Fernanda Herrera-Mesías, Imen Kharrat Ep Jarboui, Alexander M. Weigand

Data type: table (excel file)

Explanation note: Mean *in silico* penalty score and transformed mean penalty score (T-Score) within each wild bee genus considered in this study. Number of MOTUs used as weights in the ANOVA analysis are also given.

Copyright notice: This dataset is made available under the Open Database License (<http://opendatacommons.org/licenses/odbl/1.0/>). The Open Database License (ODbL) is a license agreement intended to allow users to freely share, modify, and use this Dataset while maintaining this same freedom for others, provided that the original source and author(s) are credited.

Link: <https://doi.org/10.3897/jhr.94.84617.suppl2>

Supplementary material 3

Summary and metadata of the wild bee samples from Luxembourg and Germany used in the mock communities

Authors: Fernanda Herrera-Mesías, Imen Kharrat Ep Jarboui, Alexander M. Weigand

Data type: table (excel file)

Explanation note: Information sheet regarding the wild bee specimens used in the mock communities. Morphological identification, molecular identification, % of identity with their best BOLD match, concentration category and set-up in which they were used are included.

Copyright notice: This dataset is made available under the Open Database License (<http://opendatacommons.org/licenses/odbl/1.0/>). The Open Database License (ODbL) is a license agreement intended to allow users to freely share, modify, and use this Dataset while maintaining this same freedom for others, provided that the original source and author(s) are credited.

Link: <https://doi.org/10.3897/jhr.94.84617.suppl3>

Supplementary material 4

Tagged primer combinations used in the mock community experiment

Authors: Fernanda Herrera-Mesías, Imen Kharrat Ep Jarboui, Alexander M. Weigand

Data type: table (excel file)

Explanation note: Primer tags. Combinations from Elbrecht V, Leese F (2017) Validation and development of COI metabarcoding primers for freshwater macroinvertebrate bioassessment. *Frontiers in Environmental Science* 5: 11. Specifications about the tag combinations used in each mock community replicate are also given.

Copyright notice: This dataset is made available under the Open Database License (<http://opendatacommons.org/licenses/odbl/1.0/>). The Open Database License (ODbL) is a license agreement intended to allow users to freely share, modify, and use this Dataset while maintaining this same freedom for others, provided that the original source and author(s) are credited.

Link: <https://doi.org/10.3897/jhr.94.84617.suppl4>

Supplementary material 5

Overview of MOTU data per mock community

Authors: Fernanda Herrera-Mesías, Imen Kharrat Ep Jarboui, Alexander M. Weigand

Data type: table (excel file)

Explanation note: Number of reads per MOTU found in each mock community after applying the 0.01% filters. Includes non Hymenoptera MOTUs.

Copyright notice: This dataset is made available under the Open Database License (<http://opendatacommons.org/licenses/odbl/1.0/>). The Open Database License (ODbL) is a license agreement intended to allow users to freely share, modify, and use this Dataset while maintaining this same freedom for others, provided that the original source and author(s) are credited.

Link: <https://doi.org/10.3897/jhr.94.84617.suppl5>

Supplementary material 6

Mock community metabarcoding results

Authors: Fernanda Herrera-Mesías, Imen Kharrat Ep Jarboui, Alexander M. Weigand

Data type: table (excel file)

Explanation note: Sequencing results of the three PCR replicates of each mock community. Only Hymenoptera MOTUs identified to species level are considered. Number of input species detected in each set-up is also given.

Copyright notice: This dataset is made available under the Open Database License (<http://opendatacommons.org/licenses/odbl/1.0/>). The Open Database License (ODbL) is a license agreement intended to allow users to freely share, modify, and use this Dataset while maintaining this same freedom for others, provided that the original source and author(s) are credited.

Link: <https://doi.org/10.3897/jhr.94.84617.suppl6>

Supplementary material 7

Species delimitation congruence, comparing Linnaean species assignment of the original sequences retrieved from BOLD v/s results of MOTU clustering

Authors: Fernanda Herrera-Mesías, Imen Kharrat Ep Jarboui, Alexander M. Weigand

Data type: Image (JPG file)

Explanation note: The number of species presenting incongruent clustering and the type of anomaly is shown in each case. Cases in which the incongruence may be due to sequences uploaded under incorrect species names in the database are shown in light gray.

Copyright notice: This dataset is made available under the Open Database License (<http://opendatacommons.org/licenses/odbl/1.0/>). The Open Database License (ODbL) is a license agreement intended to allow users to freely share, modify, and use this Dataset while maintaining this same freedom for others, provided that the original source and author(s) are credited.

Link: <https://doi.org/10.3897/jhr.94.84617.suppl7>

Supplementary material 8

***In silico* primer performance evaluation using PrimerMiner with MOTU data sorted by wild bee genus**

Authors: Fernanda Herrera-Mesías, Imen Kharrat Ep Jarboui, Alexander M. Weigand

Data type: Image (JPG file)

Explanation note: Amplification success rates are shown for each genus (dark yellow areas = successful cases with a penalty score below 100; light yellow areas = failed cases, khaki colored areas = missing information). Missing data was excluded from calculations. Mean amplification success rates based on the whole dataset are indicated at the bottom.

Copyright notice: This dataset is made available under the Open Database License (<http://opendatacommons.org/licenses/odbl/1.0/>). The Open Database License (ODbL) is a license agreement intended to allow users to freely share, modify, and use this Dataset while maintaining this same freedom for others, provided that the original source and author(s) are credited.

Link: <https://doi.org/10.3897/jhr.94.84617.suppl8>

Supplementary material 9

Primer pair amplification success rates based on Linnaean species

Authors: Fernanda Herrera-Mesías, Imen Kharrat Ep Jarboui, Alexander M. Weigand

Data type: Image (JPG file)

Explanation note: Squares correspond to distinct morphospecies. Dark yellow areas represent species with a penalty score below 100, light yellow areas represent species above the threshold and striped squares represent cases of discrepancy (i.e. having MOTUs in both categories). Only sequences with full length target regions were considered.

Copyright notice: This dataset is made available under the Open Database License (<http://opendatacommons.org/licenses/odbl/1.0/>). The Open Database License (ODbL) is a license agreement intended to allow users to freely share, modify, and use this Dataset while maintaining this same freedom for others, provided that the original source and author(s) are credited.

Link: <https://doi.org/10.3897/jhr.94.84617.suppl9>

Integrative approach resolves the taxonomy of *Eulaema cingulata* (Hymenoptera, Apidae), an important pollinator in the Neotropics

Tamires de Oliveira Andrade¹, Kelli dos Santos Ramos¹,
Margarita M. López-Uribe², Michael G. Branstetter³, Carlos Roberto F. Brandão¹

1 University of São Paulo, Museum of Zoology, Laboratory of Hymenoptera, São Paulo, Brazil **2** The Pennsylvania State University, Center for Pollinator Research, Department of Entomology, University Park, Pennsylvania 16802, USA **3** U.S. Department of Agriculture, Agricultural Research Service, Pollinating Insects Research Unit, Utah State University, Logan, Utah 84322, USA

Corresponding author: Tamires de Oliveira Andrade (tamiresdeoliveirandrade@gmail.com)

Academic editor: Christopher K. Starr | Received 29 July 2022 | Accepted 26 October 2022 | Published 20 December 2022

<https://zoobank.org/D2556958-A478-4508-8FEF-FF4B78FBB532>

Citation: Andrade TO, Ramos KS, López-Uribe MM, Branstetter MG, Brandão CRF (2022) Integrative approach resolves the taxonomy of *Eulaema cingulata* (Hymenoptera, Apidae), an important pollinator in the Neotropics. Journal of Hymenoptera Research 94: 247–269. <https://doi.org/10.3897/jhr.94.91001>

Abstract

Species delimitation is a rich scientific field that often uses different sources of data to identify independently evolving lineages that might be recognized as species. Here, we use an integrative approach based on morphometrics, COI-barcoding, and phylogenomics using ultraconserved elements (UCEs) to investigate whether the orchid bee species *Eulaema cingulata* (Fabricius, 1804) and *E. pseudocingulata* Oliveira, 2006 represent a single variable taxon or two different species. We analyzed 126 specimens across the geographical range of these nominal species to test species hypotheses using the general lineage concept. We found substantial overlap in wing and head morphometrics, and both taxa form one phylogenetic lineage based on COI mitochondrial and UCE data. Our results support the recognition of both forms as members of the same evolutionary unit and *E. pseudocingulata* is herein recognized as a junior synonym of *E. cingulata*.

Keywords

DNA barcoding, morphometrics, orchid bees, phylogenomics, species delimitation, synonymy, ultraconserved elements

Introduction

Accurate species diagnosis remains a major challenge for many groups of organisms and is often described as the “taxonomic bottleneck” (Kim and Byrne 2006). On one hand, species identification can be challenging for evolutionary units that diverged recently because they may exhibit very similar morphology making them difficult to differentiate based on morphological traits alone. Difficulty in properly identifying cryptic species leads to underestimation of species diversity. On the other hand, conspecific individuals can display discrete polymorphism in morphological characters (e.g., Quezada-Euán et al. 2015; Lepeco and Gonçalves 2018) that, if used for taxonomic identification, may lead to the erroneous description of different species.

In order to circumvent some of the limitations of taxonomic classifications exclusively based on discrete qualitatively morphological characters, integrative taxonomy incorporates evidence from multiple independent datasets such as geometric morphometrics and molecular markers to inform species recognition and species boundaries (Goldstein and DeSalle 2010; Padial et al. 2010; Schlick-Steiner et al. 2010). Basing a species description on a variety of characters from different and independent datasets is generally regarded as the best practice (DeSalle et al. 2005). When species are considered as independently evolving lineages different lines of evidence are additive to each other (de Queiroz 2007).

Orchid bees (Hymenoptera: Apidae: Euglossini) are endemic to the Neotropical region. They receive their common name because males of these bees actively collect volatile compounds from orchids, and in the process pollinate the flowers (Dressler 1982). A variety of social behaviors are found among the euglossine genera, from solitary behavior to relatively complex social interactions in some species (Cameron 2004; Faria and Melo 2020). Five genera have been described in the tribe Euglossini: *Euglossa* Latreille, 1802, *Eufriesea* Cockerell, 1908, *Eulaema* Lepeletier, 1841, *Exaeret* Hoffmannsegg, 1817, and *Aglae* Lepeletier and Serville, 1825, encompassing approximately 240 species (Michener 2007; Moure et al. 2012). The genus *Eulaema* includes the largest orchid bees, with total body size varying from 18 to 30 mm in length (Oliveira 2000; Melo 2014), and is divided into two subgenera, *Apeulaema* and *Eulaema*, which are easily recognizable. Males of *Apeulaema* differ from *Eulaema* in having whitish-yellow spots on the clypeous, parocular areas and terga integument black, the latter sometimes turning to blue-violet (Moure 2000).

Eulaema (Apeulaema) cingulata (Fabricius, 1804) has a widespread distribution (from southern Brazil to southern Mexico), where it is associated mainly with wet and dry forested areas (Fig. 1A–C). This species is frequently sampled in faunistic inventories (e.g. Pires et al. 2013; Silveira et al. 2015; Machado et al. 2018) and reported in a wide range of ecological studies related to pollination in agroecosystems (Marques et al. 2017; Gutiérrez-Chacón et al. 2018), pollination of plants in Amazon rainforest (Martel et al. 2019; Watteyn et al. 2021), and as vectors of cleptoparasitic beetles (Rocha-Filho and Garófalo 2015).

Eulaema cingulata was initially described as *Centris cingulata* with no information on the number and sex of the specimens studied. The only information about these

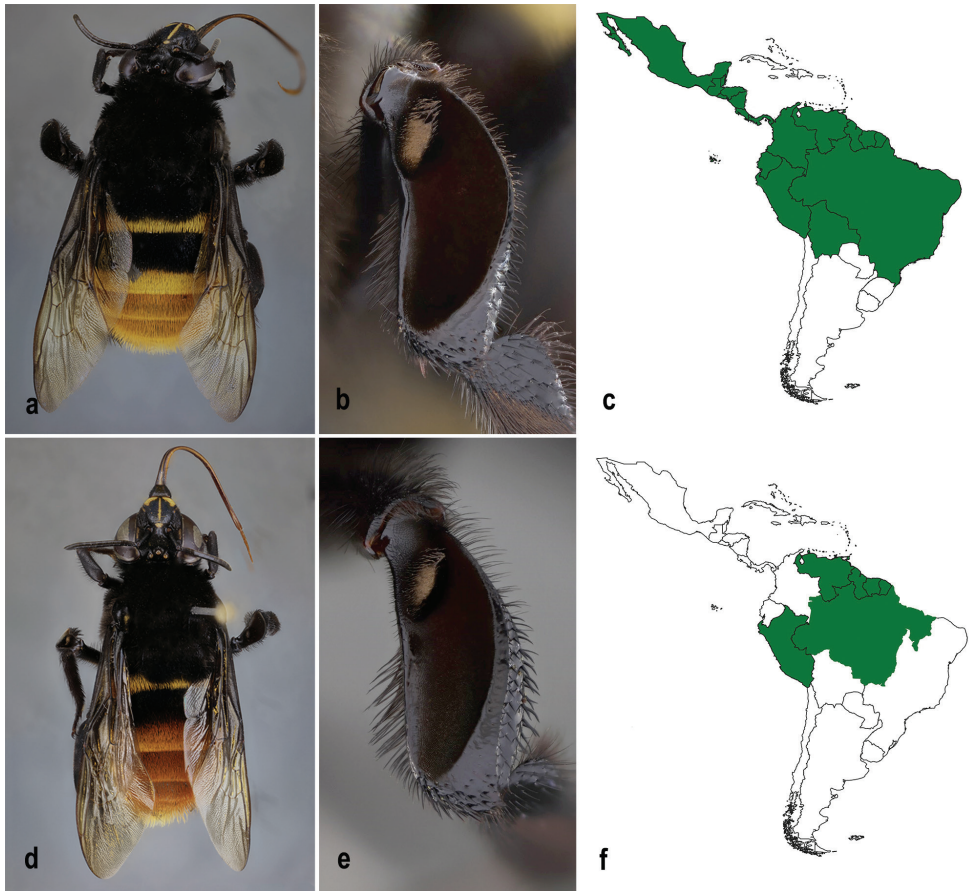


Figure 1. **A, B** male specimen of *Eulaema cingulata* from Sergipe, Brazil **A** body in dorsal view **B** velvety area in the mid tibia **C** geographical distribution of *E. cingulata* in green **D, E** male specimen of *E. pseudocingulata* from Pará, Brazil **D** body in dorsal view **E** velvety area in the mid tibia **F** geographical distribution of *E. pseudocingulata* in green.

specimens is their location as “*America meridionalis*” (according to Moure (1960) probably Guyana) and the institution in which they were deposited, the Zoologisk Museum in Copenhagen. In the species description, the first tergum and the base of the second are described as a single tergum, which led some authors to subsequent identification mistakes related to the color pattern of these terga. Lepeletier (1841), having specimens of *C. cingulata*, did not recognize them as such and described them as *E. fasciata*, based on a female, and *E. cajennensis*, based on a male (Moure 1960, 2000). Oliveira (2006) described *E. (Apeulaema) pseudocingulata* for specimens from the Amazon Forest (Fig. 1D–F) that show a morphologically distinct feature in the velvety area of the mid-leg of males. Males of *E. cingulata* have a wider posterior edge in the velvety area of the middle tibia than in *E. pseudocingulata* (Fig. 1B, E). In addition, the coloration of the male abdomen is darker in *E. pseudocingulata* than in *E. cingulata*.

Morphological differences between females of these two forms have not yet been found (Moure et al. 2012) and the female of *E. pseudocingulata* remains undescribed. Nemésio (2009) synonymized *E. pseudocingulata* under *E. cingulata* and proposed a new species (*E. marcii*) for the Atlantic Forest population, based on the misunderstood conclusion that this latter form had not been found in the type locality of *E. cingulata* (Melo in Moure et al. 2012). Moure et al. (2012) recently placed *Eulaema marcii* in synonymy with *E. cingulata* and adopted *E. pseudocingulata* as a taxonomically valid species as proposed by Oliveira (2006).

Despite the distinct differences in coloration and the velvety area of the mid-leg between males of *E. cingulata* and *E. pseudocingulata*, the taxonomic status of these nominal species has not been investigated with additional datasets. A comparative phylogeographic study of *E. cingulata* based on mitochondrial and nuclear markers revealed a lack of structure for *E. cingulata* throughout the whole range of the species (López-Urbe et al. 2014). That study included a small set of specimens from both *E. cingulata* and *E. pseudocingulata* and did not indicate genetic differentiation between these species. In the present study, we incorporate morphometric data (wings and heads) and molecular data from mitochondrial and genome-wide markers to test the status of both species. We used the character of the velvety area of the mid-leg of males for species identification of the specimens. Genetic and/or morphological clustering of specimens taxonomically identified based on this morphological character would support the presence of two evolutionary units.

Materials and methods

Morphometric data

We studied 107 specimens of *E. cingulata* and *E. pseudocingulata* from across their geographic ranges. Most of the specimens were collected in the Amazon forest where both species are sympatrically distributed (Fig. 2A, Suppl. material 1: table S1). Using a Leica DFC 295 camera, we photographed specimens attached to a stereomicroscope Leica M205C. For the analysis of wing morphometrics, we separated the right forewing from the body at the base of the radial vein using forceps and fixed it on glass microscopy slides. The heads were photographed in frontal view. For the image analysis, we saved photographs into TPS files using the software TpsUtil 1.60 (Rohlf 2013) and identified landmarks using the software tpsDig version 2.26 (Rohlf 2006). We selected 10 landmarks for the head (Fig. 3A), and 18 landmarks on the vein intersections for the wing (Fig. 3B). We choose the landmarks based on previous studies of bees (Quezada-Euán et al. 2015; Souza et al. 2015; Costa et al. 2020).

For comparisons of the overall wing and head sizes between species, we extracted the centroid size and used a generalized Procrustes analysis to capture shape variables without the effects of orientation and position of the images. A regression analysis between size and shape was performed to quantify the effect of allometry. Afterwards, we

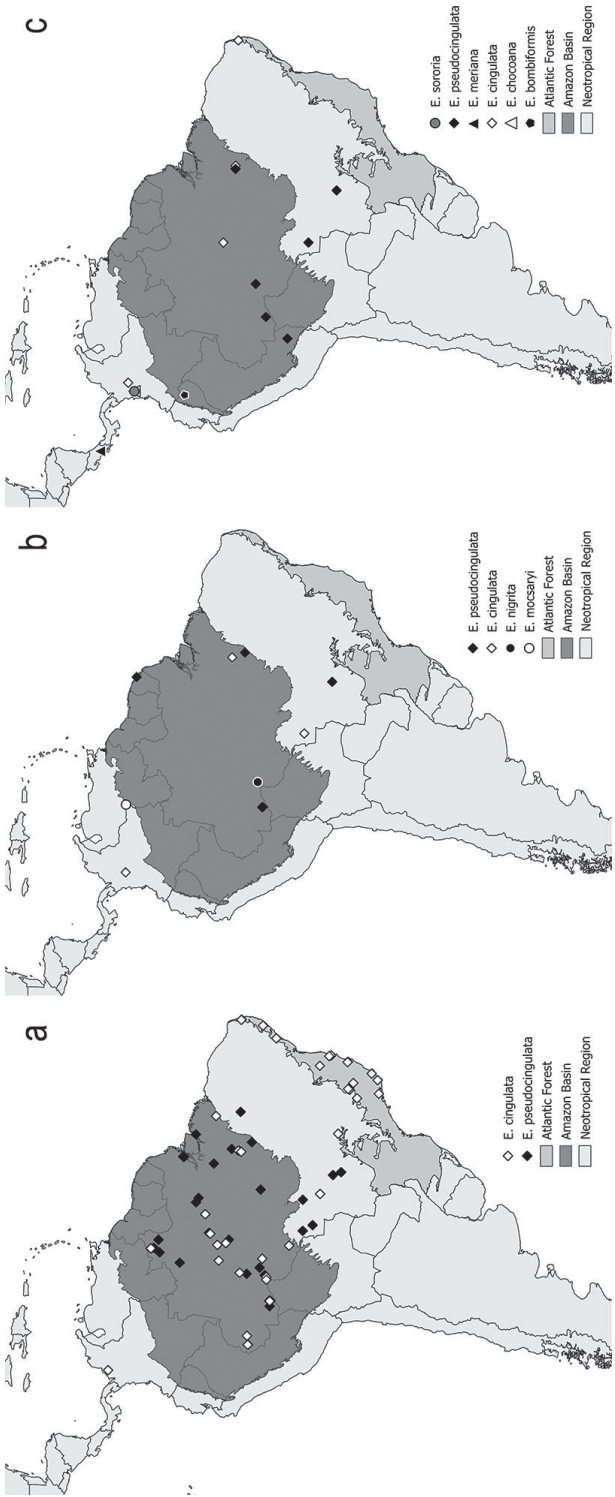


Figure 2. Geographical locality of the specimens used in each analysis of the present study **A** geometric morphometrics **B** COI-barcoding and pairwise genetic p-distance **C** phylogenomics using Ultraconserved elements.

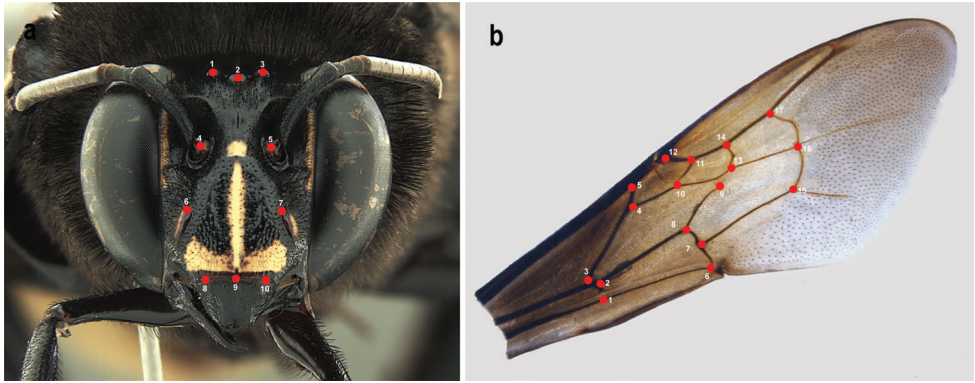


Figure 3. Landmarks used in the geometric morphometric analyses of *Eulaema cingulata* and *E. pseudocingulata* **A** head of male in frontal view and **B** forewing of male.

removed this allometric effect to independently quantify shape variation. The resulting landmark configurations retained only shape information (Klingenberg 2015).

To visually compare all individuals in multivariate trait space, we used a Principal Component Analysis (PCA) using the relative Cartesian coordinates of each landmark after alignment. The shape difference between species were tested using a Discriminant Analysis followed by a leave-one-out cross-validation test (Lachenbruch 1967). All analyses were performed using the software MorphoJ (Klingenberg 2011). Additionally, we used the percentages of correct classification to evaluate the discriminatory power of wing and head shapes.

DNA sampling, extraction, amplification, and sequencing

We extracted total genomic DNA from the hind legs or thoracic muscles of specimens using Qiagen DNeasy Kit (Qiagen) with modifications to maximize DNA yield for dry specimens as incorporated in Evangelista et al. (2012). Before extraction, we placed pinned specimens in a humid chamber for 24 hours to facilitate the removal of the leg or abdomen muscle without damaging the whole specimen. For tissue digestion, we added ATL buffer and 20 μ L of proteinase K (20 mg/ml) for the first six hours, and 10 μ L additionally after six hours of incubation at 55 °C .

We amplified sequences of the cytochrome oxidase I (COI) region using universal barcoding primers LCO (5'-GGTCAACAAATCATAAAGATATTGG-3') and HCO (5'-TAAACTTCAGGGTGACCAAAAATCA-3') (Folmer et al. 1994). Polymerase Chain Reaction (PCR) amplifications were performed in a final volume of 17 μ l including 0.13 μ L of Taq Polymerase (Qiagen) , 2 μ L of genomic DNA, 1.3 μ L of each primer (10 μ M), 3.4 μ L of dNTPs (10mM), 0.85 μ L of MgCl, 1.7 μ L of 10 \times Qiagen Buffer and 6.32 μ L of purified water. We performed amplification with an initial step of three minutes at 94 °C, followed by 40 cycles of 30 seconds at 94 °C, 30 seconds for annealing at 50 °C and 1 min at 72 °C. After 40 cycles, we performed a final step at 72 °C for 10 minutes. We performed all steps related to DNA extraction and COI

amplification at the Molecular Biology Laboratory of the Museu de Zoologia da Universidade de São Paulo, Brazil (MZSP). We sent the amplified COI fragments to Macrogen (Seoul, South Korea) for post-PCR purification and Sanger sequencing. We corroborated sequence quality by the quality scores provided by Macrogen and by visually examining the chromatograms using the software Ugene (Okonechnikov et al. 2012).

To include genome-wide markers in our dataset, we sequenced 2,180 Ultra Conserved Element (UCE) loci using a recently published bait set specific to bees, ants, and other apoid wasps (“hym-v2-bee-ant-specific”; Grab et al. 2019). This bait set is a subset of the principal Hymenoptera bait set first reported in Branstetter et al. (2017). For each sample, we sheared the DNA using a Qsonica Q800R2 acoustic sonicator, with the target fragment size range being 400–600 bp (60–120 secs shear time, 25% amplitude, 10–10 sec pulse). For older samples with more degraded DNA, we adjusted the shearing times to between 30–60 seconds. We cleaned fragmented DNA at 3× volume using a homemade SPRI-bead substitute (“speedbeads”; Rohland and Reich 2012). We generated Illumina sequencing libraries for each sample using Kapa Hyper Prep Kits (Roche Sequencing and Life Science, Wilmington, MA) and custom, dual-indexing adapters (Glenn et al. 2019).

We amplified libraries for 12 cycles, purified them using speedbeads (Rohland and Reich 2012), and quantified them using a Qubit 3.0 fluorometer (Thermo Fisher Scientific, Waltham, MA). To enrich UCE loci, we pooled 10 libraries at equimolar concentrations. Then, up to 500 ng of each pool was enriched following the manufacturer’s protocol for day 1 (MYcroarray enrichment protocol v3.02) and the standard UCE protocol for day 2 (enrichment protocol v1.5 available at ultraconserved.org). The custom bait set was diluted 1:4 (1 µL bait, 4 µL H₂O) with enrichment incubation at 65 °C for 24 hours using strip tubes and a PCR thermal cycler. For the second day of enrichment, we used 50 µL of streptavidin beads per sample and performed on-bead PCR following the three heated (65 °C) wash steps. We amplified the enriched pools for 18 cycles and the resulting products were purified with SPRI beads at 1× volume. We sent the sequencing pools to the University of Utah Genomics Core for sequencing on an Illumina HiSeq 2500 (2×125, v4 chemistry).

Molecular approaches for species phylogeny and delimitation

For the molecular analyses, we generated DNA sequences from 19 males (less than 10 years old after collection) for the amplification of COI and UCEs. We preserved remaining body parts and associated DNA extractions for future studies (Suppl. material 1: table S2). Two sequences of the mitochondrial gene COI were obtained from GenBank and one sequence was obtained from BOLD Systems. We added the following other *Eulaema* species as outgroups: *E. meriana* (Olivier, 1789), *E. mocsaryi* (Friese, 1899) and *E. nigrita* Lepeletier, 1841 for COI analysis, and *E. bombiformis* (Packard, 1869), *E. chocoana* Ospina-Torres & Sandino-Franco, 1997, *E. meriana*, and *E. sororia* Dressler & Ospina-Torres, 1997 for the phylogenomic analysis (Suppl. material 1: table S2).

For the mitochondrial data, we aligned COI sequences using the multiple sequence alignment online tool MAFFT (Katoh et al. 2019) and manually edited them using

the software Ugene (Okonechnikov et al. 2012). We inferred a phylogenetic tree using Bayesian Inference (BI) method. Genetic distances within and between species were calculated in MEGA-X (Kumar et al. 2018) using 10,000 bootstraps. We performed Bayesian phylogenetic analyses in MrBayes v.3.2 (Ronquist et al. 2012) with COI sequences using the best nucleotide model estimated by PartitionFinder2 (Lanfear et al. 2017). The Markov Chain Monte Carlo (MCMC) was run for 20 million generations sampled every 1000th generation. We discarded 25 percent of the first trees as burnin. We visualized and edited the Bayesian trees in FigTree v. 1.4.4 (Rambaut 2018).

For the UCE dataset, we performed most data processing steps using the software package Phyluce (Faircloth 2016). We cleaned the reads for adapter contamination and low-quality bases using Illumiprocessor (Faircloth 2013), which functions as a wrapper around the software Trimmomatic (Bolger et al. 2014). We assembled cleaned reads *de novo* for each individual using SPAdes v. 3.12.0 (Bankevich et al. 2012). To identify UCE regions from the bulk of assembled contigs and to remove paralogs, we used the Phyluce script `match_contigs_to_pobes` and the HymV2-bee-ant UCE bait files from Grab et al. (2019). We aligned all the loci individually using MAFFT (Kato and Standley 2013) as implemented in Phyluce package, and trimmed resulting alignments using Gblocks with reduced stringency parameters (Castresana 2000). We removed loci that had data for fewer than 75% of taxa and generated a concatenated matrix from the resulting alignment set.

For phylogenetic reconstruction using UCE data, we inferred phylogenetic trees using Maximum Likelihood (ML), and multi-species coalescence reconstruction. We performed maximum likelihood analyses using two different strategies: single concatenated alignment and partitioned based on the best-fitting partitioning scheme. For the concatenated alignment, we obtained the substitution model (TVM+F+R2) using ModelFinder (Kalyaanamoorthy et al. 2017) which is part of the IQ-TREE v2.1.1 software (Nguyen et al. 2015). The best-fitting partitioning scheme was obtained using Sliding-Window Site Characteristics (SWSC), which divides each UCE into three data blocks corresponding to the right flank, core, and left flank (Tagliacollo and Lanfear 2018). We analyzed the resulting data subsets using PartitionFinder2 (Lanfear et al. 2017) using the `rclusterf` algorithm with AICc model selection criterion and GTR+G model of sequence evolution obtained by ModelFinder. We used the likelihood-based program IQ-Tree v2.1.1 for phylogenetic reconstruction of both partitioning schemes. To assess branch support, we performed 1000 replicates of the ultrafast bootstrap approximation (UFBoot; Hoang et al. 2018) and 1000 replicates of the branch-based Shimodaira-Hasegawa approximate likelihood-rate test (SH-aLRT; Guindon et al. 2010) using the command ‘-alrt’. Only clades with support values of UFBoot ≥ 0.95 and SH-aLRT ≥ 0.80 were considered robust. To account for heterogeneous gene histories that may influence phylogenetic accurate resolution, we inferred a species tree under the multi-species coalescent model using the program ASTRAL-III v.5.7.3 (Zhang et al. 2018), using gene trees provided by IQ-Tree as input. Support was assessed as local posterior probability, with ≥ 0.95 considered robust.

We also estimated a coalescent-based species tree using *Beast (Heled and Drummond 2010) and the BEAST2 package (Bouckert et al. 2019). Due to computational constraints, we selected a subset of loci for the *BEAST analysis. We ran the command

'phyluce_align_get_informative_sites' from Phyluce to identify the 100 most informative genes. From these most informative genes, we then selected those that were present in all samples, resulting in 88 UCEs. The analysis was run for 100 million generations sampling every 10,000 generations under a strict clock model with a constant population model, and a Yule model as a tree prior. We used a GTR model (unlinked across loci) for the nucleotide substitution model that was provided by PartitionFinder2 (Lanfear et al. 2017). To examine the convergence across the four runs performed and the ESS values of sampled parameters, we used Tracer v1.7 (Rambaut et al. 2018). A maximum clade credibility was constructed in TreeAnnotator and visualized the tree using Densitree, both included in the BEAST package (Bouckert et al. 2019).

Data availability

The raw UCE sequence reads have been uploaded to the NCBI Sequence Read Archive under BioProject accession PRJNA875942.

Results

Morphometric geometrics

Individuals identified as *E. cingulata* and *E. pseudocingulata* formed one cluster based on the shape of the head and wings (Fig. 4). The PCA captured the variation of head and wing shape in 8 and 32 PCs, respectively. The first three components of the head variation explained 45.28%, 19.16%, and 12.37% of the covariance, respectively, totaling 76.81% (Suppl. material 1: table S3). The cross-validation test correctly located

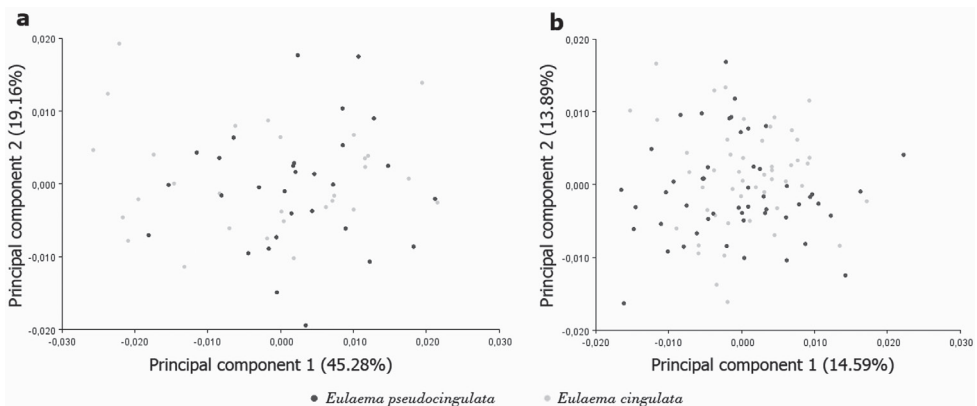


Figure 4. Shape variation of males of *Eulaema* species grouped considering **A** the shape of the head, and **B** the shape of the wings: The percentage explained by each Principal Components (PC) is in parenthesis. The negative and positive extremes of both PC1 and PC2 are shown below and besides of the graph (Factor scale: left -0.03, right 0.03).

Table 1. Cross-validated classification rates of correct group assignments between male specimens of *Eulaema cingulata* and *Eulaema pseudocingulata* based on head and wing shapes.

	Head			%
	<i>E. cingulata</i>	<i>E. pseudocingulata</i>	Total	
<i>E. cingulata</i>	18	11	29	62.07
<i>E. pseudocingulata</i>	10	20	30	66.67
	Wing			%
	<i>E. cingulata</i>	<i>E. pseudocingulata</i>	Total	
<i>E. cingulata</i>	33	17	50	66
<i>E. pseudocingulata</i>	16	34	50	68

62.07% and 66.67% of specimens of *E. cingulata* and *E. pseudocingulata*, respectively. The first three components of the wing shape explained 13.32%, 10.84%, and 10.02% of the variance, respectively, explaining a total of 34.18% of the variation (Suppl. material 1: table S4). Similar to the head results, the cross-validation test correctly located 66% and 68% of specimens of *E. cingulata* and *E. pseudocingulata*, respectively (Table 1). The multivariate regression analysis showed that, after 10,000 permutation rounds, the influence of the allometric effect was statically significant ($P < 0.0001$) with 32.28% and 3.07% predicted shape variation of the head and wing shape, respectively. Nonetheless, even after removing this allometric effect, the groups remained undifferentiated.

Genetic distance

The 655 bp fragment of the mitochondrial COI region resulted in an average pairwise genetic p-distance within *E. cingulata* of 1.3% and within *E. pseudocingulata* of 0.7%, while between the two species was 0.9%. The greater amount of genetic differentiation within the group of *E. cingulata* than between specimens from the two nominal species indicated no support for the presence of two evolutionarily independent units. The average pairwise genetic distances among *E. cingulata* and the outgroups (*Eulaema mocsaryi*, *E. nigrita*, and *E. meriana*) are greater than 5.6% (Table 2).

Table 2. Average pairwise genetic p-distance between species of *Eulaema* employing COI sequences with 655pb aligned.

Species	<i>Eulaema cingulata</i>	<i>Eulaema pseudocingulata</i>
<i>Eulaema cingulata</i>	1.3%*	0.9%
<i>Eulaema pseudocingulata</i>	0.9%	0.7%*
<i>Eulaema mocsaryi</i>	5.6%	5.3%
<i>Eulaema nigrita</i>	9.3%	9.0%
<i>Eulaema meriana</i>	11.2%	11.3%

*Average pairwise genetic p-distance within each species.

Phylogenetic relationships

Both the COI and UCE phylogenetic reconstructions provided no support for the species differentiation of *E. cingulata* and *E. pseudocingulata* (Figs 5, 6). For COI, PartitionFinder2 identified GTR+I as the best nucleotide substitution mod-

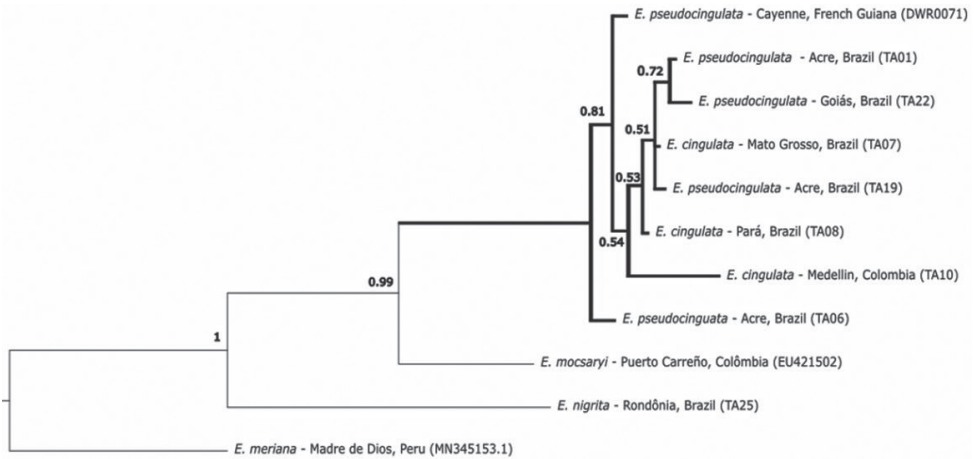


Figure 5. Consensus tree for *Eulaema cingulata* and *E. pseudocingulata* resulting from a Bayesian analysis of molecular data from the gene COI. Numbers on branches indicate posterior probability support. Geographical location of each individual is shown in each tip.

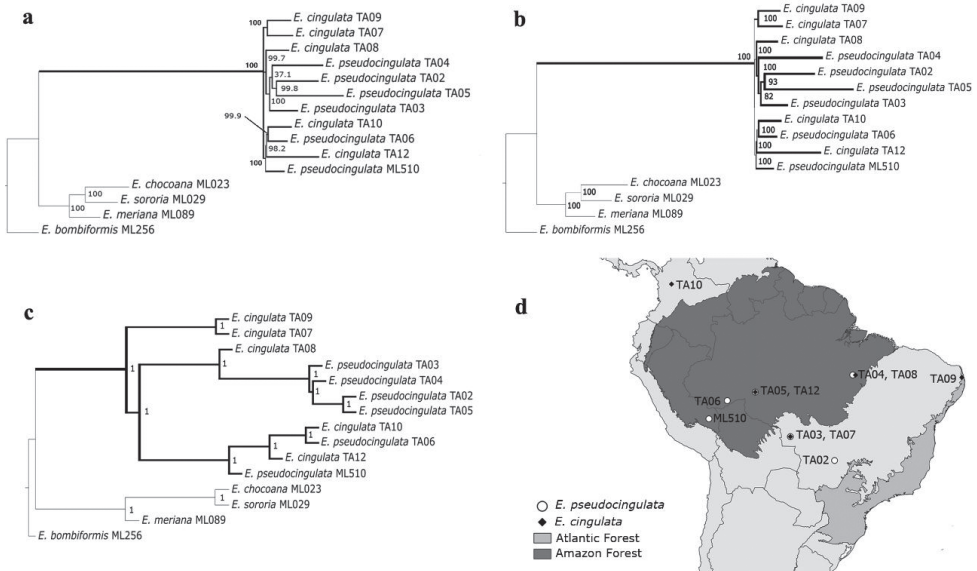


Figure 6. Phylogenetic trees for *Eulaema cingulata* and *E. pseudocingulata* obtained with Ultraconserved Elements (UCE) **A** maximum likelihood phylogenetic tree obtained with concatenated dataset in IQ-Tree. Numbers on nodes correspond to ultrafast bootstrap **B** maximum likelihood phylogenetic tree obtained with partitioned dataset in IQ-Tree. Numbers on nodes correspond to ultrafast bootstrap **C** species delimitation analyses based on multispecies-coalescent model obtained with ASTRAL. Number on nodes corresponds to posterior probabilities **D** map showing the distribution of the analyzed material (ingroup).

el. The consensus tree obtained from MrBayes showed that the COI fragments grouped *E. cingulata* and *E. pseudocingulata* into one highly supported clade sister to *E. mocsaryi* (Fig. 5). For the UCE data, we recovered a total of 21,470,135 reads

with an average of 1,431,342 reads per sample (range = 513,594 – 2,585,935). These reads were assembled into an average of 186,700 contigs per sample (range = 34,358 – 441,504), having an average length of 167bp. An average (per sample) of 2,217 of contigs match UCE loci from the target capture probes used. Following alignment, trimming, and filtering of the UCE loci, our final UCE matrix consisted of 2,180 loci and 1,509,760 bp of sequence data, of which 33,722 bp are informative. The average length of UCE contigs post alignment and trimming is about 692 bp (range = 229 – 1,831).

The maximum likelihood inference of the UCEs markers recovered identical topologies from both partitioned and concatenated schemes, with most nodes showing high support (Fig. 6A, B). Individuals identified as *E. cingulata* and *E. pseudocingulata* form a monophyletic group with maximum support value. The difference between these topologies is limited to the phylogenetic position of *E. pseudocingulata* TA03 and TA04 within a small *pseudocingulata* clade. The only individual from the Atlantic Forest (*E. cingulata* TA09) is recovered with maximum support as sister to the individual from Mato Grosso (*E. cingulata* TA07), a state in the Amazon Forest. The ASTRAL and *Beast species tree showed maximum support values and both recovered the same topology (illustrated by the ASTRAL tree on Fig. 6C). Even though the COI and UCE data included different samples, both methods present very similar topologies with no significant differences between the individuals grouped in the two nominal species. Both trees showed one clade with individuals from the two species with high statistical support.

Discussion

Our results indicate that specimens identified as *E. cingulata* and *E. pseudocingulata* do not show morphological or genetic differentiation. Geometric morphometrics of the forewings has been previously used as a powerful technique to discriminate bee species (Francoy et al. 2012; Combey et al. 2013), subspecies (Oleksa and Tofilski 2014; Silva et al. 2015), cryptic species (Francisco et al. 2008; Hurtado-Burillo et al. 2016) and geographical ecotypes (Francoy et al. 2011; Grassi-Sella et al. 2018; Carneiro et al. 2019). Using both landmarks and outlined-based methodologies, Francoy et al. (2012) showed that the use of this approach to discriminate *Euglossa* species was more effective than studies using allozymes and restriction patterns of mitochondrial genes. Quezada-Euán et al. (2015) identified differences in wing shape of the two different morphs of *Euglossa viridissima* Friese, 1899 that had been only otherwise identified by the number of mandibular teeth. We applied the same methodology to this study to assess the taxonomic status of the two focal species in the genus *Eulaema*. Similarly, the results obtained with the head measurements were congruent with the results obtained with the forewings. Despite being used less frequently than the wings, the use of landmarks on the head has also been informative to recognize intercastes in honey bees (Souza et al. 2015), and to discriminate the morphologically indistinguishable females of the *Psychodopygus* complex (Diptera) (Godoy et al. 2018).

Because the level of morphological differentiation among recently divergent lineages is sometimes insufficient to recognize species, we used mitochondrial and UCE data to test the presence of genetically distinct groups of individuals among the specimens studied. DNA barcodes are increasingly becoming a standard tool used by taxonomists and its association with morphological characters has proven useful at discriminating species in several groups of bees (Gibbs 2009). Although this method has been criticized by some authors (Rubinoff et al. 2006; Wheeler 2008), it gives additional support to the recognition of species when considered along with other data sources (Padial and De La Riva 2007; Packer et al. 2009). Based on our data, the pair wise sequence divergences within and between the two species were below 3%, which according to Hebert et al. (2003) is a result compatible with the expected variation within a single species. More importantly, specimens of *E. cingulata* and *E. pseudocingulata* did not form a distinct monophyletic clades and the genetic distance among individuals of *E. cingulata* was greater than the genetic distance among individuals of *E. cingulata* and *E. pseudocingulata*. Dick et al. (2004) found that mtDNA divergences within Euglossini species were consistently low, with divergences among populations separated by the Andes averaging 1.1% (collection sites cover 3,000km). These findings and other studies have indicated the presence of high levels of long-distance gene flow between orchid bee populations. Rocha-Filho et al. (2013) observed a comparatively high dispersal ability in *E. cingulata* through genetic analyses comparing mainland and island populations. López-Urbe et al. (2014) also found low values of mitochondrial nucleotide divergence between populations of three species of *Eulaema*, showing a minimum value of 0.39% within species divergence in *E. cingulata*. According to the authors, the low sequence divergence between populations of *E. cingulata* was partially explained by the recent origin of this species.

The topology obtained with genomic data also supports the monophyly and recognition of one clade that comprises *E. cingulata* and *E. pseudocingulata*. UCEs have been successfully used as a tool for species discrimination as they provide sufficient variation at shallow time scales (Smith et al. 2013; Gueuning et al. 2020). Combined phylogenetic and population genetic approaches have been effectively used to investigate boundaries between complexes of wild European bees suspected to harbor cryptic diversity, mitochondrial introgression, or mitochondrial paraphyly (Gueuning et al. 2020). Using COI and UCEs with the multispecies coalescent method (BPP), Gueuning et al. (2020) also concluded that UCEs can provide robust species hypotheses and outperform COI in species delimitation. The adoption of delimitation methods based on the multispecies coalescent model has been criticized by Sukumaran and Knowles (2017), who argued that these methods tend to delimit population structure instead of species. The authors' concern was raised by the possibility of taxonomic inflation if species are described based only on molecular data. However, most studies using genetic data in species delimitation also incorporate additional sources of data such as morphology or morphometrics.

Herein, we conclude that *E. pseudocingulata* is not an independent evolutionary lineage from *E. cingulata* suggesting that the morphological differences observed in the



Figure 7. Color of the pilosity on the metasoma of males from Amazon Forest **A** *Eulaema cingulata* (Brazil, Pará, Cachimbó) **B** *Eulaema cingulata* (Brazil, Pará) **C** *Eulaema pseudocingulata* (Brazil, Pará, Canaã dos Carajás) **D** *Eulaema pseudocingulata* (Brazil, Acre, Rio Branco).

velvety area of the mid-leg of males are a species polymorphism in *E. cingulata*. The difference in the shape of the mid tibia velvety area, proposed as the diagnostic character between the species, can be interpreted as a variable condition: it can be narrower and farther from the rear edge in some morphs occurring in the Amazon forest, or wider and closer to the rear edge in morphs occurring throughout the species distribution. Initially, the color of the abdomen was also proposed as a diagnostic character to differentiate *E. cingulata* and *E. pseudocingulata*, but a gradient can be observed in the two morphs, varying from a yellowish tone to orange (Fig. 7A–D). Additionally, color can be a highly variable trait within bees making it a difficult character for taxonomic identification. Variable color patterns on the abdomen have been described for several species of bumble bees (e.g., Carolan et al. 2012; Huang et al. 2015). Color variation in Eucerini bees was reported by Grando et al. (2018), in which they found two distinct color patterns in sympatric populations of *Melissodes nigroaenea* (Smith, 1854) in Brazil. Variation in color and shape was observed in *Augochlora amphitrite* (Schtottky, 1909) by Lepeco and Gonçalves (2018) using morphometric analyses and studying the male genital capsules. The authors did not find any character that support the recognition of distinct color morphs and macrocephalic females as different species. Similar to our findings, a genetic study of different color morphs of *Euglossa* species from the Atlantic Forest did not support the recognition of different species (Ferrari and Melo 2014).

The mechanisms responsible for maintaining the variation of the velvety area of the mid tibia in individuals of *E. cingulata* in the Amazon Forest remain unknown. However, a plausible explanation for the lack of differentiation in morphological and genetic markers is that there is an ongoing speciation process driven by sexual selection in the Amazonian population of *E. cingulata*. Such a rapid speciation process has been described in two sympatric *Euglossa* species from southern Mexico: *E. viridissima* and *E. dilemma* (Eltz et al. 2011). These sister species can be partially differentiated by the number of mandibular teeth: *E. dilemma* males possess three teeth on the mandibles while *E. viridissima* mostly show two teeth with some individuals expressing three teeth. However, these species are unequivocally distinguished by chemical characters (cuticular hydrocarbons found in the hind tibia) as well as by highly variable DNA markers (microsatellites and SNPs) (Pokorny et al. 2014; Quezada-Euán et al. 2015).

A similar process could be occurring in *E. cingulata* and *E. pseudocingulata* but chemical information and characterization of genetic polymorphism across the entire genome of these bees would be necessary to properly investigate these questions. Further investigations are necessary to understand potential processes of incipient speciation in characters that have been characterized thus far.

Taxonomy

Eulaema (Apeulaema) cingulata (Fabricius 1804)

Centris cingulata Fabricius 1804: 355. Lectotype female, 'America meridionalis' (probably Guyana according to Moure 1960).

Eulaema cajennensis Lepeletier 1841: 14. Lectotype male, French Guiana, Cayenne.

Eulaema fasciata Lepeletier 1841: 12. Lectotype female, French Guiana, Cayenne.

Eulaema (Apeulaema) marcii Nemésio 2009: 175. Holotype male, Brazil, Minas Gerais.

Eulaema (Apeulaema) pseudocingulata Oliveira 2006: 122. Holotype male, Brazil: Amazonas. New synonymy.

Diagnosis and comments. We recognized the taxon present in the Amazon forest under the name *E. pseudocingulata* as a junior synonym of *E. cingulata*, in light of the morphometric and phylogenetic data presented here. *E. cingulata* includes individuals with velvety areas of the midtibia that vary in width of the smooth area near the posterior edge (Fig. 1B, E). The basal tuft can be narrower or wider and slightly sloping. Other characters in this species include the labrum with lateral carina smoothly curved at the apex and ending distantly the edge of the clypeus, and the middle carina much shorter than lateral carina. The color of the metasomal hairs varies from orange to a light yellowish color (Fig. 7A–D). The material examined is the same as referenced in the Suppl. material 1: tables S1, S2. Lectotype of *Eulaema cingulata* was examined by the images available in Nemésio (2009) and the holotype of *E. pseudocingulata* in Almeida et al. (2020).

Conclusion

We tested the species hypothesis of *Eulaema cingulata* and *E. pseudocingulata* by integrating multiple independent datasets: geometric morphometrics, phylogenetics using mitochondrial DNA, and phylogenomics using ultraconserved elements. All results across methods were congruent, showing no separation between morphs previously recognized as different species. Our results also suggest that the morphology of the mid tibia of *E. pseudocingulata*, proposed as the diagnostic character between the morphs, appears as a variable condition in some individuals of *E. cingulata* from the Amazon basin. Besides the variation in the mid leg, there is also color variation across samples. The evolutionary drivers of this variability are currently unknown. In the interests of nomenclatural stability, we have designated *E. pseudocingulata* as a junior synonym of

E. cingulata. Orchid bees are important pollinators in Neotropical forests, being widely used in environmental quality studies, and they have become a good model for evolutionary genetics studies. However, as shown here, there is still a need to improve knowledge of the alpha taxonomy of these important group of Neotropical pollinators. Integration of DNA sequence analyses with geometric morphometrics of heads and wings can more rigorously test species boundaries than traditional morphological assessments alone and can ultimately improve species descriptions and identification tools.

Acknowledgements

We thank the curators and technicians of the collections for the loan of bee specimens: Elder Morato (Universidade Federal do Acre), Beatriz Coelho and Orlando Silveira (Museu Paraense Emílio Goeldi), Márcio Oliveira (Instituto Nacional de Pesquisas da Amazônia), Fernando Silveira and José Eustáquio (Universidade Federal de Minas Gerais), Maria Cristina Gaglianone (Universidade Estadual do Norte Fluminense Darcy Ribeiro). We thank José Villavicencio (Museu de Zoologia da Universidade de São Paulo - MZSP) for the support with the morphometric analyses, and Nathaniel Pope (Pennsylvania State University), Sergio Bolivar and Luz Eneida (MZSP) for the assistance with genomic data. This work was supported by Coordenação de Aperfeiçoamento de Pessoal de Nível Superior (Capes), funding code 001 (TOA), Fundação de Amparo à Pesquisa do Estado de São Paulo (Fapesp), process 17/07366-1 and 2016/50378-8 (CRFB and TOA). MML-U was funded through the USDA NIFA Appropriations under Projects PEN04716 and PEN04620. MGB and part of the sequencing work was funded through USDA project 2080-21000-019-000-D and NSF grant DEB-2127744. USDA is an equal opportunity provider and employer.

References

- Almeida EAB, Costa AM, Filho JAT, Zichinelli MMP, Quintero FB (2020) Illustrated catalogue of type specimens of insects (Hexapoda) at Coleção Entomológica “Prof. J.M.F. Camargo” (RPSP), Universidade de São Paulo, Brazil. *Zootaxa* 4842(1): 1–204. <https://doi.org/10.11646/zootaxa.4842.1.1>
- Bankevich A, Nurk S, Antipov D, Gurevich AA, Dvorkin M, Kulikov AS, Lesin VM, Nikolenko SI, Pham S, Prjibelski AD, Pyshkin AV, Sirotkin AV, Vyahhi N, Tesler G, Alekseyev MA, Pevzner PA (2012) SPAdes: a new genome assembly algorithm and its applications to single-cell sequencing. *Journal of Computational Biology* 19: 455–477 <https://doi.org/10.1089/cmb.2012.0021>
- Bolger AM, Lohse M, Usadel B (2014) Trimmomatic: a flexible trimmer for Illumina sequence data. *Bioinformatics* 30: 2114–2120. <https://doi.org/10.1093/bioinformatics/btu170>
- Bouckaert RR, Vaughan TG, Barido-Sottani J, Duchene S, Fourment M, Gavryushina A, Heled J, Jones G, Kühnert D, Maio N, Matschiner M, Mendes FK, Müller NE, Ogilvie HA, Plessis L, Poppinga A, Rambaut A, Rasmussen D, Siveroni I, Suchard MA, Wu C-H, Xie D, Zhang C, Stadler T, Drummond AJ (2019) BEAST 2.5: An advanced software

- platform for Bayesian evolutionary analysis. *PLoS Computational Biology* 15: e1006650. <https://doi.org/10.1371/journal.pcbi.1006650>
- Branstetter MG, Longino JT, Ward PS, Faircloth BC (2017) Enriching the ant tree of life: enhanced UCE bait set for genome-scale phylogenetics of ants and other Hymenoptera. *Methods in Ecology and Evolution* 8: 768–776. <https://doi.org/10.1111/2041-210x.12742>
- Cameron SA (2004) Phylogeny and biology of neotropical orchid bees (Euglossini). *Annual Review of Entomology* 49: 377–404. <https://doi.org/10.1146/annurev.ento.49.072103.115855>
- Carneiro LS, Aguiar CML, Aguiar WM, Aniceto ES, Nunes LA, Ferreira VS (2019) Morphometric variability among populations of *Euglossa cordata* (Hymenoptera: Apidae: Euglossini) from different phytophysiognomies. *Sociobiology* 66(4): 575–581. <https://doi.org/10.13102/sociobiology.v66i4.4675>
- Carolan JC, Murray TE, Fitzpatrick Ú, Crossley J, Schmidt H, Cederberg B, McNally L, Paxton RJ, Williams PH, Brown MJF (2012) Color patterns do not diagnose species: quantitative evaluation of a DNA barcode cryptic bumblebee complex. *PLoS ONE* 7: e29251. <https://doi.org/10.1371/journal.pone.0029251>
- Castresana J (2000) Selection of conserved blocks from multiple alignments for their use in phylogenetic analysis. *Molecular Biology and Evolution* 17: 540–552. <https://doi.org/10.1093/oxfordjournals.molbev.a026334>
- Combey R, Teixeira JSG, Bonatti V, Kapwong P, Francoy TM (2013) Geometric morphometrics reveals morphological differentiation within four African stingless bee species. *Annals of Biological Research* 4: 95–105.
- Costa CP, Machado CAS, Santiago WMS, Dallacqua RP, Garófalo CA, Francoy TM (2020) Biome variation, not distance between populations, explains morphological variability in the orchid bee *Eulaema nigrita* (Hymenoptera, Apidae, Euglossini). *Apidologie* 51: 984–996. <https://doi.org/10.1007/s13592-020-00776-z>
- DeSalle R, Egan MG, Siddall M (2005) The unholy trinity: taxonomy, species delimitation and DNA barcoding. *Philosophical Transactions of the Royal Society B* 360: 1905–1916. <https://doi.org/10.1098/rstb.2005.1722>
- De Queiroz K (2007) Species concepts and species delimitation. *Systematic Biology* 56: 879–886. <https://doi.org/10.1080/10635150701701083>
- Dick CW, Roubik DW, Gruber KF, Bermingham E (2004) Long-distance gene flow and cross-Andean dispersal of lowland rainforest bees (Apidae: Euglossini) revealed by comparative mitochondrial DNA phylogeography. *Molecular Ecology* 13: 3775–3785. <https://doi.org/10.1111/j.1365-294X-2004.02374.x>
- Eltz T, Fritsch F, Pech JR, Zimmermann Y, Ramírez SR, Quezada-Euán JJG, Bembé B (2011) Characterization of the orchid bee *Euglossa viridissima* (Apidae: Euglossini) and a novel cryptic sibling species, by morphological, chemical, and genetic characters. *Zoological Journal of the Linnean Society* 163: 1064–1076. <https://doi.org/10.1111/j.1096-3642.2011.00740.x>
- Evangelista O, Sakakibara AM, Cryan JR, Urban JM (2012) A phylogeny of the treehopper subfamily Heteronotinae reveals convergent pronotal traits (Hemiptera: Auchenorrhyncha: Membracidae). *Systematic Entomology* 42: 410–428. <https://doi.org/10.1111/syen.12221>
- Faircloth BC (2013) Illumiprocessor: a trimmomatic wrapper for parallel adapter and quality trimming. <https://doi.org/10.6079/J9ILL>

- Faircloth BC (2016) PHYLUCE is a software package for the analysis of conserved genomic loci. *Bioinformatics* 32: 786–788. <https://doi.org/10.1093/bioinformatics/btv646>
- Faria LRR, Melo GAR (2020) Orchid bees (Euglossini). In: Starr C (Ed.) *Encyclopedia of Social Insects*. Springer, Cham, 1–6. https://doi.org/10.1007/978-3-319-90306-4_91-1
- Ferrari BR, Melo GAR (2014) Deceiving colors: recognition of color morphs as separate species in orchid bees is not supported by molecular evidence. *Apidologie* 45: 641–652. <https://doi.org/10.1007/s13592-014-0280-7>
- Folmer O, Black M, Hoeh W, Lutz R, Vrijenhoek R (1994) DNA primers for amplification of mitochondrial cytochrome c oxidase subunit I from diverse metazoan invertebrates. *Molecular Marine Biology and Biotechnology* 3: 294–299.
- Francisco FO, Nunes-Silva P, Francoy TM, Wittmann D, Imperatriz-Fonseca VL, Arias MC, Morgan ED (2008) Morphometrical, biochemical and molecular tools for assessing biodiversity. An example in *Plebeia remota* (Holmberg, 1903) (Apidae, Meliponini). *Insectes Sociaux* 55: 231–237. <https://doi.org/10.1007/s0004-008-0992-7>
- Francoy TM, de Faria Franco F, Roubik DW (2012) Integrated landmark and outline-based morphometric methods efficiently distinguish species of *Euglossa* (Hymenoptera, Apidae, Euglossini). *Apidologie* 43: 609–617. <https://doi.org/10.1007/s13592-012-0132-2>
- Francoy TM, Grassi ML, Imperatriz-Fonseca VL, May-Itzá WJ, Quezada-Euán JGG (2011) Geometric morphometrics of the wing as a tool for assigning genetic lineages and geographic origin to *Melipona beecheii* (Hymenoptera: Meliponini). *Apidologie* 42: 499–507. <https://doi.org/10.1007/s13592-011-0013-0>
- Gibbs J (2009) Integrative taxonomy identifies new (and old) species in the *Lasioglossum* (*Dialictus*) *tegulare* (Robertson) species group (Hymenoptera, Halictidae). *Zootaxa* 2032: 1–38. <https://doi.org/10.11646/zootaxa.2032.1.1>
- Glenn TC, Pierson TW, Bayona-Vásquez NJ, Kieran TJ, Hoffberg SL, Thomas IVJC, Lefever DE, Finger JJW, Gao B, Bian X, Louha S, Kolli RT, Bentley K, Rushmore J, Wong K, Shaw TI, Rothrock JMJ, McKee AM, Guo TL, Mauricio R, Molina M, Cummings BS, Lash LH, Lu K, Gilbert GS, Hubbell SP, Faircloth BC (2019) Adapterama II: universal amplicon sequencing on Illumina platforms (TaggiMatrix). *PeerJ* 7: e7786. <https://doi.org/10.7717/peerj.7786>
- Godoy RE, Shimabukuro PHF, Santos TV, Pessoa FAC, Cunha AEFL, Santos FKM, Vilela ML, Rangel EF, Galati EAB (2018) Geometric morphometry of the head in sand flies (Diptera: Psychodidae: Phlebotominae), an alternative approach to taxonomy studies. *Zootaxa* 4504: 566–576. <https://doi.org/10.11646/zootaxa.4504.4.7>
- Goldstein PZ, DeSalle R (2010) Integrating DNA barcode data and taxonomic practice: determination, discovery, and description. *Bioessays* 33: 135–147. <https://doi.org/10.1002/bies.201000036>
- Grab H, Branstetter MG, Amon N, Urban-Mead KR, Park MG, Gibbs J, Blitzer EJ, Poveda K, Loeb G, Danforth BN (2019) Agriculturally dominated landscapes reduce bee phylogenetic diversity and pollination services. *Science* 363: 282–284. <https://doi.org/10.1126/Science.aat6016>
- Grando C, Amon ND, Clough SJ, Guo N, Wei W, Azevedo P, López-Uribe MM, Zucchi MI (2018) Two colors, one species: the case of *Melissodes nigroaenea* (Apidae: Eucerini), an important pollinator of cotton fields in Brazil. *Sociobiology* 65: 645–653. <https://doi.org/10.13102/sociobiology.v65i4.3464>

- Grassi-Sella ML, Garófalo CA, Francoy TM (2018) Morphological similarity of widely separated populations of two Euglossini (Hymenoptera; Apidae) species based on geometric morphometrics wings. *Apidologie* 49: 151–161. <https://doi.org/10.1007/s13592-017-0536-0>
- Gueuning M, Frey JE, Praz C (2020) Ultraconserved yet informative for species delimitation: UCEs resolve long-standing systematic enigma in Central European bees. *Molecular Ecology* 29: 4203–4220. <https://doi.org/10.1111/mec.15629>
- Guindon S, Dufayard JF, Lefort V, Anisimova M, Hordijk W, Gascuel O (2010) New algorithms and methods to estimate maximum likelihood phylogenies: assessing the performance of phylml 3.0. *Systematic Biology* 59: 307–321. <https://doi.org/10.1093/sysbio/syq010>
- Gutiérrez-Chacón C, Fornoff F, Ospina-Torres R, Klein A-M (2018) Pollination of *Granadilla* (*Passiflora ligularis*) benefits from large wild insects. *Journal of Economic Entomology* 111: 1526–1534. <https://doi.org/10.1093/jee/toy133>
- Hebert PDN, Cywinska A, Ball SL, de Waard JR (2003) Biological identifications through DNA barcodes. *Proceedings of the Royal Society Biological Sciences* 270: 313–321. <https://doi.org/10.1098/rspb.2002.2218>
- Heled J, Drummond AJ (2010) Bayesian inference of species trees from multilocus data. *Molecular Biology and Evolution* 27: 570–580. <https://doi.org/10.1093/molbev/msp274>
- Hoang DT, Chernomor O, von Haeseler A, Minh BQ, Vinh LS (2018) UFBoot2: Improving the ultrafast bootstrap approximation. *Molecular Biology and Evolution* 35: 518–522. <https://doi.org/10.1093/molbev/msx281>
- Huang J, Wu J, An J, Williams PH (2015) Newly discovered colour-pattern polymorphism of *Bombus koreanus* females (Hymenoptera: Apidae) demonstrated by DNA barcoding. *Apidologie* 46: 250–261. <https://doi.org/10.1007/s13592-014-0319-9>
- Hurtado-Burillo M, Jara L, May-Itzá WJ, Quezada-Euán JGG, Ruiz C, Rúa P (2016) A geometric morphometric and microsatellite analyses of *Scaptotrigona mexicana* and *S. pectoralis* (Apidae: Meliponini) sheds light on the biodiversity of Mesoamerican stingless bees. *Journal of Insect Conservation* 20: 753–763. <https://doi.org/10.1007/s10841-016-9899-1>
- Kalyaanamoorthy S, Minh BQ, Wong TKF, von Haeseler A, Jermiin LS (2017) ModelFinder: Fast model selection for accurate phylogenetic estimates. *Nature Methods* 14: 587–589. <https://doi.org/10.1038/nmeth.4285>
- Katoh K, Standley DM (2013) MAFFT multiple sequence alignment software version 7: improvements in performance and usability. *Molecular Biology and Evolution* 30: 772–780. <https://doi.org/10.1093/molbev/mst010>
- Katoh K, Rozewicki J, Yamada KD (2019) MAFFT online service: multiple sequence alignment, interactive sequence choice and visualization. *Briefings in Bioinformatics* 20: 1160–1166. <https://doi.org/10.1093/bib/bbx108>
- Kim CK, Byrne LB (2006) Biodiversity loss and the taxonomic bottleneck: emerging biodiversity science. *Ecological Research* 21: 794–810. <https://doi.org/10.1007/s11284-006-0035-7>
- Klingenberg CP (2011) MorphoJ: an integrated software package for geometric morphometrics. *Molecular Ecology Resources* 11: 353–357. <https://doi.org/10.1111/j.1755-0998.2010.02924.x>
- Klingenberg CP (2015) Analyzing fluctuating asymmetry with geometric morphometrics: concepts, methods, and applications. *Symmetry* 7: 843–934. <https://doi.org/10.3390/sym7020843>

- Kumar S, Stecher G, Li M, Knyaz C, Tamura K (2018) Mega X. Molecular evolutionary genetics analysis across computing platforms. *Molecular Biology and Evolution* 35: 1547–1549. <https://doi.org/10.1093/molbev/msy096>
- Lachenbruch PA (1967) An almost unbiased method of obtaining confidence intervals for the probability of misclassification in discriminant analysis. *Biometrics* 23: 639–645. <https://doi.org/10.2307/2528418>
- Lanfear R, Frandsen PB, Wright AM, Senfeld T, Calcott B (2017) PartitionFinder 2: new methods for selecting partitioned models of evolution for molecular and morphological phylogenetic analyses. *Molecular Biology and Evolution* 34: 772–773. <https://doi.org/10.1093/molbev/msw2560>
- Lepeco A, Gonçalves RB (2018) The colour and the shape: Morphological variation on a facultatively eusocial bee *Augochlora (Augochlora) amphitrite* (Schrottky). *Sociobiology* 65: 662–670. <https://doi.org/10.13102/sociobiology.v65i4.3388>
- Lepeletier de Saint Fargeau, A LM (1841) *Histoire Naturelle des Insectes, Hyménoptères, Vol. 2*. Librairie Encyclopédique de Roret, Paris, 680 pp.
- López-Urbe MM, Zamudio KR, Cardoso CF, Danforth BN (2014) Climate, physiological tolerance and sex-biased dispersal shape genetic structure of Neotropical orchid bees. *Molecular Ecology* 23: 1874–1890. <https://doi.org/10.1111/mec.12689>
- Machado C, Costa CP, Franco TM (2018) Different physiognomies and the structure of Euglossini bee (Hymenoptera: Apidae) communities. *Sociobiology* 65: 471–481. <https://doi.org/10.13102/sociobiology.v65i3.2718>
- Marques MF, Hautequest AP, Oliveira UB, Manhães-Tavares VF, Perles OR, Zappes CA, Gaglianone MC (2017) Local knowledge on native bees and their role as pollinators in agricultural communities. *Journal of Insect Conservation* 21: 345–356. <https://doi.org/10.1007/s10841-017-9981-3>
- Martel C, Gerlach G, Ayasse M, Milet-Pinheiro P (2019) Pollination ecology of the Neotropical gesneriad *Gloxinia perennis*: chemical composition and temporal fluctuation of floral perfume. *Plant Biology* 21: 723–731. <https://doi.org/10.1111/plb.12974>
- Melo GAR (2014) Notes on the systematics of the orchid bee genus *Eulaema* (Hymenoptera: Apidae). *Revista Brasileira de Entomologia* 58: 235–240. <https://doi.org/10.1590/S0085-56262014000300003>
- Michener CD (2007) *The Bees of the World*, 2nd Edn. Johns Hopkins University Press, Baltimore.
- Moure JS (1960) Notes on the types of Neotropical bees described by Fabricius (Hymenoptera: Apoidea). *Studia Entomologica* 3: 97–160.
- Moure JS (2000) As espécies do gênero *Eulaema* Lepeletier, 1841 (Hymenoptera, Apidae, Euglossinae). *Acta Biologica Paranaense* 29: 1–70. <https://doi.org/10.5380/abpr.v29i0.582>
- Moure JS, Melo GAR (2022) Euglossini Latreille, 1802. In: Moure JS, Urban D, Melo GAR (Orgs) *Catalogue of Bees (Hymenoptera, Apoidea) in the Neotropical Region - online version*. <http://www.moure.cria.org.br/catalogue> [Accessed Aug/27/2022. Online since: 23 Jul 2008. Last update: 14 Apr 2022]
- Nemésio A (2009) Orchid bees (Hymenoptera: Apidae) of the Brazilian Atlantic Forest. *Zootaxa* 2041: 1–242. <https://doi.org/10.11646/zootaxa.2041.1.1>
- Nguyen LT, Schmidt HA, von Haeseler A, Minh BQ (2015) IQ-TREE: A fast and effective stochastic algorithm for estimating maximum likelihood phylogenies. *Molecular Biology and Evolution* 32: 268–274. <https://doi.org/10.1093/molbev/msu300>

- Okonechnikov K, Golosova O, Fursov M (2012) Unipro UGENE: a unified bioinformatics toolkit. *Bioinformatics* 28: 1166–1167. <https://doi.org/10.1093/bioinformatics/bts091>
- Oleksa A, Tofilski A (2014) Wing geometric morphometrics and microsatellite analysis provide similar discrimination of honey bee subspecies. *Apidologie* 46: 49–60. <https://doi.org/10.1007/s13592-014-0300-7>
- Oliveira ML (2000) O gênero *Eulaema* Lepeletier, 1841 (Hymenoptera: Apidae: Euglossini): filogenia, biogeografia e relações com as Orchidaceae. PHD Thesis. Universidade de São Paulo (Brazil), 160 pp.
- Oliveira ML (2006) Três novas espécies de abelhas da Amazônia pertencentes ao gênero *Eulaema* Lepeletier, 1841 (Hymenoptera: Apidae: Euglossini). *Acta Amazonica* 36: 273–286. <https://doi.org/10.1590/S0044-59672006000100015>
- Packer L, Gibbs J, Sheffield C, Hanner R (2009) DNA barcoding and the mediocrity of morphology. *Molecular Ecology Resources* 9: 42–50. <https://doi.org/10.1111/j.1755-0998.2009.02631.x>
- Padial JM, De La Riva I (2007) Integrative taxonomists should use and produce DNA barcodes. *Zootaxa* 1586: 67–68. <https://doi.org/10.11646/ZOOTAXA.1586.1.7>
- Padial JM, Miralles A, De La Riva I, Vences M (2010) The integrative future of taxonomy. *Frontiers in Zoology* 7: 16. <https://doi.org/10.1186/1742-9994-7-16>
- Pires EP, Morgado LN, Souza B, Carvalho CF, Nemésio A (2013) Community of orchid bees (Hymenoptera: Apidae) in transitional vegetation between Cerrado and Atlantic Forest in southeastern Brazil. *Brazilian Journal of Biology* 73: 507–513. <https://doi.org/10.1590/S1519-69842013000300007>
- Pokorny T, Lunau K, Quezada-Euán JJG, Eltz T (2014) Cuticular hydrocarbons distinguish cryptic sibling species in *Euglossa* orchid bees. *Apidologie* 45: 276–283. <https://doi.org/10.1007/s13592-013-0250-5>
- Quezada-Euán JJG, Sheets HD, de Luna E, Eltz T (2015) Identification of cryptic species and morphotypes in male *Euglossa*: Morphometric analysis of forewings (Hymenoptera: Euglossini). *Apidologie* 46: 787–795. <https://doi.org/10.1007/s13592-015-0369-7>
- Rambaut A (2018) Figtree: tree figure drawing tool version 1.4.4. <http://tree.bio.ed.ac.uk/software/figtree>
- Rambaut A, Drummond AJ, Xie D, Baele G, Suchard MA (2018) Posterior summarization in Bayesian phylogenetics using Tracer 1.7. *Systematic Biology* 67(5): 901–904. <https://doi.org/10.1093/sysbio/syy032>
- Rocha-Filho LC, Garófalo CA (2015) Males of the orchid bee *Eulaema cingulata* (Hymenoptera: Apidae) as important vectors of the cleptoparasitic beetle *Meloetyphlus fuscatus* (Coleoptera: Meloidae). *Apidologie* 46: 286–291. <https://doi.org/10.1007/s13592-014-0322-1>
- Rocha-Filho LC, Cerântola NCM, Garófalo CA, Imperatriz-Fonseca VL, Del Lama MA (2013) Genetic differentiation of the Euglossini (Hymenoptera, Apidae) populations on a mainland coastal plain and an island in southeastern Brazil. *Genetica* 141: 65–74. <https://doi.org/10.1007/s10709-013-9706-9>
- Rohland N, Reich D (2012) Cost-effective, high-throughput DNA sequencing libraries for multiplexed target capture. *Genome Resources* 22: 939–946. <https://doi.org/10.1101/gr.128124.111>

- Rohlf FJ (2006) TpsDig, 2.0. Department of Ecology and Evolution, State Univ. of New York at Stony Brook, Stony Brook, NY.
- Rohlf FJ (2013) TpsUtil. Department of Ecology and Evolution, State University of New York, Stony Brook, NY, USA. <http://life.bio.sunysb.edu/morph/>
- Ronquist F, Teslenko M, Mark PVD, Ayres DL, Darling A, Höhna S, Larget B, Liu L, Suchard MA, Huelsenbeck J (2012) MrBayes 3.2: Efficient Bayesian phylogenetic inference and model choice across a large model space. *Systematic Biology* 61: 539–542. <https://doi.org/10.1093/sysbio/sys029>
- Rubinoff D, Cameron S, Will K (2006) A genomic perspective on the shortcomings of mitochondrial DNA for “barcoding” identification. *Journal of Heredity* 97: 581–594. <https://doi.org/10.1093/jhered/esl036>
- Schlick-Steiner BC, Steiner FM, Seifert B, Stauffer C, Christian E, Crozier RH (2010) Integrative taxonomy: a multisource approach to exploring biodiversity. *Annual Review of Entomology* 55: 421–438. <https://doi.org/10.1146/annurev-ento-112408-085432>
- Silva FL, Grassi-Sella ML, Francoy TM, Costa AHR (2015) Evaluating classification and feature selection techniques for honeybee subspecies identification using wing images. *Computers and Electronics in Agriculture* 114: 68–77. <https://doi.org/10.1016/j.compag.2015.03.012>
- Silveira GC, Freitas RF, Tosta THA, Rabelo LC, Gaglianone MC, Augusto SC (2015) The orchid bee fauna in the Brazilian savanna: do forest formations contribute to higher species diversity? *Apidologie* 46: 197–208. <https://doi.org/10.1007/s13592-014-0314-1>
- Smith BT, Harvey MG, Faircloth BC, Glenn TC, Brumfield RT (2013) Target capture and massively parallel sequencing of ultraconserved elements (UCEs) for comparative studies at shallow evolutionary time scales. *Systematic Biology* 63: 83–95. <https://doi.org/10.1093/sysbio/syt061>
- Souza DA, Wang Y, Kaftanoglu O, De Jong D, Amdam GV, Gonçalves LS, Francoy TM (2015) Morphometric identification of queens, workers and intermediates in *In Vitro* reared honey bees (*Apis mellifera*). *PLoS ONE* 10: e0123663. <https://doi.org/10.1371/journal.pone.0123663>
- Sukumaran J, Knowles LL (2017) Multispecies coalescent delimits structure, not species. *Proceedings of the National Academy of Sciences* 114: 1607–1612. <https://doi.org/10.1073/pnas.1607921114>
- Tagliacollo VA, Lanfear R (2018) Estimating improved partitioning schemes for ultraconserved elements. *Molecular Biology and Evolution* 35: 1798–1811. <https://doi.org/10.1093/molbev/msy069>
- Watteyn C, Scaccabarozzi D, Muys B, Meerbeek K, Ackerman JD, Fonseca MVC, Alvarado IFC, Reubens B, Huarcaya RP, Cuzzolino S, Karremans AP (2021) Trick or treat? Pollinator attraction in *Vanilla pompona* (Orchidaceae). *Biotropica* 54: 268–274. <https://doi.org/10.1111/btp.13034>
- Wheeler QD (2008) Undisciplined thinking: morphology and Hennig’s unfinished revolution. *Systematic Entomology* 33: 2–7. <https://doi.org/10.1111/j.1365-3113.2007.00411.x>
- Zhang C, Rabiee M, Sayyari E, Mirarab S (2018) ASTRAL-III: polynomial time species tree reconstruction from partially resolved gene trees. *BMC Bioinformatics* 19: 153. <https://doi.org/10.1186/s12859-018-2129-y>

Supplementary material I

Integrative taxonomy of *Eulaema cingulata*

Authors: Tamires de Oliveira Andrade, Kelli dos Santos Ramos, Margarita M. López-Uribe, Michael G. Branstetter, Carlos Roberto F. Brandão

Data type: tables (ms word file)

Explanation note: tables: Voucher ID, locality data, and institutional repositories of the male specimens of *Eulaema* used in Geometric Morphometric analyses; Voucher ID, locality data, and institutional repositories of the specimens used both in COI and phylogenomic analyses; Results of the Principal Component Analysis (PCA) of head analysis with their respective percentage of variance; Results of the Principal Component Analysis (PCA) of wing analysis with their respective percentage of variance.

Copyright notice: This dataset is made available under the Open Database License (<http://opendatacommons.org/licenses/odbl/1.0/>). The Open Database License (ODbL) is a license agreement intended to allow users to freely share, modify, and use this Dataset while maintaining this same freedom for others, provided that the original source and author(s) are credited.

Link: <https://doi.org/10.3897/jhr.94.91001.suppl1>

A checklist of South Dakota bumble bees (Hymenoptera, Apidae)

Abigail P. Martens^{1,2}, Paul J. Johnson², Eric A. Beckendorf¹,
Louis S. Hesler¹, Jesse D. Daniels¹, Karl A. Roeder¹

1 USDA, Agricultural Research Service, North Central Agricultural Research Laboratory, Brookings, SD 57006, USA **2** South Dakota State University, Insect Biodiversity Lab, Severin-McDaniel Insect Research Collection, Brookings, SD 57007, USA

Corresponding author: Karl A. Roeder (karl.roeder@usda.gov)

Academic editor: C.K. Starr | Received 7 September 2022 | Accepted 18 November 2022 | Published 20 December 2022

<https://zoobank.org/27EF03AB-8145-4906-90DF-AAE312531151>

Citation: Martens AP, Johnson PJ, Beckendorf EA, Hesler LS, Daniels JD, Roeder KA (2022) A checklist of South Dakota bumble bees (Hymenoptera, Apidae). *Journal of Hymenoptera Research* 94: 271–286. <https://doi.org/10.3897/jhr.94.94584>

Abstract

Several bumble bee species (*Bombus* Latreille) are declining and efforts to conserve populations will be strengthened by an improved knowledge of their geographic distribution. Knowledge gaps exist, however, especially in central portions of North America. Here we report 29 species of bumble bees from South Dakota in the north-central USA, based on 130 years of records from 1891 to 2021. Specimens or observations were available for >90% of the 66 counties, though they were not distributed evenly as most records came from Pennington, Lawrence, Custer, Brookings, and Day Counties. The five most commonly collected or reported bumble bee species were *B. griseocollis* (54 counties), *B. pensylvanicus* (41 counties), *B. fervidus* (39 counties), *B. huntii* (27 counties), and *B. bimaculatus* (25 counties). Twenty species were recorded from 10 or fewer counties. Despite differences in occurrence, 66% of the *Bombus* species in South Dakota were collected or observed since 2020, including six of the nine species of conservation concern (*B. fraternus*, *B. pensylvanicus*, *B. fervidus*, *B. occidentalis*, *B. terricola*, and *B. morrisoni*). However, the critically endangered *B. affinis*, *B. variabilis*, and *B. suckleyi* have not been collected or observed for over 50 years. While this checklist is the first for South Dakota bumble bees in nearly 100 years, data are still lacking as ~55% of counties had fewer than five species reported. We suggest future efforts should focus on these under-sampled areas to fill in baseline knowledge of the wild bee fauna towards completing a more holistic view of bumble bee distributions across the Great Plains.

Keywords

Bombus, community science, conservation, faunal inventory, IUCN Red List, museum collections, natural history, pollinator

Introduction

There are more than 20,000 described species of bees (Hymenoptera: Apoidea, Anthophila) worldwide exhibiting a vast diversity of morphology, diet, and social structure (Michener 2007; Danforth et al. 2013; Engel et al. 2021). Roughly 5,200 bee species are known from North America north of Mexico (Ascher and Pickering 2020). Bee diversity is critical for ecosystem function (Genung et al. 2017; Winfree et al. 2018) and is essential for conserving many habitats by way of generalist and specialist plant-pollinator interactions (Kearns et al. 1998; Biesmeijer et al. 2006). Indeed, bees are vital pollinators of native vegetation and cultivated plants in most habitats throughout the world (Losey et al. 2006; Ollerton et al. 2011; Reilly et al. 2020) with certain groups like bumble bees (*Bombus* spp.) providing pollination services worth \$963 USD per hectare on average (Kleijn et al. 2015). Important crops pollinated by bumble bees include blueberries, cranberries, cucumbers, field beans, melons, peppers, and tomatoes (Stubbs and Drummond 2001; Goulson et al. 2008; Cooley and Vallejo-Marín 2021). However, despite their economic importance, charisma, large size, and conspicuous nature, little is known about the abundance, diversity, and distribution of bumble bees across much of the Great Plains.

The status of bumble bees in a substantial portion of the Great Plains remains an open question, as the distributions of many species must be interpolated from published records for species known east of the Mississippi River and from the Rocky Mountains westward (Colla et al. 2011; Koch et al. 2012). Such data discrepancies limit the ability to infer population changes at local and landscape levels despite well-documented bumble bee declines elsewhere (Colla and Packer 2008; Grixti et al. 2009; Cameron et al. 2011; Wood et al. 2019; Hemberger et al. 2021; Novotny et al. 2021). Moreover, the International Union for Conservation of Nature (IUCN) lists five bumble bee species as critically endangered, two species as endangered, five as vulnerable, and one as near threatened in North America, suggesting that almost 30% of the 46 bumble bee species in the continental United States may be at risk (Williams et al. 2014; IUCN 2022). Bumble bees are clearly a group of conservation concern (Goulson et al. 2008; Potts et al. 2010; Colla et al. 2012; Graves et al. 2020; Mola et al. 2021) and knowledge gaps in states like South Dakota are especially apparent as comprehensive statewide pollinator surveys have not been conducted.

South Dakota is a promising state for studying bumble bees as it is situated in the geographic center of North America. Species distribution patterns in the state reflect the classic post-Pleistocene models showing eastern species moving into eastern deglaciated areas from southern and eastern periglacial regions, and western species inhabiting the Black Hills, Rocky Mountains, and peripheral central plains forested areas then moving eastward post-glacially (Hines 2008) or with scattered relict populations. Prior to Euro-American colonization, the South Dakota landscape was dominated by diverse assemblages of native showy forbs and grasses. Settlement of the state east of the Missouri River began in the late 1850's and by the late 1870's nearly all arable land in the eastern portion of the state had been converted from tallgrass prairie to pasture grazing and cultivated land for crops (Gartner and Sieg 1996; Witt et al. 2013). The central and western

regions of the state, excepting the Black Hills, were primarily composed of shortgrass prairie prior to intensive colonization in the 1880's, but were subjected to intensive open range grazing by cattle and sheep. The Black Hills were and remain a mosaic of dense conifer forest, meadows, and fire-maintained aspen expanses and conifer savannas.

The near elimination of bison in favor of cattle and resultant overgrazing severely degraded the native vegetation and landscape. This was followed by the introduction of and subsequent invasion by exotic cool-season grasses like smooth brome (*Bromus inermis*) and Kentucky bluegrass (*Poa pratensis*) which were introduced for cattle forage and erosion control (Grant et al. 2020; Palit et al. 2021). These exotic grass species have invaded almost all remnant prairie sites of the Prairie Coteau region in the northeastern portion of the state, choking out the native grasses and forbs necessary to preserve and support native species diversity (Grant et al. 2009; Toledo et al. 2014). Substantial natural habitat loss has occurred in the state over the last 170 years due to agricultural intensification and colonization with up to 5% of grasslands in the Western Corn Belt being converted to row crop agriculture annually (Wright and Wimberly 2013). This is especially prevalent in eastern South Dakota where prairie remnant sites are at risk of conversion to cropland (Wimberly et al. 2017). More recently, the amount of undisturbed Conservation Reserve Program land, which could act as an important resource for pollinators, has likewise declined nationally since 2007.

As the landscape of South Dakota continues to change, baseline knowledge of the wild bee fauna will be essential for understanding biodiversity, species distributions, and population trajectories, as well as for focusing conservation strategies (LeBuhn et al. 2012; Kilpatrick et al. 2020). Thorough faunal inventories also aid in identifying knowledge gaps (e.g., under-sampled areas, seasons, and species), thus improving targeted sampling in future studies (Kilpatrick et al. 2020). The last comprehensive checklist of the bumble bees of South Dakota (Severin 1925) is nearly 100 years old and reported 20 species from the state. Since then, bumble bees have been sampled as part of smaller regional surveys, graduate research projects, and community science efforts in South Dakota, leading to thousands of records within institutional collections, online databases, and research publications (Andress 1971; Milliron 1971, 1973a, b; Drons 2012; Koch et al. 2015; Martens and Johnson 2021; Vilella-Arnizaut et al. 2022).

Here we present a revised list of bumble bee species by consolidating published records and observations to present a comprehensive checklist of bumble bees from South Dakota. This complements the old list from Nebraska (Laberge and Webb 1962), the recent list from Montana (Dolan et al. 2017), and broader distributions given by Williams et al. (2014) and online databases and identification tools.

Materials and methods

We compiled historical South Dakota bumble bee records from 1891 to 2021 from 23 institutional insect collections and two community-science observational databases. Records of South Dakota bumble bees at 21 of the institutions are from searches of two online databases: the Symbiota Collections of Arthropods Network (SCAN) and

the Global Biodiversity Information Facility (GBIF). Additional data were derived from offline digital records of bumble bee specimens at the Severin-McDaniel Insect Research Collection, Brookings, South Dakota, and at the North Central Agricultural Research Laboratory, Brookings, South Dakota. Williams et al. (2014) was also consulted about overall *Bombus* distributions throughout the state. Observational data were compiled from authoritatively identified records of bumble bees posted online at iNaturalist.org and BugGuide.net. Specimens were considered authoritatively identified if they possessed ‘Research Grade’ status on iNaturalist or were identified by a recognized bumble bee taxonomic expert. We compiled data on county and year in which individual bumble bees were collected. New bumble bee specimens from a survey on the Prairie Coteau and sampling in the Fort Pierre National Grassland were vouchered into the Severin-McDaniel Insect Research Collection and are available for further study. New specimens from surveys were identified with the bumble bee key on DiscoverLife.org, Williams et al. (2014), and comparisons with specimens authoritatively identified by Sam Droege, and John Ascher on iNaturalist.org and BugGuide.net. Bumble bee nomenclature in this paper follows Williams et al. (2014).

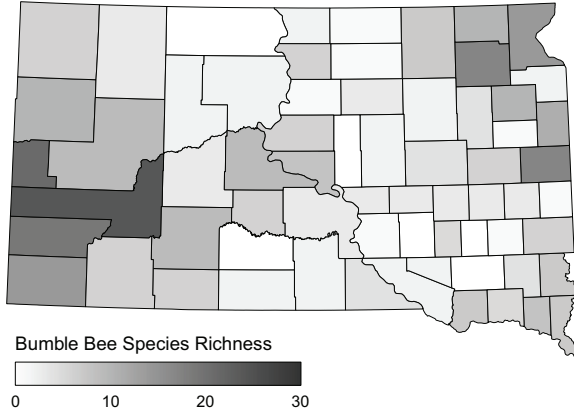
Results and discussion

We report 29 *Bombus* species in South Dakota based on a total of 9,202 records composed of 8,509 specimens from institutional collections and 693 community science observational records. Specimen records dated from 1891 to 2021, while observational records ranged from 2002 to 2021. All 29 bumble bee species were included among the institutional records, whereas only 19 species were recorded by observation (Figs 1, 2a). By comparison, South Dakota has more *Bombus* species than the surrounding states of Iowa (14 spp.), Minnesota (24 spp.), Montana (28 spp.), Nebraska (20 spp.), North Dakota (23 spp.), and Wyoming (24 spp.) (Colla et al. 2011; Koch et al. 2012; Williams et al. 2014; Dolan et al. 2017; Hartman et al. 2019; Bell and Tronstad 2021; Pei et al. 2022; Xerces Bumble Bee Atlas projects for IA, ND, NE, MN).

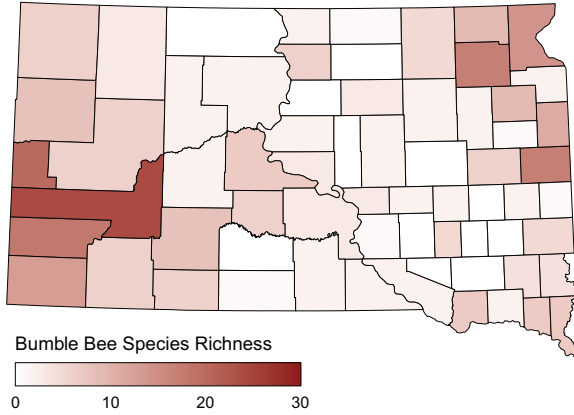
Spatial patterns and sampling biases

Specimens and observations of bumble bee species were recorded from 60 of the 66 counties in South Dakota, though they were not distributed evenly (Fig. 1). Most records were skewed toward Pennington, Lawrence, Custer, Brookings, and Day Counties. Those five counties had the most bumble bee records in the state due to tourist attractions (Black Hills National Forest, Custer State Park, Badlands National Park, and state recreation areas), the state land grant institution, and dedicated sampling efforts. Observations occurred primarily in or near population centers with the majority coming from the Black Hills counties of Pennington, Custer, Fall River, and Lawrence in western South Dakota (Fig. 1). In contrast, 36 of the 66 counties (54.5%) had fewer than five bumble bee species reported. Because most of these counties are in more remote regions of the state, we attribute their lower species richness to under-

Specimens + Observations



Specimens



Observations

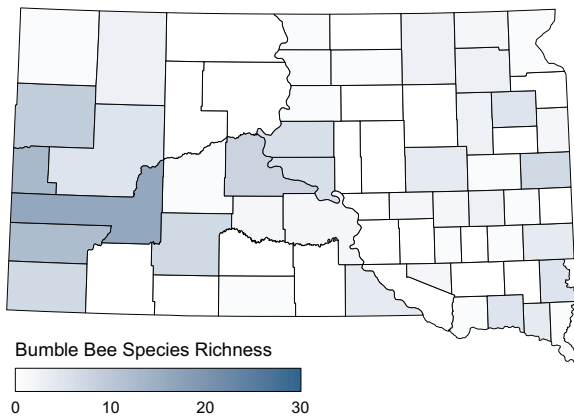


Figure 1. Geographic distribution of bumble bees (*Bombus* spp.) in South Dakota. Panels show either the combined records from specimens and observations (top/grey), just specimen records from insect collections (middle/red), or just observation records from community science databases (bottom/blue).

sampling. We anticipate these counties to have species diversity similar to adjacent and better-sampled counties though this can only be confirmed with focused sampling efforts. Because ~80% of land is privately-owned in the state, sampling *Bombus* diversity effectively in many areas will require developing relationships with private landowners.

The number of county records varied considerably among *Bombus* species. For instance, the most common and widespread bumble bee in South Dakota, *B. griseocollis*, was recorded from 54 counties. *Bombus fervidus* and *B. pensylvanicus* showed distribution patterns similar to *B. griseocollis*, with both species occurring statewide in 39 and 41 counties respectively. Conversely, 20 species were recorded from only 10 or fewer counties (Fig. 2). The majority (83%) of *Bombus* species from the state have been collected or observed after 1994 with 19 of the 29 known species being recorded since 2020, including six of the nine species of conservation concern (*B. fraternus*, *B. pensylvanicus*, *B. fervidus*, *B. occidentalis*, *B. terricola*, and *B. morrisoni*). However, five species have not been recovered since 1974 or earlier (Fig. 2b) including the three remaining species of conservation concern: *B. affinis* (critically endangered, not since 1952), *B. variabilis* (critically endangered, not since 1958), and *B. suckleyi* (critically endangered, not since 1969). In addition, *B. melanopygus*, *B. bohemicus*, and *B. citrinus* have not been reported in South Dakota since 1963, 1974, and 1994. The status of

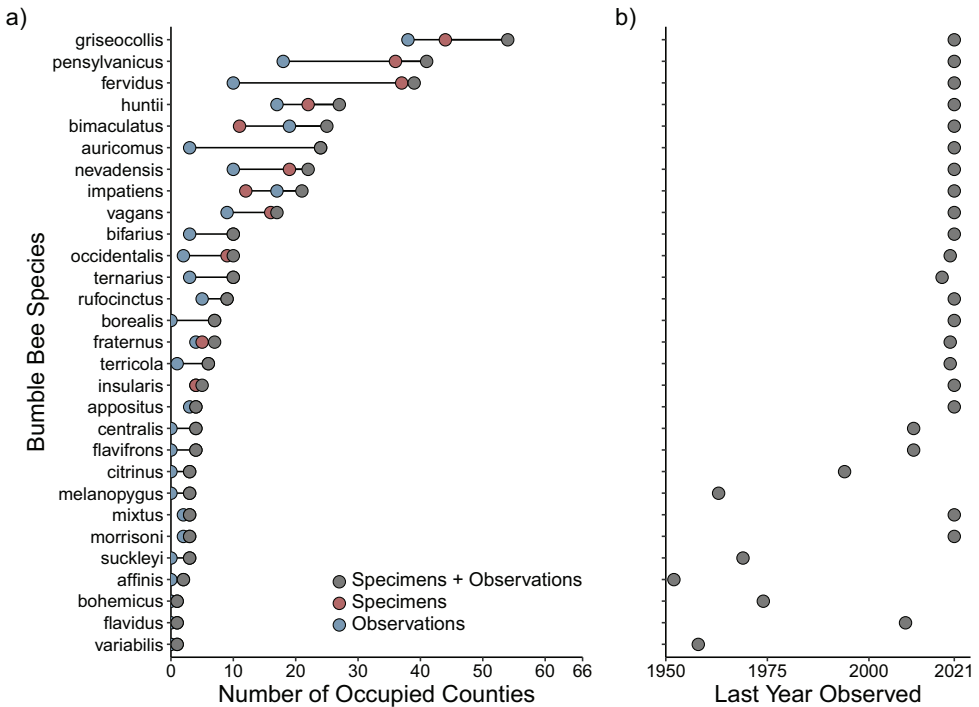


Figure 2. Number of occupied counties and last year observed for each of the 29 bumble bee species (*Bombus* spp.) in South Dakota. Panel **a** shows the number of counties (out of 66) that a bumble bee species has been either observed (blue), collected (red), or both (grey). Panel **b** shows the last year each bumble bee species was collected and/or observed in South Dakota.

B. melanopygus and *B. bohemicus* in the state today is unknown, however we anticipate *B. citrinus* to still occur in South Dakota due to its more recent sighting.

Several *Bombus* species are restricted to the western portion of the state, particularly Pennington, Lawrence, and Custer counties. This is due, in part, to the drastic landscape and elevational transitions encountered in these counties from the mixed and short-grass prairie-dominated landscape of the Great Plains and Badlands to the ponderosa pine and spruce-aspen communities of the Black Hills. *Bombus* species from the Black Hills include species from the eastern United States like *B. impatiens* and western species that are often restricted to higher elevations such as *B. appositus*, *B. mixtus*, and *B. occidentalis*. While South Dakota has extensive overlap with the *Bombus* species from neighboring states, the following species are known from the region only in Montana and Wyoming: *B. balteatus*, *B. frigidus*, *B. sitkensis*, and *B. sylvicola*. *Bombus frigidus* is also known from iNaturalist observations in northern Minnesota. These species are primarily boreal-alpine specialists and prefer elevations higher than those found in the Black Hills. While most of these species are unlikely to occur in South Dakota due to a lack of suitable high-elevation habitat, *Bombus sylvicola* is reported historically from Crook County, Wyoming near the South Dakota border and could also occur in montane meadows in the South Dakota Black Hills. *Bombus sandersoni* was collected in north central Minnesota and across the Canadian Great Plains but is not reported from South Dakota. *Bombus perplexus* was collected in Minnesota and North Dakota and, though there appear to be small areas of suitable habitat in eastern South Dakota, has not been reported from the state.

All species of cuckoo bumble bees from the United States are historically reported from South Dakota i.e. *B. bohemicus*, *B. citrinus*, *B. flavidus*, *B. insularis*, *B. suckleyi*, and *B. variabilis*. Similarly, the hosts of these bees are also present in the state including widespread species like *B. pensylvanicus*, *B. fervidus*, and *B. rufocinctus*. *Bombus flavidus* is the most recent cuckoo species reported from South Dakota and is known from a series of four specimens collected in Pennington County in 2009. Similarly, *B. bohemicus* records are from a series of seven specimens collected in 1974 from Lawrence County. Records for *B. citrinus* span from 1929 to 1994 and are centered primarily in the eastern and northeastern counties of Brookings, Marshall, and Roberts. *Bombus insularis* and *B. suckleyi* are known from more than 50 specimens each with records dating from 1924 to 2021 and 1925 to 1969 respectively. Both species are primarily from western counties (Pennington, Lawrence, Fall River, and Custer) with two aberrant records of *B. insularis* from Clay County. The final cuckoo species, *B. variabilis* is known only from a single specimen reported from Brookings County in 1958.

Species of conservation concern

Nine IUCN-listed *Bombus* species are known from South Dakota (Fig. 3), comprising approximately one-third of the total species from the state. These include the critically endangered species *Bombus affinis*, *B. suckleyi*, and *B. variabilis*, the endangered species *B. fraternus*, and the vulnerable species *B. fervidus*, *B. morrisoni*, *B. occidentalis*, *B. pensylvanicus*, and *B. terricola*. Six of the nine IUCN-listed species, including

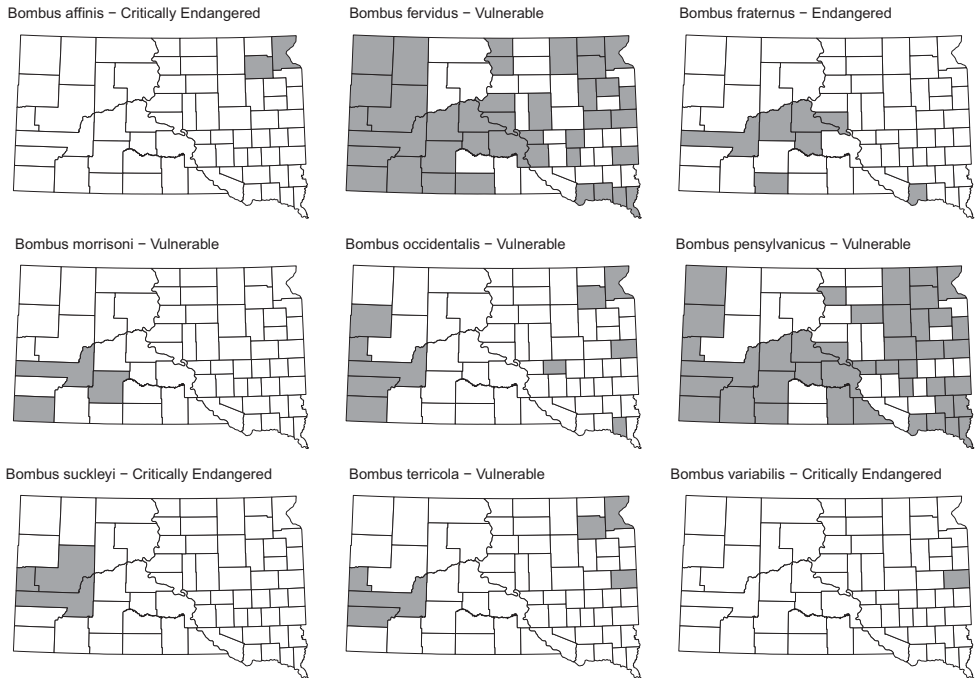


Figure 3. Geographic distribution for the nine critically endangered, endangered, and vulnerable bumble bee species in South Dakota from the International Union for Conservation of Nature (IUCN) Red List of Threatened Species.

B. fraternus, *B. fervidus*, *B. morrisoni*, *B. occidentalis*, *B. pensylvanicus*, and *B. terricola* were reported on observation-based platforms since 2020 highlighting the importance of community science in monitoring threatened species. Most of the IUCN-listed species have small geographic distributions in South Dakota with the critically endangered species *B. variabilis*, *B. affinis* and *B. suckleyi* observed in only one, two and three counties, respectively (Fig. 3). Moreover, the last records of *B. affinis*, *B. variabilis*, and *B. suckleyi* in South Dakota are from 1952, 1958, and 1969. Thus, we regard *B. affinis*, *B. suckleyi*, and *B. variabilis* as likely extirpated from South Dakota. The endangered species *B. fraternus* was reported from seven counties in the central and western parts of the state (Fig. 3). Three of the five vulnerable species, *B. morrisoni*, *B. terricola*, and *B. occidentalis*, were from occurrence records from three, six, and ten counties (Fig. 3). The remaining two vulnerable species, *B. fervidus* and *B. pensylvanicus*, were recorded from 39 and 41 counties and appear to have a nearly statewide distribution (Fig. 3).

Future work

The number of *Bombus* records from the state has slowly increased over time, with an exponential increase since the early 2000s corresponding to various pollinator research

projects. Yet we still lack records for ~10% of counties in South Dakota and fewer than five species records are available from ~55% of counties. Community science projects like the Great Plains Bumble Bee Atlas from the Xerces Society will undoubtedly help, but additional coordinated sampling efforts are needed to document *Bombus* species in under-sampled counties. Though we only anticipate reporting one or two additional new species from the state, possibly *B. perplexus* and *B. sylvicola*, adding new county records is important for understanding the distributions of species and will be necessary when considering the potential declines of these species. Moreover, future sampling efforts will need to take into consideration the vast tracts of private land and scattered small areas of public land available for surveying bumble bees in South Dakota. Establishing relationships with private landowners and communicating the importance of bumble bee species will be imperative for promoting the conservation of these charismatic and beneficial pollinators.

Acknowledgements

We thank all the bumble bee biologists who made this work possible. Harold Ikerd, Jonathan Koch, and Tommy McElrath were especially helpful in locating specimen records from the USDA Bee Biology and Systematics Laboratory and the Illinois Natural History Survey. John Ascher provided essential authoritative identifications of bumble bees, especially on iNaturalist.org and BugGuide.net. APM and PJJ are indebted to Savannah Allard, Vicki Kieszek, and Anne Bartz for their assistance in collecting and preparing bee specimens for the South Dakota Prairie Coteau project. Charlene Miller and the Sisseton-Wahpeton Oyate are thanked for their interest in the project and providing access to tribal lands during the project. Sam Droege, US Geological Survey, Native Bee Inventory and Monitoring Program, generously shared specimen identifications and locality data for specimens from Badlands National Park. Daniel Kim and Charlene Bessken (retired), U.S. Fish and Wildlife Service, Pierre, provided many records to online databases and generously shared observations. Eileen Dowd Stukel and the South Dakota Department of Game Fish and Parks Non-Game Program generously provided funding for surveys of native bees in the Black Hills and Prairie Coteau regions, and specimen processing. The USDA National Institutes of Food and Agriculture (NIFA) provided general support for this and other studies conducted in the Severin-McDaniel Insect Research Collection through the South Dakota Agricultural Experiment Station. EAB, LSH, JJD, and KAR were supported by base funds from USDA-ARS CRIS Project 3080-21220-006-00D. All authors would like to thank the anonymous reviewers that improved this manuscript. Mentions of trade names or commercial products in this publication is solely for the purpose of providing specific information and does not imply recommendation or endorsement by the U.S. Department of Agriculture or South Dakota State University. USDA and SDSU are equal opportunity providers and employers.

References

- Andress FP (1972) Biological studies of the bumblebees of eastern South Dakota. MS Thesis. South Dakota State University (Brookings).
- Ascher JS, Pickering J (2020) Discover Life bee species guide and world checklist (Hymenoptera: Apoidea: Anthophila). http://www.discoverlife.org/mp/20q?guide=Apoidea_species [accessed 14 June 2022]
- Bell C, Tronstad LM (2021) Distribution of declining bumble bees in central and eastern Wyoming. Report prepared by the Wyoming Natural Diversity Database for the Wyoming Office of the Bureau of Land Management, 1–13.
- Biesmeijer JC, Roberts SPM, Reemer M, Ohlemüller R, Edwards M, Peeters T, Schaffers AP, Potts SG, Kleukers R, Thomas CD, Settele J, Kunin WE (2006) Parallel declines in pollinators and insect-pollinated plants in Britain and the Netherlands. *Science* 313: 351–354. <https://doi.org/10.1126/science.1127863>
- BugGuide (2022) BugGuide. <https://bugguide.net/node/view/15740> [accessed 10 June 2022]
- Cameron SA, Lozier JD, Strange JP, Koch JB, Cordes N, Solter LF, Griswold TL (2011) Patterns of widespread decline in North American bumble bees. *Proceedings of the National Academy of Sciences of the United States of America* 108: 662–667. <https://doi.org/10.1073/pnas.1014743108>
- Colla SR, Packer L (2008) Evidence for decline in eastern North American bumblebees (Hymenoptera: Apidae), with special focus on *Bombus affinis* Cresson. *Biodiversity and Conservation* 17: 1379–1391. <https://doi.org/10.1007/s10531-008-9340-5>
- Colla SR, Richardson L, Williams PH (2011) Bumble Bees of the Eastern United States. Washington (DC): US Forest Service and the Pollinator Partnership, 1–104.
- Colla SR, Gadallah F, Richardson L, Wagner D, Gall L (2012) Assessing declines of North American bumble bees (*Bombus* spp.) using museum specimens. *Biodiversity and Conservation* 21: 3585–3595. <https://doi.org/10.1007/s10531-012-0383-2>
- Cooley H, Vallejo-Marin M (2021) Buzz-pollinated crops: a global review and meta-analysis of the effects of supplemental bee pollination in tomato. *Journal of Economic Entomology* 114: 505–519. <https://doi.org/10.1093/jee/toab009>
- Danforth BN, Cardinal S, Praz C, Almeida EAB, Michez D (2013) The impact of molecular data on our understanding of bee phylogeny and evolution. *Annual Review of Entomology* 58: 57–78. <https://doi.org/10.1146/annurev-ento-120811-153633>
- Dolan AC, Delphia CM, O’Neill KM, Ivie MA (2017) Bumble bees (Hymenoptera: Apidae) of Montana. *Annals of the Entomological Society of America* 110: 129–144. <https://doi.org/10.1093/aesa/saw064>
- Drons DJ (2012) An inventory of native bees (Hymenoptera: Apiformes) in the Black Hills of South Dakota and Wyoming. MS Thesis. South Dakota State University (Brookings).
- Engel MS, Rasmussen C, Gonzalez VH (2021) Bees, Phylogeny and Classification. In: Starr CK (Ed.) *Encyclopedia of Social Insects*. Springer, Cham, 93–109. https://doi.org/10.1007/978-3-030-28102-1_14
- Gartner RF, Seig CH (1996) South Dakota rangelands: more than a sea of grass. *Rangelands* 18: 212–216.

- GBIF (2022) Global Biodiversity Information Facility. <https://www.gbif.org> [accessed 10 June 2022]
- Genung MA, Fox J, Williams NM, Kremen C, Ascher J, Gibbs J, Winfree R (2017) The relative importance of pollinator abundance and species richness for the temporal variance of pollination services. *Ecology* 98: 1807–1816. <https://doi.org/10.1002/ecy.1876>
- Goulson D, Lye GC, Darvill B (2008) Decline and conservation of bumble bees. *Annual Review of Entomology* 53: 191–208. <https://doi.org/10.1146/annurev.ento.53.103106.093454>
- Grant TA, Flanders-Wanner B, Shaffer TL, Murphy RK, Knutsen GA (2009) An emerging crisis across northern prairie refuges: Prevalence of invasive plants and a plan for adaptive management. *Ecological Restoration* 27: 58–65. <https://doi.org/10.3368/er.27.1.58>
- Grant TA, Shaffer TL, Flanders B (2020) Patterns of smooth brome, Kentucky bluegrass, and shrub invasion in the Northern Great Plains vary with temperature and precipitation. *Natural Areas Journal* 40: 11–22. <https://doi.org/10.3375/043.040.0103>
- Graves TA, Janousek WM, Gaulke SM, Nicholas AC, Keinath DA, Bell CM, Cannings S, Hatfield RG, Heron JM, Koch JB, Loffland HL, Richardson LL, Rohde AT, Rykken J, Strange JP, Tronstad LM, Sheffield CF (2020) Western bumble bee: declines in the continental United States and range-wide information gaps. *Ecosphere* 11: e03141. <https://doi.org/10.1002/ecs2.3141>
- Grixti JC, Wong LT, Cameron SA, Favret C (2009) Decline of bumble bees (*Bombus*) in the North American Midwest. *Biological Conservation* 142: 75–84. <https://doi.org/10.1016/j.biocon.2008.09.027>
- Hartman K, Archambault A, Hall A, Sand-Driver T, Johnson PJ (2019) The native bees (Hymenoptera: Apiformes) associated with Juneberry (*Amelanchier alnifolia*) on the Fort Berthold Indian Reservation, North Dakota. *Tribal College and University Research Journal* 4: 51–64.
- Hemberger J, Crossley MS, Gratton C (2021) Historical decrease in agricultural landscape diversity is associated with shifts in bumble bee species occurrence. *Ecology Letters* 24: 1800–1813. <https://doi.org/10.1111/ele.13786>
- Hines HM (2008) Historical biogeography, divergence times, and diversification patterns of bumble bees (Hymenoptera: Apidae: *Bombus*). *Systematic Biology* 57: 58–75. <https://doi.org/10.1080/10635150801898912>
- iNaturalist (2022) iNaturalist. <https://www.inaturalist.org> [accessed June 10 2022]
- IUCN (2022) The IUCN Red List of Threatened Species. Version 2022-1. <https://www.iucn-redlist.org> [accessed 10 June 2022]
- Kearns CA, Inouye DW, Waser NM (1998) Endangered mutualisms: the conservation of plant-pollinator interactions. *Annual Review of Ecology and Systematics* 29: 83–112. <https://doi.org/10.1146/annurev.ecolsys.29.1.83>
- Kilpatrick SK, Gibbs J, Mikulas MM, Spichiger SE, Ostiguy N, Biddinger DJ, Lopez-Uribe MM. (2020) An updated checklist of the bees (Hymenoptera, Apoidea, Anthophila) of Pennsylvania, United States of America. *Journal of Hymenoptera Research* 77: 1–86. <https://doi.org/10.3897/jhr.77.49622>
- Kleijn D, Winfree R, Bartomeus I, Carvalheiro LG, Henry M, Isaacs R, Klein AM, Kremen C, M'Gonigle LK, Rader R, Ricketts TH, Williams NM, Adamson NL, Ascher JS, Báldi

- A, Batáry P, Benjamin F, Biesmeijer JC, Blitzer EJ, Bommarco R, Brand MR, Bretagnolle V, Button L, Cariveau DP, Chifflet R, Colville JF, Danforth BN, Elle E, Garratt MPD, Herzog F, Holzschuh A, Howlett BG, Jauker F, Jha S, Knop E, Krewenka KM, Le Féon V, Mandelik Y, May EA, Park MG, Pisanty G, Reemer M, Riedinger V, Rollin O, Rundlöf M, Sardiñas HS, Scheper J, Sciligo AR, Smith HG, Steffan-Dewenter I, Thorp R, Tscharrntke T, Verhulst J, Viana BE, Vaissière BE, Veldtman R, Ward KL, Westphal C, Potts SG (2015) Delivery of crop pollination services is an insufficient argument for wild pollinator conservation. *Nature Communications* 6: 7414. <https://doi.org/10.1038/ncomms8414>
- Koch JB, Strange JP, Williams P (2012) *Bumble Bees of the Western United States*. Washington (DC): US Forest Service and the Pollinator Partnership, 1–144.
- Koch JB, Lozier J, Strange JP, Ikerd H, Griswold T, Cordes N, Solter L, Stewart I, Cameron SA (2015) US *Bombus*, a database of contemporary survey data for North American Bumble Bees (Hymenoptera, Apidae, *Bombus*) distributed in the United States. *Biodiversity Data Journal* 3: e6833. <https://doi.org/10.3897/BDJ.3.e6833>
- LaBerge WE, Webb MC (1962) *The Bumblebees of Nebraska*. University of Nebraska College of Agriculture Research Bulletin 205: 1–38.
- LeBuhn G, Droege S, Connor EF, Gemmill-Herren B, Potts SG, Minckley RL, Griswold T, Jean R, Kula E, Roubik DW, Cane J, Wright KW, Frankie G, Parker F (2013) Detecting insect pollinator declines on regional and global scales. *Conservation Biology* 27: 113–120. <https://doi.org/10.1111/j.1523-1739.2012.01962.x>
- Losey JE, Vaughan M (2006) The economic value of ecological services provided by insects. *Bioscience* 56: 311–323. [https://doi.org/10.1641/0006-3568\(2006\)56\[311:TEVOES\]2.0.CO;2](https://doi.org/10.1641/0006-3568(2006)56[311:TEVOES]2.0.CO;2)
- Martens AP, Johnson PJ (2021) Prairie remnant bumble bee diversity on the Prairie Coteau (Hymenoptera: Apidae: *Bombus* spp.). *Proceedings of the South Dakota Academy of Science* 100: 126.
- Michener CD (2007) *The Bees of the World*. 2nd Edn. Johns Hopkins University Press (Baltimore), 1–953.
- Milliron HE (1971) A monograph of the western hemisphere bumblebees (Hymenoptera: Apidae; Bombinae) I. *The Memoirs of the Entomological Society of Canada* 82: 1–80. <https://doi.org/10.4039/entm10382fv>
- Milliron HE (1973a) A monograph of the western hemisphere bumblebees (Hymenoptera: Apidae; Bombinae) II. *The Memoirs of the Entomological Society of Canada* 89: 81–235. <https://doi.org/10.4039/entm10589fv>
- Milliron HE (1973b) A monograph of the western hemisphere bumblebees (Hymenoptera: Apidae; Bombinae) III. *The Memoirs of the Entomological Society of Canada* 91: 236–333.
- Mitchell TB (1962) *Bees of the Eastern United States: Volume II*. North Carolina Agricultural Experimental Station Technical Bulletin 152: 1–557.
- Mola JM, Hemberger J, Kochanski J, Richardson LL, Pearse IS (2021) The importance of forests in bumble bee biology and conservation. *Bioscience* 71: 1234–1248. <https://doi.org/10.1093/biosci/biab121>
- Novotny JL, Reeher P, Varvaro M, Lybbert A, Smith J, Mitchell RJ, Goodell K (2021) Bumble bee species distributions and habitat associations in the Midwestern USA, a region of

- declining diversity. *Biodiversity and Conservation* 30: 865–887. <https://doi.org/10.1007/s10531-021-02121-x>
- Ollerton J, Winfree R, Tarrant S (2011) How many flowering plants are pollinated by animals? *Oikos* 120: 321–326. <https://doi.org/10.1111/j.1600-0706.2010.18644.x>
- Palit R, Gramig G, DeKeyser ES (2021) Kentucky bluegrass invasion in the Northern Great Plains and prospective management approaches to mitigate its spread. *Plants* 10: 817. <https://doi.org/10.3390/plants10040817>
- Pei CK, Hovick TJ, Limb RF, Harmon JP, Geaumont BA (2022) Bumble bee (*Bombus*) species distribution, phenology, and diet in North Dakota. *Prairie Naturalist Special Issue 1*: 11–29.
- Potts SG, Biesmeijer JC, Kremen C, Neumann P, Schweiger O, Kunin WE (2010) Global pollinator declines: trends, impacts, and drivers. *Trends in Ecology & Evolution* 25: 345–353. <https://doi.org/10.1016/j.tree.2010.01.007>
- Reilly JR, Artz DR, Biddinger D, Bobiwash K, Boyle NK, Brittain C, Brokaw J, Campbell JW, Daniels J, Elle E, Ellis JD, Fleischer SJ, Gibbs J, Gillespie RL, Gundersen KB, Gut L, Hoffman G, Joshi N, Lundin O, Mason K, McGrady CM, Peterson SS, Pitts-Singer TL, Rao S, Rothwell N, Rowe L, Ward KL, Williams NM, Wilson JK, Isaacs R, Winfree R (2020) Crop production in the USA is frequently limited by a lack of pollinators. *Proceedings of the Royal Society B* 287: 20200922. <https://doi.org/10.1098/rspb.2020.0922>
- SCAN (2022) Symbiota Collections of Arthropods Network. <https://scan-bugs.org/portal> [accessed June 10 2022]
- Severin HC (1925) The Bumble-Bees of South Dakota. 16th Annual Report of the State Entomologist of South Dakota. South Dakota State College, Brookings, 17–20.
- Stubbs CS, Drummond FA (2001) *Bombus impatiens* (Hymenoptera: Apidae): an alternative to *Apis mellifera* (Hymenoptera: Apidae) for lowbush blueberry pollination. *Journal of Economic Entomology* 94: 609–616. <https://doi.org/10.1603/0022-0493-94.3.609>
- Toledo D, Sanderson M, Spaeth K, Hendrickson J, Printz J (2014) Extent of Kentucky bluegrass and its effect on native plant species diversity and ecosystem services in the Northern Great Plains of the United States. *Invasive Plant Science and Management* 7: 543–552. <https://doi.org/10.1614/IPSM-D-14-00029.1>
- Williams PH, Cameron SA, Hines HM, Cederberg B, Rasmont P (2008) A simplified subgeneric classification of the bumblebees (genus *Bombus*). *Apidologie* 39: 46–74. <https://doi.org/10.1051/apido:2007052>
- Williams PH, Thorp RW, Richardson LL, Colla SR (2014) Bumble Bees of North America. An Identification Guide. Princeton University Press, Princeton, 1–208.
- Wimberly MC, Janssen LL, Hennessy DA, Luri M, Chowdhury NM, Feng H (2017) Crop-land expansion and grassland loss in the eastern Dakotas: new insights from a farm-level survey. *Land Use Policy* 63: 160–173. <https://doi.org/10.1016/j.landusepol.2017.01.026>
- Winfree R, Reilly JR, Bartomeus I, Cariveau DP, Williams NM, Gibbs J (2018) Species turnover promotes the importance of bee diversity for crop pollination at regional scales. *Science* 359: 791–793. <https://doi.org/10.1126/science.aao2117>
- Witt T, Corbett K, Norton H, Steely J (2013) The history of agriculture in South Dakota: components for a fully developed historic context. South Dakota State Historic Preservation Office, Pierre, 1–137.

- Wood TJ, Gibbs J, Graham KK, Isaacs R (2019) Narrow pollen diets are associated with declining Midwestern bumble bee species. *Ecology* 100: e02697. <https://doi.org/10.1002/ecy.2697>
- Wright CK, Wimberly MC (2013) Recent land use change in the Western Corn Belt threatens grasslands and wetlands. *Proceedings of the National Academy of Sciences* 110: 4134–4139. <https://doi.org/10.1073/pnas.1215404110>
- Vilella-Arnizaut IB, Roeder DV, Fenster CB (2022) Use of botanical gardens as arks for conserving pollinators and plant-pollinator interactions: a case study from the United States Northern Great Plains. *Journal of Pollination Ecology* 31: 53–69. [https://doi.org/10.26786/1920-7603\(2022\)645](https://doi.org/10.26786/1920-7603(2022)645)

Appendix I

Checklist of the *Bombus* spp. of South Dakota

All records for *Bombus* species reported from South Dakota are presented here, organized alphabetically by subgenus, then species epithet. Each species record consists of the counties for which a voucher specimen or verifiable observational record had been confirmed. The year of the most recent record for each species is presented at the end of the county list.

Family Apidae

Subfamily Apinae

Tribe Bombini

Genus *Bombus* Latreille 1802

Taxonomy: Milliron (1971, 1973a, b); Mitchell (1962); Williams et al. (2008, 2014).

Subgenus *Bombias* Robertson, 1903

Bombus (Bombias) auricomus (Robertson, 1903) – Bennett, Bon Homme, Brookings, Brown, Butte, Charles Mix, Clay, Codington, Custer, Day, Deuel, Jackson, Jones, Lake, Lawrence, Lincoln, Marshall, Minnehaha, Oglala Lakota, Pennington, Roberts, Stanley, Turner, Union. Last recorded 2021.

Bombus (Bombias) nevadensis Cresson, 1874 – Brookings, Butte, Codington, Custer, Day, Deuel, Dewey, Fall River, Harding, Hughes, Jackson, Jones, Lawrence, Marshall, Meade, Moody, Oglala Lakota, Pennington, Roberts, Stanley, Sully, Ziebach. Last recorded 2021.

Subgenus *Bombus* Latreille, 1802

Bombus (Bombus) affinis Cresson, 1863 – Day, Roberts. Last recorded 1952.

Bombus (Bombus) occidentalis Greene, 1858 – Brookings, Butte, Clay, Custer, Day, Fall River, Jerauld, Lawrence, Pennington, Roberts. Last recorded 2020.

Bombus (Bombus) terricola Kirby, 1837 – Brookings, Custer, Day, Lawrence, Pennington, Roberts. Last recorded 2020.

Subgenus *Cullumanobombus* Vogt, 1911

Bombus (Cullumanobombus) fraternus (Smith, 1854) – Bennett, Bon Homme, Haakon, Hughes, Jones, Pennington, Stanley. Last recorded 2020.

Bombus (Cullumanobombus) griseocollis (De Geer, 1773) – Beadle, Bennett, Bon Homme, Brookings, Brown, Buffalo, Butte, Charles Mix, Clark, Clay, Codington, Custer, Davison, Day, Deuel, Dewey, Douglas, Edmunds, Fall River, Faulk, Grant, Gregory, Hand, Harding, Hughes, Jackson, Jerauld, Jones, Kingsbury, Lake, Lawrence, Lincoln, Lyman, Marshall, McPherson, Meade, Miner, Minnehaha, Oglala Lakota, Pennington, Perkins, Potter, Roberts, Sanborn, Spink, Stanley, Sully, Todd, Tripp, Turner, Union, Walworth, Yankton, Ziebach. Last recorded 2021.

Bombus (Cullumanobombus) morrisoni Cresson, 1878 – Fall River, Jackson, Pennington. Last recorded 2021.

Bombus (Cullumanobombus) rufocinctus Cresson, 1863 – Brookings, Butte, Custer, Day, Fall River, Harding, Jackson, Lawrence, Pennington. Last recorded 2021.

Subgenus *Psithyrus* Lepeletier, 1833

Bombus (Psithyrus) bohemicus Seidl, 1837 – Lawrence. Last recorded 1974.

Bombus (Psithyrus) citrinus (Smith, 1854) – Brookings, Marshall, Roberts. Last recorded 1994.

Bombus (Psithyrus) flavidus Eversmann, 1852 – Pennington. Last recorded 2009.

Bombus (Psithyrus) insularis (Smith, 1861) – Clay, Custer, Fall River, Lawrence, Pennington. Last recorded 2021.

Bombus (Psithyrus) suckleyi Greene, 1860 – Lawrence, Meade, Pennington. Last recorded 1969.

Bombus (Psithyrus) variabilis (Cresson, 1872) – Brookings. Last recorded 1958.

Subgenus *Pyrobombus* Dalla Torre, 1880

Bombus (Pyrobombus) bifarius Cresson, 1878 – Brookings, Custer, Davison, Day, Deuel, Fall River, Kingsbury, Lawrence, Meade, Pennington. Last recorded 2021.

Bombus (Pyrobombus) bimaculatus Cresson, 1863 – Brookings, Brown, Butte, Clay, Codington, Custer, Day, Deuel, Douglas, Gregory, Hughes, Jackson, Kingsbury, Lawrence, Lincoln, Marshall, Meade, Miner, Minnehaha, Pennington, Roberts, Stanley, Sully, Turner, Yankton. Last recorded 2021.

Bombus (Pyrobombus) centralis Cresson, 1864 – Custer, Fall River, Lawrence, Pennington. Last recorded 2011.

***Bombus (Pyrobombus) flavifrons* Cresson, 1863** – Custer, Fall River, Lawrence, Pennington. Last recorded 2011.

***Bombus (Pyrobombus) huntii* Greene, 1860** – Beadle, Bennett, Brookings, Brown, Butte, Campbell, Clark, Codington, Custer, Day, Deuel, Fall River, Faulk, Harding, Hughes, Jackson, Lawrence, Lincoln, Meade, Oglala Lakota, Pennington, Perkins, Roberts, Stanley, Sully, Union, Walworth. Last recorded 2021.

***Bombus (Pyrobombus) impatiens* Cresson, 1863** – Beadle, Bon Homme, Brookings, Clay, Codington, Davison, Day, Deuel, Gregory, Hughes, Kingsbury, Lake, Lincoln, Marshall, Miner, Minnehaha, Pennington, Stanley, Sully, Union, Yankton. Last recorded 2021.

***Bombus (Pyrobombus) melanopygus* Nylander, 1848** – Custer, Lawrence, Pennington. Last recorded 1963.

***Bombus (Pyrobombus) mixtus* Cresson, 1878** – Custer, Lawrence, Pennington. Last recorded 2021.

***Bombus (Pyrobombus) ternarius* Say, 1837** – Brookings, Custer, Day, Fall River, Grant, Lawrence, Meade, Pennington, Roberts, Walworth. Last recorded 2018.

***Bombus (Pyrobombus) vagans* Smith, 1854** – Bon Homme, Brookings, Brown, Butte, Codington, Custer, Day, Deuel, Fall River, Hamlin, Lawrence, Lincoln, Marshall, Meade, Pennington, Roberts, Union. Last recorded 2021.

Subgenus *Subterraneobombus* Vogt, 1911

***Bombus (Subterraneobombus) appositus* Cresson, 1879** – Custer, Day, Lawrence, Pennington. Last recorded 2021.

***Bombus (Subterraneobombus) borealis* Kirby, 1837** – Brookings, Codington, Day, Deuel, Marshall, Roberts, Walworth. Last recorded 2021.

Subgenus *Thoracobombus* Dalla Torre, 1880

***Bombus (Thoracobombus) fervidus* (Fabricius, 1798)** – Bennett, Bon Homme, Brookings, Brown, Brule, Buffalo, Butte, Campbell, Clark, Clay, Codington, Custer, Davison, Day, Deuel, Fall River, Haakon, Hand, Harding, Hughes, Jackson, Jones, Kingsbury, Lawrence, Lyman, Marshall, Meade, Minnehaha, Oglala Lakota, Pennington, Perkins, Roberts, Sanborn, Stanley, Sully, Todd, Union, Walworth, Yankton. Last recorded 2021.

***Bombus (Thoracobombus) pensylvanicus* (De Geer, 1773)** – Beadle, Bennett, Bon Homme, Brookings, Brown, Buffalo, Butte, Clark, Clay, Codington, Custer, Davison, Day, Deuel, Fall River, Faulk, Gregory, Haakon, Harding, Hughes, Jackson, Jerauld, Jones, Kingsbury, Lawrence, Lincoln, Lyman, Marshall, McCook, Minnehaha, Oglala Lakota, Pennington, Roberts, Sanborn, Spink, Stanley, Tripp, Turner, Union, Walworth, Yankton. Last recorded 2021.